Aspects of the determination of the platinum group elements and arsenic by inductively coupled plasma mass spectrometry

by

Lilian Olga Schmidt

Submitted in partial fulfilment
of the requirements for the degree

Philosophiae Doctor

in the Faculty of Natural and Agricultural Sciences
University of Pretoria

Pretoria
January 2001

ACKNOWLEDGEMENTS

The author wishes to thank the following:

Professors CJ Rademeyer and CA Strydom for their guidance.

The Foundation for Research and Development, the University of Pretoria and her parents for financial assistance.

The Forensic Science Laboratory of the South African Police Service for the use of their equipment and instrumentation.

Her husband, Heinrich Schmidt, for his advice and assistance.

Her family for their encouragement.

CONTENTS

SUMMARY

Aspects of the determination of the platinum group elements and arsenic by inductively coupled plasma mass spectrometry

Lilian Olga Schmidt
Supervisor: Professor CJ Rademeyer
Co-supervisor: Professor CA Strydom
Chemistry Department of the University of Pretoria
Submitted in the partial fulfilment of the requirements for the degree
Philosophiae Doctor

Inductively coupled plasma mass spectrometry is an extremely sensitive analytical technique for the detection of the isotopes of the elements.

The principles of the technique and the instrumentation associated with it were discussed with emphasis being placed on the inductively coupled plasma, ion extraction, ion focusing, quadrupole mass spectrometers and ion detection.

In order to set up a procedure for the optimisation of the inductively coupled plasma mass spectrometer and due to the complex nature of the technique a study was made of the effects of instrument parameters on the signals of the light elements, the heavy elements, the background intensities and the formation of interferences, for example polyatomic oxides and doubly charged ions. The parameters investigated include torch adjustment in the x, y and z directions, the coolant and auxiliary gas flow rates, the power, the aerosol carrier gas flow rate as well as ion lens settings.

An attempt was made to optimise and refine the method of quantitative determination of the platinum group elements (iridium, palladium, platinum, rhodium, ruthenium) and gold by means of inductively coupled plasma mass spectrometry. Selected isotopes of argon, scandium, yttrium and lanthanum were considered as possible internal standards for such determinations. The effect of the concentration of aqua regia present in solution on the ratios of the isotopes of the analytes to the isotopes of the internal standards was determined. Extensive regression data were compiled for calibrations involving the isotopes of the platinum group elements and gold with the mentioned isotopes as internal standards. The accuracy of quantitative determinations using these calibration curves was then determined in matrices comprising of various concentrations of aqua regia.

The quantitative determination of mono-isotopic arsenic in acidic matrices was investigated. Interferences render the quantitative determination of arsenic in a chloride containing matrix almost impossible. The reason for this is the fact that the argon isotope of mass 40, which is present due to the plasma, and the chlorine isotopes of masses 35 and 37, which is usually present due to the sample matrix or introduced via reagents, combine to form polyatomic ions at masses 75 and 77. The only naturally occurring isotope of arsenic is detected at mass 75. Various procedures for the correction of these polyatomic interferences on the analyte signal of arsenic were investigated in an attempt to make the accurate detection of low levels of arsenic by means of inductively coupled plasma mass spectrometry possible. In order to test the viability of using these correction procedures and to verify the accuracy thereof, molecular correction factors, employing the formation of polyatomic ions at masses 75 and 77, were determined in a number of acidic matrices. The effects of these correction factors combined with the use of several isotopes of chlorine, argon, scandium, yttrium and lanthanum as internal standards, on the quantitative determination of arsenic in various acidic matrices, including nitric acid, hydrochloric acid and combinations thereof, were monitored.

Certified reference materials were analysed in order to verify the validity of the developed methods.

SAMEVATTING

Aspekte van die bepaling van die platinum groep elemente en arseen deur middel van induktief gekoppelde plasma massaspektrometrie

Lilian Olga Schmidt
Studieleier: Professor CJ Rademeyer
Mede-studieleier: Professor CA Strydom
Departement Chemie van die Universiteit van Pretoria
Voorgelê ter vervulling van 'n deel van die vereistes vir die graad
Philosophiae Doctor

Induktief gekoppelde plasma massaspektrometrie is 'n baie sensitiewe analitiese tegniek vir die bepaling van die isotope van die elemente.

Die basiese beginsels van die tegniek en die instrumentasie wat daarmee geassosieer word, is bespreek en klem is gelê op die induktief gekoppelde plasma, ioon-ekstraksie, ioon-fokusering, kwadrupool massaspektrometers en ioon-deteksie.

Ten einde 'n prosedure daar te stel vir die optimisering van die induktief gekoppelde plasma massaspektrometer en as gevolg van die komplekse aard van die tegniek, is 'n studie gemaak van die effek van instrument veranderlikes op die seine van die ligte elemente, die swaarder elemente, die agtergrond intensiteite en die vorming van steurders, byvoorbeeld poli-atomiese oksides en dubbel gelaaide ione. Die veranderlikes wat ondersoek is, is onder andere verstelling van die fakkel in die *x*-, *y*- en *z*-rigtings, die vloeitempo's van die verkoelings- en plasmagasse, die plasmadrywing, die vloeitempo van die verstuiwergas asook die verstellings van die ioon-lense.

'n Poging is aangewend om die metode van kwantitatiewe bepaling van die platinum groep elemente (iridium, palladium, platinum, rodium, rutenium) en goud deur middel van induktief gekoppelde plasma massaspektrometrie te optimiseer en te verfyn. Sekere isotope van argon, skandium, yttrium en lantaan is oorweeg as moontlike interne standaarde vir sodanige bepalings. Die effek van die konsentrasie van koningswater teenwoordig in oplossing op die verhoudings van die isotope van die analiete tot die isotope van die interne standaarde, is bepaal. Omvattende regressie data vir kalibrasies van die isotope van die platinum groep elemente en goud met die genoemde isotope as interne standaarde, is bepaal. Die akkuraatheid van kwantitatiewe bepalings

deur van hierdie kalibrasie kurwes gebruik te maak, in matrikse wat uit verskeie konsentrasies van koningswater bestaan, is vasgestel.

Die kwantitatiewe bepaling van arseen, wat slegs een isotoop het, in verskillende suurmatrikse is ondersoek. Steurders maak die kwantitatiewe bepaling van arseen in 'n chloried-bevattende matriks bykans onmoontlik. Die rede hiervoor is die feit dat die argon-isotoop van massa 40, teenwoordig as gevolg van die plasma, en die chloor-isotope van massas 35 en 37, teenwoordig as gevolg van die monster se matriks of as gevolg van reagense gebruik, kombineer om poli-atomiese ione van massas 75 en 77 te vorm. Die enigste isotoop van arseen wat natuurlik voorkom, word waargeneem by massa 75. Verskeie prosedures om die korreksie van hierdie poli-atomiese steurders op die analiet-sein van arseen te bewerkstellig, is ondersoek. Dit is gedoen in 'n poging om die akkurate bepaling van lae vlakke van arseen deur middel van induktief gekoppelde plasma massa spektrometrie moontlik te maak. Om die haalbaarheid van hierdie korreksie-prosedures te toets en die akkuraatheid daarvan te verifieer, is molekulêre korreksie-faktore, wat berus op die vorming van poli-atomiese ione van massas 75 en 77, bepaal in 'n aantal suurmatrikse. Die effek van hierdie korreksie-faktore, gekombineer met die gebruik van verskeie isotope van argon, chloor, skandium, yttrium en lantaan as interne standaarde, op die kwantitatiewe bepaling van arseen in verskeie suurmatrikse, insluitende salpetersuur, soutsuur en kombinasies daarvan, is vasgestel.

Gesertifiseerde verwysingsmateriale is geanaliseer om die geldigheid van die ontwikkelde metodes te toets.

LIST OF ABBREVIATIONS USED

ICP-MS:	Inductively coupled plasma mass spectrometry or Inductively coupled plasma mass spectrometer
ICP-AES:	Inductively coupled plasma atomic emission spectrometry or Inductively coupled plasma atomic emission spectrometer
RF:	Radio frequency
RSD:	Relative standard deviation
XRF:	X-ray fluorescence spectrometry
AAS:	Atomic absorption spectrometry
GFAAS:	Graphite furnace atomic absorption spectrometry

CHAPTER 1

THE TECHNIQUE OF INDUCTIVELY COUPLED PLASMA MASS SPECTROMETRY

1.1 The inductively coupled plasma *[1]*

There is basically no difference between the characteristics of the inductively coupled plasma as used in ICP-MS and those of the plasma as used in the ICP-AES. Knowledge of the nature of the inductively coupled plasma is important to an understanding of the basis and characteristics of ICP-MS and therefore an outline is given below.

1.1.1 Torch and plasma [1]

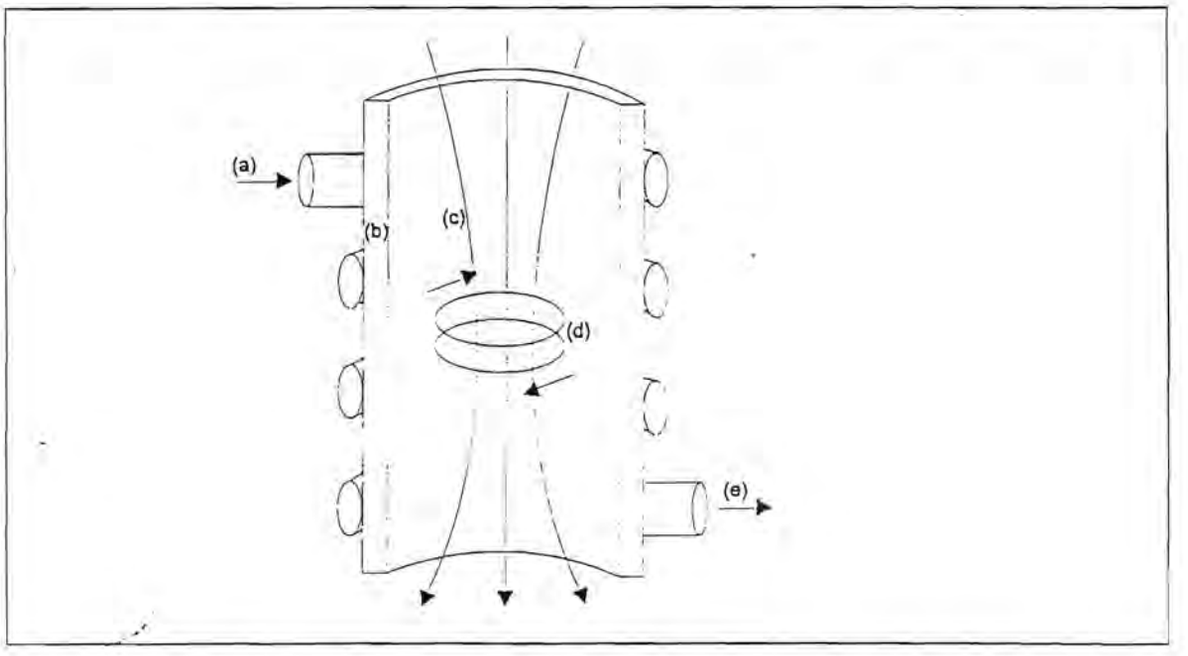

Figure 1.1: Operation of an inductively coupled plasma source. (a) Passing current through a coil (b) wrapped around a quartz tube (c) sets up a magnetic field, (d) which causes an eddy current of ions and electrons (e) whose motion generates intense heat in a continuously ionised flow of gas.

The inductively coupled plasma is an electrodeless discharge in a gas at atmospheric pressure, maintained by energy coupled to it from a radio frequency generator. This is achieved by a suitable coupling coil, which functions as the primary of a radio frequency transformer and the discharge itself acts as the secondary. The argon plasma is generated inside and at the open end of an assembly of quartz tubes known as the torch. The operation of an inductively coupled

plasma source is shown in figure 1.1 *[2]*. Minor changes have been made in the systems used for mass spectrometry – this includes the mounting of the torch with the axis horizontal which is done for convenience and some changes are made to the grounding point of the coupling (load) coil circuit to control the plasma electrical potential with respect to the mass spectrometer system which is grounded. The torch commonly used, based on the "Scott Fassel" design (see figure 1.2), has an outer tube of diameter 18 mm and the tube is about 100 mm long. Within this are two concentric tubes of 13 mm and 1.5 mm inner diameter which terminate short of the torch mouth. Each annular region formed by the tubes is supplied with gas by a side tube entering tangentially in such a way that it creates a vorticular flow. The center tube, through which the sample is introduced to the plasma, is brought out along the axis. The outer gas flow (termed the coolant flow) protects the tube walls and acts as the main plasma support and it is usually set between 10 and 15 $dm^3\ min^{-1}$. The main use of the second gas flow (termed the auxiliary flow), which is introduced to the inner annular space, is to ensure that the hot plasma is kept clear of the tip of the central capillary injector tube to prevent its being melted and its flow is usually set between 0 and 1.5 $dm^3\ min^{-1}$. The central gas flow (termed the injector, nebuliser or carrier flow) conveys the aerosol from the sample introduction system and is usually set at approximately 1 $dm^3\ min^{-1}$. This is sufficient, in the small diameter injector tube, to produce a high velocity jet of gas which then punches a cooler hole through the center of the plasma (termed the central or axial channel).

The load coil which consists of 2 - 4 turns of fine copper tube, cooled by a water or gas flow, is located with its outer turn a few millimeters below the mouth of the torch. The RF current which is supplied by the generator, produces a magnetic field which varies in time at the generator frequency (27 MHz), so that within the torch, the field lies along the axis. A spark from a Tesla coil initiates a discharge in a cold torch, thereby providing free electrons to couple with the magnetic field. Electrons in the plasma precess around the magnetic field lines in circular orbits and the electrical energy supplied to the coil is inverted into kinetic energy of electrons. At atmospheric pressure a free electron moves approximately 10^{-3} mm before it collides with an argon atom, to which its energy is transferred, thereby heating the plasma and forming a bright discharge. The skin effect which occurs in RF induction heating ensures that most of the energy is coupled into the outer or induction region of the plasma. The cool injector gas flow, which carries most of the sample aerosol, punches a channel through the center of the plasma so that little appears in the outer annular part of the plasma. Radiation and conduction from the annulus are mainly responsible for the heating of the gas in the center channel and

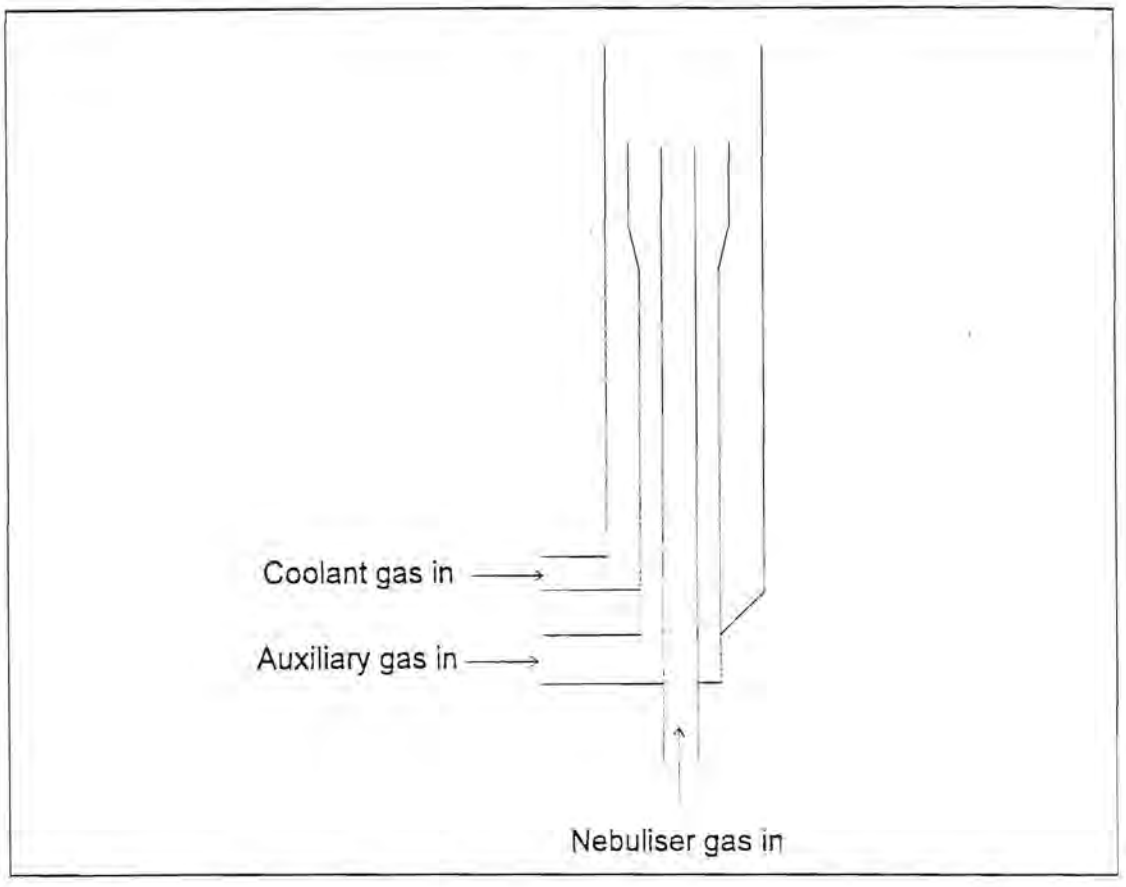

Figure 1.2: Fassel type inductively coupled plasma torch.

while the temperature in the induction region of the plasma may be as high as 10000 K, in the central channel the gas kinetic temperature is probably between 5000 and 7000 K at the mouth of the torch. The chemical composition of the sample solution can vary substantially without greatly affecting the electrical processes that sustain the plasma. This is mainly because the power is coupled mainly into the outer region which is physically distinct from the central channel through which the sample aerosol travels. The fact that the physical and chemical interferences in the inductively coupled plasma are not as severe compared to those seen in most other spectrochemical processes *[1]* may be attributed to this physical separation between the region where the electrical energy is added and the region containing the sample.

1.1.2 RF coupling [1]

The load coil and plasma present a low electrical impedance to the RF generator which feeds them energy. A matched load at the end of the coupling line to the load coil is necessary in order to provide efficient energy transfer and avoid mismatches which could produce high potentials from the reflected power. The load coil is essentially resistive and thus it absorbs the power delivered. The power required to maintain such a plasma is usually varies between 0.75

and 2.0 kW.

Mainly two types of generator are used. These include 1) free running systems, where the frequency is controlled by the oscillating circuit and load coil parameters and 2) crystal controlled systems where the operating frequency is determined by an oscillating quartz crystal and a servo controlled matching circuit is used to ensure correct matching of the load.

1.1.3 Sample introduction [1]

A sample which is introduced into central channel gas flow of the inductively coupled plasma needs to be a gas, vapour or aerosol of fine droplets or solid particles. A wide variety of methods and techniques may be used to produce these such as pneumatic or ultrasonic nebulisation for solutions, laser or spark ablation from a solid and generation of volatile hydrides or oxides from a reaction vessel among others. In a standard pneumatic nebuliser a fine droplet dispersion of the analyte solution is produced by a high velocity gas stream. A spray chamber removes the larger droplets and allows only those below approximately 8 μm to pass on to the plasma. These small droplets which reach the plasma carry only about 1% of the solution which is usually metered to the nebuliser by a peristaltic pump.

1.1.4 Sample history [1]

The ultimate aim of sample introduction is to produce sample ions at the entrance to the mass spectrometer. This is usually achieved by volatilisating, atomising and ionising a dispersion of fine solid particles in a carrier gas stream. In the most common case of pneumatic nebulisation the aerosol leaving the injector tube in the torch may still contain small liquid droplets, but these are quickly dried to produce solid microparticulates and at the increasingly higher temperatures which are experienced these are vaporised and the resulting vapour phase compounds dissociated. The transit through the center of the plasma takes several milliseconds and once atomised the sample is substantially ionised at the high temperature experienced.

Only 10^{-6} or less of the total atom population of the plasma consist of sample atoms. The degree of ionisation of the sample atoms is dependent on the ionisation conditions in the plasma, which in turn are dominated by the major constituents, usually argon, hydrogen, oxygen and electrons, as well as the ionisation constant and partition functions for the atom concerned. The temperature in the central channel is high enough to produce almost complete ionisation of many elements and a significant level for those elements of higher ionisation energy.

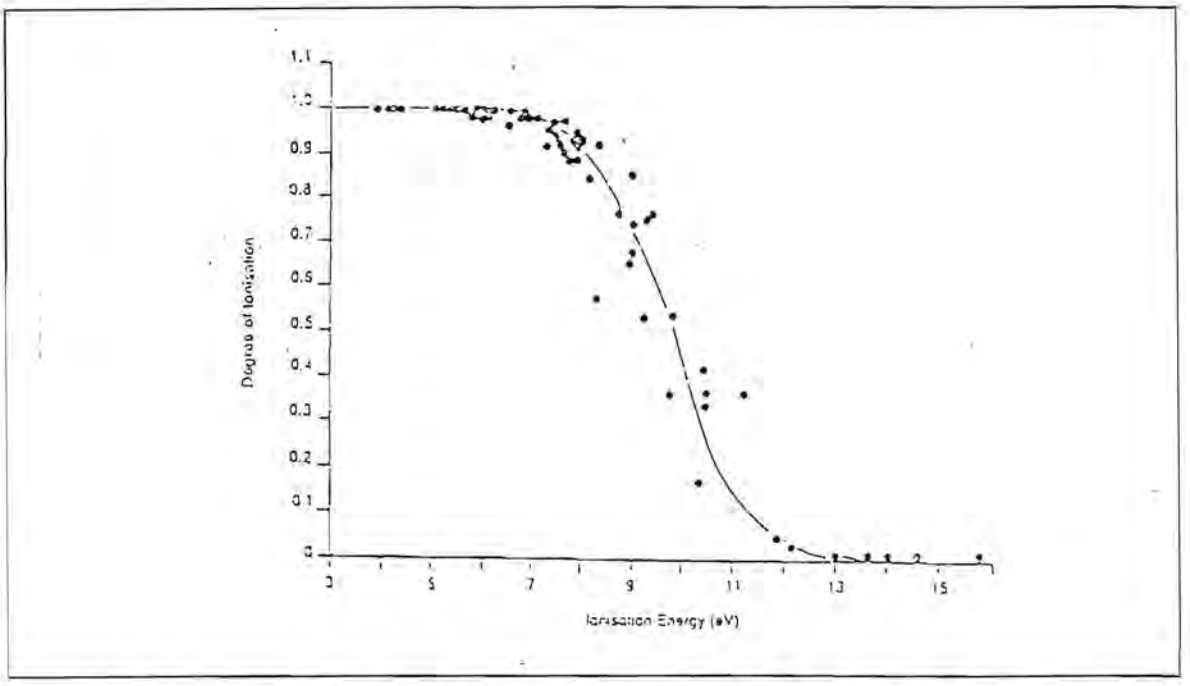

Figure 1.3: Degree of ionisation versus ionisation energy for singly charged ions in the inductively coupled plasma.

Although thermal equilibrium is not strictly achieved, it is approached at the plasma powers usually used. If it is however assumed, a reasonable estimate of experimental values for degree of ionisation may be obtained from the Saha equation. This is done using the generally accepted values from the literature for ionisation temperature T_i and electron population n_e. Values for most of the elements of the periodic table *[3]* are given in table 1.1. The general form of the dependence of degree of ionisation on ionisation energy for singly charged ions *[4]* is shown in figure 1.3, from which it may be seen that the response falls rapidly above 9 eV.

Table 1.1: Calculated values for degree of ionisation (%) of M^+ and M^{2+} at T_i = 7500 K, $n_e = 1x10^{18}$ dm^{-3}. Elements marked by an asterisk yield significant amounts of M^{2+} but partition functions are not available. (Values in brackets indicate % M^{2+} formed.)

H 0.1																He
Li 100	Be 75											B 58	C 5	N 0.1	O 0.1	F $9x10^{-4}$	Ne $6x10^{-6}$
Na 100	Mg 98											Al 98	Si 85	P 33	S 14	Cl 0.9	Ar 0.04
K 100	Ca 99(1)	Sc 100	Ti 99	V 99	Cr 98	Mn 95	Fe 96	Co 93	Ni 91	Cu 90	Zn 75	Ga 98	Ge 90	As 52	Se 33	Br 5	Kr 0.6
Rb 100	Sr 96(4)	Y 98	Zr 99	Nb 98	Mo 98	Tc	Ru 96	Rh 94	Pd 93	Ag 93	Cd 85	In 99	Sn 96	Sb 78	Te 66	I 29	Xe 8.5
Cs 100	Ba 91(9)	La 90(10)	Hf 98	Ta 95	W 94	Re 93	Os 78	Ir	Pt 62	Au 51	Hg 38	Tl 100	Pb 97(0.01)	Bi 92	Po	At	Rn
Fr	Ra	Ac	Unq	Unp	Unh	Uns	Uno										

Ce 98(2)	Pr 90(10)	Nd 99*	Pm	Sm 97(3)	Eu 100*	Gd 93(7)	Tb 99*	Dy 100*	Ho	Er 99*	Tm 91(9)	Yb 92(8)	Lu
Th 100*	Pa	U 100*	Np	Pu	Am	Cm	Bk	Cf	Es	Fm	Md	No	Lr

Table 1.2: Distribution of ionisation energies among the elements for singly and doubly charged ions at 1 eV intervals.

Ionisation energy (eV)	**Elements**	**2^+ ions**
<7	Li, Na, Al, K, Ca, Sc, Ti, V, Cr, Ga, Rb, Sr, Y, Zr, Nb, In, Cs, Ba, La, Ce, Pr, Nd, Pm, Sm, Eu, Gd, Tb, Dy, Ho, Er, Tm, Yb, Lu, Hf, Tl, Ra, Ac, Th, U	
7 – 8	Mg, Mn, Fe, Co, Ni, Cu, Ge, Mo, Tc, Ru, Rh, Ag, Sn, Sb, Ta, W, Re, Pb, Bi	
8 – 9	B, Si, Pd, Cd, Os, Ir, Pt, Po	
9 –10	Be, Zn, As, Se, Te, Au	
10 - 11	P, S, I, Hg, Rn	Ba, Ce, Pr, Nd, Ra
11 - 12	C, Br	Ca, Sr, La, Sm, Eu, Tb, Dy, Ho, Er
12 - 13	Xe	Sc, Y, Gd, Tm, Yb, Th, U, Ac
13 - 14	H, O, Cl, Kr	Ti, Zr, Lu
14 - 15	N	V, Nb, Hf
15 - 16	Ar	Mg, Mn, Ge, Pb
> 16	He, F, Ne	All other elements

It is clear from table 1.2 that most elements have first ionisation energies below 10 eV, corresponding to more than 50% ionisation while there are none whose second ionisation energies fall below 10 eV. Thus, although there are a number of elements such as the alkaline and rare earths, thorium and uranium which undergo some double ionisation, the majority do not and doubly charged ions should not present serious problems.

1.1.5 Plasma populations [1]

The gas pressure is 1 bar and at a gas kinetic temperature of 5000 K the total particle density is calculated from the gas laws to be 1.5×10^{21} dm^{-3}. The majority of this is argon. At an ionisation temperature of 7500 K the degree of ionisation of argon is calculated to be about 0.1%. As the second ionisation energy of argon is very high at 27 eV, the population of Ar^{2+} ions is negligible. In a "dry" plasma a typical value would be $n_{Ar+} = n_e = 1 \times 10^{18}$ dm^{-3}, but if a nebulised solution is introduced additional electrons are contributed by the ionisation of hydrogen and oxygen from the solvent, as well as H^+ and O^+ ions. At a nebuliser uptake of 1×10^{-3} dm^3 min^{-1} and an efficiency of 1% the populations of H^+ and O^+ are respectively about 2×10^{17} dm^{-3} and 1×10^{17} dm^{-3}. In addition, if the solution had been acidified with 1% nitric acid, as is usually done, there would be a population of N^+ of about 1×10^{15} dm^{-3}. These all contribute to the electron population and the value of n_e rises to about 1.3×10^{18} dm^{-3}. It is thus clear that the presence of water vapour in the aerosol contributes significantly to the ion and electron population of the axial channel.

The addition of trace elements to the nebulised solution produces far lower populations of the elements to be determined against this background of the "permanent" ions. An element at a concentration of 1 mg dm^{-3} in the sample solution, which is fully ionised in the plasma, contributes about 1×10^{13} ions dm^{-3} and accordingly the number is even lower for elements of higher ionisation energy. Thus, a fully ionised matrix element at 5 g dm^{-3} in the solution only contributes about 5×10^{16} dm^{-3} to the total level of n_e of 1.3×10^{18} dm^{-3} and produces a barely significant shift in the equilibrium. Thus, unless the concentration of the matrix element is extremely high, ionisation suppression in the plasma is generally not a major cause of matrix interference *[5]*.

1.1.6 Distribution of ions in the plasma [1]

As the plasma leaves the mouth of the torch it becomes accessible for ion extraction into the mass spectrometer. A simple visualization of the distribution of ions in the plasma may be

obtained from spatially resolved profiles made by moving the plasma across the ion extraction interface of an ICP-MS system. When no sample is introduced and the central channel contains only dry argon, the transverse profile of Ar^+ ions across the mouth of the torch is shown by the Ar^+ response in figure 1.4 *[1]*. On the torch axis the cooler central gas stream shows a relatively low Ar^+ population. A higher degree of ionisation of Ar occurs in the hotter induction region (plasma annulus) each side of the center. The ion population drops sharply at the edge of the plasma. If a similar plot is performed across the narrow central channel when a sample is being introduced, a profile such as that shown for Co^+ in figure 1.4 is obtained. The ions are concentrated mainly within 1 mm of the axis. Further along the axis away from the torch, the central channel diffuses into the annulus and similar profiles for Co at 5, 10 and 15 mm from the load coil are shown in figure 1.5 *[1]*.

From the distribution plots in figure 1.5 it seems as if the optimum position of the orifice is as close to the torch mouth as the load coil permits. However, it must be kept in mind that during its passage along the central channel of the plasma the sample must be converted to atomic ions as completely as possible and the processes of desolvation, volatilisation, dissociation and ionisation take several milliseconds. The time required depends particularly on the size of the initially desolvated microparticulates in the aerosol, which in turn depends on the level of dissolved solids in a nebulised sample solution, and on the bond strengths of the molecular species (which may be refractory) in the sample *[1]*. The time the sample resides in the hottest part of the plasma depends on the plasma operating parameters, but especially on plasma power and central channel gas flow.

The inductively coupled plasma thus forms a very convenient ion source with a high yield of singly charged analyte ions, few doubly charged and oxide or other molecular and adduct ions*[1]*.

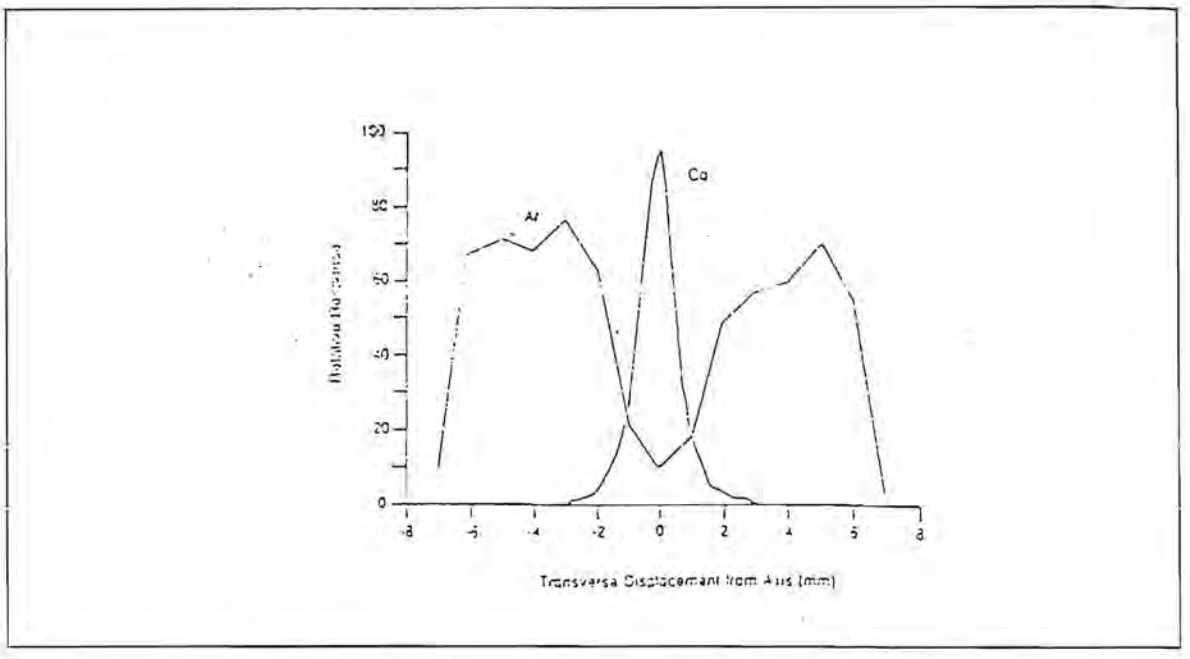

Figure 1.4: Transverse profiles of ions across the mouth of the plasma torch. Profile for Ar^+ shown for dry argon only. Profile for Co^+ from a nebulised solution at 100 μg dm^{-3}.

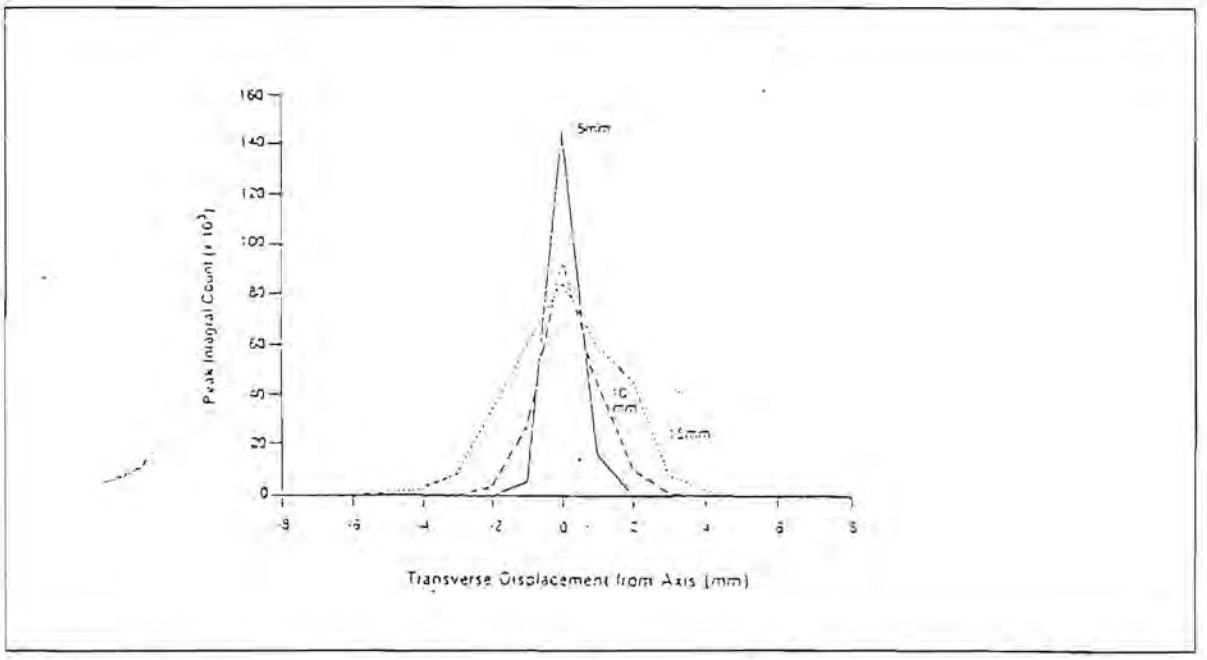

Figure 1.5: Transverse profiles across plasma flame at 5, 10 and 15 mm from load coil in steps of 1 mm. Nebulised solution containing Co at 100 μg dm^{-3}.

1.2 Ion extraction *[1]*

The extraction of ions from the plasma into the vacuum system is of critical importance in ICP-MS. Figure 1.6 shows a typical extraction interface. The ions first flow through a sampling orifice (diameter approximately 1 mm) into a mechanically pumped vacuum system, where a supersonic jet forms. The central section of the jet flows through the orifice of a skimmer cone (diameter also approximately 1 mm). The extracted gas containing the ions attains supersonic velocities as it expands into the vacuum chamber and reaches the skimmer orifice in only a few microseconds *[6]*. The sample ions change little in nature or relative proportions during the extraction process. To a first approximation, they simply flow through the orifice of the sampler cone and then through the orifice of the skimmer cone.

1.2.1 Boundary layer and sheath [1]

Figure 1.7 shows the two ways in which the plasma interacts with the sampling cone. Firstly, the plasma is deflected and cooled when it comes into contact with the metal cone. The temperature in the boundary layer of gas that forms between the plasma and the side of the cone is intermediate between the temperature of the plasma and that of the cone. Chemical reactions, such as oxide formation, occur readily in the boundary layer. However, in modern ICP-MS instruments the orifice of the sampler cone is large enough for the gas flow to puncture the boundary layer. Thus, the sampled gas is not cooled much while it is outside the sampler cone. There is still a thin, oblique boundary layer inside the lip of the orifice and care is taken in the design of the interface to ensure that oxides formed in this layer do not pass through the orifice of the skimmer cone. Oxide response is minimised if the diameter of the skimmer is less than that of the sampler *[7]*.

There is also an electrical interaction between the plasma and the conducting sampler cone. The plasma is electrically neutral since it contains equal numbers of positive ions and electrons (ignoring the negligible number of doubly charged and negative ions). A surface immersed in the plasma will collect both positive ions and electrons. Since the mobility of the electrons is much higher than that of the positive ions, the electron flux (current) to the surface is much higher than the positive ion flux. Thus, the potential of the surface of the sampler cone becomes negative with respect to the plasma. The sheath region that forms over the surface of the sampler cone is depleted in electrons, and positive ions are in excess. The negative potential of the surface of the sampler cone with respect to the plasma repels electrons and attracts ions to balance the two fluxes.

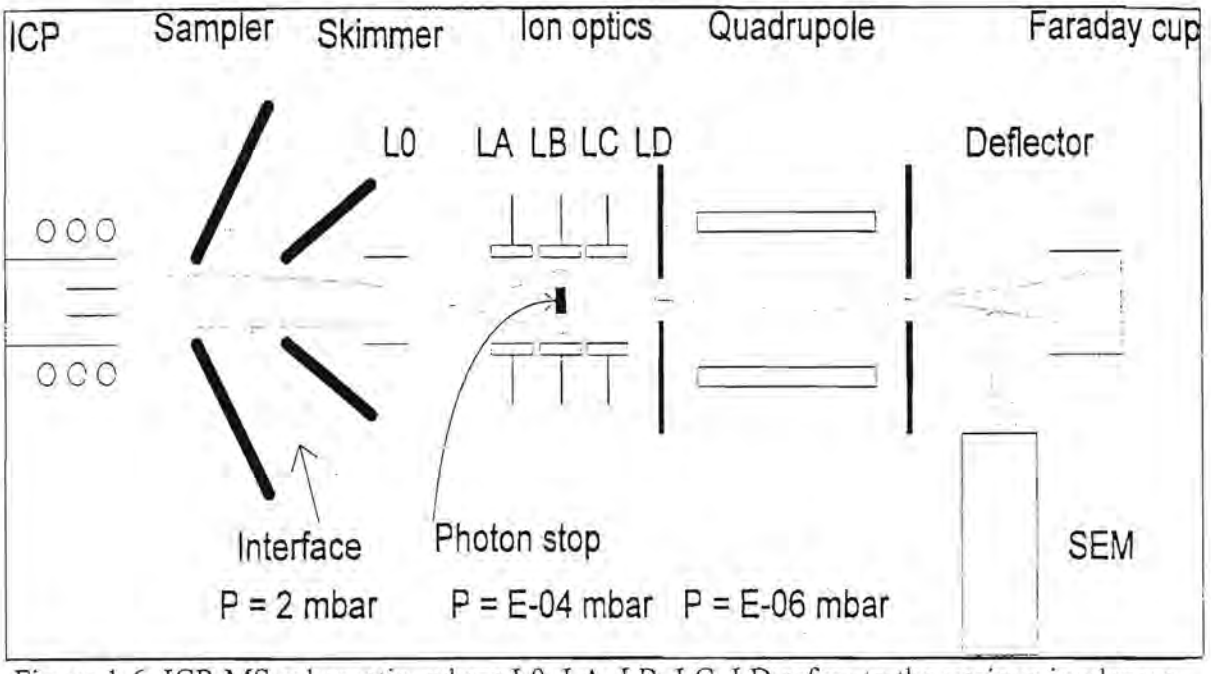

Figure 1.6: ICP-MS schematic, where L0, LA, LB, LC, LD refers to the various ion lenses and SEM refers to a secondary electron multiplier.

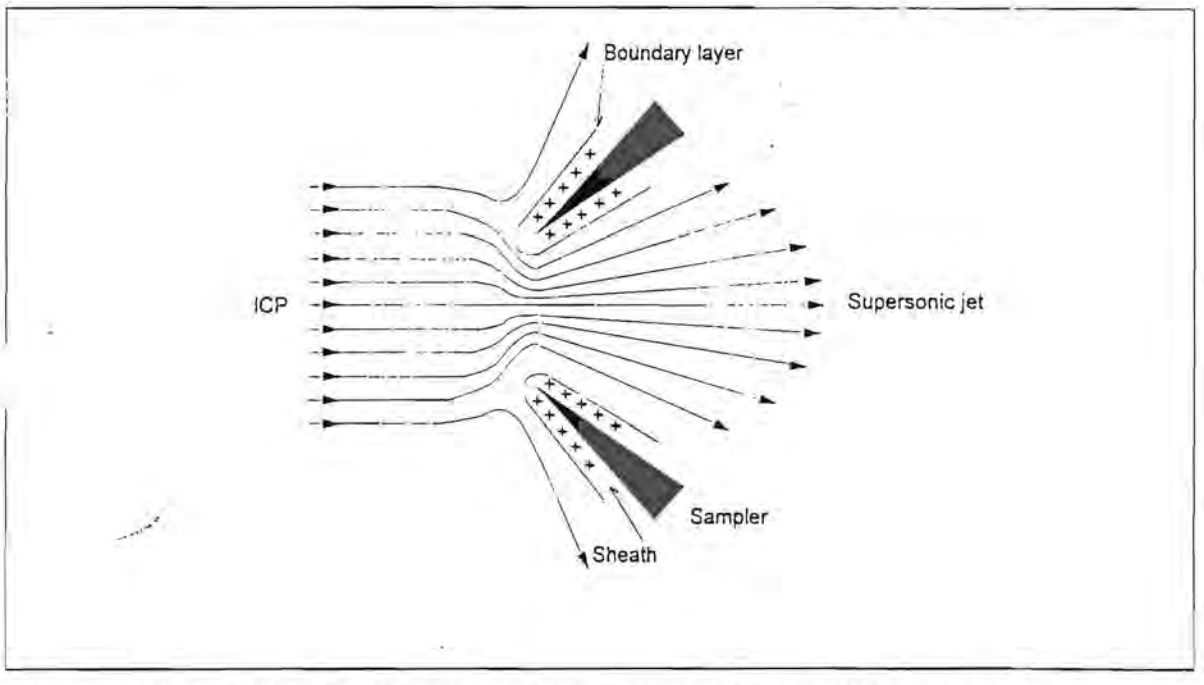

Figure 1.7: Interaction of inductively coupled plasma with sampling cone showing boundary layer, sheath and flow field into orifice. (Boundary layer not drawn to scale.) *[1]*

In ICP-MS the metal sampler cone is usually grounded. Since the potential of the sampler cone is fixed, the plasma appears to float at a positive potential, which is known as the plasma potential. The sheath co-exists with the boundary layer. The number of uncharged particles greatly exceeds the numbers of either positive ions or electrons, so the sheath is a dynamic region with particles constantly moving in or out via collisions. Although calculations indicate

the sheath to be much thinner than the boundary layer *[6]*, it still influences the ion extraction process by its interaction with the RF potential in the plasma, as described in the next section.

1.2.2 *Plasma potential and secondary discharge [1]*

The plasma is maintained by RF energy coupled to it by the load coil. Thus, current circulate at this frequency through the plasma, which is a good conductor. In addition to this inductive (magnetic) coupling, the load coil is also coupled capacitively (electrostatically) through the torch wall by the capacitance between the coil and the plasma. The arrangement of the electrical connections to the coil influences this capacitive coupling process *[1]*.

Normally, the one end of the load coil is connected to the high voltage RF source while the other end of the load coil is grounded. A potential gradient thus exists along the load coil, except at the moment when the field polarity reverses. When the plasma contacts the sampler cone and part of it is drawn through the orifice, the plasma is coupled to the sampler cone through the very thin sheath. Since the impedance of this sheath layer is much lower than that of the capacitive coupling between the plasma and load coil, the plasma acquires an RF potential which is determined by the ratio of these two impedances which act as a potential divider. An RF current flows through this coupling from the load coil. However, the RF current flow to the grounded cone is modified by the different mobilities of ions and electrons in the sheath layer. During negative half cycles, the current is carried mainly by electrons, which can flow to ground far more readily than the positive ions that carry current during positive half cycles.

These effects cause the plasma to assume a net mean positive DC potential. This offset or bias potential may be considerably larger than the floating potential due to the sheath alone *[8, 9]*.

If the plasma potential is high enough, it can cause an electrical discharge between the plasma and the sampler cone. This secondary discharge is manifest as a crackling discharge into the orifice. A severe discharge is detrimental in that it erodes the orifice, generates multiply charged ions, and induces high kinetic energies and a wide spread of kinetic energy in the extracted ion beam *[8, 10]*.

Minimising this secondary discharge was a key step in the early development of ICP-MS. Modification of the load coil arrangement was one successful approach. The plasma potential

can also be reduced by: a) use of a low aerosol gas flow rate (0.5 - 0.9 dm^3 min^{-1}), b) reducing the solvent load to the plasma, c) moving the sampling orifice close to the load coil and d) substituting a two-turn load coil (instead of the original three turns). These measures weaken the discharge but do not eliminate it fully, because the ion kinetic energy and certain properties of the spectra such as the ratio M^{2+}/M^{+} vary with operating conditions in a fashion that is not consistent with the expected changes in the plasma. The fundamental reasons why the plasma potential is sensitive to sampling position and operating conditions are not clear at this time*[1]*.

The center tapped load coil arrangement *[8,11]*, as well as the Colpitts oscillator circuit *[12]*, seems to eliminate almost totally the secondary discharge. With the widespread use of aerosol desolvation, dry sample introduction, and other empirical ways to minimise plasma potential with unbalanced load coils, excellent results can be obtained from either type of coil arrangement *[13]*.

1.2.3 Supersonic jet [1]

The gas flowing through the sampler cone expands into the first stage of the vacuum chamber, which is evacuated by a mechanical pump. The pressure ratio is more than sufficient for a supersonic jet to be formed inside the first stage. The supersonic jet consists of a freely expanding region often called the zone of silence surrounded by shock waves called the barrel shock and Mach disc. Figure 1.8 graphically depicts the sampler and skimmer cones as well as the shock waves. The barrel shock and Mach disc are caused by collisions between fast atoms from the jet and the background gas, which reheat the atoms and induce emission. The position of the onset of the Mach disc is given by:

$$X_M = 0.67\, D_0\, (P_0/P_1)^{1/2}$$

where X_M is the position of the Mach disc from the sampling orifice along the central axis,

D_0 is the diameter of the sampling orifice,

P_0 is the pressure in the inductively coupled plasma and

P_1 is the background pressure in the extraction chamber *[14]*.

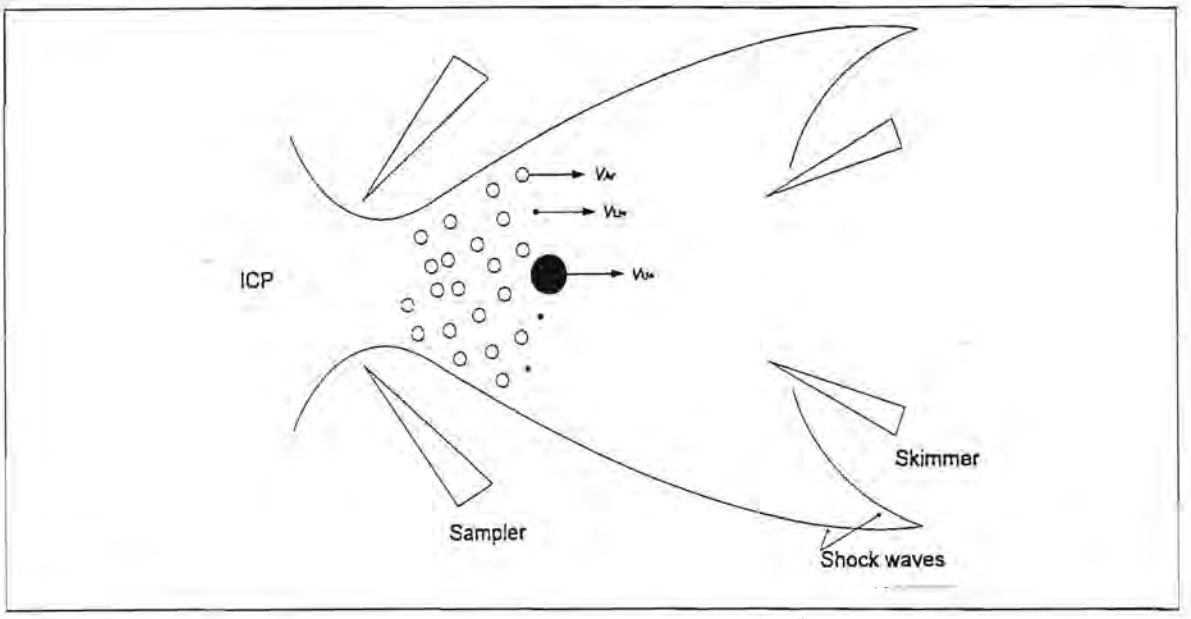

Figure 1.8: Sampler, skimmer and shock waves showing how light ions (·) and heavy ions (•) are all accelerated to the same velocity (v) as neutral Ar (○) in the supersonic jet.

In order to avoid losses of positive ions due to collisions and scattering, the skimmer cone is positioned with its tip open inside the Mach disc. This is done to ensure that the central core of the zone of silence passes through the skimmer cone into the second vacuum stage. The Mach disc is now replaced by a shock wave that forms outside the skimmer downstream from the tip. A sampler-skimmer separation of roughly two thirds of the distance to the onset of the Mach disc usually provides optimum positive ion transmission *[6, 15]*.

1.2.4 *Gas dynamics [1]*

The gas dynamic properties of the extraction process have been described *[6]*. Some of the points are given below.

The sampler collects gas from a region in the plasma of cross-sectional diameter roughly eight times that of the orifice of the sampler cone. The gas flow rate of an argon plasma at 5000 K is 10^{21} atoms s^{-1}. Of the gas that passes through the sampler, only about 1% (~10^{19} atoms s^{-1}) also traverses the skimmer. Furthermore, only the centerline flow gets through the skimmer, resulting in a spatial resolution in the plasma comparable to the diameter of the skimmer cone.

When the orifice of the sampler cone is large, the flow punctures the boundary layer cleanly and the gas is cooled very little until it gets inside the orifice. The presence of the metal sampler cone has little effect on the upstream plasma unless the secondary discharge is intense. Once

the sampled gas passes through the orifice of the sampler cone, collisions occur for the first few orifice diameters, after which the atoms continue to flow under essentially collisionless conditions. It is estimated that approximately 250 collisions occur between neutral argon atoms and other species during extraction. The extraction process takes roughly 3 μs and therefore there is little opportunity for ion loss by recombination between positive ions and electrons. There is also substantial experimental evidence for the lack of ion-electron recombination during extraction *[10, 16, 17]*.

The low number of collisions during the expansion and the short time duration thereof suggest that the sampling process is not complicated by extensive chemical reactions, and the ions extracted is more or less representative of the ions in the plasma *[6]*. The oxide ions (MO^+) observed are probably present mainly in the plasma, particularly if the orifice of the sampler cone is too close to the initial radiation zone. Some MO^+ ions can be formed from M^+ ions by reactions in the cool boundary layer in front of or inside the orifice of the sampler cone. Use of a skimmer orifice that is smaller than the sampling orifice helps prevent these additional MO^+ ions from passing through the skimmer to the mass spectrometer *[7]*. The origins of the other polyatomic ions are less clearly established.

1.3 Ion focusing *[1]*

After the positive ions leave the skimmer cone they are conveyed to the mass analyser by means of ion lenses.

1.3.1 Operation of ion lenses [1]

The general problem of transmitting and focusing ions through an ion lens are shown in figure 1.9. Suppose a positive ion of charge z is formed in a region of potential $V_{initial}$. It has a potential energy $zV_{initial}$. This ion will travel through a given region as long as the potential in that region is below $V_{initial}$, otherwise it will turn around and go back towards the source. This implies that the ion in figure 1.9 will travel to the right if the potentials V_1 and V_2 are less than $V_{initial}$.

When the ion moves into a region of potential V, the kinetic energy of the ion becomes $z(V_{initial} - V)$. The velocity (v) of the ion is therefore $v = [2z(V_{initial} - V)/m]$, where m refers to the mass of the positive ion. Consider the first cylinder (V_1) in figure 1.9. Once inside the cylinder, the ion

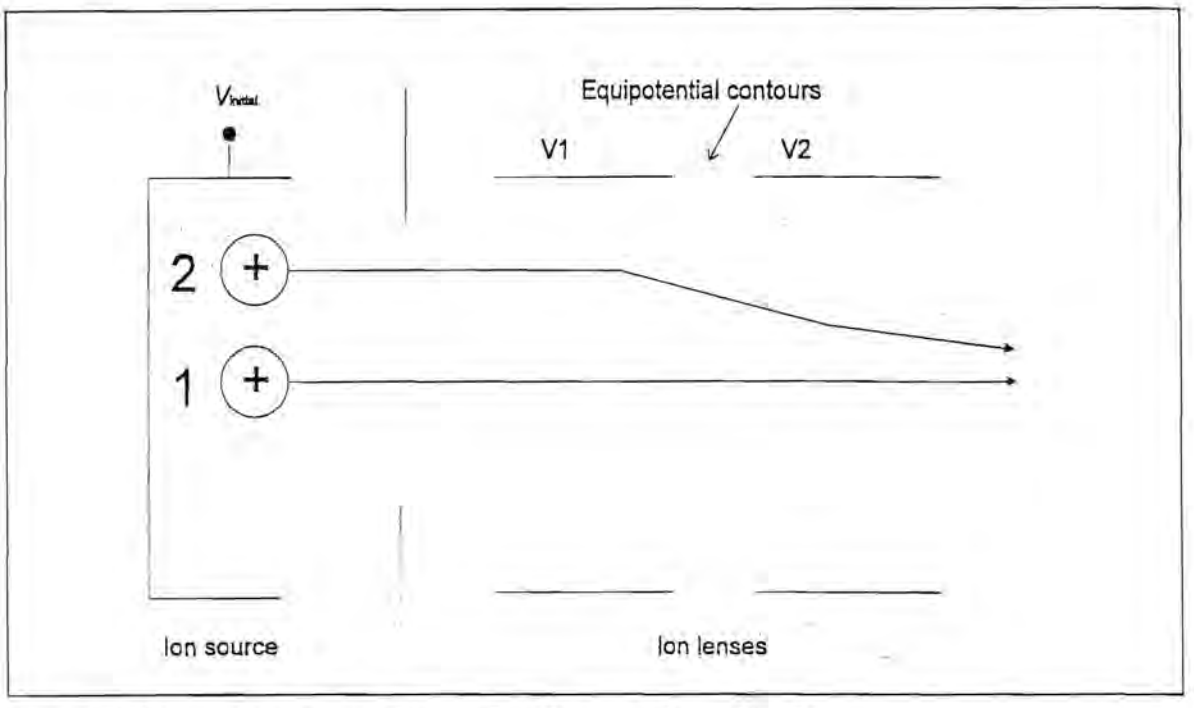

Figure 1.9 Schematic diagram illustrating the operation of ion lens.

experiences a uniform potential and moves at constant velocity in the same direction as when it entered the cylinder. By imparting a directed velocity to the ion, the lens draws it toward the mass analyser and retains it inside the vacuum system while the unwanted neutral particles flow to the pump. As the ion nears the exit of the first cylinder, it enters a new field region, which may be used as a lens to constrict or focus the stream of ions. This focusing action can improve the fraction of ions leaving the source that are transmitted downstream to the mass analyser.

Consider the region between the two cylinders in figure 1.9. If V_1 is not equal to V_2, the potential between the cylinders varies in space. The figure depicts curved equipotential contours in this region. These curved equipotential surfaces between cylinders provide the focusing action. Ion 1, which leaves the source on center, is acted upon symmetrically and passes straight through the lens. This ion is easily collected anyway. The real improvement lies for ion 2, which initially leaves the source displaced from the axis of the lens. The forces acting on ion 2 in the region between the two cylinders are unbalanced. If V_1 and V_2 are adjusted properly, ion 2 can be deflected closer to the axis. Once inside the second cylinder, the ion travels along a straight path, which may cross the axis and diverge again. More electrodes can be used downstream from V_2 to provide additional focusing action and to further adjust the ion path.

1.3.2 *Ion lenses in ICP-MS [1]*

In each lens several electrodes are strung together in order to confine the ions on their way to the mass analyser. Each lens incorporates a central disc in order to prevent photons originating from the plasma from reaching the detector. The sampler and skimmer cones stare into the heart of the inductively coupled plasma, which is a good source of vacuum ultraviolet radiation that can activate the detector. 50 - 80% of the positive ions are probably lost here, as shown by measurements of ion current with the stop removed.

Generally, the skimmer cone is grounded. The positive ions gain kinetic energy during extraction from both the gas dynamic effect of the supersonic expansion and any plasma potential above that of the sampler cone. The positive ion beam also has an energy spread of a few electron volts. Also, positive ions of different masses have different kinetic energies and thus follow different paths through the lens.

Different ion optical conditions are required to transmit positive ions of different *m/z* and the sensitivity for different elements is not as even across the mass range as the high ionisation efficiencies of the different elements would indicate. The extent of the mass discrimination effect depends on ion lens settings and ion energy, the latter of which can be influenced by plasma potential and plasma operating conditions.

1.3.3 *Space charge effects [1]*

A few ions are lost due to recombination during the extraction process and thus the ion current through the sampler cone remains quite high at about 0.1 A. The current through the skimmer cone is about 1 mA. In the plasma and in the supersonic jet, an equal electron current balances this ion current, so the beam acts more or less as if it was neutral *[6]*. As the beam leaves the skimmer cone, the electric field due to the lens collects positive ions and repels electrons. The electrons are no longer present to keep the positive ions confined in a narrow beam, resulting in the beam not being quasi-neutral, and the ion density still being very high. The mutual repulsion of ions of like charge limits the total number of positive ions that can be compressed into a beam of a given size. Space charge effects should become substantial in ICP-MS at total beam currents of the order of 1 μA *[18, 19]*, roughly three orders of magnitude below the actual beam current cited above. A simplified description of ion lenses, using the Laplace equation, assumes that the positive ions do not interact while in the ion lens, so the high ion current causes space-charge effects that are further reasons for non-ideal behaviour in ion optics in ICP-MS.

Ion trajectory calculations *[19]* show that the ion beam expands greatly due to space-charge effects. This expansion makes it difficult to collect all the ions leaving the skimmer cone and is probably a major source of ion loss in ICP-MS. Also, if the same space-charge force acts on all the positive ions, the light ions are affected the most and are deflected more severely. A greater fraction of light ions is deflected outside the acceptance volume of the ion lens than is the case for heavy ions, which could contribute to the generally poorer sensitivity for light elements and for the need for different focusing voltages for light and heavy ions.

The transmission of the ion lens now depends on the total beam current and the mass of the positive ions comprising the beam. Gillson et al. *[19]* showed that even a small change in the total ion current caused by addition of just a modest amount of matrix element can change the fraction of analyte ions that passes through the lens. Heavy matrix ions are deflected to a lesser extent and stay closer to the center of the ion beam where they can do the most damage.

These space-charge effects are a major cause of matrix interferences in ICP-MS. Many workers have reported that matrix effects are more severe in ICP-MS than in inductively coupled plasma emission spectrometry *[20 - 23]*. The masses of both the interferent and the analyte are of importance. Heavy matrix ions suppress analyte signals more extensively than matrices comprising of light ions, and heavy analyte ions are suppressed less severely than light ones *[19, 24 - 26]*. Most of these observations can be explained via the space-charge phenomenon. Alleviation of these effects and their analytical symptoms would greatly improve the analytical capabilities of ICP-MS. Caruso and co-workers have described a scheme in which the ion lens voltage is adjusted to maximise the analyte signal with the sample matrix present *[27]*.

1.4 Quadrupole mass spectrometers *[1]*

The ion lens provides little or no *m/z* separation of the extracted ion beam. In most ICP-MS instruments this function is performed by a quadrupole mass analyser. This section describes the operating principles and pertinent properties of these mass analysers.

1.4.1 Quadrupole configuration [1]

Figure 1.10 shows a diagram of a typical quadrupole mass filter. Four straight metal rods or metallised surfaces are suspended parallel to and equidistant from the axis. Ideally, the surfaces of these rods have a hyperbolic shape, although round rods that approximate hyperbola are usually used instead. Opposite pairs are connected together. DC and RF voltages of amplitude

U and V, respectively, are applied to each pair. The DC voltage is positive for one pair and negative for the other pair. The RF voltages on each pair have the same amplitude but of opposite sign, i.e. they are 180° out of phase.

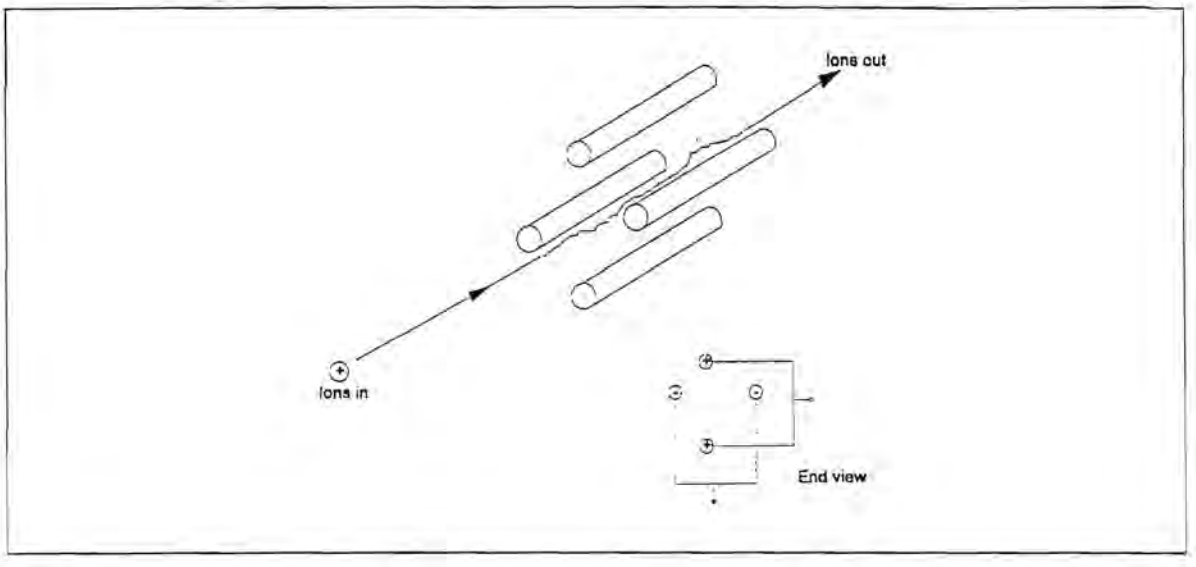

Figure 1.10: Diagram of quadrupole rods showing ion trajectory and applied voltages.

The ions to be separated are introduced along the axis into one end of the quadrupole system at velocities determined by their energy and mass. Due to the applied RF voltages all the ions are deflected into oscillatory paths through the rods. If the RF and DC voltages are selected properly, only ions of a given m/z ratio will have stable paths through the rods and will pass through the quadrupole system. Other ions will be deflected too much and will strike the rods and be neutralized and lost there. Thus, the dimensions of the ion trajectories relative to the boundaries of the rods are of critical importance.

1.4.2 *Ion trajectories [1]*

In the positive rod plane (figure 1.11), the lighter ions tend to be deflected too much and strike the rods, while the ions of interest and the heavier ions have stable paths. In this plane the quadrupole acts like a high pass mass filter. In the negative rod plane the heavier ions tend to be lost preferentially and the analyte ions and the lighter ions have stable paths. Thus the quadrupole acts like a low pass mass filter in the negative plane. The negative and positive planes are superimposed physically, so these filtering actions occur on the same ion beam at the same time. This juxtaposition of high pass and low pass mass filtering produces a structure that transmits ions only at the m/z value of interest.

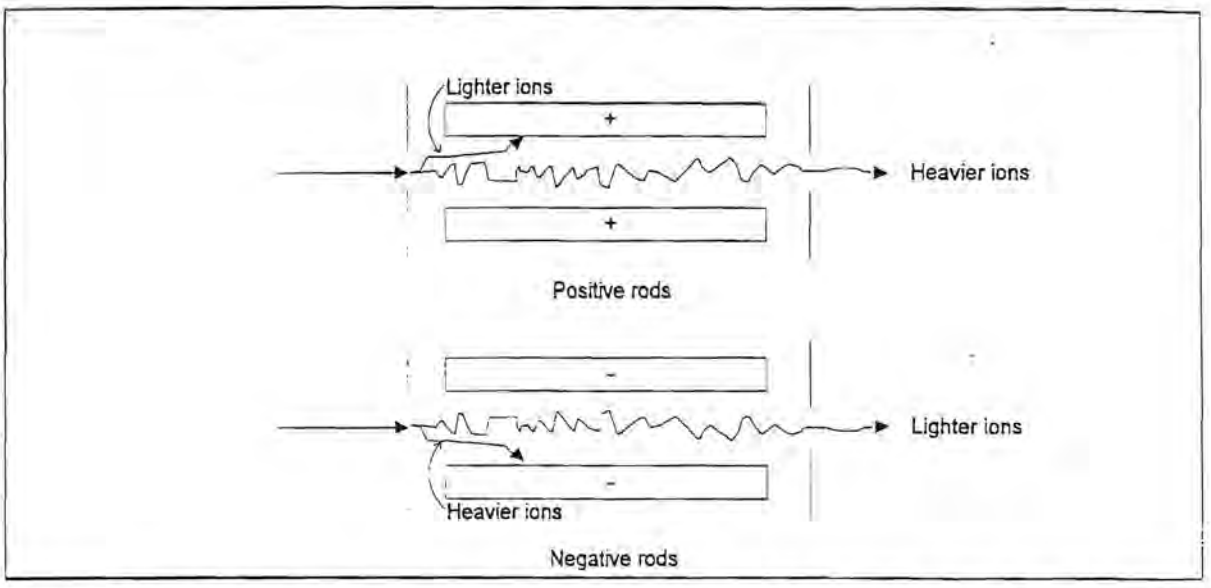

Figure 1.11: Side views of the ion separation processes in the two rod planes of a quadrupole.

1.4.3 *Characteristics of mass spectra from quadrupoles [1]*

Quadrupoles can operate at fairly high pressures (~1.3×10^{-2} Pa) as long as the mean free path is greater than the length of the device and the pressure is low enough to prevent electrical discharges inside the rods. Since the inductively coupled plasma operates at atmospheric pressure this causes the gas load to be high and the tolerance of the quadrupole to relatively high operating pressures simplifies the vacuum requirements. The typical operating pressures in ICP-MS instruments are limited largely by the detector (electron multiplier) rather than by the mass analyser system.

Quadrupoles perform best with positive ions that have low kinetic energies. The resolution is not greatly sensitive to the ion energy spread in the axial direction if the maximum ion energy stays below a certain value, usually about 20 eV. In the case of the ions having a too high energy they pass through the quadrupole system too quickly and do not experience enough RF cycles for proper resolution. The peaks resulting from such high-energy ions tend to be broad and/or split.

Only ions of a given *m/z* value are transmitted at any given time. The *m/z* value can be scanned or switched very rapidly, but ions of different *m/z* cannot be simultaneously monitored with a conventional quadrupole.

1.4.4 Scanning and data acquisition [1]

If U and V are not changed, the mass filter transmits only one m/z value continuously. This mode is called selected ion monitoring or single ion monitoring. It provides a 100% duty cycle on the m/z value of interest but precludes acquisition of spectral information elsewhere. For multi-element measurements, the values of U and V can be changed continuously in one scan. Also, U and V can be changed under computer control rapidly between selected discrete values (peak hopping), or the quadrupole can be scanned repetitively through the m/z region of interest (multi-channel scanning).

1.5 Ion detection *[1]*

1.5.1 Channeltron electron multipliers [1]

These are the most common detectors used in ICP-MS instruments. Figure 1.12 shows a diagram of such a Channeltron electron multiplier. The operating principles are similar to those of a photomultiplier, but there are no discrete dynodes. Instead, an open glass tube with a cone at one end is used. The interior of the tube and cone is coated with a lead oxide semiconducting material whose exact composition is proprietary. Electrical connections are made to the semiconducting coating through metal strips. For detection of positive ions, the cone is biased at a high negative potential (~-3 kV) and the back of the tube near the collector is held near ground. Relative to either end, the resistance of the interior coating varies continuously with position. Thus, when a voltage is applied across the tube, a continuous gradient of potential exists with position inside the tube.

When a positive ion leaves the quadrupole system it is attracted to the high negative potential at the cone. As the ion hits this surface it causes one or more secondary electrons to be ejected. Inside the tube, the potential varies continuously with position, so the secondary electron(s) move further into the tube to regions closer to ground. The secondary electrons hit another section of the coating causing more secondary electrons to be emitted. This process is repeated many times as the secondary electrons pass down the tube. The result is a discrete pulse containing as many as 10^8 electrons at the collector after an ion strikes the entrance of the detector.

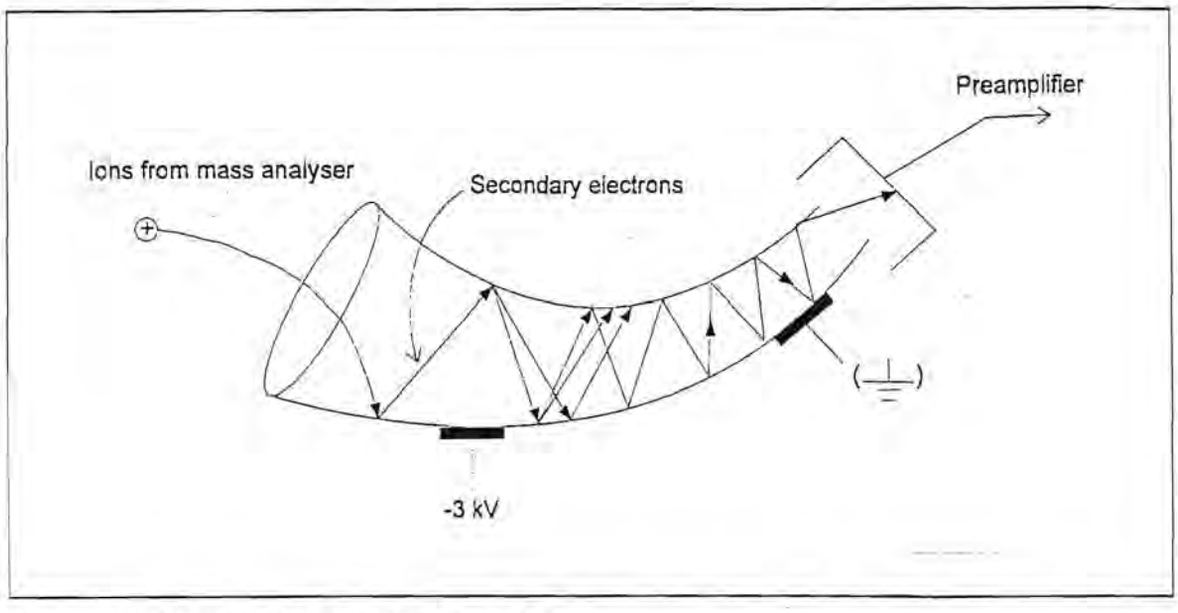

Figure 1.12: Channeltron electron multiplier.

As long as the high voltage is switched off first Channeltrons can be vented to air repeatedly without damage. A pressure below a value of approximately 6.7×10^{-3} Pa is required during operation, else spurious discharges form in the detector chamber.

1.5.2 *Signal measurement by pulse counting [1]*

Despite the use of pulse counting and careful blocking of the optical axis (in order to block photons that can activate the detector) between the detector and plasma, the actual background during operation is generally 10 to 50 counts s^{-1}, substantially higher than the dark count rate of the multiplier. The phenomena responsible for this background are not known precisely *[28]*.

The upper end of the dynamic range is limited by two phenomena. Firstly, the electron multiplier can only sustain a given maximum current flow. At a gain of 10^8 and an ion count rate of 10^6 ions s^{-1}, the current flow at the collector is about 16 μA. At high count rates the gain decreases because the electron current exceeds the standing current in the semiconducting coating of the detector. The fraction of ion pulses that are too low to be counted therefore increases. Secondly, pulse pile-up (the arrival of two pulses in a time interval shorter than the response time constants of the counting circuit) is a problem that could also limit linearity.

Both these effects cause the calibration curve to droop toward the horizontal axis at relatively high count rates. A peak that is split in the center is another symptom of count rates that exceed the linear range of the system.

CHAPTER 2

OPTIMISATION OF INSTRUMENT PARAMETERS IN INDUCTIVELY COUPLED PLASMA MASS SPECTROMETRY

2.1 Introduction

In ICP-MS various instrument parameters need to be set in order to optimise for analyte signals and to minimise background, doubly ionised and oxide signals. The plasma is optimised for the production of a large population of ions and the efficient transport of these ions through the interface with minimum interferences. Analyte signals may further be divided into intensities for light elements, argon and heavier elements. Some of the instrument parameters that need to be considered are: 1) horizontal, vertical and axial setting of the torch, 2) coolant, auxiliary and aerosol carrier gas flow rates, 3) power and 4) ion lens settings.

The effects of these various parameters on the different signals were investigated and the results presented were compared with the results of other researchers.

2.2 Experimental

2.2.1 Instrument

The instrument used for this study was a Spectromass-ICP. The free running generator operates at a frequency of 27.12 MHz. It has a three stage vacuum system consisting of two turbomolecular pumps and two rotating pumps. The following were used: a Fassel torch, a Scott-type double-pass spray chamber, a Meinhard nebuliser, Ni sampler and skimmer cones with diameters of about 1 mm and <1 mm. The solution uptake rate was $1x10^{-3}$ dm^3 min^{-1}.

Since mainly the way in which the signals vary with inductively coupled plasma and mass spectrometer parameters were of interest for this study, the study was started with a specific set of conditions, one parameter was varied, set optimally and then the next parameter was varied. Values and scales used for torch settings and gas flow rates are "arbitrary scales" as used by the instrument manufacturers, i.e. they do not refer to specific units of measurement. According to the manufacturers the scales for gas flow rates may be converted to dm^3 min^{-1} in the following way: For the coolant gas flow rate (arbitrary scale unit x 0.40), for the auxiliary gas

flow rate (arbitrary scale unit x 0.05) and for the aerosol carrier gas flow rate (arbitrary scale unit x 0.033).

2.2.2 *Multi-element solution*

The analyte solution consisted of a 1 mg dm^{-3} multi-element solution in 1% v/v HNO_3. According to some workers *[29, 30]* it is inadvisable to optimise ICP parameters in isolation to the mass spectrometer since the interface links together directly and synergistically two instrument components operating at totally different pressures and temperatures (inductively coupled plasma at atmospheric pressure and 5000 - 7000 K while the mass spectrometer is at 10^3 to 10^1 Pa and ambient temperature). Potential problems with spectral overlap interferences may result from the individual or combined effects of background intensities, isotopes or different concomitant elements, doubly ionised ions, oxide ions or other polyatomic ions. These form in either the plasma or the interface or during the sampling process.

Table 2.1: List of *m/z* values at which signals were monitored.

Element / ion monitored	**Isotope / *m/z* monitored**
Li^+	^{7}Li
Na^+	^{23}Na
Mg^+	^{24}Mg
Ar^+	^{36}Ar
Cu^+	^{63}Cu
In^+	^{115}In
Ce^+	^{140}Ce
Pb^+	^{208}Pb
Background	^{93}Nb
Background	^{100}Tc
Ce^{2+}	*m/z* 70
CeO^+	*m/z* 156

Background values in ICP-MS results from scattered photons or stray ions in the mass spectrometer. Background positions were chosen as positions where no analyte species in the multi-element solution would interfere or be monitored. The mass positions chosen were mass 93 and mass 100.

The doubly ionised and oxide ions of Ce were monitored as interferences, i.e. Ce^{2+} and CeO^+ at masses 70 and 156, respectively.

Signals monitored were divided into: low mass elements (Li^+, Na^+, Mg^+), Ar^+, heavier elements (Cu^+, In^+, Ce^+, Pb^+), background positions ($^{100}Tc^+$, $^{93}Nb^+$) and interferences (Ce^{2+}, CeO^+). The Ce^{2+}/Ce^+ and CeO^+/Ce^+ ratios were also calculated. A list of the masses at which signals were monitored are shown in table 2.1.

2.3 Effect of parameters on ICP-MS signals

2.3.1 Effect of torch adjustment

Effect of torch adjustment on light elements

The effect of the horizontal adjustment of the torch on the light elements can be seen in figure 2.1. An amount of "1000 units" on the x-axis corresponds to a distance of 0.492 mm moved. As the plasma is moved horizontally across the aperture of the sampler cone the analyte signals increase, reach a maximum and then decrease again. This is as expected since the analyte flow through the centre of the torch constitutes only a small part of the total plasma. The maximum analyte signals are observed at the torch setting of approximately "-2500 units". Although the system is sensitive to variations in the horizontal setting of the torch, this parameter does not seem to be critical since at distances of 1.2 mm away from the maximum Mg^+ intensities are still about 0.5×10^6 and intensities for Li^+ and Na^+ are about 1.5×10^6.

Figure 2.2 shows the effect of the vertical displacement of the torch on the response curves for the light elements. An amount of "1000 units" on the x-axis corresponds to a distance of 0.396 mm moved. Maximum analyte signals are observed at a setting of "-6500 units". As with the horizontal variation of the plasma, the signals increase, reach a maximum and then decrease again. At distances of about 1 mm from the optimum position a decrease in signal intensity of approximately 40% can be seen.

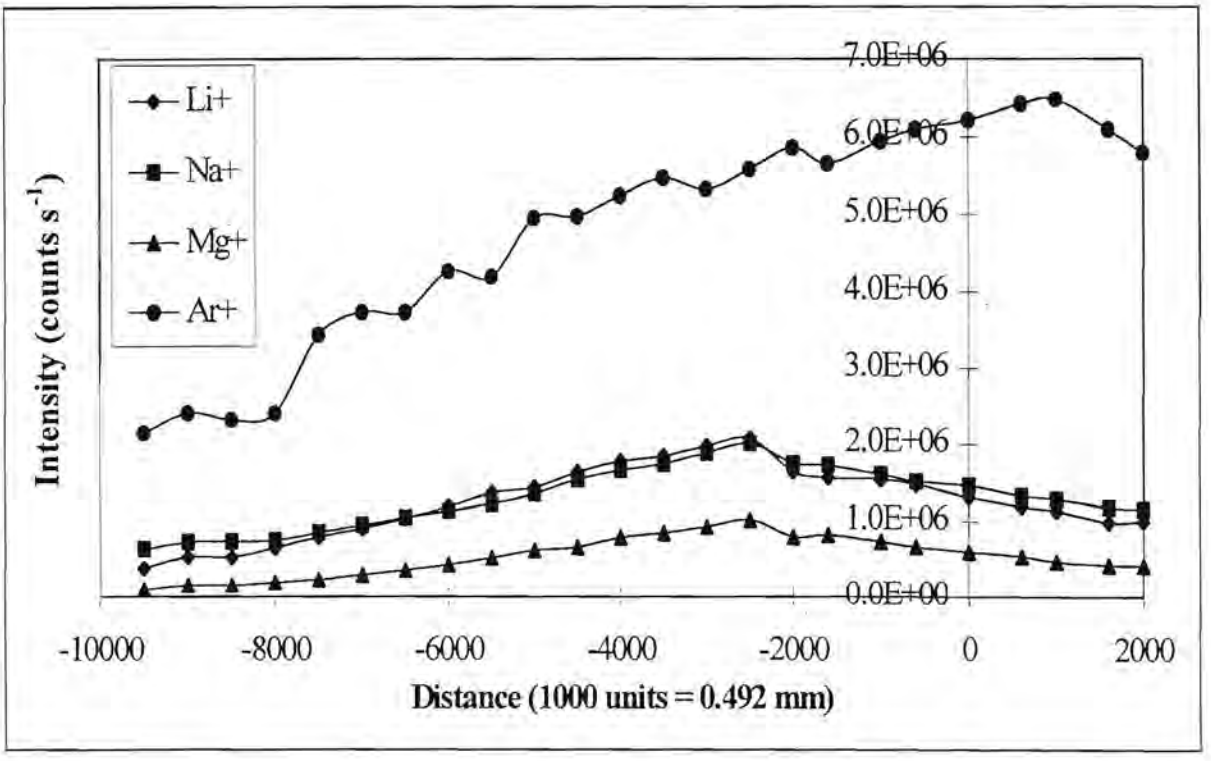

Figure 2.1: Effect of horizontal displacement of the torch on the response curves of light elements and argon.

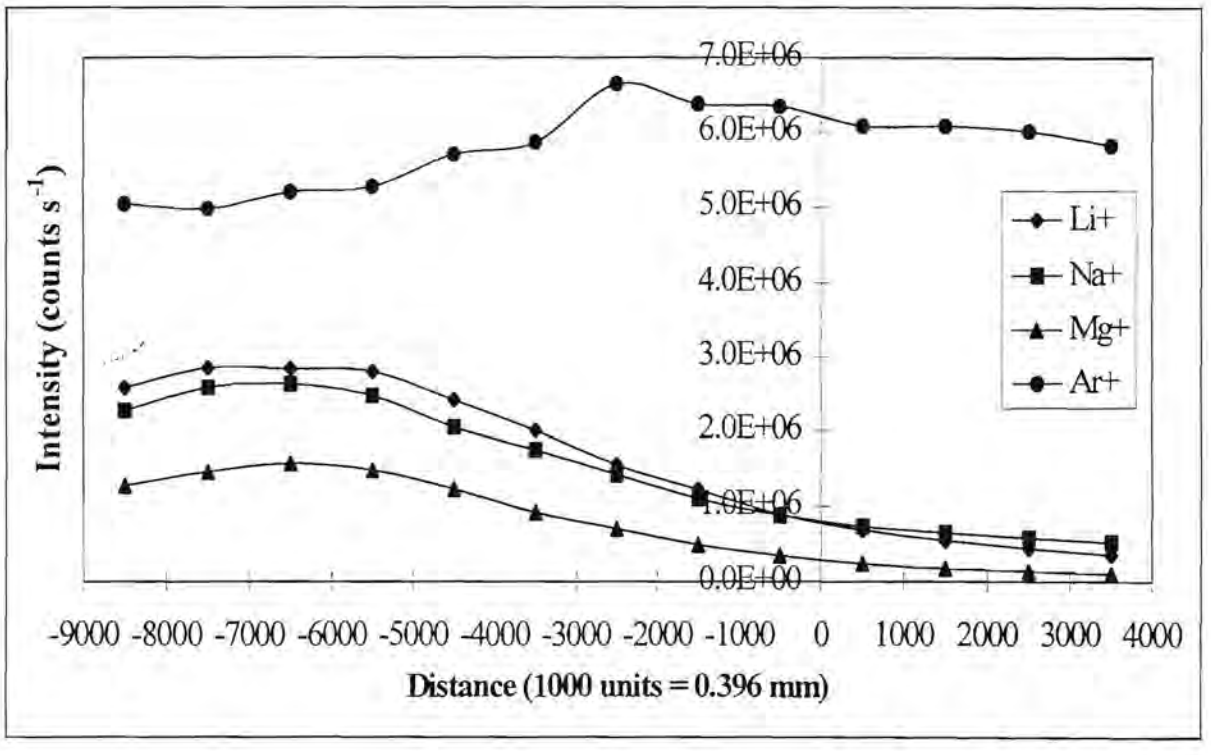

Figure 2.2: Effect of vertical displacement of the torch on the response curves of light elements and argon.

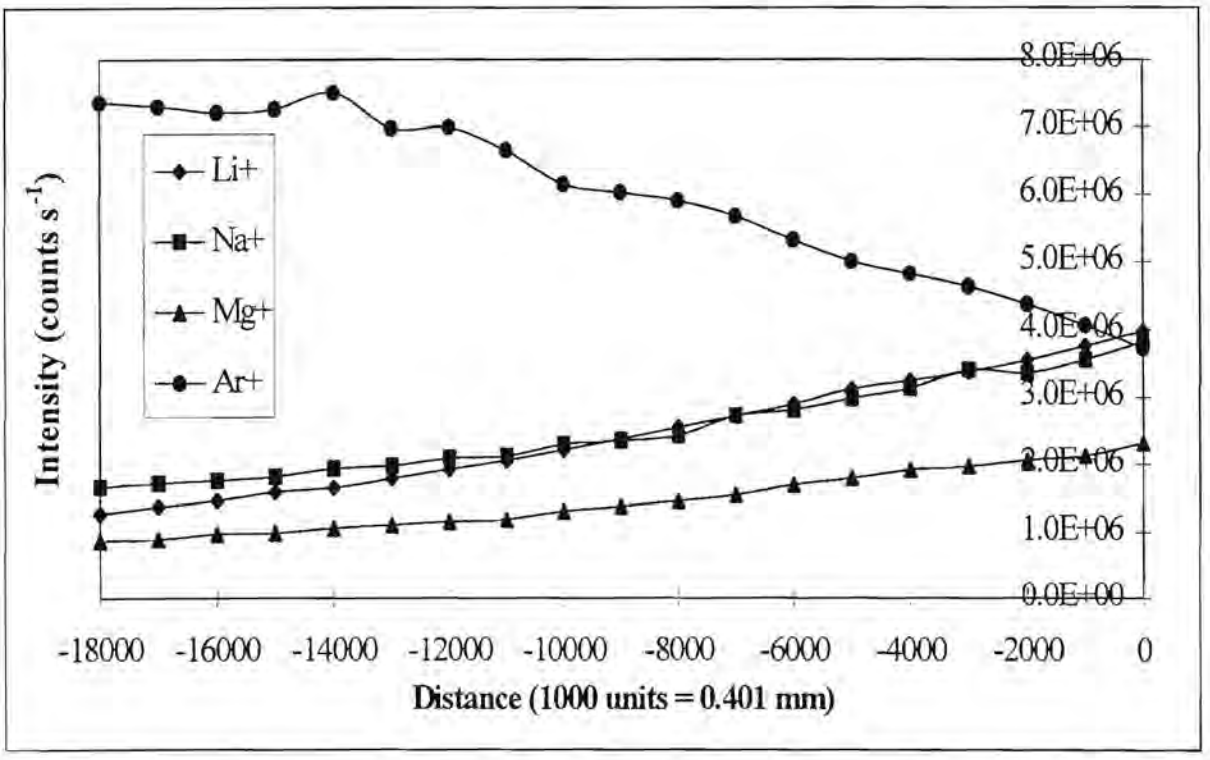

Figure 2.3: Effect of axial displacement of the torch on the response curves of light elements and argon.

From figure 2.3 the effect of the axial displacement of the torch on the analyte signal can be seen. "1000 units" on the x-axis corresponds to a distance of 0.401 mm moved. At the setting "0 units" the torch-sampler cone separation is 8.3 mm. As the torch is moved away from the sampling aperture, the analyte signals decrease and the argon signal increases. This can be explained by the fact that as the plasma is moved away less analyte ions reach the aperture and more argon reaches the sampler as the argon flow tends to enfold the analyte gas flow. Although higher analyte intensities are recorded nearer to the sampling aperture, other factors also have to be considered, e.g. lifetime of the sampler cone, time spent in the plasma by the analyte for processes such as desolvation, volatilisation, dissociation and ionisation to occur. The torch is usually set between "-3000 units" and "-6000 units". Many workers *[29 - 31]* also reported relative little change over a range of depths (axial displacement) with increasing signal loss at greater depths.

Effect of torch adjustment on heavier elements

Figure 2.4 shows the response of the heavier elements on the horizontal displacement of the torch. Similar trends are observed as for the light elements.

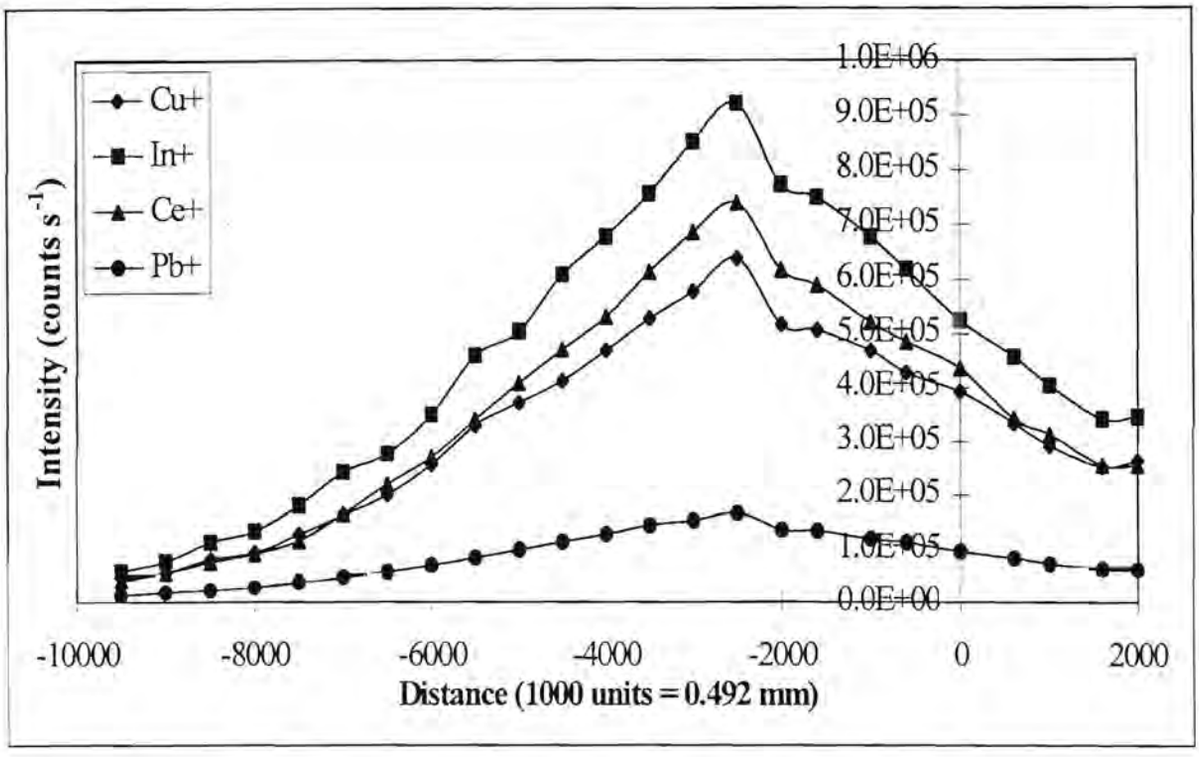

Figure 2.4: Effect of horizontal displacement of the torch on the response curves of heavier elements.

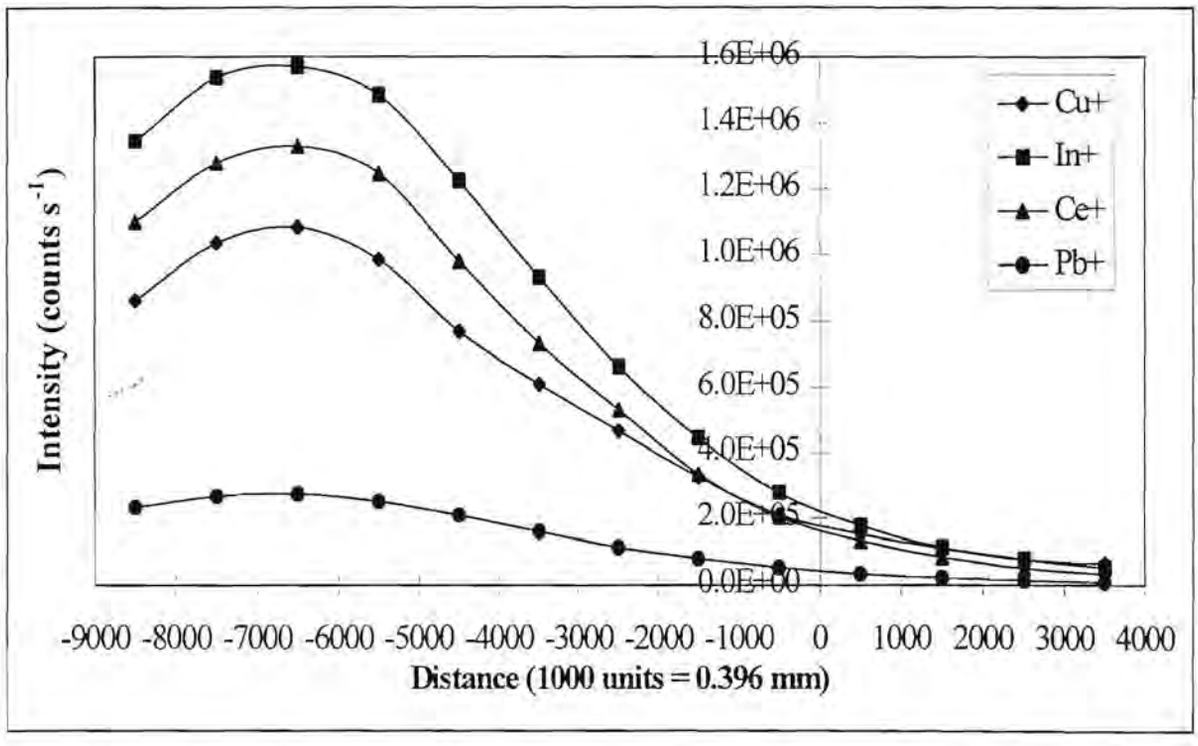

Figure 2.5: Effect of vertical displacement of the torch on the response curves of heavier elements.

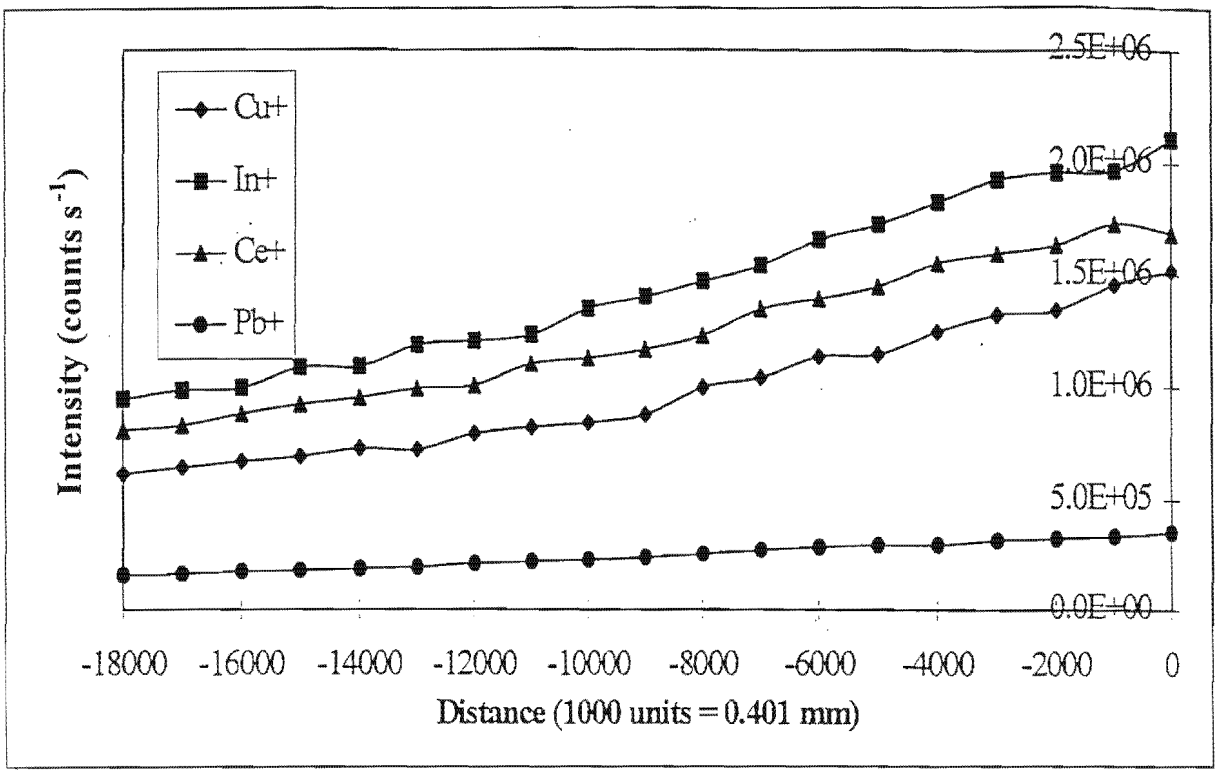

Figure 2.6: Effect of axial displacement of the torch on the response curves of heavier elements.

As the plasma is moved across the aperture the maximum analyte intensities are also observed at "-2500 units". At distances of 1.2 mm away from the maximum position the analyte signals decrease by about 40%. Even at these settings the signals observed are still above 1 x10^5.

The optimum vertical setting of the torch appears to be at "-6500 units" as can be seen from figure 2.5. The same trends as for the horizontal variation are observed.

Figure 2.6 shows the effect of axial displacement of the torch on the response curves of heavier elements. The trends observed are similar to those seen for the light elements. This is in accordance with results from Horlick *et al. [29]* and Vaughan *et al. [30]*.

Effect of torch adjustment on background intensities

From figure 2.7 the background intensities at various horizontal displacements can be seen. The background signals do not follow a specific trend but are below 80 counts s^{-1} over the whole range.

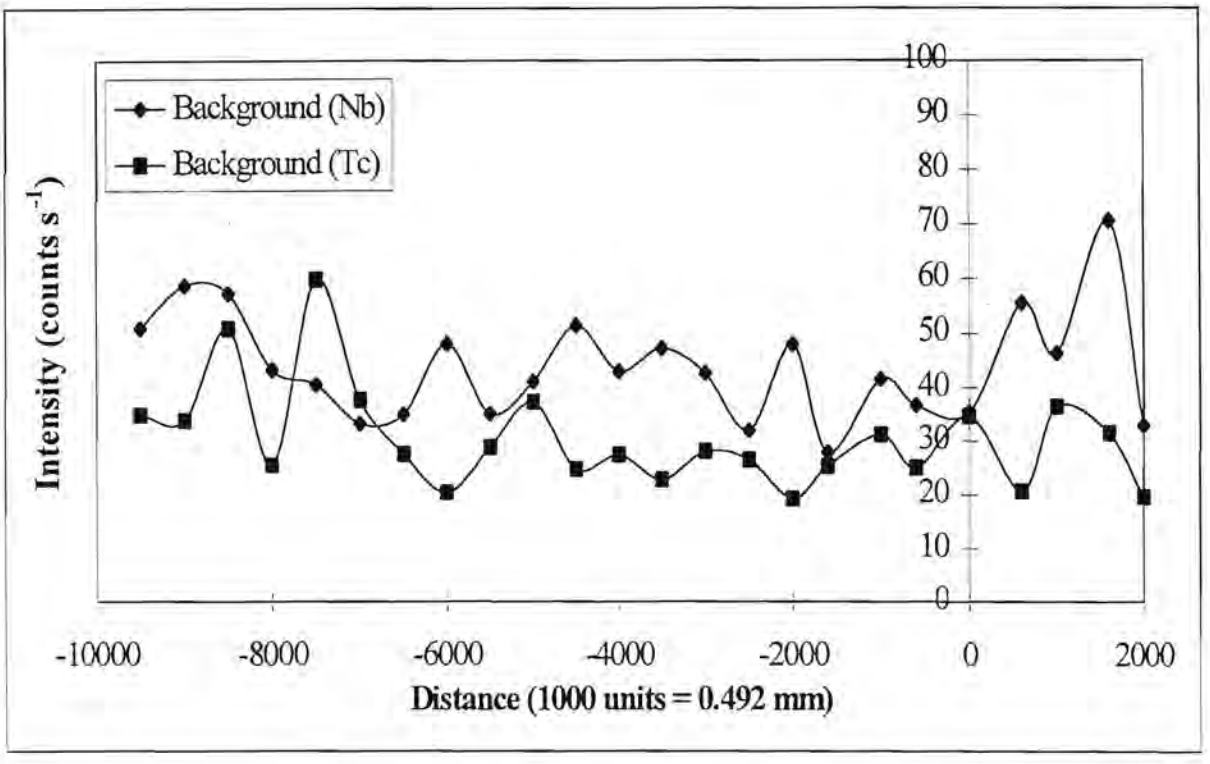

Figure 2.7: Effect of horizontal displacement of the torch on background intensities.

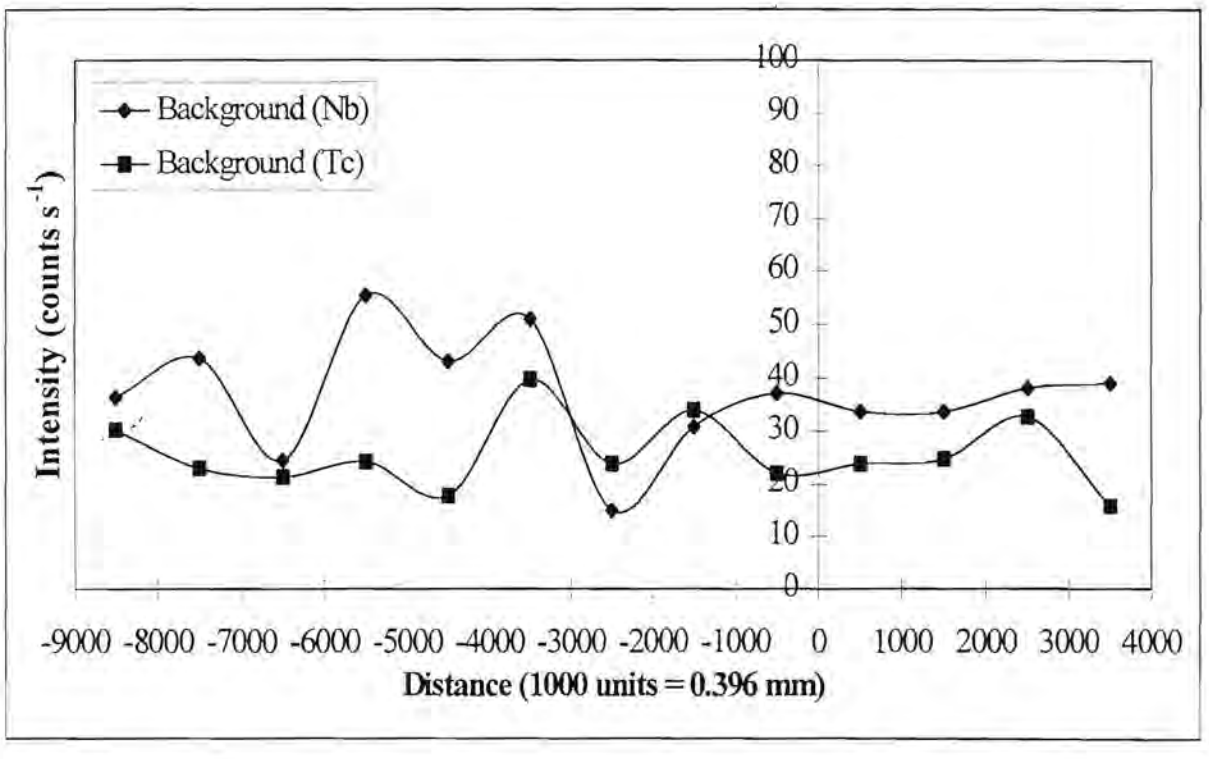

Figure 2.8: Effect of vertical displacement of the torch on background intensities.

Figure 2.8 shows that the background signals are below 50 counts s^{-1} for vertical displacement settings of the torch.

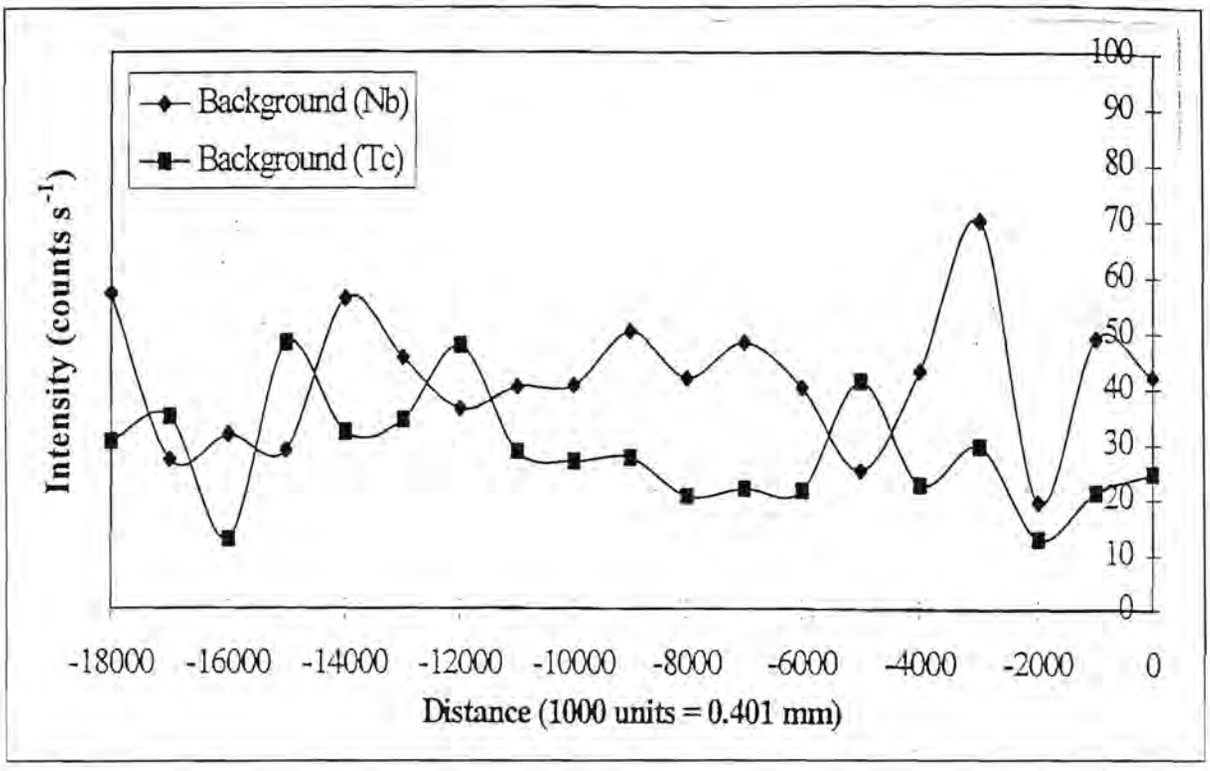

Figure 2.9: Effect of axial displacement of the torch on background intensities.

Axial settings of the torch have little or no effect on the intensities of the background signals. This can be seen from figure 2.9. Acceptable values of below 100 counts s^{-1} are observed over the whole range of axial displacements.

Effect of torch adjustment on doubly ionised ions and oxides

From figure 2.10 the signals from doubly ionised Ce and CeO^+ can be seen. Optimum values for these interferences are also obtained at a setting of "-2500 units". Figure 2.11 shows that the setting of the horizontal displacement of the torch has no significant effect on the M^{2+}/M^+ and MO^+/M^+ ratios. The Ce^{2+}/Ce^+ ratio is below the acceptable value of 2.5% and the CeO^+/Ce^+ ratio is about the acceptable value of 1% *[32]*.

The vertical displacement of the torch shows similar effects on the Ce^{2+} and CeO^+ signals (figure 2.12) and on analyte signals. Figure 2.13 shows that the vertical displacement of the torch does not have a significant effect on the Ce^{2+}/Ce^+ and CeO^+/Ce^+ ratios, except for the Ce^{2+}/Ce^+ ratio which increases significantly at settings of "500 units" to "3500 units".

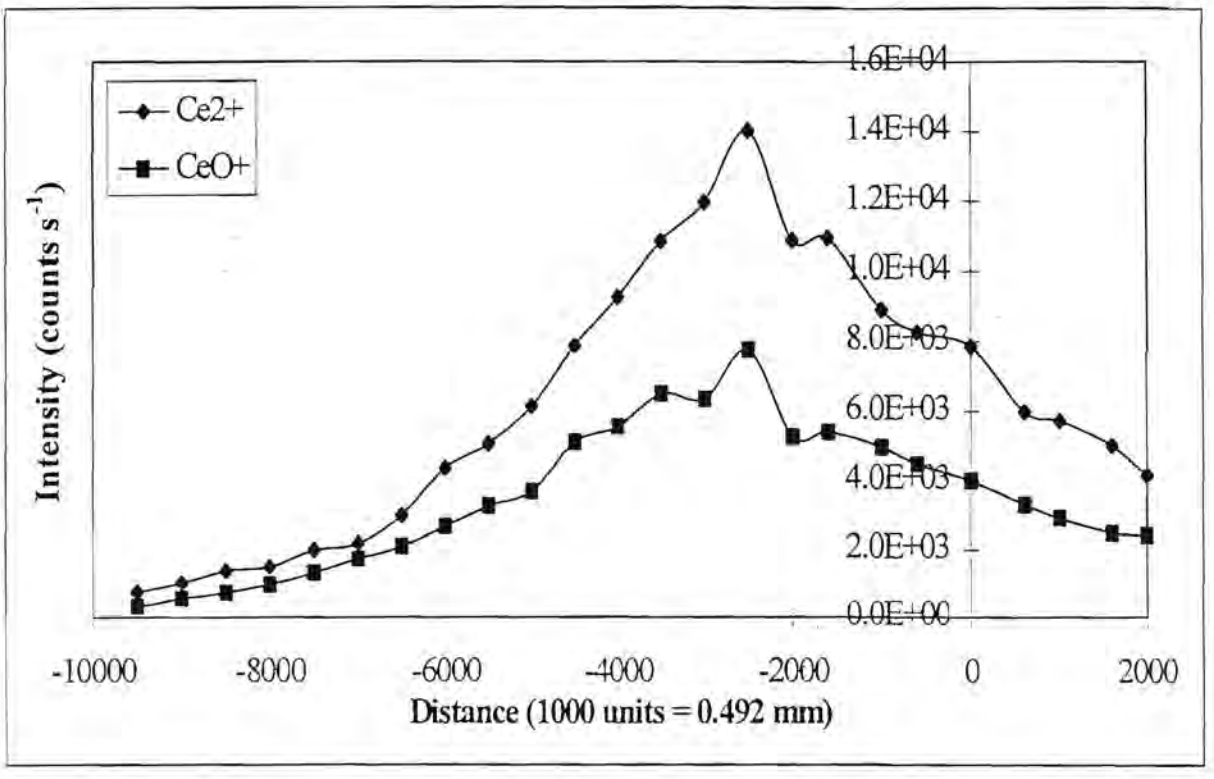

Figure 2.10: Effect of horizontal displacement of the torch on the response curves of doubly ionised and oxide ions.

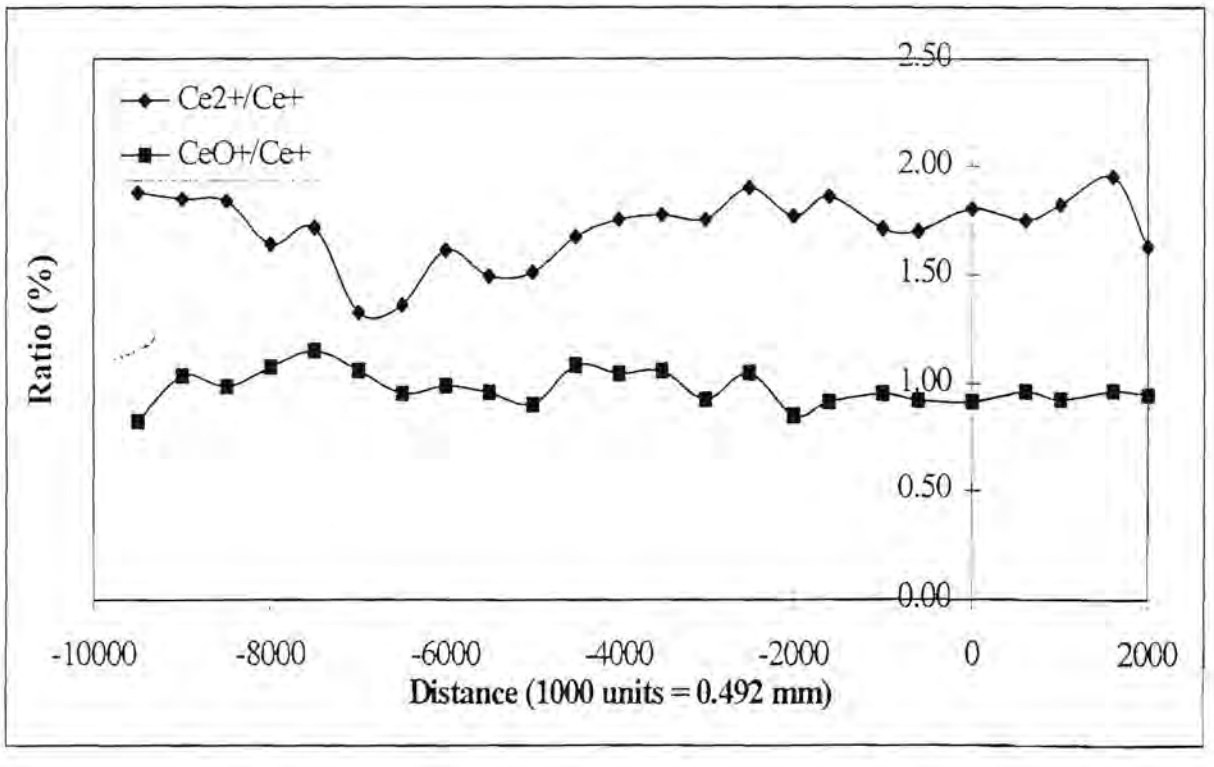

Figure 2.11: Effect of horizontal displacement of the torch on the ratios Ce^{2+}/Ce^{+} and CeO^{+}/Ce^{+}.

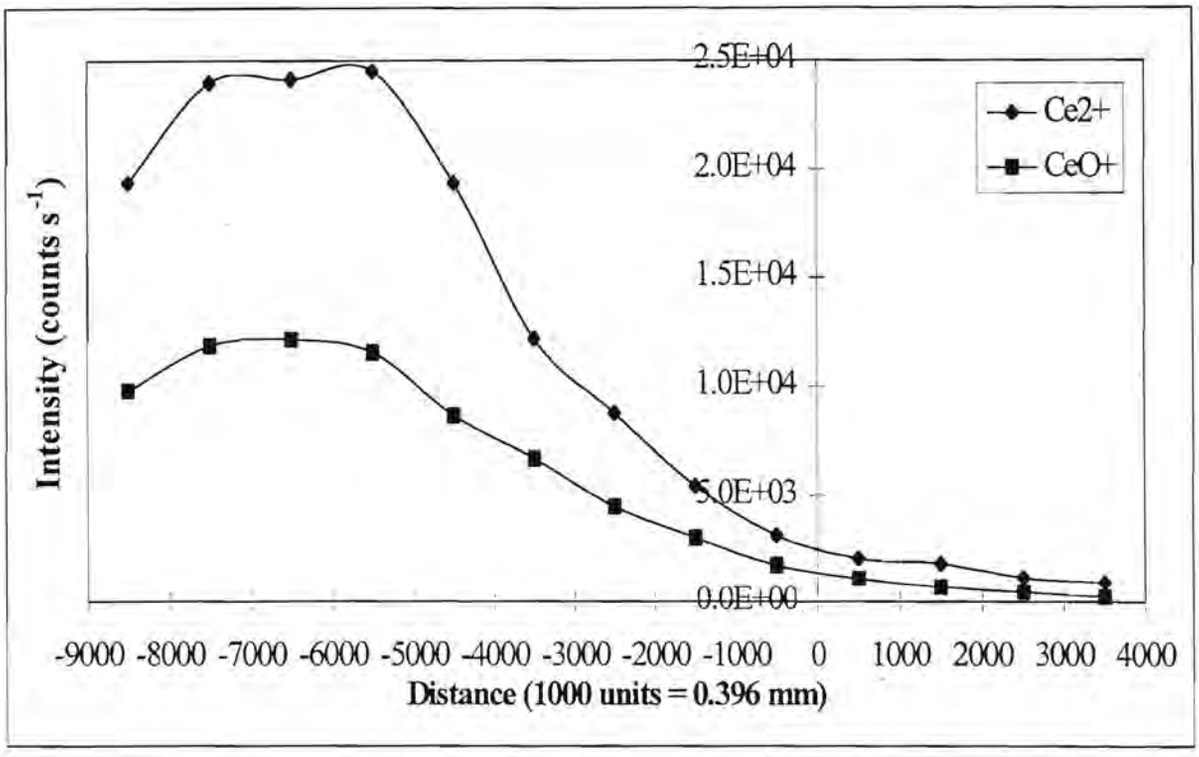

Figure 2.12: Effect of vertical displacement of the torch on the response curves of doubly ionised and oxide ions.

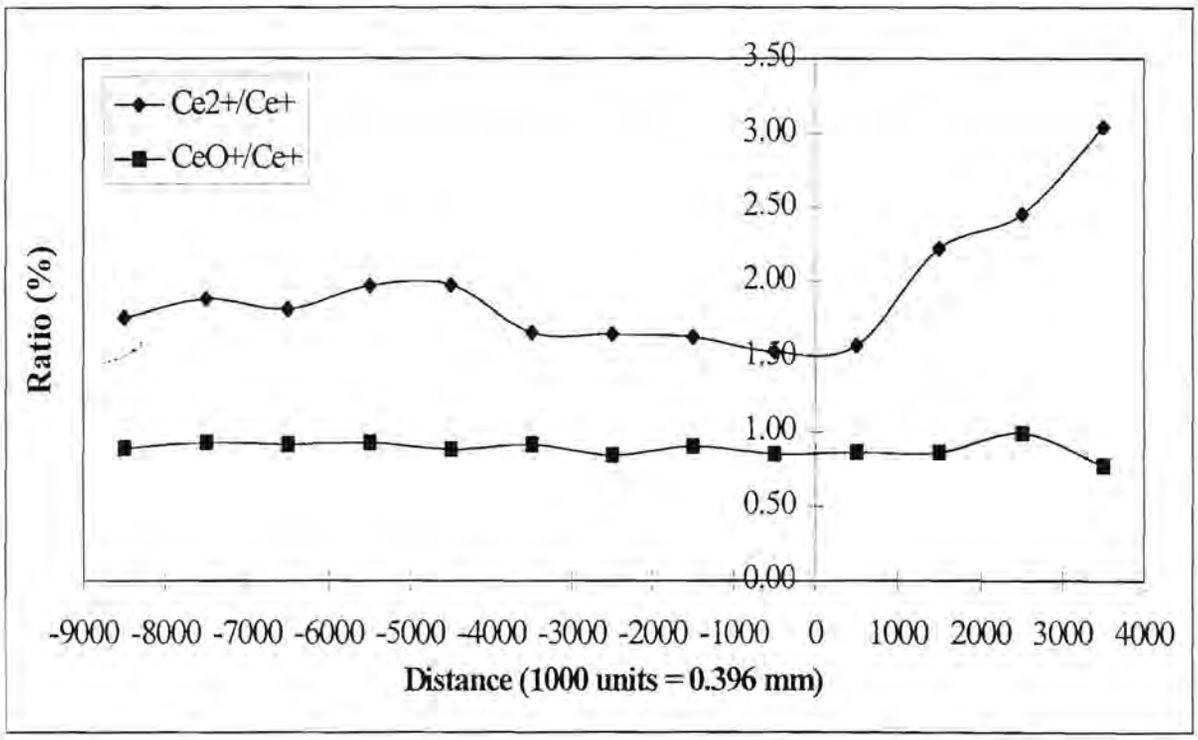

Figure 2.13: Effect of vertical displacement of the torch on the ratios Ce^{2+}/Ce^{+} and CeO^{+}/Ce^{+}.

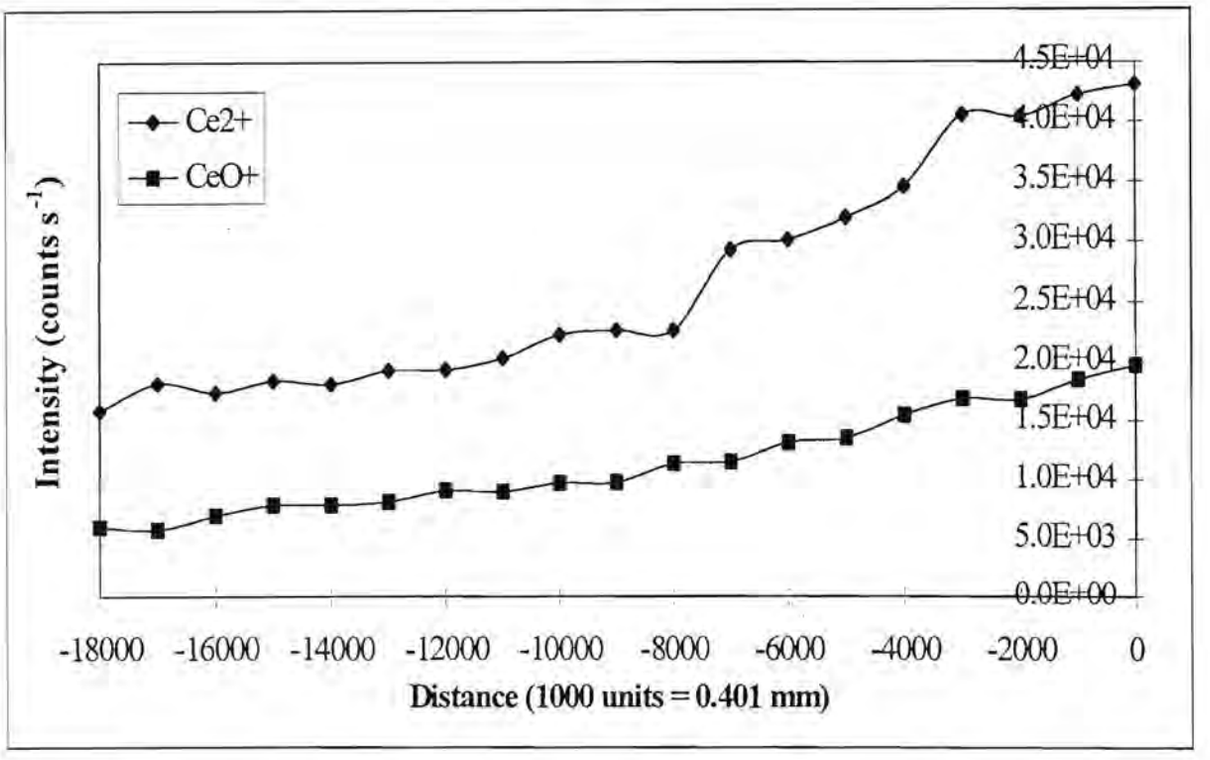

Figure 2.14: Effect of axial displacement of the torch on the response curves of doubly ionised and oxide ions.

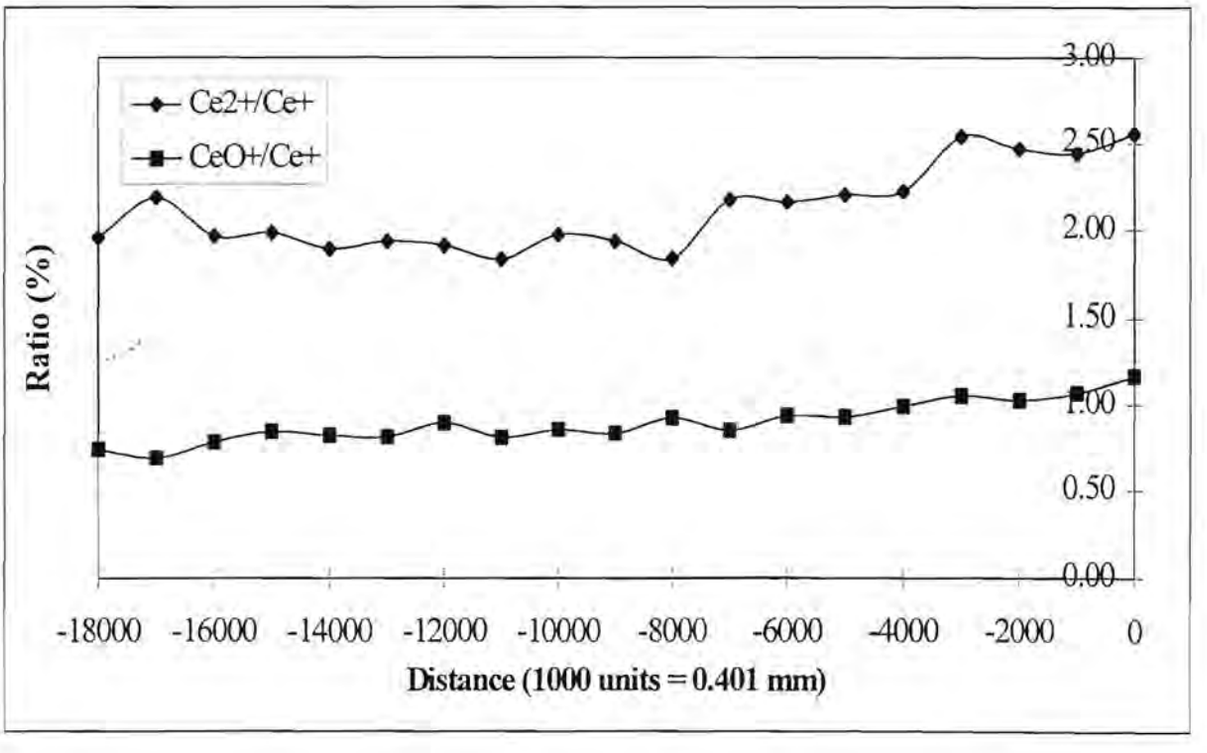

Figure 2.15: Effect of axial displacement of the torch on the ratios Ce^{2+}/Ce^{+} and CeO^{+}/Ce^{+}.

Figure 2.14 and figure 2.15 show that the amounts of Ce^{2+} and CeO^{+} produced, as well as the ratio of CeO^{+} to Ce^{+}, are not significantly affected by the axial displacement of the torch. The Ce^{2+}/Ce^{+} ratio increases slightly as the torch is moved closer to the sampling aperture. Distances closer than "-3000 units" should thus be avoided.

2.3.2 *Effects of coolant and auxiliary gas flow rates*

Effect of coolant and auxiliary gas flow rates on light elements

The effects of coolant and auxiliary gas flow rates on the light elements are shown in figure 2.16 and figure 2.17. The analyte signals increase with an increase in coolant gas flow rate and decrease with an increase in the auxiliary gas flow rate. Contrary to these results Horlick *et al. [29]* reported a slight increase in analyte signals with an increase in the auxiliary gas flow rate. The auxiliary gas flow rate has a smaller effect on the intensity of the signals than the coolant gas flow rate.

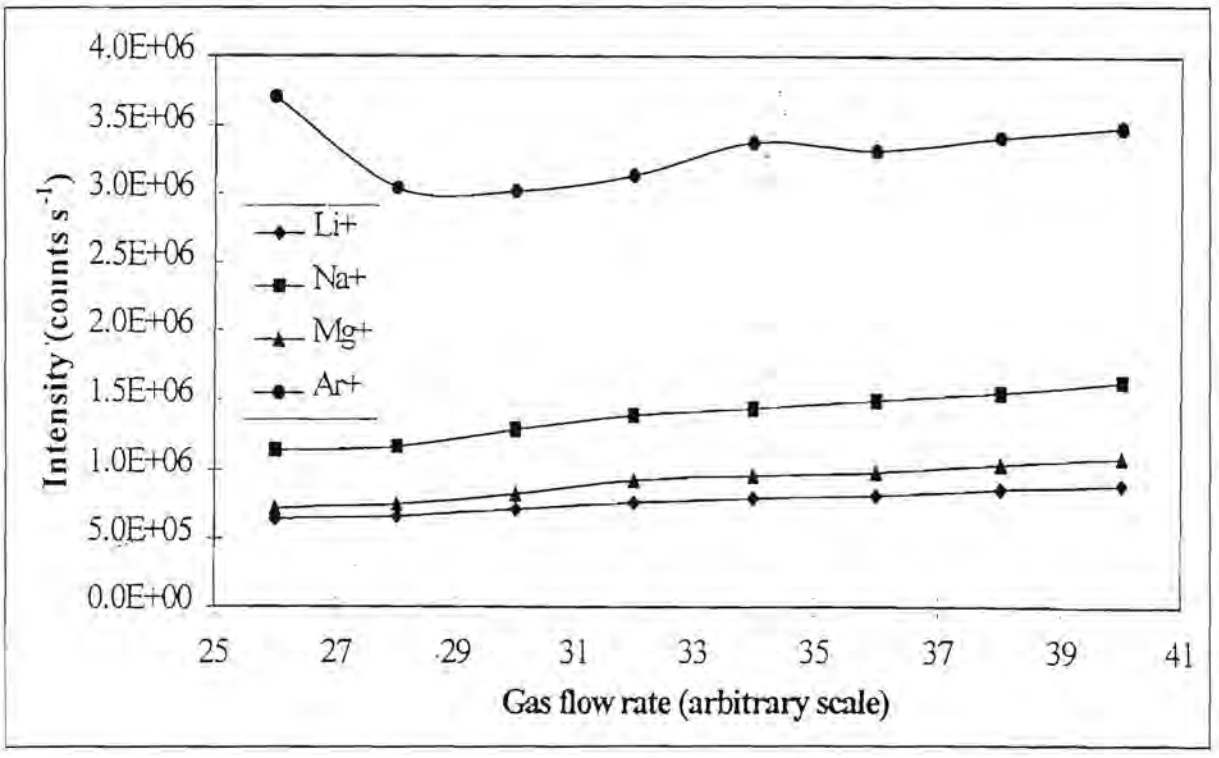

Figure 2.16: Effect of the coolant gas flow rate on the response curves of the light elements and argon.

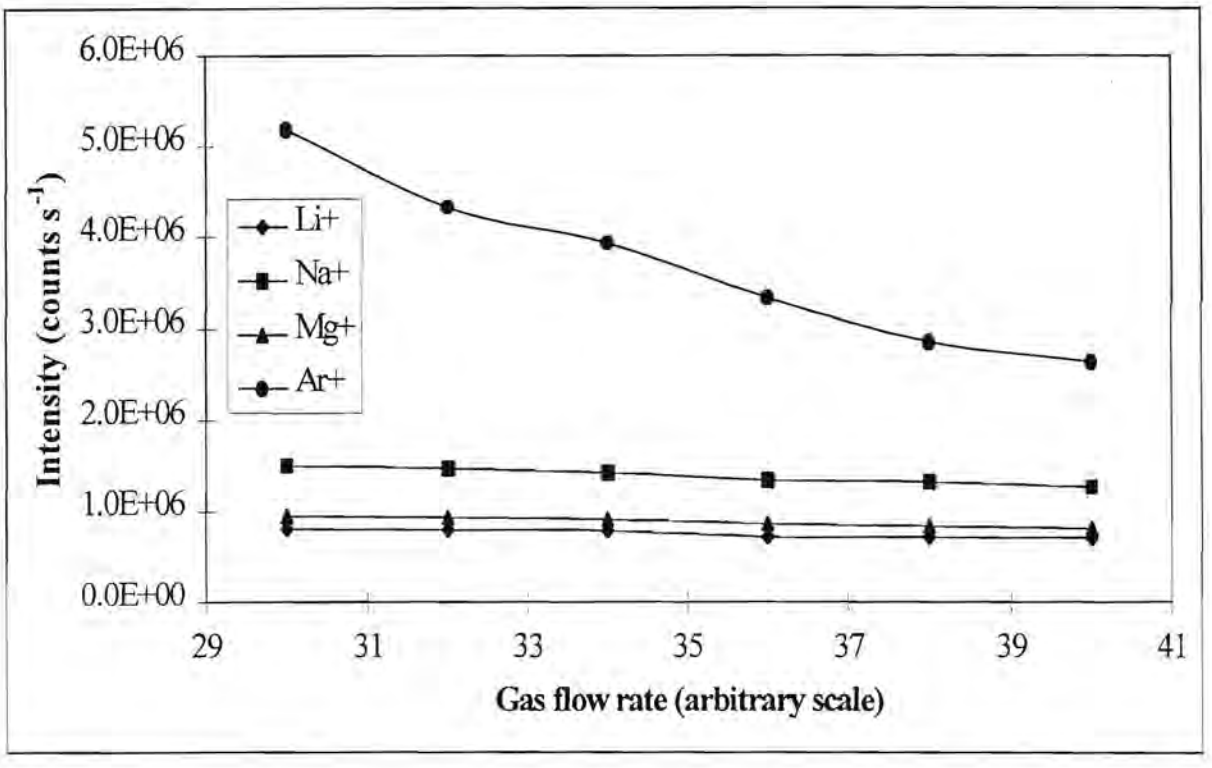

Figure 2.17: Effect of the auxiliary gas flow rate on the response curves of the light elements and argon.

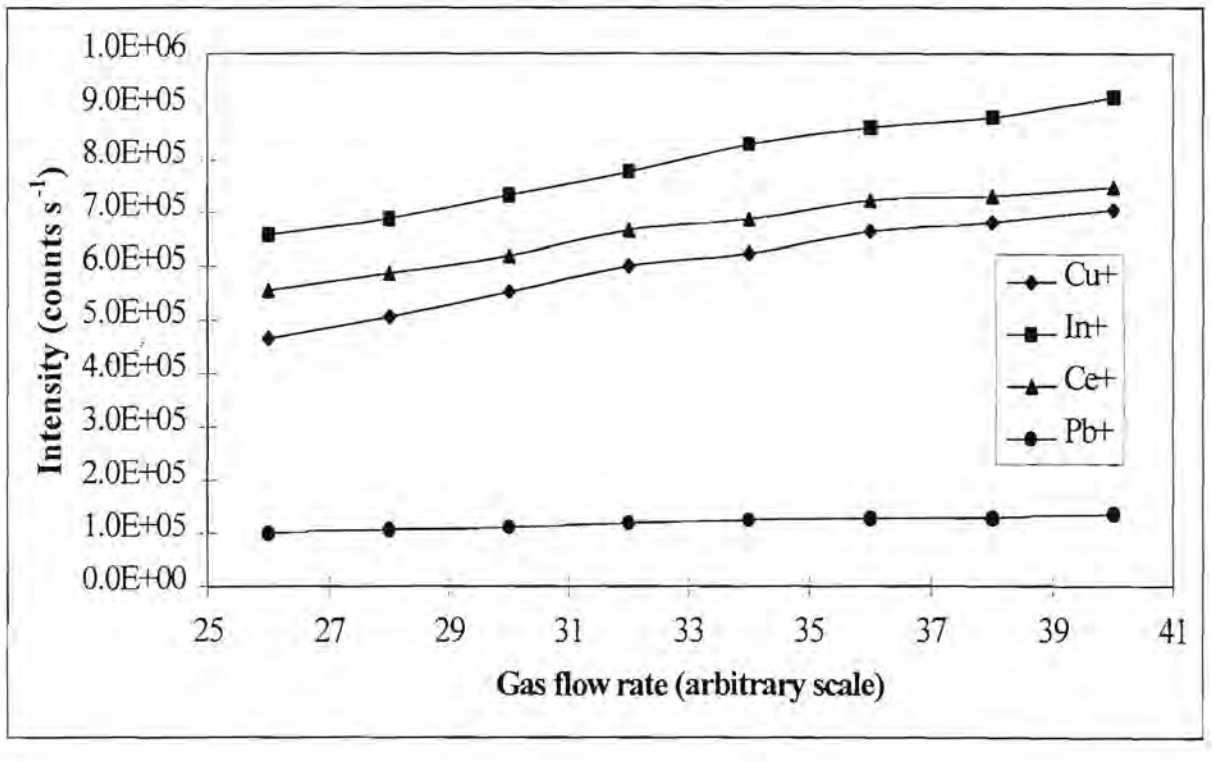

Figure 2.18: Effect of the coolant gas flow rate on the response curves of the heavier elements.

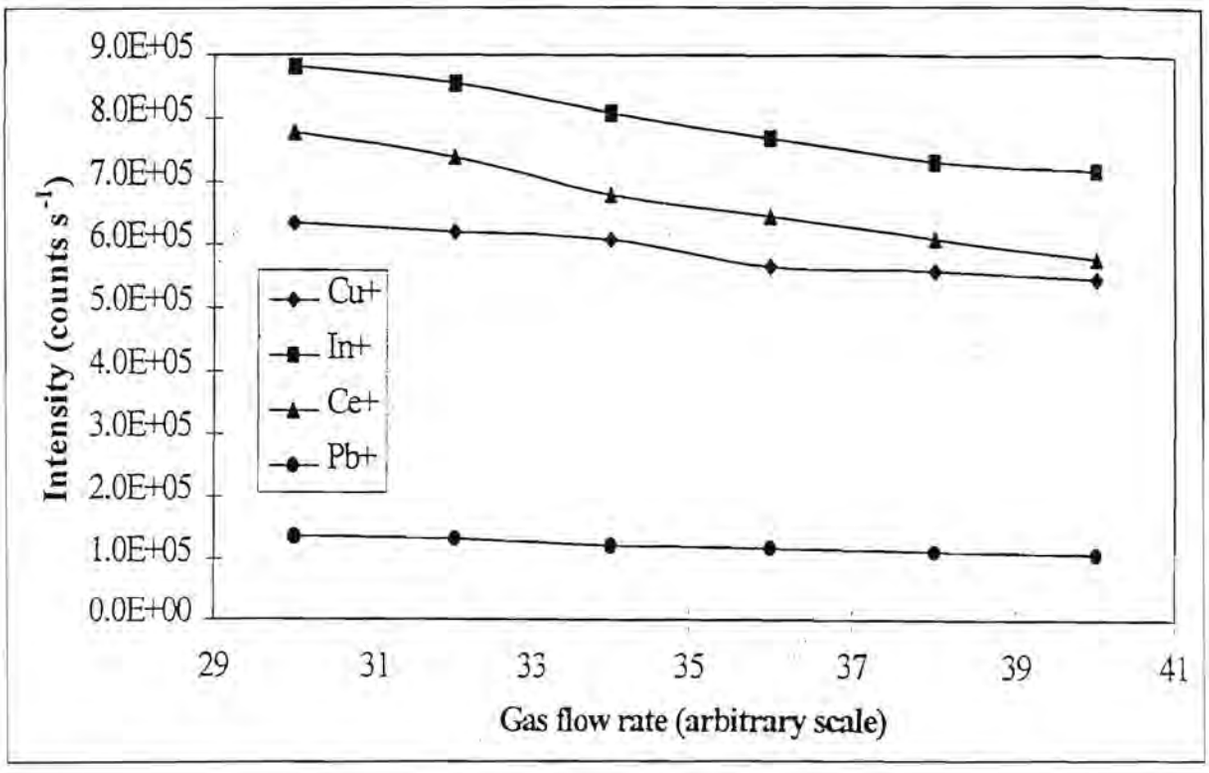

Figure 2.19: Effect of the auxiliary gas flow rate on the response curves of the heavier elements.

Effect of coolant and auxiliary gas flow rates on heavier elements

Figures 2.18 and 2.19 show similar trends for the heavier elements as for the light elements with increases in the coolant and auxiliary gas flow rates. Results from Long and Brown *[33]* show similar trends with the coolant flow identified as not having a great effect on analyte signals. They also found low auxiliary gas flow rates to be preferable.

Effect of coolant and auxiliary gas flow rates on background intensities

Changes in the coolant and auxiliary gas flow rates do not have a significant effect on the background intensities, which remain at approximately 50 counts s^{-1}. This is shown in figure 2.20 and figure 2.21.

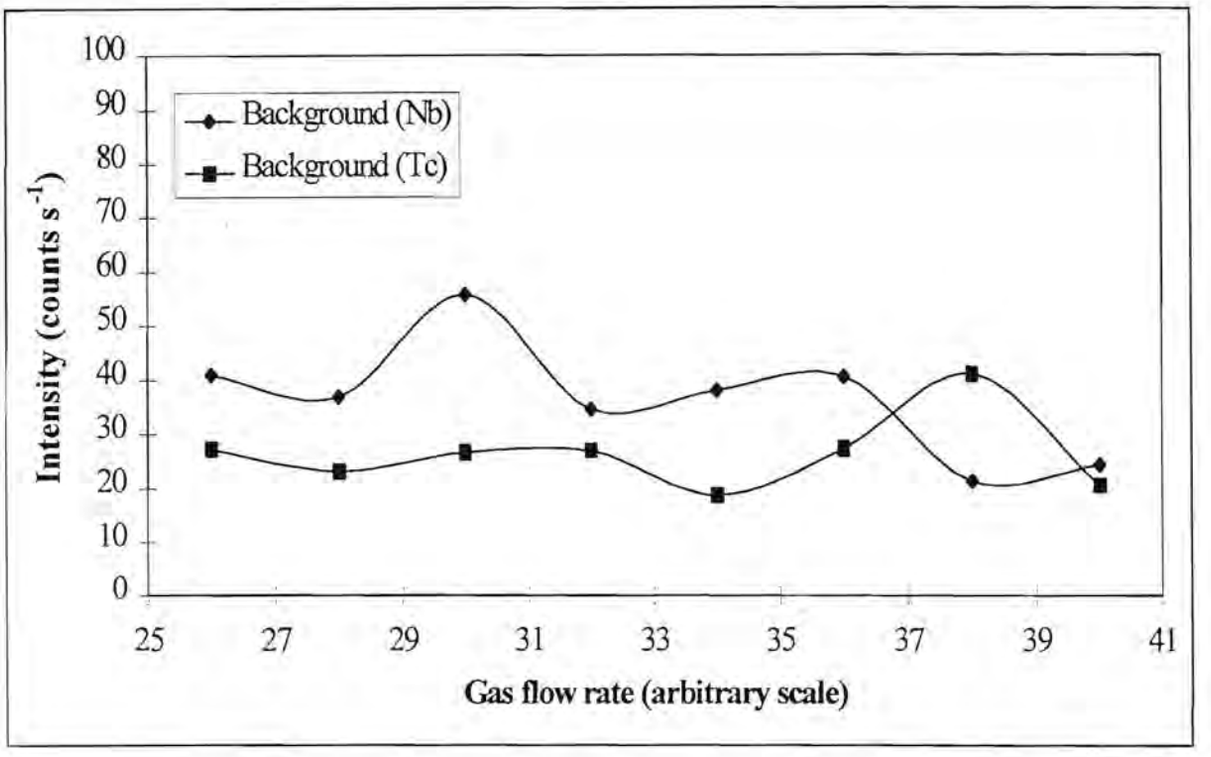

Figure 2.20: Effect of coolant gas flow rate on background intensities.

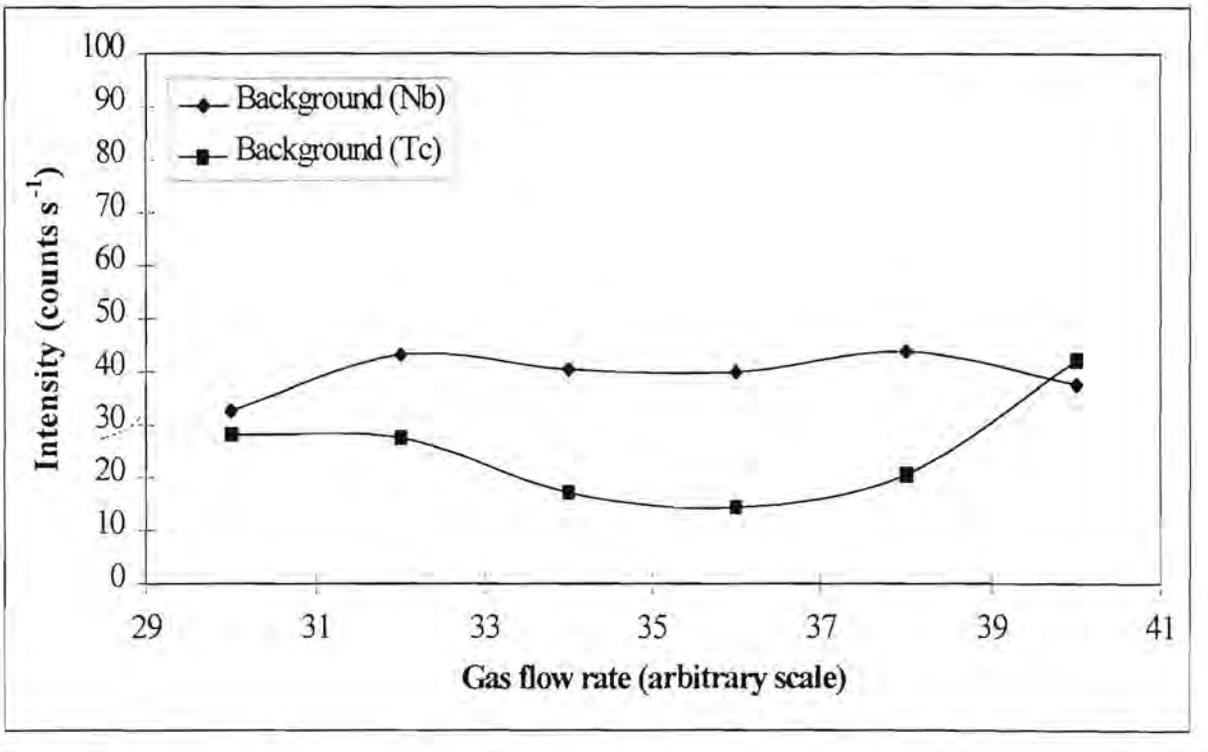

Figure 2.21: Effect of auxiliary gas flow rate on background intensities.

Effect of coolant and auxiliary gas flow rates on doubly ionised ions and oxides

Figures 2.22 and 2.23 show that the intensity of CeO^+ does not change much with variations in the coolant and auxiliary gas flow rates. The Ce^{2+} signal increases with increases in the coolant and auxiliary gas flow rates.

Figures 2.24 and 2.25 put these values into perspective by showing changes in the Ce^{2+}/Ce^+ and CeO^+/Ce^+ ratios with changes in the gas flow rates. Although the CeO^+/Ce^+ ratio remains unchanged at about 1%, the Ce^{2+}/Ce^+ ratio increases with increases in the gas flow rates.

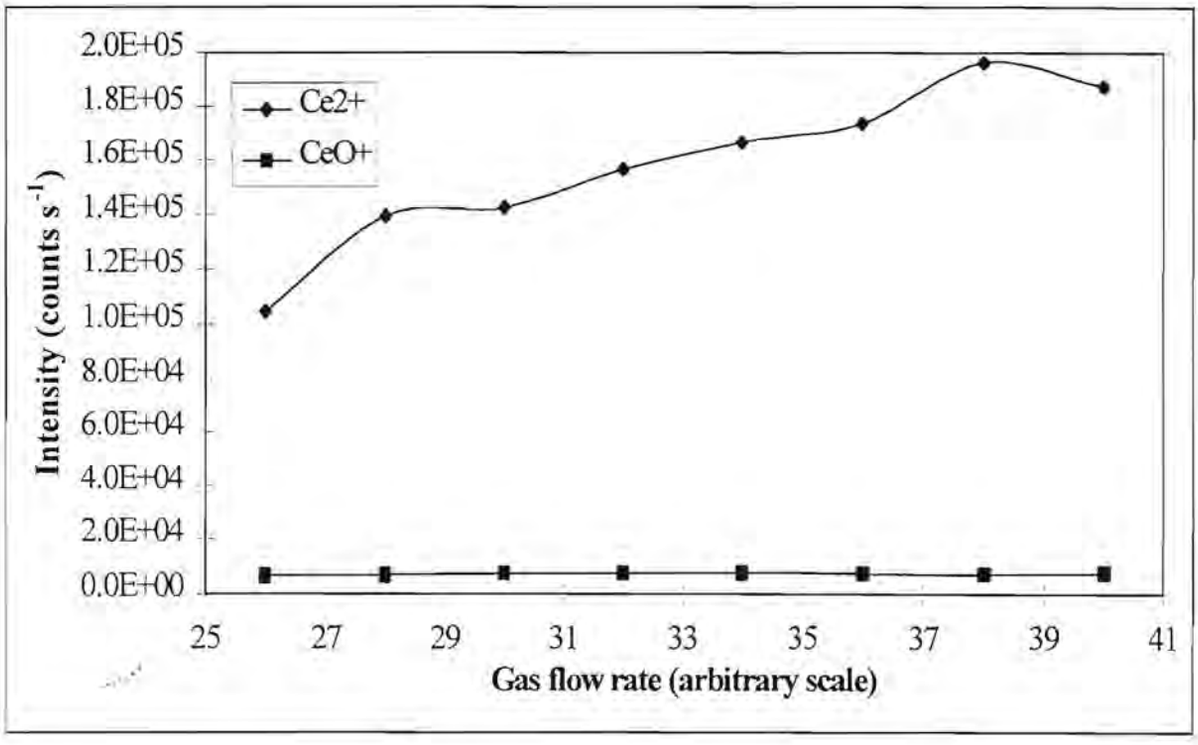

Figure 2.22: Effect of coolant gas flow rate on the response curves of doubly ionised and oxide ions.

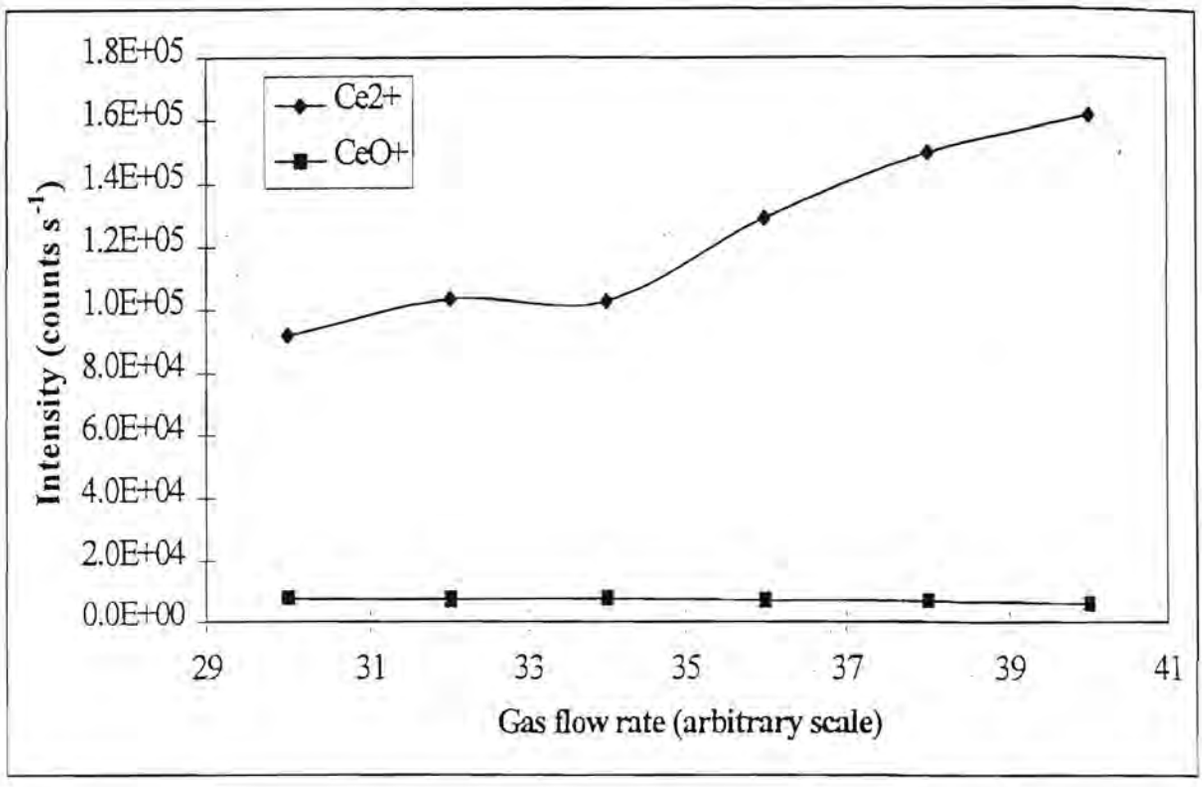

Figure 2.23: Effect of auxiliary flow on the response curves of doubly ionised and oxide ions.

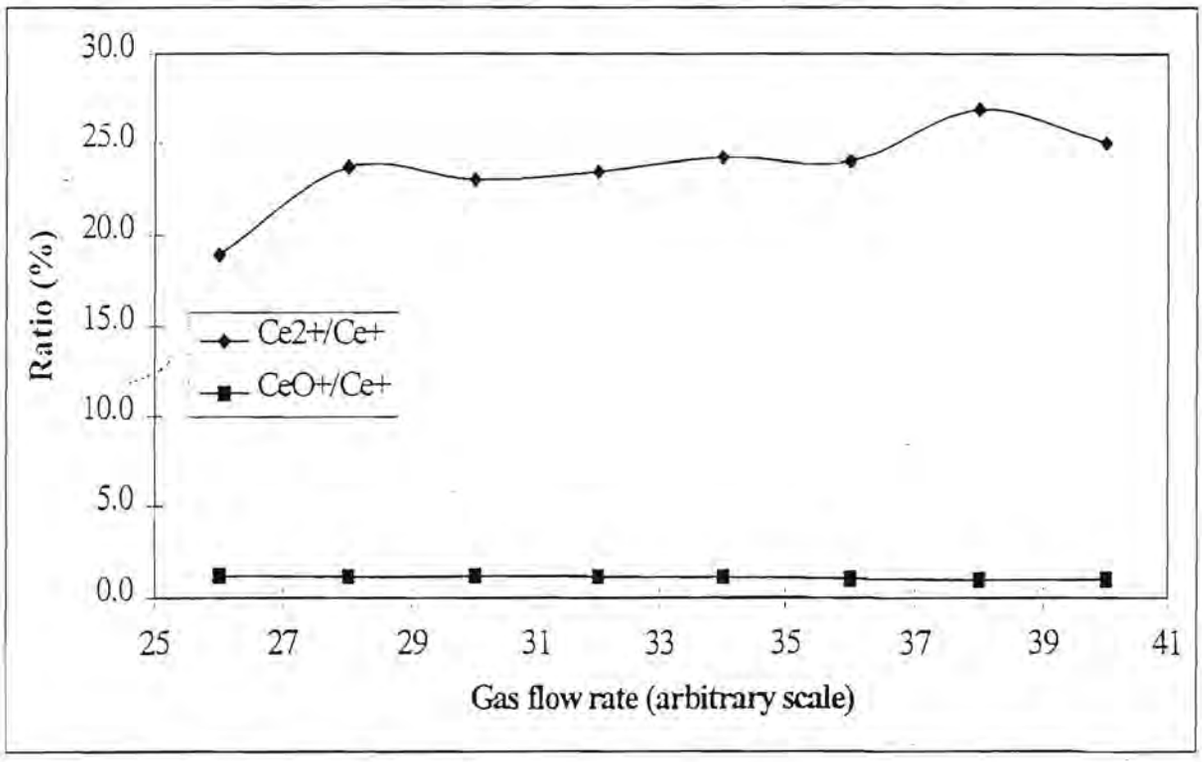

Figure 2.24: Effect of coolant flow on the response curves of the ratios Ce^{2+}/Ce^{+} and CeO^{+}/Ce^{+}.

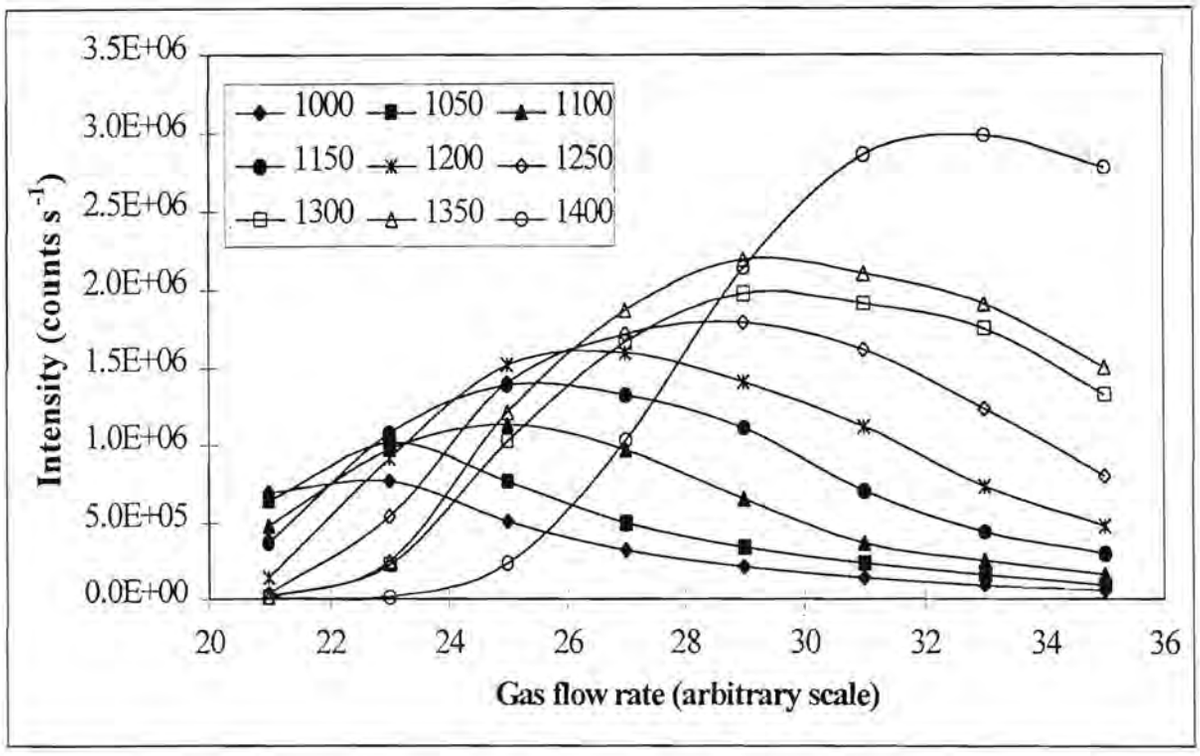

Figure 2.26: Effect of the aerosol carrier gas flow rate on the Li^+ signal at different power settings.

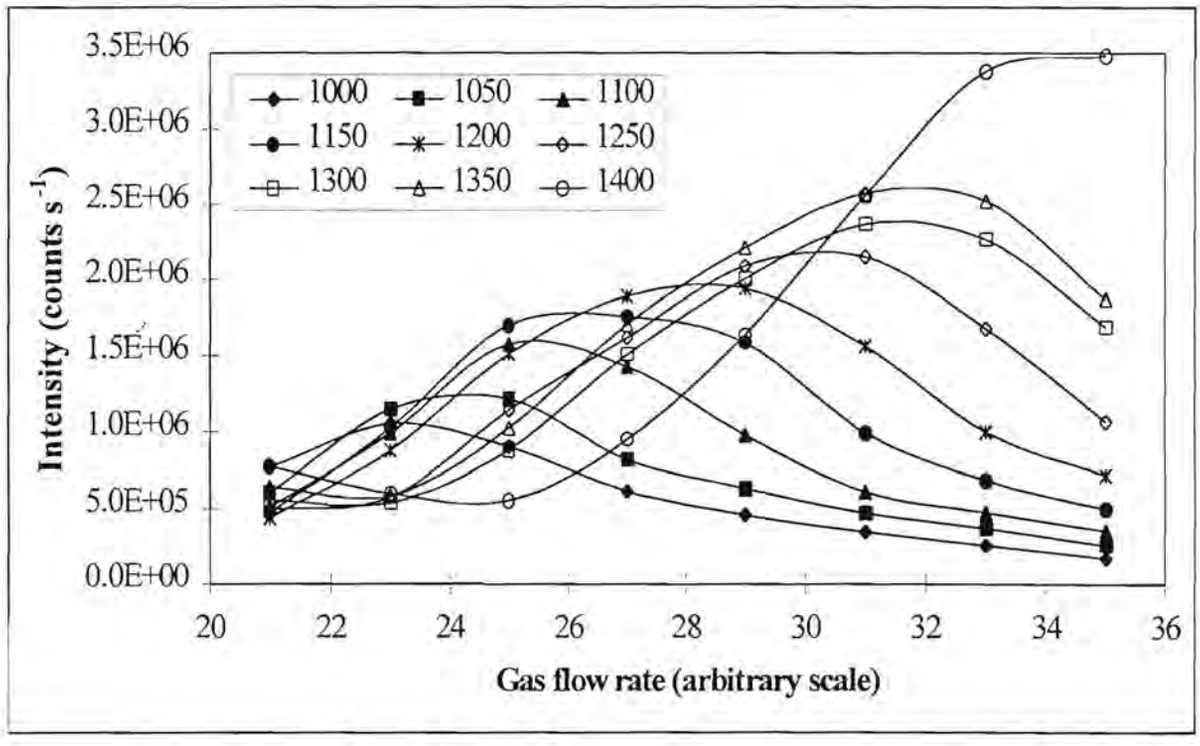

Figure 2.27: Effect of the aerosol carrier gas flow rate on the Na^+ signal at different power settings.

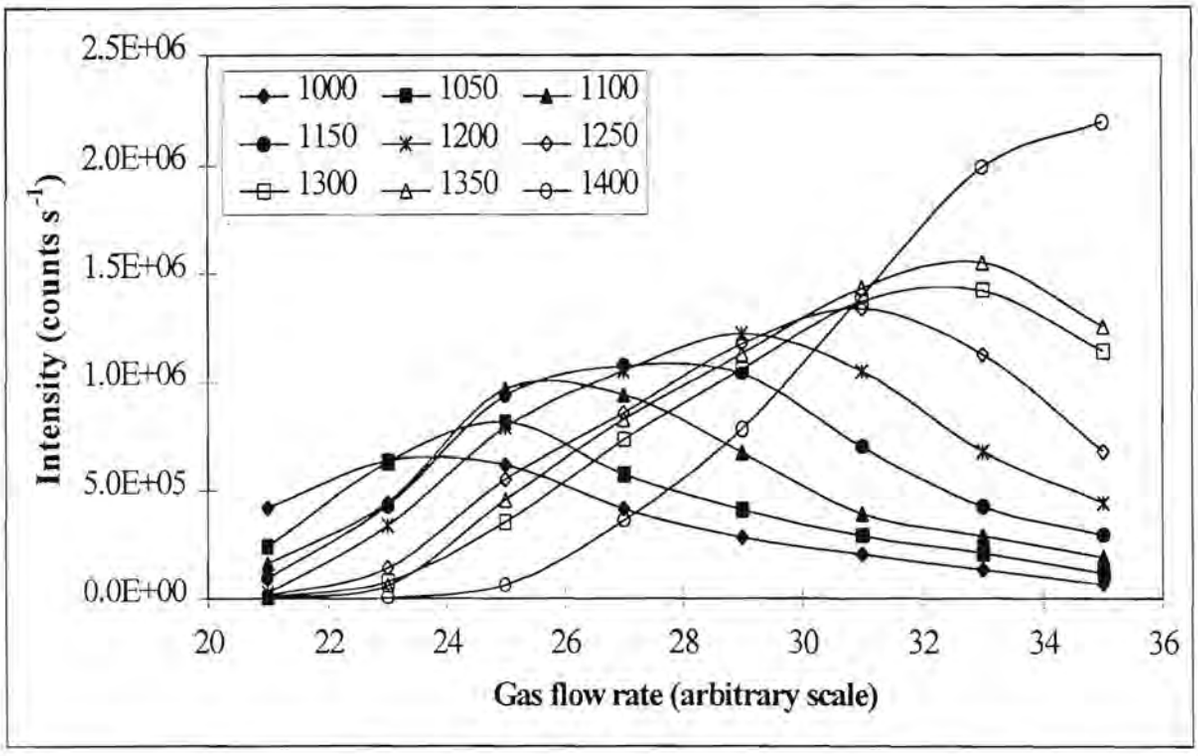

Figure 2.28: Effect of the aerosol carrier gas flow rate on the Mg^+ signal at different power settings.

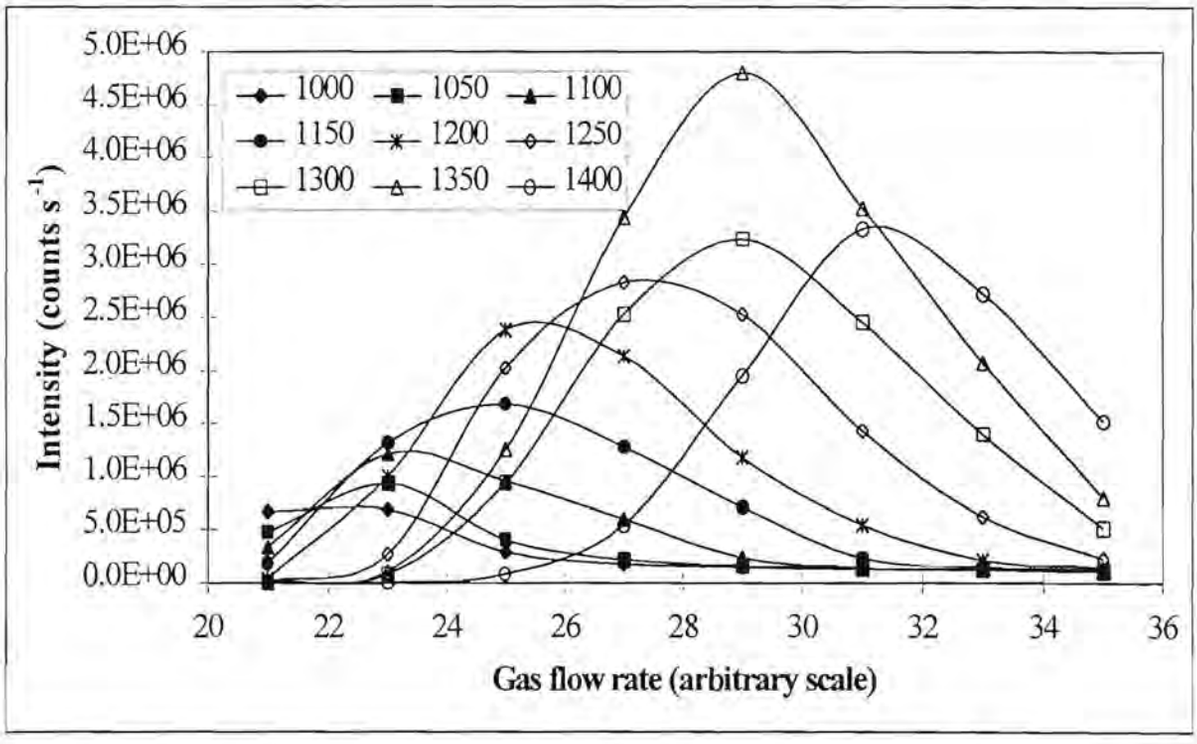

Figure 2.29: Effect of the aerosol carrier gas flow rate on the Ar^+ signal at different power settings.

Table 2.2: Aerosol carrier gas flow rates ("arbitrary scale" as used by instrument manufacturer) at which a maximum analyte signal is obtained for the power settings investigated.

Power setting	Li^+	Na^+	Mg^+	Ar^+	Cu^+	In^+	Ce^+	Pb^+	Ce^{2+}	CeO^+
1000 W	23	23	23	23	23	23	23	23	27	23
1050 W	23	25	25	23	25	23	23	23	29	25
1100 W	25	25	25	23	25	25	25	25	31	27
1150 W	25	27	27	25	27	27	25	25	33	27
1200 W	27	29	29	25	29	27	29	27	-	29
1250 W	29	31	31	27	31	29	29	29	-	29
1300 W	29	31	33	29	33	31	31	31	-	31
1350 W	29	31	33	29	33	31	31	31	-	31
1400 W	33	-	-	31	-	-	33	33	-	-

As the maximum intensity observed for an element increases with the power setting, it seems preferable to work at higher power settings. The curves show that the analyte signals are very sensitive to changes in the aerosol carrier gas flow rate at a specific power setting. Care should thus be taken when optimising the aerosol carrier gas flow rate.

Effect of power and aerosol carrier gas flow rate on heavier elements

Curves showing the effect of the aerosol carrier gas flow rate at different power settings can be seen in figures 2.30, 2.31, 2.32 and 2.33 for Cu^+, In^+, Ce^+ and Pb^+. The same trends as for the light elements are observed for the heavier elements. Table 2.2 shows that for the heavier elements the optimal aerosol carrier gas flow rate at a power setting of 1350 W is also about 31 ("arbitrary scale" as used by instrument manufacturer). As for the light elements, the data plotted indicate that analyte signals are very sensitive to changes in the aerosol carrier gas flow rate and higher power settings are preferable.

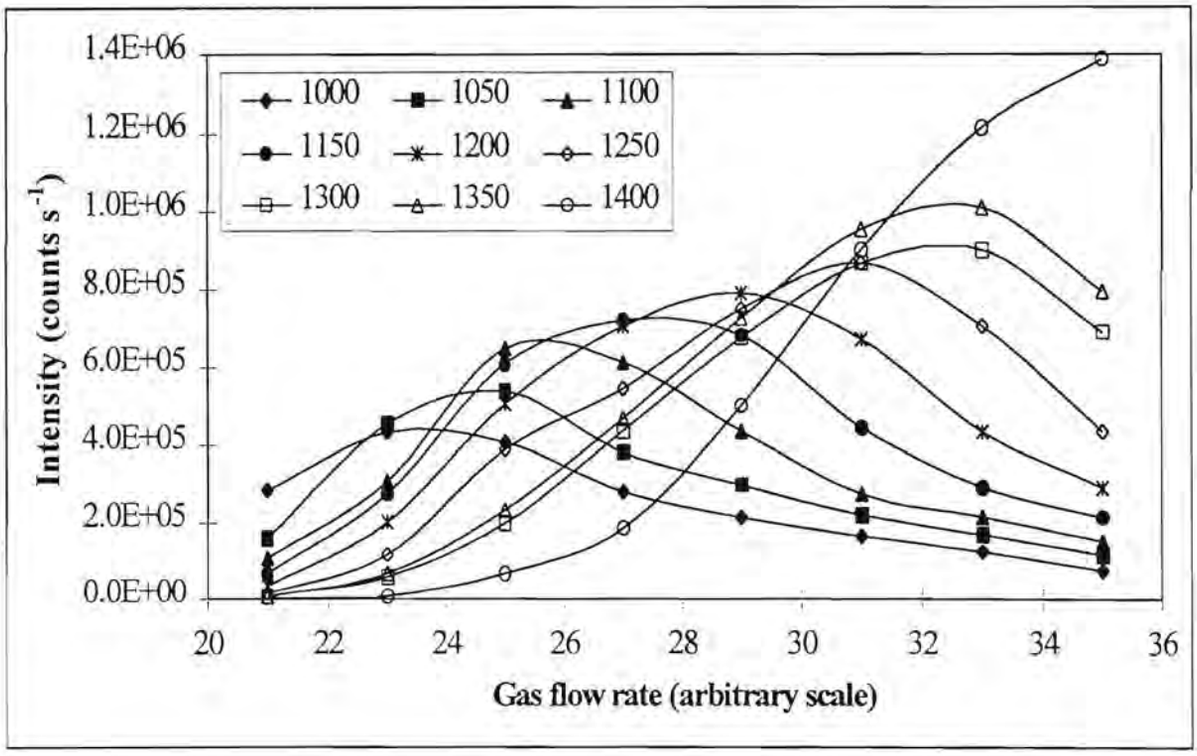

Figure 2.30: Effect of the aerosol carrier gas flow rate on the Cu^+ signal at different power settings.

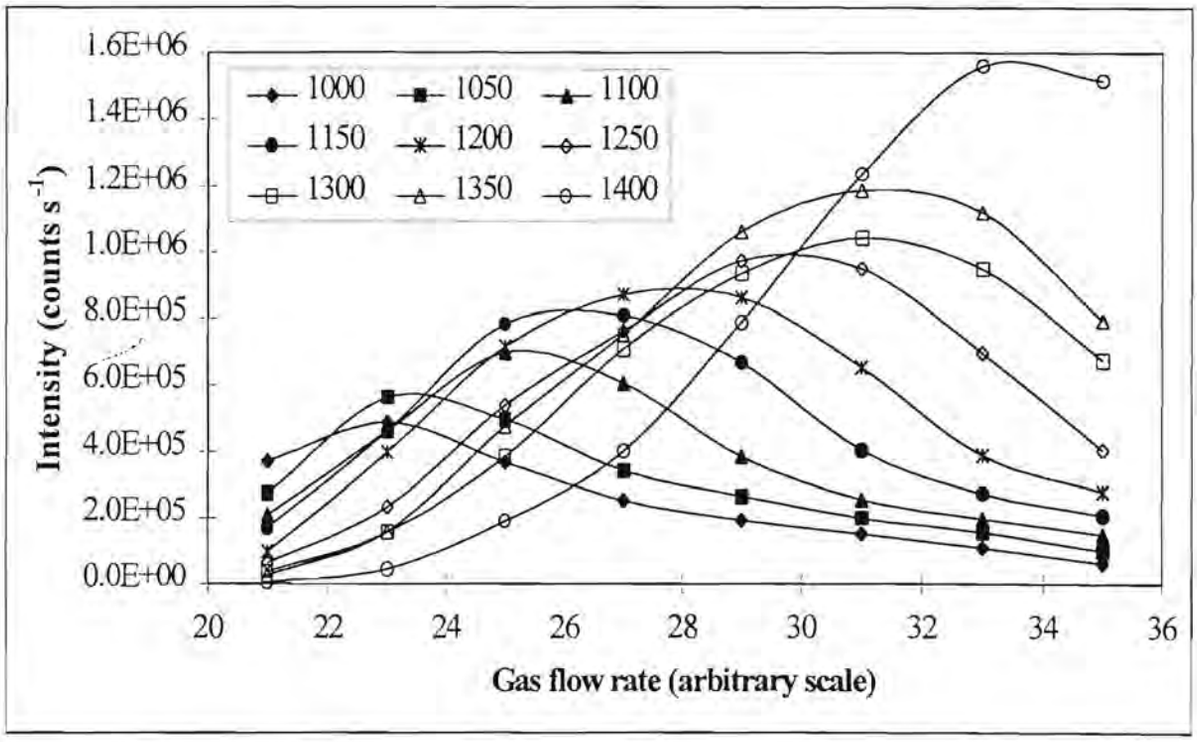

Figure 2.31: Effect of the aerosol carrier gas flow rate on the In^+ signal at different power settings.

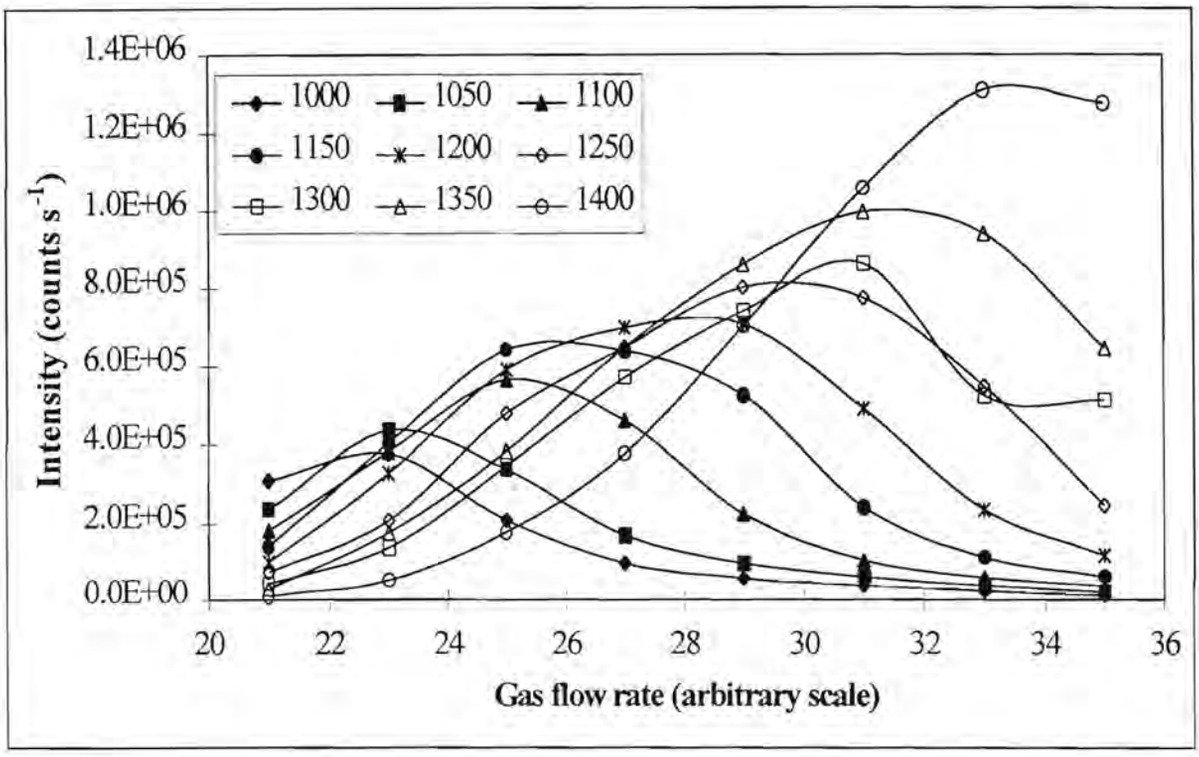

Figure 2.32: Effect of the aerosol carrier gas flow rate on the Ce^+ signal at different power settings.

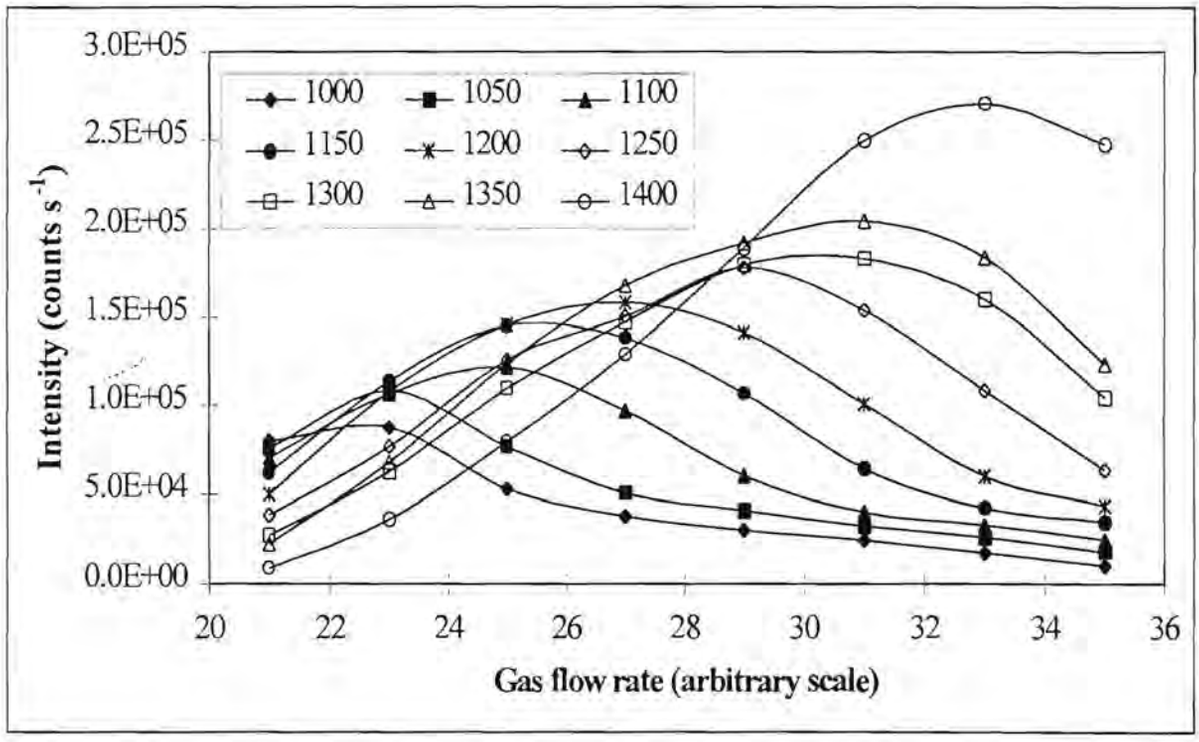

Figure 2.33: Effect of the aerosol carrier gas flow rate on the Pb^+ signal at different power settings.

Long and Brown *[33]* also found the aerosol carrier gas pressure to be of critical importance with definite settings for maximum analyte intensities. Their results showed that a compromise setting may be used that allowed multi-element analysis within 10% of the optimum sensitivity. In accordance to the results reported here, Long and Brown *[33]* further showed analyte signals to increase with an increase in power, to reach maximum values in the range 1.2 to 1.4 kW and then to decrease again. Their results, as well as those of other workers *[29, 30]*, also showed the optimum aerosol carrier gas pressure to increase with an increase in power. Zhu and Browner *[31]* reported that the response behaviour for aerosol carrier gas flow rate is largely independent of the concentration of the solution.

Effect of power and aerosol carrier gas flow rate on background intensities

Even though figures 2.34 and 2.35 indicate that the aerosol carrier gas flow rate does not have a significant effect on the background signals (values below 100 counts s^{-1}), lower background intensities are observed at lower power settings.

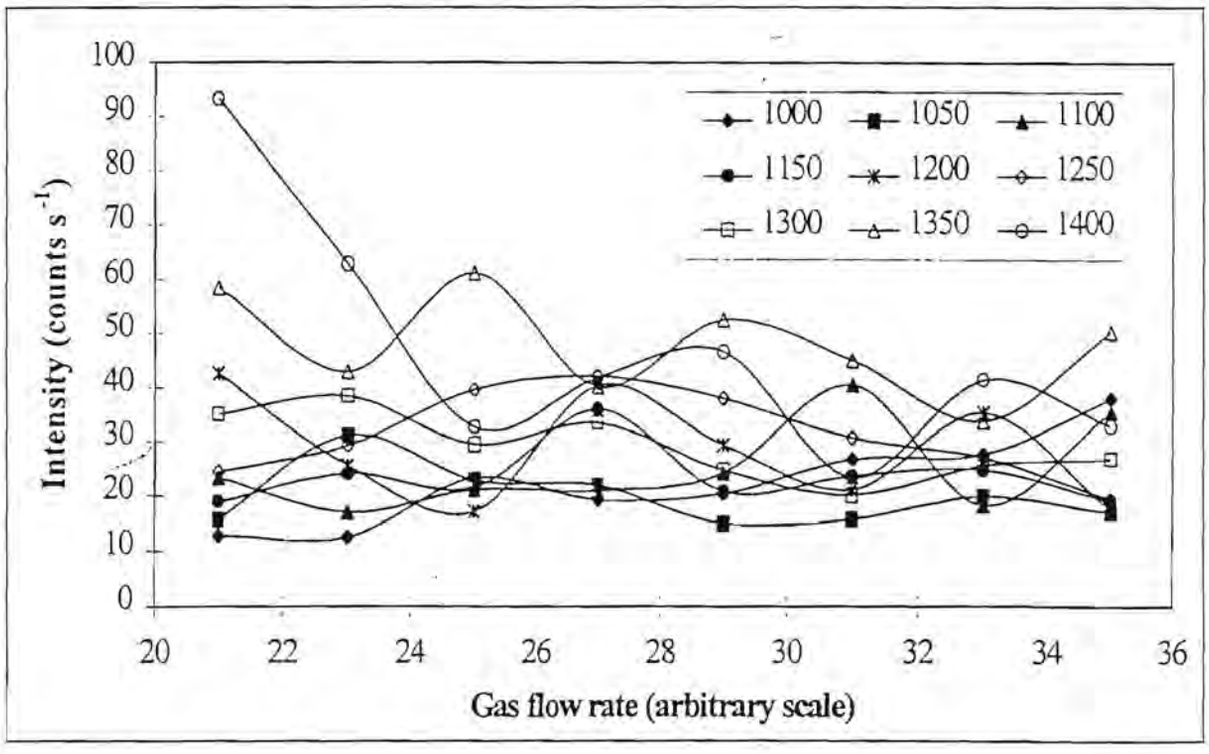

Figure 2.34: Effect of the aerosol carrier gas flow rate on background(Nb) signal at different power settings.

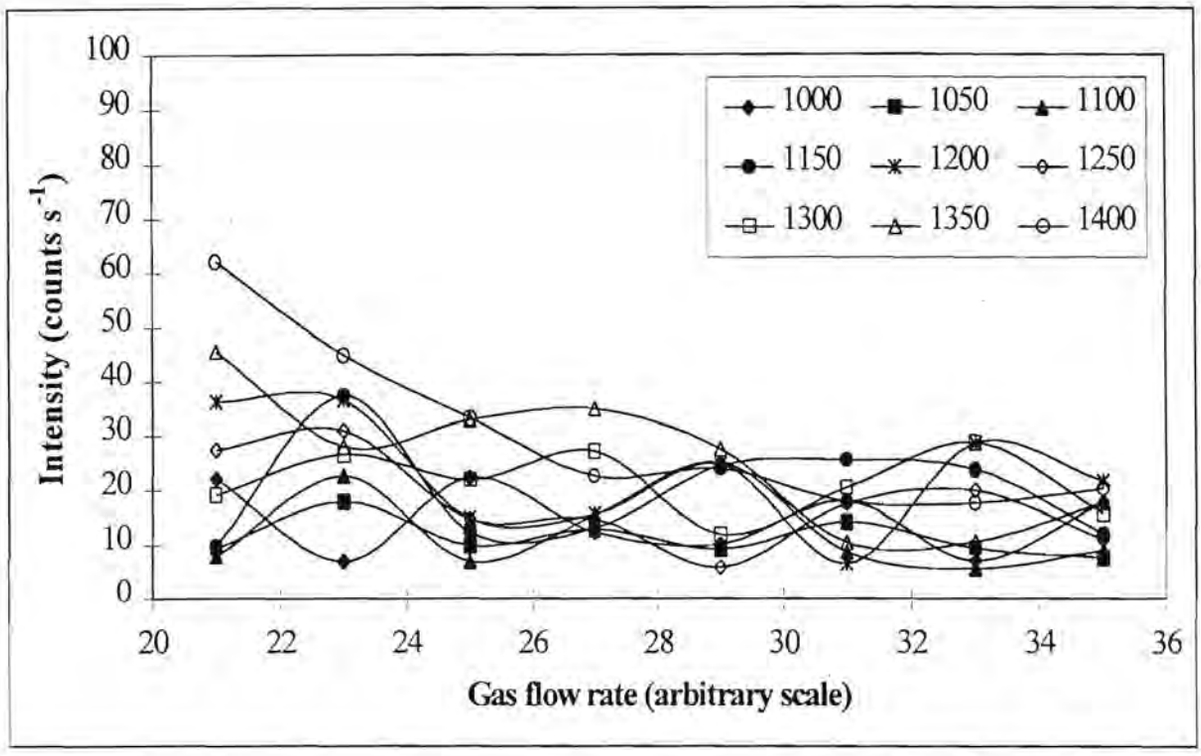

Figure 2.35: Effect of the aerosol carrier gas flow rate on background(Tc) signal at different power settings.

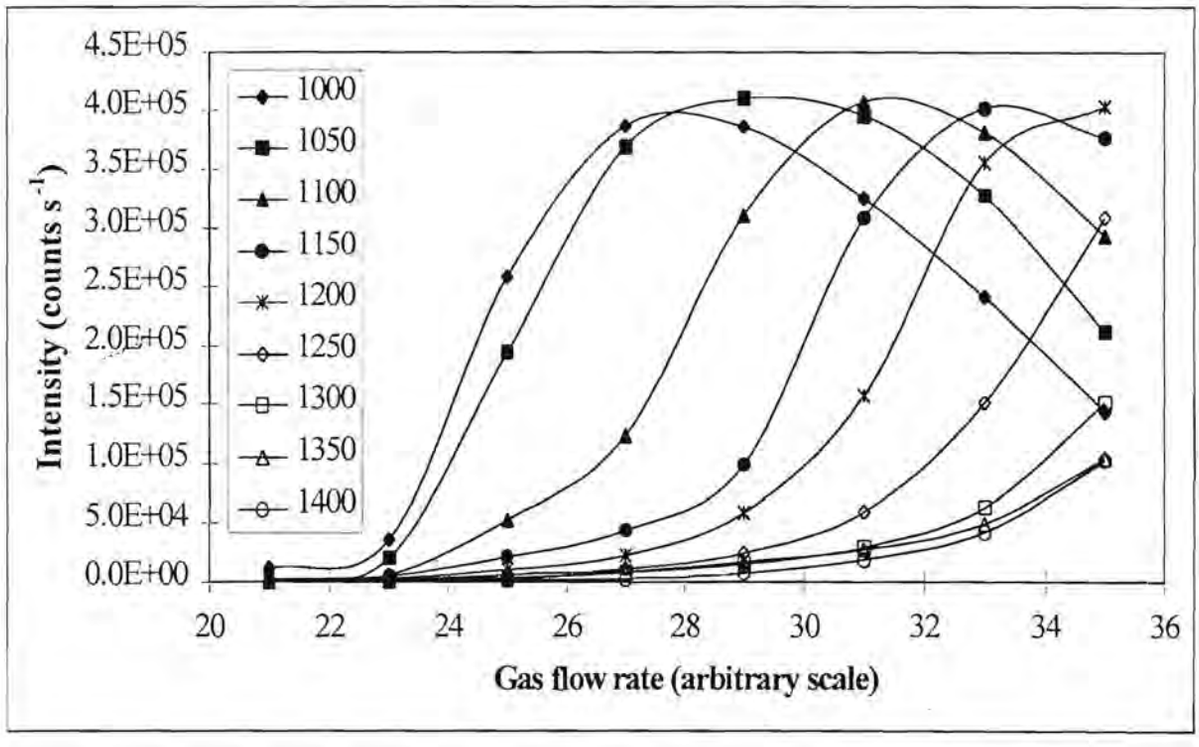

Figure 2.36: Effect of the aerosol carrier gas flow rate on the Ce^{2+} signal at different power settings.

Some workers *[33]* monitored background values at mass 130 and found a linear response with an increase in power. They found this to be more or less the same at 80 - 240 amu. They also reported a decrease in background intensity with an increase in aerosol carrier gas pressure. They stated that presumably, at high pressures the increased gas flow rate lowers the temperature in the plasma, thus increasing the number of scattered photons that are detected.

Effect of power and aerosol carrier gas flow rate on doubly ionised ions and oxides

According to Long and Brown *[33]* the three main reasons for decreases in the analyte signals as aerosol carrier gas pressure or power move away from the optimum are: 1) reduction in ion formation as a result of less efficient energy transfer from the RF load coil, via the plasma, to the analyte, 2) formation of neutrally charged species (not detected) and 3) formation of analyte oxide ions and doubly charged analyte ions. The effect of the aerosol carrier gas flow at various power settings on Ce^{2+} and CeO^{+} can be seen in figures 2.36 and 2.37. For Ce^{2+} signal maxima of approximately the same value can be seen for all power settings 1000 W to 1200 W. CeO^{+} curves show more or less the same trends as for the light and heavier elements.

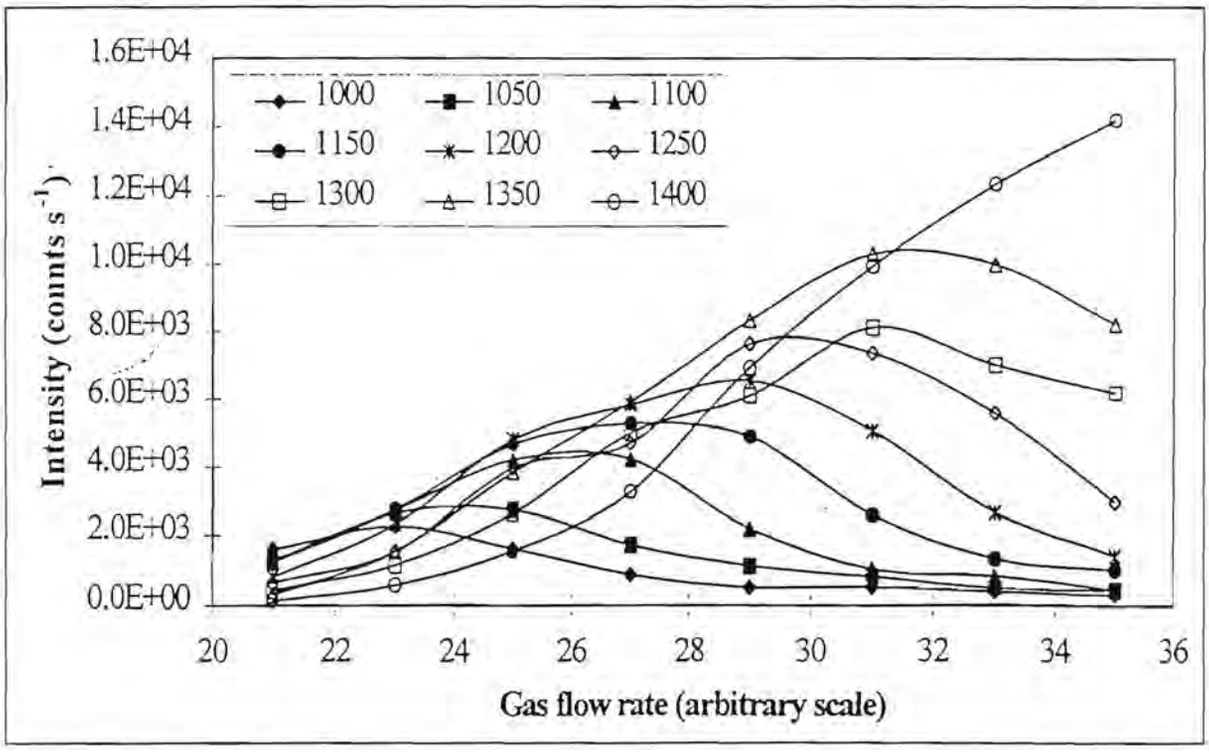

Figure 2.37: Effect of the aerosol carrier gas flow rate on the CeO^{+} signal at different power settings.

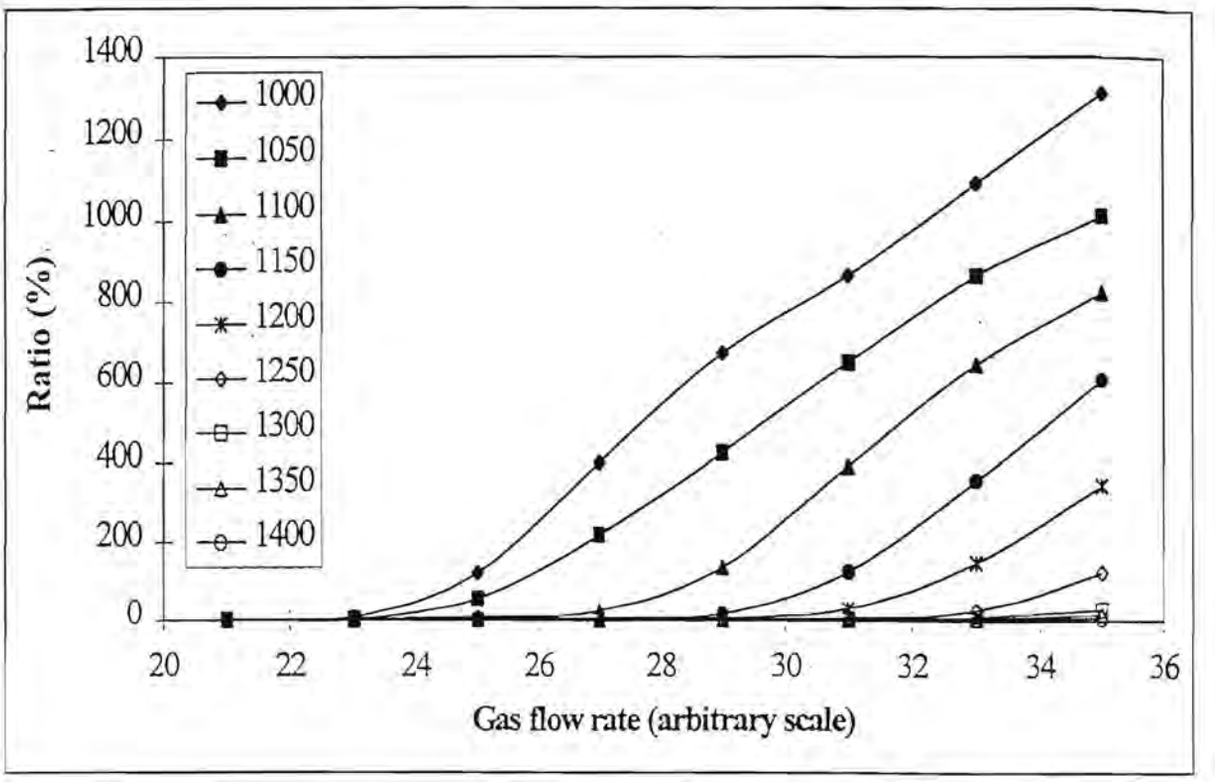

Figure 2.38(a): Effect of the aerosol carrier gas flow rate on the Ce^{2+}/Ce^{+} ratio at different power settings.

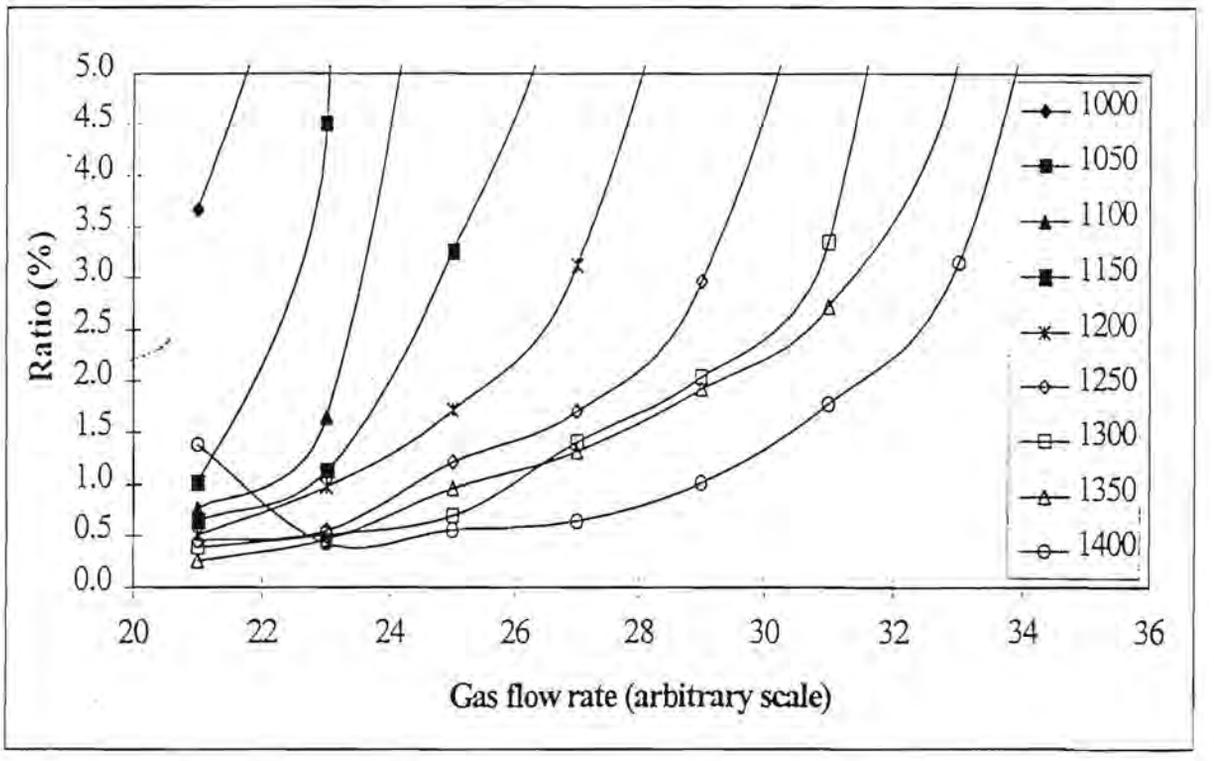

Figure 2.38(b): Effect of the aerosol carrier gas flow rate on the Ce^{2+}/Ce^{+} ratio at different power settings. (Only the 0 - 5% range is showed.)

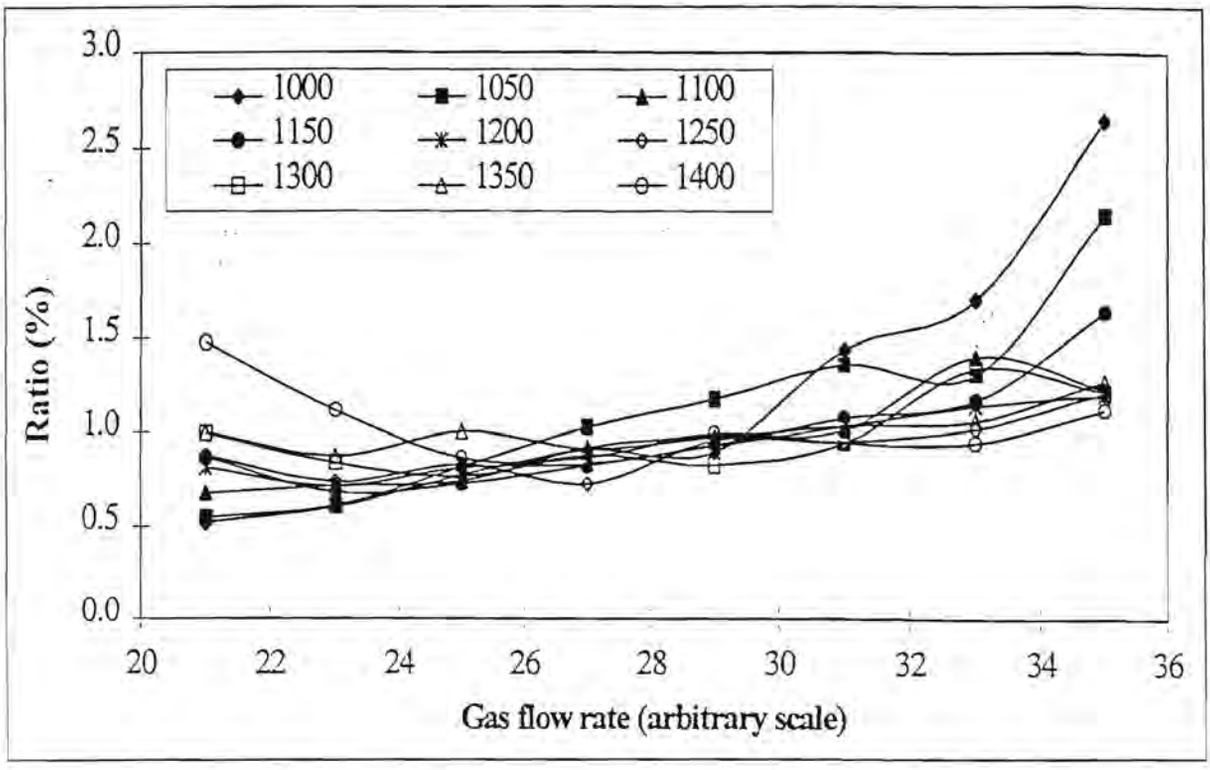

Figure 2.39: Effect of the aerosol carrier gas flow rate on the CeO^+/Ce^+ ratio at different power settings.

Figures 2.38(a), 2.38(b) and 2.39 give the trends followed by the Ce^{2+}/Ce^+ and CeO^+/Ce^+ ratios when the aerosol carrier gas flow rate is varied. Figure 2.38(b) shows that these parameters are critical in minimising the doubly ionised interferences. Table 2.3 gives the maximum flow rates that may be employed in order to maintain the Ce^{2+}/Ce^+ and CeO^+/Ce^+ ratios below the acceptable values of 2.5% and 1%.

These ratios are extremely sensitive to changes in the flow rate and great care must be taken in not choosing too high flow rates. For a power setting of 1350 W the maximum allowable flow rate seems to be 29 which is lower than the value of 31 for the analyte signals. Relative to these ratios the changes caused in the analyte signals by reducing the flow rate to 29 are small. Generally, the optimal flow rates for the analyte signals would not cause the CeO^+/Ce^+ ratio to increase above 1%, but lower flow rates have to be employed in order to minimise the Ce^{2+}/Ce^+ ratio. Long and Brown *[33]* reported M^+/MO^+ and M^+/M^{2+} ratios for Cs, Sm, Ba, Pb with variations in aerosol carrier gas pressure or power. They reported optimum aerosol carrier gas pressures with $M^+/MO^+ >$ 300 and $M^+/M^{2+} > 100$. They also concluded that lower pressures are preferable. Other researchers *[31]* obtained CeO^+/Ce^+ and Ce^{2+}/Ce^+ ratios of both lower than

3%. Similar to the results reported here, they found the CeO^+/Ce^+ ratio to increase slightly with increases in the aerosol carrier gas flow rate and decrease slightly with increases in the power settings. They also found the Ce^{2+}/Ce^+ ratio to increase with an increase in the aerosol carrier gas flow rate and decrease with an increase in power. Horlick *et al. [29]* stated that in order to minimise the CeO^+/Ce^+ ratio one has to lower the aerosol carrier gas pressure to a value lower than that providing maximum analyte counts. Gray and Williams *[34]* reported values of about 1% for the CeO^+/Ce^+ ratio.

Table 2.3: Maximum aerosol carrier gas flow rates ("arbitrary scale" as used by instrument manufacturer) at which acceptable values for Ce^{2+}/Ce^+ (2.5%) and CeO^+/Ce^+ (1%) ratios are still obtained for the power settings investigated.

Power setting	Ce^{2+}/Ce^+	CeO^+/Ce^+
1000 W	-	29
1050 W	21	25
1100 W	23	29
1150 W	23	29
1200 W	25	29
1250 W	27	31
1300 W	29	31
1350 W	29	29
1400 W	31	33

2.3.4 *Effect of ion lens settings*

Effect of ion lens settings on light elements

Figures 2.40(a) - (h) show the effects of various ion lens settings such as: lens parameters, field axis voltage and detector inner and outer diameter voltages on the response curves of the light elements. All the light elements appear to reach maximum values at more or less the same ion lens settings. The settings to which the analyte intensities are the most sensitive are: LA, LB, LC, ID and OD.

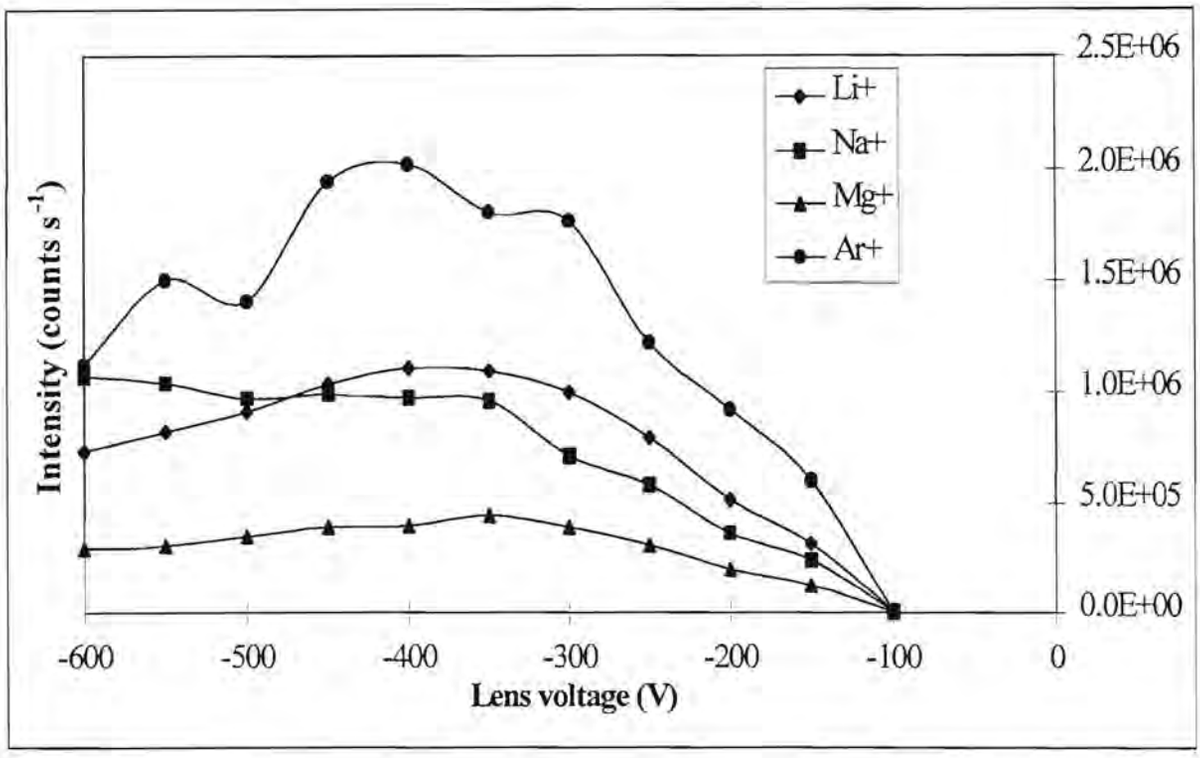

Figure 2.40(a): Effect of the lens parameter LO on the response curves of the light elements and argon.

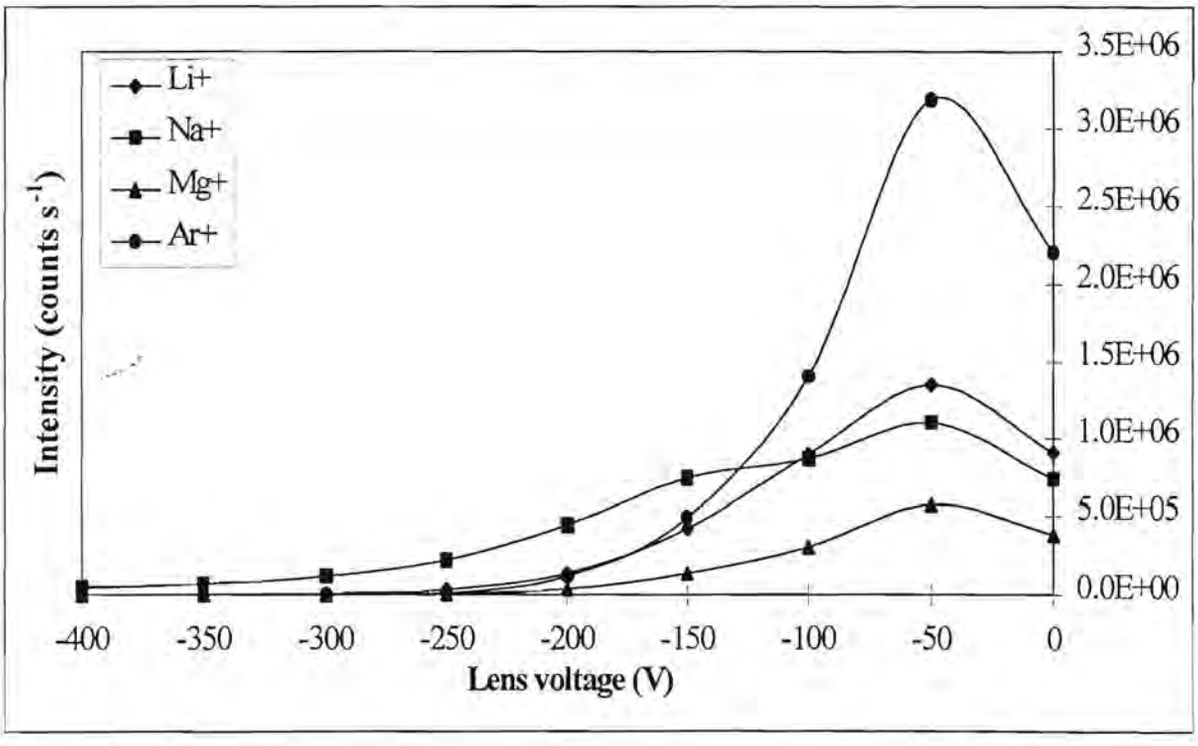

Figure 2.40(b): Effect of the lens parameter LA on the response curves of the light elements and argon.

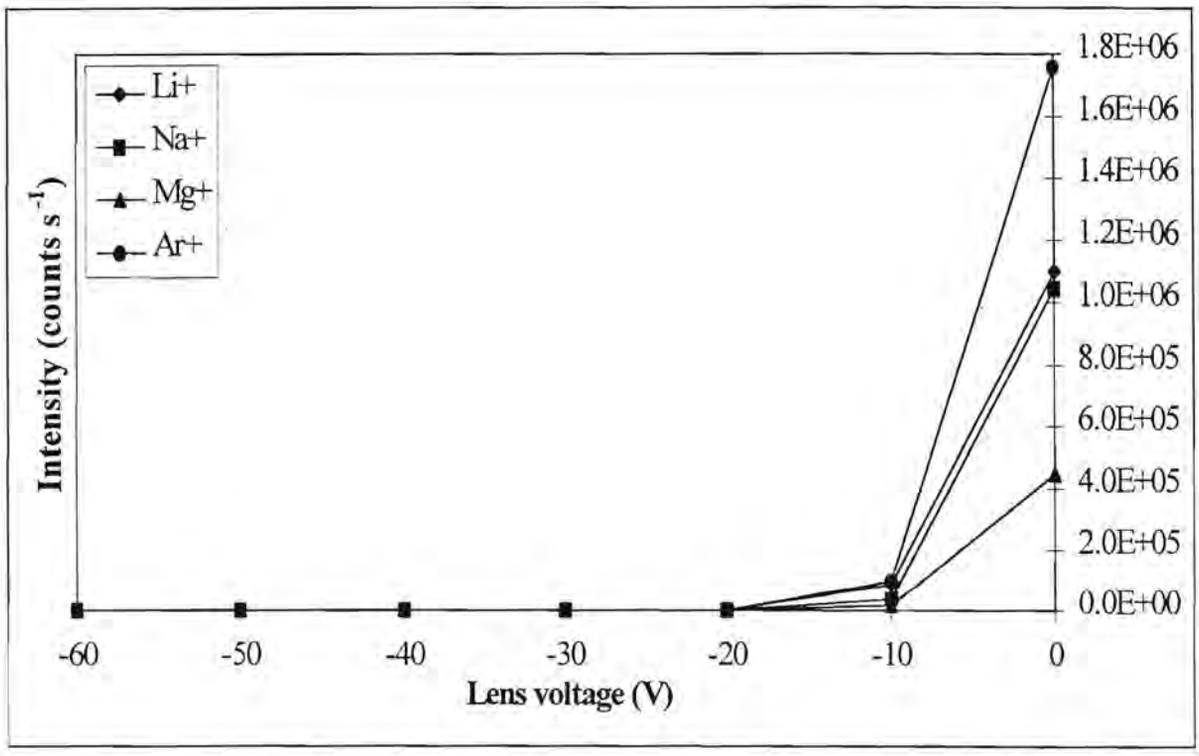

Figure 2.40(c): Effect of the lens parameter LB on the response curves of the light elements and argon.

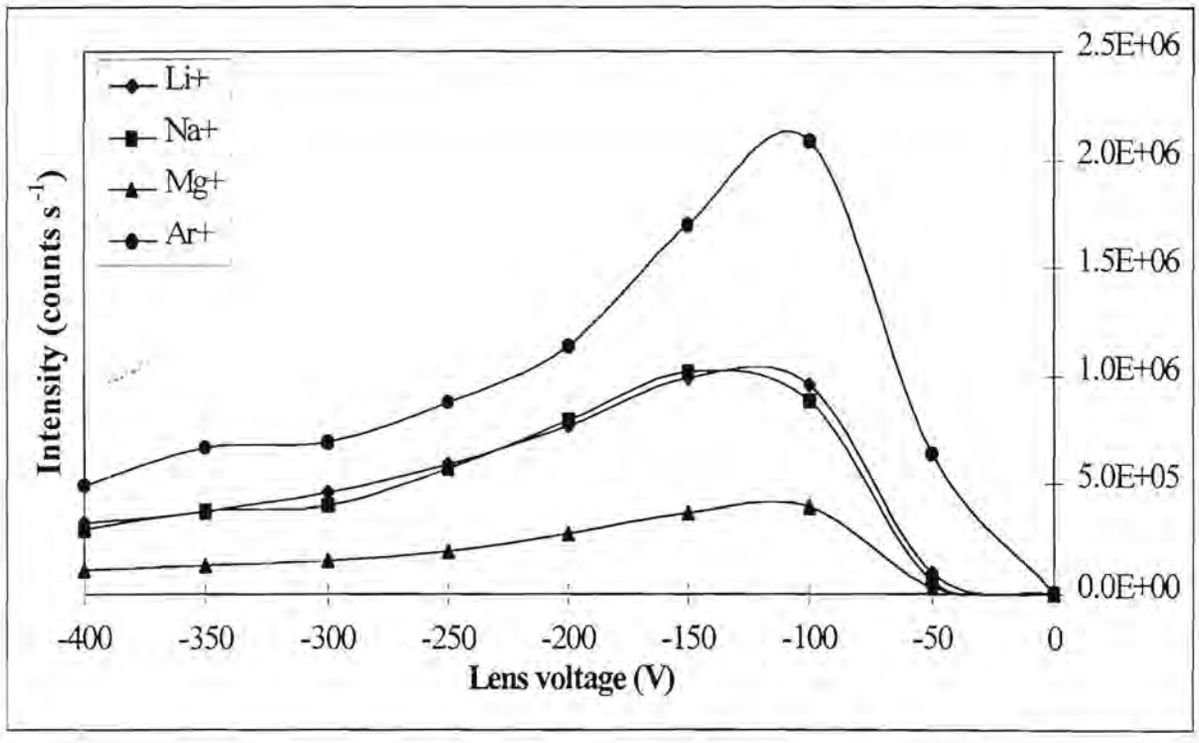

Figure 2.40(d): Effect of the lens parameter LC on the response curves of the light elements and argon.

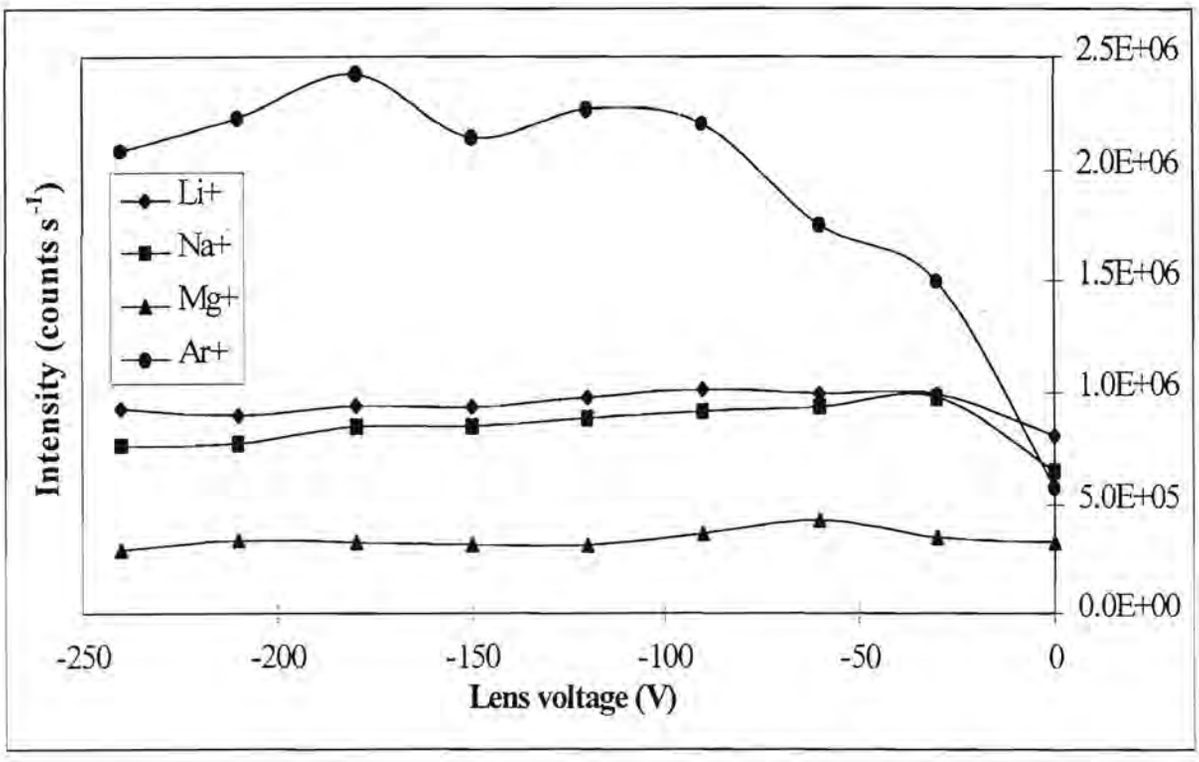

Figure 2.40(e): Effect of the lens parameter LD on the response curves of the light elements and argon.

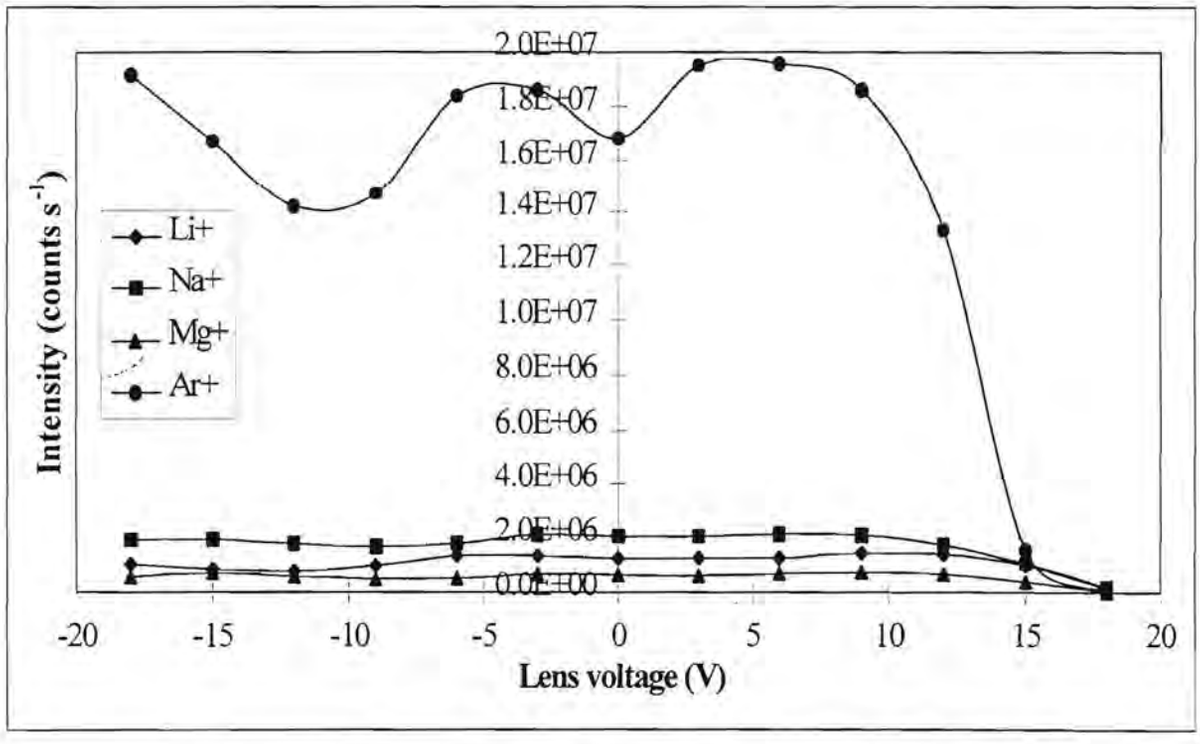

Figure 2.40(f): Effect of the field axis voltage FA on the response curves of the light elements and argon.

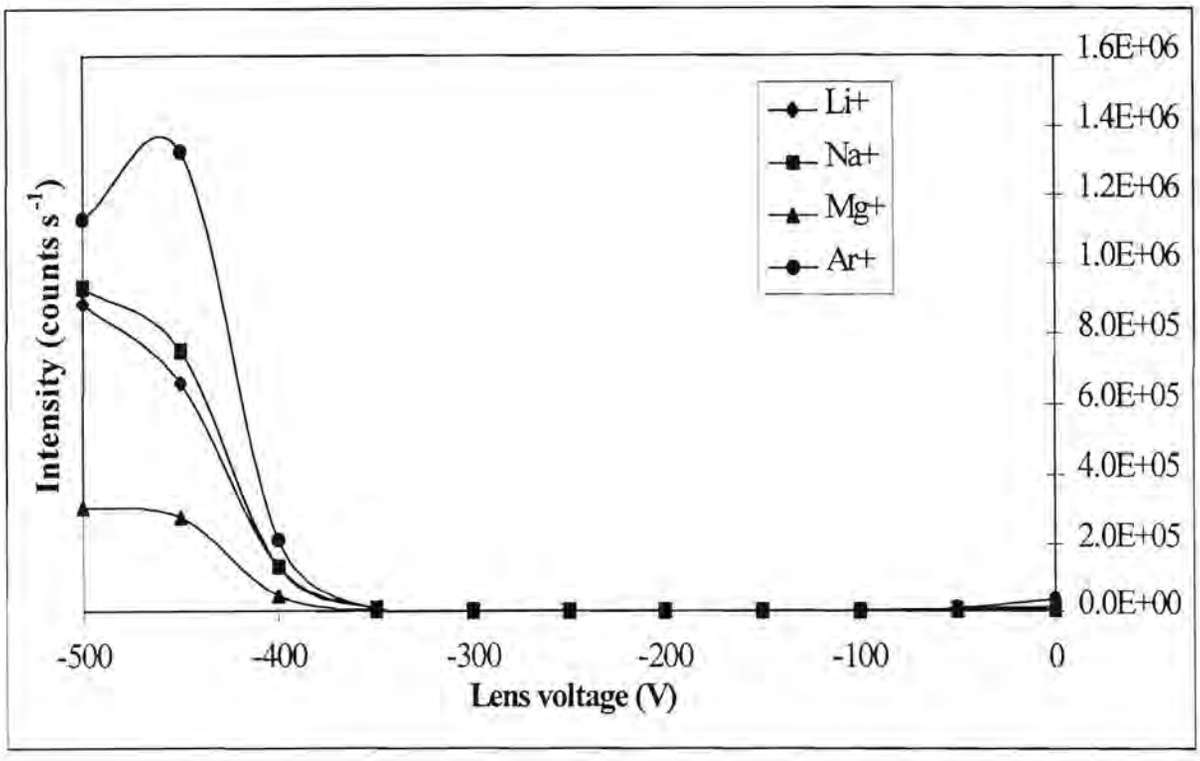

Figure 2.40(g): Effect of the detector inner diameter voltage ID on the response curves of the light elements and argon.

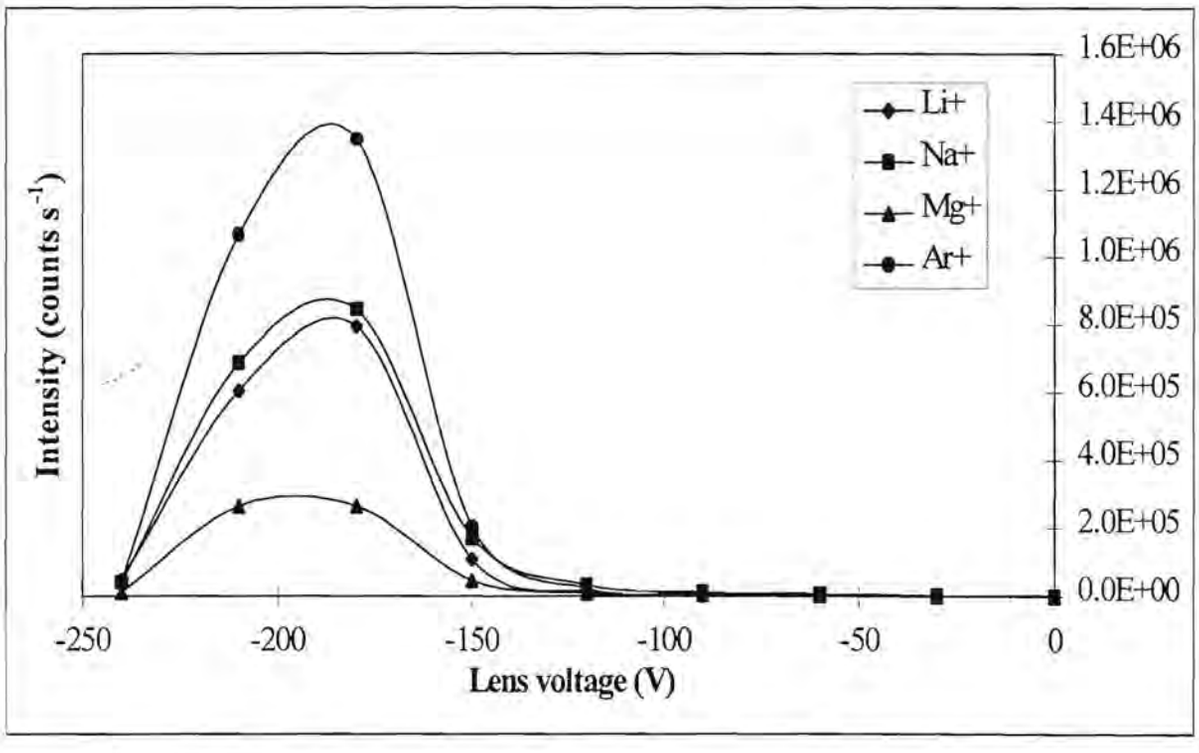

Figure 2.40(h): Effect of the detector outer diameter voltage OD on the response curves of the light elements and argon.

Effect of ion lens settings on heavier elements

From figures 2.41(a) - (h) it can be seen that the curves for the heavier elements show maxima at approximately the same ion lens settings than for the light elements. In some cases slightly more negative voltages are preferred. i.e. for the LO, LC and LD parameters.

Effect of ion lens settings on background intensities

Figures 2.42(a) - (h) show that none of the preferred ion lens settings for the light and heavier elements would cause the background signals to increase to values higher than 100 counts s^{-1}.

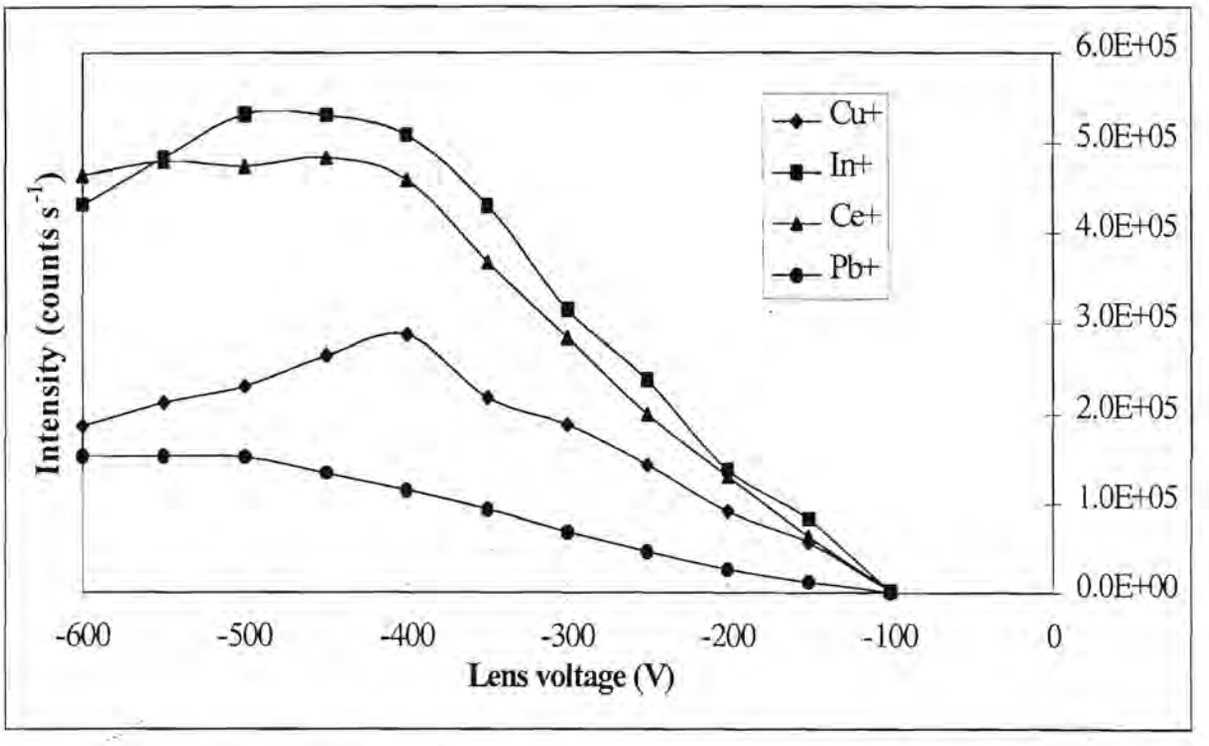

Figure 2.41(a): Effect of the lens parameter LO on the response curves of the heavier elements.

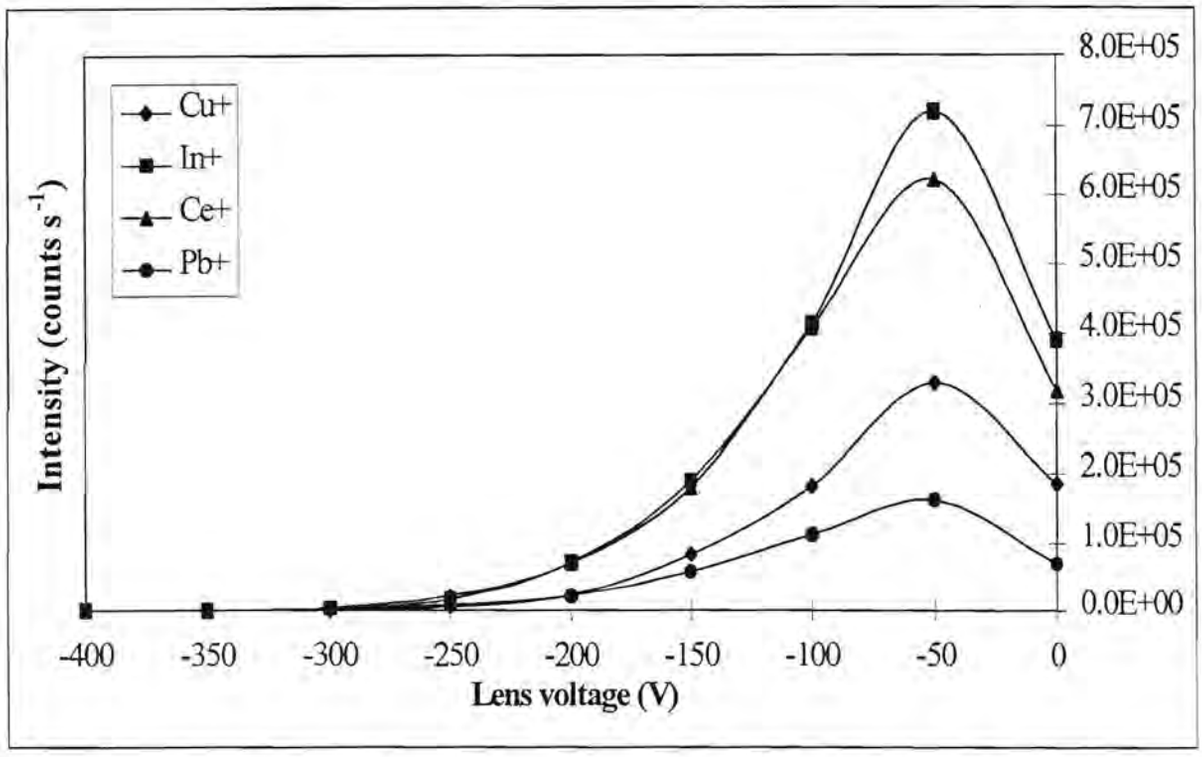

Figure 2.41(b): Effect of the lens parameter LA on the response curves of the heavier elements.

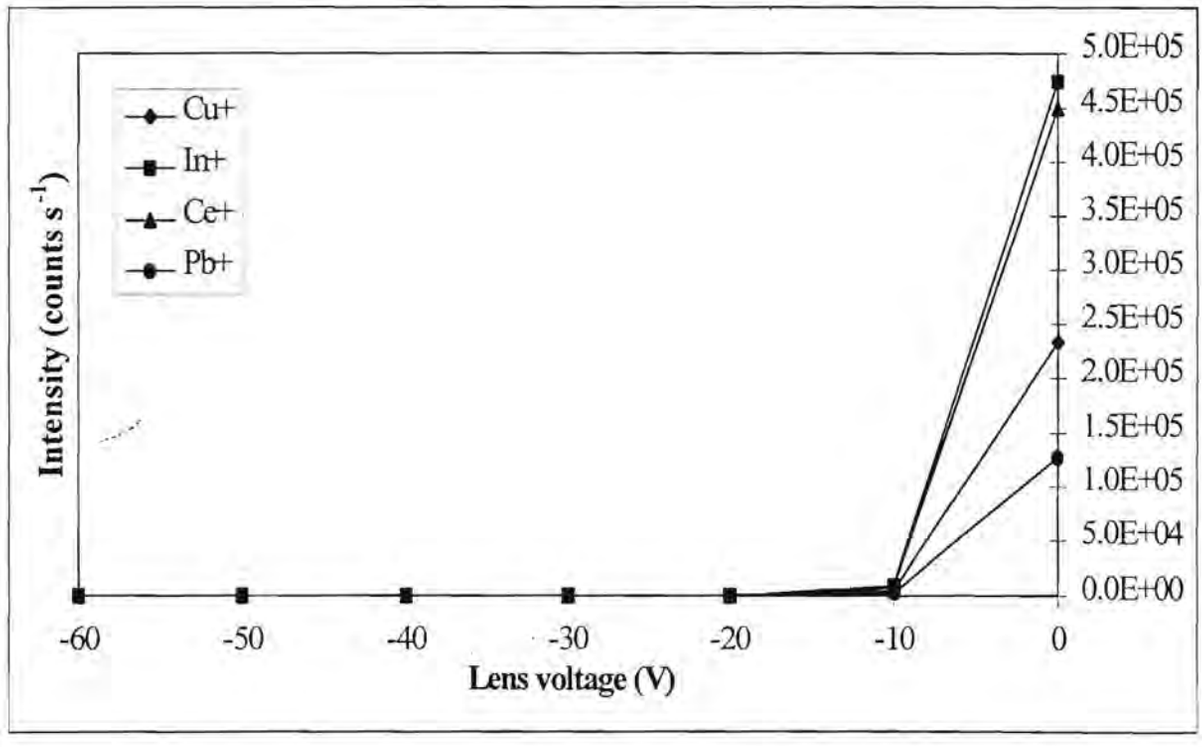

Figure 2.41(c): Effect of the lens parameter LB on the response curves of the heavier elements.

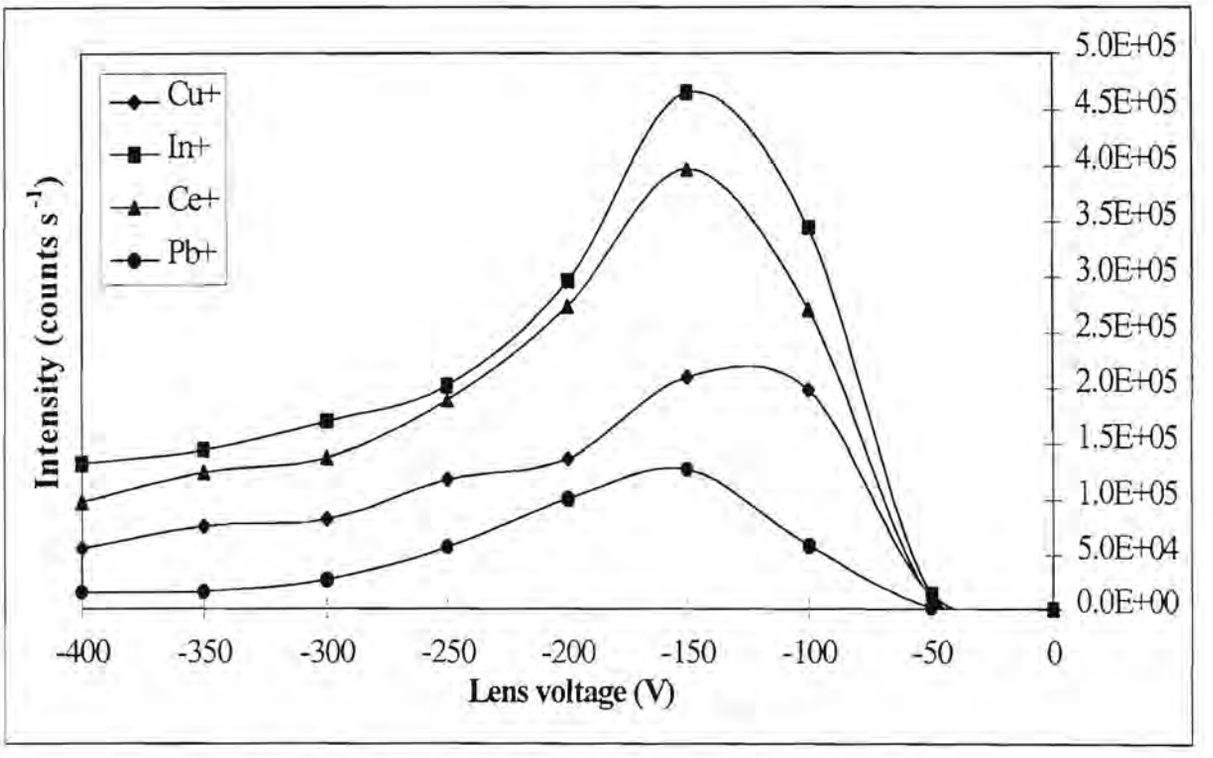

Figure 2.41(d): Effect of the lens parameter LC on the response curves of the heavier elements.

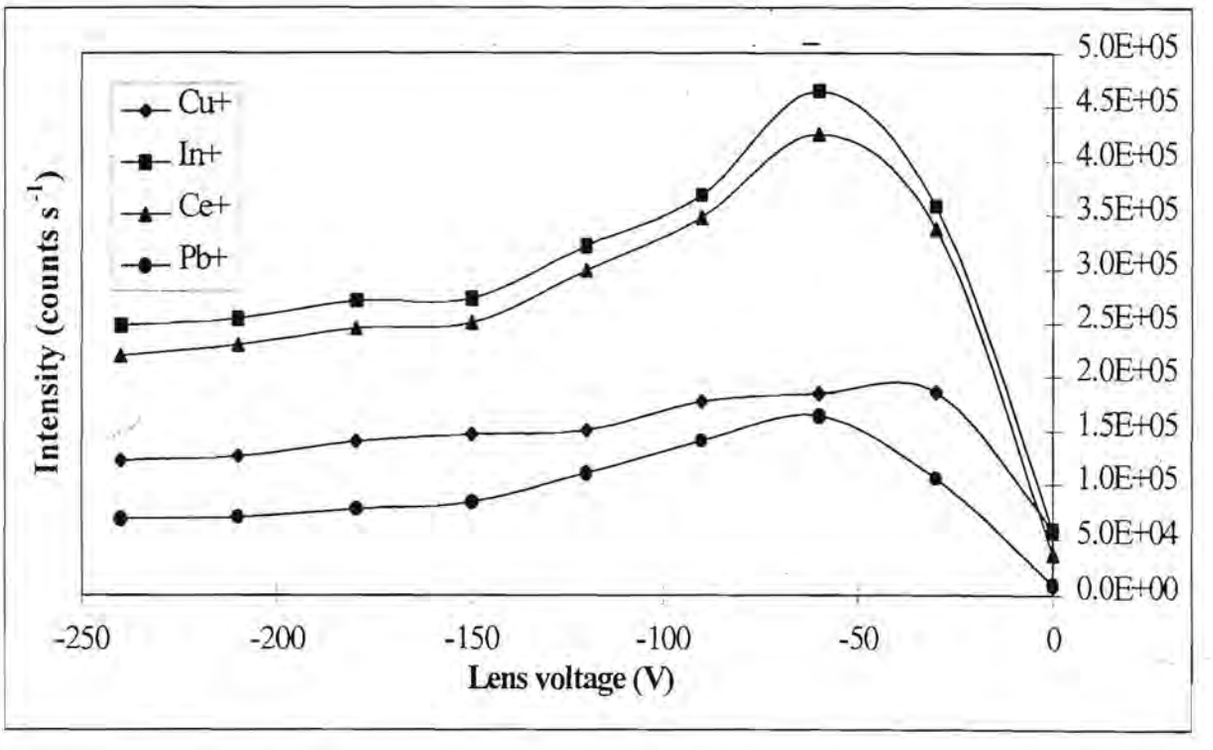

Figure 2.41(e): Effect of the lens parameter LD on the response curves of the heavier elements.

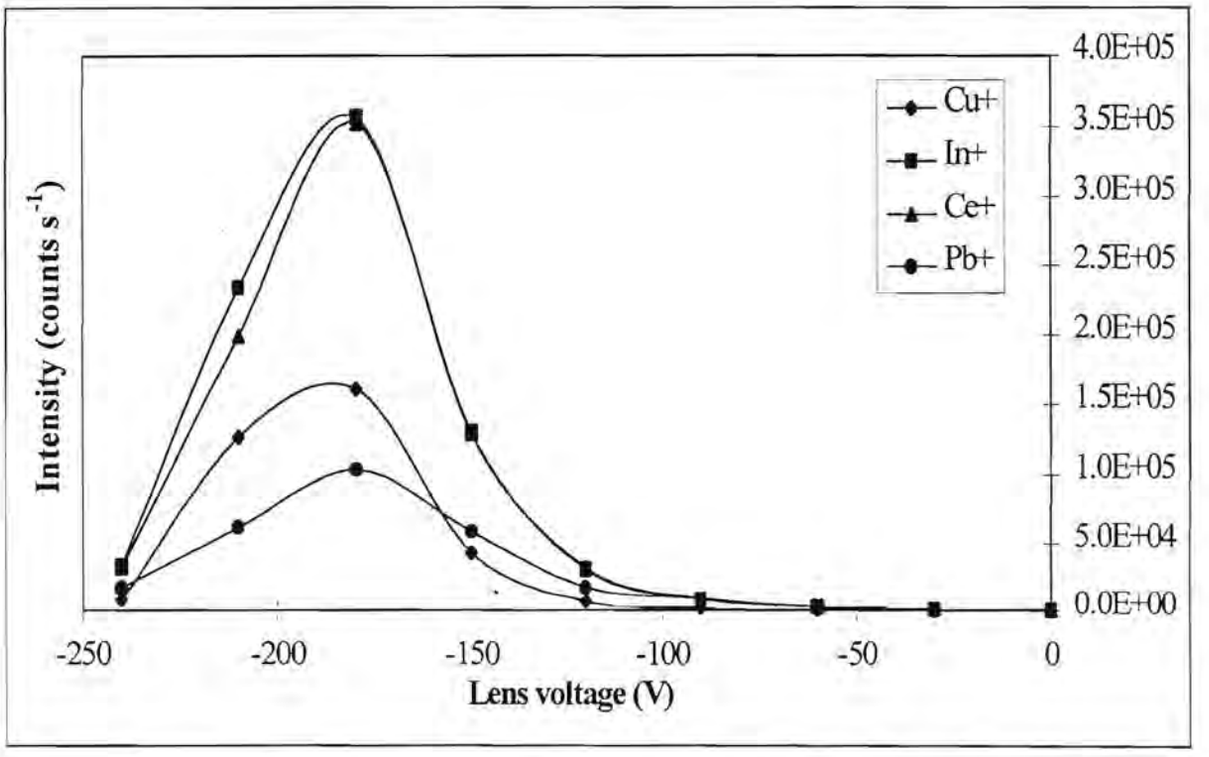

Figure 2.41(h): Effect of the detector outer diameter voltage OD on the response curves of the heavier elements.

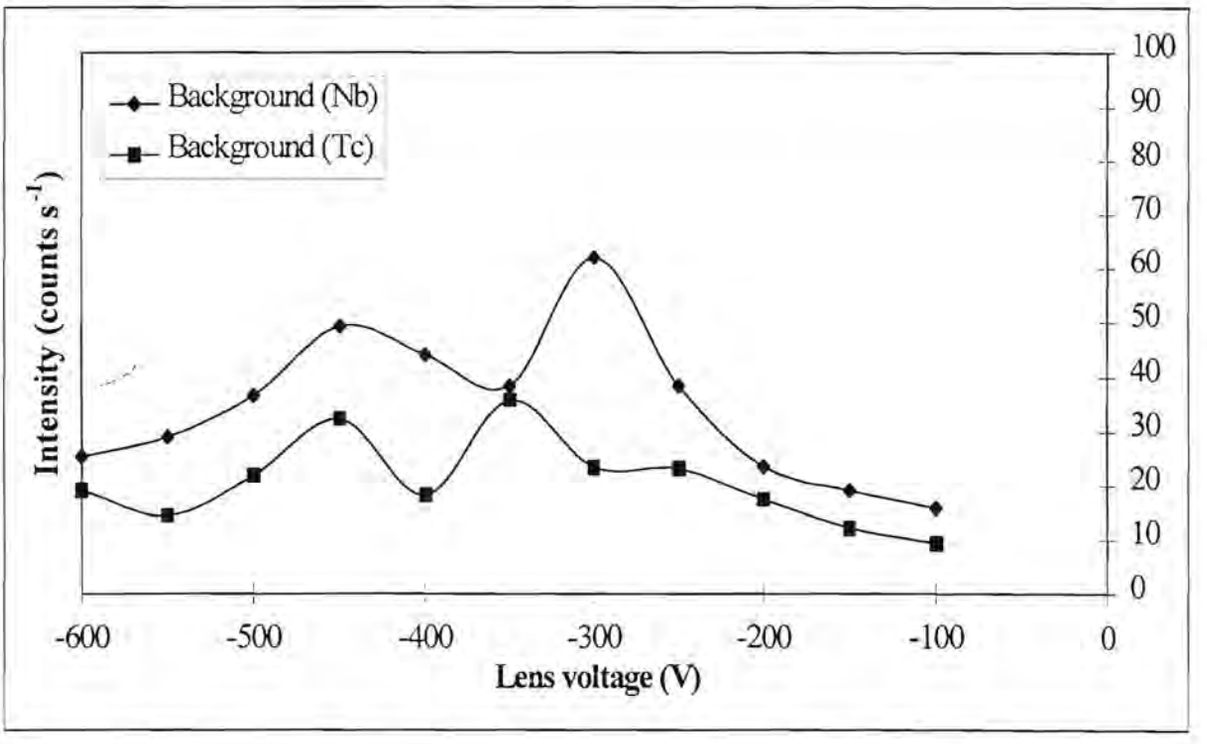

Figure 2.42(a): Effect of the lens parameter LO on the background intensities.

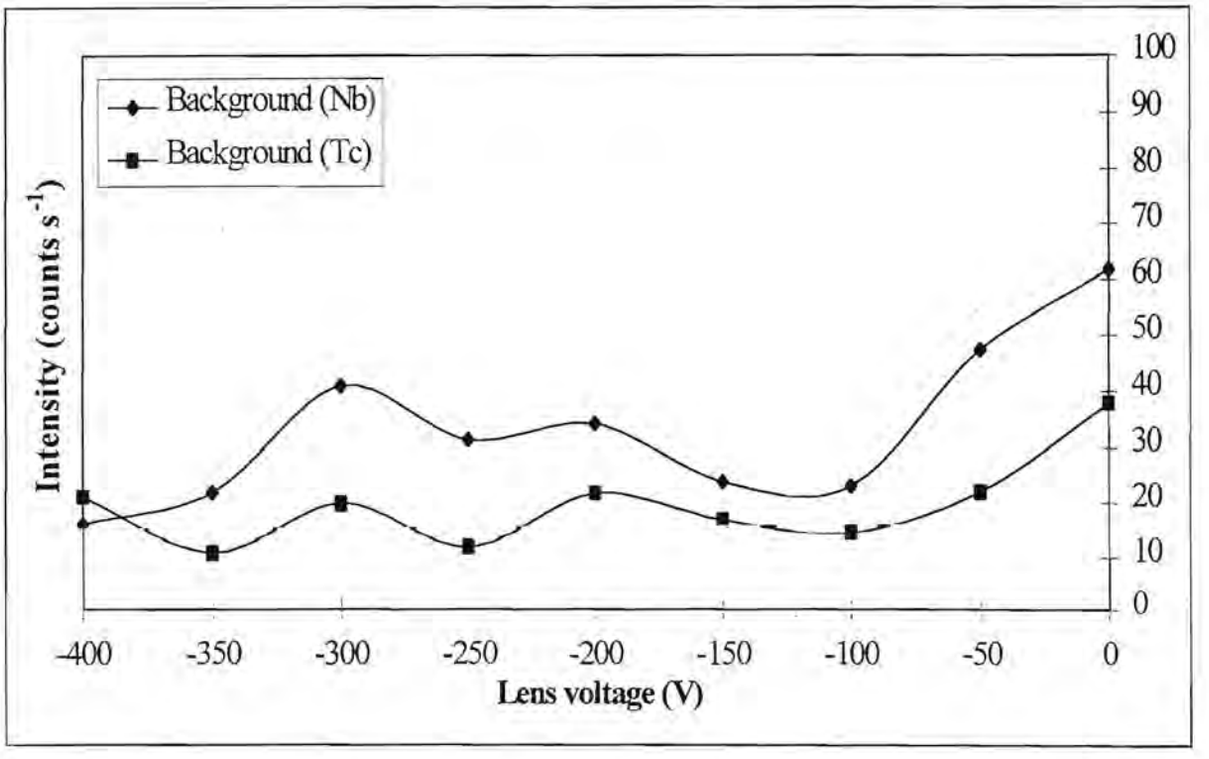

Figure 2.42(b): Effect of the lens parameter LA on the background intensities.

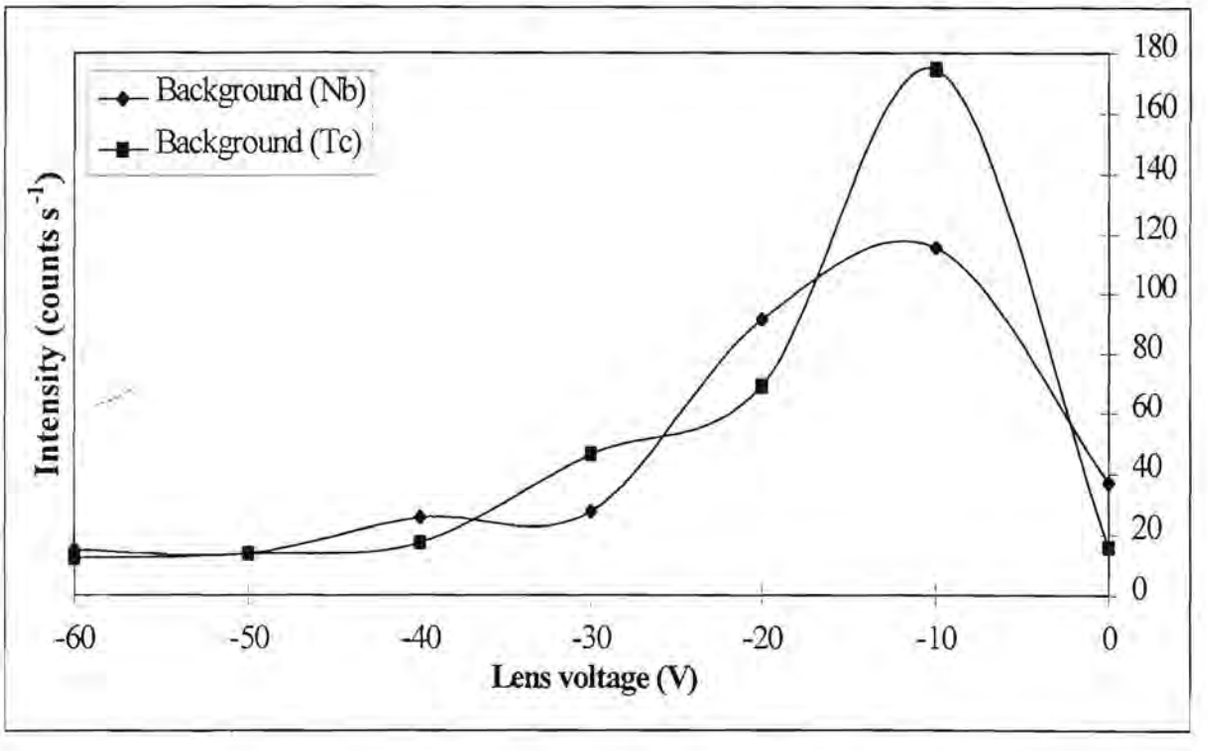

Figure 2.42(c): Effect of the lens parameter LB on the background.

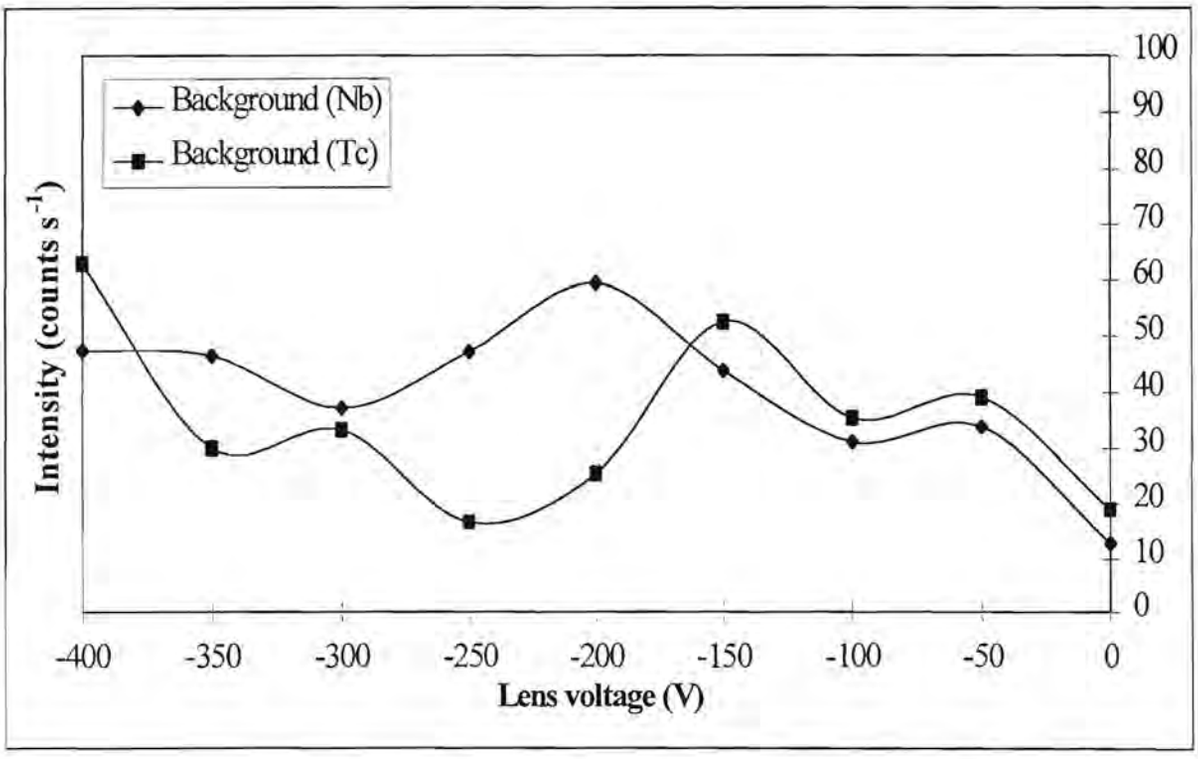

Figure 2.42(d): Effect of the lens parameter LC on the background intensities.

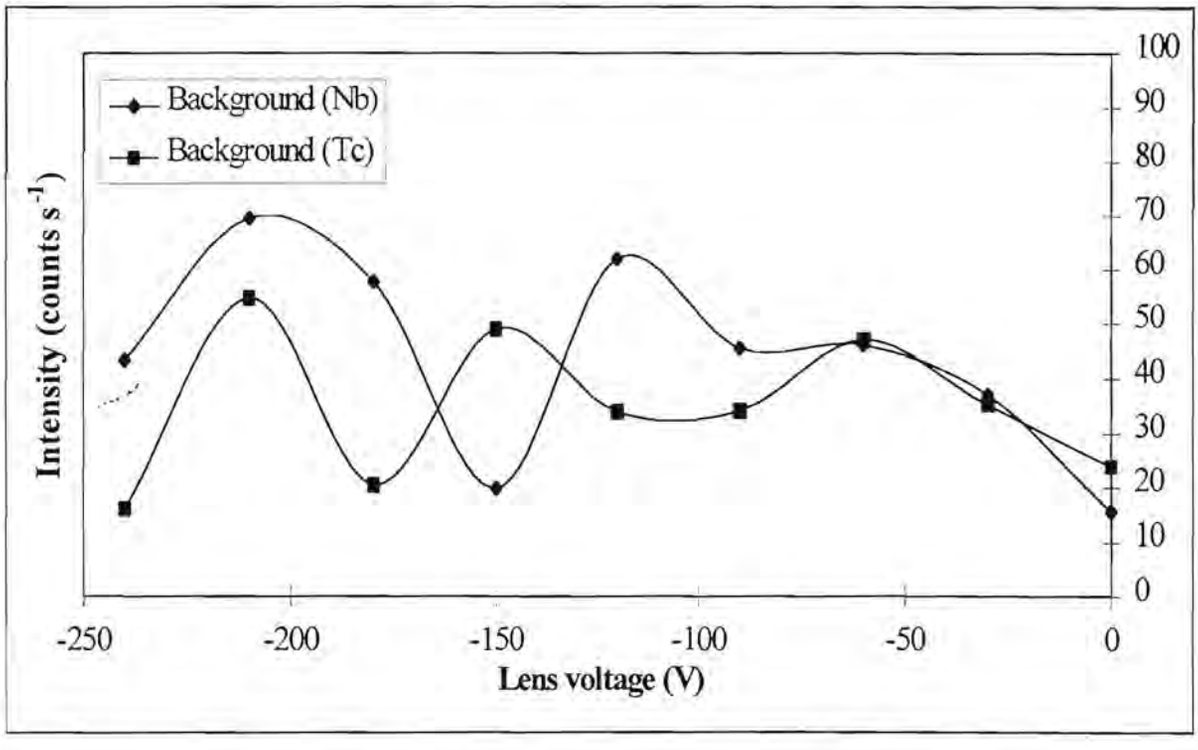

Figure 2.42(e): Effect of the lens parameter LD on the background intensities.

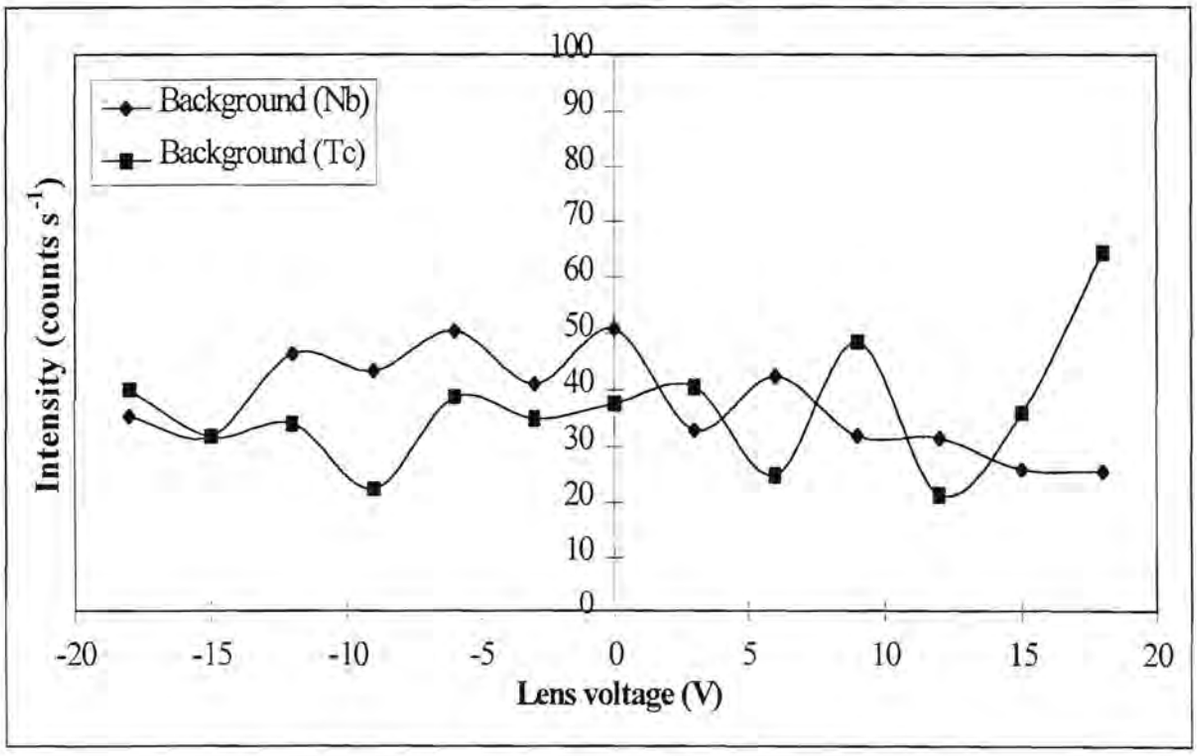

Figure 2.42(f): Effect of the field axis voltage FA on the background intensities.

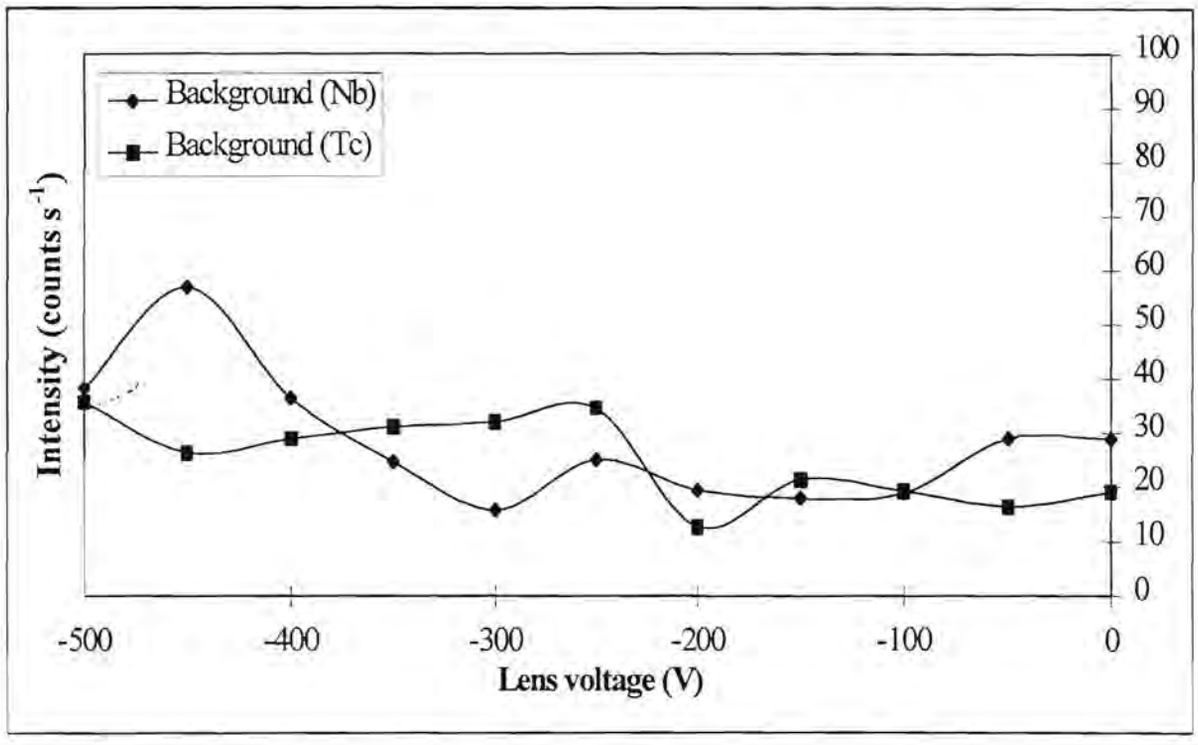

Figure 2.42(g): Effect of the detector inner diameter voltage ID on the background intensities.

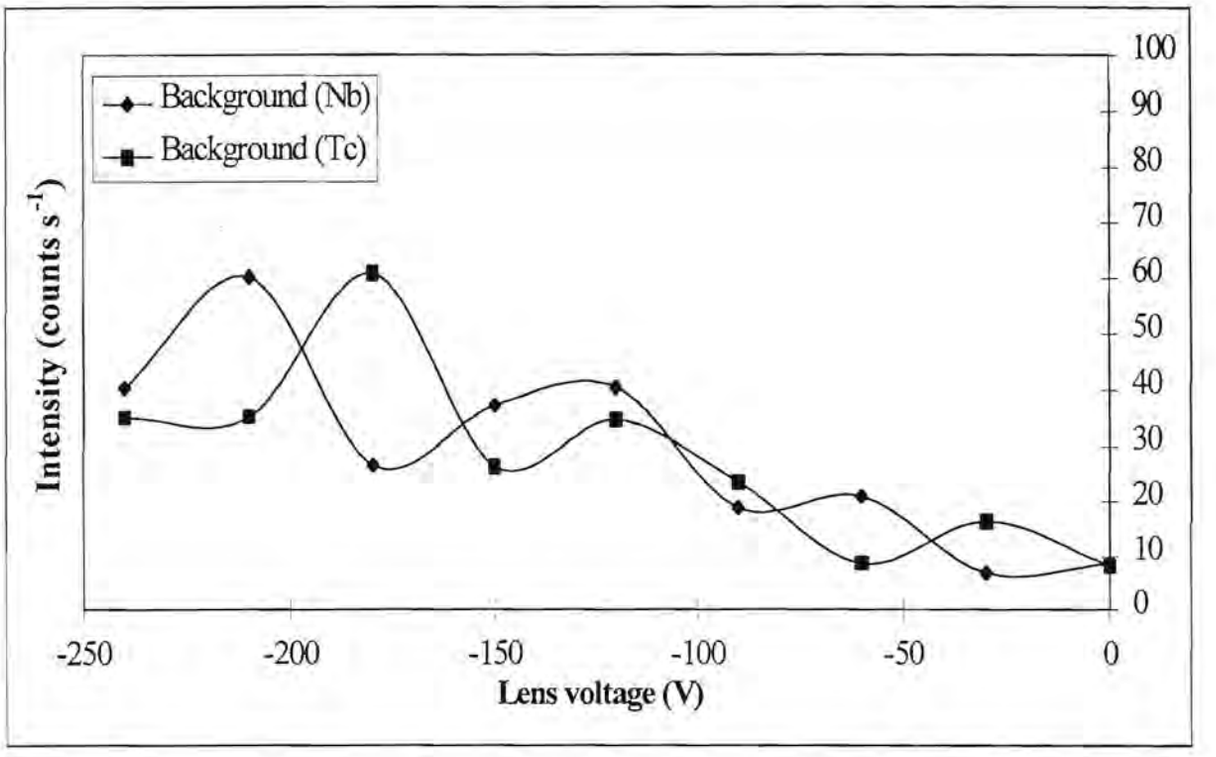

Figure 2.42(h): Effect of the detector outer diameter voltage OD on the background intensities.

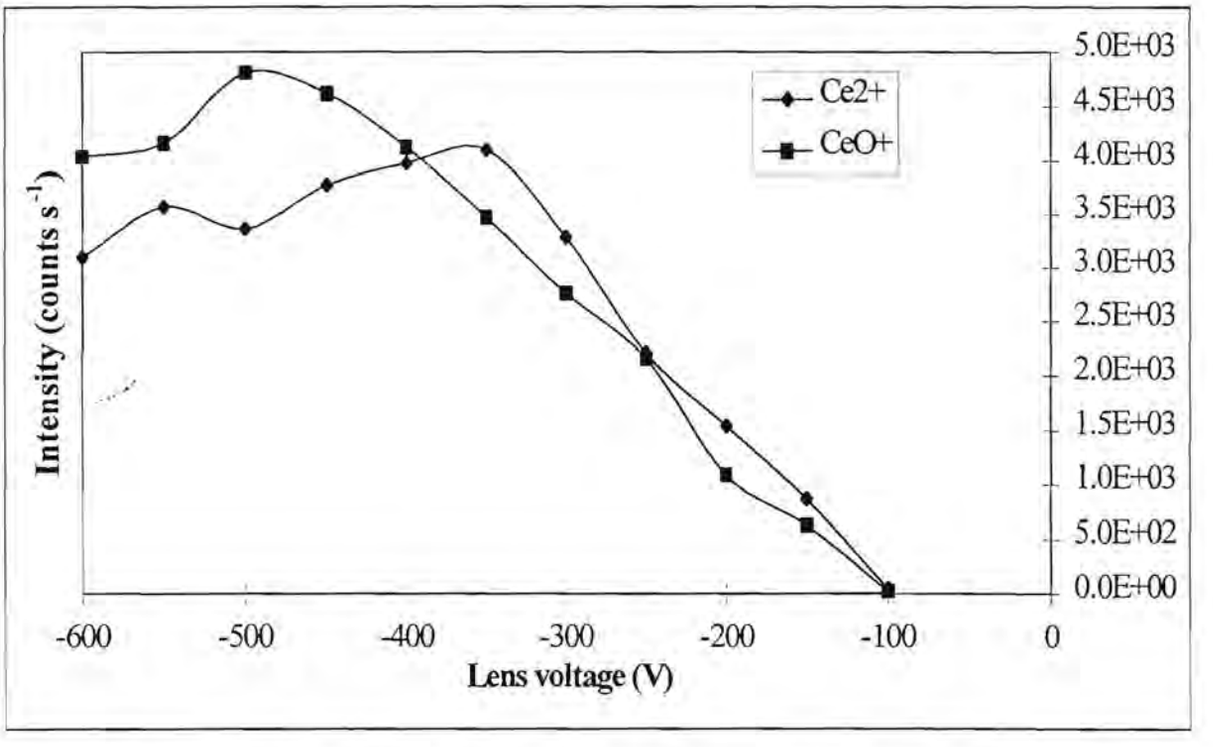

Figure 2.43(a): Effect of the lens parameter LO on the response curves of the doubly ionised and oxide ions.

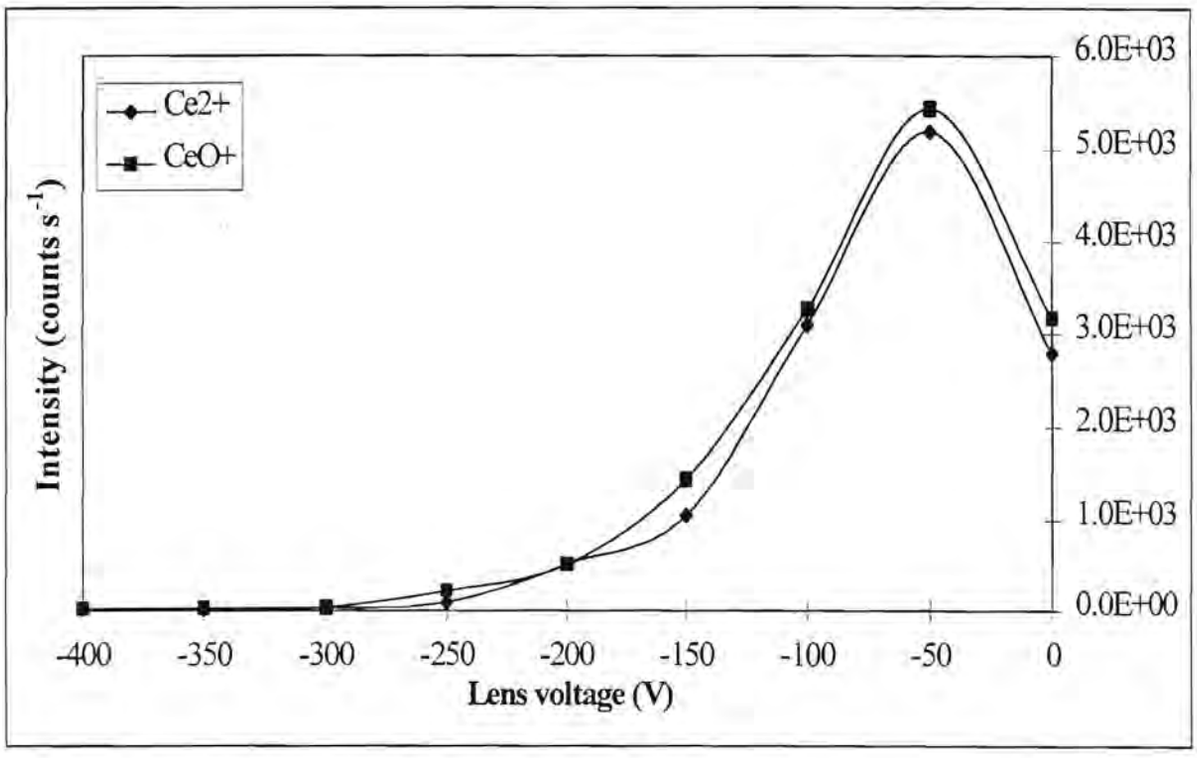

Figure 2.43(b): Effect of the lens parameter LA on the response curves of the doubly ionised and oxide ions.

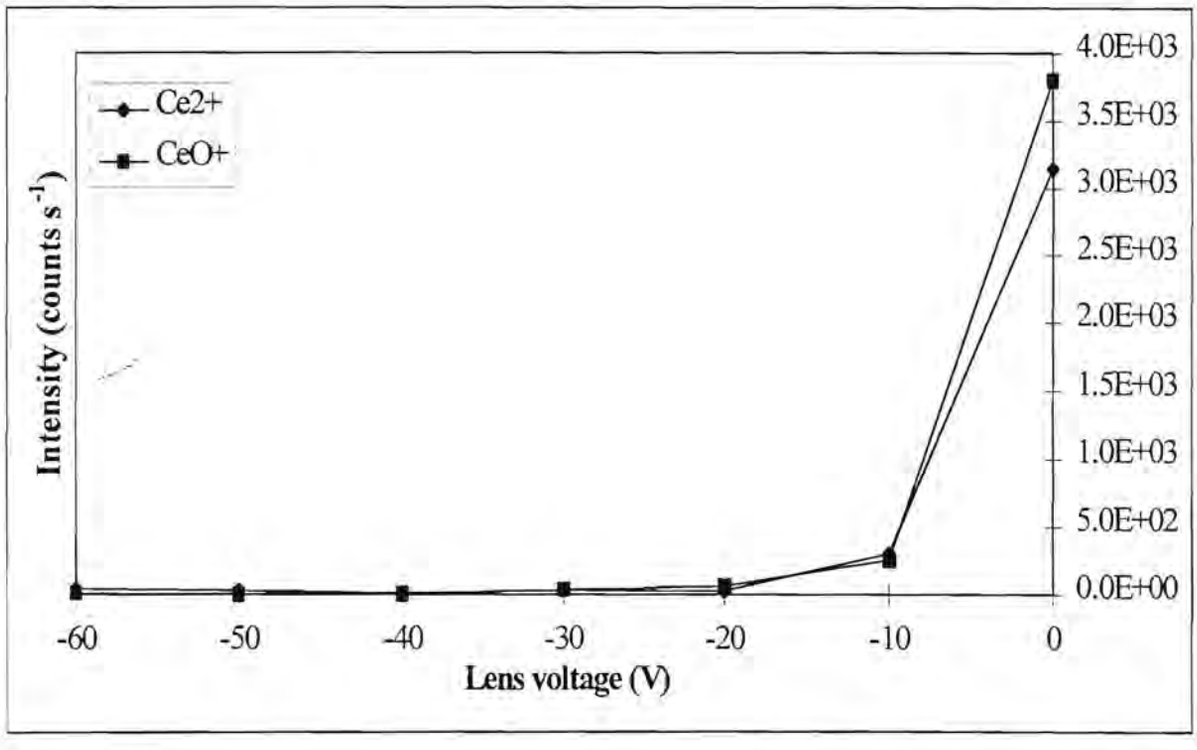

Figure 2.43(c): Effect of the lens parameter LB on the response curves of the doubly ionised and oxide ions.

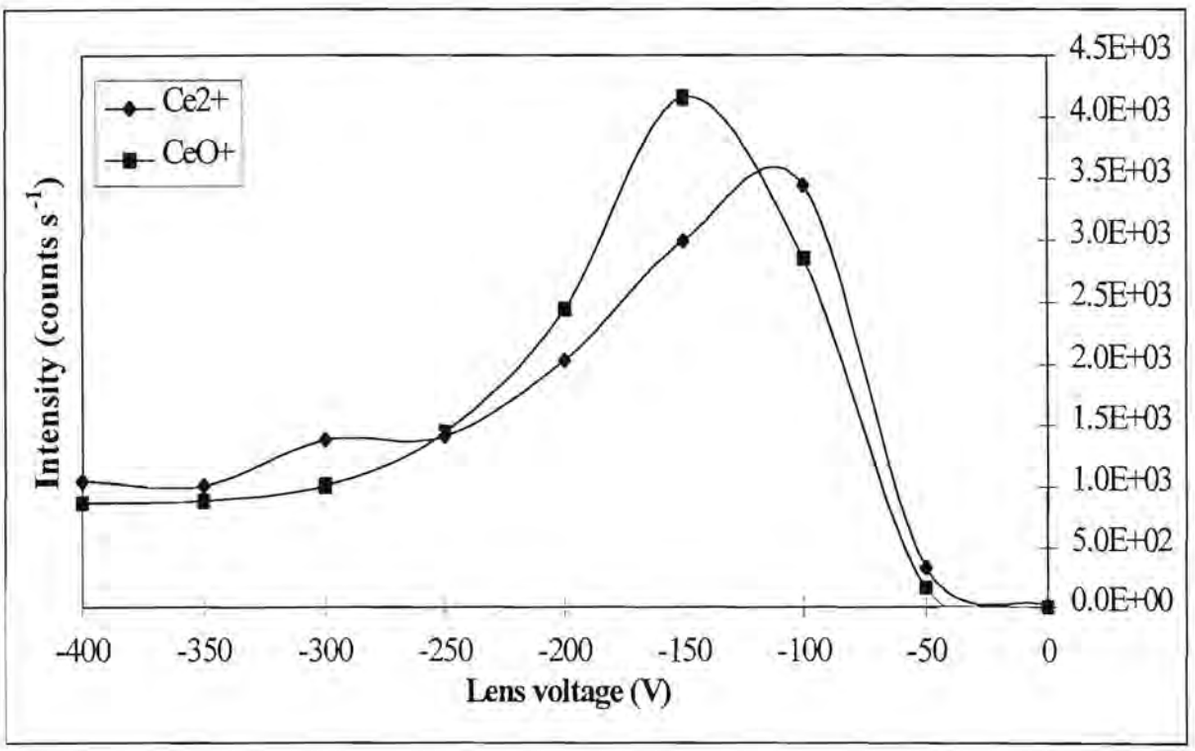

Figure 2.43(d): Effect of the lens parameter LC on the response curves of the doubly ionised and oxide ions.

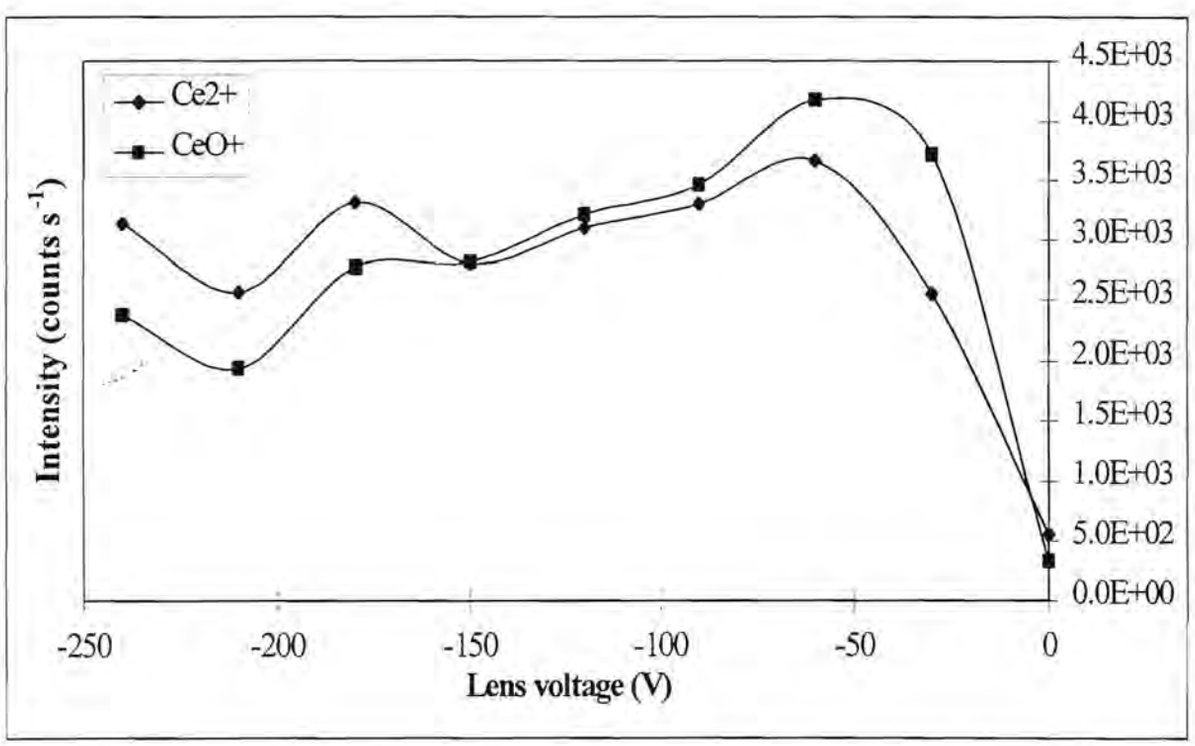

Figure 2.43(e): Effect of the lens parameter LD on the response curves of the doubly ionised and oxide ions.

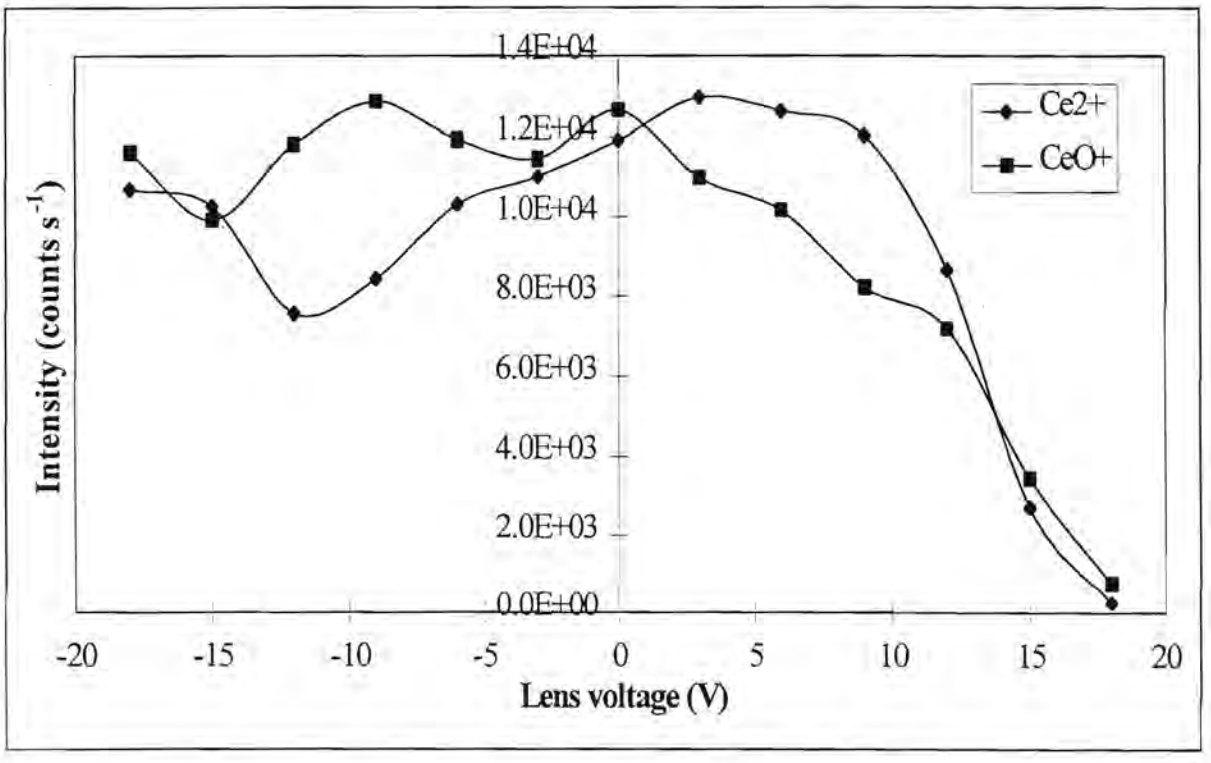

Figure 2.43(f): Effect of the field axis voltage FA on the response curves of the doubly ionised and oxide ions.

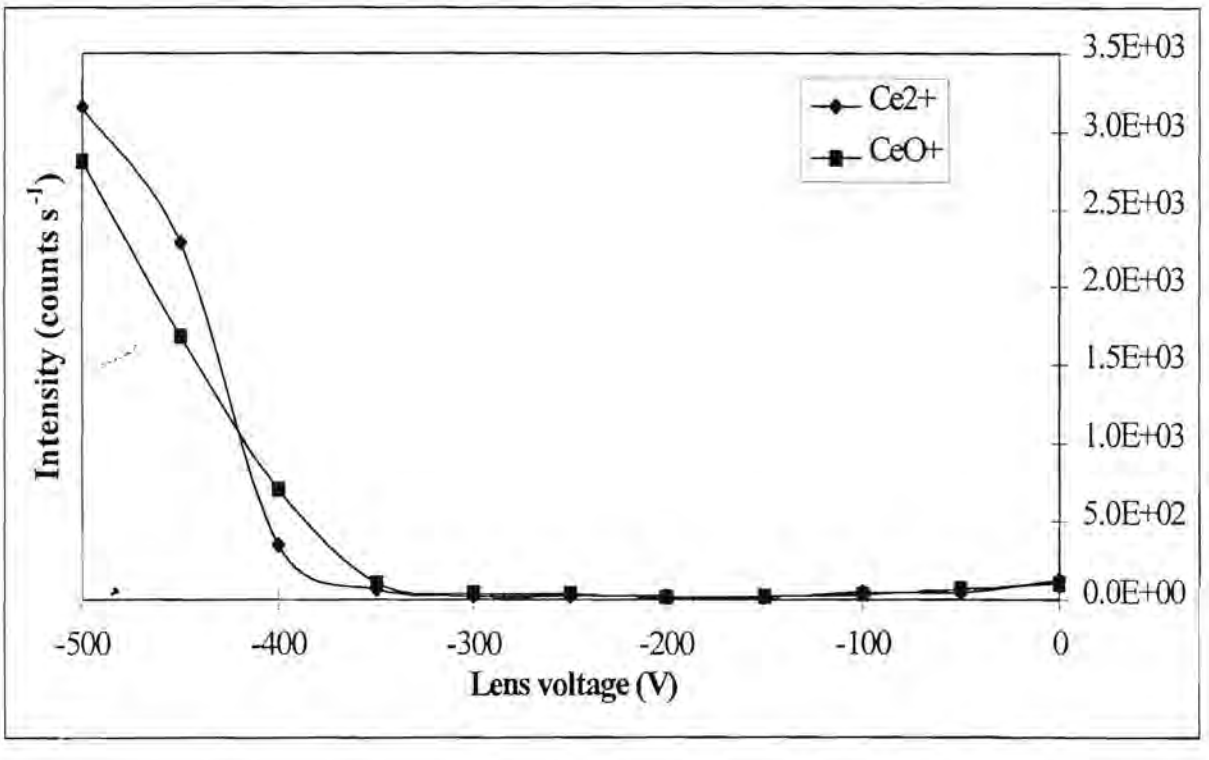

Figure 2.43(g): Effect of the detector inner diameter voltage ID on the response curves of the doubly ionised and oxide ions.

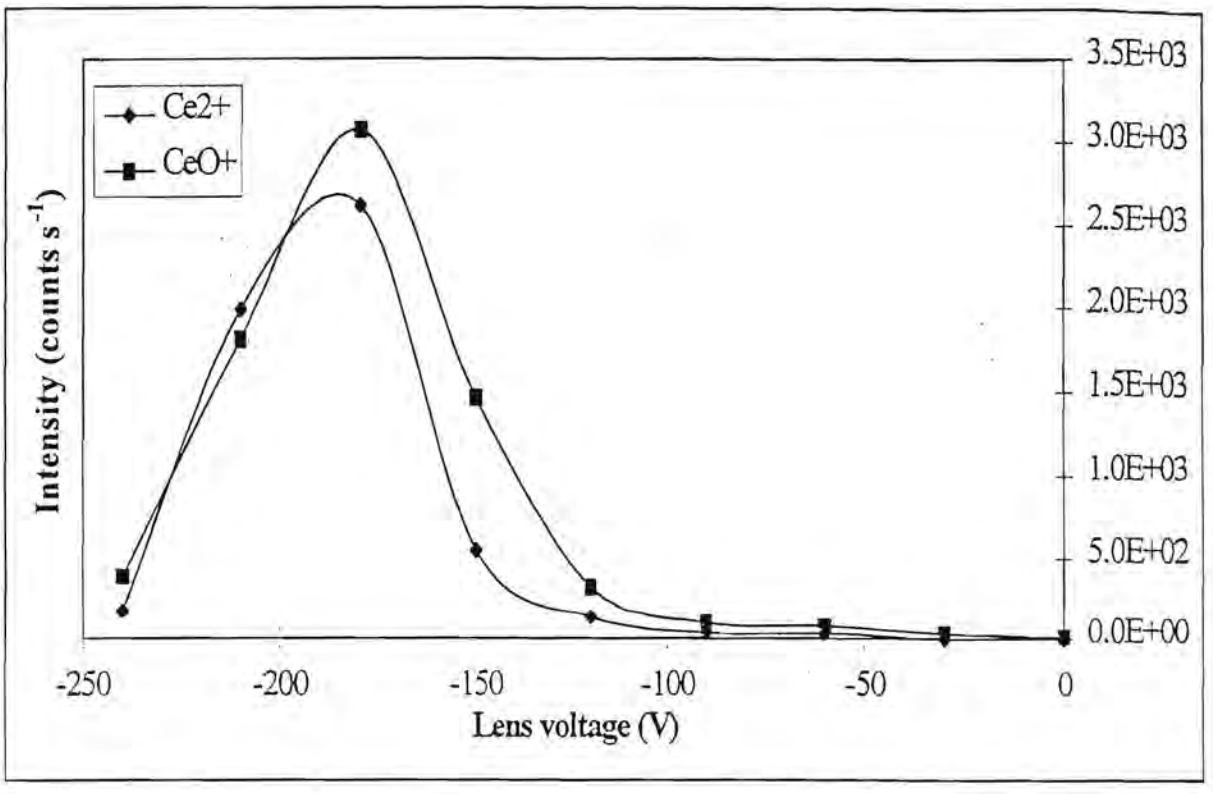

Figure 2.43(h): Effect of the detector outer diameter voltage OD on the response curves of the doubly ionised and oxide ions.

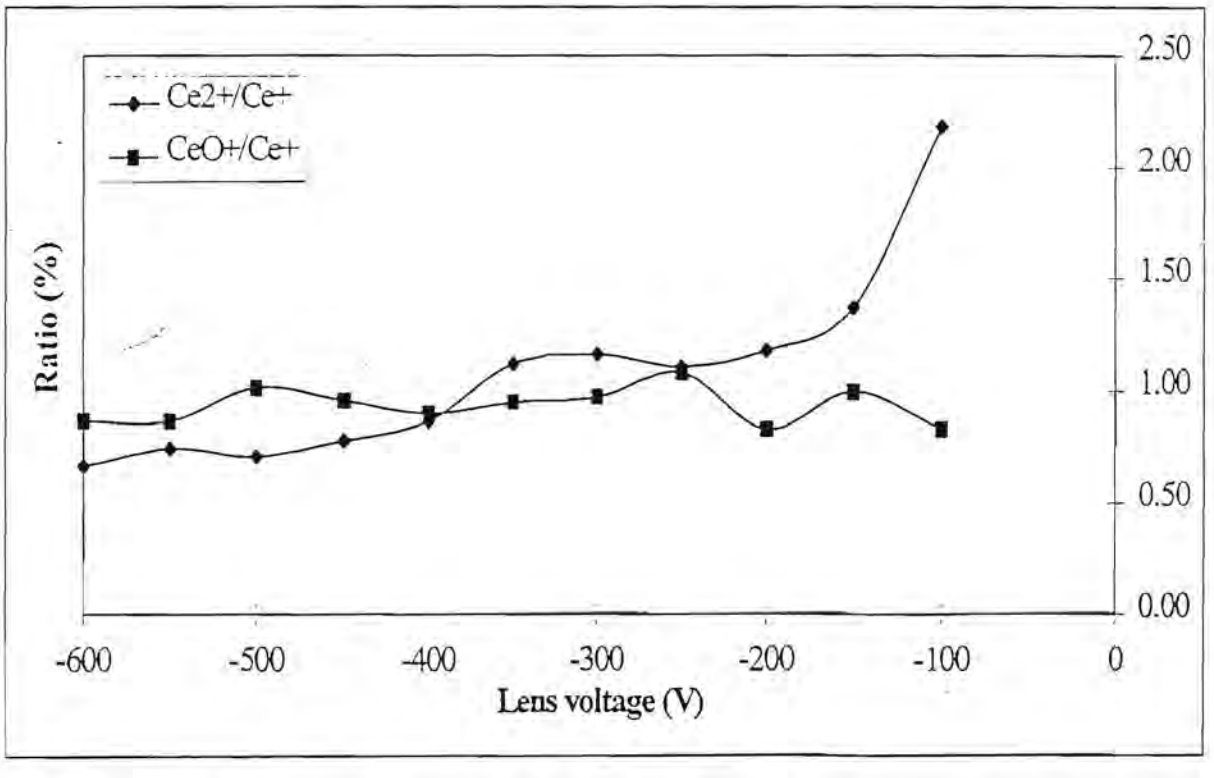

Figure 2.44(a): Effect of the lens parameter LO on the response curves of the Ce^{2+}/Ce^{+} and CeO^{+}/Ce^{+} ratios.

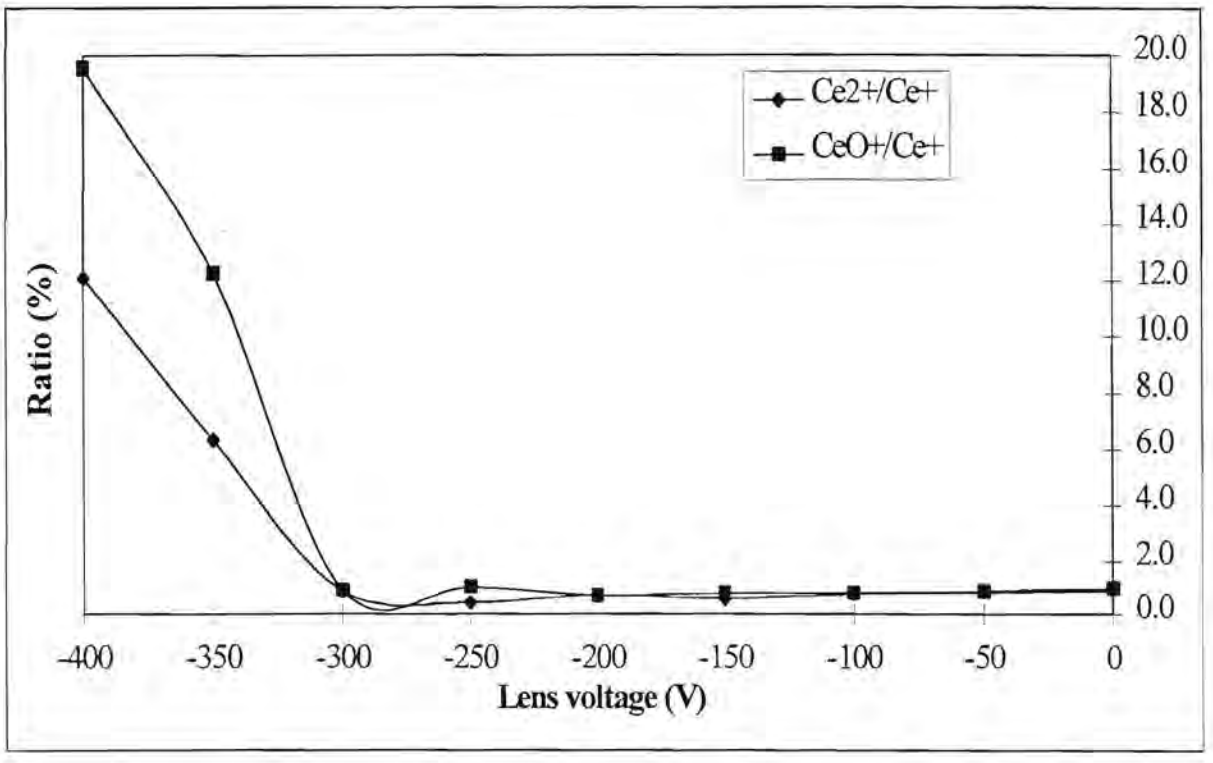

Figure 2.44(b): Effect of the lens parameter LA on the response curves of the Ce^{2+}/Ce^{+} and CeO^{+}/Ce^{+} ratios.

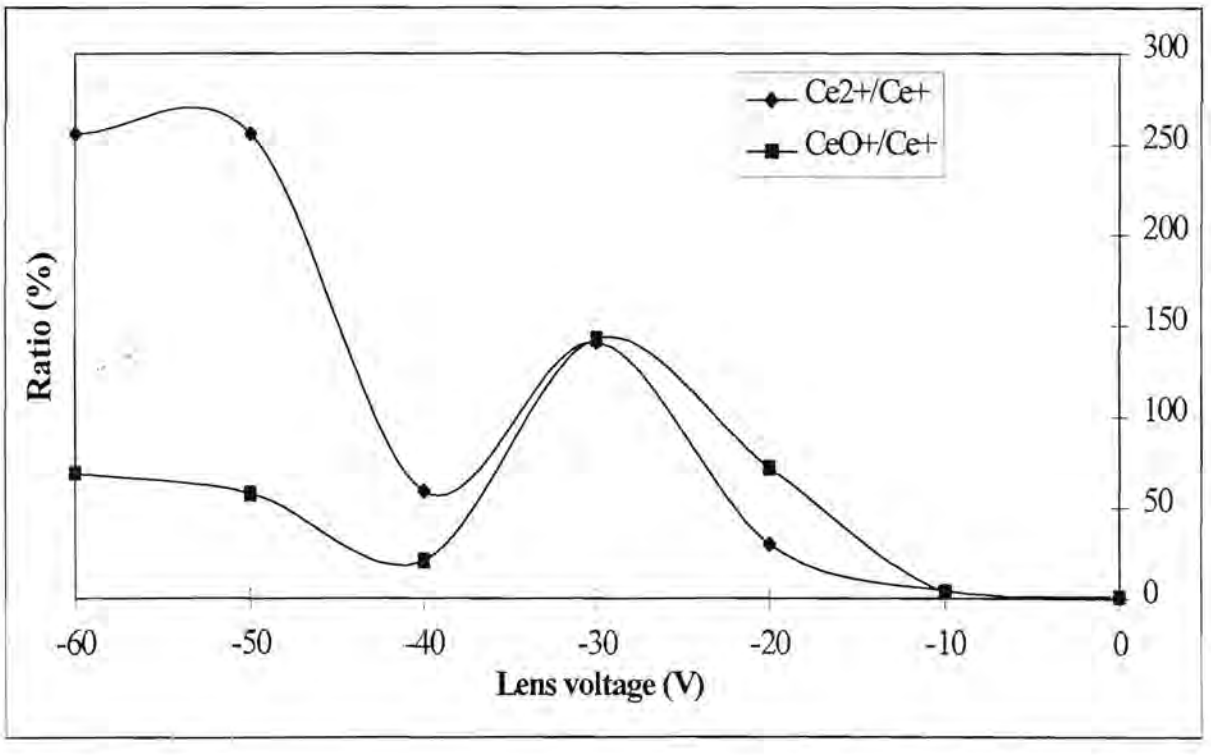

Figure 2.44(c): Effect of the lens parameter LB on the response curves of the Ce^{2+}/Ce^{+} and CeO^{+}/Ce^{+} ratios.

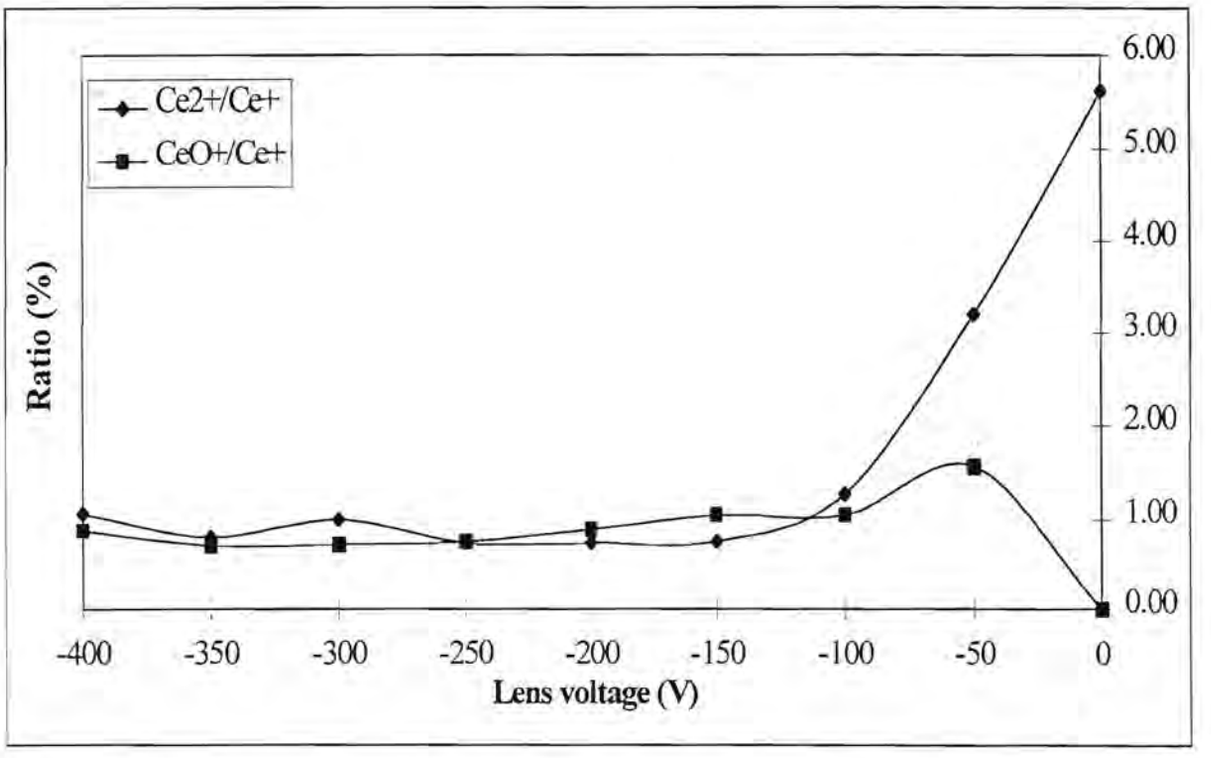

Figure 2.44(d): Effect of the lens parameter LC on the response curves of the Ce^{2+}/Ce^{+} and CeO^{+}/Ce^{+} ratios.

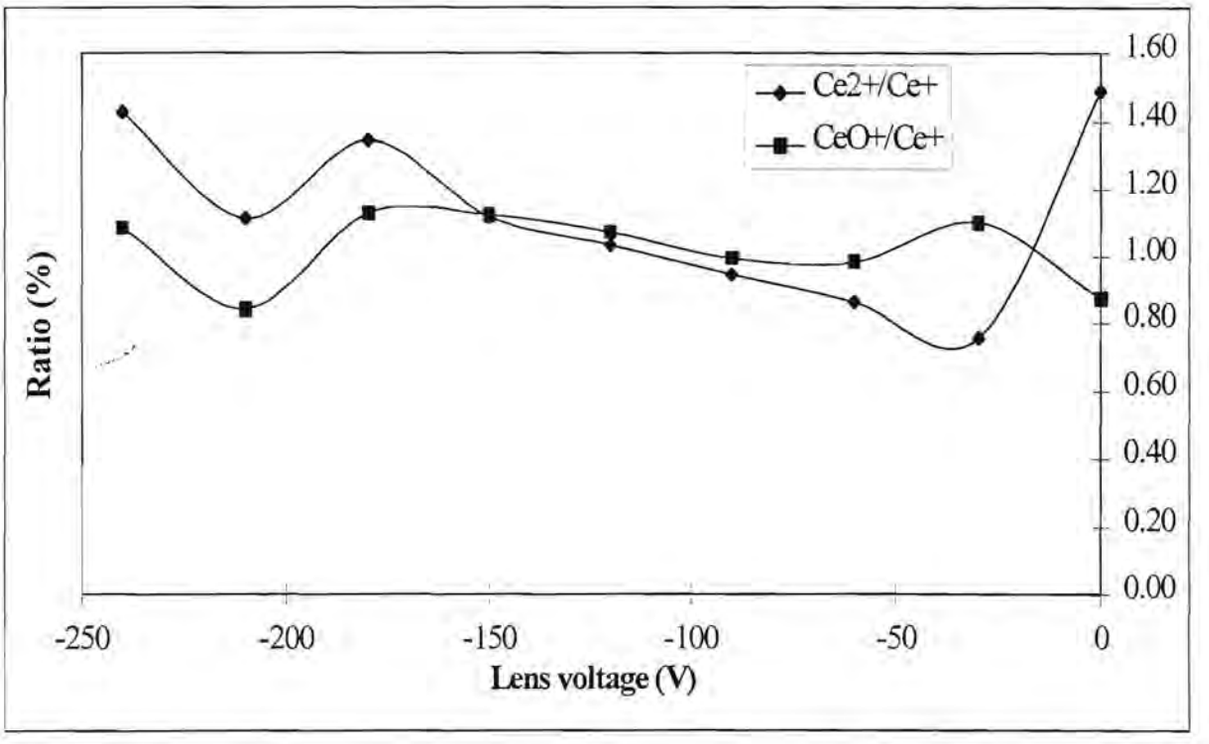

Figure 2.44(e): Effect of the lens parameter LD on the response curves of the Ce^{2+}/Ce^{+} and CeO^{+}/Ce^{+} ratios.

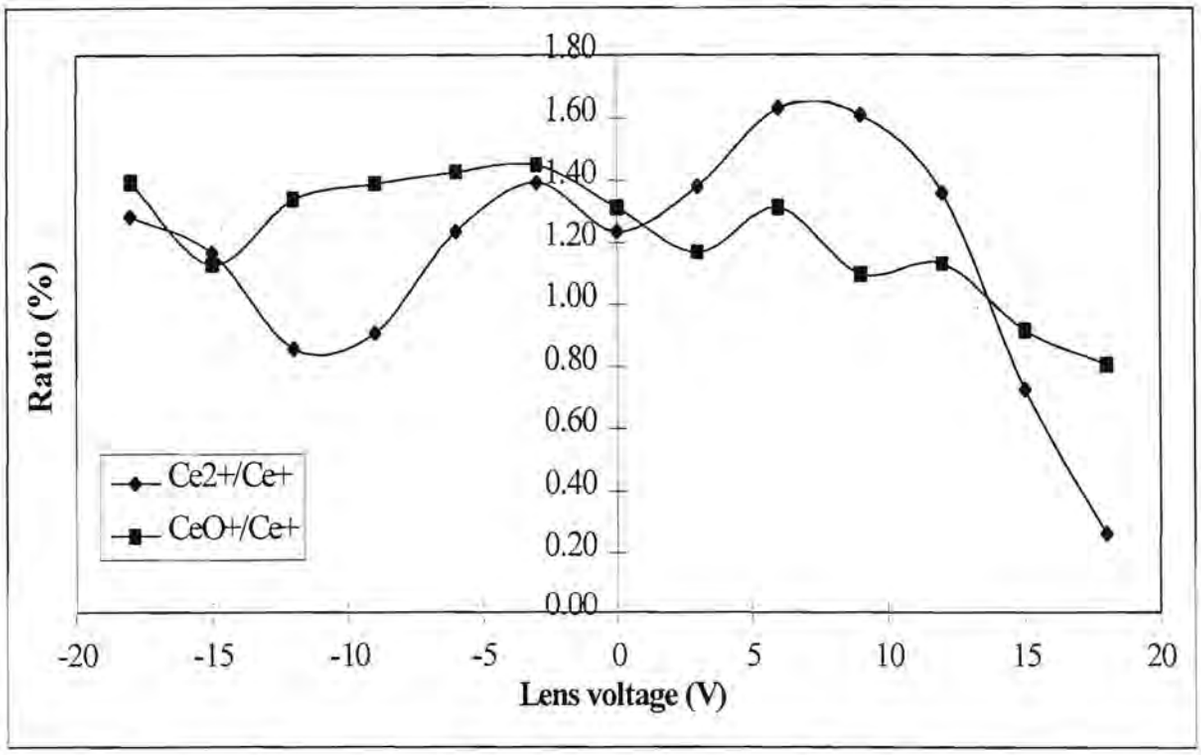

Figure 2.44(f): Effect of the field axis voltage FA on the response curves of the Ce^{2+}/Ce^{+} and CeO^{+}/Ce^{+} ratios.

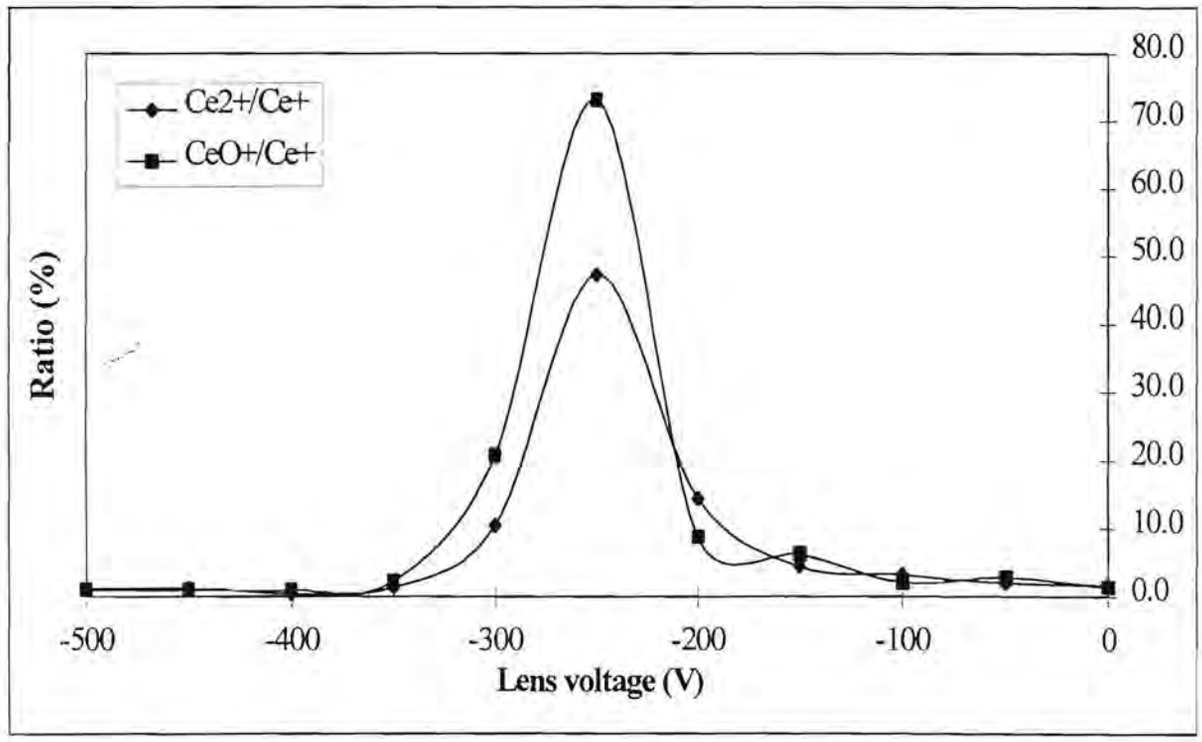

Figure 2.44(g): Effect of the detector inner diameter voltage ID on the response curves of the Ce^{2+}/Ce^{+} and CeO^{+}/Ce^{+} ratios.

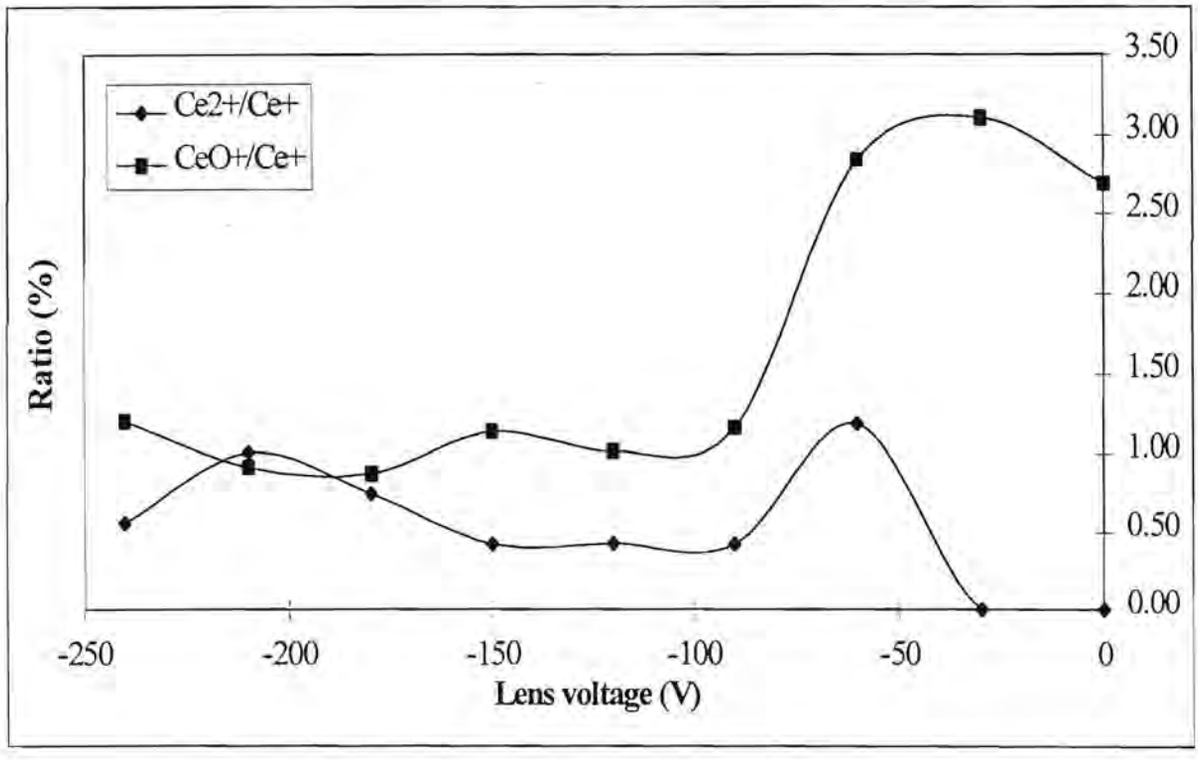

Figure 2.44(h): Effect of the detector outer diameter voltage OD on the response curves of the Ce^{2+}/Ce^{+} and CeO^{+}/Ce^{+} ratios.

Effect of ion lens settings on doubly ionised ions and oxides

Figures 2.43(a) - (h) and 2.44(a) - (h) give the effects of ion lens settings on the response curves of Ce^{2+} and CeO^{+} ions, as well as for the Ce^{2+}/Ce^{+} and CeO^{+}/Ce^{+} ratios. According to figures 2.43(a) - (h) the interference ions follow more or less the same trends as the light and heavier elements. Figures 2.44(a) - (h) show that the optimum lens settings for the analyte signals would not cause the Ce^{2+}/Ce^{+} and CeO^{+}/Ce^{+} ratios to exceed the acceptable values of 2.5% and 1%.

2.4 Conclusion

Table 2.4: Optimum values for parameters. Gas flow rates in arbitrary scales as used by the instrument manufacturer.

Parameter	Light elements and argon	Heavier elements	Background	Ratio of doubly charged to mono-charged ions	Ratio of oxide ions to mono-charged ions
Horizontal displacement of torch	"-2500" units	"-2500" units	Acceptable at all settings	"-2500" units	"-2500" units
Vertical displacement of torch	"-6500" units	"-6500" units	Acceptable at all settings	Acceptable at all settings except "500" to "3000" units	Acceptable at all settings
Axial displacement of torch	"-3000" to "-6000" units	"-3000" to "-6000" units	Acceptable at all settings	Acceptable at all settings except at values closer than "-3000" units to sampling aperture	Acceptable at all settings excepts at values closer than "-3000" units to sampling aperture
Coolant gas flow rate	40	40	Acceptable at all settings	26	Acceptable at all settings
Auxiliary gas flow rate	30	30	Acceptable at all settings	30	Acceptable at all settings
Aerosol carrier gas flow rate at a power setting of 1350 W	31	31	Acceptable at all settings	Maximum value of 29	Maximum value of 29
Lens setting: LO	-350 V	-450 V	Acceptable at all settings	-600 V	-550 V
Lens setting: LA	-50 V	-50 V	Acceptable at all settings	0 to -200 V	0 to -200 V

Parameter	Light elements and argon	Heavier elements	Background	Ratio of doubly charged to mono-charged ions	Ratio of oxide ions to mono-charged ions
Lens setting: LB	0 V	0 V	Acceptable at all settings	0 V	0 V
Lens setting: LC	-120 V	-150 V	Acceptable at all settings	-300 to -150 V	-350 to -250 V
Lens setting: LD	-25 V	-60 V	Acceptable at all settings	-30 V	-210 V
Lens setting: FA	0 V	0 V	Acceptable at all settings	18 V	18 V
Lens setting: ID	-500 V	-500 V	Acceptable at all settings	-500 to -400 V	-500 to -400 V
Lens setting: OD	-190 V	-180 V	Acceptable at all settings	0 to -30 V	-200 V

A final set of conditions that may seen as the optimised parameters can be taken from table 2.4 and can be listed as set out in table 2.5.

Table 2.5: Optimised set of parameters for the ICP-MS.

Parameter	Setting
Horizontal displacement of torch	"-2500" units
Vertical displacement of torch	"-6500" units
Axial displacement of torch	"-3000" to "-6000" units
Coolant gas flow rate	40
Auxiliary gas flow rate	30
Aerosol carrier gas flow rate at a power setting of 1350 W	29
Lens setting: LO	-500 V
Lens setting: LA	-50 V
Lens setting: LB	0 V
Lens setting: LC	-150 V

Parameter	Setting
Lens setting: LD	-60 V
Lens setting: FA	0 V
Lens setting: ID	-500 V
Lens setting: OD	-190 V

The following optimisation strategy is proposed for the instrument and setup investigated:

a) Prepare a solution containing the analytes to be investigated as well as light elements and heavier elements. The concentration of the elements in the solution should be approximately 1 mg dm^{-3} in 1% HNO_3.

b) Set the parameters of the instrument to the values as set out in table 2.5.

c) Scan the prepared solution while monitoring the magnitudes of the signals of the analytes to be investigated, light elements, heavier elements, background masses, oxide interferences and doubly charged interferences.

d) While keeping the other parameters constant, adjust the first parameter as listed in table 2.5. Monitor the magnitudes of the signals as listed in c). Optimise the parameter value, i.e. adjust in order to increase element signals and decrease background and interference signals.

e) Continue with the above mentioned for the other parameters as listed in table 2.5.

Optimised instrument settings are valid for a specific torch - load coil arrangement. This implies that as soon as the torch is replaced or is put in the load coil in a different manner, the parameters have to be optimised again.

Analyte signals in ICP-MS depend in a complex manner on instrument parameters. Parameters such as torch position, coolant and auxiliary gas flow rates and ion lens settings are important and should be optimised. However, aerosol carrier gas flow rate and power settings proved to be of critical importance for the optimisation of analyte signals and the minimisation of doubly ionised and oxide interferences.

The main conclusion drawn from this optimisation study is that similar optimum conditions are valid for most elements. The optimal parameters for minimal potential interferences correspond very closely to the optimal set of conditions for mono-ionised analyte ions.

CHAPTER 3

THE QUANTITATIVE DETERMINATION OF THE PLATINUM GROUP ELEMENTS AND GOLD BY ICP-MS

3.1 Introduction

Non-spectroscopic interferences, matrix effects and drift of calibration curves and analyte sensitivities are well known problems in ICP-MS and if not properly compensated for can lead to a degradation in analytical precision and accuracy *[5, 20, 22, 35 - 41]*. These interference effects are generally believed to be due to the physical and chemical behaviour of the matrix elements (and analytes) in the sample introduction system, the interface region and the ion optics. These include transport effects, ionisation equilibrium effects and ion sampling effects *[25, 42, 43]*. Moderate amounts (0.1 - 1%) of a matrix ion can change analyte signals significantly *[5, 21, 25, 41]*. Standard addition and isotope dilution methods have been tried to minimise matrix effects in ICP-MS *[44]*. However, standard addition is time consuming and isotope dilution is not applicable to mono-isotopic elements *[22, 45]*. In this study the feasibility of using an internal standard as a possible solution to the above-mentioned problems was investigated.

Some investigations into trends in non-spectroscopic interferences and signal drift in ICP-MS have appeared in literature *[5, 25, 46]*. The general consensus is that internal standardisation is most effective when the internal standards and analytes are closely matched in terms of mass and first stage ionisation potential. Some caution has been suggested even when these selection criteria are used *[22]*. In this study the different isotopes of Sc, Y and La were considered as possible internal standards in the quantitative determination of the platinum group elements and gold.

A variety of internal standards that span the *m/z* range are often employed *[47, 48]*. This procedure requires spikes and usually precludes determination of the spike elements in the original sample. As an alternative, ions that are already present in the spectrum can be used. Several researchers *[25, 48, 49]* have published results where polyatomic ions have successfully

been employed as internal standards. In this study the use of the ^{36}Ar isotope, which is always present in the spectrum, was investigated as a possible internal standard.

Table 3.1: Relevant data of the platinum group elements, gold and the internal standards investigated *[50]*.

Atomic no.	**Element**	**Mass no.**	**Relative abundance**	**Atomic mass (g mol^{-1})**	**First ionisation potential (eV)**	**Second ionisation potential (eV)**
18	Argon	36 38 40	0.337 0.063 99.600	39.948	15.76	27.63
21	Scandium	45	100.0	44.956	6.56	12.80
39	Yttrium	89	100.0	88.905	6.53	12.23
57	Lanthanum	138 139	0.089 99.911	138.91	5.61	11.06
44	Ruthenium	96 98 99 100 101 102 104	5.51 1.87 12.72 12.62 17.07 31.63 18.58	101.07	7.36	16.76
45	Rhodium	103	100.0	102.905	7.45	18.07
46	Palladium	102 104 105 106 108 110	0.96 10.97 22.23 27.33 26.71 11.81	106.4	8.33	19.42
77	Iridium	191 193	37.3 62.7	192.2	9.1	
78	Platinum	190 192 194 195 196 198	0.013 0.78 32.9 33.8 25.3 7.21	195.09	8.96	18.56
79	Gold	197	100.0	196.967	9.23	20.5

One of the dissolution methods employed in the analysis of the platinum group metals and gold involves an aqua regia (3:1 mixture of concentrated HCl and concentrated HNO_3) leaching procedure *[51, 52]*. This has the effect that the matrix of the final sample solution is mainly

diluted aqua regia. The standard solutions from which the calibration curves are constructed however is in a 1.0% v/v HCl matrix. The effect of matrices consisting of different concentrations of aqua regia on the quantitative analysis of sample solutions was investigated.

Table 3.1 shows the relative abundances of the naturally occurring isotopes of the platinum group elements, gold and the internal standards investigated, as well as the first and second ionisation potentials of the various elements. From this table it can be seen that the mass of the isotope of Y is relatively well matched to those of the isotopes of Ru, Pd and Rh. The masses of the isotopes of La are relatively well matched to those of Ir, Pt and Au. The first ionisation potentials of Sc, Y and La are relatively close to those of the platinum group elements and gold. Some elements have overlapping isotopes, e.g. ^{102}Ru and ^{102}Pd, as well as ^{104}Ru and ^{104}Pd. The feasibility of using isotopes of very low abundance, e.g. ^{138}La and ^{192}Pt was also investigated.

3.2 Experimental

3.2.1 Preparation of solutions

Tables 3.2 and 3.3 show the results of calculations performed in order to prepare stock solutions of the platinum group elements, gold, the internal standards, as well as standard solutions for the preparation of calibration curves in the range 0 to 150 μg dm^{-3} and 50 μg dm^{-3} sample solutions in matrices containing aqua regia from 0.35 to 2.50% v/v. Higher acid concentrations were not considered as this would shorten the lifetime of the nickel sampler and skimmer cones considerably.

Certified solutions of the platinum group elements and gold each containing 1000 mg dm^{-3} of the element in 4.9% HCl were employed for the preparation of the calibration and sample solutions (Spectrascan, Teknolab A/S, Dröbak, Norway). Certified solutions of Sc and Y each containing 1000 mg dm^{-3} of the element in 2.5% HCl were used (Spectrascan, Teknolab A/S, Dröbak, Norway). A certified solution of La containing 5000 mg dm^{-3} of the element in 2.5% HNO_3 was used for the preparation of a stock solution (Spectrascan, Teknolab A/S, Dröbak, Norway). High purity hydrochloric acid (> 32%) and nitric acid (> 65%) (Fluka) were used for the preparation of acidic solutions. High purity water with resistivity 18.2 MΩ cm (Millipore Corporation, United States of America) was used for dilutions.

All solutions were prepared in pre-conditioned plastic laboratory ware. A-grade pipettes and volume adjustable pipettes were used for the transfer of solutions. The calibration standard solutions as well as the sample solutions were transferred to clean PTFE holders which were placed on the sample rack of the autosampler of the instrument.

3.2.2 *Optimisation of the ICP-MS*

The instrument was optimised as described in chapter 2. A warm-up time of one hour was allowed before any analyses were performed in order for instrumental conditions to equilibrate.

3.2.3 *Mass scans of the platinum group elements and gold*

Mass scans of a 100 μg dm^{-3} solution of the platinum group elements and gold in 1.00% v/v HCl were performed in order to verify the validity of 1) the isotopic ratios used and 2) the mass calibration of the instrument.

3.2.4 *Data acquisition*

The intensities of the various isotopes of the internal standards, ^{36}Ar, the platinum group elements and gold were measured. The operating conditions of the inductively coupled plasma mass spectrometer and settings for data acquisition are listed in table 3.4. The data was then used to construct calibration curves and perform quantitative analysis of the platinum group elements and gold.

3.3 Results and discussion

3.3.1 *Mass scans of a solution of the platinum group elements and gold*

Figures 3.1 and 3.2 show the mass scans of the platinum group elements and gold. The heights of the bars, indicating the isotopic ratios, were calculated using the relative abundances of the isotopes (see table 3.1). From both figures it can be seen that the isotopic patterns fit the scan indicating the validity of the mass calibration of the instrument. The intensities at masses 102 and 104 (for Ru and Pd) also fit the theoretical patterns reasonably well. From figure 3.2 it can be seen that the peak shape at mass 192 (for ^{192}Pt) could lead to imprecise and inaccurate readings due to the low abundance of this isotope.

Table 3.2: Preparation of stock solutions of Au, Ir, Pd, Pt, Rh, Ru, Sc, Y and La.

Solution to prepare	**[Element] (mg dm^{-3})**	**[HCl] (% v/v)**	**[HNO_3] (% v/v)**	**Dilution factor**	**Volume of certified solution to transfer (10^{-3} dm^3)**	**Volume of flask (10^{-3} dm^3)**	**Volume of HCl to add (10^{-3} dm^3)**	**Volume of HNO_3 to add (10^{-3} dm^3)**
Certified platinum group element solution	1000	4.9	0.0	0	0.00	0	0.000	0.000
Stock platinum group element solution	10	5.0	0.0	100	5.00	500	23.530	0.000
Certified Sc solution	1000	2.5	0.0	0	0.00	0	0.000	0.000
Certified Y solution	1000	2.5	0.0	0	0.00	0	0.000	0.000
Certified La solution	5000	0.0	2.5	0	0.00	0	0.000	0.000
Stock La solution	1000	0.0	2.5	5	10.00	50	0.000	1.000

Table 3.3: Preparation of A.: Platinum group elements and gold calibration standards with internal standards in 1% v/v HCl and

B.: Sample solutions to study the effect of aqua regia concentration on the quantitative analysis of the platinum group elements and gold.

	[platinum group element] (μg dm^{-3})	[HCl] (% v/v)	[HNO_3] (% v/v)	[aqua regia] (% v/v)	Dilution factor	Volume of platinum group element stock solution to transfer (10^{-3} dm^3)	Volume of flask (10^{-3} dm^3)	Volume of HCl to add (10^{-3} dm^3)	Volume of HNO_3 to add (10^{-3} dm^3)	[internal standard] (mg dm^{-3})	Dilution factor	Volume of each internal standard solution to transfer (10^{-3} dm^3)
A.	Blank	1.00	0.00	0.00	-	0.000	1000	9.950	-	1.00	1000	1.000
	10	1.00	0.00	0.00	1000	1.000	1000	9.900	-	1.00	1000	1.000
	50	1.00	0.00	0.00	200	5.000	1000	9.700	-	1.00	1000	1.000
	100	1.00	0.00	0.00	100	10.000	1000	9.450	-	1.00	1000	1.000
	150	1.00	0.00	0.00	67	15.000	1000	9.200	-	1.00	1000	1.000
B.	50	0.26	0.09	0.35	200	5.000	1000	2.325	0.850	1.00	1000	1.000
	50	0.38	0.13	0.50	200	5.000	1000	3.450	1.225	1.00	1000	1.000
	50	0.75	0.25	1.00	200	5.000	1000	7.200	2.475	1.00	1000	1.000
	50	1.13	0.38	1.50	200	5.000	1000	10.950	3.725	1.00	1000	1.000
	50	1.50	0.50	2.00	200	5.000	1000	14.700	4.975	1.00	1000	1.000
	50	1.88	0.63	2.50	200	5.000	1000	18.450	6.225	1.00	1000	1.000

Table 3.4: Operating conditions of the inductively coupled plasma mass spectrometer and settings for data acquisition.

Instrument	Spectromass-ICP
Torch	Fassel
Spray chamber	Scott-type double-pass
Nebuliser	Meinhard
Sampler cone	Ni with diameter approximately 1 mm
Skimmer cone	Ni with diameter approximately 1 mm
RF power	1350 W
Coolant argon gas flow rate	16 dm^3 min^{-1}
Auxiliary argon gas flow rate	1.5 dm^3 min^{-1}
Aerosol carrier argon gas flow rate	0.96 dm^3 min^{-1}
Sample introduction	$1.0x10^{-3}$ dm^3 min^{-1}
Dwell time	2 s
Resolution	Normal
Readings per measurement	5
Rinse time with water between samples to avoid contamination	120 s
Total pre-flush time with sample before measurement	120 s (of which the first 20 s was set at an uptake rate of approximately $3x10^{-3}$ dm^3 min^{-1})
Isotopes monitored	^{36}Ar, ^{45}Sc, ^{89}Y, ^{138}La, ^{139}La, ^{96}Ru, ^{98}Ru, ^{99}Ru, ^{100}Ru, ^{101}Ru, ^{102}Ru, ^{104}Ru, ^{103}Rh, ^{102}Pd, ^{104}Pd, ^{105}Pd, ^{106}Pd, ^{108}Pd, ^{110}Pd, ^{191}Ir, ^{193}Ir, ^{192}Pt, ^{194}Pt, ^{195}Pt, ^{196}Pt, ^{198}Pt, ^{197}Au

3.3.2 *Intensities as measured*

Tables 3.5 to 3.7 (Addendum A) show the averages of the intensities measured for the isotopes of the internal standards, the platinum group elements and gold.

3.3.3 *The effect of aqua regia concentration on the ratios of the isotopes of the platinum group elements and gold to the isotopes of the internal standards*

The values from tables 3.5 to 3.7 (Addendum A) were used to calculate the effect of the aqua regia concentration in the solution on the ratios of the isotopes of the platinum group elements and gold to those of the internal standards. This was done in order to see whether the isotopes of the platinum group elements and gold and those of the internal standards behave in a similar manner in aqua regia matrix.

Effect of aqua regia concentration on the ratios of the isotopes of the platinum group elements and gold to ^{36}Ar

From figures 3.3 to 3.8 it can be seen that the analyte to internal standard isotope ratios generally decrease with an increase in aqua regia concentration. The decreases in the isotope ratios are about 20%. The relative standard deviations for the various isotopes are about 10%. The isotopes of the platinum group elements and gold are thus not affected in the same way as the ^{36}Ar isotope. These preliminary results are an indication that ^{36}Ar would possibly not serve as a good internal standard for the platinum group elements and gold.

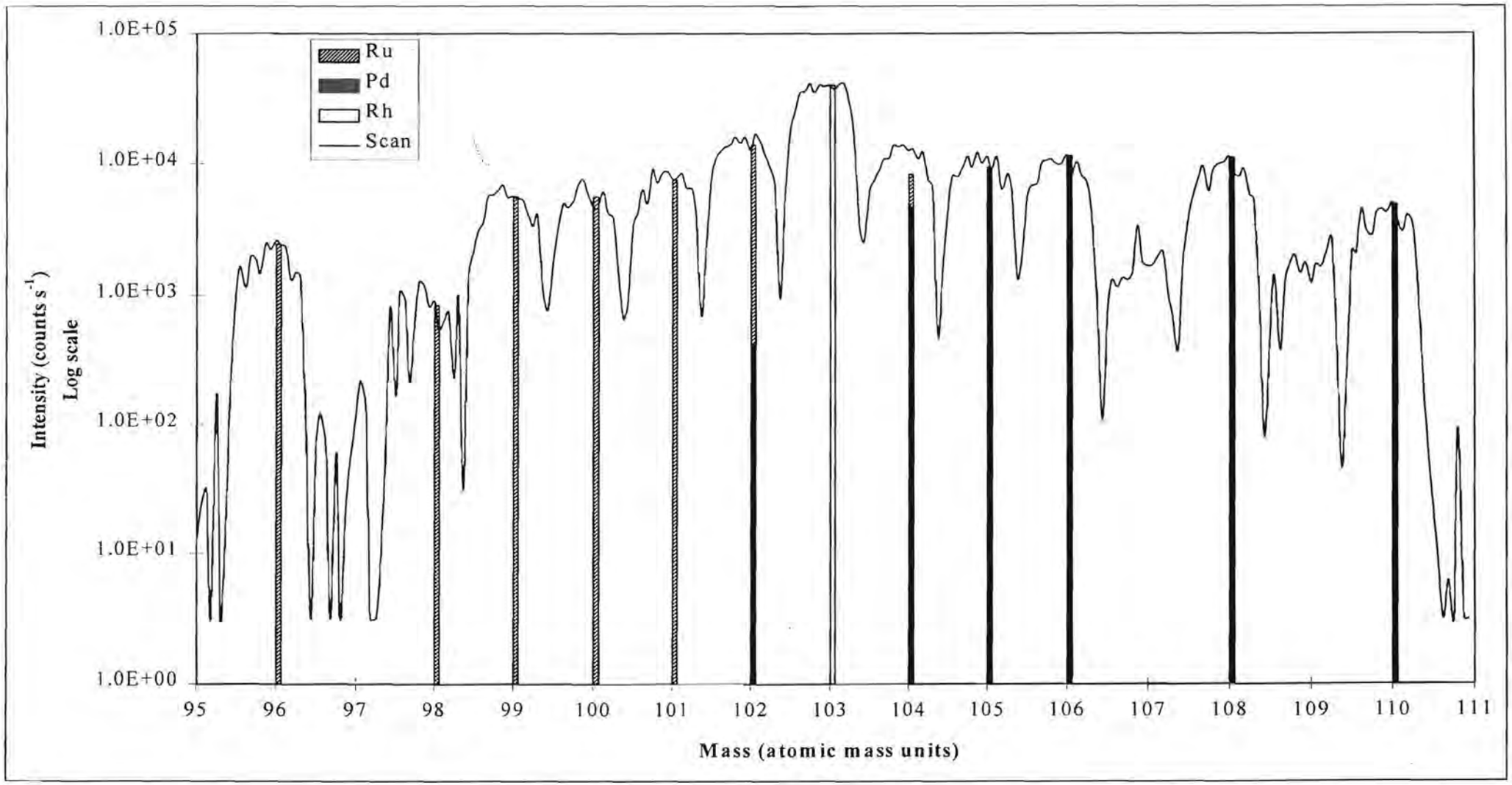

Figure 3.1: Mass scan (at normal resolution) of a solution containing 100 μg dm^{-3} platinum group elements and gold in 1.00% v/v HCl. The theoretical relative abundances of the isotopes of Ru, Pd and Rh are shown.

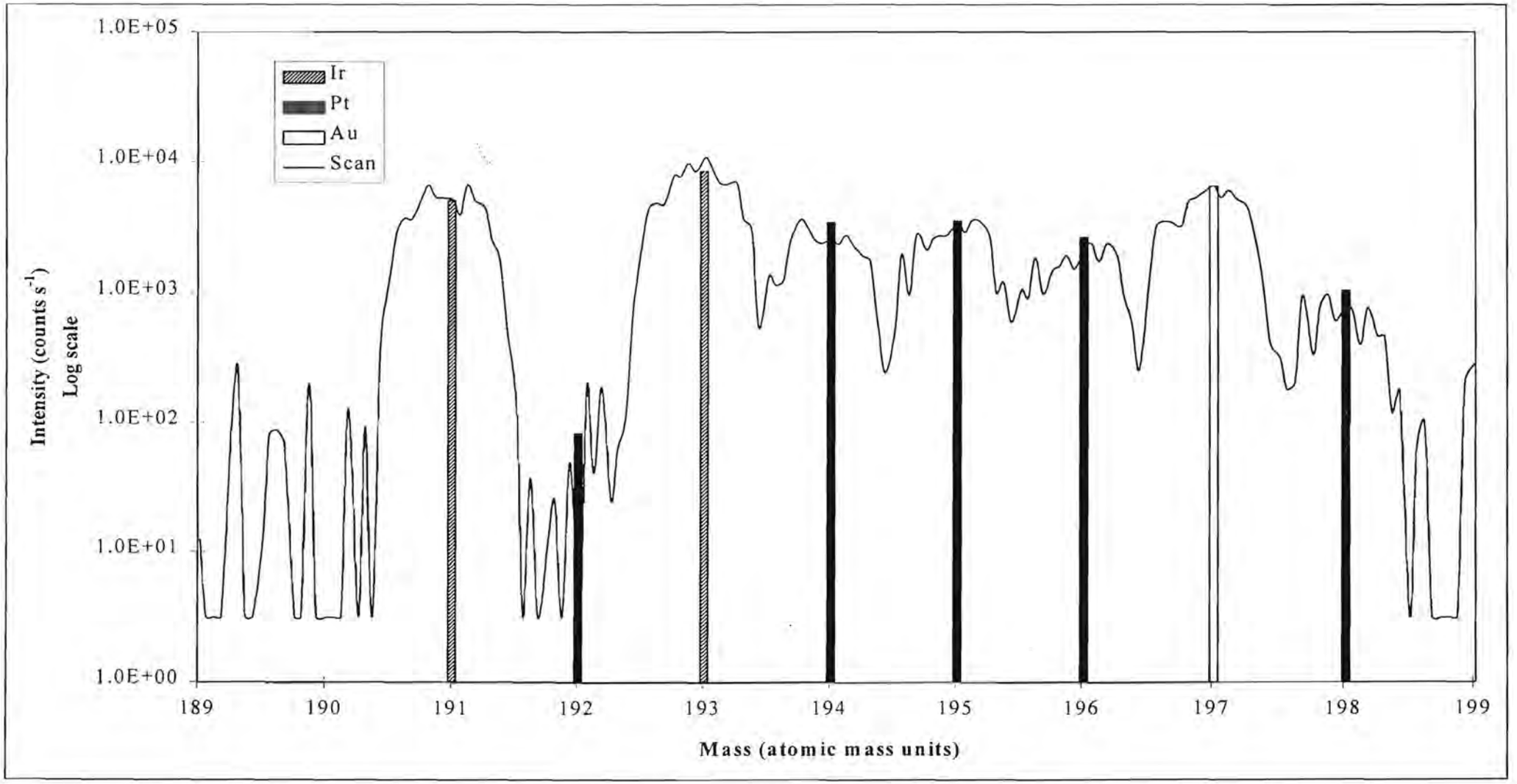

Figure 3.2: Mass scan (at normal resolution) of a solution containing 100 μg dm^{-3} platinum group elements and gold in 1.00% v/v HCl. The theoretical relative abundances of the isotopes of Ir, Pt and Au are shown.

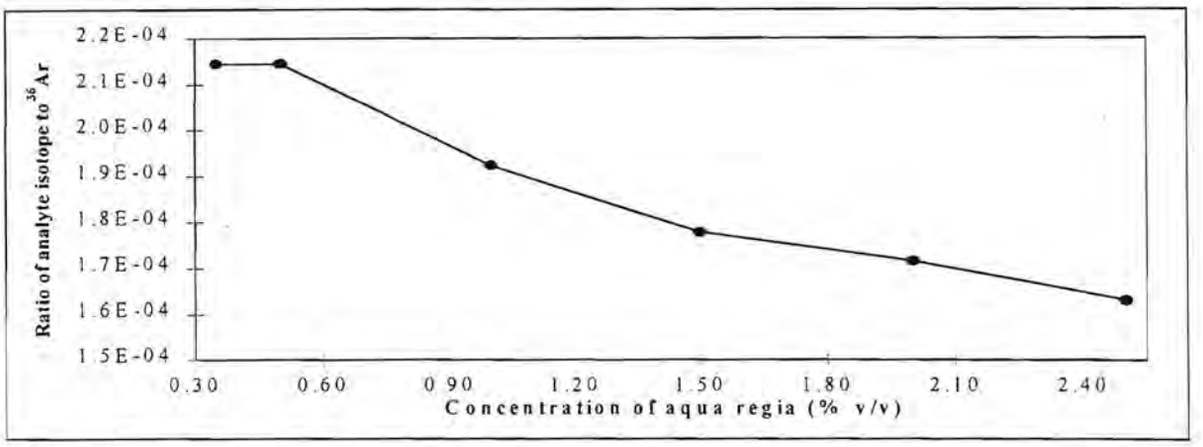

Figure 3.3: Effect of aqua regia concentration on the ratio of the gold isotope to the ^{36}Ar isotope. RSD for ^{197}Au to ^{36}Ar ratio is 12%.

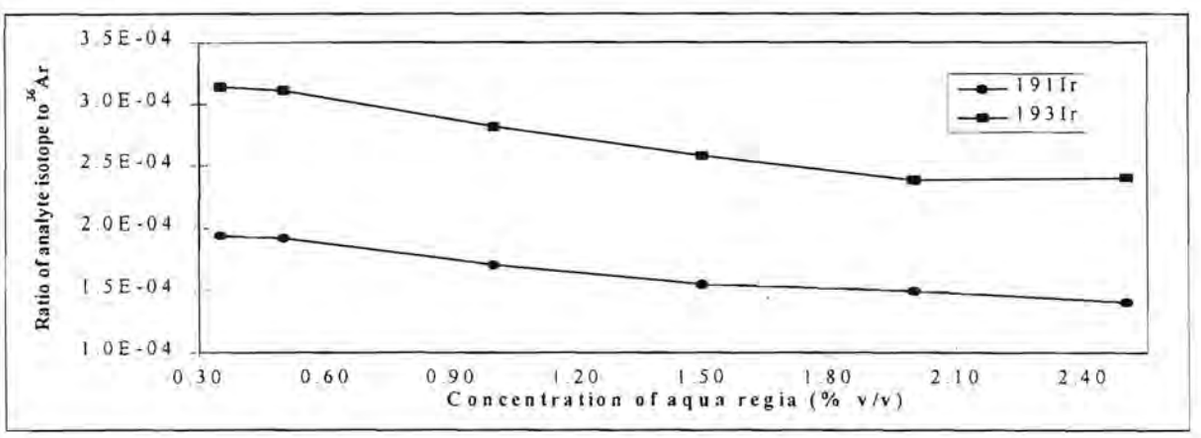

Figure 3.4: Effect of aqua regia concentration on the ratios of the iridium isotopes to the ^{36}Ar isotope. RSD for analytes to ^{36}Ar ratios is ^{191}Ir: 13% and ^{193}Ir: 12%.

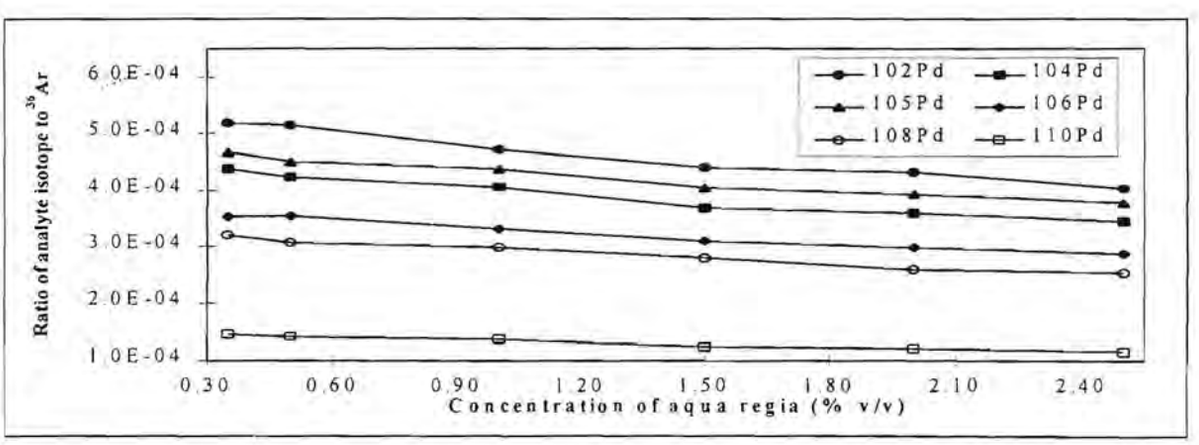

Figure 3.5: Effect of aqua regia concentration on the ratios of the palladium isotopes to the ^{36}Ar isotope. RSD for analytes to ^{36}Ar ratios is ^{102}Pd: 10%, ^{104}Pd: 10%, ^{105}Pd: 8%, ^{106}Pd: 9%, ^{108}Pd: 9% and ^{110}Pd: 9%.

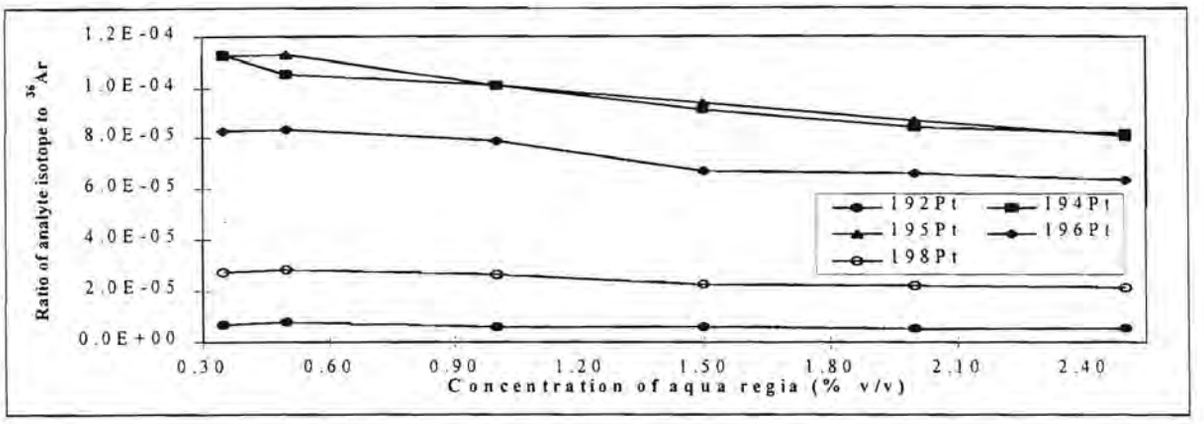

Figure 3.6: Effect of aqua regia concentration on the ratios of the platinum isotopes to the ^{36}Ar isotope. RSD for analytes to ^{36}Ar ratios is ^{192}Pt: 16%, ^{194}Pt: 13%, ^{195}Pt: 14%, ^{196}Pt: 12% and ^{198}Pt: 12%.

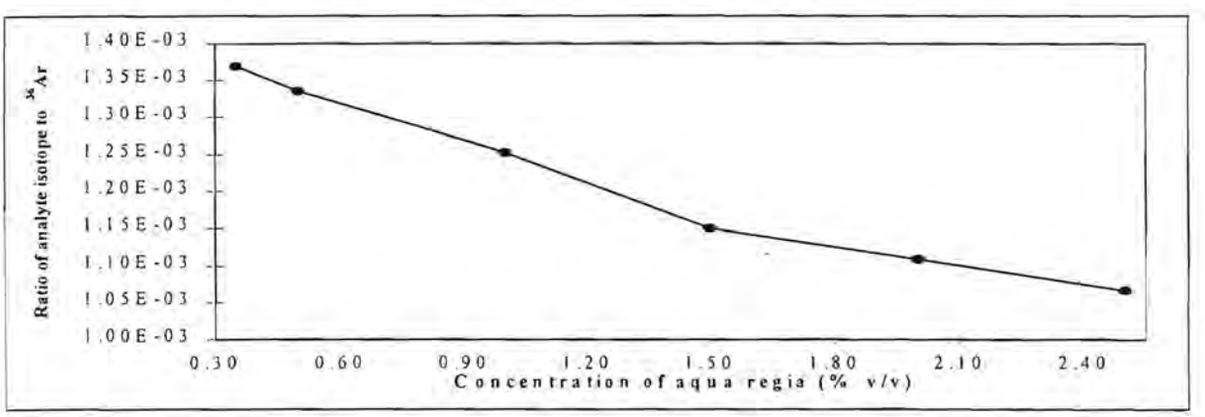

Figure 3.7: Effect of aqua regia concentration on the ratio of the rhodium isotope to the ^{36}Ar isotope. RSD for ^{103}Rh to ^{36}Ar ratio is 10%.

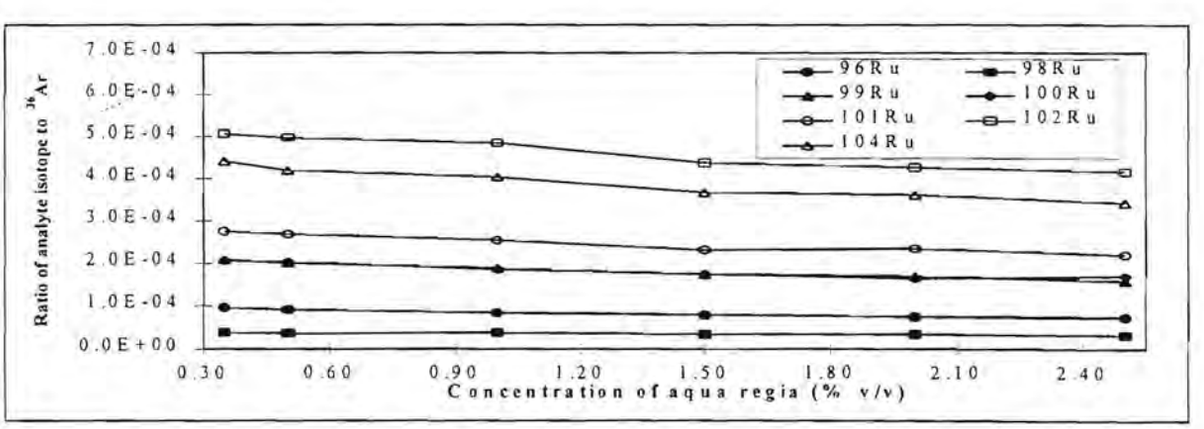

Figure 3.8: Effect of aqua regia concentration on the ratios of the ruthenium isotopes to the ^{36}Ar isotope. RSD for analytes to ^{36}Ar ratios is ^{96}Ru: 11%, ^{98}Ru: 7%, ^{99}Ru: 11%, ^{100}Ru: 10%, ^{101}Ru: 9%, ^{102}Ru: 9% and ^{104}Ru: 10%.

Effect of aqua regia concentration on the ratios of the isotopes of the platinum group elements and gold to ^{45}Sc

Figures 3.9 to 3.14 show a reasonably good correlation in the behaviour of the analyte isotopes relative to that of Sc. In general, a decrease in the ratio with an increase in aqua regia concentration is also observed. The decreases in the ratios over the concentration range studied was below 10% for Ru, Pd and Rh, i.e. the elements of lower mass. Relative standard deviations of less than 4% are observed for Ru, Pd and Rh and 5 - 7% for Au, Ir and Pt, with the exception of the low abundant ^{192}Pt isotope. From these curves it is seen that Sc could serve as a possible internal standard for the quantitative determination of the platinum group elements and gold, especially those of lower mass.

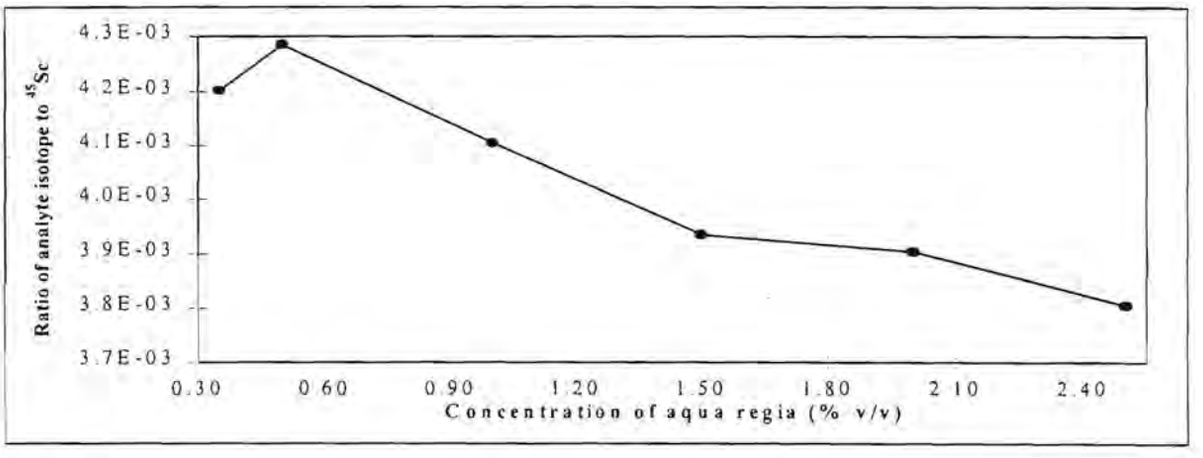

Figure 3.9: Effect of aqua regia concentration on the ratio of the gold isotope to the ^{45}Sc isotope. RSD for ^{197}Au to ^{45}Sc ratio is 5%.

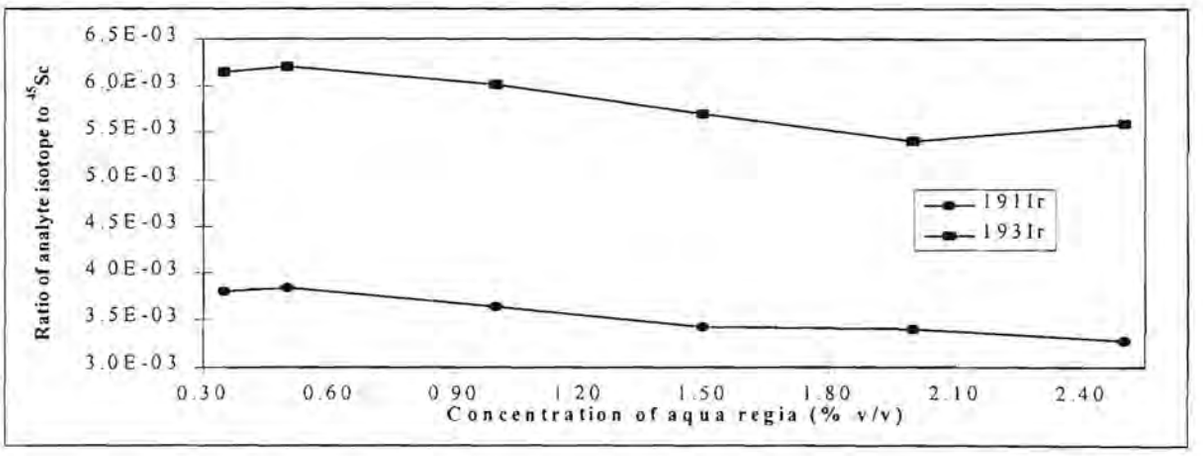

Figure 3.10: Effect of aqua regia concentration on the ratios of the iridium isotopes to the ^{45}Sc isotope. RSD for analytes to ^{45}Sc ratios is ^{191}Ir: 6% and ^{193}Ir: 6%.

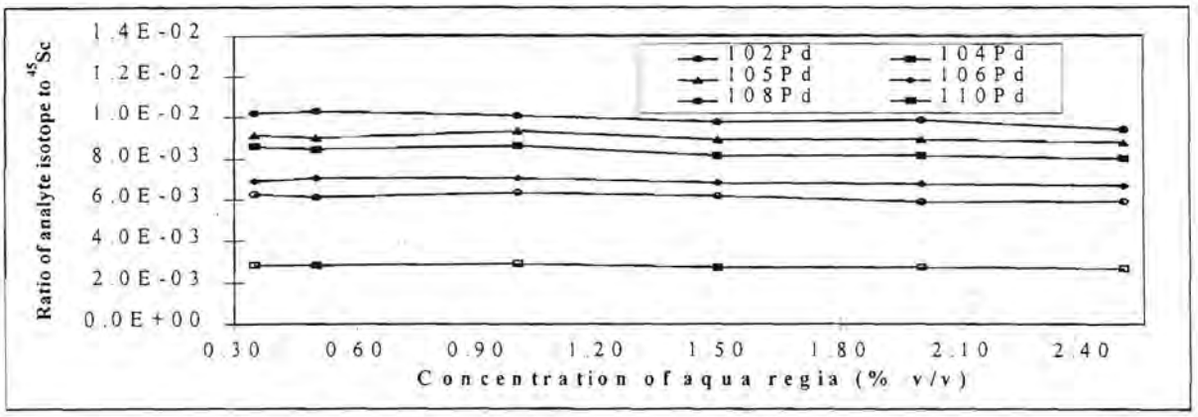

Figure 3.11: Effect of aqua regia concentration on the ratios of the palladium isotopes to the ^{45}Sc isotope. RSD for analytes to ^{45}Sc ratios is ^{102}Pd: 3%, ^{104}Pd: 3%, ^{105}Pd: 2%, ^{106}Pd: 2%, ^{108}Pd: 3% and ^{110}Pd: 3%.

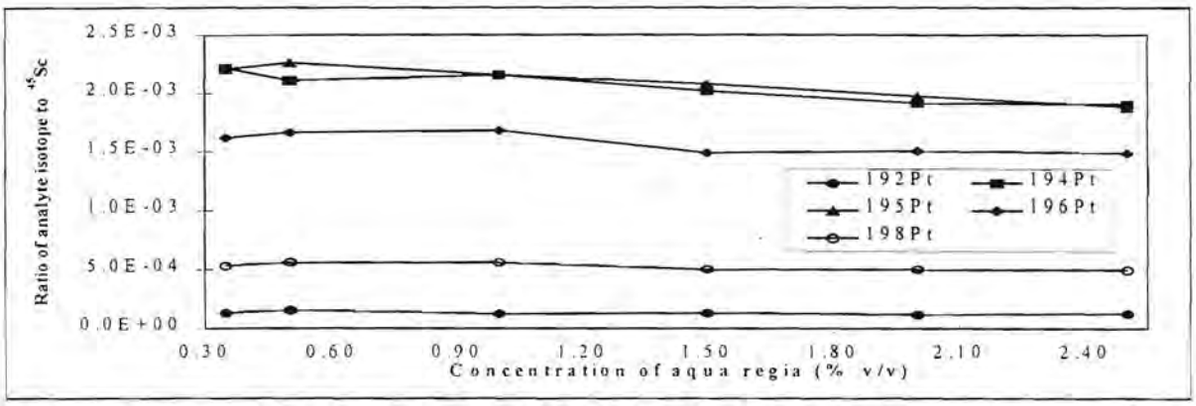

Figure 3.12: Effect of aqua regia concentration on the ratios of the platinum isotopes to the ^{45}Sc isotope. RSD for analytes to ^{45}Sc ratios is ^{192}Pt: 10%, ^{194}Pt: 6%, ^{195}Pt: 7%, ^{196}Pt: 6% and ^{198}Pt: 6%.

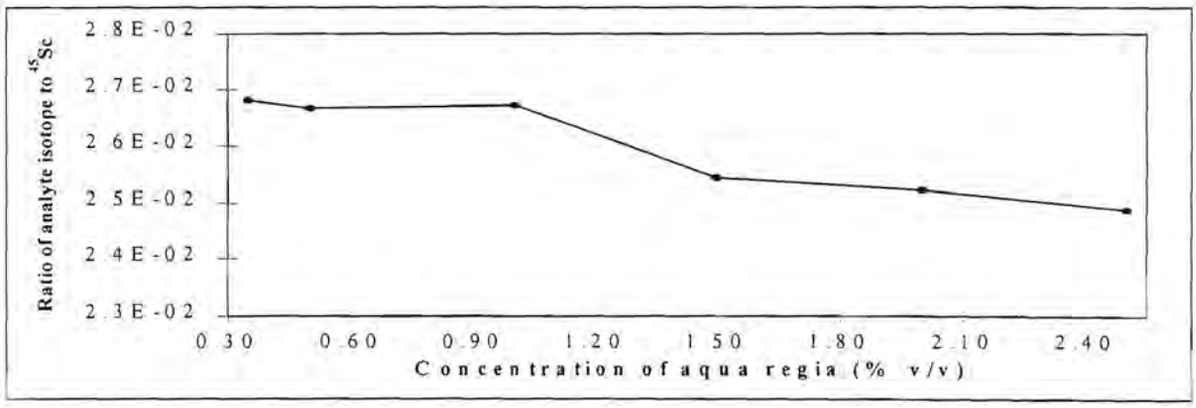

Figure 3.13: Effect of aqua regia concentration on the ratio of the rhodium isotope to the ^{45}Sc isotope. RSD for ^{103}Rh to ^{45}Sc ratio is 3%.

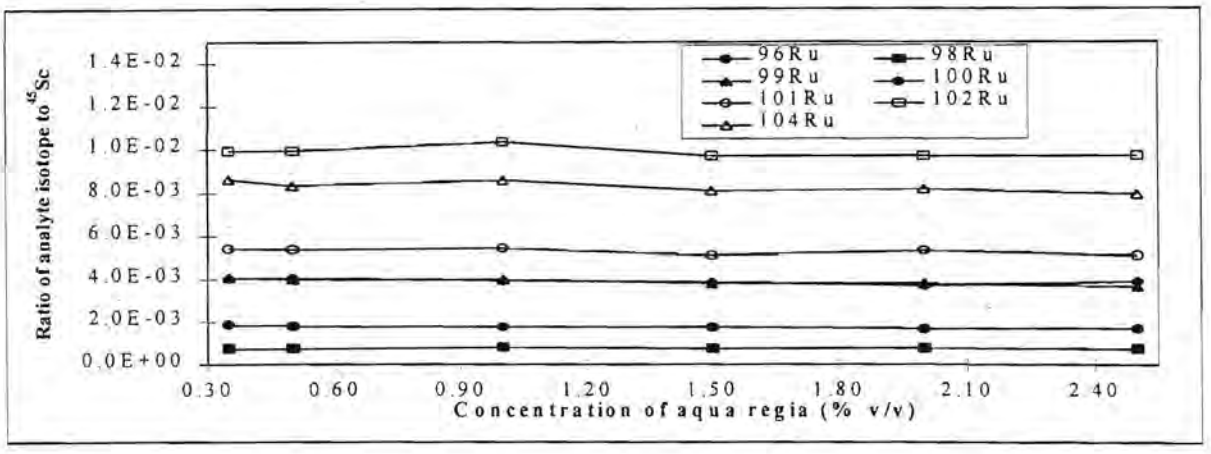

Figure 3.14: Effect of aqua regia concentration on the ratio of the ruthenium isotopes to the ^{45}Sc isotope. RSD for analytes to ^{45}Sc ratios is ^{96}Ru: 4%, ^{98}Ru: 3%, ^{99}Ru: 4%, ^{100}Ru: 3%, ^{101}Ru: 3%, ^{102}Ru: 3% and ^{104}Ru: 3%.

Effect of aqua regia concentration on the ratios of the isotopes of the platinum group elements and gold to ^{89}Y

Figures 3.15 to 3.20 show an excellent correlation between the behaviour of the platinum group elements and gold isotopes and the Y isotope. A maximum relative standard deviation of 3% for the ratios of the analytes to Y was observed for the platinum group elements of lighter mass. For Au, Ir and Pt (with the exception of ^{192}Pt) the corresponding value is 5%. Y shows great potential as an internal standard for the platinum group elements and gold, and more so for those of lighter mass.

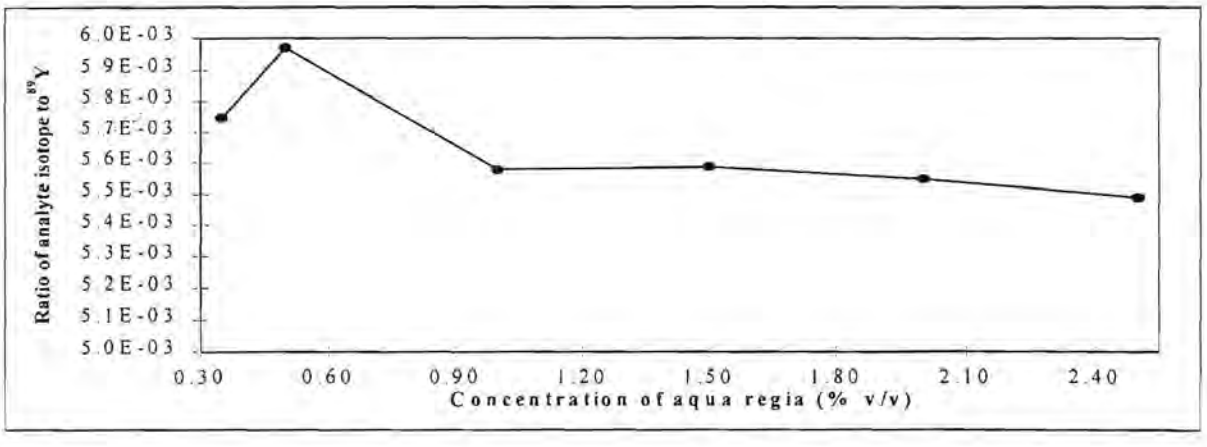

Figure 3.15: Effect of aqua regia concentration on the ratio of the gold isotope to the ^{89}Y isotope. RSD for ^{197}Au to ^{89}Y ratio is 3%.

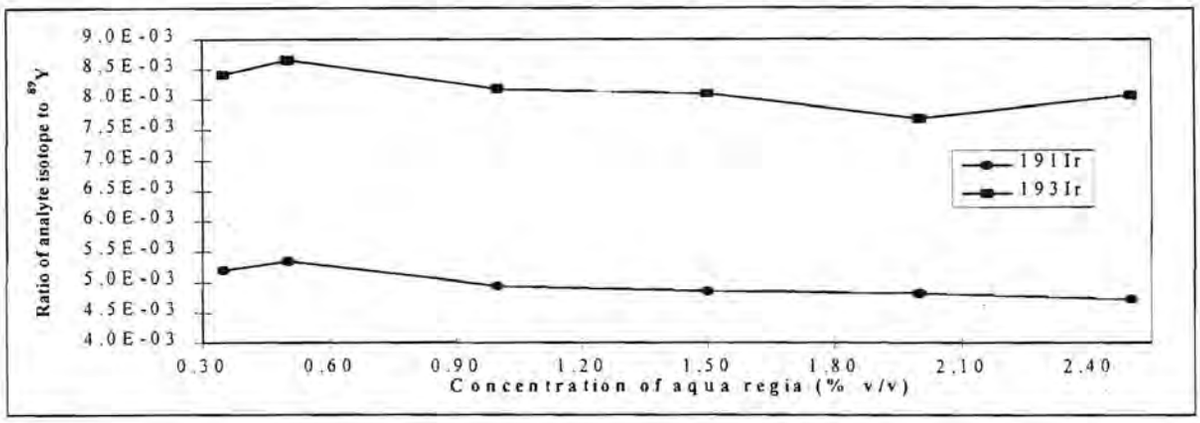

Figure 3.16: Effect of aqua regia concentration on the ratios of the iridium isotopes to the ^{89}Y isotope. RSD for analytes to ^{89}Y ratios is ^{191}Ir: 5% and ^{193}Ir: 4%.

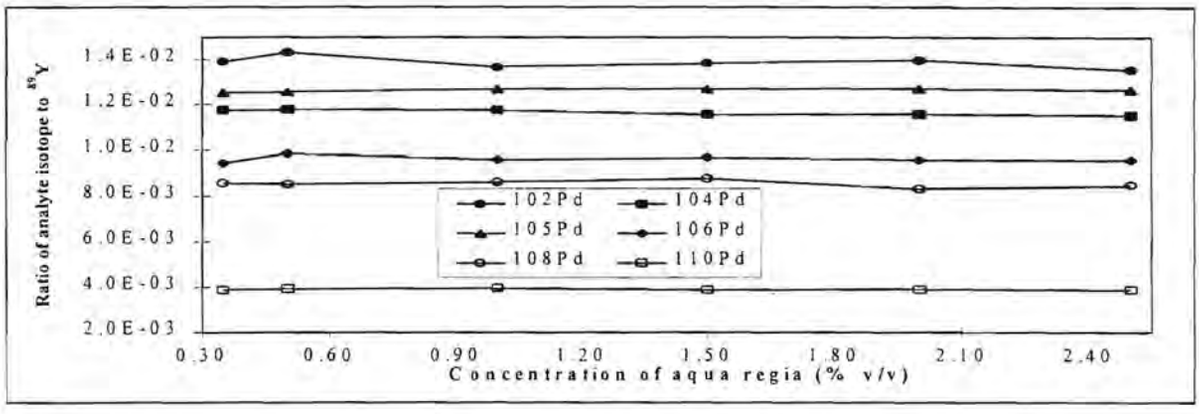

Figure 3.17: Effect of aqua regia concentration on the ratios of the palladium isotopes to the ^{89}Y isotope. RSD for analytes to ^{89}Y ratios is ^{102}Pd: 2%, ^{104}Pd: 1%, ^{105}Pd: 1%, ^{106}Pd: 1%, ^{108}Pd: 2% and ^{110}Pd: 1%.

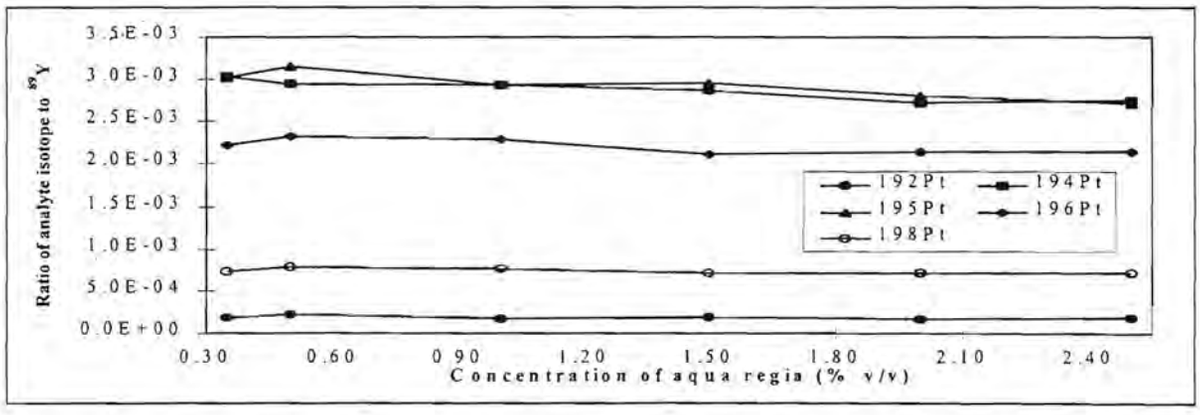

Figure 3.18: Effect of aqua regia concentration on the ratios of the platinum isotopes to the ^{89}Y isotope. RSD for analytes to ^{89}Y ratios is ^{192}Pt: 10%, ^{194}Pt: 4%, ^{195}Pt: 5%, ^{196}Pt: 4% and ^{198}Pt: 4%.

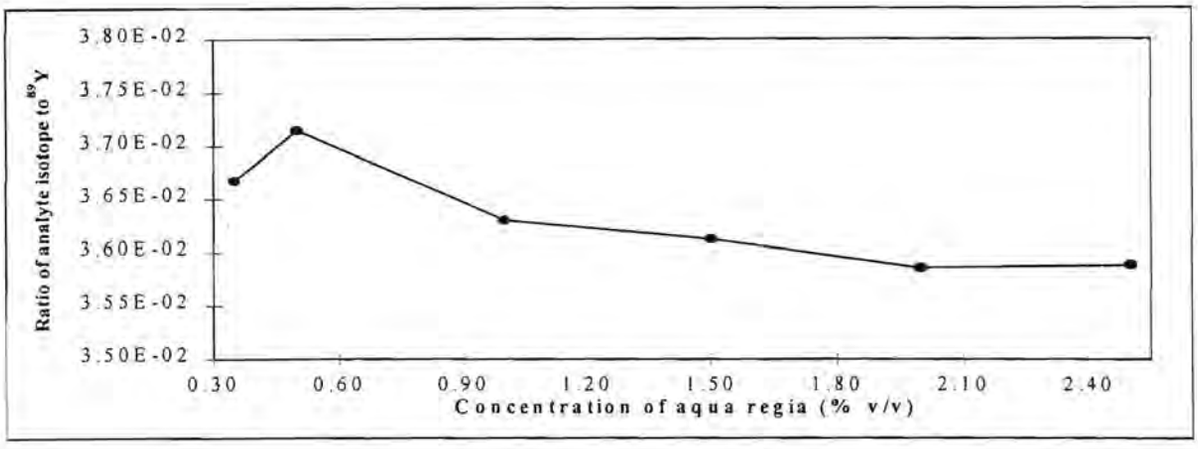

Figure 3.19: Effect of aqua regia concentration on the ratio of the rhodium isotope to the ^{89}Y isotope. RSD for ^{103}Rh to ^{89}Y ratio is 1%.

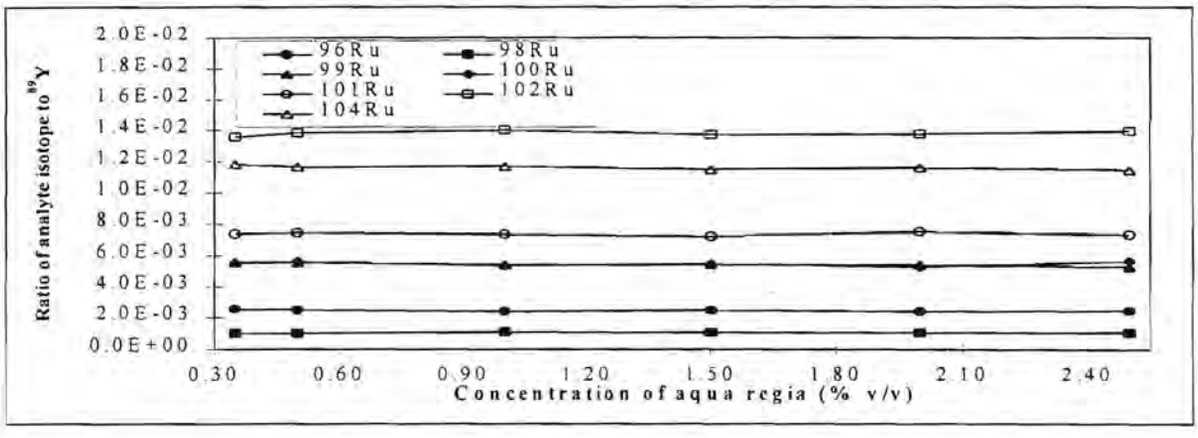

Figure 3.20: Effect of aqua regia concentration on the ratios of the ruthenium isotopes to the ^{89}Y isotope. RSD for analytes to ^{89}Y ratios is ^{96}Ru: 3%, ^{98}Ru: 3%, ^{99}Ru: 2%, ^{100}Ru: 3%, ^{101}Ru: 1%, ^{102}Ru: 1% and ^{104}Ru: 1%.

Effect of aqua regia concentration on the ratios of the isotopes of the platinum group elements and gold to ^{138}La

The ratios of the analytes to ^{138}La over the concentration range studied can be seen in figures 3.21 to 3.26. The less abundant isotope of La shows great potential as an internal standard for the analytes investigated since the variation in the ratios in aqua regia appears to be less than 6% (except for ^{192}Pt).

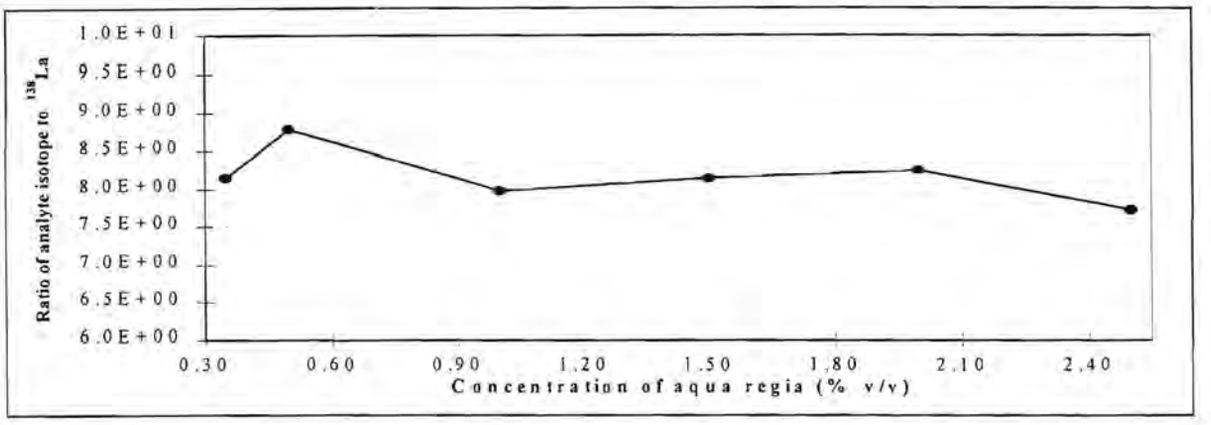

Figure 3.21: Effect of aqua regia concentration on the ratio of the gold isotope to the ^{138}La isotope. RSD for ^{197}Au to ^{138}La ratio is 4%.

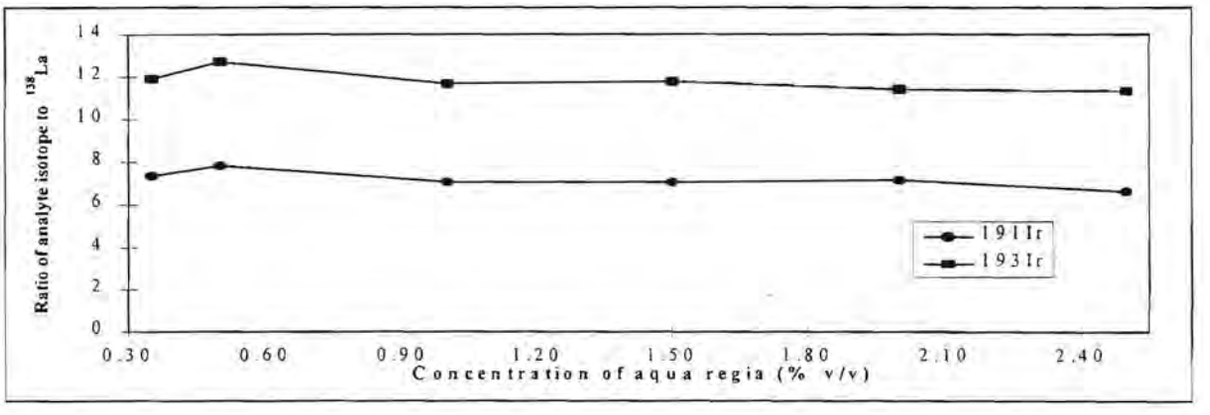

Figure 3.22: Effect of aqua regia concentration on the ratios of the iridium isotopes to the ^{138}La isotope. RSD for analytes to ^{138}La ratios is ^{191}Ir: 6% and ^{193}Ir: 4%.

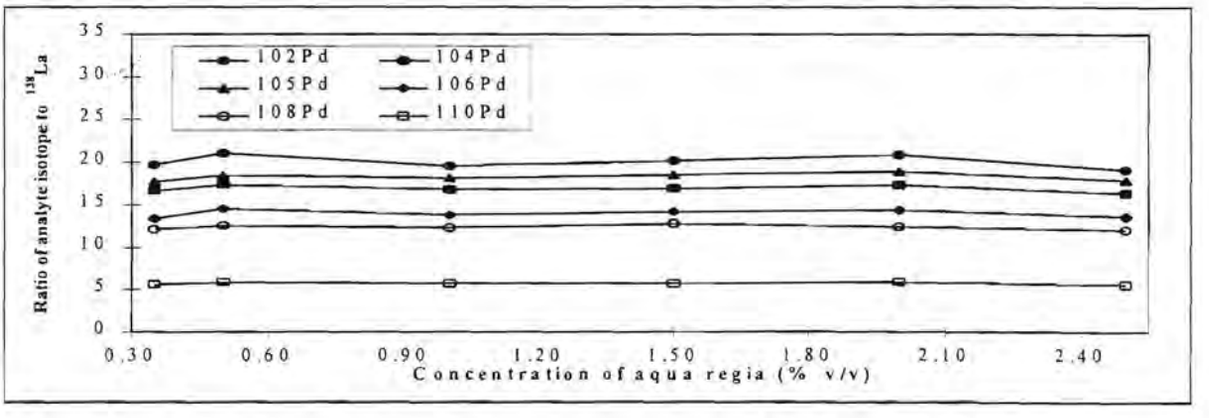

Figure 3.23: Effect of aqua regia concentration on the ratios of the palladium isotopes to the ^{138}La isotope. RSD for analytes to ^{138}La ratios is ^{102}Pd: 2%, ^{104}Pd: 2%, ^{105}Pd: 3%, ^{106}Pd: 3%, ^{108}Pd: 3% and ^{110}Pd: 3%.

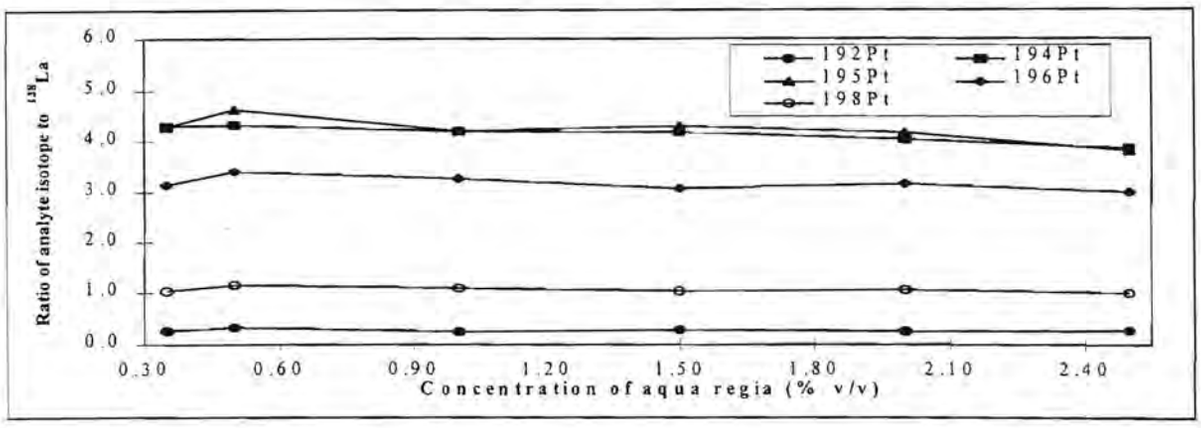

Figure 3.24: Effect of aqua regia concentration on the ratios of the platinum isotopes to the ^{138}La isotope. RSD for analytes to ^{138}La ratios is ^{192}Pt: 11%, ^{194}Pt: 4%, ^{195}Pt: 6%, ^{196}Pt: 5% and ^{198}Pt: 5%.

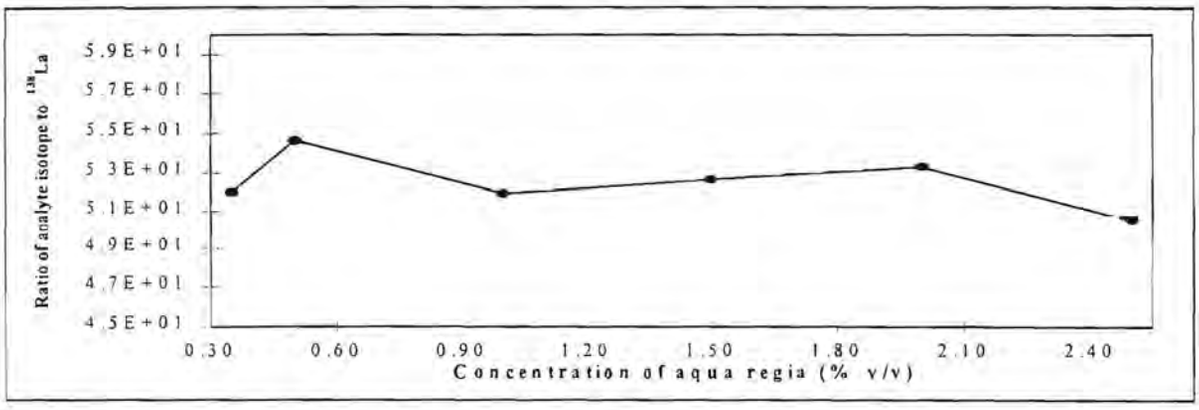

Figure 3.25: Effect of aqua regia concentration on the ratio of the rhodium isotope to the ^{138}La isotope. RSD for ^{103}Rh to ^{138}La ratio is 3%.

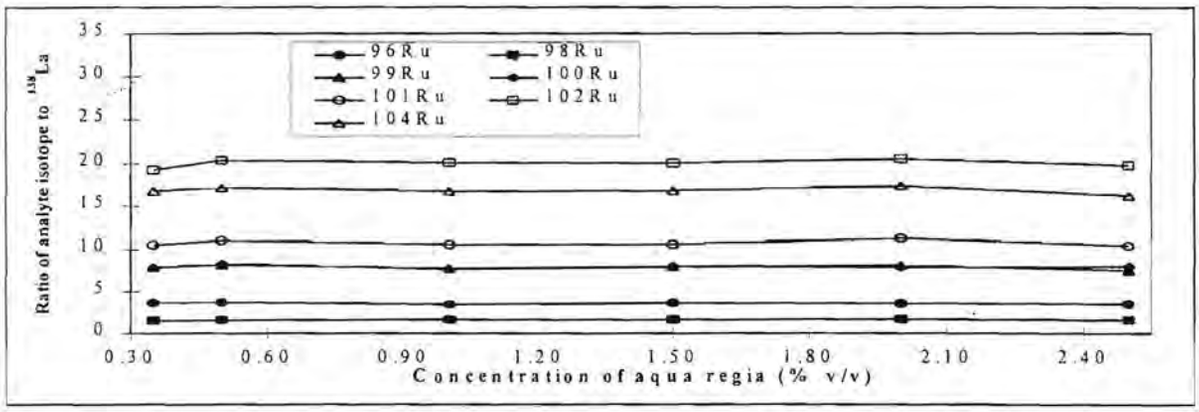

Figure 3.26: Effect of aqua regia concentration on the ratios of the ruthenium isotopes to the ^{138}La isotope. RSD for analytes to ^{138}La ratios is ^{96}Ru: 3%, ^{98}Ru: 4%, ^{99}Ru: 3%, ^{100}Ru: 3%, ^{101}Ru: 3%, ^{102}Ru: 2% and ^{104}Ru: 2%.

Effect of aqua regia concentration on the ratios of the isotopes of the platinum group elements and gold to ^{139}La

Figures 3.27 to 3.32 show the behaviour of the ^{139}La isotope relative to those of the analytes investigated in solutions containing 0.35 to 2.50% aqua regia. Excellent agreement in the various behaviour patterns is observed. This is also reflected in the relative standard deviations which are generally ≤ 3%.

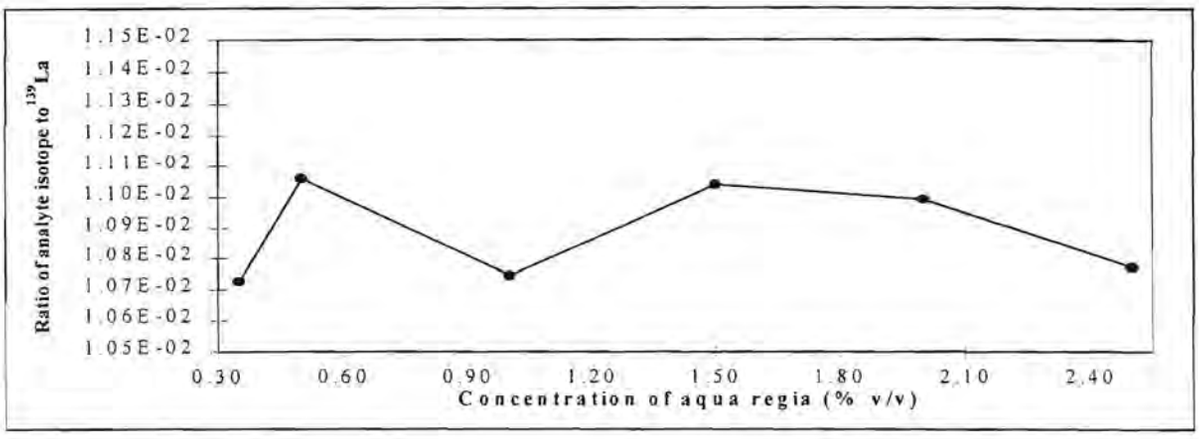

Figure 3.27: Effect of aqua regia concentration on the ratio of the gold isotope to the ^{139}La isotope. RSD for ^{197}Au to ^{139}La ratio is 1%.

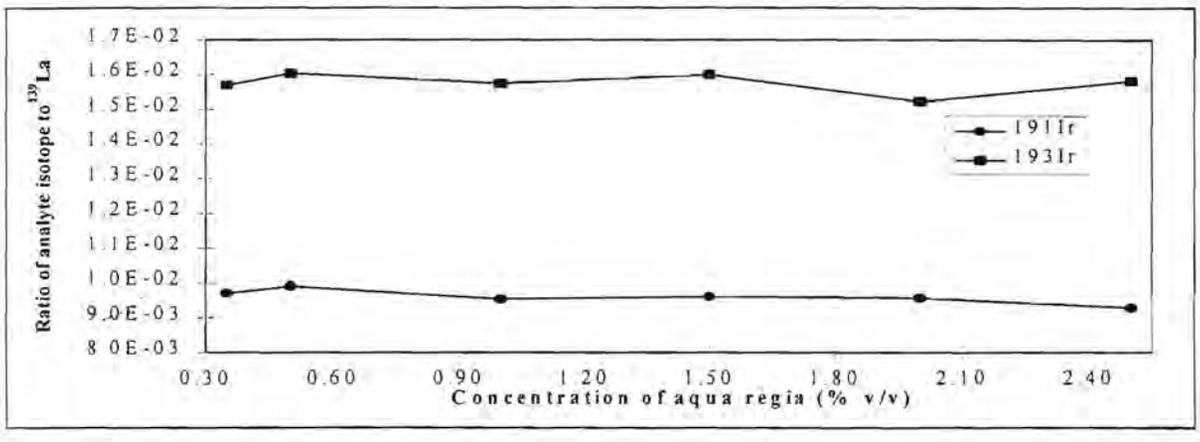

Figure 3.28: Effect of aqua regia concentration on the ratios of the iridium isotopes to the ^{139}La isotope. RSD for analytes to ^{139}La ratios is ^{191}Ir: 2% and ^{193}Ir: 2%.

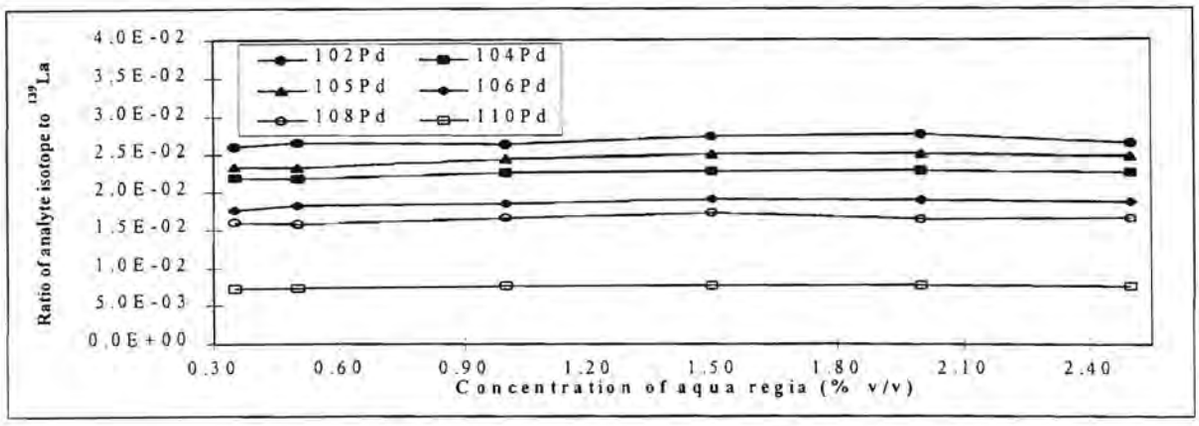

Figure 3.29: Effect of aqua regia concentration on the ratios of the palladium isotopes to the ^{139}La isotope. RSD for analytes to ^{139}La ratios is ^{102}Pd: 2%, ^{104}Pd: 2%, ^{105}Pd: 3%, ^{106}Pd: 3%, ^{108}Pd: 3% and ^{110}Pd: 3%.

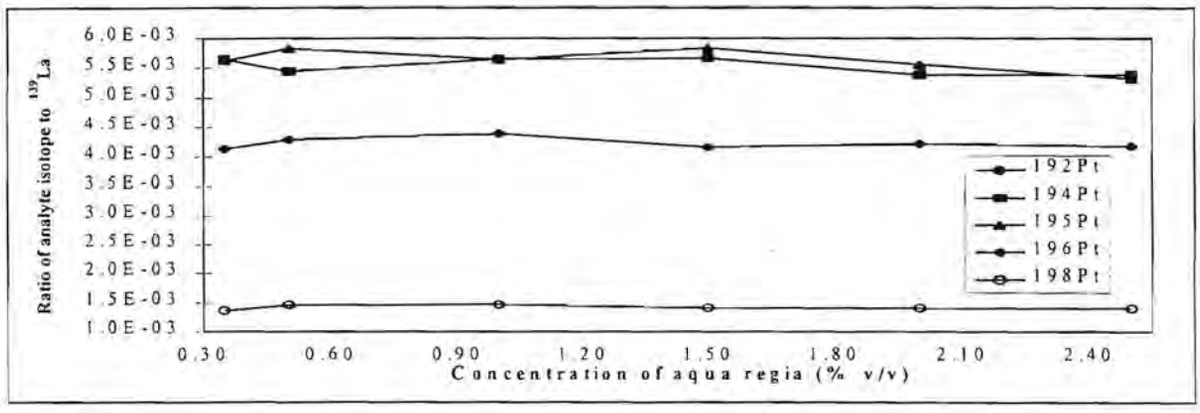

Figure 3.30: Effect of aqua regia concentration on the ratios of the platinum isotopes to the ^{139}La isotope. RSD for analytes to ^{139}La ratios is ^{192}Pt: 9%, ^{194}Pt: 2%, ^{195}Pt: 3%, ^{196}Pt: 2% and ^{198}Pt: 3%.

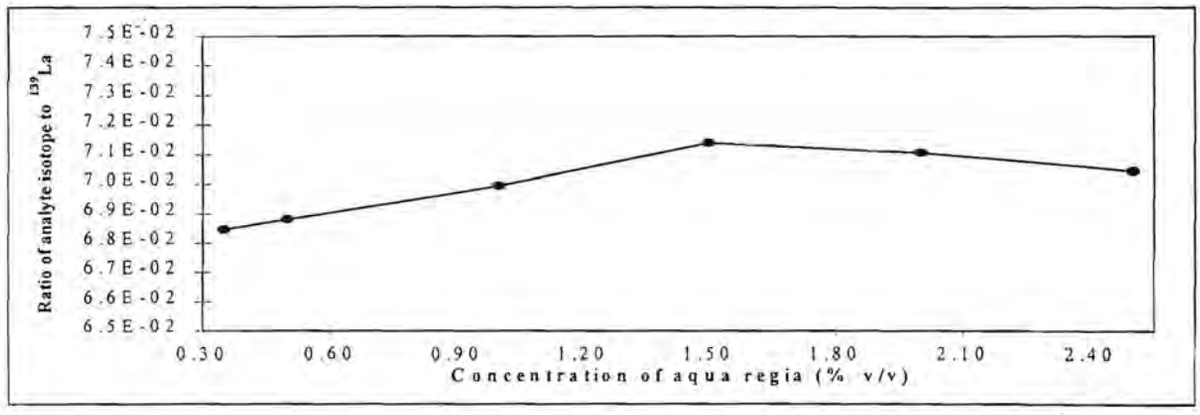

Figure 3.31: Effect of aqua regia concentration on the ratio of the rhodium isotope to the ^{139}La isotope. RSD for ^{103}Rh to ^{139}La ratio is 2%.

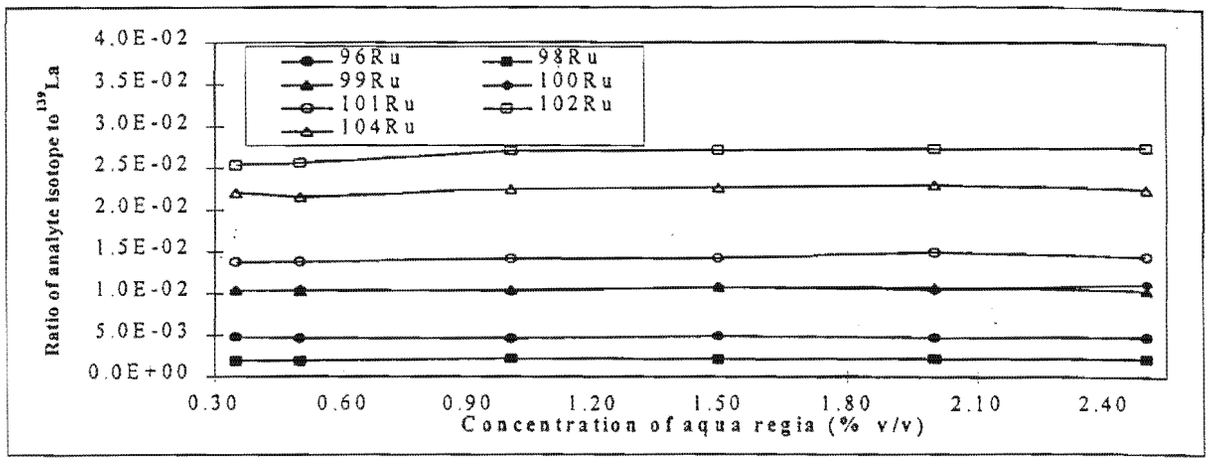

Figure 3.32: Effect of aqua regia concentration on the ratios of the ruthenium isotopes to the ^{139}La isotope. RSD for analytes to ^{139}La ratios is ^{96}Ru: 2%, ^{98}Ru: 6%, ^{99}Ru: 2%, ^{100}Ru: 3%, ^{101}Ru: 3%, ^{102}Ru: 3% and ^{104}Ru: 2%.

3.3.4 Calibration curves

For each of the isotopes of the platinum group elements and gold the following calibration data were compiled: 1) correlation coefficient of the curve, 2) slope of the calibration curve, 3) intercept of the calibration curve, 4) detection limit of the calibration curve and 5) the standard error of the predicted y-value. In the cases of 2) and 3) the x-range was taken as the concentration in μg dm^{-3} and the y-range was taken as the measured intensity. In 4) the detection limit (in μg dm^{-3}) was calculated as [(3 x s) / slope of the calibration curve] where s is the standard deviation of the blank standard. 5) refers to the standard error of the predicted y-value for each x in the regression. The standard error is a measure of the amount of error in the prediction of y for an individual x. For these calculations the y-range is taken as the concentration in μg dm^{-3} and the x-range is taken as the measured intensities. Also, the concentration was calculated using the measured intensity and the regression statistics; this value was compared to the "certified" concentration value of the standard and the % difference calculated. The above-mentioned data were compiled for the following cases: 1) no internal standard (tables 3.8 to 3.15, Addendum B), 2) ^{36}Ar as internal standard (tables 3.16 to 3.23, Addendum B), 3) ^{45}Sc as internal standard (tables 3.24 to 3.31, Addendum B), 4) ^{89}Y as internal standard (tables 3.32 to 3.39, Addendum B), 5) ^{138}La as internal standard (tables 3.40 to 3.47, Addendum B) and 6) ^{139}La as internal standard (tables 3.48 to 3.55, Addendum B).

Regression data with no internal standard

Correlation coefficients were 0.999 or better, except for ^{105}Pd, ^{192}Pt, ^{198}Pt and ^{98}Ru. Detection limits ranged from ≤ 1 $\mu g\ dm^{-3}$ for most of the isotopes to 13 $\mu g\ dm^{-3}$ for ^{105}Pd, 26 $\mu g\ dm^{-3}$ for ^{192}Pt, 5 $\mu g\ dm^{-3}$ for ^{198}Pt and 7 $\mu g\ dm^{-3}$ for ^{98}Ru. The standard error of the predicted y-value generally proved to be ≤ 4%. Calibration curves in the concentration range 0 to 150 $\mu g\ dm^{-3}$ in 1% v/v HCl produced good regression statistics when no internal standard was employed.

Regression data with ^{36}Ar as internal standard

When ^{36}Ar is employed as internal standard the correlation coefficients of the calibration curves were 0.99 or better, except for ^{192}Pt. Detection limits similar to the case where no internal standard was used, were observed. In this case the standard errors of the predicted y-values were generally ≤ 4%, but for individual isotopes higher standard errors were observed than for the above-mentioned case where no internal standard was employed. Worse regression data were observed in the case of ^{36}Ar as internal standard than for the case when no internal standard was used.

Regression data with ^{45}Sc as internal standard

Correlation coefficients were 0.999 or better, except for ^{192}Pt and ^{198}Pt. Although similar detection limits were observed as in the cases where no internal standard was used and when ^{36}Ar was used as internal standard, the standard errors of the predicted y-values were lower in the case of ^{45}Sc as internal standard. Calibration curve data for the platinum group elements and gold suggest that ^{45}Sc could be used as an internal standard in quantitative analysis.

Regression data with ^{89}Y as internal standard

Except for a few cases correlation coefficients were 0.9999 or better. The standard errors of the predicted y-values were generally ≤ 2%. In the low concentration range studied for the platinum group elements and gold, i.e. 0 to 150 $\mu g\ dm^{-3}$, ^{89}Y shows great potential as an internal standard for quantitative determinations of these analytes.

Regression data with ^{138}La as internal standard

Correlation coefficients calculated for calibration curves when ^{138}La is used as internal standard were in most cases between 0.990 and 0.999. Standard errors of predicted y-values were

generally quite high and values between 5 and 10% are observed. The calculated regression data does not prove ^{138}La a good reference element for the analytes investigated.

Regression data with ^{139}La as internal standard

Generally, correlation coefficients of 0.9999 or better were calculated. The standard errors of the predicted y-values proved to be more or less the same as in the case when ^{89}Y was used as internal standard. The very good regression statistics obtained suggests that ^{139}La could also be used as an internal standard for the quantitative determination of the platinum group elements and gold.

3.3.5 Concentrations as calculated from the calibration curves

The accuracy of quantitative determinations using the calibration curves of the various internal standards are illustrated in figures 3.33 to 3.54.

Quantitative values obtained for Au

With no internal standard the 50 μg dm^{-3} calibration standard showed values slightly higher than 50 μg dm^{-3} which could be due to a slight drift in the calibration curve. From figure 3.33 it can be seen that with an aqua regia concentration of $\leq$ 1% v/v values slightly lower than 50 μg dm^{-3} were obtained.

With ^{36}Ar as internal standard the calibration standard quantitated at about 50 μg dm^{-3} but at aqua regia concentrations of $\leq$ 1% v/v too high values were observed while too low values were observed at higher aqua regia concentrations. Similar trends were observed for ^{45}Sc as internal standard although the deviations from the 50 μg dm^{-3} value were not as severe as in the case of ^{36}Ar.

With ^{89}Y as internal standard the solutions with aqua regia concentrations of $\geq$ 1.50% v/v were quantitated at values lower than 50 μg dm^{-3}. With ^{138}La as internal standard deviations from the accepted value of 50 μg dm^{-3} were observed for the calibration standard as well as for the solutions containing 50 μg dm^{-3} Au in other matrices. ^{139}La showed to be the best internal standard for Au analyses as the 50 μg dm^{-3} calibration standard and the sample solutions all returned values of about 50 μg dm^{-3}.

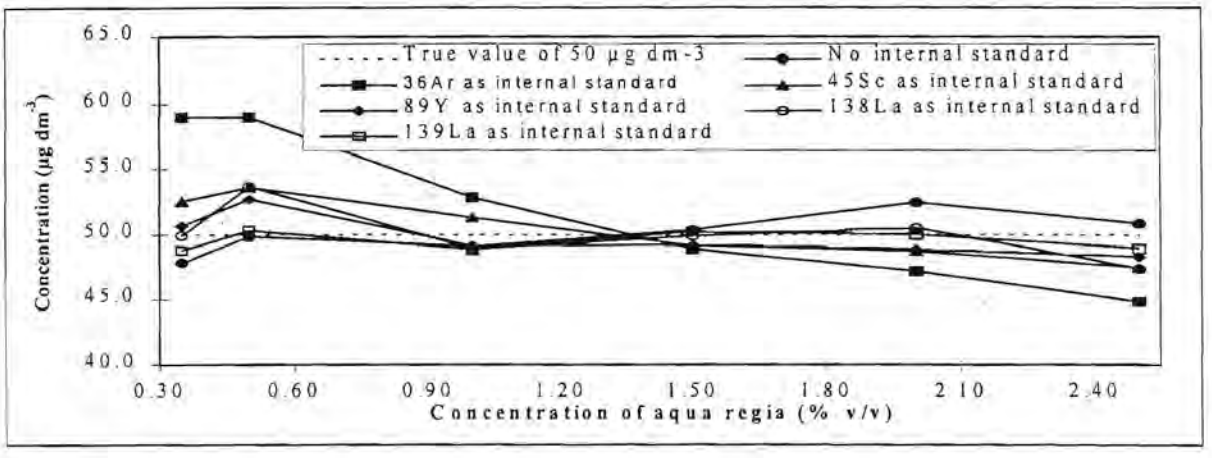

Figure 3.33: Effect of the concentration of aqua regia on the quantitative determination of Au (as ^{197}Au) using different internal standards.

Quantitative values obtained for Ir

Both the isotopes of Ir returned values of 50 μg dm^{-3} for solutions containing aqua regia when no internal standard was employed (see figures 3.34 and 3.35). The calibration standard in 1% v/v HCl however showed values higher than 50 μg dm^{-3} also possibly due to calibration curve drift.

^{36}Ar did not prove a good internal standard for Ir as both isotopes returned too high values at aqua regia concentrations of less than 1% v/v and too low values at concentrations of more than 1.5% v/v . ^{45}Sc showed similar trends as ^{36}Ar for Ir determinations but the deviations from 50 μg dm^{-3} were not as severe.

With ^{89}Y as internal standard too low values were observed for both the Ir isotopes at higher aqua regia concentrations. With ^{138}La as reference isotope, generally too low values were observed for the Ir containing solution. ^{139}La proved to be the best internal standard for the quantitative determination of Ir as both isotopes returned values close to 50 μg dm^{-3}.

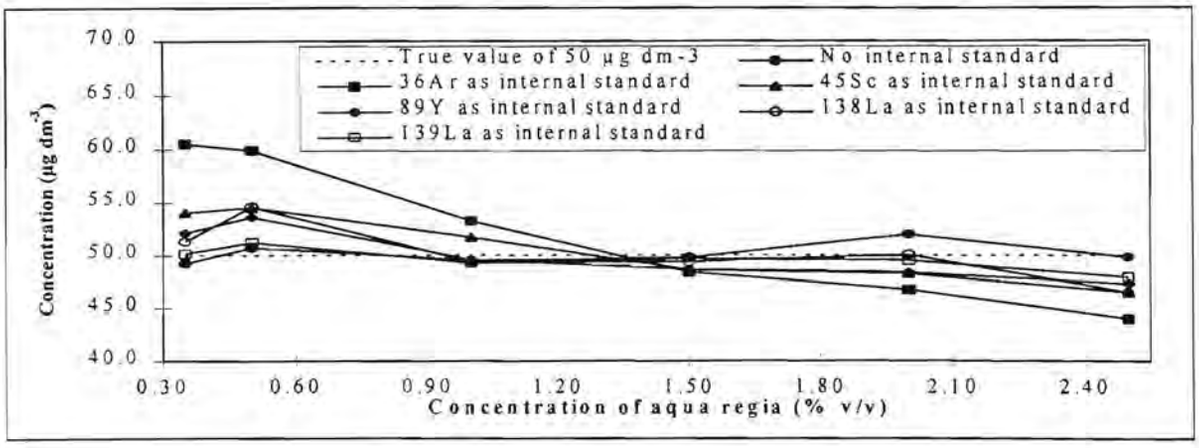

Figure 3.34: Effect of the concentration of aqua regia on the quantitative determination of Ir (as ^{191}Ir) using different internal standards.

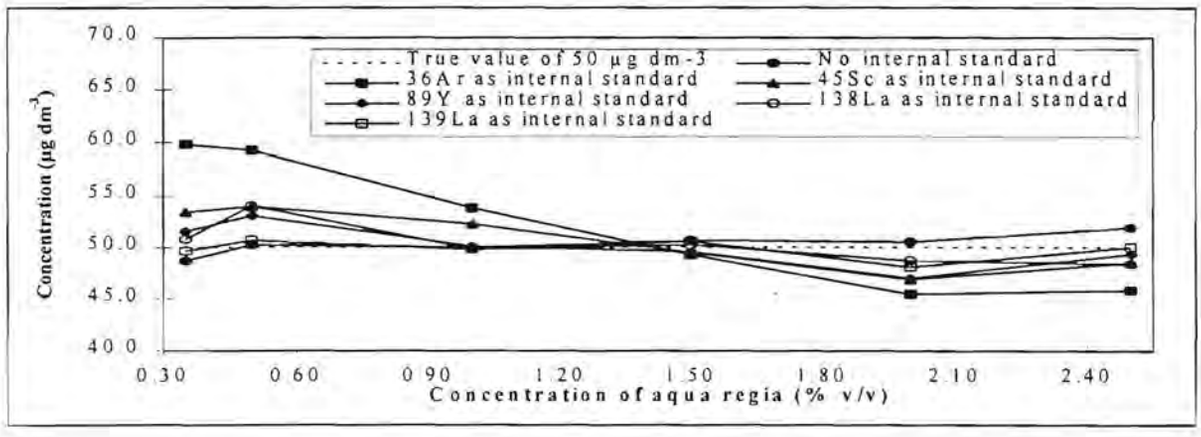

Figure 3.35: Effect of the concentration of aqua regia on the quantitative determination of Ir (as ^{193}Ir) using different internal standards.

Quantitative values obtained for Pd

Figures 3.36 to 3.41 show the effect of aqua regia on the quantitative determination of the various isotopes of Pd. In general too low values are observed for the Pd isotopes when no internal standard is used at aqua regia concentrations of less than 1% v/v .

With ^{36}Ar as internal standard too high values are observed at aqua regia concentrations of less than 1% v/v and too low values at higher aqua regia concentrations. Again ^{45}Sc showed similar trends as ^{36}Ar but the effect is less severe and reasonably good quantitative values were observed.

^{89}Y as reference element for Pd showed values very close to 50 μg dm^{-3} especially for the ^{104}Pd and ^{105}Pd isotopes. ^{138}La performed worse than ^{139}La as a possible internal standard for the isotopes of Pd and the values close to 50 μg dm^{-3} were observed for ^{104}Pd with ^{139}La as internal standard.

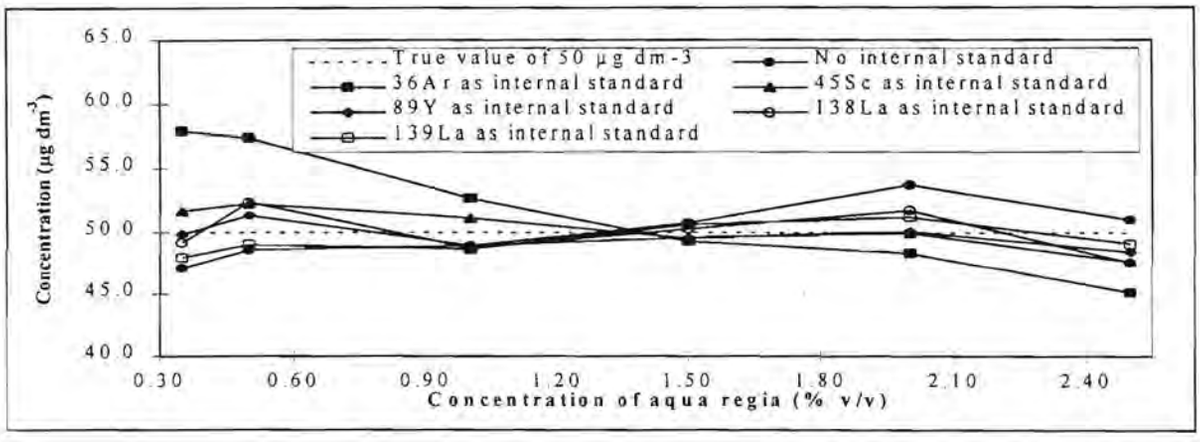

Figure 3.36: Effect of the concentration of aqua regia on the quantitative determination of Pd (as ^{102}Pd) using different internal standards.

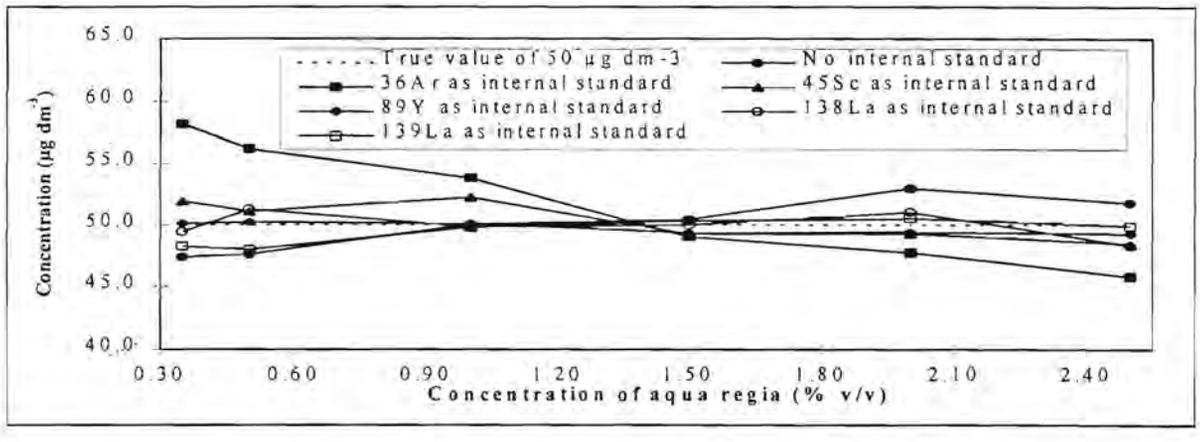

Figure 3.37: Effect of the concentration of aqua regia on the quantitative determination of Pd (as ^{104}Pd) using different internal standards.

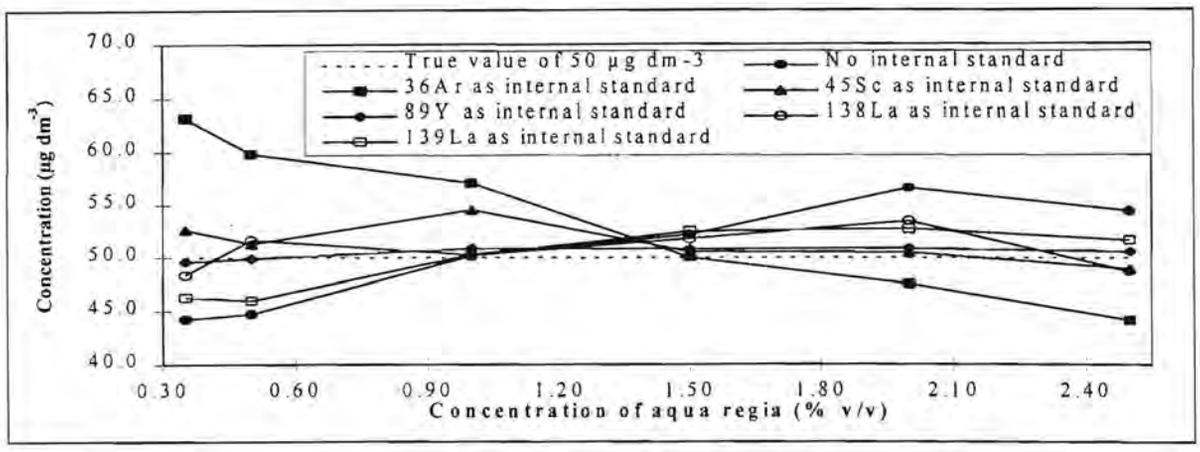

Figure 3.38: Effect of the concentration of aqua regia on the quantitative determination of Pd (as ^{105}Pd) using different internal standards.

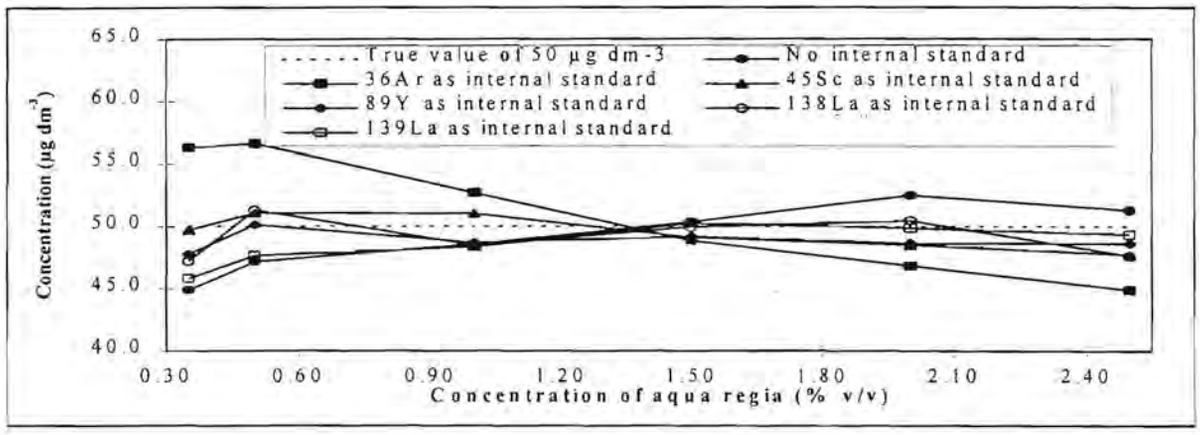

Figure 3.39: Effect of the concentration of aqua regia on the quantitative determination of Pd (as ^{106}Pd) using different internal standards.

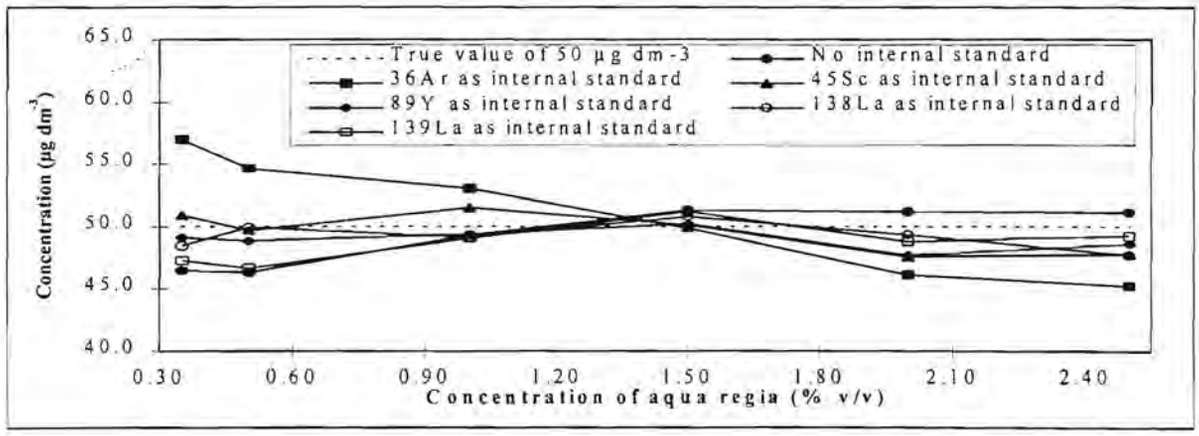

Figure 3.40: Effect of the concentration of aqua regia on the quantitative determination of Pd (as ^{108}Pd) using different internal standards.

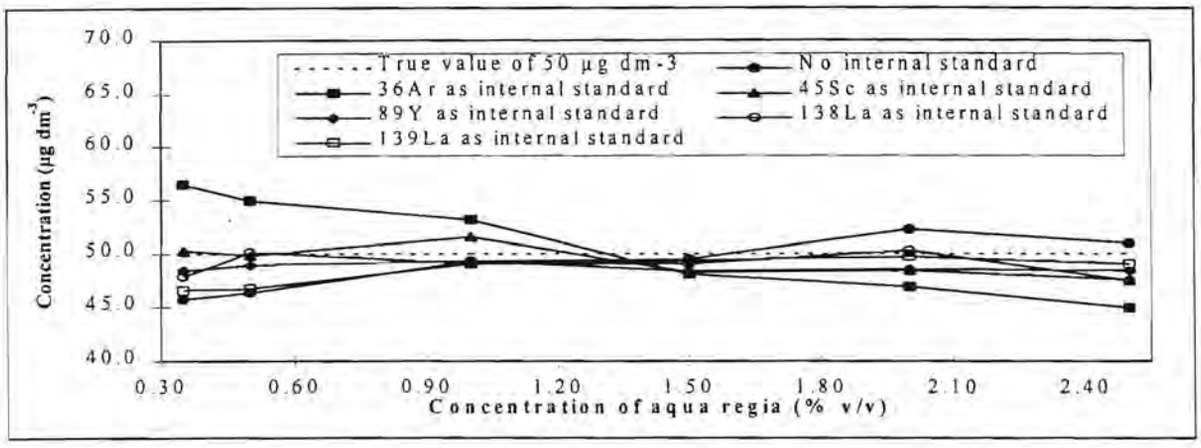

Figure 3.41: Effect of the concentration of aqua regia on the quantitative determination of Pd (as ^{110}Pd) using different internal standards.

Quantitative values obtained for Pt

The values observed for ^{192}Pt deviated very much from 50 μg dm^{-3} and this isotope of Pt was not considered any further.

With no internal standard employed too low values were observed at low aqua regia concentrations and the 50 μg dm^{-3} calibration standard also showed a drift (see figures 3.42 to 3.46).

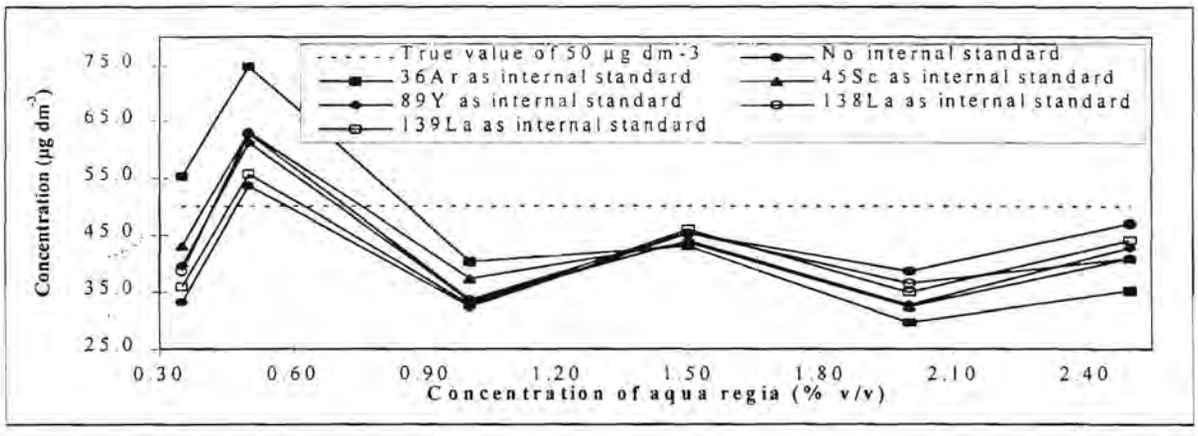

Figure 3.42: Effect of the concentration of aqua regia on the quantitative determination of Pt (as ^{192}Pt) using different internal standards.

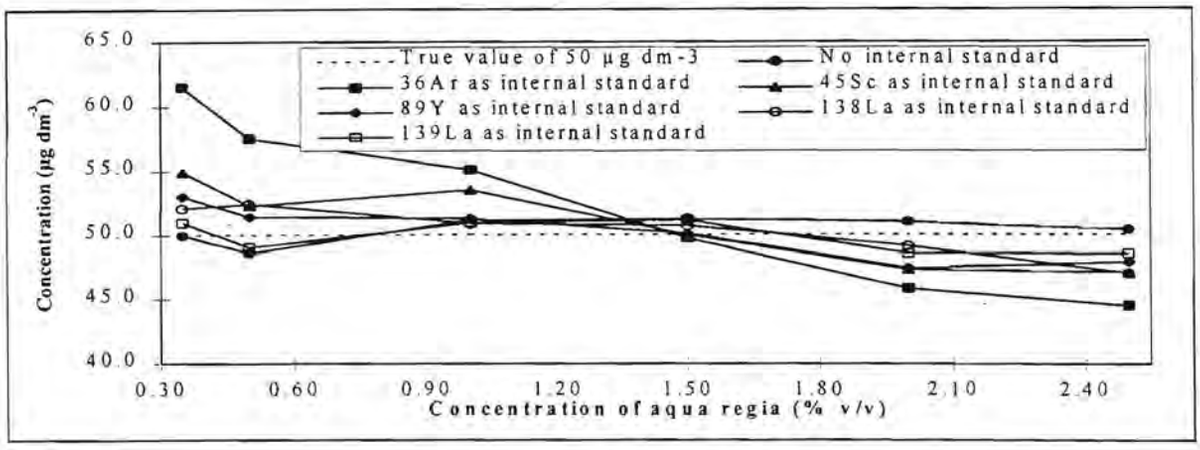

Figure 3.43: Effect of the concentration of aqua regia on the quantitative determination of Pt (as ^{194}Pt) using different internal standards.

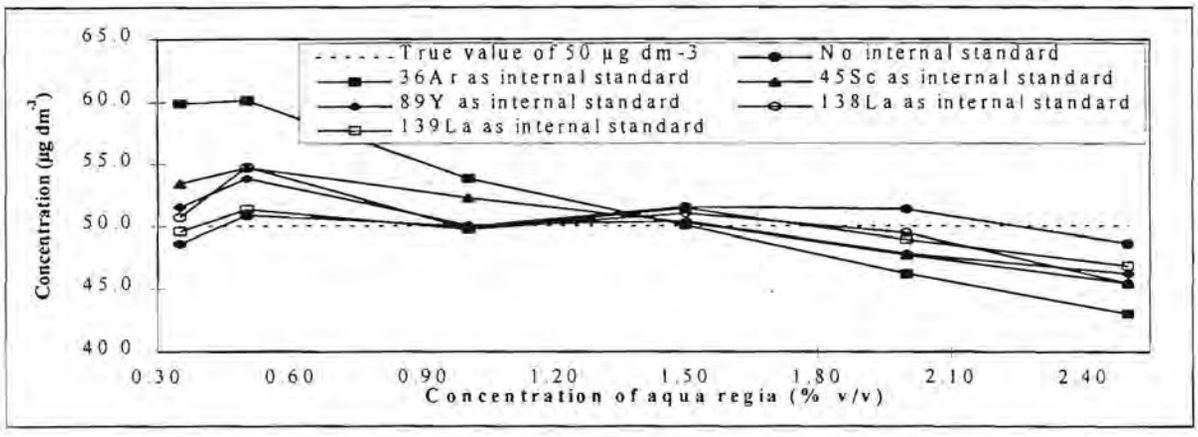

Figure 3.44: Effect of the concentration of aqua regia on the quantitative determination of Pt (as ^{195}Pt) using different internal standards.

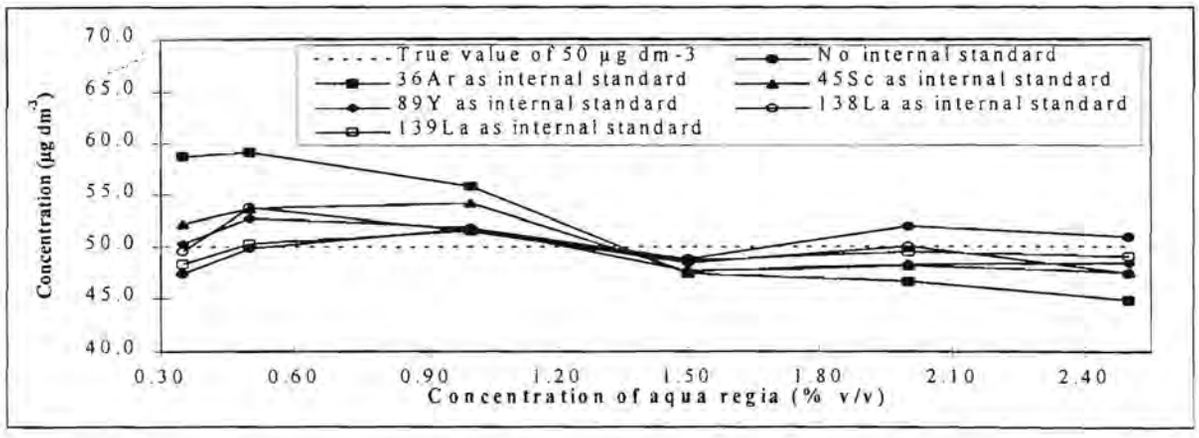

Figure 3.45: Effect of the concentration of aqua regia on the quantitative determination of Pt (as ^{196}Pt) using different internal standards.

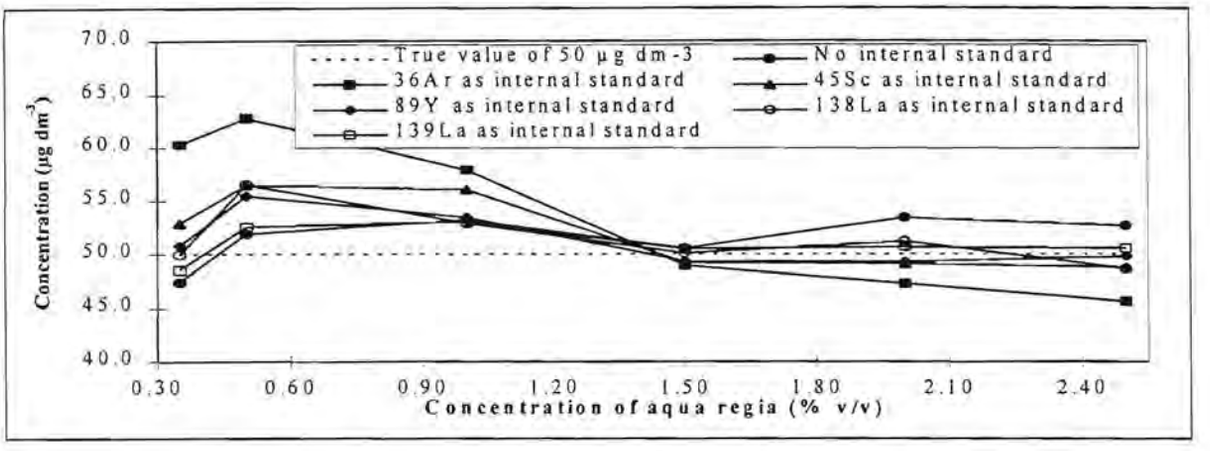

Figure 3.46: Effect of the concentration of aqua regia on the quantitative determination of Pt (as ^{198}Pt) using different internal standards.

^{36}Ar as reference element returned too high values at low aqua regia concentrations and too low values at higher aqua regia concentrations. Although ^{45}Sc and ^{89}Y returned similar trends as ^{36}Ar when employed as internal standards, the deviations were not so great as with ^{36}Ar. Of the two isotopes of La, ^{139}La showed the most potential as an internal standard for the quantitative determination of Pt, especially with ^{194}Pt, ^{195}Pt and ^{196}Pt.

Quantitative values obtained for Rh

See figure 3.47 for the effect of aqua regia on the quantitative determination of Rh when using different internal standards. When no internal standard is employed, slightly low values were recovered for Rh at low aqua regia concentrations and slightly high values at higher aqua regia concentrations.

^{36}Ar as internal standard returned too high values at low aqua regia concentrations and too low values when the matrices of the solutions consisted of higher aqua regia concentrations. ^{45}Sc and ^{89}Y showed good recovery values for Rh although the values for Y as reference element were closer to 50 μg dm^{-3} than for ^{45}Sc. Of ^{138}La and ^{139}La, ^{139}La returned values closer to 50 μg dm^{-3} when employed as internal standard for Rh analyses.

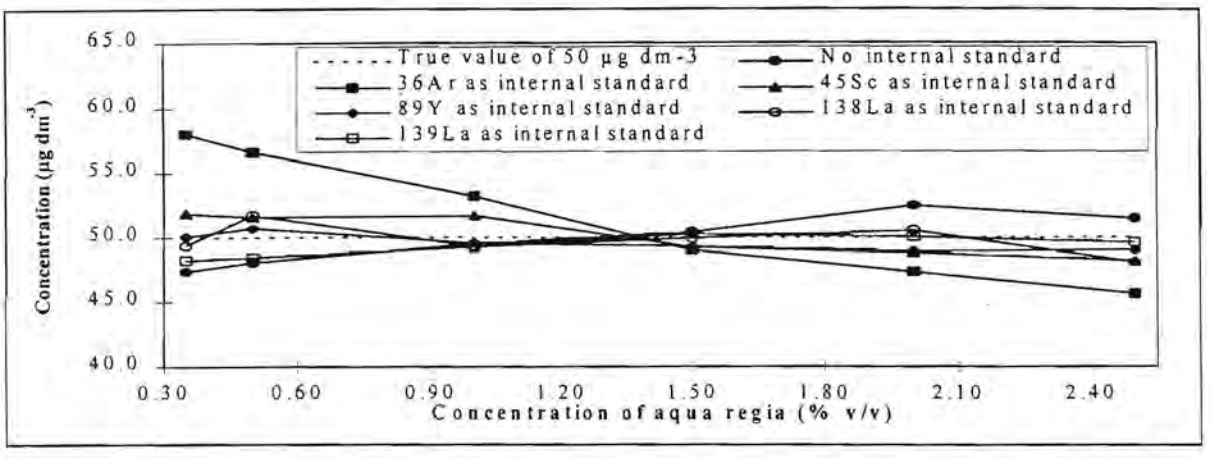

Figure 3.47: Effect of the concentration of aqua regia on the quantitative determination of Rh (as ^{103}Rh) using different internal standards.

Quantitative values obtained for Ru

Figures 3.48 to 3.54 show the effect of aqua regia on Ru analyses. Quantitative values for Ru isotopes are lower than 50 μg dm^{-3} at low aqua regia concentrations and higher than 50 μg dm^{-3} at higher concentrations of aqua regia, when no internal standard is used.

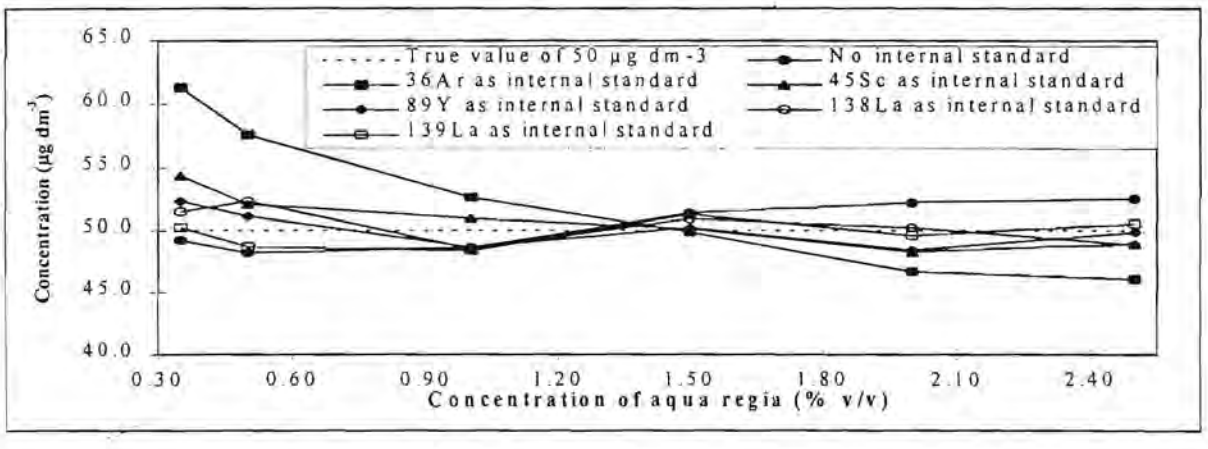

Figure 3.48: Effect of the concentration of aqua regia on the quantitative determination of Ru (as ^{96}Ru) using different internal standards.

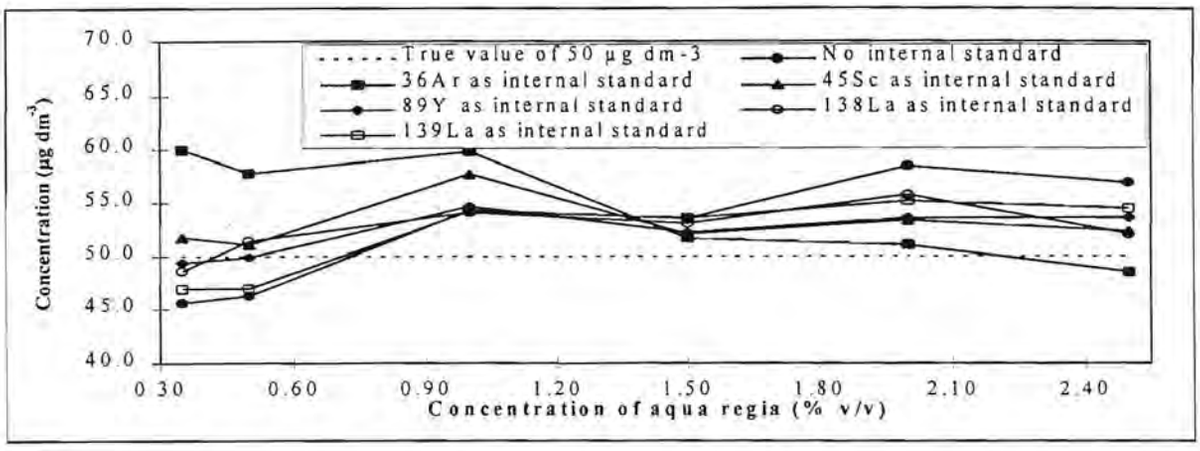

Figure 3.49: Effect of the concentration of aqua regia on the quantitative determination of Ru (as ^{98}Ru) using different internal standards.

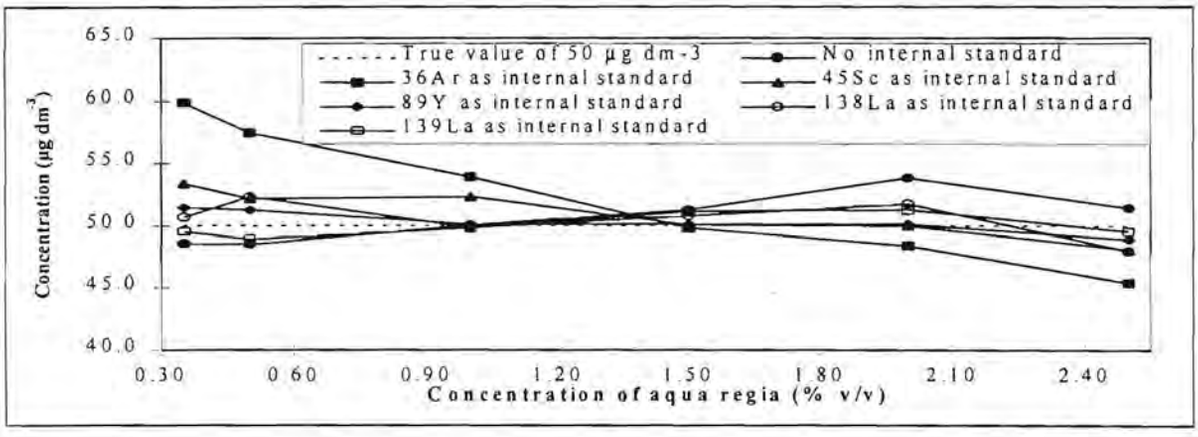

Figure 3.50: Effect of the concentration of aqua regia on the quantitative determination of Ru (as ^{99}Ru) using different internal standards.

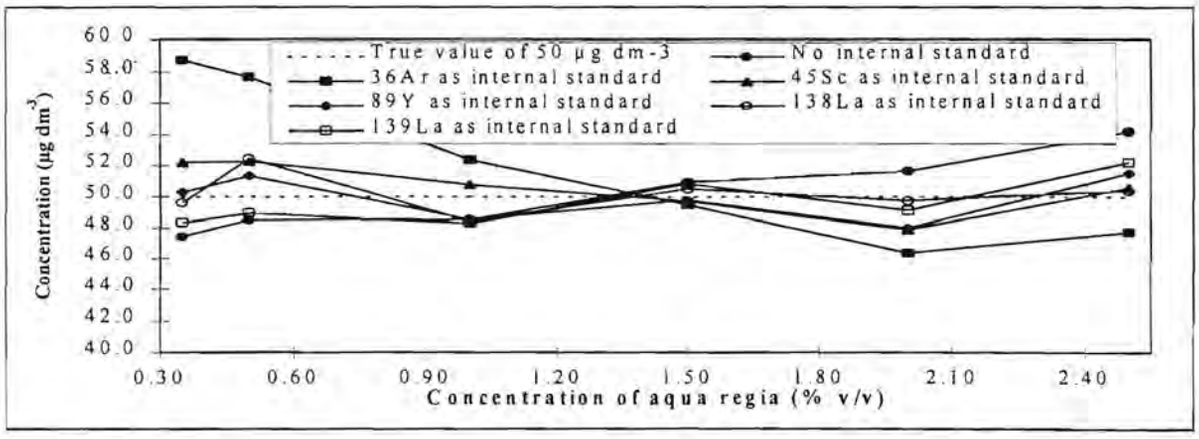

Figure 3.51: Effect of the concentration of aqua regia on the quantitative determination of Ru (as ^{100}Ru) using different internal standards.

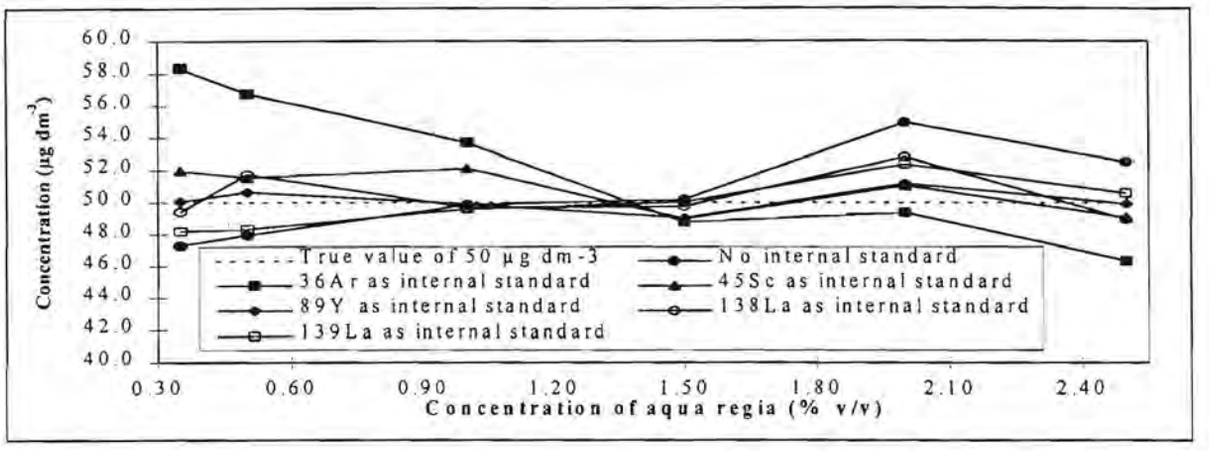

Figure 3.52: Effect of the concentration of aqua regia on the quantitative determination of Ru (as ^{101}Ru) using different internal standards.

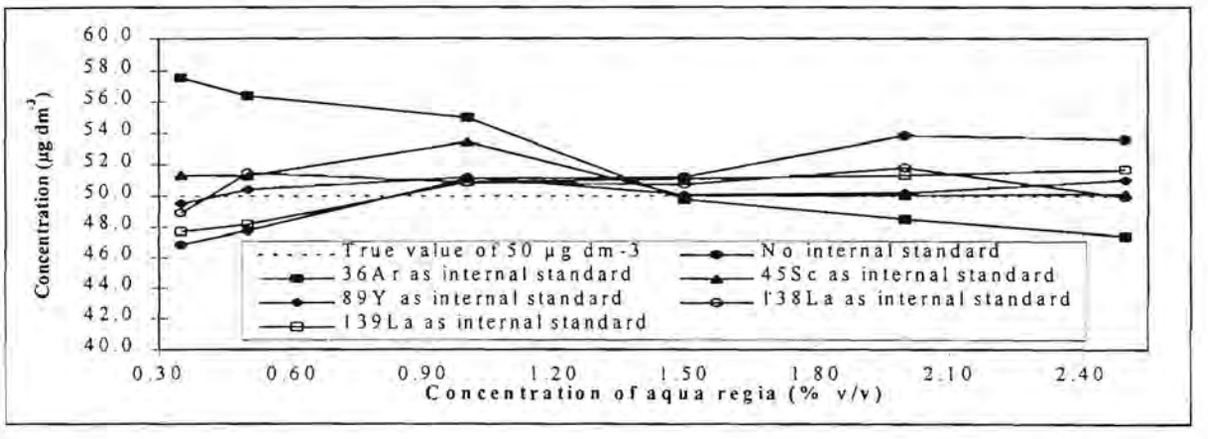

Figure 3.53: Effect of the concentration of aqua regia on the quantitative determination of Ru (as ^{102}Ru) using different internal standards.

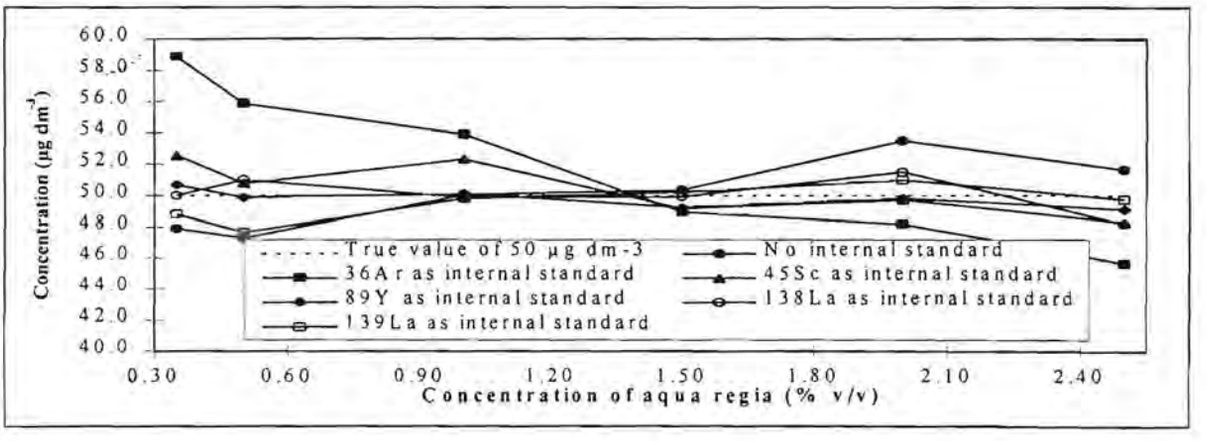

Figure 3.54: Effect of the concentration of aqua regia on the quantitative determination of Ru (as ^{104}Ru) using different internal standards.

^{36}Ar as internal standard returns too high and too low recovery values at lower and higher aqua regia concentrations, respectively. As internal standard ^{45}Sc returned values close to 50 μg dm^{-3} for ^{101}Ru and ^{102}Ru over the aqua regia concentration range studied. Except for ^{96}Ru and ^{98}Ru, ^{89}Y showed to be a good internal standard for the quantitative determination of Ru. For most isotopes of Ru, both the isotopes of La returned values fairly close to 50 μg dm^{-3} when used as internal standards.

3.4 Conclusion

As some drift was observed in the calibration curves of most of the isotopes of the platinum group elements and gold, it is necessary to employ one or more internal standards when performing quantitative analysis of these analytes.

Plots of the ratios of analyte isotopes to internal standard isotopes versus the aqua regia concentration present in solution showed: 1) ^{36}Ar not to be a possible internal standard, 2) ^{45}Sc to be a possible internal standard for Ru, Pd and Rh, 3) ^{89}Y to be possible internal standard for the lighter platinum group elements, 4) ^{138}La to be possible internal standard for the platinum group elements and gold and 5) ^{139}La to be a possible reference element for all the analytes investigated.

Calibration curves were constructed and very good regression data were obtained when ^{89}Y and ^{139}La were employed as reference elements for the platinum group elements and gold.

Quantitative values were calculated for the various calibration curves and from the results ^{139}La proved to be an excellent internal standard in the determination of Au, Ir, Pt and ^{89}Y proved to be a very good reference element for Ru, Pd, Rh. This confirms the need for the matching of the masses of the internal standards to the masses of the analytes analysed. The low abundant ^{192}Pt isotope returned values that deviated too much from the "true" value and should not be used in the quantitative determination of Pt.

CHAPTER 4

THE QUANTITATIVE DETERMINATION OF MONO-ISOTOPIC ARSENIC IN ACIDIC MATRICES

4.1 Introduction

4.1.1 Aspects of the toxicity of arsenic

Inorganic arsenics have a toxicity rating reported to be 100 times higher than in organic forms *[53]*. The clinical manifestations of arsenic overdose are polymorphous, in particular, digestive, cardiovascular, neurologic, cutaneous and renal *[54 - 58]*. In the case of acute suicidal arsenic intoxication death can occur one week after digestion, despite intensive care *[59]*. The trivalent derivates are more toxic than the pentavalent forms and soluble forms (arsenites and arsenates) are more toxic than nonsoluble forms *[53]*. At cell level, arsenic toxicity is mainly due to an inhibition of enzymatic cell reactions, through an effect on the sulphydryl groups in enzymes *[59]*. Gradual increasing tolerance to arsenic appears to be significant *[59]*. Further effects of arsenic on the body are discussed in detail in literature *[59]* .

4.1.2 Levels of arsenic in the human body

Cutaneous absorption is low except in the case of damaged skin *[60]*. Arsenic accumulates mainly in hair, nails and teeth *[59]*. Elimination is both through the digestive and urinary systems *[54]*.

Normal arsenic values in hair (from 4.55 mg $(100\ g)^{-1}$ to 33.08 mg $(100\ g)^{-1}$ depending on the type of hair), normal arsenic values in various body parts (levels ranging from 0.002 mg dm^{-3} to 0.3 mg dm^{-3} depending on the topography), values in cases of acute intoxications (ranged from 0.7 ng g^{-1} in the brain to 654.0 ng g^{-1} in the stomach) are reported in references *[61, 62]*. Blood toxic levels are quoted as $\geq$ 1 mg dm^{-3} and lethal blood levels as $\geq$ 10 mg dm^{-3} *[63]*. Normal "unexposed" values for arsenic content as reported by some researchers *[64 - 66]* are < 2 mg dm^{-3} in hair and < 1.5 mg dm^{-3} in nails. Arsenic concentrations in blood of normal subjects range from 0.002 to 0.062 g dm^{-3} according to Heydorn *[67]*.

Although arsenic poisoning is usually associated with foul play, these elements may be consumed in connection with cultural and lifestyle preferences as showed in an examination of traditional Chinese medicines *[68]*. The arsenic content in the herbal balls varied from 0.1 mg to 36.6 mg per ball where the masses of the balls varied from 2.5 g to 9.0 g. The prescribed adult dose of two balls daily leads to a maximum elemental intake of 73.2 mg arsenic. Chronic and acute arsenic poisoning of 74 traditional Chinese medicine consumers in Singapore was reported in 1975 *[69]*.

4.1.3 Techniques employed

Several techniques are commonly employed for the qualitative and quantitative determination of arsenic. Some of these include: the Gutzeit method and the Reinsch Test *[70 - 73]*, silver diethylcarbamate colorimetric method *[74]*, radioactive methods *[75]*, XRF *[68]*, AAS *[68]*, GFAAS *[59]*, ICP-AES *[76]* and ICP-MS *[77 - 81]*.

After they compared results obtained by AA and ICP-MS, Tanaka *et al. [77]* concluded that the sensitivity of AAS for arsenic determination is inferior to that of ICP-MS. Other workers showed the advantages of ICP-MS as compared to ICP-AES for the determination of arsenic *[82]*.

4.2 Polyatomic ion interferences

4.2.1 Characteristics of polyatomic ions

Compared to elemental isobaric overlap, polyatomic or adduct ions cause more serious problems to ICP-MS analysis. In this form of spectroscopic interference the polyatomic ions result from the short-lived combination of two or more atomic species. Argon, hydrogen and oxygen are the dominant species in the plasma and they may combine with one another or with elements in the analyte matrix to form polyatomic ions. Although the composition of the gas extracted from the plasma at the interface is effectively frozen within approximately 1μs of leaving the plasma, fast ion molecule reactions can occur between species present in the gas. Although a large number of polyatomic ions can form, they are only significantly detected below 82 *m/z [83]*.

A number of authors *[29, 30, 34, 84 - 86]* have examined the factors affecting the formation of polyatomic ion interferences; these include: extraction geometry, operating parameters for

plasma and nebuliser systems, specific instrument design and most importantly the acid and sample matrix.

The polyatomic ion peaks in both HNO_3 and H_2O_2 are identical to those identified in deionised water and these media are thus considered ideal matrices. Additional peaks are seen in the more complex spectra of HCl and H_2SO_4 matrices. Mono-isotopic arsenic has a mass of 75, the same mass as that at which the peak of the polyatomic ion $^{40}Ar^{35}Cl$ occurs.

4.2.2 *Possible procedures for the correction of polyatomic interferences*

Usually a correction may be made for the overlap of a polyatomic ion peak with an elemental peak, e.g. by using a reagent blank. However, these peaks may be relatively large compared to the analyte contribution at any given mass and a significant error may occur when a correction is applied *[83]*. In addition, polyatomic ion peaks are less stable than analyte ion peaks, introducing a further source of errors *[83]*.

Sakata and Kawabata *[84]* proposed the electrical decoupling of the plasma from the load coil (using a special device) and then changing the plasma conditions to attenuate ionisation of the polyatomic ions in order to effectively reduce the polyatomic ions. A high resolution ICP-MS was employed by Prohaska and co-workers and a separation of the peaks of $^{40}Ar^{35}Cl$ and As peak was obtained, that effectively rendered the As peak free from interference *[87]*. Some researchers *[78, 81]* used the $^{16}O^{35}Cl$ polyatomic ion to correct for chloride interference when determining As by means of ICP-MS. Other workers proposed a matrix matching technique which minimises differences in acidity and carbon loading in order to overcome the problem *[79]*. The addition of nitrogen to the aerosol carrier gas flow decreases the formation of the $^{40}Ar^{35}Cl$ polyatomic ion to negligible levels *[80, 88]*, but the nitrogen addition has the disadvantage of reducing analyte sensitivity *[89]*. Other workers developed a method of matrix elimination that facilitates determination of arsenic by means of ICP-MS without interference from polyatomic ions *[90]*. This method involves the retention of the analytes as anions on activated alumina (acidic form) in a microcolumn using an on-line flow injection system, with simultaneous matrix removal. Anderson and co-workers *[89]* suggested that hydride generation be employed as a means of eliminating chloride interferences while maintaining sufficient analyte sensitivity for the determination of arsenic by means of ICP-MS.

Since the problem of the $^{40}Ar^{35}Cl$ interference on ^{75}As is recognised by many ICP-MS users *[49, 91]*, many chose to work in a nitric acid matrix when determining arsenic *[49, 77, 82, 91]*.

4.3 Arsenic determinations in biological samples

Usually hair, nail and other biological samples are digested in nitric acid using a microwave method *[92 - 94]* and the resulting solutions can be used for ICP-MS determinations when very low levels of arsenic has to be determined. In the case of more indigestible inorganic samples hydrochloric acid also has to be employed in the sample preparation procedures. It is thus the aim of this work to investigate the determination of arsenic at $\mu g\ dm^{-3}$ levels in nitric acid and hydrochloric acid matrices. The effects of different correction procedures, similar to those proposed by Nixon, Lásztity and others *[81, 94]*, as well as internal standards on the quantitative determination of arsenic by ICP-MS will also be monitored.

The feasibility of using the following isotopes as internal standards in arsenic determination was investigated: ^{45}Sc, ^{89}Y, ^{139}La, ^{36}Ar, ^{35}Cl and ^{37}Cl. ^{45}Sc, ^{89}Y and ^{139}La were added to the solutions and ^{36}Ar, ^{35}Cl and ^{37}Cl were present due to the argon plasma and the nature of the matrices of the solutions. Table 4.1 shows the relevant data of arsenic and the internal standards investigated.

The determination of arsenic in the following acidic matrices were investigated: concentrations of HNO_3 ranging from 0.10% v/v to 2.50% v/v HNO_3, concentrations of HCl ranging from 0.10% v/v to 2.50% v/v, mixtures of HNO_3 and HCl with combined concentrations of 0.20% v/v to 2.00% v/v.

4.4 Experimental

4.4.1 Preparation of solutions

Table 4.2 shows the results of the calculations performed in order to prepare stock solutions of arsenic and the internal standards added. Table 4.3 shows the results of similar calculations for the preparation of arsenic calibration standards in 1.00% v/v HNO_3 and 20 $\mu g\ dm^{-3}$ arsenic samples in various acidic matrices. Arsenic calibration standards were prepared in the range from 0 to 100 $\mu g\ dm^{-3}$ and 20 $\mu g\ dm^{-3}$ arsenic sample solutions were prepared in matrices of 0.10% v/v to 2.50% v/v HNO_3 and HCl.

Table 4.1: Relevant data of arsenic and the internal standards investigated *[50]*.

Atomic no.	Element	Mass no.	Relative abundance	Atomic mass (g mol^{-1})	First ionisation potential (eV)	Second ionisation potential (eV)
17	Chlorine	35 37	75.53 24.47	35.453	13.02	23.80
18	Argon	36 38 40	0.337 0.063 99.600	39.948	15.76	27.63
21	Scandium	45	100.0	44.956	6.56	12.80
33	Arsenic	75	100.0	74.922	9.82	18.63
39	Yttrium	89	100.0	88.905	6.53	12.23
57	Lanthanum	138 139	0.089 99.911	138.91	5.61	11.06

A certified solution of As containing 1000 mg dm^{-3} of the element in 2.5% HNO_3 was employed for the preparation of the calibration and sample solutions (Spectrascan, Teknolab A/S, Dröbak, Norway). Certified solutions of Sc and Y each containing 1000 mg dm^{-3} of the element in 2.5% HCl were used (Spectrascan, Teknolab A/S, Dröbak, Norway). A certified solution of La containing 5000 mg dm^{-3} of the element in 2.5% HNO_3 was used for the preparation of a stock solution (Spectrascan, Teknolab A/S, Dröbak, Norway). A stock solution of La containing 1000 mg dm^{-3} of the element in 2.5% HNO_3 was prepared. High purity hydrochloric acid (> 32%) and nitric acid (> 65%) (Fluka) were used for the preparation of acidic solutions. High purity water with resistivity 18.2 MΩ cm (Millipore Corporation, United States of America) was used for dilutions.

All solutions were prepared in pre-conditioned plastic laboratory ware. A-grade pipettes and volume adjustable pipettes were used for the transfer of solutions. All solutions were transferred to clean PTFE holders which were placed on the sample rack of the autosampler of the instrument.

4.4.2 *Optimisation of the instrument*

The instrument was optimised as described in chapter 2. A warm-up time of three hours was allowed before any analyses were performed in order for instrumental conditions to equilibrate.

Table 4.2: Preparation of stock solutions of As, Sc, Y and La.

Element	[Element] in certified solution (mg dm^{-3})	[HNO_3] in certified solution (% v/v)	[HCl] in certified solution (% v/v)	[Element] in stock solution ($\mu g\ dm^{-3}$)	[HNO_3] in stock solution (% v/v)	[HCl] in stock solution (% v/v)	Volume of flask ($10^{-3}\ dm^3$)	Volume of certified solution to transfer ($10^{-3}\ dm^3$)	Volume of concentrated HNO_3 to add ($10^{-3}\ dm^3$)	Volume concentrated HCl to add ($10^{-3}\ dm^3$)
As	1000	2.50	0.00	1000	1.00	0.00	1000	1.00	9.98	0.00
La	1000	2.50	0.00							
Y	1000	0.00	2.50							
Sc	1000	0.00	2.50							
Internal standards (i.s.)				10000	1.00	1.00	500	5.00	4.88	4.75

Table 4.3: Preparation of A.: Arsenic calibration standards with internal standards in 1.00% v/v HNO_3,
B.1: 20 μg dm^{-3} arsenic sample solutions to study the effects of HNO_3,
B.2: 20 μg dm^{-3} arsenic sample solutions to study the effects of HCl and
B.3: 20 μg dm^{-3} arsenic sample solutions to study the effects of HNO_3 and HCl on the quantitative analysis of arsenic.

	[As] (μg dm^{-3})	Volume of flask (10^{-3} dm^3)	[HNO_3] (% v/v)	[HCl] (% v/v)	Volume of As to transfer (10^{-3} dm^3)	[internal standard] (μg dm^{-3})	Volume of internal standard solution to transfer (10^{-3} dm^3)	Volume of concentrated HNO_3 to add (10^{-3} dm^3)	Volume of concentrated HCl to add (10^{-3} dm^3)
A.	0	100	1.00	0.00	0.00	100	1.00	0.99	0.00
	5	100	1.00	0.00	0.50	100	1.00	0.99	0.00
	10	100	1.00	0.00	1.00	100	1.00	0.98	0.00
	20	100	1.00	0.00	2.00	100	1.00	0.97	0.00
	50	100	1.00	0.00	5.00	100	1.00	0.94	0.00
	100	100	1.00	0.00	10.00	100	1.00	0.89	0.00
B.1	20	100	0.10	0.00	2.00	100	1.00	0.07	0.00
	20	100	0.50	0.00	2.00	100	1.00	0.47	0.00
	20	100	1.00	0.00	2.00	100	1.00	0.97	0.00
	20	100	1.50	0.00	2.00	100	1.00	1.47	0.00
	20	100	2.00	0.00	2.00	100	1.00	1.97	0.00
	20	100	2.50	0.00	2.00	100	1.00	2.47	0.00
B.2	20	100	0.00	0.10	2.00	100	1.00	0.00	0.08
	20	100	0.00	0.50	2.00	100	1.00	0.00	0.48
	20	100	0.00	1.00	2.00	100	1.00	0.00	0.98
	20	100	0.00	1.50	2.00	100	1.00	0.00	1.48
	20	100	0.00	2.00	2.00	100	1.00	0.00	1.98
	20	100	0.00	2.50	2.00	100	1.00	0.00	2.48
B.3	20	100	0.10	0.10	2.00	100	1.00	0.07	0.08
	20	100	0.50	0.50	2.00	100	1.00	0.47	0.48
	20	100	1.00	1.00	2.00	100	1.00	0.97	0.98

Table 4.4: Operating conditions of the inductively coupled plasma mass spectrometer and settings for data acquisition.

Instrument	Spectromass-ICP
Torch	Fassel
Spray chamber	Scott-type double-pass
Nebuliser	Meinhard
Sampler cone	Ni with diameter approximately 1 mm
Skimmer cone	Ni with diameter approximately 1 mm
RF power	1350 W
Coolant argon gas flow rate	16 dm^3 min^{-1}
Auxiliary argon gas flow rate	1.5 dm^3 min^{-1}
Aerosol carrier argon gas flow rate	0.96 dm^3 min^{-1}
Sample introduction	$1.0x10^{-3}$ dm^3 min^{-1}
Dwell time	1 s
Resolution	Normal
Readings per measurement	6
Rinse time with water between samples to avoid contamination	180 s
Total pre-flush time with sample before measurement	120 s (of which the first 20 s was set at an uptake rate of approximately $3x10^{-3}$ dm^3 min^{-1})
Isotopes / masses monitored	^{35}Cl, ^{37}Cl, ^{36}Ar, ^{45}Sc, ^{89}Y, ^{139}La, mass 75, mass 77

4.4.3 *Mass scans of arsenic and the internal standards in the various acidic matrices*

Various mass scans of 20 μg dm^{-3} As in different acidic media were measured. They were performed in order to verify the validity of 1) the isotopic ratios used and 2) the mass calibration of the instrument.

4.4.4 *Data acquisition*

The intensities of the various isotopes of the internal standards and arsenic were measured. The data was then used to construct calibration curves and perform quantitative analysis of the arsenic. The operating conditions of the inductively coupled plasma mass spectrometer and

settings for data acquisition are listed in table 4.4.

4.5 Results and discussion

4.5.1 Mass scans of a 20 μg dm^{-3} As solution in various acidic media

From figure 4.1 it can be seen that there is an increase in the intensities recorded for the isotopes of chlorine when the matrix contains a small amount of chloride. From figures 4.1 to 4.4 it can be seen that the intensities of ^{36}Ar, ^{45}Sc, ^{89}Y and ^{139}La are not affected by a change in the matrix. Figure 4.5 clearly shows the effect that a chloride containing matrix has on the intensity of the ^{75}As isotope as $^{40}Ar^{35}Cl$ forms.

From figures 4.1 to 4.5 it can also be seen that the theoretical relative abundance values correspond to the experimental values obtained thus confirming the validity of the mass calibration of the instrument.

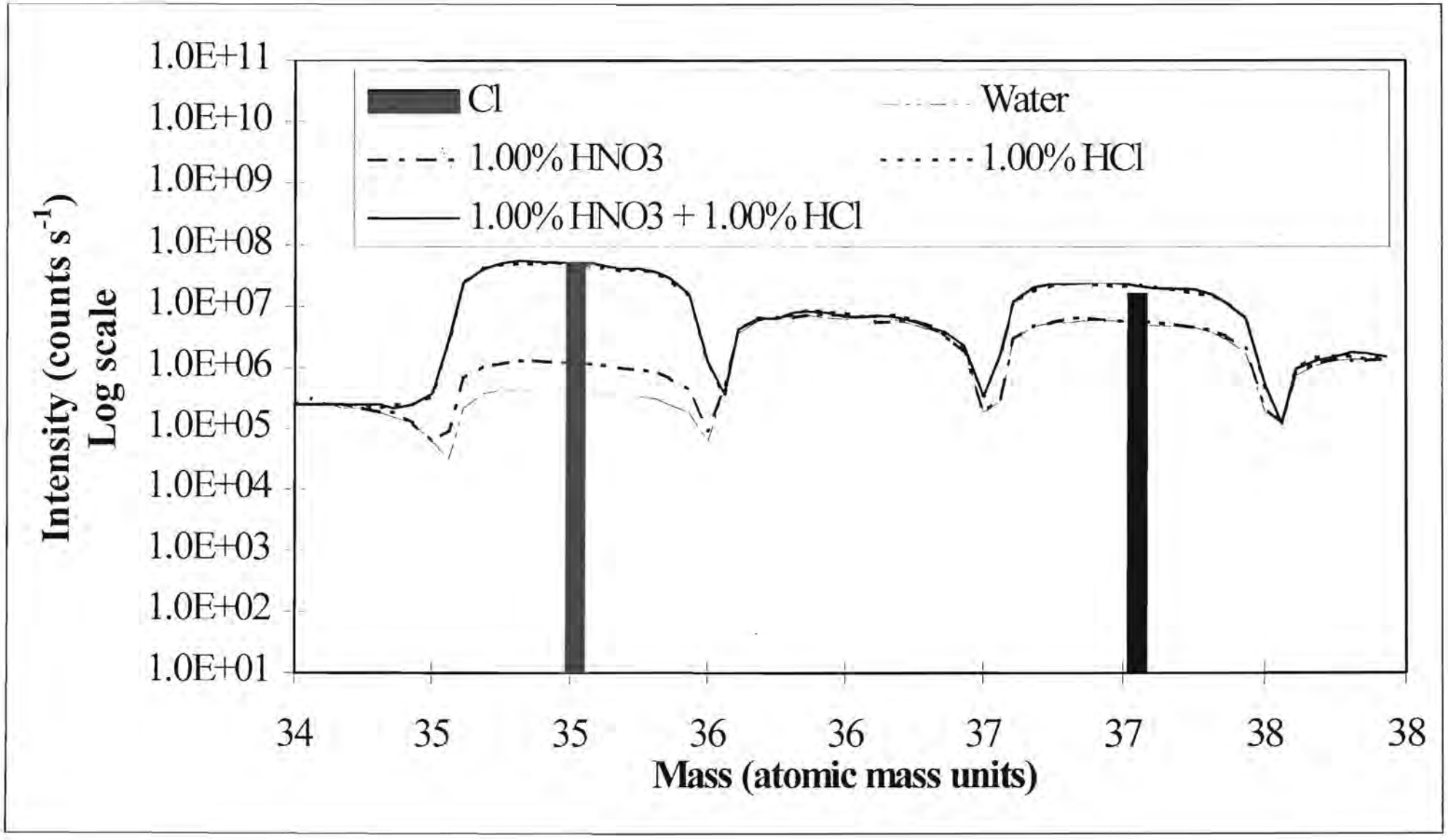

Figure 4.1: Mass scan of a solution containing 20 μg dm^{-3} As in various acidic matrices. The theoretical relative abundances of the ^{35}Cl and ^{37}Cl isotopes are shown.

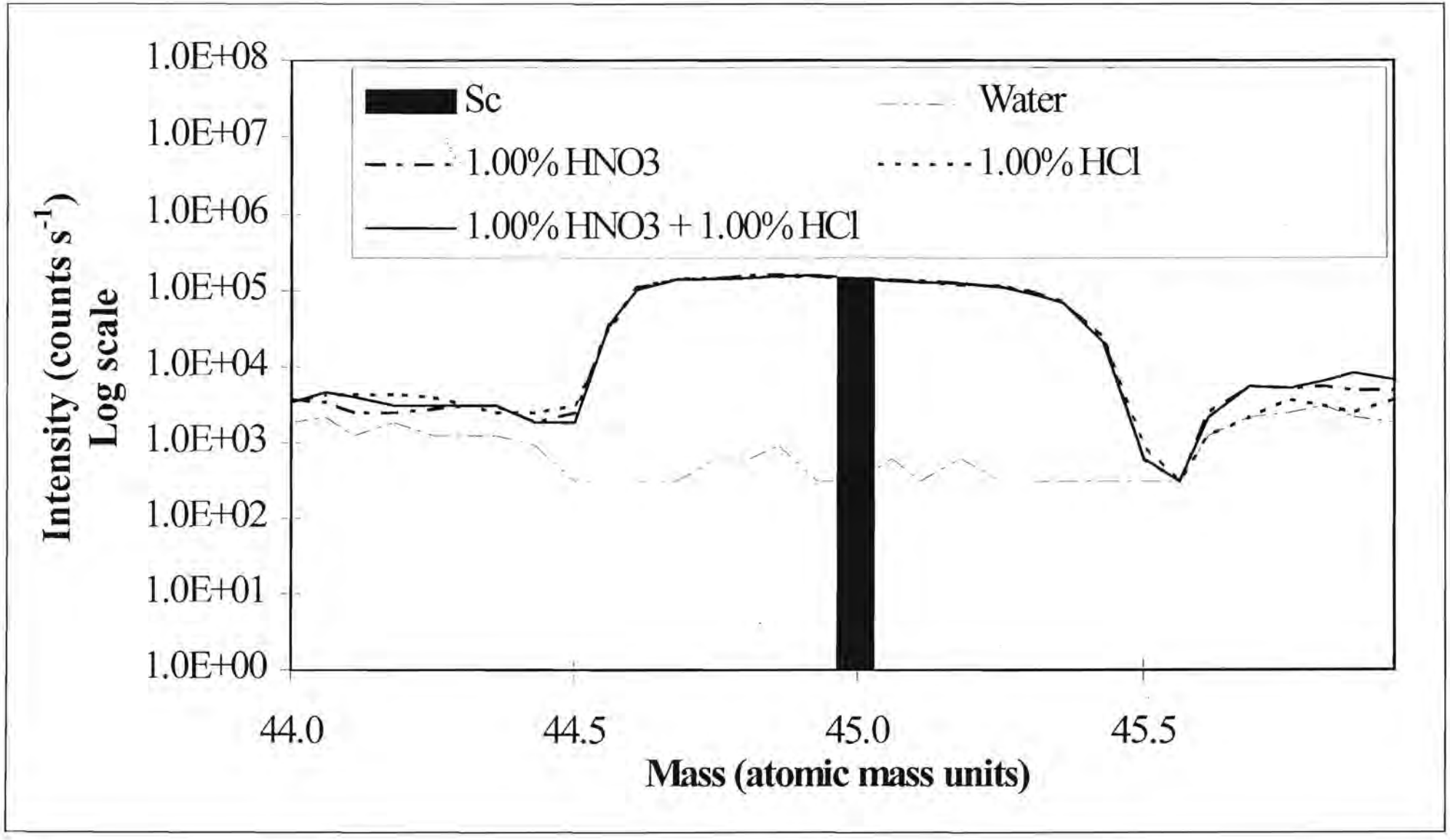

Figure 4.2: Mass scan of a solution containing 20 μg dm^{-3} As in various acidic matrices. The theoretical relative abundance of the ^{45}Sc isotope is shown.

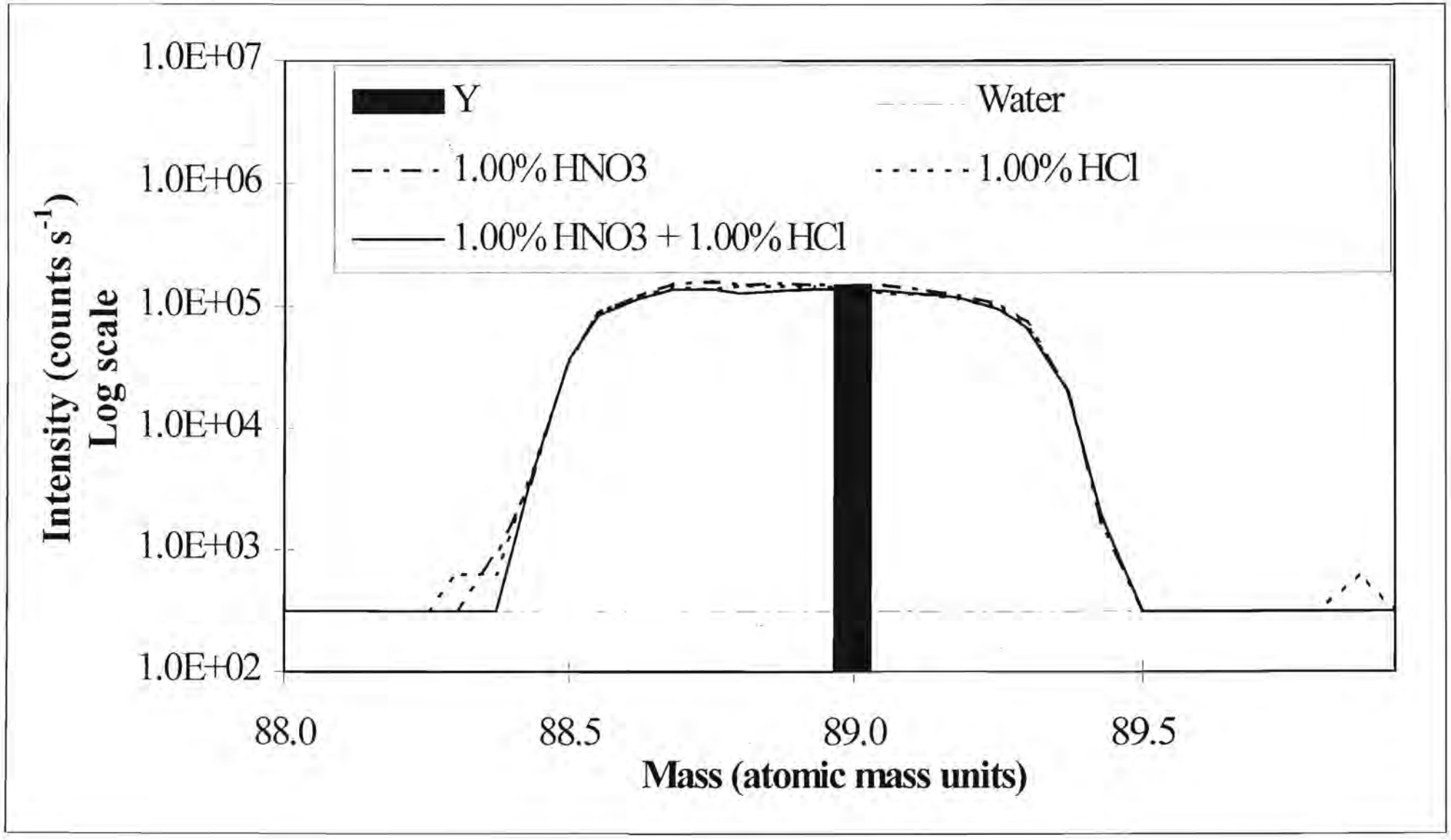

Figure 4.3: Mass scan of a solution containing 20 μg dm^{-3} As in various acidic matrices. The theoretical relative abundance of the ^{89}Y isotope is shown.

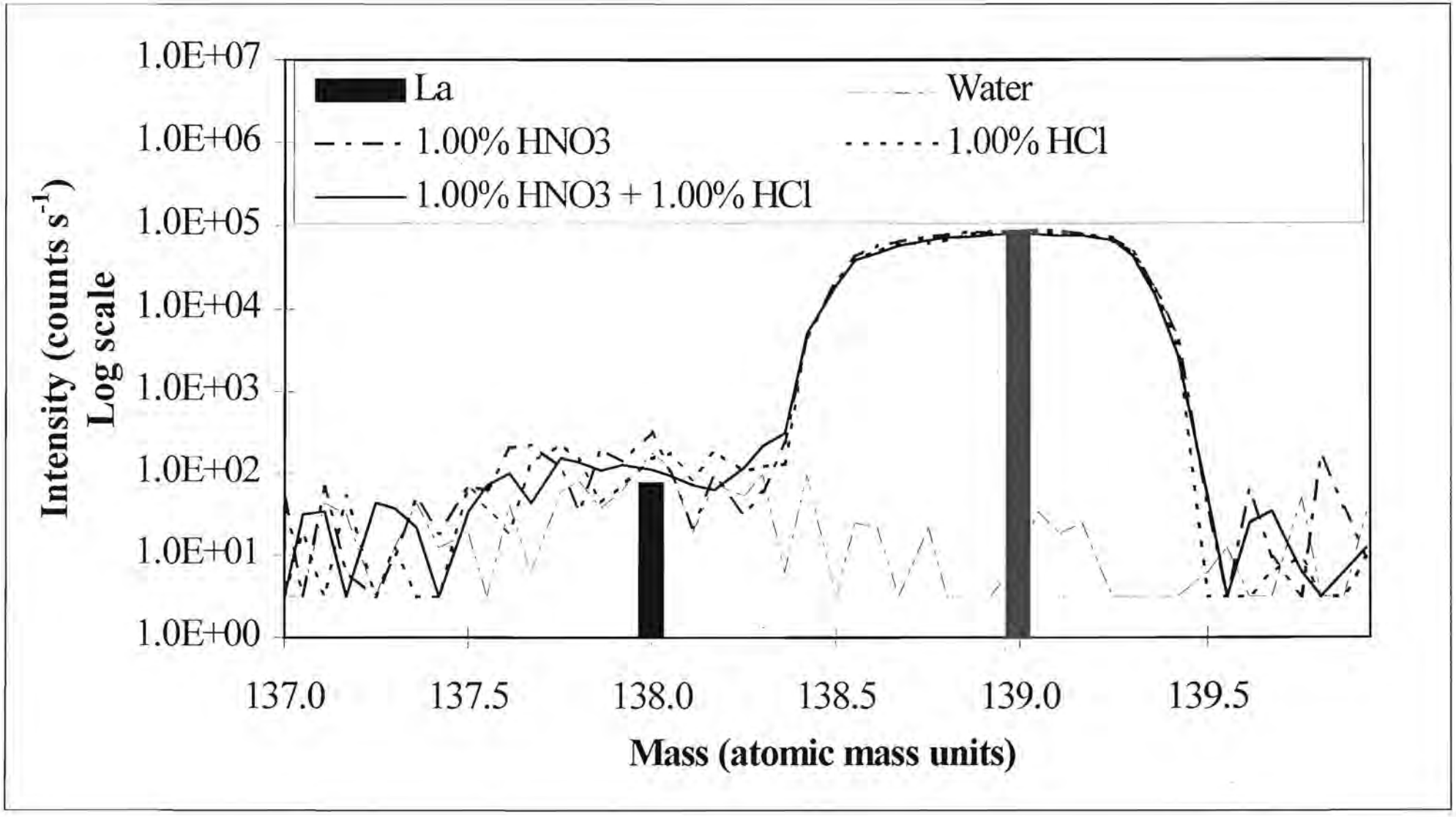

Figure 4.4: Mass scan of a solution containing 20 μg dm^{-3} As in various acidic matrices. The theoretical relative abundances of the ^{138}La and ^{139}La isotopes are shown.

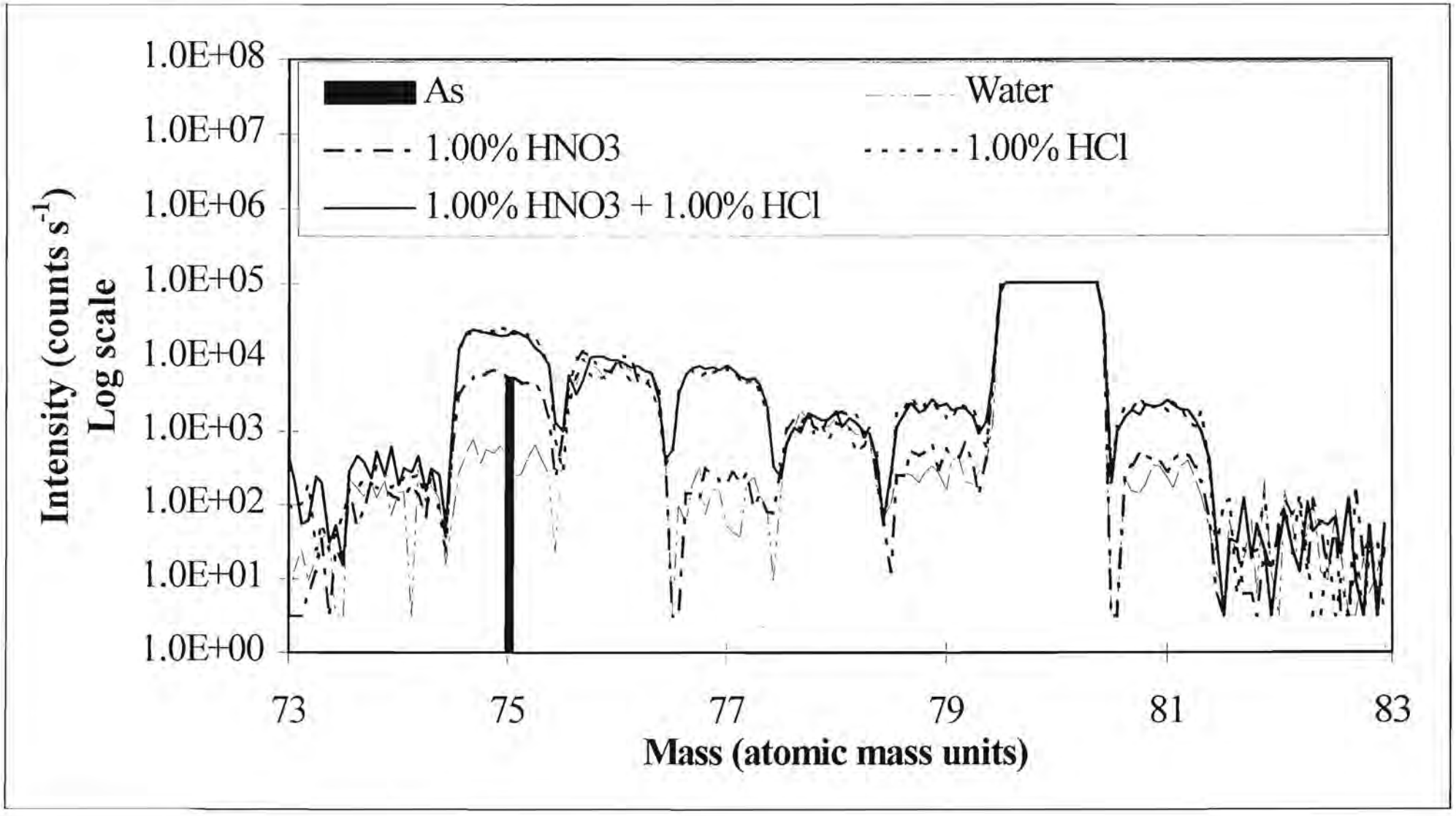

Figure 4.5: Mass scan of a solution containing 20 μg dm^{-3} As in various acidic matrices. The theoretical relative abundance of the ^{75}As isotope is shown.

4.5.2 Analysis without employing correction factors

As it is known that in inductively coupled plasma spectrometry a drift in the values with time occurs, it was decided to monitor such instrumental drift and to correct the values obtained from analysis for such drift. The following procedure was followed: A solution of 20 μg dm^{-3} As in 1.00% v/v HNO_3 was used to monitor the drift of the instrument with time. This solution was analysed at regular intervals during the course of the experimental run. The time difference from the analysis of the first sample was recorded in each case. First and second order mathematical curves were then fitted to the data and the obtained equations were then used to correct all the values for any time drift phenomena.

No internal standard

Calibration with the six calibration standards yielded a calibration curve with a correlation coefficient of 0.9999 and a detection limit of 0.996 μg dm^{-3} As. The results of the analysis of the prepared samples, the first and second order mathematical functions, which fitted the data of the drift control sample, and the results after drift correction was applied, can be seen in table 4.5.

It can be seen from the results that in the absence of hydrochloric acid the concentration of the nitric acid in the matrix had no effect on the analysis of the arsenic in solution. Values of approximately 20 μg dm^{-3} were obtained in matrices containing nitric acid from 0.10% v/v to 2.50% v/v. As expected the hydrochloric acid containing matrices yielded unacceptable high values.

Table 4.5: Results of quantitative determination of As using the intensities of the calibration standards for calibration. No internal standard was used. Results are also shown for time drift corrected values. First order equation used: ($y = 0.0351x + 19.435$) and second order equation used: ($y = -0.0002x^2 + 0.0875x + 16.681$)

Time difference (minutes)	**Sample name**	**[As] (μg dm^{-3})**	**Corrected with first order drift curve (μg dm^{-3})**	**Corrected with second order drift curve (μg dm^{-3})**
44.57	Drift control - 20 μg dm^{-3} As	20.12	19.17	19.86
51.83	20 μg dm^{-3} As in 0.10% v/v HNO_3	19.73	18.57	18.99

Time difference (minutes)	Sample name	[As] (μg dm^{-3})	Corrected with first order drift curve (μg dm^{-3})	Corrected with second order drift curve (μg dm^{-3})
59.10	20 μg dm^{-3} As in 0.50% v/v HNO_3	20.70	19.24	19.44
66.42	20 μg dm^{-3} As in 1.00% v/v HNO_3	20.95	19.25	19.23
73.68	20 μg dm^{-3} As in 1.50% v/v HNO_3	20.95	19.02	18.82
80.95	20 μg dm^{-3} As in 2.00% v/v HNO_3	20.10	18.05	17.70
88.22	20 μg dm^{-3} As in 2.50% v/v HNO_3	20.99	18.63	18.13
142.48	20 μg dm^{-3} As in 0.10% v/v HCl	40.02	32.76	30.90
149.82	20 μg dm^{-3} As in 0.50% v/v HCl	126.81	102.70	96.80
157.18	20 μg dm^{-3} As in 1.00% v/v HCl	235.23	188.54	177.65
164.55	20 μg dm^{-3} As in 1.50% v/v HCl	327.20	259.57	244.66
171.92	20 μg dm^{-3} As in 2.00% v/v HCl	429.43	337.21	318.15
179.30	20 μg dm^{-3} As in 2.50% v/v HCl	515.49	400.71	378.67
188.58	Drift control - 20 μg dm^{-3} As	28.69	22.02	20.87
220.02	20 μg dm^{-3} As in (0.10% v/v HNO_3 + 0.10% v/v HCl)	45.43	33.46	32.23
227.40	20 μg dm^{-3} As in (0.50% v/v HNO_3 + 0.50% v/v HCl)	151.83	110.76	107.28
234.78	20 μg dm^{-3} As in (1.00% v/v HNO_3 + 1.00% v/v HCl)	268.09	193.73	188.76
244.08	Drift control - 20 μg dm^{-3} As	26.79	19.13	18.80
296.78	Drift control - 20 μg dm^{-3} As	29.31	19.64	20.53

^{45}Sc, ^{89}Y and ^{139}La as internal standards

The calibration curve obtained when using ^{45}Sc as internal standard yielded a correlation coefficient of 0.9999 and a detection limit of 1.066 μg dm^{-3} As. In the case of ^{89}Y as internal standard a correlation coefficient of 0.9999 was obtained with a detection limit of 0.887 μg dm^{-3} As. For ^{139}La the correlation coefficient was also 0.9999 and the detection limit was calculated

to be 1.010 μg dm^{-3} As. The results of the analysis as well as the time drift corrected values can be seen in tables 4.6 to 4.8.

In all three cases the matrices containing only nitric acid resulted in acceptable values of approximately 20 μg dm^{-3}, while the hydrochloric acid containing matrices resulted in unacceptably high values.

Table 4.6: Results of quantitative determination of As using ^{45}Sc as internal standard. Results are also shown for time drift corrected values. First order equation used: ($y = 0.0138x + 19.097$) and second order equation used: ($y = -0.0001x^2 + 0.0489x + 17.255$)

Time difference (minutes)	**Sample name**	**[As] (μg dm^{-3})**	**Corrected with first order drift curve (μg dm^{-3})**	**Corrected with second order drift curve (μg dm^{-3})**
44.57	Drift control - 20 μg dm^{-3} As	19.11	19.39	19.89
51.83	20 μg dm^{-3} As in 0.10% v/v HNO_3	18.45	18.62	18.92
59.10	20 μg dm^{-3} As in 0.50% v/v HNO_3	19.62	19.70	19.84
66.42	20 μg dm^{-3} As in 1.00% v/v HNO_3	19.34	19.33	19.31
73.68	20 μg dm^{-3} As in 1.50% v/v HNO_3	19.48	19.37	19.21
80.95	20 μg dm^{-3} As in 2.00% v/v HNO_3	19.10	18.90	18.62
88.22	20 μg dm^{-3} As in 2.50% v/v HNO_3	19.92	19.62	19.22
142.48	20 μg dm^{-3} As in 0.10% v/v HCl	33.44	31.75	30.33
149.82	20 μg dm^{-3} As in 0.50% v/v HCl	107.49	101.57	96.92
157.18	20 μg dm^{-3} As in 1.00% v/v HCl	198.93	187.09	178.43
164.55	20 μg dm^{-3} As in 1.50% v/v HCl	272.73	255.27	243.46
171.92	20 μg dm^{-3} As in 2.00% v/v HCl	347.81	324.01	309.18
179.30	20 μg dm^{-3} As in 2.50% v/v HCl	414.84	384.62	367.39
188.58	Drift control - 20 μg dm^{-3} As	23.59	21.75	20.81

Time difference (minutes)	Sample name	[As] (μg dm^{-3})	Corrected with first order drift curve (μg dm^{-3})	Corrected with second order drift curve (μg dm^{-3})
220.02	20 μg dm^{-3} As in (0.10% v/v HNO_3 + 0.10% v/v HCl)	36.71	33.17	32.15
227.40	20 μg dm^{-3} As in (0.50% v/v HNO_3 + 0.50% v/v HCl)	123.26	110.87	107.92
234.78	20 μg dm^{-3} As in (1.00% v/v HNO_3 + 1.00% v/v HCl)	221.72	198.53	194.17
244.08	Drift control - 20 μg dm^{-3} As	21.47	19.12	18.82
296.78	Drift control - 20 μg dm^{-3} As	22.91	19.76	20.51

Table 4.7: Results of quantitative determination of As using ^{89}Y as internal standard. Results are also shown for time drift corrected values. First order equation used: ($y = 0.0223x + 18.810$) and second order equation used: ($y = -0.0001x^2 + 0.0679x + 16.414$)

Time difference (minutes)	Sample name	[As] (μg dm^{-3})	Corrected with first order drift curve (μg dm^{-3})	Corrected with second order drift curve (μg dm^{-3})
44.57	Drift control - 20 μg dm^{-3} As	19.07	19.26	19.90
51.83	20 μg dm^{-3} As in 0.10% v/v HNO_3	18.64	18.67	19.06
59.10	20 μg dm^{-3} As in 0.50% v/v HNO_3	20.03	19.91	20.09
66.42	20 μg dm^{-3} As in 1.00% v/v HNO_3	19.37	19.09	19.07
73.68	20 μg dm^{-3} As in 1.50% v/v HNO_3	19.75	19.31	19.11
80.95	20 μg dm^{-3} As in 2.00% v/v HNO_3	19.15	18.57	18.23
88.22	20 μg dm^{-3} As in 2.50% v/v HNO_3	19.92	19.18	18.69
142.48	20 μg dm^{-3} As in 0.10% v/v HCl	35.79	32.55	30.76
149.82	20 μg dm^{-3} As in 0.50% v/v HCl	120.47	108.78	102.68
157.18	20 μg dm^{-3} As in 1.00% v/v HCl	233.19	209.00	197.18
164.55	20 μg dm^{-3} As in 1.50% v/v HCl	322.11	286.59	270.42
171.92	20 μg dm^{-3} As in 2.00% v/v HCl	423.95	374.45	353.60

Time difference (minutes)	Sample name	[As] (μg dm^{-3})	Corrected with first order drift curve (μg dm^{-3})	Corrected with second order drift curve (μg dm^{-3})
179.30	20 μg dm^{-3} As in 2.50% v/v HCl	510.18	447.36	423.04
188.58	Drift control - 20 μg dm^{-3} As	25.07	21.79	20.66
220.02	20 μg dm^{-3} As in (0.10% v/v HNO_3 + 0.10% v/v HCl)	41.16	34.71	33.43
227.40	20 μg dm^{-3} As in (0.50% v/v HNO_3 + 0.50% v/v HCl)	140.89	117.99	114.23
234.78	20 μg dm^{-3} As in (1.00% v/v HNO_3 + 1.00% v/v HCl)	260.14	216.37	210.69
244.08	Drift control - 20 μg dm^{-3} As	23.57	19.44	19.08
296.78	Drift control - 20 μg dm^{-3} As	24.82	19.52	20.41

Table 4.8: Results of quantitative determination of As using ^{139}La as internal standard. Results are also shown for time drift corrected values. First order equation used: ($y = 0.0292x + 18.726$) and second order equation used: ($y = -0.0002x^2 + 0.0824x + 15.932$)

Time difference (minutes)	Sample name	[As] (μg dm^{-3})	Corrected with first order drift curve (μg dm^{-3})	Corrected with second order drift curve (μg dm^{-3})
44.57	Drift control - 20 μg dm^{-3} As	19.17	19.14	19.88
51.83	20 μg dm^{-3} As in 0.10% v/v HNO_3	19.31	19.08	19.54
59.10	20 μg dm^{-3} As in 0.50% v/v HNO_3	20.22	19.77	19.98
66.42	20 μg dm^{-3} As in 1.00% v/v HNO_3	19.50	18.87	18.85
73.68	20 μg dm^{-3} As in 1.50% v/v HNO_3	19.81	18.98	18.76
80.95	20 μg dm^{-3} As in 2.00% v/v HNO_3	19.32	18.33	17.94
88.22	20 μg dm^{-3} As in 2.50% v/v HNO_3	20.16	18.92	18.37
142.48	20 μg dm^{-3} As in 0.10% v/v HCl	37.64	32.89	30.87
149.82	20 μg dm^{-3} As in 0.50% v/v HCl	130.66	113.13	106.06
157.18	20 μg dm^{-3} As in 1.00% v/v HCl	261.15	224.01	209.91

Time difference (minutes)	Sample name	[As] (μg dm^{-3})	Corrected with first order drift curve (μg dm^{-3})	Corrected with second order drift curve (μg dm^{-3})
164.55	20 μg dm^{-3} As in 1.50% v/v HCl	360.85	306.70	287.48
171.92	20 μg dm^{-3} As in 2.00% v/v HCl	481.37	405.44	380.38
179.30	20 μg dm^{-3} As in 2.50% v/v HCl	599.61	500.48	470.32
188.58	Drift control - 20 μg dm^{-3} As	26.70	22.04	20.77
220.02	20 μg dm^{-3} As in (0.10% v/v HNO_3 + 0.10% v/v HCl)	43.98	34.97	33.55
227.40	20 μg dm^{-3} As in (0.50% v/v HNO_3 + 0.50% v/v HCl)	156.97	123.76	119.40
234.78	20 μg dm^{-3} As in (1.00% v/v HNO_3 + 1.00% v/v HCl)	297.13	232.30	225.54
244.08	Drift control - 20 μg dm^{-3} As	24.94	19.30	18.90
296.78	Drift control - 20 μg dm^{-3} As	26.73	19.51	20.47

^{36}Ar, ^{35}Cl and ^{37}Cl as internal standards

Correlation coefficients of 0.9999 were obtained when using the ^{36}Ar and ^{37}Cl isotopes as internal standards. In the case of ^{35}Cl the correlation coefficient was 1.0000. The detection limits were calculated to be 1.062 μg dm^{-3} As, 0.493 μg dm^{-3} As and 1.057 μg dm^{-3} As in the cases of ^{36}Ar, ^{35}Cl and ^{37}Cl. The results of the analysis can be seen in tables 4.9 to 4.11.

For ^{36}Ar slightly lower values than 20 μg dm^{-3} were obtained in the case of matrices only containing various amounts of nitric acid, but after drift correction was applied acceptable values were obtained. In the case of ^{35}Cl, values of approximately 20 μg dm^{-3} were obtained for matrices containing only nitric acid, but after drift correction, values higher than 20 μg dm^{-3} were mostly obtained. ^{37}Cl as internal standard yielded values of approximately 20 μg dm^{-3} for acidic matrices not containing hydrochloric acid.

In all the cases with all three the internal standards, unacceptable values were obtained when hydrochloric acid was present in the matrix.

Table 4.9: Results of quantitative determination of As using ^{36}Ar as internal standard. Results are also shown for time drift corrected values. First order equation used: ($y = -0.0038x + 19.008$) and second order equation used: ($y = -6x10^{-5}x^2 + 0.016x + 17.969$)

Time difference (minutes)	Sample name	[As] ($\mu g\ dm^{-3}$)	Corrected with first order drift curve ($\mu g\ dm^{-3}$)	Corrected with second order drift curve ($\mu g\ dm^{-3}$)
44.57	Drift control - 20 $\mu g\ dm^{-3}$ As	18.47	19.61	19.90
51.83	20 $\mu g\ dm^{-3}$ As in 0.10% v/v HNO_3	17.18	18.26	18.43
59.10	20 $\mu g\ dm^{-3}$ As in 0.50% v/v HNO_3	18.02	19.19	19.27
66.42	20 $\mu g\ dm^{-3}$ As in 1.00% v/v HNO_3	18.04	19.24	19.23
73.68	20 $\mu g\ dm^{-3}$ As in 1.50% v/v HNO_3	17.85	19.06	18.96
80.95	20 $\mu g\ dm^{-3}$ As in 2.00% v/v HNO_3	17.15	18.34	18.18
88.22	20 $\mu g\ dm^{-3}$ As in 2.50% v/v HNO_3	18.28	19.57	19.32
142.48	20 $\mu g\ dm^{-3}$ As in 0.10% v/v HCl	29.70	32.17	31.21
149.82	20 $\mu g\ dm^{-3}$ As in 0.50% v/v HCl	92.60	100.44	97.37
157.18	20 $\mu g\ dm^{-3}$ As in 1.00% v/v HCl	159.76	173.55	168.15
164.55	20 $\mu g\ dm^{-3}$ As in 1.50% v/v HCl	212.49	231.19	223.95
171.92	20 $\mu g\ dm^{-3}$ As in 2.00% v/v HCl	268.59	292.67	283.53
179.30	20 $\mu g\ dm^{-3}$ As in 2.50% v/v HCl	300.65	328.11	318.00
188.58	Drift control - 20 $\mu g\ dm^{-3}$ As	19.65	21.49	20.85
220.02	20 $\mu g\ dm^{-3}$ As in (0.10% v/v HNO_3 + 0.10% v/v HCl)	30.91	34.02	33.26
227.40	20 $\mu g\ dm^{-3}$ As in (0.50% v/v HNO_3 + 0.50% v/v HCl)	100.96	111.29	109.12
234.78	20 $\mu g\ dm^{-3}$ As in (1.00% v/v HNO_3 + 1.00% v/v HCl)	173.39	191.42	188.28
244.08	Drift control - 20 $\mu g\ dm^{-3}$ As	17.09	18.91	18.68
296.78	Drift control - 20 $\mu g\ dm^{-3}$ As	17.90	20.03	20.54

Table 4.10: Results of quantitative determination of As using ^{35}Cl as internal standard. Results are also shown for time drift corrected values. First order equation used: ($y = -0.040x + 19.880$) and second order equation used: ($y = 0.0003x^2 - 0.1458x + 25.435$)

Time difference (minutes)	Sample name	[As] ($\mu g\ dm^{-3}$)	Corrected with first order drift curve ($\mu g\ dm^{-3}$)	Corrected with second order drift curve ($\mu g\ dm^{-3}$)
44.57	Drift control - 20 $\mu g\ dm^{-3}$ As	19.81	21.89	20.24
51.83	20 $\mu g\ dm^{-3}$ As in 0.10% v/v HNO_3	19.43	21.82	20.73
59.10	20 $\mu g\ dm^{-3}$ As in 0.50% v/v HNO_3	20.08	22.93	22.38
66.42	20 $\mu g\ dm^{-3}$ As in 1.00% v/v HNO_3	19.85	23.05	23.11
73.68	20 $\mu g\ dm^{-3}$ As in 1.50% v/v HNO_3	20.30	23.97	24.69
80.95	20 $\mu g\ dm^{-3}$ As in 2.00% v/v HNO_3	19.59	23.54	24.89
88.22	20 $\mu g\ dm^{-3}$ As in 2.50% v/v HNO_3	20.36	24.91	27.01
142.48	20 $\mu g\ dm^{-3}$ As in 0.10% v/v HCl	2.16	3.04	3.86
149.82	20 $\mu g\ dm^{-3}$ As in 0.50% v/v HCl	0.14	0.20	0.26
157.18	20 $\mu g\ dm^{-3}$ As in 1.00% v/v HCl	-0.17	-0.25	-0.32
164.55	20 $\mu g\ dm^{-3}$ As in 1.50% v/v HCl	-0.42	-0.63	-0.82
171.92	20 $\mu g\ dm^{-3}$ As in 2.00% v/v HCl	-0.47	-0.72	-0.95
179.30	20 $\mu g\ dm^{-3}$ As in 2.50% v/v HCl	-0.60	-0.94	-1.24
188.58	Drift control - 20 $\mu g\ dm^{-3}$ As	7.47	12.12	15.92
220.02	20 $\mu g\ dm^{-3}$ As in (0.10% v/v HNO_3 + 0.10% v/v HCl)	2.67	4.82	5.98
227.40	20 $\mu g\ dm^{-3}$ As in (0.50% v/v HNO_3 + 0.50% v/v HCl)	0.46	0.85	1.02
234.78	20 $\mu g\ dm^{-3}$ As in (1.00% v/v HNO_3 + 1.00% v/v HCl)	0.03	0.06	0.07
244.08	Drift control - 20 $\mu g\ dm^{-3}$ As	11.87	23.47	26.29
296.78	Drift control - 20 $\mu g\ dm^{-3}$ As	9.37	23.39	17.80

Table 4.11: Results of quantitative determination of As using ^{37}Cl as internal standard. Results are also shown for time drift corrected values. First order equation used: ($y = 0.0072x + 18.948$) and second order equation used: ($y = -3x10^{-5}x^2 + 0.0185x + 18.353$)

Time difference (minutes)	Sample name	[As] ($\mu g\ dm^{-3}$)	Corrected with first order drift curve ($\mu g\ dm^{-3}$)	Corrected with second order drift curve ($\mu g\ dm^{-3}$)
44.57	Drift control - 20 $\mu g\ dm^{-3}$ As	19.06	19.78	19.94
51.83	20 $\mu g\ dm^{-3}$ As in 0.10% v/v HNO_3	18.69	19.35	19.44
59.10	20 $\mu g\ dm^{-3}$ As in 0.50% v/v HNO_3	19.11	19.73	19.76
66.42	20 $\mu g\ dm^{-3}$ As in 1.00% v/v HNO_3	18.96	19.52	19.49
73.68	20 $\mu g\ dm^{-3}$ As in 1.50% v/v HNO_3	18.72	19.22	19.14
80.95	20 $\mu g\ dm^{-3}$ As in 2.00% v/v HNO_3	17.82	18.25	18.14
88.22	20 $\mu g\ dm^{-3}$ As in 2.50% v/v HNO_3	18.56	18.96	18.80
142.48	20 $\mu g\ dm^{-3}$ As in 0.10% v/v HCl	27.36	27.40	26.85
149.82	20 $\mu g\ dm^{-3}$ As in 0.50% v/v HCl	45.34	45.28	44.34
157.18	20 $\mu g\ dm^{-3}$ As in 1.00% v/v HCl	51.20	50.99	49.90
164.55	20 $\mu g\ dm^{-3}$ As in 1.50% v/v HCl	51.20	50.87	49.75
171.92	20 $\mu g\ dm^{-3}$ As in 2.00% v/v HCl	52.92	52.43	51.26
179.30	20 $\mu g\ dm^{-3}$ As in 2.50% v/v HCl	51.55	50.94	49.79
188.58	Drift control - 20 $\mu g\ dm^{-3}$ As	21.06	20.74	20.27
220.02	20 $\mu g\ dm^{-3}$ As in (0.10% v/v HNO_3 + 0.10% v/v HCl)	29.71	28.94	28.34
227.40	20 $\mu g\ dm^{-3}$ As in (0.50% v/v HNO_3 + 0.50% v/v HCl)	51.28	49.82	48.82
234.78	20 $\mu g\ dm^{-3}$ As in (1.00% v/v HNO_3 + 1.00% v/v HCl)	56.79	55.03	53.98
244.08	Drift control - 20 $\mu g\ dm^{-3}$ As	20.17	19.48	19.14
296.78	Drift control - 20 $\mu g\ dm^{-3}$ As	21.08	19.99	19.88

4.5.3 Effect of using molecular (mass 75 / mass 77) corrections in a 0.10% v/v HCl matrix on the quantitative determination of arsenic

This factor depends upon the formation of the $^{40}Ar^{35}Cl$ and $^{40}Ar^{37}Cl$ molecular interferences at masses 75 and 77. It is calculated by measuring the intensities at masses 75 and 77 for a blank solution containing no arsenic or chlorine and for a solution containing a small amount of chlorine but no arsenic. The ratio of the intensities at the two masses is then determined after the blank values have been subtracted. It is then assumed that the formation of the dimers is constant in the plasma and the intensity at mass 75 can subsequently be corrected for the contribution by the $^{40}Ar^{35}Cl$ dimer at mass 75.

The correction factor when a blank and a 0.10% v/v HCl solution were measured was 3.275. (The theoretical ratio of the relative abundances of the ^{35}Cl to the ^{37}Cl isotopes is 3.087.)

No internal standard

When only the correction factor of 3.275 was used with no internal standard the correlation coefficient of the calibration curve was 1.0000 and the detection limit was 1.706 μg dm^{-3} As. The results of the analysis can be seen in table 4.12.

The matrices containing only nitric acid and no hydrochloric acid yielded values of approximately 20 μg dm^{-3}. Due to the applied correction the values obtained for the solutions containing 0.10% v/v to 1.00% v/v HCl, (0.10% v/v HNO_3 + 0.10% v/v HCl) and (1.00% v/v HNO_3 + 1.00% v/v HCl) were acceptable.

Table 4.12: Results of quantitative determination of As using no internal standard and the molecular correction factor (mass 75 / mass 77) at 0.10% v/v HCl. Results are also shown for time drift corrected values. First order equation used: ($y = 0.0081x + 20.274$) and second order equation used: ($y = -1x10^{-5}x^2 + 0.0125x + 20.039$)

Time difference (minutes)	Sample name	[As] (μg dm^{-3})	Corrected with first order drift curve (μg dm^{-3})	Corrected with second order drift curve (μg dm^{-3})
44.57	Drift control - 20 μg dm^{-3} As	20.59	19.96	20.01
51.83	20 μg dm^{-3} As in 0.10% v/v HNO_3	19.98	19.31	19.35

Time difference (minutes)	Sample name	[As] (μg dm^{-3})	Corrected with first order drift curve (μg dm^{-3})	Corrected with second order drift curve (μg dm^{-3})
59.10	20 μg dm^{-3} As in 0.50% v/v HNO_3	21.12	20.36	20.37
66.42	20 μg dm^{-3} As in 1.00% v/v HNO_3	21.44	20.60	20.59
73.68	20 μg dm^{-3} As in 1.50% v/v HNO_3	21.02	20.15	20.11
80.95	20 μg dm^{-3} As in 2.00% v/v HNO_3	20.44	19.53	19.48
88.22	20 μg dm^{-3} As in 2.50% v/v HNO_3	21.22	20.22	20.15
142.48	20 μg dm^{-3} As in 0.10% v/v HCl	20.21	18.86	18.70
149.82	20 μg dm^{-3} As in 0.50% v/v HCl	18.26	17.00	16.84
157.18	20 μg dm^{-3} As in 1.00% v/v HCl	18.30	16.99	16.82
164.55	20 μg dm^{-3} As in 1.50% v/v HCl	10.61	9.82	9.72
171.92	20 μg dm^{-3} As in 2.00% v/v HCl	15.55	14.36	14.21
179.30	20 μg dm^{-3} As in 2.50% v/v HCl	9.35	8.61	8.52
188.58	Drift control - 20 μg dm^{-3} As	21.77	19.97	19.75
220.02	20 μg dm^{-3} As in (0.10% v/v HNO_3 + 0.10% v/v HCl)	19.98	18.12	17.92
227.40	20 μg dm^{-3} As in (0.50% v/v HNO_3 + 0.50% v/v HCl)	16.80	15.19	15.02
234.78	20 μg dm^{-3} As in (1.00% v/v HNO_3 + 1.00% v/v HCl)	19.44	17.53	17.34
244.08	Drift control - 20 μg dm^{-3} As	22.51	20.23	20.01
296.78	Drift control - 20 μg dm^{-3} As	22.47	19.82	19.65

^{45}Sc, ^{89}Y and ^{139}La as internal standards

Calibration curves constructed when employing ^{45}Sc, ^{89}Y and ^{139}La as internal standards each resulted in a correlation coefficients of 1.0000 with detection limits of 1.759 μg dm^{-3} As, 1.718 μg dm^{-3} As and 1.711 μg dm^{-3} As respectively. The results of the analysis can be seen in tables 4.13 to 4.15.

In all three cases the nitric acid matrices yielded values of approximately 20 μg dm^{-3} As.

Table 4.13: Results of quantitative determination of As using ^{45}Sc as internal standard and the molecular correction factor (mass 75 / mass 77) at 0.10% v/v HCl. Results are also shown for time drift corrected values. First order equation used: ($y = 0.0059x + 19.915$) and second order equation used: ($y = 2x10^{-5}x^2 - 0.0128x + 20.277$)

Time difference (minutes)	Sample name	[As] ($\mu g\ dm^{-3}$)	Corrected with first order drift curve ($\mu g\ dm^{-3}$)	Corrected with second order drift curve ($\mu g\ dm^{-3}$)
44.57	Drift control - 20 $\mu g\ dm^{-3}$ As	19.77	20.12	20.02
51.83	20 $\mu g\ dm^{-3}$ As in 0.10% v/v HNO_3	18.94	19.32	19.26
59.10	20 $\mu g\ dm^{-3}$ As in 0.50% v/v HNO_3	20.24	20.69	20.66
66.42	20 $\mu g\ dm^{-3}$ As in 1.00% v/v HNO_3	20.10	20.59	20.60
73.68	20 $\mu g\ dm^{-3}$ As in 1.50% v/v HNO_3	19.82	20.35	20.39
80.95	20 $\mu g\ dm^{-3}$ As in 2.00% v/v HNO_3	19.64	20.20	20.27
88.22	20 $\mu g\ dm^{-3}$ As in 2.50% v/v HNO_3	20.36	20.99	21.09
142.48	20 $\mu g\ dm^{-3}$ As in 0.10% v/v HCl	17.23	18.07	18.28
149.82	20 $\mu g\ dm^{-3}$ As in 0.50% v/v HCl	15.61	16.41	16.60
157.18	20 $\mu g\ dm^{-3}$ As in 1.00% v/v HCl	15.58	16.41	16.61
164.55	20 $\mu g\ dm^{-3}$ As in 1.50% v/v HCl	8.94	9.44	9.55
171.92	20 $\mu g\ dm^{-3}$ As in 2.00% v/v HCl	12.72	13.45	13.62
179.30	20 $\mu g\ dm^{-3}$ As in 2.50% v/v HCl	7.64	8.10	8.20
188.58	Drift control - 20 $\mu g\ dm^{-3}$ As	18.42	19.59	19.83
220.02	20 $\mu g\ dm^{-3}$ As in (0.10% v/v HNO_3 + 0.10% v/v HCl)	16.52	17.75	17.93
227.40	20 $\mu g\ dm^{-3}$ As in (0.50% v/v HNO_3 + 0.50% v/v HCl)	13.80	14.86	15.00
234.78	20 $\mu g\ dm^{-3}$ As in (1.00% v/v HNO_3 + 1.00% v/v HCl)	16.19	17.48	17.63
244.08	Drift control - 20 $\mu g\ dm^{-3}$ As	18.67	20.21	20.36
296.78	Drift control - 20 $\mu g\ dm^{-3}$ As	18.21	20.05	19.96

Table 4.14: Results of quantitative determination of As using ^{89}Y as internal standard and the molecular correction factor (mass 75 / mass 77) at 0.10% v/v HCl. Results are also shown for time drift corrected values. First order equation used: ($y = 4x10^{-5}x + 19.686$) and second order equation used: ($y = -3x10^{-6}x^2 + 0.0009x + 19.638$)

Time difference (minutes)	Sample name	[As] ($\mu g\ dm^{-3}$)	Corrected with first order drift curve ($\mu g\ dm^{-3}$)	Corrected with second order drift curve ($\mu g\ dm^{-3}$)
44.57	Drift control - 20 $\mu g\ dm^{-3}$ As	19.71	20.03	20.04
51.83	20 $\mu g\ dm^{-3}$ As in 0.10% v/v HNO_3	19.09	19.39	19.40
59.10	20 $\mu g\ dm^{-3}$ As in 0.50% v/v HNO_3	20.58	20.90	20.91
66.42	20 $\mu g\ dm^{-3}$ As in 1.00% v/v HNO_3	20.10	20.42	20.42
73.68	20 $\mu g\ dm^{-3}$ As in 1.50% v/v HNO_3	20.03	20.35	20.35
80.95	20 $\mu g\ dm^{-3}$ As in 2.00% v/v HNO_3	19.65	19.96	19.96
88.22	20 $\mu g\ dm^{-3}$ As in 2.50% v/v HNO_3	20.33	20.65	20.65
142.48	20 $\mu g\ dm^{-3}$ As in 0.10% v/v HCl	18.31	18.60	18.58
149.82	20 $\mu g\ dm^{-3}$ As in 0.50% v/v HCl	17.41	17.68	17.67
157.18	20 $\mu g\ dm^{-3}$ As in 1.00% v/v HCl	18.14	18.43	18.41
164.55	20 $\mu g\ dm^{-3}$ As in 1.50% v/v HCl	10.45	10.62	10.61
171.92	20 $\mu g\ dm^{-3}$ As in 2.00% v/v HCl	15.36	15.60	15.59
179.30	20 $\mu g\ dm^{-3}$ As in 2.50% v/v HCl	9.26	9.40	9.40
188.58	Drift control - 20 $\mu g\ dm^{-3}$ As	19.39	19.70	19.69
220.02	20 $\mu g\ dm^{-3}$ As in (0.10% v/v HNO_3 + 0.10% v/v HCl)	18.30	18.59	18.59
227.40	20 $\mu g\ dm^{-3}$ As in (0.50% v/v HNO_3 + 0.50% v/v HCl)	15.67	15.91	15.92
234.78	20 $\mu g\ dm^{-3}$ As in (1.00% v/v HNO_3 + 1.00% v/v HCl)	18.88	19.18	19.19
244.08	Drift control - 20 $\mu g\ dm^{-3}$ As	20.19	20.50	20.52
296.78	Drift control - 20 $\mu g\ dm^{-3}$ As	19.48	19.78	19.84

Table 4.15: Results of quantitative determination of As using ^{139}La as internal standard and the molecular correction factor (mass 75 / mass 77) at 0.10% v/v HCl. Results are also shown for time drift corrected values. First order equation used: ($y = 0.0048x + 19.636$) and second order equation used: ($y = -2x10^{-5}x^2 + 0.011x + 19.308$)

Time difference (minutes)	Sample name	[As] ($\mu g\ dm^{-3}$)	Corrected with first order drift curve ($\mu g\ dm^{-3}$)	Corrected with second order drift curve ($\mu g\ dm^{-3}$)
44.57	Drift control - 20 $\mu g\ dm^{-3}$ As	19.79	19.94	20.03
51.83	20 $\mu g\ dm^{-3}$ As in 0.10% v/v HNO_3	19.65	19.76	19.82
59.10	20 $\mu g\ dm^{-3}$ As in 0.50% v/v HNO_3	20.73	20.81	20.85
66.42	20 $\mu g\ dm^{-3}$ As in 1.00% v/v HNO_3	20.20	20.25	20.26
73.68	20 $\mu g\ dm^{-3}$ As in 1.50% v/v HNO_3	20.09	20.10	20.08
80.95	20 $\mu g\ dm^{-3}$ As in 2.00% v/v HNO_3	19.80	19.78	19.73
88.22	20 $\mu g\ dm^{-3}$ As in 2.50% v/v HNO_3	20.53	20.47	20.40
142.48	20 $\mu g\ dm^{-3}$ As in 0.10% v/v HCl	19.19	18.88	18.75
149.82	20 $\mu g\ dm^{-3}$ As in 0.50% v/v HCl	18.85	18.52	18.38
157.18	20 $\mu g\ dm^{-3}$ As in 1.00% v/v HCl	20.27	19.88	19.74
164.55	20 $\mu g\ dm^{-3}$ As in 1.50% v/v HCl	11.68	11.44	11.36
171.92	20 $\mu g\ dm^{-3}$ As in 2.00% v/v HCl	17.40	17.01	16.88
179.30	20 $\mu g\ dm^{-3}$ As in 2.50% v/v HCl	10.81	10.55	10.47
188.58	Drift control - 20 $\mu g\ dm^{-3}$ As	20.49	19.95	19.82
220.02	20 $\mu g\ dm^{-3}$ As in (0.10% v/v HNO_3 + 0.10% v/v HCl)	19.46	18.81	18.75
227.40	20 $\mu g\ dm^{-3}$ As in (0.50% v/v HNO_3 + 0.50% v/v HCl)	17.40	16.79	16.75
234.78	20 $\mu g\ dm^{-3}$ As in (1.00% v/v HNO_3 + 1.00% v/v HCl)	21.50	20.71	20.69
244.08	Drift control - 20 $\mu g\ dm^{-3}$ As	21.19	20.37	20.38
296.78	Drift control - 20 $\mu g\ dm^{-3}$ As	20.77	19.73	19.96

^{36}Ar, ^{35}Cl and ^{37}Cl as internal standards

Correlation coefficients of 0.9998, 1.0000 and 0.9999 and detection limits of 1.939 μg dm^{-3} As, 1.207 μg dm^{-3} As and 1.824 μg dm^{-3} As respectively were obtained when using ^{36}Ar, ^{35}Cl and ^{37}Cl as internal standards for the calibration curves. Tables 4.16 to 4.18 show the results of the analysis.

The matrices containing only nitric acid yielded values of approximately 20 μg dm^{-3} As. The correction procedure resulted in values below 20 μg dm^{-3} for matrices containing hydrochloric acid.

Table 4.16: Results of quantitative determination of As using ^{36}Ar as internal standard and the molecular correction factor (mass 75 / mass 77) at 0.10% v/v HCl. Results are also shown for time drift corrected values. First order equation used: ($y = 0.0183x + 19.898$) and second order equation used: ($y = 6x10^{-5}x^2 - 0.0369x + 20.874$)

Time difference (minutes)	Sample name	[As] (μg dm^{-3})	Corrected with first order drift curve (μg dm^{-3})	Corrected with second order drift curve (μg dm^{-3})
44.57	Drift control - 20 μg dm^{-3} As	19.36	20.29	20.02
51.83	20 μg dm^{-3} As in 0.10% v/v HNO_3	18.01	19.01	18.84
59.10	20 μg dm^{-3} As in 0.50% v/v HNO_3	19.02	20.22	20.13
66.42	20 μg dm^{-3} As in 1.00% v/v HNO_3	19.14	20.49	20.48
73.68	20 μg dm^{-3} As in 1.50% v/v HNO_3	18.59	20.04	20.12
80.95	20 μg dm^{-3} As in 2.00% v/v HNO_3	18.13	19.68	19.83
88.22	20 μg dm^{-3} As in 2.50% v/v HNO_3	19.10	20.89	21.12
142.48	20 μg dm^{-3} As in 0.10% v/v HCl	15.25	17.64	18.12
149.82	20 μg dm^{-3} As in 0.50% v/v HCl	12.96	15.11	15.53
157.18	20 μg dm^{-3} As in 1.00% v/v HCl	11.99	14.09	14.48
164.55	20 μg dm^{-3} As in 1.50% v/v HCl	6.41	7.59	7.80
171.92	20 μg dm^{-3} As in 2.00% v/v HCl	9.27	11.06	11.37

Time difference (minutes)	Sample name	[As] ($\mu g\ dm^{-3}$)	Corrected with first order drift curve ($\mu g\ dm^{-3}$)	Corrected with second order drift curve ($\mu g\ dm^{-3}$)
179.30	20 $\mu g\ dm^{-3}$ As in 2.50% v/v HCl	5.01	6.03	6.19
188.58	Drift control - 20 $\mu g\ dm^{-3}$ As	15.76	19.16	19.64
220.02	20 $\mu g\ dm^{-3}$ As in (0.10% v/v HNO_3 + 0.10% v/v HCl)	13.87	17.47	17.71
227.40	20 $\mu g\ dm^{-3}$ As in (0.50% v/v HNO_3 + 0.50% v/v HCl)	10.82	13.75	13.88
234.78	20 $\mu g\ dm^{-3}$ As in (1.00% v/v HNO_3 + 1.00% v/v HCl)	12.15	15.58	15.67
244.08	Drift control - 20 $\mu g\ dm^{-3}$ As	15.50	20.09	20.08
296.78	Drift control - 20 $\mu g\ dm^{-3}$ As	14.81	20.47	19.47

Table 4.17: Results of quantitative determination of As using ^{35}Cl as internal standard and the molecular correction factor (mass 75 / mass 77) at 0.10% v/v HCl. Results are also shown for time drift corrected values. First order equation used: ($y = -0.0432x + 20.304$) and second order equation used: ($y = 0.0003x^2 - 0.1481x + 25.714$)

Time difference (minutes)	Sample name	[As] ($\mu g\ dm^{-3}$)	Corrected with first order drift curve ($\mu g\ dm^{-3}$)	Corrected with second order drift curve ($\mu g\ dm^{-3}$)
44.57	Drift control - 20 $\mu g\ dm^{-3}$ As	20.04	21.81	20.24
51.83	20 $\mu g\ dm^{-3}$ As in 0.10% v/v HNO_3	19.45	21.53	20.53
59.10	20 $\mu g\ dm^{-3}$ As in 0.50% v/v HNO_3	20.32	22.89	22.42
66.42	20 $\mu g\ dm^{-3}$ As in 1.00% v/v HNO_3	20.21	23.18	23.31
73.68	20 $\mu g\ dm^{-3}$ As in 1.50% v/v HNO_3	20.20	23.60	24.37
80.95	20 $\mu g\ dm^{-3}$ As in 2.00% v/v HNO_3	19.73	23.48	24.89
88.22	20 $\mu g\ dm^{-3}$ As in 2.50% v/v HNO_3	20.41	24.75	26.93
142.48	20 $\mu g\ dm^{-3}$ As in 0.10% v/v HCl	2.99	4.23	5.45
149.82	20 $\mu g\ dm^{-3}$ As in 0.50% v/v HCl	1.26	1.83	2.39
157.18	20 $\mu g\ dm^{-3}$ As in 1.00% v/v HCl	1.08	1.60	2.13

Time difference (minutes)	Sample name	[As] (μg dm^{-3})	Corrected with first order drift curve (μg dm^{-3})	Corrected with second order drift curve (μg dm^{-3})
164.55	20 μg dm^{-3} As in 1.50% v/v HCl	0.98	1.48	1.99
171.92	20 μg dm^{-3} As in 2.00% v/v HCl	0.98	1.53	2.08
179.30	20 μg dm^{-3} As in 2.50% v/v HCl	0.95	1.51	2.07
188.58	Drift control - 20 μg dm^{-3} As	7.50	12.34	16.99
220.02	20 μg dm^{-3} As in (0.10% v/v HNO_3 + 0.10% v/v HCl)	2.95	5.45	7.28
227.40	20 μg dm^{-3} As in (0.50% v/v HNO_3 + 0.50% v/v HCl)	1.22	2.32	3.04
234.78	20 μg dm^{-3} As in (1.00% v/v HNO_3 + 1.00% v/v HCl)	1.09	2.14	2.73
244.08	Drift control - 20 μg dm^{-3} As	11.39	23.34	28.74
296.78	Drift control - 20 μg dm^{-3} As	8.87	23.69	20.20

Table 4.18: Results of quantitative determination of As using ^{37}Cl as internal standard and the molecular correction factor (mass 75 / mass 77) at 0.10% v/v HCl. Results are also shown for time drift corrected values. First order equation used: ($y = -0.0108x + 19.876$) and second order equation used: ($y = 7x10^{-5}x^2 - 0.0344x + 21.114$)

Time difference (minutes)	Sample name	[As] (μg dm^{-3})	Corrected with first order drift curve (μg dm^{-3})	Corrected with second order drift curve (μg dm^{-3})
44.57	Drift control - 20 μg dm^{-3} As	19.78	20.40	20.06
51.83	20 μg dm^{-3} As in 0.10% v/v HNO_3	19.20	19.88	19.68
59.10	20 μg dm^{-3} As in 0.50% v/v HNO_3	19.87	20.66	20.56
66.42	20 μg dm^{-3} As in 1.00% v/v HNO_3	19.83	20.70	20.72
73.68	20 μg dm^{-3} As in 1.50% v/v HNO_3	19.24	20.17	20.29
80.95	20 μg dm^{-3} As in 2.00% v/v HNO_3	18.61	19.59	19.81
88.22	20 μg dm^{-3} As in 2.50% v/v HNO_3	19.26	20.35	20.68
142.48	20 μg dm^{-3} As in 0.10% v/v HCl	14.32	15.62	16.25

Time difference (minutes)	Sample name	[As] (μg dm^{-3})	Corrected with first order drift curve (μg dm^{-3})	Corrected with second order drift curve (μg dm^{-3})
149.82	20 μg dm^{-3} As in 0.50% v/v HCl	6.93	7.60	7.91
157.18	20 μg dm^{-3} As in 1.00% v/v HCl	4.39	4.83	5.03
164.55	20 μg dm^{-3} As in 1.50% v/v HCl	1.99	2.20	2.30
171.92	20 μg dm^{-3} As in 2.00% v/v HCl	2.30	2.55	2.66
179.30	20 μg dm^{-3} As in 2.50% v/v HCl	1.28	1.43	1.49
188.58	Drift control - 20 μg dm^{-3} As	16.69	18.71	19.50
220.02	20 μg dm^{-3} As in (0.10% v/v HNO_3 + 0.10% v/v HCl)	13.55	15.48	16.00
227.40	20 μg dm^{-3} As in (0.50% v/v HNO_3 + 0.50% v/v HCl)	6.02	6.91	7.12
234.78	20 μg dm^{-3} As in (1.00% v/v HNO_3 + 1.00% v/v HCl)	4.51	5.20	5.34
244.08	Drift control - 20 μg dm^{-3} As	17.71	20.54	20.97
296.78	Drift control - 20 μg dm^{-3} As	16.93	20.31	19.83

4.5.4 Effect of using molecular (mass 75 / mass 77) corrections in a 0.50% v/v HCl matrix on the quantitative determination of arsenic

No internal standard

Correction factor of 3.202 was calculated after measuring a blank and a 0.50% v/v HCl solution. When not using an internal standard a correlation coefficient of 1.0000 was calculated with a detection limit of 1.687 μg dm^{-3} As. The results are in table 4.19.

The time drift corrected values obtained for the samples containing only nitric acid as matrix yielded acceptable values of approximately 20 μg dm^{-3} As. Acceptable values were obtained for samples containing 0.10% v/v HCl and 0.50% v/v HCl.

Table 4.19: Results of quantitative determination of As using no internal standard and the molecular correction factor (mass 75 / mass 77) at 0.50% v/v HCl. Results are also shown for time drift corrected values. First order equation used: ($y = 0.0087x + 20.256$) and second order equation used: ($y = -2x10^{-5}x^2 + 0.0142x + 19.965$)

Time difference (minutes)	Sample name	[As] ($\mu g\ dm^{-3}$)	Corrected with first order drift curve ($\mu g\ dm^{-3}$)	Corrected with second order drift curve ($\mu g\ dm^{-3}$)
44.57	Drift control - 20 $\mu g\ dm^{-3}$ As	20.58	19.94	20.02
51.83	20 $\mu g\ dm^{-3}$ As in 0.10% v/v HNO_3	19.98	19.30	19.35
59.10	20 $\mu g\ dm^{-3}$ As in 0.50% v/v HNO_3	21.11	20.33	20.36
66.42	20 $\mu g\ dm^{-3}$ As in 1.00% v/v HNO_3	21.43	20.57	20.58
73.68	20 $\mu g\ dm^{-3}$ As in 1.50% v/v HNO_3	21.02	20.12	20.11
80.95	20 $\mu g\ dm^{-3}$ As in 2.00% v/v HNO_3	20.43	19.50	19.48
88.22	20 $\mu g\ dm^{-3}$ As in 2.50% v/v HNO_3	21.22	20.18	20.15
142.48	20 $\mu g\ dm^{-3}$ As in 0.10% v/v HCl	20.64	19.21	19.13
149.82	20 $\mu g\ dm^{-3}$ As in 0.50% v/v HCl	20.64	19.15	19.08
157.18	20 $\mu g\ dm^{-3}$ As in 1.00% v/v HCl	23.07	21.34	21.26
164.55	20 $\mu g\ dm^{-3}$ As in 1.50% v/v HCl	17.57	16.20	16.15
171.92	20 $\mu g\ dm^{-3}$ As in 2.00% v/v HCl	24.65	22.67	22.60
179.30	20 $\mu g\ dm^{-3}$ As in 2.50% v/v HCl	20.47	18.77	18.73
188.58	Drift control - 20 $\mu g\ dm^{-3}$ As	21.92	20.02	19.99
220.02	20 $\mu g\ dm^{-3}$ As in (0.10% v/v HNO_3 + 0.10% v/v HCl)	20.54	18.53	18.57
227.40	20 $\mu g\ dm^{-3}$ As in (0.50% v/v HNO_3 + 0.50% v/v HCl)	19.77	17.78	17.84
234.78	20 $\mu g\ dm^{-3}$ As in (1.00% v/v HNO_3 + 1.00% v/v HCl)	24.90	22.34	22.44
244.08	Drift control - 20 $\mu g\ dm^{-3}$ As	22.60	20.20	20.33
296.78	Drift control - 20 $\mu g\ dm^{-3}$ As	22.62	19.81	20.18

^{45}Sc, ^{89}Y and ^{139}La as internal standards

Regression correlation coefficients of 1.0000 were obtained for the calibration curves and detection limits of 1.730 μg dm^{-3} As, 1.697 μg dm^{-3} As and 1.689 μg dm^{-3} As were calculated respectively for ^{45}Sc, ^{89}Y and ^{139}La as internal standards. The results of the analyses can be seen in tables 4.20 to 4.22.

In all three cases acceptable values of approximately 20 μg dm^{-3} As were obtained when the matrices contained only nitric acid. In all three cases some of the matrices containing hydrochloric acid yielded values of approximately 20 μg dm^{-3} As, but the correction procedure was not successful for all these matrices.

Table 4.20: Results of quantitative determination of As using ^{45}Sc as internal standard and the molecular correction factor (mass 75 / mass 77) at 0.50% v/v HCl. Results are also shown for time drift corrected values. First order equation used: ($y = -0.0055x + 19.897$) and second order equation used: ($y = 2x10^{-5}x^2 - 0.0115x + 20.210$)

Time difference (minutes)	Sample name	[As] (μg dm^{-3})	Corrected with first order drift curve (μg dm^{-3})	Corrected with second order drift curve (μg dm^{-3})
44.57	Drift control - 20 μg dm^{-3} As	19.75	20.10	20.02
51.83	20 μg dm^{-3} As in 0.10% v/v HNO_3	18.93	19.31	19.25
59.10	20 μg dm^{-3} As in 0.50% v/v HNO_3	20.23	20.67	20.64
66.42	20 μg dm^{-3} As in 1.00% v/v HNO_3	20.08	20.56	20.56
73.68	20 μg dm^{-3} As in 1.50% v/v HNO_3	19.82	20.33	20.36
80.95	20 μg dm^{-3} As in 2.00% v/v HNO_3	19.62	20.18	20.22
88.22	20 μg dm^{-3} As in 2.50% v/v HNO_3	20.35	20.96	21.03
142.48	20 μg dm^{-3} As in 0.10% v/v HCl	17.59	18.40	18.54
149.82	20 μg dm^{-3} As in 0.50% v/v HCl	17.63	18.49	18.62
157.18	20 μg dm^{-3} As in 1.00% v/v HCl	19.60	20.60	20.75
164.55	20 μg dm^{-3} As in 1.50% v/v HCl	14.73	15.51	15.62

Time difference (minutes)	Sample name	[As] ($\mu g\ dm^{-3}$)	Corrected with first order drift curve ($\mu g\ dm^{-3}$)	Corrected with second order drift curve ($\mu g\ dm^{-3}$)
171.92	20 $\mu g\ dm^{-3}$ As in 2.00% v/v HCl	20.07	21.18	21.33
179.30	20 $\mu g\ dm^{-3}$ As in 2.50% v/v HCl	16.58	17.53	17.65
188.58	Drift control - 20 $\mu g\ dm^{-3}$ As	18.53	19.65	19.77
220.02	20 $\mu g\ dm^{-3}$ As in (0.10% v/v HNO_3 + 0.10% v/v HCl)	16.96	18.15	18.19
227.40	20 $\mu g\ dm^{-3}$ As in (0.50% v/v HNO_3 + 0.50% v/v HCl)	16.20	17.38	17.39
234.78	20 $\mu g\ dm^{-3}$ As in (1.00% v/v HNO_3 + 1.00% v/v HCl)	20.71	22.26	22.25
244.08	Drift control - 20 $\mu g\ dm^{-3}$ As	18.73	20.19	20.15
296.78	Drift control - 20 $\mu g\ dm^{-3}$ As	18.31	20.05	19.73

Table 4.21: Results of quantitative determination of As using ^{89}Y as internal standard and the molecular correction factor (mass 75 / mass 77) at 0.50% v/v HCl. Results are also shown for time drift corrected values. First order equation used: ($y = 0.0005x + 19.667$) and second order equation used: ($y = -6x10^{-6}x^2 + 0.0024x + 19.568$)

Time difference (minutes)	Sample name	[As] ($\mu g\ dm^{-3}$)	Corrected with first order drift curve ($\mu g\ dm^{-3}$)	Corrected with second order drift curve ($\mu g\ dm^{-3}$)
44.57	Drift control - 20 $\mu g\ dm^{-3}$ As	19.70	20.01	20.04
51.83	20 $\mu g\ dm^{-3}$ As in 0.10% v/v HNO_3	19.08	19.38	19.39
59.10	20 $\mu g\ dm^{-3}$ As in 0.50% v/v HNO_3	20.56	20.88	20.89
66.42	20 $\mu g\ dm^{-3}$ As in 1.00% v/v HNO_3	20.08	20.39	20.39
73.68	20 $\mu g\ dm^{-3}$ As in 1.50% v/v HNO_3	20.03	20.33	20.32
80.95	20 $\mu g\ dm^{-3}$ As in 2.00% v/v HNO_3	19.64	19.93	19.92
88.22	20 $\mu g\ dm^{-3}$ As in 2.50% v/v HNO_3	20.32	20.62	20.60
142.48	20 $\mu g\ dm^{-3}$ As in 0.10% v/v HCl	18.69	18.94	18.90
149.82	20 $\mu g\ dm^{-3}$ As in 0.50% v/v HCl	19.67	19.93	19.88

Time difference (minutes)	Sample name	[As] (μg dm^{-3})	Corrected with first order drift curve (μg dm^{-3})	Corrected with second order drift curve (μg dm^{-3})
157.18	20 μg dm^{-3} As in 1.00% v/v HCl	22.87	23.16	23.10
164.55	20 μg dm^{-3} As in 1.50% v/v HCl	17.30	17.52	17.47
171.92	20 μg dm^{-3} As in 2.00% v/v HCl	24.34	24.64	24.58
179.30	20 μg dm^{-3} As in 2.50% v/v HCl	20.26	20.51	20.46
188.58	Drift control - 20 μg dm^{-3} As	19.52	19.75	19.71
220.02	20 μg dm^{-3} As in (0.10% v/v HNO_3 + 0.10% v/v HCl)	18.80	19.02	18.99
227.40	20 μg dm^{-3} As in (0.50% v/v HNO_3 + 0.50% v/v HCl)	18.42	18.62	18.60
234.78	20 μg dm^{-3} As in (1.00% v/v HNO_3 + 1.00% v/v HCl)	24.18	24.45	24.43
244.08	Drift control - 20 μg dm^{-3} As	20.26	20.48	20.47
296.78	Drift control - 20 μg dm^{-3} As	19.60	19.78	19.84

Table 4.22: Results of quantitative determination of As using ^{139}La as internal standard and the molecular correction factor (mass 75 / mass 77) at 0.50% v/v HCl. Results are also shown for time drift corrected values. First order equation used: ($y = 0.0053x + 19.616$) and second order equation used: ($y = -2x10^{-5}x^2 + 0.0126x + 19.234$)

Time difference (minutes)	Sample name	[As] (μg dm^{-3})	Corrected with first order drift curve (μg dm^{-3})	Corrected with second order drift curve (μg dm^{-3})
44.57	Drift control - 20 μg dm^{-3} As	19.77	19.92	20.02
51.83	20 μg dm^{-3} As in 0.10% v/v HNO_3	19.64	19.75	19.81
59.10	20 μg dm^{-3} As in 0.50% v/v HNO_3	20.72	20.79	20.81
66.42	20 μg dm^{-3} As in 1.00% v/v HNO_3	20.19	20.22	20.21
73.68	20 μg dm^{-3} As in 1.50% v/v HNO_3	20.08	20.07	20.03
80.95	20 μg dm^{-3} As in 2.00% v/v HNO_3	19.79	19.74	19.67
88.22	20 μg dm^{-3} As in 2.50% v/v HNO_3	20.52	20.43	20.33

Time difference (minutes)	Sample name	[As] (μg dm^{-3})	Corrected with first order drift curve (μg dm^{-3})	Corrected with second order drift curve (μg dm^{-3})
142.48	20 μg dm^{-3} As in 0.10% v/v HCl	19.59	19.23	19.00
149.82	20 μg dm^{-3} As in 0.50% v/v HCl	21.30	20.88	20.61
157.18	20 μg dm^{-3} As in 1.00% v/v HCl	25.56	25.00	24.68
164.55	20 μg dm^{-3} As in 1.50% v/v HCl	19.36	18.89	18.64
171.92	20 μg dm^{-3} As in 2.00% v/v HCl	27.59	26.88	26.52
179.30	20 μg dm^{-3} As in 2.50% v/v HCl	23.75	23.09	22.78
188.58	Drift control - 20 μg dm^{-3} As	20.62	20.01	19.74
220.02	20 μg dm^{-3} As in (0.10% v/v HNO_3 + 0.10% v/v HCl)	20.00	19.25	19.01
227.40	20 μg dm^{-3} As in (0.50% v/v HNO_3 + 0.50% v/v HCl)	20.47	19.66	19.43
234.78	20 μg dm^{-3} As in (1.00% v/v HNO_3 + 1.00% v/v HCl)	27.56	26.42	26.13
244.08	Drift control - 20 μg dm^{-3} As	21.28	20.35	20.15
296.78	Drift control - 20 μg dm^{-3} As	20.90	19.73	19.71

^{36}Ar, ^{35}Cl and ^{37}Cl as internal standards

In the cases of ^{36}Ar, ^{35}Cl and ^{37}Cl as internal standards regression correlation coefficients of 0.9998, 1.0000 and 0.9999 were obtained. It resulted in detection limits of 1.915 μg dm^{-3} As, 1.182 μg dm^{-3} As and 1.803 μg dm^{-3} As respectively. Tables 4.23 to 4.25 show the results of the analyses.

Nitric acid matrices yielded values of 20 μg dm^{-3} in the cases of ^{36}Ar and ^{37}Cl. Time drift corrected values for ^{35}Cl resulted in too high values for the 20 μg dm^{-3} As samples. For ^{36}Ar the results show slightly too low values for hydrochloric acid containing matrices. In the cases of ^{35}Cl and ^{37}Cl as internal standards very poor results were obtained for hydrochloric acid containing matrices.

Table 4.23: Results of quantitative determination of As using ^{36}Ar as internal standard and the molecular correction factor (mass 75 / mass 77) at 0.50% v/v HCl. Results are also shown for time drift corrected values. First order equation used: ($y = -0.018x + 19.878$) and second order equation used: ($y = 5x10^{-5}x^2 - 0.0357x + 20.810$)

Time difference (minutes)	Sample name	[As] ($\mu g\ dm^{-3}$)	Corrected with first order drift curve ($\mu g\ dm^{-3}$)	Corrected with second order drift curve ($\mu g\ dm^{-3}$)
44.57	Drift control - 20 $\mu g\ dm^{-3}$ As	19.34	20.28	20.03
51.83	20 $\mu g\ dm^{-3}$ As in 0.10% v/v HNO_3	18.00	19.00	18.85
59.10	20 $\mu g\ dm^{-3}$ As in 0.50% v/v HNO_3	19.00	20.20	20.13
66.42	20 $\mu g\ dm^{-3}$ As in 1.00% v/v HNO_3	19.11	20.46	20.49
73.68	20 $\mu g\ dm^{-3}$ As in 1.50% v/v HNO_3	18.57	20.02	20.13
80.95	20 $\mu g\ dm^{-3}$ As in 2.00% v/v HNO_3	18.10	19.66	19.84
88.22	20 $\mu g\ dm^{-3}$ As in 2.50% v/v HNO_3	19.08	20.86	21.14
142.48	20 $\mu g\ dm^{-3}$ As in 0.10% v/v HCl	15.57	17.98	18.60
149.82	20 $\mu g\ dm^{-3}$ As in 0.50% v/v HCl	14.70	17.11	17.73
157.18	20 $\mu g\ dm^{-3}$ As in 1.00% v/v HCl	15.22	17.86	18.52
164.55	20 $\mu g\ dm^{-3}$ As in 1.50% v/v HCl	10.92	12.91	13.40
171.92	20 $\mu g\ dm^{-3}$ As in 2.00% v/v HCl	14.94	17.80	18.50
179.30	20 $\mu g\ dm^{-3}$ As in 2.50% v/v HCl	11.48	13.78	14.33
188.58	Drift control - 20 $\mu g\ dm^{-3}$ As	15.84	19.22	19.98
220.02	20 $\mu g\ dm^{-3}$ As in (0.10% v/v HNO_3 + 0.10% v/v HCl)	14.24	17.89	18.52
227.40	20 $\mu g\ dm^{-3}$ As in (0.50% v/v HNO_3 + 0.50% v/v HCl)	12.79	16.21	16.75
234.78	20 $\mu g\ dm^{-3}$ As in (1.00% v/v HNO_3 + 1.00% v/v HCl)	15.68	20.04	20.65
244.08	Drift control - 20 $\mu g\ dm^{-3}$ As	15.54	20.07	20.61
296.78	Drift control - 20 $\mu g\ dm^{-3}$ As	14.87	20.47	20.35

Table 4.24: Results of quantitative determination of As using ^{35}Cl as internal standard and the molecular correction factor (mass 75 / mass 77) at 0.50% v/v HCl. Results are also shown for time drift corrected values. First order equation used: ($y = -0.0431x + 20.294$) and second order equation used: ($y = 0.0003x^2 - 0.1461x + 25.708$)

Time difference (minutes)	Sample name	[As] ($\mu g\ dm^{-3}$)	Corrected with first order drift curve ($\mu g\ dm^{-3}$)	Corrected with second order drift curve ($\mu g\ dm^{-3}$)
44.57	Drift control - 20 $\mu g\ dm^{-3}$ As	20.03	21.81	20.24
51.83	20 $\mu g\ dm^{-3}$ As in 0.10% v/v HNO_3	19.45	21.54	20.54
59.10	20 $\mu g\ dm^{-3}$ As in 0.50% v/v HNO_3	20.31	22.89	22.42
66.42	20 $\mu g\ dm^{-3}$ As in 1.00% v/v HNO_3	20.20	23.17	23.31
73.68	20 $\mu g\ dm^{-3}$ As in 1.50% v/v HNO_3	20.20	23.60	24.38
80.95	20 $\mu g\ dm^{-3}$ As in 2.00% v/v HNO_3	19.72	23.47	24.89
88.22	20 $\mu g\ dm^{-3}$ As in 2.50% v/v HNO_3	20.41	24.75	26.94
142.48	20 $\mu g\ dm^{-3}$ As in 0.10% v/v HCl	2.98	4.21	5.42
149.82	20 $\mu g\ dm^{-3}$ As in 0.50% v/v HCl	1.24	1.79	2.35
157.18	20 $\mu g\ dm^{-3}$ As in 1.00% v/v HCl	1.06	1.56	2.08
164.55	20 $\mu g\ dm^{-3}$ As in 1.50% v/v HCl	0.95	1.43	1.93
171.92	20 $\mu g\ dm^{-3}$ As in 2.00% v/v HCl	0.95	1.48	2.01
179.30	20 $\mu g\ dm^{-3}$ As in 2.50% v/v HCl	0.91	1.45	1.99
188.58	Drift control - 20 $\mu g\ dm^{-3}$ As	7.50	12.33	17.00
220.02	20 $\mu g\ dm^{-3}$ As in (0.10% v/v HNO_3 + 0.10% v/v HCl)	2.94	5.44	7.27
227.40	20 $\mu g\ dm^{-3}$ As in (0.50% v/v HNO_3 + 0.50% v/v HCl)	1.20	2.28	3.00
234.78	20 $\mu g\ dm^{-3}$ As in (1.00% v/v HNO_3 + 1.00% v/v HCl)	1.06	2.09	2.68
244.08	Drift control - 20 $\mu g\ dm^{-3}$ As	11.40	23.33	28.79
296.78	Drift control - 20 $\mu g\ dm^{-3}$ As	8.88	23.66	20.24

Table 4.25: Results of quantitative determination of As using ^{37}Cl as internal standard and the molecular correction factor (mass 75 / mass 77) at 0.50% v/v HCl. Results are also shown for time drift corrected values. First order equation used: ($y = -0.0105x + 19.856$) and second order equation used: ($y = 7x10^{-5}x^2 - 0.0332x + 21.053$)

Time difference (minutes)	Sample name	[As] ($\mu g\ dm^{-3}$)	Corrected with first order drift curve ($\mu g\ dm^{-3}$)	Corrected with second order drift curve ($\mu g\ dm^{-3}$)
44.57	Drift control - 20 $\mu g\ dm^{-3}$ As	19.77	20.39	20.05
51.83	20 $\mu g\ dm^{-3}$ As in 0.10% v/v HNO_3	19.19	19.87	19.66
59.10	20 $\mu g\ dm^{-3}$ As in 0.50% v/v HNO_3	19.85	20.64	20.53
66.42	20 $\mu g\ dm^{-3}$ As in 1.00% v/v HNO_3	19.81	20.68	20.68
73.68	20 $\mu g\ dm^{-3}$ As in 1.50% v/v HNO_3	19.23	20.15	20.25
80.95	20 $\mu g\ dm^{-3}$ As in 2.00% v/v HNO_3	18.59	19.56	19.75
88.22	20 $\mu g\ dm^{-3}$ As in 2.50% v/v HNO_3	19.24	20.33	20.61
142.48	20 $\mu g\ dm^{-3}$ As in 0.10% v/v HCl	14.61	15.91	16.47
149.82	20 $\mu g\ dm^{-3}$ As in 0.50% v/v HCl	7.78	8.51	8.81
157.18	20 $\mu g\ dm^{-3}$ As in 1.00% v/v HCl	5.41	5.95	6.16
164.55	20 $\mu g\ dm^{-3}$ As in 1.50% v/v HCl	3.07	3.39	3.52
171.92	20 $\mu g\ dm^{-3}$ As in 2.00% v/v HCl	3.41	3.77	3.91
179.30	20 $\mu g\ dm^{-3}$ As in 2.50% v/v HCl	2.38	2.65	2.75
188.58	Drift control - 20 $\mu g\ dm^{-3}$ As	16.79	18.78	19.43
220.02	20 $\mu g\ dm^{-3}$ As in (0.10% v/v HNO_3 + 0.10% v/v HCl)	13.90	15.84	16.22
227.40	20 $\mu g\ dm^{-3}$ As in (0.50% v/v HNO_3 + 0.50% v/v HCl)	7.01	8.03	8.19
234.78	20 $\mu g\ dm^{-3}$ As in (1.00% v/v HNO_3 + 1.00% v/v HCl)	5.66	6.51	6.61
244.08	Drift control - 20 $\mu g\ dm^{-3}$ As	17.76	20.54	20.75
296.78	Drift control - 20 $\mu g\ dm^{-3}$ As	17.02	20.33	19.60

4.5.5 *Effect of using molecular (mass 75 / mass 77) corrections in a 1.00% v/v HCl matrix on the quantitative determination of arsenic*

No internal standard

A correction factor of 3.145 was obtained in the case of a matrix of 1.00% v/v HCl. A calibration correlation coefficient of 1.0000 and a detection limit of 1.671 μg dm^{-3} As resulted. The results of the analysis of the 20 μg dm^{-3} As samples are tabulated in table 4.26.

Good results were obtained for matrices only containing 20 μg dm^{-3} As and nitric acid. Acceptable results were obtained for samples in the cases of hydrochloric acid matrices of low concentration.

Table 4.26: Results of quantitative determination of As using no internal standard and the molecular correction factor (mass 75 / mass 77) at 1.00% v/v HCl. Results are also shown for time drift corrected values. First order equation used: ($y = 0.0091x + 20.241$) and second order equation used: ($y = -2x10^{-5}x^2 + 0.0155x + 19.906$)

Time difference (minutes)	**Sample name**	**[As] (μg dm^{-3})**	**Corrected with first order drift curve (μg dm^{-3})**	**Corrected with second order drift curve (μg dm^{-3})**
44.57	Drift control - 20 μg dm^{-3} As	20.57	19.93	20.01
51.83	20 μg dm^{-3} As in 0.10% v/v HNO_3	19.97	19.29	19.34
59.10	20 μg dm^{-3} As in 0.50% v/v HNO_3	21.10	20.31	20.34
66.42	20 μg dm^{-3} As in 1.00% v/v HNO_3	21.42	20.55	20.55
73.68	20 μg dm^{-3} As in 1.50% v/v HNO_3	21.02	20.10	20.08
80.95	20 μg dm^{-3} As in 2.00% v/v HNO_3	20.43	19.48	19.43
88.22	20 μg dm^{-3} As in 2.50% v/v HNO_3	21.21	20.16	20.09
142.48	20 μg dm^{-3} As in 0.10% v/v HCl	20.99	19.49	19.34
149.82	20 μg dm^{-3} As in 0.50% v/v HCl	22.55	20.88	20.71
157.18	20 μg dm^{-3} As in 1.00% v/v HCl	26.88	24.81	24.61
164.55	20 μg dm^{-3} As in 1.50% v/v HCl	23.13	21.28	21.11

Time difference (minutes)	Sample name	[As] (μg dm^{-3})	Corrected with first order drift curve (μg dm^{-3})	Corrected with second order drift curve (μg dm^{-3})
171.92	20 μg dm^{-3} As in 2.00% v/v HCl	31.92	29.28	29.05
179.30	20 μg dm^{-3} As in 2.50% v/v HCl	29.37	26.86	26.65
188.58	Drift control - 20 μg dm^{-3} As	22.04	20.08	19.93
220.02	20 μg dm^{-3} As in (0.10% v/v HNO_3 + 0.10% v/v HCl)	20.99	18.87	18.78
227.40	20 μg dm^{-3} As in (0.50% v/v HNO_3 + 0.50% v/v HCl)	22.14	19.85	19.77
234.78	20 μg dm^{-3} As in (1.00% v/v HNO_3 + 1.00% v/v HCl)	29.27	26.16	26.09
244.08	Drift control - 20 μg dm^{-3} As	22.68	20.19	20.16
296.78	Drift control - 20 μg dm^{-3} As	22.74	19.83	20.00

^{45}Sc, ^{89}Y and ^{139}La as internal standards

All the calibration curves yielded correlation coefficients of 1.0000 and detection limits of 1.724 μg dm^{-3} As, 1.680 μg dm^{-3} As and 1.673 μg dm^{-3} As were calculated respectively for the three internal standards. The results of the analyses are listed in tables 4.27 to 4.29.

In all three cases values of 20 μg dm^{-3} As were obtained for samples containing only nitric acid as matrix. When using any of these three elements as internal standards for arsenic analysis of solutions containing hydrochloric acid in the matrix, the correction procedure proved to be successful only when the hydrochloric acid is present at low concentrations.

Table 4.27: Results of quantitative determination of As using ^{45}Sc as internal standard and the molecular correction factor (mass 75 / mass 77) at 1.00% v/v HCl. Results are also shown for time drift corrected values. First order equation used: ($y = -0.0052x + 19.883$) and second order equation used: ($y = 2x10^{-5}x^2 - 0.0104x + 20.157$)

Time difference (minutes)	Sample name	[As] (μg dm^{-3})	Corrected with first order drift curve (μg dm^{-3})	Corrected with second order drift curve (μg dm^{-3})
44.57	Drift control - 20 μg dm^{-3} As	19.74	20.09	20.01
51.83	20 μg dm^{-3} As in 0.10% v/v HNO_3	18.92	19.30	19.24

Time difference (minutes)	Sample name	[As] (μg dm^{-3})	Corrected with first order drift curve (μg dm^{-3})	Corrected with second order drift curve (μg dm^{-3})
59.10	20 μg dm^{-3} As in 0.50% v/v HNO_3	20.22	20.65	20.62
66.42	20 μg dm^{-3} As in 1.00% v/v HNO_3	20.07	20.54	20.52
73.68	20 μg dm^{-3} As in 1.50% v/v HNO_3	19.81	20.32	20.32
80.95	20 μg dm^{-3} As in 2.00% v/v HNO_3	19.61	20.16	20.17
88.22	20 μg dm^{-3} As in 2.50% v/v HNO_3	20.34	20.94	20.97
142.48	20 μg dm^{-3} As in 0.10% v/v HCl	17.87	18.67	18.73
149.82	20 μg dm^{-3} As in 0.50% v/v HCl	19.24	20.15	20.21
157.18	20 μg dm^{-3} As in 1.00% v/v HCl	22.82	23.94	24.00
164.55	20 μg dm^{-3} As in 1.50% v/v HCl	19.36	20.35	20.39
171.92	20 μg dm^{-3} As in 2.00% v/v HCl	25.96	27.34	27.38
179.30	20 μg dm^{-3} As in 2.50% v/v HCl	23.73	25.04	25.06
188.58	Drift control - 20 μg dm^{-3} As	18.62	19.71	19.70
220.02	20 μg dm^{-3} As in (0.10% v/v HNO_3 + 0.10% v/v HCl)	17.32	18.48	18.39
227.40	20 μg dm^{-3} As in (0.50% v/v HNO_3 + 0.50% v/v HCl)	18.12	19.38	19.25
234.78	20 μg dm^{-3} As in (1.00% v/v HNO_3 + 1.00% v/v HCl)	24.32	26.06	25.84
244.08	Drift control - 20 μg dm^{-3} As	18.78	20.18	19.97
296.78	Drift control - 20 μg dm^{-3} As	18.39	20.06	19.53

Table 4.28: Results of quantitative determination of As using ^{89}Y as internal standard and the molecular correction factor (mass 75 / mass 77) at 1.00% v/v HCl. Results are also shown for time drift corrected values. First order equation used: ($y = 0.0009x + 19.652$) and second order equation used: ($y = -8x10^{-6}x^2 + 0.0036x + 19.511$)

Time difference (minutes)	Sample name	[As] ($\mu g\ dm^{-3}$)	Corrected with first order drift curve ($\mu g\ dm^{-3}$)	Corrected with second order drift curve ($\mu g\ dm^{-3}$)
44.57	Drift control - 20 $\mu g\ dm^{-3}$ As	19.69	20.00	20.03
51.83	20 $\mu g\ dm^{-3}$ As in 0.10% v/v HNO_3	19.07	19.36	19.38
59.10	20 $\mu g\ dm^{-3}$ As in 0.50% v/v HNO_3	20.56	20.86	20.87
66.42	20 $\mu g\ dm^{-3}$ As in 1.00% v/v HNO_3	20.07	20.36	20.36
73.68	20 $\mu g\ dm^{-3}$ As in 1.50% v/v HNO_3	20.02	20.31	20.29
80.95	20 $\mu g\ dm^{-3}$ As in 2.00% v/v HNO_3	19.63	19.91	19.88
88.22	20 $\mu g\ dm^{-3}$ As in 2.50% v/v HNO_3	20.32	20.59	20.56
142.48	20 $\mu g\ dm^{-3}$ As in 0.10% v/v HCl	19.00	19.21	19.13
149.82	20 $\mu g\ dm^{-3}$ As in 0.50% v/v HCl	21.48	21.71	21.62
157.18	20 $\mu g\ dm^{-3}$ As in 1.00% v/v HCl	26.64	26.92	26.81
164.55	20 $\mu g\ dm^{-3}$ As in 1.50% v/v HCl	22.78	23.00	22.90
171.92	20 $\mu g\ dm^{-3}$ As in 2.00% v/v HCl	31.51	31.82	31.68
179.30	20 $\mu g\ dm^{-3}$ As in 2.50% v/v HCl	29.06	29.33	29.21
188.58	Drift control - 20 $\mu g\ dm^{-3}$ As	19.62	19.79	19.71
220.02	20 $\mu g\ dm^{-3}$ As in (0.10% v/v HNO_3 + 0.10% v/v HCl)	19.21	19.35	19.29
227.40	20 $\mu g\ dm^{-3}$ As in (0.50% v/v HNO_3 + 0.50% v/v HCl)	20.62	20.77	20.70
234.78	20 $\mu g\ dm^{-3}$ As in (1.00% v/v HNO_3 + 1.00% v/v HCl)	28.42	28.62	28.54
244.08	Drift control - 20 $\mu g\ dm^{-3}$ As	20.32	20.45	20.41
296.78	Drift control - 20 $\mu g\ dm^{-3}$ As	19.69	19.77	19.82

Table 4.29: Results of quantitative determination of As using ^{139}La as internal standard and the molecular correction factor (mass 75 / mass 77) at 1.00% v/v HCl. Results are also shown for time drift corrected values. First order equation used: ($y = 0.0057x + 19.600$) and second order equation used: ($y = -2x10^{-5}x^2 + 0.0138x + 19.175$)

Time difference (minutes)	Sample name	[As] ($\mu g\ dm^{-3}$)	Corrected with first order drift curve ($\mu g\ dm^{-3}$)	Corrected with second order drift curve ($\mu g\ dm^{-3}$)
44.57	Drift control - 20 $\mu g\ dm^{-3}$ As	19.76	19.91	20.01
51.83	20 $\mu g\ dm^{-3}$ As in 0.10% v/v HNO_3	19.64	19.74	19.80
59.10	20 $\mu g\ dm^{-3}$ As in 0.50% v/v HNO_3	20.71	20.77	20.79
66.42	20 $\mu g\ dm^{-3}$ As in 1.00% v/v HNO_3	20.18	20.20	20.17
73.68	20 $\mu g\ dm^{-3}$ As in 1.50% v/v HNO_3	20.08	20.06	19.99
80.95	20 $\mu g\ dm^{-3}$ As in 2.00% v/v HNO_3	19.78	19.72	19.62
88.22	20 $\mu g\ dm^{-3}$ As in 2.50% v/v HNO_3	20.51	20.41	20.27
142.48	20 $\mu g\ dm^{-3}$ As in 0.10% v/v HCl	19.91	19.51	19.21
149.82	20 $\mu g\ dm^{-3}$ As in 0.50% v/v HCl	23.27	22.75	22.38
157.18	20 $\mu g\ dm^{-3}$ As in 1.00% v/v HCl	29.80	29.07	28.58
164.55	20 $\mu g\ dm^{-3}$ As in 1.50% v/v HCl	25.49	24.82	24.39
171.92	20 $\mu g\ dm^{-3}$ As in 2.00% v/v HCl	35.74	34.74	34.11
179.30	20 $\mu g\ dm^{-3}$ As in 2.50% v/v HCl	34.09	33.06	32.46
188.58	Drift control - 20 $\mu g\ dm^{-3}$ As	20.73	20.06	19.68
220.02	20 $\mu g\ dm^{-3}$ As in (0.10% v/v HNO_3 + 0.10% v/v HCl)	20.43	19.59	19.24
227.40	20 $\mu g\ dm^{-3}$ As in (0.50% v/v HNO_3 + 0.50% v/v HCl)	22.92	21.94	21.54
234.78	20 $\mu g\ dm^{-3}$ As in (1.00% v/v HNO_3 + 1.00% v/v HCl)	32.40	30.95	30.40
244.08	Drift control - 20 $\mu g\ dm^{-3}$ As	21.34	20.33	19.99
296.78	Drift control - 20 $\mu g\ dm^{-3}$ As	21.01	19.73	19.53

^{36}Ar, ^{35}Cl and ^{37}Cl as internal standards

Calibration curves constructed using these three internal standards yielded correlation coefficients of 0.9998, 1.0000 and 0.9999 respectively. Detection limits were calculated to be 1.895 μg dm^{-3} As, 1.162 μg dm^{-3} As and 1.786 μg dm^{-3} As for the cases of ^{36}Ar, ^{35}Cl and ^{37}Cl as internal standards. Results of analyses using these internal standards are listed in tables 4.30 to 4.32.

Samples containing only nitric acid as matrix yielded good results in all three cases, but after drift correction was applied results for ^{35}Cl as internal standard yielded too high values. In the cases of samples containing hydrochloric acid in the matrix, ^{35}Cl and ^{37}Cl as internal standards yielded very poor results. However, in the case of ^{36}Ar acceptable results were obtained except in the matrices: 2.00% v/v HCl and (1.00% v/v HNO_3 + 1.00% v/v HCl).

Table 4.30: Results of quantitative determination of As using ^{36}Ar as internal standard and the molecular correction factor (mass 75 / mass 77) at 1.00% v/v HCl. Results are also shown for time drift corrected values. First order equation used: ($y = -0.0177x + 19.863$) and second order equation used: ($y = 5x10^{-5}x^2 - 0.0348x + 20.759$)

Time difference (minutes)	Sample name	[As] (μg dm^{-3})	Corrected with first order drift curve (μg dm^{-3})	Corrected with second order drift curve (μg dm^{-3})
44.57	Drift control - 20 μg dm^{-3} As	19.33	20.27	20.02
51.83	20 μg dm^{-3} As in 0.10% v/v HNO_3	17.98	18.98	18.84
59.10	20 μg dm^{-3} As in 0.50% v/v HNO_3	18.98	20.18	20.11
66.42	20 μg dm^{-3} As in 1.00% v/v HNO_3	19.09	20.44	20.46
73.68	20 μg dm^{-3} As in 1.50% v/v HNO_3	18.56	20.00	20.10
80.95	20 μg dm^{-3} As in 2.00% v/v HNO_3	18.09	19.63	19.80
88.22	20 μg dm^{-3} As in 2.50% v/v HNO_3	19.07	20.83	21.09
142.48	20 μg dm^{-3} As in 0.10% v/v HCl	15.82	18.24	18.81
149.82	20 μg dm^{-3} As in 0.50% v/v HCl	16.10	18.70	19.31
157.18	20 μg dm^{-3} As in 1.00% v/v HCl	17.81	20.85	21.55

Time difference (minutes)	Sample name	[As] (μg dm^{-3})	Corrected with first order drift curve (μg dm^{-3})	Corrected with second order drift curve (μg dm^{-3})
164.55	20 μg dm^{-3} As in 1.50% v/v HCl	14.52	17.13	17.72
171.92	20 μg dm^{-3} As in 2.00% v/v HCl	19.48	23.16	23.96
179.30	20 μg dm^{-3} As in 2.50% v/v HCl	16.65	19.95	20.65
188.58	Drift control - 20 μg dm^{-3} As	15.91	19.26	19.92
220.02	20 μg dm^{-3} As in (0.10% v/v HNO_3 + 0.10% v/v HCl)	14.54	18.21	18.73
227.40	20 μg dm^{-3} As in (0.50% v/v HNO_3 + 0.50% v/v HCl)	14.37	18.14	18.62
234.78	20 μg dm^{-3} As in (1.00% v/v HNO_3 + 1.00% v/v HCl)	18.50	23.56	24.11
244.08	Drift control - 20 μg dm^{-3} As	15.56	20.03	20.42
296.78	Drift control - 20 μg dm^{-3} As	14.93	20.44	20.13

Table 4.31: Results of quantitative determination of As using ^{35}Cl as internal standard and the molecular correction factor (mass 75 / mass 77) at 1.00% v/v HCl. Results are also shown for time drift corrected values. First order equation used: ($y = -0.0431x + 20.287$) and second order equation used: ($y = 0.0003x^2 - 0.1461x + 25.703$)

Time difference (minutes)	Sample name	[As] (μg dm^{-3})	Corrected with first order drift curve (μg dm^{-3})	Corrected with second order drift curve (μg dm^{-3})
44.57	Drift control - 20 μg dm^{-3} As	20.03	21.81	20.25
51.83	20 μg dm^{-3} As in 0.10% v/v HNO_3	19.45	21.55	20.54
59.10	20 μg dm^{-3} As in 0.50% v/v HNO_3	20.31	22.89	22.42
66.42	20 μg dm^{-3} As in 1.00% v/v HNO_3	20.19	23.18	23.31
73.68	20 μg dm^{-3} As in 1.50% v/v HNO_3	20.21	23.62	24.39
80.95	20 μg dm^{-3} As in 2.00% v/v HNO_3	19.72	23.48	24.90
88.22	20 μg dm^{-3} As in 2.50% v/v HNO_3	20.41	24.76	26.95
142.48	20 μg dm^{-3} As in 0.10% v/v HCl	2.96	4.19	5.40

Time difference (minutes)	Sample name	[As] (μg dm^{-3})	Corrected with first order drift curve (μg dm^{-3})	Corrected with second order drift curve (μg dm^{-3})
149.82	20 μg dm^{-3} As in 0.50% v/v HCl	1.22	1.76	2.31
157.18	20 μg dm^{-3} As in 1.00% v/v HCl	1.03	1.53	2.04
164.55	20 μg dm^{-3} As in 1.50% v/v HCl	0.92	1.40	1.88
171.92	20 μg dm^{-3} As in 2.00% v/v HCl	0.93	1.44	1.96
179.30	20 μg dm^{-3} As in 2.50% v/v HCl	0.88	1.41	1.93
188.58	Drift control - 20 μg dm^{-3} As	7.50	12.33	17.00
220.02	20 μg dm^{-3} As in (0.10% v/v HNO_3 + 0.10% v/v HCl)	2.93	5.43	7.26
227.40	20 μg dm^{-3} As in (0.50% v/v HNO_3 + 0.50% v/v HCl)	1.19	2.26	2.97
234.78	20 μg dm^{-3} As in (1.00% v/v HNO_3 + 1.00% v/v HCl)	1.04	2.05	2.63
244.08	Drift control - 20 μg dm^{-3} As	11.41	23.36	28.83
296.78	Drift control - 20 μg dm^{-3} As	8.89	23.71	20.27

Table 4.32: Results of quantitative determination of As using ^{37}Cl as internal standard and the molecular correction factor (mass 75 / mass 77) at 1.00% v/v HCl. Results are also shown for time drift corrected values. First order equation used: ($y = -0.0101x + 19.839$) and second order equation used: ($y = 7x10^{-5}x^2 - 0.0323x + 21.005$)

Time difference (minutes)	Sample name	[As] (μg dm^{-3})	Corrected with first order drift curve (μg dm^{-3})	Corrected with second order drift curve (μg dm^{-3})
44.57	Drift control - 20 μg dm^{-3} As	19.75	20.38	20.05
51.83	20 μg dm^{-3} As in 0.10% v/v HNO_3	19.18	19.86	19.65
59.10	20 μg dm^{-3} As in 0.50% v/v HNO_3	19.84	20.62	20.52
66.42	20 μg dm^{-3} As in 1.00% v/v HNO_3	19.80	20.66	20.65
73.68	20 μg dm^{-3} As in 1.50% v/v HNO_3	19.22	20.13	20.22
80.95	20 μg dm^{-3} As in 2.00% v/v HNO_3	18.58	19.53	19.71

Time difference (minutes)	Sample name	[As] (μg dm^{-3})	Corrected with first order drift curve (μg dm^{-3})	Corrected with second order drift curve (μg dm^{-3})
88.22	20 μg dm^{-3} As in 2.50% v/v HNO_3	19.23	20.30	20.57
142.48	20 μg dm^{-3} As in 0.10% v/v HCl	14.84	16.13	16.65
149.82	20 μg dm^{-3} As in 0.50% v/v HCl	8.45	9.22	9.53
157.18	20 μg dm^{-3} As in 1.00% v/v HCl	6.23	6.83	7.06
164.55	20 μg dm^{-3} As in 1.50% v/v HCl	3.94	4.33	4.48
171.92	20 μg dm^{-3} As in 2.00% v/v HCl	4.29	4.74	4.90
179.30	20 μg dm^{-3} As in 2.50% v/v HCl	3.26	3.62	3.74
188.58	Drift control - 20 μg dm^{-3} As	16.86	18.81	19.38
220.02	20 μg dm^{-3} As in (0.10% v/v HNO_3 + 0.10% v/v HCl)	14.18	16.10	16.41
227.40	20 μg dm^{-3} As in (0.50% v/v HNO_3 + 0.50% v/v HCl)	7.81	8.90	9.04
234.78	20 μg dm^{-3} As in (1.00% v/v HNO_3 + 1.00% v/v HCl)	6.57	7.53	7.61
244.08	Drift control - 20 μg dm^{-3} As	17.80	20.50	20.59
296.78	Drift control - 20 μg dm^{-3} As	17.09	20.30	19.44

4.5.6 Effect of using molecular (mass 75 / mass 77) corrections in a 1.50% v/v HCl matrix on the quantitative determination of arsenic

No internal standard

A correction factor of 3.240 was obtained using a 1.50% v/v HCl solution. In the case of no internal standard, the calibration curve yielded a correlation coefficient of 1.0000 and a detection limit of 1.697 μg dm^{-3} As was calculated. The results of the analyses are shown in table 4.33.

Samples prepared from only arsenic and nitric acid yielded values of near to 20 μg dm^{-3}. Acceptable values were obtained for samples containing 0.10% v/v to 1.00% v/v HCl and the two samples with matrices (0.10% v/v HNO_3 + 0.10% v/v HCl) and (1.00% v/v HNO_3 + 1.00% v/v HCl).

Table 4.33: Results of quantitative determination of As using no internal standard and the molecular correction factor (mass 75 / mass 77) at 1.50% v/v HCl. Results are also shown for time drift corrected values. First order equation used: ($y = 0.0084x + 20.265$) and second order equation used: ($y = -2x10^{-5}x^2 + 0.0133x + 20.004$)

Time difference (minutes)	Sample name	[As] ($\mu g\ dm^{-3}$)	Corrected with first order drift curve ($\mu g\ dm^{-3}$)	Corrected with second order drift curve ($\mu g\ dm^{-3}$)
44.57	Drift control - 20 $\mu g\ dm^{-3}$ As	20.58	19.95	20.03
51.83	20 $\mu g\ dm^{-3}$ As in 0.10% v/v HNO_3	19.98	19.31	19.36
59.10	20 $\mu g\ dm^{-3}$ As in 0.50% v/v HNO_3	21.12	20.34	20.38
66.42	20 $\mu g\ dm^{-3}$ As in 1.00% v/v HNO_3	21.43	20.59	20.61
73.68	20 $\mu g\ dm^{-3}$ As in 1.50% v/v HNO_3	21.02	20.13	20.14
80.95	20 $\mu g\ dm^{-3}$ As in 2.00% v/v HNO_3	20.44	19.52	19.51
88.22	20 $\mu g\ dm^{-3}$ As in 2.50% v/v HNO_3	21.22	20.20	20.19
142.48	20 $\mu g\ dm^{-3}$ As in 0.10% v/v HCl	20.42	19.03	19.00
149.82	20 $\mu g\ dm^{-3}$ As in 0.50% v/v HCl	19.40	18.03	18.01
157.18	20 $\mu g\ dm^{-3}$ As in 1.00% v/v HCl	20.58	19.07	19.05
164.55	20 $\mu g\ dm^{-3}$ As in 1.50% v/v HCl	13.94	12.88	12.87
171.92	20 $\mu g\ dm^{-3}$ As in 2.00% v/v HCl	19.90	18.34	18.34
179.30	20 $\mu g\ dm^{-3}$ As in 2.50% v/v HCl	14.67	13.48	13.49
188.58	Drift control - 20 $\mu g\ dm^{-3}$ As	21.84	19.99	20.04
220.02	20 $\mu g\ dm^{-3}$ As in (0.10% v/v HNO_3 + 0.10% v/v HCl)	20.25	18.32	18.44
227.40	20 $\mu g\ dm^{-3}$ As in (0.50% v/v HNO_3 + 0.50% v/v HCl)	18.22	16.43	16.57
234.78	20 $\mu g\ dm^{-3}$ As in (1.00% v/v HNO_3 + 1.00% v/v HCl)	22.05	19.83	20.02
244.08	Drift control - 20 $\mu g\ dm^{-3}$ As	22.56	20.22	20.45
296.78	Drift control - 20 $\mu g\ dm^{-3}$ As	22.54	19.81	20.32

^{45}Sc, ^{89}Y and ^{139}La as internal standards

In all these three cases correlation coefficients of 1.0000 were obtained for the calibration curves. Detection limits of 1.750 μg dm^{-3} As, 1.708 μg dm^{-3} As and 1.701 μg dm^{-3} As were calculated respectively. The results of the analyses when using the blank correction factor of a 1.50% v/v HCl solution together with ^{45}Sc, ^{89}Y and ^{139}La as internal standards can be seen in tables 4.34 to 4.36.

Using any of the three isotopes as internal standards values of approximately 20 μg dm^{-3} were obtained when the matrices of the samples comprised of only nitric acid. In some cases where the sample matrix contained hydrochloric acid the correction procedure proved to be successful for all three isotopes as internal standards, especially when the concentration of the hydrochloric acid was low.

Table 4.34: Results of quantitative determination of As using ^{45}Sc as internal standard and the molecular correction factor (mass 75 / mass 77) at 1.50% v/v HCl. Results are also shown for time drift corrected values. First order equation used: ($y = -0.0057x + 19.906$) and second order equation used: ($y = 2x10^{-5}x^2 - 0.0122x + 20.245$)

Time difference (minutes)	Sample name	[As] (μg dm^{-3})	Corrected with first order drift curve (μg dm^{-3})	Corrected with second order drift curve (μg dm^{-3})
44.57	Drift control - 20 μg dm^{-3} As	19.76	20.11	20.02
51.83	20 μg dm^{-3} As in 0.10% v/v HNO_3	18.94	19.31	19.26
59.10	20 μg dm^{-3} As in 0.50% v/v HNO_3	20.23	20.68	20.65
66.42	20 μg dm^{-3} As in 1.00% v/v HNO_3	20.09	20.58	20.58
73.68	20 μg dm^{-3} As in 1.50% v/v HNO_3	19.82	20.34	20.38
80.95	20 μg dm^{-3} As in 2.00% v/v HNO_3	19.63	20.19	20.25
88.22	20 μg dm^{-3} As in 2.50% v/v HNO_3	20.35	20.98	21.06
142.48	20 μg dm^{-3} As in 0.10% v/v HCl	17.40	18.23	18.40
149.82	20 μg dm^{-3} As in 0.50% v/v HCl	16.58	17.40	17.57
157.18	20 μg dm^{-3} As in 1.00% v/v HCl	17.50	18.41	18.60

Time difference (minutes)	Sample name	[As] (μg dm^{-3})	Corrected with first order drift curve (μg dm^{-3})	Corrected with second order drift curve (μg dm^{-3})
164.55	20 μg dm^{-3} As in 1.50% v/v HCl	11.71	12.34	12.47
171.92	20 μg dm^{-3} As in 2.00% v/v HCl	16.23	17.15	17.33
179.30	20 μg dm^{-3} As in 2.50% v/v HCl	11.91	12.62	12.74
188.58	Drift control - 20 μg dm^{-3} As	18.47	19.62	19.81
220.02	20 μg dm^{-3} As in (0.10% v/v HNO_3 + 0.10% v/v HCl)	16.73	17.94	18.06
227.40	20 μg dm^{-3} As in (0.50% v/v HNO_3 + 0.50% v/v HCl)	14.95	16.06	16.16
234.78	20 μg dm^{-3} As in (1.00% v/v HNO_3 + 1.00% v/v HCl)	18.35	19.77	19.86
244.08	Drift control - 20 μg dm^{-3} As	18.70	20.20	20.26
296.78	Drift control - 20 μg dm^{-3} As	18.26	20.05	19.86

Table 4.35: Results of quantitative determination of As using ^{89}Y as internal standard and the molecular correction factor (mass 75 / mass 77) at 1.50% v/v HCl. Results are also shown for time drift corrected values. First order equation used: ($y = 0.0003x + 19.677$) and second order equation used: ($y = -4x10^{-6}x^2 + 0.0017x + 19.605$)

Time difference (minutes)	Sample name	[As] (μg dm^{-3})	Corrected with first order drift curve (μg dm^{-3})	Corrected with second order drift curve (μg dm^{-3})
44.57	Drift control - 20 μg dm^{-3} As	19.71	20.02	20.03
51.83	20 μg dm^{-3} As in 0.10% v/v HNO_3	19.08	19.46	19.39
59.10	20 μg dm^{-3} As in 0.50% v/v HNO_3	20.57	21.02	20.89
66.42	20 μg dm^{-3} As in 1.00% v/v HNO_3	20.09	20.58	20.40
73.68	20 μg dm^{-3} As in 1.50% v/v HNO_3	20.03	20.56	20.33
80.95	20 μg dm^{-3} As in 2.00% v/v HNO_3	19.65	20.21	19.93
88.22	20 μg dm^{-3} As in 2.50% v/v HNO_3	20.33	20.95	20.61
142.48	20 μg dm^{-3} As in 0.10% v/v HCl	18.49	19.37	18.71

Time difference (minutes)	Sample name	[As] (μg dm^{-3})	Corrected with first order drift curve (μg dm^{-3})	Corrected with second order drift curve (μg dm^{-3})
149.82	20 μg dm^{-3} As in 0.50% v/v HCl	18.49	19.41	18.70
157.18	20 μg dm^{-3} As in 1.00% v/v HCl	20.40	21.46	20.63
164.55	20 μg dm^{-3} As in 1.50% v/v HCl	13.73	14.47	13.88
171.92	20 μg dm^{-3} As in 2.00% v/v HCl	19.65	20.77	19.87
179.30	20 μg dm^{-3} As in 2.50% v/v HCl	14.52	15.38	14.68
188.58	Drift control - 20 μg dm^{-3} As	19.45	20.66	19.67
220.02	20 μg dm^{-3} As in (0.10% v/v HNO_3 + 0.10% v/v HCl)	18.54	19.88	18.74
227.40	20 μg dm^{-3} As in (0.50% v/v HNO_3 + 0.50% v/v HCl)	16.98	18.25	17.17
234.78	20 μg dm^{-3} As in (1.00% v/v HNO_3 + 1.00% v/v HCl)	21.42	23.07	21.65
244.08	Drift control - 20 μg dm^{-3} As	20.22	21.84	20.44
296.78	Drift control - 20 μg dm^{-3} As	19.54	21.45	19.78

Table 4.36: Results of quantitative determination of As using ^{139}La as internal standard and the molecular correction factor (mass 75 / mass 77) at 1.50% v/v HCl. Results are also shown for time drift corrected values. First order equation used: ($y = 0.005x + 19.626$) and second order equation used: ($y = -2x10^{-5}x^2 + 0.0118x + 19.273$)

Time difference (minutes)	Sample name	[As] (μg dm^{-3})	Corrected with first order drift curve (μg dm^{-3})	Corrected with second order drift curve (μg dm^{-3})
44.57	Drift control - 20 μg dm^{-3} As	19.78	19.93	20.02
51.83	20 μg dm^{-3} As in 0.10% v/v HNO_3	19.65	19.76	19.81
59.10	20 μg dm^{-3} As in 0.50% v/v HNO_3	20.72	20.81	20.83
66.42	20 μg dm^{-3} As in 1.00% v/v HNO_3	20.20	20.24	20.23
73.68	20 μg dm^{-3} As in 1.50% v/v HNO_3	20.08	20.09	20.05
80.95	20 μg dm^{-3} As in 2.00% v/v HNO_3	19.79	19.76	19.70

Time difference (minutes)	Sample name	[As] (μg dm^{-3})	Corrected with first order drift curve (μg dm^{-3})	Corrected with second order drift curve (μg dm^{-3})
88.22	20 μg dm^{-3} As in 2.50% v/v HNO_3	20.52	20.46	20.36
142.48	20 μg dm^{-3} As in 0.10% v/v HCl	19.38	19.06	18.86
149.82	20 μg dm^{-3} As in 0.50% v/v HCl	20.02	19.65	19.45
157.18	20 μg dm^{-3} As in 1.00% v/v HCl	22.80	22.34	22.10
164.55	20 μg dm^{-3} As in 1.50% v/v HCl	15.35	15.01	14.85
171.92	20 μg dm^{-3} As in 2.00% v/v HCl	22.27	21.74	21.51
179.30	20 μg dm^{-3} As in 2.50% v/v HCl	16.99	16.56	16.38
188.58	Drift control - 20 μg dm^{-3} As	20.55	19.98	19.78
220.02	20 μg dm^{-3} As in (0.10% v/v HNO_3 + 0.10% v/v HCl)	19.72	19.03	18.87
227.40	20 μg dm^{-3} As in (0.50% v/v HNO_3 + 0.50% v/v HCl)	18.87	18.17	18.04
234.78	20 μg dm^{-3} As in (1.00% v/v HNO_3 + 1.00% v/v HCl)	24.40	23.46	23.30
244.08	Drift control - 20 μg dm^{-3} As	21.23	20.37	20.26
296.78	Drift control - 20 μg dm^{-3} As	20.83	19.74	19.83

^{36}Ar, ^{35}Cl and ^{37}Cl as internal standards

Calibration correlation coefficients of 0.9998, 1.0000 and 0.9999 together with detection limits of 1.927 μg dm^{-3} As, 1.195 μg dm^{-3} As and 1.814 μg dm^{-3} As were obtained respectively in the cases of using ^{36}Ar, ^{35}Cl and ^{37}Cl as internal standards. Tables 4.37 to 4.39 show the results of the analyses.

^{36}Ar and ^{37}Cl as internal standards yielded good results for matrices containing only nitric acid, but in the case of ^{35}Cl time drift correction resulted in too high values. When the matrix contained hydrochloric acid, the values obtained in the case of ^{36}Ar were slightly too low to be considered acceptable, but ^{35}Cl and ^{37}Cl as internal standards resulted in very poor quantitative values.

Table 4.37: Results of quantitative determination of As using ^{36}Ar as internal standard and the molecular correction factor (mass 75 / mass 77) at 1.50% v/v HCl. Results are also shown for time drift corrected values. First order equation used: ($y = -0.0181x + 19.889$) and second order equation used: ($y = 6x10^{-5}x^2 - 0.0363x + 20.843$)

Time difference (minutes)	Sample name	[As] ($\mu g\ dm^{-3}$)	Corrected with first order drift curve ($\mu g\ dm^{-3}$)	Corrected with second order drift curve ($\mu g\ dm^{-3}$)
44.57	Drift control - 20 $\mu g\ dm^{-3}$ As	19.35	20.29	20.01
51.83	20 $\mu g\ dm^{-3}$ As in 0.10% v/v HNO_3	18.00	19.00	18.83
59.10	20 $\mu g\ dm^{-3}$ As in 0.50% v/v HNO_3	19.01	20.21	20.11
66.42	20 $\mu g\ dm^{-3}$ As in 1.00% v/v HNO_3	19.13	20.47	20.46
73.68	20 $\mu g\ dm^{-3}$ As in 1.50% v/v HNO_3	18.58	20.03	20.09
80.95	20 $\mu g\ dm^{-3}$ As in 2.00% v/v HNO_3	18.12	19.67	19.80
88.22	20 $\mu g\ dm^{-3}$ As in 2.50% v/v HNO_3	19.09	20.87	21.08
142.48	20 $\mu g\ dm^{-3}$ As in 0.10% v/v HCl	15.40	17.79	18.24
149.82	20 $\mu g\ dm^{-3}$ As in 0.50% v/v HCl	13.79	16.06	16.47
157.18	20 $\mu g\ dm^{-3}$ As in 1.00% v/v HCl	13.53	15.88	16.29
164.55	20 $\mu g\ dm^{-3}$ As in 1.50% v/v HCl	8.56	10.13	10.38
171.92	20 $\mu g\ dm^{-3}$ As in 2.00% v/v HCl	11.98	14.28	14.63
179.30	20 $\mu g\ dm^{-3}$ As in 2.50% v/v HCl	8.10	9.73	9.96
188.58	Drift control - 20 $\mu g\ dm^{-3}$ As	15.80	19.18	19.59
220.02	20 $\mu g\ dm^{-3}$ As in (0.10% v/v HNO_3 + 0.10% v/v HCl)	14.05	17.66	17.82
227.40	20 $\mu g\ dm^{-3}$ As in (0.50% v/v HNO_3 + 0.50% v/v HCl)	11.76	14.92	14.99
234.78	20 $\mu g\ dm^{-3}$ As in (1.00% v/v HNO_3 + 1.00% v/v HCl)	13.84	17.70	17.71
244.08	Drift control - 20 $\mu g\ dm^{-3}$ As	15.52	20.06	19.95
296.78	Drift control - 20 $\mu g\ dm^{-3}$ As	14.84	20.44	19.33

Table 4.38: Results of quantitative determination of As using ^{35}Cl as internal standard and the molecular correction factor (mass 75 / mass 77) at 1.50% v/v HCl. Results are also shown for time drift corrected values. First order equation used: ($y = -0.0431x + 20.299$) and second order equation used: ($y = 0.0003x^2 - 0.1461x + 25.712$)

Time difference (minutes)	Sample name	[As] ($\mu g\ dm^{-3}$)	Corrected with first order drift curve ($\mu g\ dm^{-3}$)	Corrected with second order drift curve ($\mu g\ dm^{-3}$)
44.57	Drift control - 20 $\mu g\ dm^{-3}$ As	20.04	21.81	20.24
51.83	20 $\mu g\ dm^{-3}$ As in 0.10% v/v HNO_3	19.45	21.53	20.53
59.10	20 $\mu g\ dm^{-3}$ As in 0.50% v/v HNO_3	20.31	22.89	22.42
66.42	20 $\mu g\ dm^{-3}$ As in 1.00% v/v HNO_3	20.20	23.17	23.31
73.68	20 $\mu g\ dm^{-3}$ As in 1.50% v/v HNO_3	20.20	23.60	24.38
80.95	20 $\mu g\ dm^{-3}$ As in 2.00% v/v HNO_3	19.73	23.47	24.89
88.22	20 $\mu g\ dm^{-3}$ As in 2.50% v/v HNO_3	20.41	24.75	26.93
142.48	20 $\mu g\ dm^{-3}$ As in 0.10% v/v HCl	2.99	4.22	5.44
149.82	20 $\mu g\ dm^{-3}$ As in 0.50% v/v HCl	1.25	1.81	2.37
157.18	20 $\mu g\ dm^{-3}$ As in 1.00% v/v HCl	1.07	1.58	2.11
164.55	20 $\mu g\ dm^{-3}$ As in 1.50% v/v HCl	0.96	1.46	1.96
171.92	20 $\mu g\ dm^{-3}$ As in 2.00% v/v HCl	0.97	1.50	2.05
179.30	20 $\mu g\ dm^{-3}$ As in 2.50% v/v HCl	0.93	1.48	2.03
188.58	Drift control - 20 $\mu g\ dm^{-3}$ As	7.50	12.32	16.99
220.02	20 $\mu g\ dm^{-3}$ As in (0.10% v/v HNO_3 + 0.10% v/v HCl)	2.94	5.44	7.27
227.40	20 $\mu g\ dm^{-3}$ As in (0.50% v/v HNO_3 + 0.50% v/v HCl)	1.21	2.30	3.02
234.78	20 $\mu g\ dm^{-3}$ As in (1.00% v/v HNO_3 + 1.00% v/v HCl)	1.07	2.11	2.71
244.08	Drift control - 20 $\mu g\ dm^{-3}$ As	11.39	23.30	28.76
296.78	Drift control - 20 $\mu g\ dm^{-3}$ As	8.87	23.63	20.22

Table 4.39: Results of quantitative determination of As using ^{37}Cl as internal standard and the molecular correction factor (mass 75 / mass 77) at 1.50% v/v HCl. Results are also shown for time drift corrected values. First order equation used: ($y = -0.0107x + 19.866$) and second order equation used: ($y = 7x10^{-5}x^2 - 0.0338x + 21.085$)

Time difference (minutes)	Sample name	[As] ($\mu g\ dm^{-3}$)	Corrected with first order drift curve ($\mu g\ dm^{-3}$)	Corrected with second order drift curve ($\mu g\ dm^{-3}$)
44.57	Drift control - 20 $\mu g\ dm^{-3}$ As	19.77	20.40	20.06
51.83	20 $\mu g\ dm^{-3}$ As in 0.10% v/v HNO_3	19.20	19.88	19.67
59.10	20 $\mu g\ dm^{-3}$ As in 0.50% v/v HNO_3	19.86	20.65	20.55
66.42	20 $\mu g\ dm^{-3}$ As in 1.00% v/v HNO_3	19.82	20.70	20.70
73.68	20 $\mu g\ dm^{-3}$ As in 1.50% v/v HNO_3	19.23	20.16	20.27
80.95	20 $\mu g\ dm^{-3}$ As in 2.00% v/v HNO_3	18.60	19.58	19.78
88.22	20 $\mu g\ dm^{-3}$ As in 2.50% v/v HNO_3	19.25	20.35	20.65
142.48	20 $\mu g\ dm^{-3}$ As in 0.10% v/v HCl	14.46	15.77	16.35
149.82	20 $\mu g\ dm^{-3}$ As in 0.50% v/v HCl	7.34	8.03	8.34
157.18	20 $\mu g\ dm^{-3}$ As in 1.00% v/v HCl	4.88	5.36	5.57
164.55	20 $\mu g\ dm^{-3}$ As in 1.50% v/v HCl	2.51	2.77	2.88
171.92	20 $\mu g\ dm^{-3}$ As in 2.00% v/v HCl	2.83	3.14	3.26
179.30	20 $\mu g\ dm^{-3}$ As in 2.50% v/v HCl	1.81	2.01	2.09
188.58	Drift control - 20 $\mu g\ dm^{-3}$ As	16.74	18.76	19.46
220.02	20 $\mu g\ dm^{-3}$ As in (0.10% v/v HNO_3 + 0.10% v/v HCl)	13.72	15.66	16.10
227.40	20 $\mu g\ dm^{-3}$ As in (0.50% v/v HNO_3 + 0.50% v/v HCl)	6.50	7.45	7.63
234.78	20 $\mu g\ dm^{-3}$ As in (1.00% v/v HNO_3 + 1.00% v/v HCl)	5.06	5.83	5.95
244.08	Drift control - 20 $\mu g\ dm^{-3}$ As	17.73	20.55	20.86
296.78	Drift control - 20 $\mu g\ dm^{-3}$ As	16.97	20.34	19.71

4.5.7 Effect of using molecular (mass 75 / mass 77) corrections in a 2.00% v/v HCl matrix on the quantitative determination of arsenic

No internal standard

In this section the calculated correction factor of 3.199 for a solution of 2.00% v/v HCl was applied. In the case of no internal standard a correlation coefficient of 1.0000 was obtained for the calibration curve and the detection limit was calculated to be 1.686 μg dm^{-3} As. Table 4.40 show the values obtained after quantitative analyses.

From the table it can be seen that values of approximately 20 μg dm^{-3} were obtained when the sample matrix consisted of only nitric acid. Although this correction procedure proved to yield correct values of near to 20 μg dm^{-3} in some of the cases where hydrochloric acid was present in the matrix, it did not prove to be successful for the matrices of 1.00% v/v to 2.00% v/v HCl and (1.00% v/v HNO_3 + 1.00% v/v HCl).

Table 4.40: Results of quantitative determination of As using no internal standard and the molecular correction factor (mass 75 / mass 77) at 2.00% v/v HCl. Results are also shown for time drift corrected values. First order equation used: ($y = 0.0087x + 20.255$) and second order equation used: ($y = -2x10^{-5}x^2 + 0.0143x + 19.962$)

Time difference (minutes)	Sample name	[As] (μg dm^{-3})	Corrected with first order drift curve (μg dm^{-3})	Corrected with second order drift curve (μg dm^{-3})
44.57	Drift control - 20 μg dm^{-3} As	20.58	19.94	20.02
51.83	20 μg dm^{-3} As in 0.10% v/v HNO_3	19.98	19.30	19.35
59.10	20 μg dm^{-3} As in 0.50% v/v HNO_3	21.11	20.33	20.36
66.42	20 μg dm^{-3} As in 1.00% v/v HNO_3	21.43	20.57	20.58
73.68	20 μg dm^{-3} As in 1.50% v/v HNO_3	21.02	20.12	20.11
80.95	20 μg dm^{-3} As in 2.00% v/v HNO_3	20.43	19.50	19.47
88.22	20 μg dm^{-3} As in 2.50% v/v HNO_3	21.22	20.18	20.14
142.48	20 μg dm^{-3} As in 0.10% v/v HCl	20.67	19.23	19.14
149.82	20 μg dm^{-3} As in 0.50% v/v HCl	20.77	19.27	19.18

Time difference (minutes)	Sample name	[As] (μg dm^{-3})	Corrected with first order drift curve (μg dm^{-3})	Corrected with second order drift curve (μg dm^{-3})
157.18	20 μg dm^{-3} As in 1.00% v/v HCl	23.32	21.57	21.47
164.55	20 μg dm^{-3} As in 1.50% v/v HCl	17.93	16.54	16.47
171.92	20 μg dm^{-3} As in 2.00% v/v HCl	25.13	23.10	23.02
179.30	20 μg dm^{-3} As in 2.50% v/v HCl	21.06	19.30	19.24
188.58	Drift control - 20 μg dm^{-3} As	21.93	20.03	19.98
220.02	20 μg dm^{-3} As in (0.10% v/v HNO_3 + 0.10% v/v HCl)	20.57	18.56	18.58
227.40	20 μg dm^{-3} As in (0.50% v/v HNO_3 + 0.50% v/v HCl)	19.92	17.92	17.96
234.78	20 μg dm^{-3} As in (1.00% v/v HNO_3 + 1.00% v/v HCl)	25.19	22.59	22.67
244.08	Drift control - 20 μg dm^{-3} As	22.61	20.21	20.31
296.78	Drift control - 20 μg dm^{-3} As	22.63	19.82	20.16

^{45}Sc, ^{89}Y and ^{139}La as internal standards

Calibration curves with these three isotopes as internal standards yielded correlation coefficients of 1.0000 and detection limits of 1.738 μg dm^{-3} As, 1.696 μg dm^{-3} As and 1.688 μg dm^{-3} As respectively. The results of the quantitative analyses when using these internal standards are shown in tables 4.41 to 4.43.

All three the internal standards proved to be successful when only nitric acid where present in the matrix of the 20 μg dm^{-3} arsenic sample. With hydrochloric acid present in solution, analyses with all three internal standards resulted in values slightly deviating from the true value of 20 μg dm^{-3}. ^{139}La as internal standard yielded good values especially at low concentrations of hydrochloric acid.

Table 4.41: Results of quantitative determination of As using ^{45}Sc as internal standard and the molecular correction factor (mass 75 / mass 77) at 2.00% v/v HCl. Results are also shown for time drift corrected values. First order equation used: ($y = -0.0082x + 21.068$) and second order equation used: ($y = 8x10^{-5}x^2 - 0.0346x + 22.456$)

Time difference (minutes)	Sample name	[As] ($\mu g\ dm^{-3}$)	Corrected with first order drift curve ($\mu g\ dm^{-3}$)	Corrected with second order drift curve ($\mu g\ dm^{-3}$)
44.57	Drift control - 20 $\mu g\ dm^{-3}$ As	19.75	19.08	18.75
51.83	20 $\mu g\ dm^{-3}$ As in 0.10% v/v HNO_3	18.93	18.34	18.13
59.10	20 $\mu g\ dm^{-3}$ As in 0.50% v/v HNO_3	20.23	19.65	19.55
66.42	20 $\mu g\ dm^{-3}$ As in 1.00% v/v HNO_3	20.08	19.57	19.58
73.68	20 $\mu g\ dm^{-3}$ As in 1.50% v/v HNO_3	19.82	19.37	19.48
80.95	20 $\mu g\ dm^{-3}$ As in 2.00% v/v HNO_3	19.62	19.23	19.45
88.22	20 $\mu g\ dm^{-3}$ As in 2.50% v/v HNO_3	20.35	20.00	20.32
142.48	20 $\mu g\ dm^{-3}$ As in 0.10% v/v HCl	17.61	17.70	18.39
149.82	20 $\mu g\ dm^{-3}$ As in 0.50% v/v HCl	17.74	17.88	18.60
157.18	20 $\mu g\ dm^{-3}$ As in 1.00% v/v HCl	19.81	20.04	20.86
164.55	20 $\mu g\ dm^{-3}$ As in 1.50% v/v HCl	15.03	15.25	15.88
171.92	20 $\mu g\ dm^{-3}$ As in 2.00% v/v HCl	20.46	20.81	21.68
179.30	20 $\mu g\ dm^{-3}$ As in 2.50% v/v HCl	17.05	17.40	18.11
188.58	Drift control - 20 $\mu g\ dm^{-3}$ As	18.54	18.99	19.75
220.02	20 $\mu g\ dm^{-3}$ As in (0.10% v/v HNO_3 + 0.10% v/v HCl)	16.99	17.63	18.15
227.40	20 $\mu g\ dm^{-3}$ As in (0.50% v/v HNO_3 + 0.50% v/v HCl)	16.33	17.01	17.44
234.78	20 $\mu g\ dm^{-3}$ As in (1.00% v/v HNO_3 + 1.00% v/v HCl)	20.94	21.88	22.35
244.08	Drift control - 20 $\mu g\ dm^{-3}$ As	18.73	19.65	19.96
296.78	Drift control - 20 $\mu g\ dm^{-3}$ As	18.32	19.66	19.05

Table 4.42: Results of quantitative determination of As using ^{89}Y as internal standard and the molecular correction factor (mass 75 / mass 77) at 2.00% v/v HCl. Results are also shown for time drift corrected values. First order equation used: ($y = 0.0006x + 19.666$) and second order equation used: ($y = -6x10^{-6}x^2 + 0.0025x + 19.564$)

Time difference (minutes)	Sample name	[As] (μg dm^{-3})	Corrected with first order drift curve (μg dm^{-3})	Corrected with second order drift curve (μg dm^{-3})
44.57	Drift control - 20 μg dm^{-3} As	19.70	20.01	20.04
51.83	20 μg dm^{-3} As in 0.10% v/v HNO_3	19.08	19.37	19.39
59.10	20 μg dm^{-3} As in 0.50% v/v HNO_3	20.56	20.88	20.89
66.42	20 μg dm^{-3} As in 1.00% v/v HNO_3	20.08	20.38	20.38
73.68	20 μg dm^{-3} As in 1.50% v/v HNO_3	20.03	20.32	20.31
80.95	20 μg dm^{-3} As in 2.00% v/v HNO_3	19.64	19.93	19.91
88.22	20 μg dm^{-3} As in 2.50% v/v HNO_3	20.32	20.61	20.59
142.48	20 μg dm^{-3} As in 0.10% v/v HCl	18.71	18.95	18.91
149.82	20 μg dm^{-3} As in 0.50% v/v HCl	19.79	20.03	19.98
157.18	20 μg dm^{-3} As in 1.00% v/v HCl	23.11	23.39	23.34
164.55	20 μg dm^{-3} As in 1.50% v/v HCl	17.66	17.87	17.82
171.92	20 μg dm^{-3} As in 2.00% v/v HCl	24.81	25.10	25.04
179.30	20 μg dm^{-3} As in 2.50% v/v HCl	20.84	21.08	21.03
188.58	Drift control - 20 μg dm^{-3} As	19.52	19.74	19.70
220.02	20 μg dm^{-3} As in (0.10% v/v HNO_3 + 0.10% v/v HCl)	18.83	19.02	19.00
227.40	20 μg dm^{-3} As in (0.50% v/v HNO_3 + 0.50% v/v HCl)	18.56	18.75	18.73
234.78	20 μg dm^{-3} As in (1.00% v/v HNO_3 + 1.00% v/v HCl)	24.46	24.70	24.68
244.08	Drift control - 20 μg dm^{-3} As	20.26	20.46	20.45
296.78	Drift control - 20 μg dm^{-3} As	19.60	19.76	19.82

Table 4.43: Results of quantitative determination of As using ^{139}La as internal standard and the molecular correction factor (mass 75 / mass 77) at 2.00% v/v HCl. Results are also shown for time drift corrected values. First order equation used: ($y = 0.0053x + 19.615$) and second order equation used: ($y = -2x10^{-6}x^2 + 0.0127x + 19.230$)

Time difference (minutes)	Sample name	[As] ($\mu g\ dm^{-3}$)	Corrected with first order drift curve ($\mu g\ dm^{-3}$)	Corrected with second order drift curve ($\mu g\ dm^{-3}$)
44.57	Drift control - 20 $\mu g\ dm^{-3}$ As	19.77	19.92	20.02
51.83	20 $\mu g\ dm^{-3}$ As in 0.10% v/v HNO_3	19.64	19.75	19.80
59.10	20 $\mu g\ dm^{-3}$ As in 0.50% v/v HNO_3	20.72	20.79	20.81
66.42	20 $\mu g\ dm^{-3}$ As in 1.00% v/v HNO_3	20.19	20.22	20.20
73.68	20 $\mu g\ dm^{-3}$ As in 1.50% v/v HNO_3	20.08	20.07	20.02
80.95	20 $\mu g\ dm^{-3}$ As in 2.00% v/v HNO_3	19.79	19.75	19.66
88.22	20 $\mu g\ dm^{-3}$ As in 2.50% v/v HNO_3	20.52	20.43	20.32
142.48	20 $\mu g\ dm^{-3}$ As in 0.10% v/v HCl	19.61	19.26	19.01
149.82	20 $\mu g\ dm^{-3}$ As in 0.50% v/v HCl	21.43	21.00	20.72
157.18	20 $\mu g\ dm^{-3}$ As in 1.00% v/v HCl	25.84	25.27	24.93
164.55	20 $\mu g\ dm^{-3}$ As in 1.50% v/v HCl	19.76	19.29	19.02
171.92	20 $\mu g\ dm^{-3}$ As in 2.00% v/v HCl	28.13	27.40	27.01
179.30	20 $\mu g\ dm^{-3}$ As in 2.50% v/v HCl	24.42	23.75	23.41
188.58	Drift control - 20 $\mu g\ dm^{-3}$ As	20.63	20.02	19.73
220.02	20 $\mu g\ dm^{-3}$ As in (0.10% v/v HNO_3 + 0.10% v/v HCl)	20.03	19.28	19.02
227.40	20 $\mu g\ dm^{-3}$ As in (0.50% v/v HNO_3 + 0.50% v/v HCl)	20.63	19.82	19.57
234.78	20 $\mu g\ dm^{-3}$ As in (1.00% v/v HNO_3 + 1.00% v/v HCl)	27.87	26.73	26.41
244.08	Drift control - 20 $\mu g\ dm^{-3}$ As	21.28	20.36	20.13
296.78	Drift control - 20 $\mu g\ dm^{-3}$ As	20.91	19.74	19.69

^{36}Ar, ^{35}Cl and ^{37}Cl as internal standards

With ^{36}Ar, ^{35}Cl and ^{37}Cl as internal standards correlation coefficients of 0.9998, 1.0000 and 0.9999 were obtained for the calibration curves. Detection limits were calculated to be 1.913 $\mu g\ dm^{-3}$ As, 1.180 $\mu g\ dm^{-3}$ As and 1.802 $\mu g\ dm^{-3}$ As respectively. Tables 4.44 to 4.46 show the results of the quantitative analyses performed with these isotopes as internal standards.

Acceptable results were obtained when the sample did not contain hydrochloric acid, but for ^{35}Cl drift correction resulted in too high values. The two chlorine isotopes as internal standards did not result in acceptable values. ^{36}Ar as internal standard resulted in values slightly below the correct value of 20 $\mu g\ dm^{-3}$.

Table 4.44: Results of quantitative determination of As using ^{36}Ar as internal standard and the molecular correction factor (mass 75 / mass 77) at 2.00% v/v HCl. Results are also shown for time drift corrected values. First order equation used: ($y = -0.018x + 19.877$) and second order equation used: ($y = 5x10^{-5}x^2 - 0.0356x + 20.807$)

Time difference (minutes)	**Sample name**	**[As] ($\mu g\ dm^{-3}$)**	**Corrected with first order drift curve ($\mu g\ dm^{-3}$)**	**Corrected with second order drift curve ($\mu g\ dm^{-3}$)**
44.57	Drift control - 20 $\mu g\ dm^{-3}$ As	19.34	20.28	20.02
51.83	20 $\mu g\ dm^{-3}$ As in 0.10% v/v HNO_3	17.99	19.00	18.85
59.10	20 $\mu g\ dm^{-3}$ As in 0.50% v/v HNO_3	19.00	20.20	20.13
66.42	20 $\mu g\ dm^{-3}$ As in 1.00% v/v HNO_3	19.11	20.46	20.48
73.68	20 $\mu g\ dm^{-3}$ As in 1.50% v/v HNO_3	18.57	20.02	20.12
80.95	20 $\mu g\ dm^{-3}$ As in 2.00% v/v HNO_3	18.10	19.66	19.84
88.22	20 $\mu g\ dm^{-3}$ As in 2.50% v/v HNO_3	19.08	20.86	21.13
142.48	20 $\mu g\ dm^{-3}$ As in 0.10% v/v HCl	15.58	18.00	18.61
149.82	20 $\mu g\ dm^{-3}$ As in 0.50% v/v HCl	14.79	17.22	17.83
157.18	20 $\mu g\ dm^{-3}$ As in 1.00% v/v HCl	15.39	18.05	18.71
164.55	20 $\mu g\ dm^{-3}$ As in 1.50% v/v HCl	11.15	13.19	13.68
171.92	20 $\mu g\ dm^{-3}$ As in 2.00% v/v HCl	15.24	18.16	18.85

Time difference (minutes)	Sample name	[As] (μg dm^{-3})	Corrected with first order drift curve (μg dm^{-3})	Corrected with second order drift curve (μg dm^{-3})
179.30	20 μg dm^{-3} As in 2.50% v/v HCl	11.81	14.19	14.74
188.58	Drift control - 20 μg dm^{-3} As	15.85	19.23	19.97
220.02	20 μg dm^{-3} As in (0.10% v/v HNO_3 + 0.10% v/v HCl)	14.26	17.92	18.53
227.40	20 μg dm^{-3} As in (0.50% v/v HNO_3 + 0.50% v/v HCl)	12.89	16.34	16.86
234.78	20 μg dm^{-3} As in (1.00% v/v HNO_3 + 1.00% v/v HCl)	15.87	20.27	20.87
244.08	Drift control - 20 μg dm^{-3} As	15.54	20.07	20.58
296.78	Drift control - 20 μg dm^{-3} As	14.88	20.47	20.32

Table 4.45: Results of quantitative determination of As using ^{35}Cl as internal standard and the molecular correction factor (mass 75 / mass 77) at 2.00% v/v HCl. Results are also shown for time drift corrected values. First order equation used: ($y = -0.0431x + 20.294$) and second order equation used: ($y = 0.0003x^2 - 0.1461x + 25.708$)

Time difference (minutes)	Sample name	[As] (μg dm^{-3})	Corrected with first order drift curve (μg dm^{-3})	Corrected with second order drift curve (μg dm^{-3})
44.57	Drift control - 20 μg dm^{-3} As	20.03	21.81	20.24
51.83	20 μg dm^{-3} As in 0.10% v/v HNO_3	19.45	21.54	20.54
59.10	Drift control - 20 μg dm^{-3} As	20.31	22.89	22.42
66.42	20 μg dm^{-3} As in 0.10% v/v HNO_3	20.20	23.17	23.31
73.68	20 μg dm^{-3} As in 0.50% v/v HNO_3	20.20	23.61	24.38
80.95	20 μg dm^{-3} As in 2.00% v/v HNO_3	19.72	23.47	24.89
88.22	20 μg dm^{-3} As in 2.50% v/v HNO_3	20.41	24.75	26.94
142.48	20 μg dm^{-3} As in 0.10% v/v HCl	2.98	4.20	5.42
149.82	20 μg dm^{-3} As in 0.50% v/v HCl	1.24	1.79	2.34
157.18	20 μg dm^{-3} As in 1.00% v/v HCl	1.05	1.56	2.08
164.55	20 μg dm^{-3} As in 1.50% v/v HCl	0.94	1.43	1.93

Time difference (minutes)	Sample name	[As] (μg dm^{-3})	Corrected with first order drift curve (μg dm^{-3})	Corrected with second order drift curve (μg dm^{-3})
171.92	20 μg dm^{-3} As in 2.00% v/v HCl	0.95	1.47	2.01
179.30	20 μg dm^{-3} As in 2.50% v/v HCl	0.91	1.45	1.99
188.58	Drift control - 20 μg dm^{-3} As	7.50	12.33	17.00
220.02	20 μg dm^{-3} As in (0.10% v/v HNO_3 + 0.10% v/v HCl)	2.94	5.44	7.27
227.40	20 μg dm^{-3} As in (0.50% v/v HNO_3 + 0.50% v/v HCl)	1.20	2.28	2.99
234.78	20 μg dm^{-3} As in (1.00% v/v HNO_3 + 1.00% v/v HCl)	1.06	2.09	2.67
244.08	Drift control - 20 μg dm^{-3} As	11.40	23.33	28.79
296.78	Drift control - 20 μg dm^{-3} As	8.88	23.66	20.24

Table 4.46: Results of quantitative determination of As using ^{37}Cl as internal standard and the molecular correction factor (mass 75 / mass 77) at 2.00% v/v HCl. Results are also shown for time drift corrected values. First order equation used: ($y = -0.0104x + 19.855$) and second order equation used: ($y = 7x10^{-5}x^2 - 0.0332x + 21.050$)

Time difference (minutes)	Sample name	[As] (μg dm^{-3})	Corrected with first order drift curve (μg dm^{-3})	Corrected with second order drift curve (μg dm^{-3})
44.57	Drift control - 20 μg dm^{-3} As	19.76	20.38	20.06
51.83	20 μg dm^{-3} As in 0.10% v/v HNO_3	19.19	19.87	19.67
59.10	20 μg dm^{-3} As in 0.50% v/v HNO_3	19.85	20.64	20.54
66.42	20 μg dm^{-3} As in 1.00% v/v HNO_3	19.81	20.67	20.69
73.68	20 μg dm^{-3} As in 1.50% v/v HNO_3	19.23	20.14	20.26
80.95	20 μg dm^{-3} As in 2.00% v/v HNO_3	18.59	19.56	19.76
88.22	20 μg dm^{-3} As in 2.50% v/v HNO_3	19.24	20.32	20.62
142.48	20 μg dm^{-3} As in 0.10% v/v HCl	14.62	15.92	16.49
149.82	20 μg dm^{-3} As in 0.50% v/v HCl	7.82	8.55	8.86

Time difference (minutes)	Sample name	[As] (μg dm^{-3})	Corrected with first order drift curve (μg dm^{-3})	Corrected with second order drift curve (μg dm^{-3})
157.18	20 μg dm^{-3} As in 1.00% v/v HCl	5.47	6.00	6.22
164.55	20 μg dm^{-3} As in 1.50% v/v HCl	3.13	3.45	3.58
171.92	20 μg dm^{-3} As in 2.00% v/v HCl	3.46	3.84	3.98
179.30	20 μg dm^{-3} As in 2.50% v/v HCl	2.44	2.71	2.81
188.58	Drift control - 20 μg dm^{-3} As	16.79	18.77	19.44
220.02	20 μg dm^{-3} As in (0.10% v/v HNO_3 + 0.10% v/v HCl)	13.92	15.85	16.25
227.40	20 μg dm^{-3} As in (0.50% v/v HNO_3 + 0.50% v/v HCl)	7.07	8.08	8.25
234.78	20 μg dm^{-3} As in (1.00% v/v HNO_3 + 1.00% v/v HCl)	5.72	6.57	6.68
244.08	Drift control - 20 μg dm^{-3} As	17.76	20.52	20.76
296.78	Drift control - 20 μg dm^{-3} As	17.02	20.31	19.61

4.5.8 Effect of using molecular (mass 75 / mass 77) corrections in a 2.50% v/v HCl matrix on the quantitative determination of arsenic

No internal standard

A correction factor of 3.169 was obtained for a solution containing 2.50% v/v HCl. With no internal standard being used, a correlation coefficient of 1.0000 was obtained together with a detection limit of 1.678 μg dm^{-3} As. Results are listed in table 4.47.

Samples containing only 20 μg dm^{-3} As and nitric acid yielded acceptable values. After drift correction was applied acceptable values for the samples containing HCl were obtained when the concentration of the hydrochloric acid was low.

Table 4.47: Results of quantitative determination of As using no internal standard and the molecular correction factor (mass 75 / mass 77) at 2.50% v/v HCl. Results are also shown for time drift corrected values. First order equation used: ($y = 0.0089x + 20.247$) and second order equation used: ($y = -2x10^{-5}x^2 + 0.0149x + 19.931$)

Time difference (minutes)	Sample name	[As] ($\mu g\ dm^{-3}$)	Corrected with first order drift curve ($\mu g\ dm^{-3}$)	Corrected with second order drift curve ($\mu g\ dm^{-3}$)
44.57	Drift control - 20 $\mu g\ dm^{-3}$ As	20.57	19.93	20.02
51.83	20 $\mu g\ dm^{-3}$ As in 0.10% v/v HNO_3	19.98	19.29	19.35
59.10	20 $\mu g\ dm^{-3}$ As in 0.50% v/v HNO_3	21.11	20.32	20.35
66.42	20 $\mu g\ dm^{-3}$ As in 1.00% v/v HNO_3	21.42	20.56	20.57
73.68	20 $\mu g\ dm^{-3}$ As in 1.50% v/v HNO_3	21.02	20.11	20.10
80.95	20 $\mu g\ dm^{-3}$ As in 2.00% v/v HNO_3	20.43	19.49	19.45
88.22	20 $\mu g\ dm^{-3}$ As in 2.50% v/v HNO_3	21.21	20.17	20.12
142.48	20 $\mu g\ dm^{-3}$ As in 0.10% v/v HCl	20.84	19.38	19.26
149.82	20 $\mu g\ dm^{-3}$ As in 0.50% v/v HCl	21.75	20.15	20.03
157.18	20 $\mu g\ dm^{-3}$ As in 1.00% v/v HCl	25.27	23.34	23.20
164.55	20 $\mu g\ dm^{-3}$ As in 1.50% v/v HCl	20.78	19.14	19.03
171.92	20 $\mu g\ dm^{-3}$ As in 2.00% v/v HCl	28.85	26.49	26.34
179.30	20 $\mu g\ dm^{-3}$ As in 2.50% v/v HCl	25.60	23.44	23.32
188.58	Drift control - 20 $\mu g\ dm^{-3}$ As	21.99	20.06	19.97
220.02	20 $\mu g\ dm^{-3}$ As in (0.10% v/v HNO_3 + 0.10% v/v HCl)	20.80	18.74	18.71
227.40	20 $\mu g\ dm^{-3}$ As in (0.50% v/v HNO_3 + 0.50% v/v HCl)	21.14	18.98	18.97
234.78	20 $\mu g\ dm^{-3}$ As in (1.00% v/v HNO_3 + 1.00% v/v HCl)	27.42	24.55	24.56
244.08	Drift control - 20 $\mu g\ dm^{-3}$ As	22.65	20.20	20.24
296.78	Drift control - 20 $\mu g\ dm^{-3}$ As	22.69	19.83	20.09

^{45}Sc, ^{89}Y and ^{139}La as internal standards

With these three isotopes as internal standards correlation coefficients of the calibration curves were all 1.0000 and the detection limits were 1.730 μg dm^{-3} As, 1.687 μg dm^{-3} As and 1.680 μg dm^{-3} As respectively. Tables 4.48 to 4.50 show the results of quantitative analyses with these three internal standards.

Samples prepared from 20 μg dm^{-3} As and various concentrations of nitric acid yielded acceptable values in the cases of ^{45}Sc, ^{89}Y and ^{139}La as internal standards. For samples containing hydrochloric acid, none of the three internal standards yielded acceptable values over the whole range of hydrochloric acid concentrations.

Table 4.48: Results of quantitative determination of As using ^{45}Sc as internal standard and the molecular correction factor (mass 75 / mass 77) at 2.50% v/v HCl. Results are also shown for time drift corrected values. First order equation used: ($y = -0.0053x + 19.889$) and second order equation used: ($y = 2x10^{-5}x^2 - 0.0108x + 20.180$)

Time difference (minutes)	Sample name	[As] (μg dm^{-3})	Corrected with first order drift curve (μg dm^{-3})	Corrected with second order drift curve (μg dm^{-3})
44.57	Drift control - 20 μg dm^{-3} As	19.75	20.10	20.01
51.83	20 μg dm^{-3} As in 0.10% v/v HNO_3	18.93	19.30	19.24
59.10	20 μg dm^{-3} As in 0.50% v/v HNO_3	20.22	20.66	20.62
66.42	20 μg dm^{-3} As in 1.00% v/v HNO_3	20.07	20.55	20.53
73.68	20 μg dm^{-3} As in 1.50% v/v HNO_3	19.81	20.32	20.33
80.95	20 μg dm^{-3} As in 2.00% v/v HNO_3	19.62	20.16	20.19
88.22	20 μg dm^{-3} As in 2.50% v/v HNO_3	20.34	20.95	20.99
142.48	20 μg dm^{-3} As in 0.10% v/v HCl	17.75	18.56	18.64
149.82	20 μg dm^{-3} As in 0.50% v/v HCl	18.56	19.44	19.53
157.18	20 μg dm^{-3} As in 1.00% v/v HCl	21.46	22.52	22.62
164.55	20 μg dm^{-3} As in 1.50% v/v HCl	17.40	18.30	18.37

Time difference (minutes)	Sample name	[As] (μg dm^{-3})	Corrected with first order drift curve (μg dm^{-3})	Corrected with second order drift curve (μg dm^{-3})
171.92	20 μg dm^{-3} As in 2.00% v/v HCl	23.47	24.73	24.81
179.30	20 μg dm^{-3} As in 2.50% v/v HCl	20.70	21.86	21.92
188.58	Drift control - 20 μg dm^{-3} As	18.59	19.68	19.72
220.02	20 μg dm^{-3} As in (0.10% v/v HNO_3 + 0.10% v/v HCl)	17.17	18.34	18.29
227.40	20 μg dm^{-3} As in (0.50% v/v HNO_3 + 0.50% v/v HCl)	17.31	18.53	18.46
234.78	20 μg dm^{-3} As in (1.00% v/v HNO_3 + 1.00% v/v HCl)	22.79	24.44	24.31
244.08	Drift control - 20 μg dm^{-3} As	18.76	20.18	20.03
296.78	Drift control - 20 μg dm^{-3} As	18.36	20.05	19.60

Table 4.49: Results of quantitative determination of As using ^{89}Y as internal standard and the molecular correction factor (mass 75 / mass 77) at 2.50% v/v HCl. Results are also shown for time drift corrected values. First order equation used: ($y = 0.0008x + 19.658$) and second order equation used: ($y = -7x10^{-6}x^2 + 0.0031x + 19.535$)

Time difference (minutes)	Sample name	[As] (μg dm^{-3})	Corrected with first order drift curve (μg dm^{-3})	Corrected with second order drift curve (μg dm^{-3})
44.57	Drift control - 20 μg dm^{-3} As	19.69	20.00	18.88
51.83	20 μg dm^{-3} As in 0.10% v/v HNO_3	19.07	19.36	18.10
59.10	20 μg dm^{-3} As in 0.50% v/v HNO_3	20.56	20.87	19.31
66.42	20 μg dm^{-3} As in 1.00% v/v HNO_3	20.07	20.37	18.67
73.68	20 μg dm^{-3} As in 1.50% v/v HNO_3	20.02	20.31	18.44
80.95	20 μg dm^{-3} As in 2.00% v/v HNO_3	19.64	19.91	17.91
88.22	20 μg dm^{-3} As in 2.50% v/v HNO_3	20.32	20.60	18.36
142.48	20 μg dm^{-3} As in 0.10% v/v HCl	18.87	19.09	15.94
149.82	20 μg dm^{-3} As in 0.50% v/v HCl	20.71	20.95	17.34

Time difference (minutes)	Sample name	[As] (μg dm^{-3})	Corrected with first order drift curve (μg dm^{-3})	Corrected with second order drift curve (μg dm^{-3})
157.18	20 μg dm^{-3} As in 1.00% v/v HCl	25.04	25.32	20.79
164.55	20 μg dm^{-3} As in 1.50% v/v HCl	20.46	20.67	16.84
171.92	20 μg dm^{-3} As in 2.00% v/v HCl	28.48	28.77	23.24
179.30	20 μg dm^{-3} As in 2.50% v/v HCl	25.34	25.59	20.51
188.58	Drift control - 20 μg dm^{-3} As	19.58	19.76	15.68
220.02	20 μg dm^{-3} As in (0.10% v/v HNO_3 + 0.10% v/v HCl)	19.04	19.19	14.75
227.40	20 μg dm^{-3} As in (0.50% v/v HNO_3 + 0.50% v/v HCl)	19.69	19.84	15.13
234.78	20 μg dm^{-3} As in (1.00% v/v HNO_3 + 1.00% v/v HCl)	26.63	26.83	20.31
244.08	Drift control - 20 μg dm^{-3} As	20.29	20.44	15.34
296.78	Drift control - 20 μg dm^{-3} As	19.65	19.75	14.11

Table 4.50: Results of quantitative determination of As using ^{139}La as internal standard and the molecular correction factor (mass 75 / mass 77) at 2.50% v/v HCl. Results are also shown for time drift corrected values. First order equation used: ($y = 0.0056x + 19.607$) and second order equation used: ($y = -2x10^{-5}x^2 + 0.0133x + 19.200$)

Time difference (minutes)	Sample name	[As] (μg dm^{-3})	Corrected with first order drift curve (μg dm^{-3})	Corrected with second order drift curve (μg dm^{-3})
44.57	Drift control - 20 μg dm^{-3} As	19.77	19.91	20.01
51.83	20 μg dm^{-3} As in 0.10% v/v HNO_3	19.64	19.74	19.80
59.10	20 μg dm^{-3} As in 0.50% v/v HNO_3	20.71	20.78	20.80
66.42	20 μg dm^{-3} As in 1.00% v/v HNO_3	20.18	20.20	20.19
73.68	20 μg dm^{-3} As in 1.50% v/v HNO_3	20.08	20.06	20.01
80.95	20 μg dm^{-3} As in 2.00% v/v HNO_3	19.78	19.72	19.64
88.22	20 μg dm^{-3} As in 2.50% v/v HNO_3	20.52	20.41	20.29

Time difference (minutes)	Sample name	[As] (μg dm^{-3})	Corrected with first order drift curve (μg dm^{-3})	Corrected with second order drift curve (μg dm^{-3})
142.48	20 μg dm^{-3} As in 0.10% v/v HCl	19.78	19.39	19.12
149.82	20 μg dm^{-3} As in 0.50% v/v HCl	22.44	21.95	21.63
157.18	20 μg dm^{-3} As in 1.00% v/v HCl	28.00	27.34	26.93
164.55	20 μg dm^{-3} As in 1.50% v/v HCl	22.89	22.30	21.96
171.92	20 μg dm^{-3} As in 2.00% v/v HCl	32.29	31.40	30.91
179.30	20 μg dm^{-3} As in 2.50% v/v HCl	29.71	28.83	28.38
188.58	Drift control - 20 μg dm^{-3} As	20.69	20.02	19.71
220.02	20 μg dm^{-3} As in (0.10% v/v HNO_3 + 0.10% v/v HCl)	20.25	19.43	19.14
227.40	20 μg dm^{-3} As in (0.50% v/v HNO_3 + 0.50% v/v HCl)	21.88	20.96	20.65
234.78	20 μg dm^{-3} As in (1.00% v/v HNO_3 + 1.00% v/v HCl)	30.35	29.01	28.61
244.08	Drift control - 20 μg dm^{-3} As	21.31	20.32	20.06
296.78	Drift control - 20 μg dm^{-3} As	20.96	19.71	19.60

^{36}Ar, ^{35}Cl and ^{37}Cl as internal standards

^{36}Ar, ^{35}Cl and ^{37}Cl as internal standards resulted in correlation coefficients of 0.9998, 1.0000 and 0.9999 together with detection limits of 1.903 μg dm^{-3} As, 1.170 μg dm^{-3} As and 1.793 μg dm^{-3} As respectively. Tables 4.51 to 4.53 show the results of the quantitative analyses when using these three isotopes as internal standards.

HNO_3 matrices resulted in acceptable values for ^{36}Ar and ^{37}Cl as internal standards, but time drift corrections resulted in too high values in the case of ^{35}Cl. ^{35}Cl and ^{37}Cl as internal standards did not result in acceptable values for samples containing HCl in the matrix. In the case of ^{36}Ar the results were generally too low.

Table 4.51: Results of quantitative determination of As using ^{36}Ar as internal standard and the molecular correction factor (mass 75 / mass 77) at 2.50% v/v HCl. Results are also shown for time drift corrected values. First order equation used: ($y = -0.0178x + 19.870$) and second order equation used: ($y = 5x10^{-5}x^2 - 0.0352x + 20.781$)

Time difference (minutes)	Sample name	[As] ($\mu g\ dm^{-3}$)	Corrected with first order drift curve ($\mu g\ dm^{-3}$)	Corrected with second order drift curve ($\mu g\ dm^{-3}$)
44.57	Drift control - 20 $\mu g\ dm^{-3}$ As	19.34	20.27	20.02
51.83	20 $\mu g\ dm^{-3}$ As in 0.10% v/v HNO_3	17.99	18.99	18.84
59.10	20 $\mu g\ dm^{-3}$ As in 0.50% v/v HNO_3	18.99	20.18	20.12
66.42	20 $\mu g\ dm^{-3}$ As in 1.00% v/v HNO_3	19.10	20.44	20.47
73.68	20 $\mu g\ dm^{-3}$ As in 1.50% v/v HNO_3	18.56	20.01	20.11
80.95	20 $\mu g\ dm^{-3}$ As in 2.00% v/v HNO_3	18.09	19.64	19.82
88.22	20 $\mu g\ dm^{-3}$ As in 2.50% v/v HNO_3	19.07	20.84	21.11
142.48	20 $\mu g\ dm^{-3}$ As in 0.10% v/v HCl	15.71	18.13	18.73
149.82	20 $\mu g\ dm^{-3}$ As in 0.50% v/v HCl	15.51	18.03	18.65
157.18	20 $\mu g\ dm^{-3}$ As in 1.00% v/v HCl	16.71	19.58	20.28
164.55	20 $\mu g\ dm^{-3}$ As in 1.50% v/v HCl	13.00	15.34	15.90
171.92	20 $\mu g\ dm^{-3}$ As in 2.00% v/v HCl	17.55	20.89	21.66
179.30	20 $\mu g\ dm^{-3}$ As in 2.50% v/v HCl	14.46	17.34	17.99
188.58	Drift control - 20 $\mu g\ dm^{-3}$ As	15.88	19.24	19.95
220.02	20 $\mu g\ dm^{-3}$ As in (0.10% v/v HNO_3 + 0.10% v/v HCl)	14.41	18.07	18.65
227.40	20 $\mu g\ dm^{-3}$ As in (0.50% v/v HNO_3 + 0.50% v/v HCl)	13.70	17.32	17.84
234.78	20 $\mu g\ dm^{-3}$ As in (1.00% v/v HNO_3 + 1.00% v/v HCl)	17.31	22.06	22.66
244.08	Drift control - 20 $\mu g\ dm^{-3}$ As	15.55	20.03	20.51
296.78	Drift control - 20 $\mu g\ dm^{-3}$ As	14.91	20.44	20.23

Table 4.52: Results of quantitative determination of As using ^{35}Cl as internal standard and the molecular correction factor (mass 75 / mass 77) at 2.50% v/v HCl. Results are also shown for time drift corrected values. First order equation used: ($y = -0.0431x + 20.290$) and second order equation used: ($y = 0.0003x^2 - 0.1461x + 25.705$)

Time difference (minutes)	Sample name	[As] ($\mu g\ dm^{-3}$)	Corrected with first order drift curve ($\mu g\ dm^{-3}$)	Corrected with second order drift curve ($\mu g\ dm^{-3}$)
44.57	Drift control - 20 $\mu g\ dm^{-3}$ As	20.03	21.81	20.25
51.83	20 $\mu g\ dm^{-3}$ As in 0.10% v/v HNO_3	19.45	21.54	20.54
59.10	20 $\mu g\ dm^{-3}$ As in 0.50% v/v HNO_3	20.31	22.89	22.42
66.42	20 $\mu g\ dm^{-3}$ As in 1.00% v/v HNO_3	20.19	23.18	23.31
73.68	20 $\mu g\ dm^{-3}$ As in 1.50% v/v HNO_3	20.20	23.61	24.39
80.95	20 $\mu g\ dm^{-3}$ As in 2.00% v/v HNO_3	19.72	23.48	24.90
88.22	20 $\mu g\ dm^{-3}$ As in 2.50% v/v HNO_3	20.41	24.76	26.94
142.48	20 $\mu g\ dm^{-3}$ As in 0.10% v/v HCl	2.97	4.19	5.41
149.82	20 $\mu g\ dm^{-3}$ As in 0.50% v/v HCl	1.23	1.77	2.33
157.18	20 $\mu g\ dm^{-3}$ As in 1.00% v/v HCl	1.04	1.54	2.05
164.55	20 $\mu g\ dm^{-3}$ As in 1.50% v/v HCl	0.93	1.41	1.90
171.92	20 $\mu g\ dm^{-3}$ As in 2.00% v/v HCl	0.94	1.45	1.98
179.30	20 $\mu g\ dm^{-3}$ As in 2.50% v/v HCl	0.90	1.43	1.96
188.58	Drift control - 20 $\mu g\ dm^{-3}$ As	7.50	12.33	17.00
220.02	20 $\mu g\ dm^{-3}$ As in (0.10% v/v HNO_3 + 0.10% v/v HCl)	2.94	5.43	7.27
227.40	20 $\mu g\ dm^{-3}$ As in (0.50% v/v HNO_3 + 0.50% v/v HCl)	1.19	2.27	2.98
234.78	20 $\mu g\ dm^{-3}$ As in (1.00% v/v HNO_3 + 1.00% v/v HCl)	1.05	2.07	2.65
244.08	Drift control - 20 $\mu g\ dm^{-3}$ As	11.40	23.35	28.81
296.78	Drift control - 20 $\mu g\ dm^{-3}$ As	8.88	23.69	20.26

Table 4.53: Results of quantitative determination of As using ^{37}Cl as internal standard and the molecular correction factor (mass 75 / mass 77) at 2.50% v/v HCl. Results are also shown for time drift corrected values. First order equation used: ($y = -0.0103x + 19.846$) and second order equation used: ($y = 7x10^{-5}x^2 - 0.0327x + 21.025$)

Time difference (minutes)	Sample name	[As] ($\mu g\ dm^{-3}$)	Corrected with first order drift curve ($\mu g\ dm^{-3}$)	Corrected with second order drift curve ($\mu g\ dm^{-3}$)
44.57	Drift control - 20 $\mu g\ dm^{-3}$ As	19.76	20.38	20.05
51.83	20 $\mu g\ dm^{-3}$ As in 0.10% v/v HNO_3	19.19	19.87	19.66
59.10	20 $\mu g\ dm^{-3}$ As in 0.50% v/v HNO_3	19.84	20.63	20.53
66.42	20 $\mu g\ dm^{-3}$ As in 1.00% v/v HNO_3	19.80	20.67	20.67
73.68	20 $\mu g\ dm^{-3}$ As in 1.50% v/v HNO_3	19.22	20.14	20.24
80.95	20 $\mu g\ dm^{-3}$ As in 2.00% v/v HNO_3	18.58	19.55	19.73
88.22	20 $\mu g\ dm^{-3}$ As in 2.50% v/v HNO_3	19.24	20.31	20.59
142.48	20 $\mu g\ dm^{-3}$ As in 0.10% v/v HCl	14.74	16.04	16.58
149.82	20 $\mu g\ dm^{-3}$ As in 0.50% v/v HCl	8.16	8.92	9.23
157.18	20 $\mu g\ dm^{-3}$ As in 1.00% v/v HCl	5.89	6.46	6.68
164.55	20 $\mu g\ dm^{-3}$ As in 1.50% v/v HCl	3.57	3.93	4.07
171.92	20 $\mu g\ dm^{-3}$ As in 2.00% v/v HCl	3.92	4.34	4.49
179.30	20 $\mu g\ dm^{-3}$ As in 2.50% v/v HCl	2.89	3.21	3.32
188.58	Drift control - 20 $\mu g\ dm^{-3}$ As	16.83	18.80	19.41
220.02	20 $\mu g\ dm^{-3}$ As in (0.10% v/v HNO_3 + 0.10% v/v HCl)	14.06	16.00	16.34
227.40	20 $\mu g\ dm^{-3}$ As in (0.50% v/v HNO_3 + 0.50% v/v HCl)	7.47	8.54	8.68
234.78	20 $\mu g\ dm^{-3}$ As in (1.00% v/v HNO_3 + 1.00% v/v HCl)	6.19	7.10	7.19
244.08	Drift control - 20 $\mu g\ dm^{-3}$ As	17.79	20.52	20.66
296.78	Drift control - 20 $\mu g\ dm^{-3}$ As	17.06	20.32	19.51

4.5.9 Effect of using molecular (mass 75 / mass 77) corrections in a (0.10% v/v HNO_3 + 0.10% v/v HCl) matrix on the quantitative determination of arsenic

No internal standard

A solution containing 0.10% v/v of nitric acid and 0.10% v/v hydrochloric acid resulted in a correction factor of 3.190. The calibration curve that was constructed, gave a correlation coefficient of 1.0000 and a detection limit of 1.683 μg dm^{-3} As was calculated. Table 4.54 shows the results of the quantitative analyses that were performed.

Nitric acid as sample matrix did not prove to be a problem and acceptable results were obtained. Reasonable results were obtained for samples containing low concentrations of hydrochloric acid.

Table 4.54: Results of quantitative determination of As using no internal standard and the molecular correction factor (mass 75 / mass 77) at (0.10% v/v HNO_3 + 0.10% v/v HCl). Results are also shown for time drift corrected values. First order equation used: ($y = 0.0088x + 20.253$) and second order equation used: ($y = -2x10^{-5}x^2 + 0.0145x + 19.952$)

Time difference (minutes)	Sample name	[As] (μg dm^{-3})	Corrected with first order drift curve (μg dm^{-3})	Corrected with second order drift curve (μg dm^{-3})
44.57	Drift control - 20 μg dm^{-3} As	20.58	19.93	20.02
51.83	20 μg dm^{-3} As in 0.10% v/v HNO_3	19.98	19.29	19.35
59.10	20 μg dm^{-3} As in 0.50% v/v HNO_3	21.11	20.33	20.36
66.42	20 μg dm^{-3} As in 1.00% v/v HNO_3	21.43	20.56	20.58
73.68	20 μg dm^{-3} As in 1.50% v/v HNO_3	21.02	20.11	20.10
80.95	20 μg dm^{-3} As in 2.00% v/v HNO_3	20.43	19.49	19.46
88.22	20 μg dm^{-3} As in 2.50% v/v HNO_3	21.22	20.18	20.13
142.48	20 μg dm^{-3} As in 0.10% v/v HCl	20.72	19.27	19.17
149.82	20 μg dm^{-3} As in 0.50% v/v HCl	21.07	19.53	19.44
157.18	20 μg dm^{-3} As in 1.00% v/v HCl	23.91	22.10	22.00
164.55	20 μg dm^{-3} As in 1.50% v/v HCl	18.80	17.33	17.25

Time difference (minutes)	Sample name	[As] (μg dm^{-3})	Corrected with first order drift curve (μg dm^{-3})	Corrected with second order drift curve (μg dm^{-3})
171.92	20 μg dm^{-3} As in 2.00% v/v HCl	26.26	24.13	24.04
179.30	20 μg dm^{-3} As in 2.50% v/v HCl	22.45	20.56	20.49
188.58	Drift control - 20 μg dm^{-3} As	21.95	20.03	19.98
220.02	20 μg dm^{-3} As in (0.10% v/v HNO_3 + 0.10% v/v HCl)	20.64	18.61	18.62
227.40	20 μg dm^{-3} As in (0.50% v/v HNO_3 + 0.50% v/v HCl)	20.29	18.24	18.27
234.78	20 μg dm^{-3} As in (1.00% v/v HNO_3 + 1.00% v/v HCl)	25.87	23.18	23.25
244.08	Drift control - 20 μg dm^{-3} As	22.62	20.20	20.29
296.78	Drift control - 20 μg dm^{-3} As	22.65	19.81	20.14

^{45}Sc, ^{89}Y and ^{139}La as internal standards

Calibration curves that were constructed with ^{45}Sc, ^{89}Y and ^{139}La as internal standards resulted in correlation coefficients of 1.0000 and detection limits of 1.736 μg dm^{-3} As, 1.693 μg dm^{-3} As and 1.686 μg dm^{-3} As respectively. The results are listed in tables 4.55 to 4.57.

Values of approximately 20 μg dm^{-3} arsenic were obtained in the case of samples with matrices of only nitric acid. In the cases of all three the internal standards, acceptable results were obtained when the hydrochloric acid in the sample solution was present at a low concentration.

Table 4.55: Results of quantitative determination of As using ^{45}Sc as internal standard and the molecular correction factor (mass 75 / mass 77) at (0.10% v/v HNO_3 + 0.10% v/v HCl). Results are also shown for time drift corrected values. First order equation used: ($y = -0.0054x + 19.894$) and second order equation used: ($y = 2x10^{-5}x^2 - 0.0112x + 20.198$)

Time difference (minutes)	Sample name	[As] (μg dm^{-3})	Corrected with first order drift curve (μg dm^{-3})	Corrected with second order drift curve (μg dm^{-3})
44.57	Drift control - 20 μg dm^{-3} As	19.75	20.10	20.01
51.83	20 μg dm^{-3} As in 0.10% v/v HNO_3	18.93	19.30	19.25
59.10	20 μg dm^{-3} As in 0.50% v/v HNO_3	20.22	20.66	20.63

Time difference (minutes)	Sample name	[As] (μg dm^{-3})	Corrected with first order drift curve (μg dm^{-3})	Corrected with second order drift curve (μg dm^{-3})
66.42	20 μg dm^{-3} As in 1.00% v/v HNO_3	20.08	20.56	20.55
73.68	20 μg dm^{-3} As in 1.50% v/v HNO_3	19.82	20.33	20.34
80.95	20 μg dm^{-3} As in 2.00% v/v HNO_3	19.62	20.17	20.21
88.22	20 μg dm^{-3} As in 2.50% v/v HNO_3	20.35	20.96	21.01
142.48	20 μg dm^{-3} As in 0.10% v/v HCl	17.65	18.46	18.57
149.82	20 μg dm^{-3} As in 0.50% v/v HCl	17.99	18.85	18.97
157.18	20 μg dm^{-3} As in 1.00% v/v HCl	20.32	21.34	21.46
164.55	20 μg dm^{-3} As in 1.50% v/v HCl	15.76	16.58	16.68
171.92	20 μg dm^{-3} As in 2.00% v/v HCl	21.38	22.54	22.67
179.30	20 μg dm^{-3} As in 2.50% v/v HCl	18.16	19.20	19.29
188.58	Drift control - 20 μg dm^{-3} As	18.55	19.66	19.74
220.02	20 μg dm^{-3} As in (0.10% v/v HNO_3 + 0.10% v/v HCl)	17.04	18.22	18.22
227.40	20 μg dm^{-3} As in (0.50% v/v HNO_3 + 0.50% v/v HCl)	16.63	17.82	17.80
234.78	20 μg dm^{-3} As in (1.00% v/v HNO_3 + 1.00% v/v HCl)	21.51	23.09	23.04
244.08	Drift control - 20 μg dm^{-3} As	18.74	20.18	20.09
296.78	Drift control - 20 μg dm^{-3} As	18.33	20.04	19.67

Table 4.56: Results of quantitative determination of As using ^{89}Y as internal standard and the molecular correction factor (mass 75 / mass 77) at (0.10% v/v HNO_3 + 0.10% v/v HCl). Results are also shown for time drift corrected values. First order equation used: ($y = 0.0006x + 19.664$) and second order equation used: ($y = -6x10^{-6}x^2 + 0.0027x + 19.555$)

Time difference (minutes)	Sample name	[As] ($\mu g\ dm^{-3}$)	Corrected with first order drift curve ($\mu g\ dm^{-3}$)	Corrected with second order drift curve ($\mu g\ dm^{-3}$)
44.57	Drift control - 20 $\mu g\ dm^{-3}$ As	19.70	20.01	20.03
51.83	20 $\mu g\ dm^{-3}$ As in 0.10% v/v HNO_3	19.08	19.37	19.39
59.10	20 $\mu g\ dm^{-3}$ As in 0.50% v/v HNO_3	20.56	20.88	20.88
66.42	20 $\mu g\ dm^{-3}$ As in 1.00% v/v HNO_3	20.08	20.38	20.38
73.68	20 $\mu g\ dm^{-3}$ As in 1.50% v/v HNO_3	20.02	20.32	20.31
80.95	20 $\mu g\ dm^{-3}$ As in 2.00% v/v HNO_3	19.64	19.93	19.90
88.22	20 $\mu g\ dm^{-3}$ As in 2.50% v/v HNO_3	20.32	20.62	20.58
142.48	20 $\mu g\ dm^{-3}$ As in 0.10% v/v HCl	18.76	19.00	18.94
149.82	20 $\mu g\ dm^{-3}$ As in 0.50% v/v HCl	20.07	20.32	20.25
157.18	20 $\mu g\ dm^{-3}$ As in 1.00% v/v HCl	23.70	23.99	23.91
164.55	20 $\mu g\ dm^{-3}$ As in 1.50% v/v HCl	18.51	18.74	18.67
171.92	20 $\mu g\ dm^{-3}$ As in 2.00% v/v HCl	25.93	26.23	26.13
179.30	20 $\mu g\ dm^{-3}$ As in 2.50% v/v HCl	22.21	22.47	22.38
188.58	Drift control - 20 $\mu g\ dm^{-3}$ As	19.54	19.76	19.69
220.02	20 $\mu g\ dm^{-3}$ As in (0.10% v/v HNO_3 + 0.10% v/v HCl)	18.89	19.09	19.03
227.40	20 $\mu g\ dm^{-3}$ As in (0.50% v/v HNO_3 + 0.50% v/v HCl)	18.91	19.10	19.04
234.78	20 $\mu g\ dm^{-3}$ As in (1.00% v/v HNO_3 + 1.00% v/v HCl)	25.12	25.37	25.30
244.08	Drift control - 20 $\mu g\ dm^{-3}$ As	20.27	20.47	20.42
296.78	Drift control - 20 $\mu g\ dm^{-3}$ As	19.62	19.77	19.79

Table 4.57: Results of quantitative determination of As using ^{139}La as internal standard and the molecular correction factor (mass 75 / mass 77) at (0.10% v/v HNO_3 + 0.10% v/v HCl). Results are also shown for time drift corrected values. First order equation used: ($y = 0.0054x + 19.612$) and second order equation used: ($y = -2x10^{-5}x^2 + 0.0129x + 19.221$)

Time difference (minutes)	Sample name	[As] ($\mu g\ dm^{-3}$)	Corrected with first order drift curve ($\mu g\ dm^{-3}$)	Corrected with second order drift curve ($\mu g\ dm^{-3}$)
44.57	Drift control - 20 $\mu g\ dm^{-3}$ As	19.77	19.92	20.02
51.83	20 $\mu g\ dm^{-3}$ As in 0.10% v/v HNO_3	19.64	19.75	19.80
59.10	20 $\mu g\ dm^{-3}$ As in 0.50% v/v HNO_3	20.72	20.79	20.81
66.42	20 $\mu g\ dm^{-3}$ As in 1.00% v/v HNO_3	20.19	20.22	20.20
73.68	20 $\mu g\ dm^{-3}$ As in 1.50% v/v HNO_3	20.08	20.07	20.02
80.95	20 $\mu g\ dm^{-3}$ As in 2.00% v/v HNO_3	19.79	19.74	19.66
88.22	20 $\mu g\ dm^{-3}$ As in 2.50% v/v HNO_3	20.52	20.43	20.31
142.48	20 $\mu g\ dm^{-3}$ As in 0.10% v/v HCl	19.66	19.29	19.04
149.82	20 $\mu g\ dm^{-3}$ As in 0.50% v/v HCl	21.74	21.29	21.00
157.18	20 $\mu g\ dm^{-3}$ As in 1.00% v/v HCl	26.50	25.91	25.54
164.55	20 $\mu g\ dm^{-3}$ As in 1.50% v/v HCl	20.72	20.21	19.92
171.92	20 $\mu g\ dm^{-3}$ As in 2.00% v/v HCl	29.40	28.63	28.20
179.30	20 $\mu g\ dm^{-3}$ As in 2.50% v/v HCl	26.04	25.31	24.93
188.58	Drift control - 20 $\mu g\ dm^{-3}$ As	20.65	20.02	19.72
220.02	20 $\mu g\ dm^{-3}$ As in (0.10% v/v HNO_3 + 0.10% v/v HCl)	20.10	19.32	19.06
227.40	20 $\mu g\ dm^{-3}$ As in (0.50% v/v HNO_3 + 0.50% v/v HCl)	21.01	20.17	19.90
234.78	20 $\mu g\ dm^{-3}$ As in (1.00% v/v HNO_3 + 1.00% v/v HCl)	28.63	27.42	27.08
244.08	Drift control - 20 $\mu g\ dm^{-3}$ As	21.29	20.34	20.11
296.78	Drift control - 20 $\mu g\ dm^{-3}$ As	20.93	19.73	19.66

^{36}Ar, ^{35}Cl and ^{37}Cl as internal standards

The calibration curves constructed with these three internal standards resulted in correlation coefficients of 0.9998, 1.0000 and 0.9999 respectively. Detection limits were calculated to be 1.910 μg dm^{-3} As, 1.177 μg dm^{-3} As and 1.799 μg dm^{-3} As. The results of the quantitative analyses are shown in tables 4.58 to 4.60.

For nitric acid samples acceptable results were obtained, but from table 4.59 it can be seen that time drift procedures resulted in too high values for ^{35}Cl as internal standard. With samples containing hydrochloric acid in the matrix the two chlorine isotopes as internal standards did not result in acceptable values. In the case of ^{36}Ar the obtained values are generally just slightly below 20 μg dm^{-3}.

Table 4.58: Results of quantitative determination of As using ^{36}Ar as internal standard and the molecular correction factor (mass 75 / mass 77) at (0.10% v/v HNO_3 + 0.10% v/v HCl). Results are also shown for time drift corrected values. First order equation used: ($y = -0.0179x + 19.875$) and second order equation used: ($y = 5x10^{-5}x^2 - 0.0355x + 20.799$)

Time difference (minutes)	Sample name	[As] (μg dm^{-3})	Corrected with first order drift curve (μg dm^{-3})	Corrected with second order drift curve (μg dm^{-3})
44.57	Drift control - 20 μg dm^{-3} As	19.34	20.28	20.03
51.83	20 μg dm^{-3} As in 0.10% v/v HNO_3	17.99	18.99	18.85
59.10	20 μg dm^{-3} As in 0.50% v/v HNO_3	19.00	20.19	20.13
66.42	20 μg dm^{-3} As in 1.00% v/v HNO_3	19.11	20.45	20.48
73.68	20 μg dm^{-3} As in 1.50% v/v HNO_3	18.57	20.01	20.12
80.95	20 μg dm^{-3} As in 2.00% v/v HNO_3	18.10	19.65	19.83
88.22	20 μg dm^{-3} As in 2.50% v/v HNO_3	19.08	20.85	21.13
142.48	20 μg dm^{-3} As in 0.10% v/v HCl	15.62	18.03	18.65
149.82	20 μg dm^{-3} As in 0.50% v/v HCl	15.01	17.46	18.08
157.18	20 μg dm^{-3} As in 1.00% v/v HCl	15.79	18.51	19.20

Time difference (minutes)	Sample name	[As] (μg dm^{-3})	Corrected with first order drift curve (μg dm^{-3})	Corrected with second order drift curve (μg dm^{-3})
164.55	20 μg dm^{-3} As in 1.50% v/v HCl	11.72	13.84	14.36
171.92	20 μg dm^{-3} As in 2.00% v/v HCl	15.94	18.98	19.72
179.30	20 μg dm^{-3} As in 2.50% v/v HCl	12.62	15.15	15.74
188.58	Drift control - 20 μg dm^{-3} As	15.86	19.22	19.97
220.02	20 μg dm^{-3} As in (0.10% v/v HNO_3 + 0.10% v/v HCl)	14.31	17.95	18.57
227.40	20 μg dm^{-3} As in (0.50% v/v HNO_3 + 0.50% v/v HCl)	13.14	16.63	17.17
234.78	20 μg dm^{-3} As in (1.00% v/v HNO_3 + 1.00% v/v HCl)	16.31	20.81	21.43
244.08	Drift control - 20 μg dm^{-3} As	15.54	20.05	20.57
296.78	Drift control - 20 μg dm^{-3} As	14.89	20.44	20.30

Table 4.59: Results of quantitative determination of As using ^{35}Cl as internal standard and the molecular correction factor (mass 75 / mass 77) at (0.10% v/v HNO_3 + 0.10% v/v HCl). Results are also shown for time drift corrected values. First order equation used: ($y = -0.0431x + 20.293$) and second order equation used: ($y = 0.0003x^2 - 0.1461x + 25.707$)

Time difference (minutes)	Sample name	[As] (μg dm^{-3})	Corrected with first order drift curve (μg dm^{-3})	Corrected with second order drift curve (μg dm^{-3})
44.57	Drift control - 20 μg dm^{-3} As	20.03	21.81	20.24
51.83	20 μg dm^{-3} As in 0.10% v/v HNO_3	19.45	21.54	20.54
59.10	20 μg dm^{-3} As in 0.50% v/v HNO_3	20.31	22.89	22.42
66.42	20 μg dm^{-3} As in 1.00% v/v HNO_3	20.20	23.17	23.31
73.68	20 μg dm^{-3} As in 1.50% v/v HNO_3	20.20	23.61	24.39
80.95	20 μg dm^{-3} As in 2.00% v/v HNO_3	19.72	23.48	24.89
88.22	20 μg dm^{-3} As in 2.50% v/v HNO_3	20.41	24.76	26.94
142.48	20 μg dm^{-3} As in 0.10% v/v HCl	2.97	4.20	5.41

Time difference (minutes)	Sample name	[As] (μg dm^{-3})	Corrected with first order drift curve (μg dm^{-3})	Corrected with second order drift curve (μg dm^{-3})
149.82	20 μg dm^{-3} As in 0.50% v/v HCl	1.23	1.78	2.34
157.18	20 μg dm^{-3} As in 1.00% v/v HCl	1.05	1.55	2.07
164.55	20 μg dm^{-3} As in 1.50% v/v HCl	0.94	1.42	1.92
171.92	20 μg dm^{-3} As in 2.00% v/v HCl	0.95	1.47	2.00
179.30	20 μg dm^{-3} As in 2.50% v/v HCl	0.91	1.44	1.98
188.58	Drift control - 20 μg dm^{-3} As	7.50	12.33	17.00
220.02	20 μg dm^{-3} As in (0.10% v/v HNO_3 + 0.10% v/v HCl)	2.94	5.44	7.27
227.40	20 μg dm^{-3} As in (0.50% v/v HNO_3 + 0.50% v/v HCl)	1.20	2.28	2.99
234.78	20 μg dm^{-3} As in (1.00% v/v HNO_3 + 1.00% v/v HCl)	1.06	2.08	2.67
244.08	Drift control - 20 μg dm^{-3} As	11.40	23.33	28.79
296.78	Drift control - 20 μg dm^{-3} As	8.88	23.67	20.24

Table 4.60: Results of quantitative determination of As using ^{37}Cl as internal standard and the molecular correction factor (mass 75 / mass 77) at (0.10% v/v HNO_3 + 0.10% v/v HCl). Results are also shown for time drift corrected values. First order equation used: ($y = -0.0104x + 19.852$) and second order equation used: ($y = 7x10^{-5}x^2 - 0.0330x + 21.043$)

Time difference (minutes)	Sample name	[As] (μg dm^{-3})	Corrected with first order drift curve (μg dm^{-3})	Corrected with second order drift curve (μg dm^{-3})
44.57	Drift control - 20 μg dm^{-3} As	19.76	21.49	20.05
51.83	20 μg dm^{-3} As in 0.10% v/v HNO_3	19.19	20.96	19.66
59.10	20 μg dm^{-3} As in 0.50% v/v HNO_3	19.85	21.77	20.53
66.42	20 μg dm^{-3} As in 1.00% v/v HNO_3	19.81	21.81	20.68
73.68	20 μg dm^{-3} As in 1.50% v/v HNO_3	19.23	21.26	20.25
80.95	20 μg dm^{-3} As in 2.00% v/v HNO_3	18.59	20.64	19.74

Time difference (minutes)	Sample name	[As] (μg dm^{-3})	Corrected with first order drift curve (μg dm^{-3})	Corrected with second order drift curve (μg dm^{-3})
88.22	20 μg dm^{-3} As in 2.50% v/v HNO_3	19.24	21.46	20.60
142.48	20 μg dm^{-3} As in 0.10% v/v HCl	14.66	16.88	16.51
149.82	20 μg dm^{-3} As in 0.50% v/v HCl	7.92	9.16	8.97
157.18	20 μg dm^{-3} As in 1.00% v/v HCl	5.59	6.50	6.36
164.55	20 μg dm^{-3} As in 1.50% v/v HCl	3.26	3.81	3.73
171.92	20 μg dm^{-3} As in 2.00% v/v HCl	3.60	4.22	4.13
179.30	20 μg dm^{-3} As in 2.50% v/v HCl	2.58	3.03	2.97
188.58	Drift control - 20 μg dm^{-3} As	16.80	19.90	19.42
220.02	20 μg dm^{-3} As in (0.10% v/v HNO_3 + 0.10% v/v HCl)	13.96	16.86	16.26
227.40	20 μg dm^{-3} As in (0.50% v/v HNO_3 + 0.50% v/v HCl)	7.19	8.72	8.38
234.78	20 μg dm^{-3} As in (1.00% v/v HNO_3 + 1.00% v/v HCl)	5.86	7.14	6.83
244.08	Drift control - 20 μg dm^{-3} As	17.77	21.79	20.71
296.78	Drift control - 20 μg dm^{-3} As	17.04	21.61	19.56

4.5.10 Effect of using molecular (mass 75 / mass 77) corrections in a (0.50% v/v HNO_3 + 0.50% v/v HCl) matrix on the quantitative determination of arsenic

No internal standard

A correction factor of 3.189 for the solution of (0.50% v/v HNO_3 + 0.50% v/v HCl) was calculated and used in the processing of the results in this section. The constructed calibration curve showed a correlation coefficient of 1.0000 and the detection limit was calculated to be 1.683 μg dm^{-3} As. The results of the quantitative analyses are shown in table 4.61.

Matrices of only nitric acid resulted in acceptable values of approximately 20 μg dm^{-3} arsenic. With hydrochloric acid present at low concentration in solution the correction procedure proved to yield acceptable results.

Table 4.61: Results of quantitative determination of As using no internal standard and the molecular correction factor (mass 75 / mass 77) at (0.50% v/v HNO_3 + 0.50% v/v HCl). Results are also shown for time drift corrected values. First order equation used: ($y = 0.0088x + 20.252$) and second order equation used: ($y = -2x10^{-5}x^2 + 0.0145x + 19.952$)

Time difference (minutes)	Sample name	[As] ($\mu g\ dm^{-3}$)	Corrected with first order drift curve ($\mu g\ dm^{-3}$)	Corrected with second order drift curve ($\mu g\ dm^{-3}$)
44.57	Drift control - 20 $\mu g\ dm^{-3}$ As	20.58	19.93	20.02
51.83	20 $\mu g\ dm^{-3}$ As in 0.10% v/v HNO_3	19.98	19.29	19.35
59.10	20 $\mu g\ dm^{-3}$ As in 0.50% v/v HNO_3	21.11	20.33	20.36
66.42	20 $\mu g\ dm^{-3}$ As in 1.00% v/v HNO_3	21.43	20.57	20.58
73.68	20 $\mu g\ dm^{-3}$ As in 1.50% v/v HNO_3	21.02	20.12	20.10
80.95	20 $\mu g\ dm^{-3}$ As in 2.00% v/v HNO_3	20.43	19.49	19.46
88.22	20 $\mu g\ dm^{-3}$ As in 2.50% v/v HNO_3	21.22	20.18	20.13
142.48	20 $\mu g\ dm^{-3}$ As in 0.10% v/v HCl	20.72	19.27	19.18
149.82	20 $\mu g\ dm^{-3}$ As in 0.50% v/v HCl	21.08	19.55	19.45
157.18	20 $\mu g\ dm^{-3}$ As in 1.00% v/v HCl	23.94	22.13	22.02
164.55	20 $\mu g\ dm^{-3}$ As in 1.50% v/v HCl	18.84	17.36	17.29
171.92	20 $\mu g\ dm^{-3}$ As in 2.00% v/v HCl	26.31	24.18	24.08
179.30	20 $\mu g\ dm^{-3}$ As in 2.50% v/v HCl	22.51	20.62	20.54
188.58	Drift control - 20 $\mu g\ dm^{-3}$ As	21.95	20.03	19.98
220.02	20 $\mu g\ dm^{-3}$ As in (0.10% v/v HNO_3 + 0.10% v/v HCl)	20.65	18.61	18.62
227.40	20 $\mu g\ dm^{-3}$ As in (0.50% v/v HNO_3 + 0.50% v/v HCl)	20.31	18.25	18.28
234.78	20 $\mu g\ dm^{-3}$ As in (1.00% v/v HNO_3 + 1.00% v/v HCl)	25.90	23.21	23.28
244.08	Drift control - 20 $\mu g\ dm^{-3}$ As	22.62	20.20	20.29
296.78	Drift control - 20 $\mu g\ dm^{-3}$ As	22.65	19.81	20.14

^{45}Sc, ^{89}Y and ^{139}La as internal standards

With ^{45}Sc, ^{89}Y and ^{139}La as internal standards the calibration curves yielded correlation coefficients of 1.0000 and detection limits were calculated at 1.736 μg dm^{-3} As, 1.693 μg dm^{-3} As and 1.686 μg dm^{-3} As respectively. Tables 4.62 to 4.64 show the values obtained after quantitative analyses.

Samples containing only nitric acid as matrix yielded values of approximately 20 μg dm^{-3} for all three internal standards. None of the three internal standards resulted in acceptable values for all concentrations of hydrochloric acid present in solution.

Table 4.62: Results of quantitative determination of As using ^{45}Sc as internal standard and the molecular correction factor (mass 75 / mass 77) at (0.50% v/v HNO_3 + 0.50% v/v HCl). Results are also shown for time drift corrected values. First order equation used: ($y = -0.0054x + 19.894$) and second order equation used: ($y = 2x10^{-5}x^2 - 0.0112x + 20.198$)

Time difference (minutes)	Sample name	[As] (μg dm^{-3})	Corrected with first order drift curve (μg dm^{-3})	Corrected with second order drift curve (μg dm^{-3})
44.57	Drift control - 20 μg dm^{-3} As	19.75	20.10	20.01
51.83	20 μg dm^{-3} As in 0.10% v/v HNO_3	18.93	19.30	19.25
59.10	20 μg dm^{-3} As in 0.50% v/v HNO_3	20.22	20.66	20.63
66.42	20 μg dm^{-3} As in 1.00% v/v HNO_3	20.08	20.56	20.55
73.68	20 μg dm^{-3} As in 1.50% v/v HNO_3	19.82	20.33	20.34
80.95	20 μg dm^{-3} As in 2.00% v/v HNO_3	19.62	20.17	20.21
88.22	20 μg dm^{-3} As in 2.50% v/v HNO_3	20.35	20.96	21.01
142.48	20 μg dm^{-3} As in 0.10% v/v HCl	17.65	18.46	18.57
149.82	20 μg dm^{-3} As in 0.50% v/v HCl	18.00	18.86	18.98
157.18	20 μg dm^{-3} As in 1.00% v/v HCl	20.34	21.36	21.49
164.55	20 μg dm^{-3} As in 1.50% v/v HCl	15.79	16.61	16.71
171.92	20 μg dm^{-3} As in 2.00% v/v HCl	21.42	22.58	22.71

Time difference (minutes)	Sample name	[As] (μg dm^{-3})	Corrected with first order drift curve (μg dm^{-3})	Corrected with second order drift curve (μg dm^{-3})
179.30	20 μg dm^{-3} As in 2.50% v/v HCl	18.21	19.25	19.34
188.58	Drift control - 20 μg dm^{-3} As	18.55	19.66	19.74
220.02	20 μg dm^{-3} As in (0.10% v/v HNO_3 + 0.10% v/v HCl)	17.04	18.22	18.23
227.40	20 μg dm^{-3} As in (0.50% v/v HNO_3 + 0.50% v/v HCl)	16.64	17.83	17.81
234.78	20 μg dm^{-3} As in (1.00% v/v HNO_3 + 1.00% v/v HCl)	21.53	23.12	23.06
244.08	Drift control - 20 μg dm^{-3} As	18.74	20.18	20.09
296.78	Drift control - 20 μg dm^{-3} As	18.33	20.04	19.67

Table 4.63: Results of quantitative determination of As using ^{89}Y as internal standard and the molecular correction factor (mass 75 / mass 77) at (0.50% v/v HNO_3 + 0.50% v/v HCl). Results are also shown for time drift corrected values. First order equation used: ($y = 0.0006x + 19.664$) and second order equation used: ($y = -6x10^{-6}x^2 + 0.0027x + 19.555$)

Time difference (minutes)	Sample name	[As] (μg dm^{-3})	Corrected with first order drift curve (μg dm^{-3})	Corrected with second order drift curve (μg dm^{-3})
44.57	Drift control - 20 μg dm^{-3} As	19.70	20.01	20.03
51.83	20 μg dm^{-3} As in 0.10% v/v HNO_3	19.08	19.37	19.39
59.10	20 μg dm^{-3} As in 0.50% v/v HNO_3	20.56	20.88	20.88
66.42	20 μg dm^{-3} As in 1.00% v/v HNO_3	20.08	20.38	20.38
73.68	20 μg dm^{-3} As in 1.50% v/v HNO_3	20.02	20.32	20.31
80.95	20 μg dm^{-3} As in 2.00% v/v HNO_3	19.64	19.93	19.90
88.22	20 μg dm^{-3} As in 2.50% v/v HNO_3	20.32	20.62	20.58
142.48	20 μg dm^{-3} As in 0.10% v/v HCl	18.77	19.00	18.94
149.82	20 μg dm^{-3} As in 0.50% v/v HCl	20.08	20.33	20.26
157.18	20 μg dm^{-3} As in 1.00% v/v HCl	23.73	24.02	23.93

Time difference (minutes)	Sample name	[As] (μg dm^{-3})	Corrected with first order drift curve (μg dm^{-3})	Corrected with second order drift curve (μg dm^{-3})
164.55	20 μg dm^{-3} As in 1.50% v/v HCl	18.55	18.77	18.70
171.92	20 μg dm^{-3} As in 2.00% v/v HCl	25.97	26.28	26.18
179.30	20 μg dm^{-3} As in 2.50% v/v HCl	22.27	22.53	22.44
188.58	Drift control - 20 μg dm^{-3} As	19.54	19.76	19.69
220.02	20 μg dm^{-3} As in (0.10% v/v HNO_3 + 0.10% v/v HCl)	18.90	19.09	19.03
227.40	20 μg dm^{-3} As in (0.50% v/v HNO_3 + 0.50% v/v HCl)	18.92	19.11	19.05
234.78	20 μg dm^{-3} As in (1.00% v/v HNO_3 + 1.00% v/v HCl)	25.15	25.40	25.33
244.08	Drift control - 20 μg dm^{-3} As	20.27	20.47	20.42
296.78	Drift control - 20 μg dm^{-3} As	19.62	19.77	19.79

Table 4.64: Results of quantitative determination of As using ^{139}La as internal standard and the molecular correction factor (mass 75 / mass 77) at (0.50% v/v HNO_3 + 0.50% v/v HCl). Results are also shown for time drift corrected values. First order equation used: ($y = 0.0054x + 19.612$) and second order equation used: ($y = -2x10^{-6}x^2 + 0.0129x + 19.221$)

Time difference (minutes)	Sample name	[As] (μg dm^{-3})	Corrected with first order drift curve (μg dm^{-3})	Corrected with second order drift curve (μg dm^{-3})
44.57	Drift control - 20 μg dm^{-3} As	19.77	19.92	20.02
51.83	20 μg dm^{-3} As in 0.10% v/v HNO_3	19.64	19.75	19.80
59.10	20 μg dm^{-3} As in 0.50% v/v HNO_3	20.72	20.79	20.81
66.42	20 μg dm^{-3} As in 1.00% v/v HNO_3	20.19	20.22	20.20
73.68	20 μg dm^{-3} As in 1.50% v/v HNO_3	20.08	20.07	20.02
80.95	20 μg dm^{-3} As in 2.00% v/v HNO_3	19.79	19.74	19.66
88.22	20 μg dm^{-3} As in 2.50% v/v HNO_3	20.52	20.43	20.31
142.48	20 μg dm^{-3} As in 0.10% v/v HCl	19.66	19.30	19.04

Time difference (minutes)	Sample name	[As] (μg dm^{-3})	Corrected with first order drift curve (μg dm^{-3})	Corrected with second order drift curve (μg dm^{-3})
149.82	20 μg dm^{-3} As in 0.50% v/v HCl	21.75	21.30	21.01
157.18	20 μg dm^{-3} As in 1.00% v/v HCl	26.53	25.93	25.57
164.55	20 μg dm^{-3} As in 1.50% v/v HCl	20.76	20.25	19.96
171.92	20 μg dm^{-3} As in 2.00% v/v HCl	29.45	28.68	28.26
179.30	20 μg dm^{-3} As in 2.50% v/v HCl	26.11	25.37	24.99
188.58	Drift control - 20 μg dm^{-3} As	20.65	20.02	19.72
220.02	20 μg dm^{-3} As in (0.10% v/v HNO_3 + 0.10% v/v HCl)	20.10	19.33	19.06
227.40	20 μg dm^{-3} As in (0.50% v/v HNO_3 + 0.50% v/v HCl)	21.03	20.18	19.91
234.78	20 μg dm^{-3} As in (1.00% v/v HNO_3 + 1.00% v/v HCl)	28.66	27.46	27.11
244.08	Drift control - 20 μg dm^{-3} As	21.29	20.34	20.11
296.78	Drift control - 20 μg dm^{-3} As	20.93	19.73	19.66

^{36}Ar, ^{35}Cl and ^{37}Cl as internal standards

These three internal standards resulted in calibration curves with correlation coefficients of 0.9998, 1.0000 and 0.9999 respectively. The detection limits were calculated to be 1.910 μg dm^{-3} As, 1.177 μg dm^{-3} As and 1.799 μg dm^{-3} As. The values obtained after quantitative analyses can be seen in tables 4.65 to 4.67.

In the cases of ^{36}Ar and ^{37}Cl good results were obtained for samples containing no hydrochloric acid. In the case of ^{35}Cl drift correction procedures resulted in too high values. With hydrochloric acid present in solution and the chlorine isotopes as internal standards too low values were obtained. In the case of ^{36}Ar as internal standard the values obtained are generally below the accepted value of 20 μg dm^{-3}.

Table 4.65: Results of quantitative determination of As using ^{36}Ar as internal standard and the molecular correction factor (mass 75 / mass 77) at (0.50% v/v HNO_3 + 0.50% v/v HCl). Results are also shown for time drift corrected values. First order equation used: ($y = -0.0179x + 19.875$) and second order equation used: ($y = 5x10^{-5}x^2 - 0.0355x + 20.798$)

Time difference (minutes)	Sample name	[As] ($\mu g\ dm^{-3}$)	Corrected with first order drift curve ($\mu g\ dm^{-3}$)	Corrected with second order drift curve ($\mu g\ dm^{-3}$)
44.57	Drift control - 20 $\mu g\ dm^{-3}$ As	19.34	20.28	20.03
51.83	20 $\mu g\ dm^{-3}$ As in 0.10% v/v HNO_3	17.99	18.99	18.85
59.10	20 $\mu g\ dm^{-3}$ As in 0.50% v/v HNO_3	19.00	20.19	20.13
66.42	20 $\mu g\ dm^{-3}$ As in 1.00% v/v HNO_3	19.11	20.45	20.48
73.68	20 $\mu g\ dm^{-3}$ As in 1.50% v/v HNO_3	18.57	20.01	20.12
80.95	20 $\mu g\ dm^{-3}$ As in 2.00% v/v HNO_3	18.10	19.65	19.83
88.22	20 $\mu g\ dm^{-3}$ As in 2.50% v/v HNO_3	19.08	20.85	21.13
142.48	20 $\mu g\ dm^{-3}$ As in 0.10% v/v HCl	15.62	18.04	18.65
149.82	20 $\mu g\ dm^{-3}$ As in 0.50% v/v HCl	15.02	17.47	18.09
157.18	20 $\mu g\ dm^{-3}$ As in 1.00% v/v HCl	15.81	18.53	19.22
164.55	20 $\mu g\ dm^{-3}$ As in 1.50% v/v HCl	11.74	13.87	14.39
171.92	20 $\mu g\ dm^{-3}$ As in 2.00% v/v HCl	15.97	19.02	19.75
179.30	20 $\mu g\ dm^{-3}$ As in 2.50% v/v HCl	12.66	15.19	15.78
188.58	Drift control - 20 $\mu g\ dm^{-3}$ As	15.86	19.22	19.97
220.02	20 $\mu g\ dm^{-3}$ As in (0.10% v/v HNO_3 + 0.10% v/v HCl)	14.31	17.96	18.57
227.40	20 $\mu g\ dm^{-3}$ As in (0.50% v/v HNO_3 + 0.50% v/v HCl)	13.15	16.64	17.18
234.78	20 $\mu g\ dm^{-3}$ As in (1.00% v/v HNO_3 + 1.00% v/v HCl)	16.33	20.83	21.45
244.08	Drift control - 20 $\mu g\ dm^{-3}$ As	15.54	20.05	20.57
296.78	Drift control - 20 $\mu g\ dm^{-3}$ As	14.89	20.45	20.30

Table 4.66: Results of quantitative determination of As using ^{35}Cl as internal standard and the molecular correction factor (mass 75 / mass 77) at (0.50% v/v HNO_3 + 0.50% v/v HCl). Results are also shown for time drift corrected values. First order equation used: ($y = -0.0431x + 20.293$) and second order equation used: ($y = 0.0003x^2 - 0.1461x + 25.707$)

Time difference (minutes)	Sample name	[As] ($\mu g\ dm^{-3}$)	Corrected with first order drift curve ($\mu g\ dm^{-3}$)	Corrected with second order drift curve ($\mu g\ dm^{-3}$)
44.57	Drift control - 20 $\mu g\ dm^{-3}$ As	20.03	21.81	20.24
51.83	20 $\mu g\ dm^{-3}$ As in 0.10% v/v HNO_3	19.45	21.54	20.54
59.10	20 $\mu g\ dm^{-3}$ As in 0.50% v/v HNO_3	20.31	22.89	22.42
66.42	20 $\mu g\ dm^{-3}$ As in 1.00% v/v HNO_3	20.20	23.17	23.31
73.68	20 $\mu g\ dm^{-3}$ As in 1.50% v/v HNO_3	20.20	23.61	24.39
80.95	20 $\mu g\ dm^{-3}$ As in 2.00% v/v HNO_3	19.72	23.48	24.89
88.22	20 $\mu g\ dm^{-3}$ As in 2.50% v/v HNO_3	20.41	24.76	26.94
142.48	20 $\mu g\ dm^{-3}$ As in 0.10% v/v HCl	2.97	4.20	5.41
149.82	20 $\mu g\ dm^{-3}$ As in 0.50% v/v HCl	1.23	1.78	2.34
157.18	20 $\mu g\ dm^{-3}$ As in 1.00% v/v HCl	1.05	1.55	2.07
164.55	20 $\mu g\ dm^{-3}$ As in 1.50% v/v HCl	0.94	1.42	1.92
171.92	20 $\mu g\ dm^{-3}$ As in 2.00% v/v HCl	0.95	1.47	2.00
179.30	20 $\mu g\ dm^{-3}$ As in 2.50% v/v HCl	0.91	1.44	1.98
188.58	Drift control - 20 $\mu g\ dm^{-3}$ As	7.50	12.33	17.00
220.02	20 $\mu g\ dm^{-3}$ As in (0.10% v/v HNO_3 + 0.10% v/v HCl)	2.94	5.44	7.27
227.40	20 $\mu g\ dm^{-3}$ As in (0.50% v/v HNO_3 + 0.50% v/v HCl)	1.20	2.28	2.99
234.78	20 $\mu g\ dm^{-3}$ As in (1.00% v/v HNO_3 + 1.00% v/v HCl)	1.06	2.08	2.67
244.08	Drift control - 20 $\mu g\ dm^{-3}$ As	11.40	23.33	28.79
296.78	Drift control - 20 $\mu g\ dm^{-3}$ As	8.88	23.67	20.25

Table 4.67: Results of quantitative determination of As using ^{37}Cl as internal standard and the molecular correction factor (mass 75 / mass 77) at (0.50% v/v HNO_3 + 0.50% v/v HCl). Results are also shown for time drift corrected values. First order equation used: ($y = -0.0104x + 19.852$) and second order equation used: ($y = 7x10^{-5}x^2 - 0.0330x + 21.042$)

Time difference (minutes)	Sample name	[As] ($\mu g\ dm^{-3}$)	Corrected with first order drift curve ($\mu g\ dm^{-3}$)	Corrected with second order drift curve ($\mu g\ dm^{-3}$)
44.57	Drift control - 20 $\mu g\ dm^{-3}$ As	19.76	20.39	20.05
51.83	20 $\mu g\ dm^{-3}$ As in 0.10% v/v HNO_3	19.19	19.87	19.66
59.10	20 $\mu g\ dm^{-3}$ As in 0.50% v/v HNO_3	19.85	20.64	20.53
66.42	20 $\mu g\ dm^{-3}$ As in 1.00% v/v HNO_3	19.81	20.67	20.68
73.68	20 $\mu g\ dm^{-3}$ As in 1.50% v/v HNO_3	19.23	20.15	20.25
80.95	20 $\mu g\ dm^{-3}$ As in 2.00% v/v HNO_3	18.59	19.56	19.74
88.22	20 $\mu g\ dm^{-3}$ As in 2.50% v/v HNO_3	19.24	20.32	20.60
142.48	20 $\mu g\ dm^{-3}$ As in 0.10% v/v HCl	14.66	15.96	16.51
149.82	20 $\mu g\ dm^{-3}$ As in 0.50% v/v HCl	7.93	8.67	8.98
157.18	20 $\mu g\ dm^{-3}$ As in 1.00% v/v HCl	5.60	6.15	6.37
164.55	20 $\mu g\ dm^{-3}$ As in 1.50% v/v HCl	3.27	3.61	3.74
171.92	20 $\mu g\ dm^{-3}$ As in 2.00% v/v HCl	3.61	4.00	4.14
179.30	20 $\mu g\ dm^{-3}$ As in 2.50% v/v HCl	2.58	2.87	2.97
188.58	Drift control - 20 $\mu g\ dm^{-3}$ As	16.81	18.79	19.42
220.02	20 $\mu g\ dm^{-3}$ As in (0.10% v/v HNO_3 + 0.10% v/v HCl)	13.97	15.90	16.27
227.40	20 $\mu g\ dm^{-3}$ As in (0.50% v/v HNO_3 + 0.50% v/v HCl)	7.20	8.23	8.39
234.78	20 $\mu g\ dm^{-3}$ As in (1.00% v/v HNO_3 + 1.00% v/v HCl)	5.87	6.74	6.84
244.08	Drift control - 20 $\mu g\ dm^{-3}$ As	17.77	20.53	20.71
296.78	Drift control - 20 $\mu g\ dm^{-3}$ As	17.04	20.32	19.57

4.5.11 Effect of using molecular (mass 75 / mass 77) corrections in a (1.00% v/v HNO_3 + 1.00% v/v HCl) matrix on the quantitative determination of arsenic

No internal standard

A correction factor of 3.252 was calculated from analysis of a solution containing (1.00% v/v HNO_3 + 1.00% v/v HCl). The calibration curve that was constructed resulted in a correlation coefficient of 1.0000 and a detection limit of 1.700 μg dm^{-3} As was calculated. Table 4.68 shows the results obtained.

With no hydrochloric acid present in solution, values of approximately 20 μg dm^{-3} arsenic were obtained. With hydrochloric acid present in solution the values obtained showed to be slightly less than 20 μg dm^{-3}.

Table 4.68: Results of quantitative determination of As using no internal standard and the molecular correction factor (mass 75 / mass 77) at (1.00% v/v HNO_3 + 1.00% v/v HCl). Results are also shown for time drift corrected values. First order equation used: ($y = 0.0083x + 20.269$) and second order equation used: ($y = -1x10^{-5}x^2 + 0.0130x + 20.016$)

Time difference (minutes)	**Sample name**	**[As] (μg dm^{-3})**	**Corrected with first order drift curve (μg dm^{-3})**	**Corrected with second order drift curve (μg dm^{-3})**
44.57	Drift control - 20 μg dm^{-3} As	20.59	19.95	20.01
51.83	20 μg dm^{-3} As in 0.10% v/v HNO_3	19.98	19.31	19.34
59.10	20 μg dm^{-3} As in 0.50% v/v HNO_3	21.12	20.35	20.36
66.42	20 μg dm^{-3} As in 1.00% v/v HNO_3	21.44	20.59	20.58
73.68	20 μg dm^{-3} As in 1.50% v/v HNO_3	21.02	20.14	20.10
80.95	20 μg dm^{-3} As in 2.00% v/v HNO_3	20.44	19.52	19.46
88.22	20 μg dm^{-3} As in 2.50% v/v HNO_3	21.22	20.21	20.13
142.48	20 μg dm^{-3} As in 0.10% v/v HCl	20.34	18.97	18.78
149.82	20 μg dm^{-3} As in 0.50% v/v HCl	19.00	17.66	17.48
157.18	20 μg dm^{-3} As in 1.00% v/v HCl	19.78	18.33	18.13

Time difference (minutes)	Sample name	[As] (μg dm^{-3})	Corrected with first order drift curve (μg dm^{-3})	Corrected with second order drift curve (μg dm^{-3})
164.55	20 μg dm^{-3} As in 1.50% v/v HCl	12.77	11.80	11.67
171.92	20 μg dm^{-3} As in 2.00% v/v HCl	18.37	16.94	16.74
179.30	20 μg dm^{-3} As in 2.50% v/v HCl	12.80	11.76	11.62
188.58	Drift control - 20 μg dm^{-3} As	21.82	19.98	19.73
220.02	20 μg dm^{-3} As in (0.10% v/v HNO_3 + 0.10% v/v HCl)	20.16	18.25	18.00
227.40	20 μg dm^{-3} As in (0.50% v/v HNO_3 + 0.50% v/v HCl)	17.72	15.99	15.78
234.78	20 μg dm^{-3} As in (1.00% v/v HNO_3 + 1.00% v/v HCl)	21.13	19.02	18.77
244.08	Drift control - 20 μg dm^{-3} As	22.54	20.22	19.95
296.78	Drift control - 20 μg dm^{-3} As	22.52	19.81	19.59

^{45}Sc, ^{89}Y and ^{139}La as internal standards

Correlation coefficients of 1.0000 were obtained when using these three isotopes as internal standards. Detection limits of 1.753 μg dm^{-3} As, 1.711 μg dm^{-3} As and 1.704 μg dm^{-3} As were obtained respectively for the three internal standards. The results obtained can be seen in tables 4.69 to 4.71.

In the cases of nitric acid sample matrices all three internal standards resulted in acceptable values of approximately 20 μg dm^{-3}. Although none of the three internal standards yielded acceptable values over the whole concentration range of hydrochloric acid used in the sample matrices, ^{139}La yielded acceptable values when the hydrochloric acid was present at low concentrations.

Table 4.69: Results of quantitative determination of As using ^{45}Sc as internal standard and the molecular correction factor (mass 75 / mass 77) at (1.00% v/v HNO_3 + 1.00% v/v HCl). Results are also shown for time drift corrected values. First order equation used: ($y = -0.0058x + 19.909$) and second order equation used: ($y = 2x10^{-5}x^2 - 0.0124x + 20.256$)

Time difference (minutes)	Sample name	[As] ($\mu g\ dm^{-3}$)	Corrected with first order drift curve ($\mu g\ dm^{-3}$)	Corrected with second order drift curve ($\mu g\ dm^{-3}$)
44.57	Drift control - 20 $\mu g\ dm^{-3}$ As	19.76	20.12	20.02
51.83	20 $\mu g\ dm^{-3}$ As in 0.10% v/v HNO_3	18.94	19.32	19.26
59.10	20 $\mu g\ dm^{-3}$ As in 0.50% v/v HNO_3	20.24	20.69	20.66
66.42	20 $\mu g\ dm^{-3}$ As in 1.00% v/v HNO_3	20.09	20.58	20.59
73.68	20 $\mu g\ dm^{-3}$ As in 1.50% v/v HNO_3	19.82	20.35	20.38
80.95	20 $\mu g\ dm^{-3}$ As in 2.00% v/v HNO_3	19.63	20.20	20.26
88.22	20 $\mu g\ dm^{-3}$ As in 2.50% v/v HNO_3	20.35	20.99	21.07
142.48	20 $\mu g\ dm^{-3}$ As in 0.10% v/v HCl	17.34	18.18	18.36
149.82	20 $\mu g\ dm^{-3}$ As in 0.50% v/v HCl	16.24	17.06	17.23
157.18	20 $\mu g\ dm^{-3}$ As in 1.00% v/v HCl	16.83	17.71	17.90
164.55	20 $\mu g\ dm^{-3}$ As in 1.50% v/v HCl	10.73	11.32	11.44
171.92	20 $\mu g\ dm^{-3}$ As in 2.00% v/v HCl	14.99	15.86	16.02
179.30	20 $\mu g\ dm^{-3}$ As in 2.50% v/v HCl	10.41	11.03	11.15
188.58	Drift control - 20 $\mu g\ dm^{-3}$ As	18.46	19.62	19.81
220.02	20 $\mu g\ dm^{-3}$ As in (0.10% v/v HNO_3 + 0.10% v/v HCl)	16.66	17.88	18.01
227.40	20 $\mu g\ dm^{-3}$ As in (0.50% v/v HNO_3 + 0.50% v/v HCl)	14.54	15.65	15.75
234.78	20 $\mu g\ dm^{-3}$ As in (1.00% v/v HNO_3 + 1.00% v/v HCl)	17.59	18.97	19.07
244.08	Drift control - 20 $\mu g\ dm^{-3}$ As	18.69	20.21	20.29
296.78	Drift control - 20 $\mu g\ dm^{-3}$ As	18.24	20.06	19.89

Table 4.70: Results of quantitative determination of As using ^{89}Y as internal standard and the molecular correction factor (mass 75 / mass 77) at (1.00% v/v HNO_3 + 1.00% v/v HCl). Results are also shown for time drift corrected values. First order equation used: ($y = 0.0002x + 19.680$) and second order equation used: ($y = -4x10^{-6}x^2 + 0.0014x + 19.617$)

Time difference (minutes)	Sample name	[As] ($\mu g\ dm^{-3}$)	Corrected with first order drift curve ($\mu g\ dm^{-3}$)	Corrected with second order drift curve ($\mu g\ dm^{-3}$)
44.57	Drift control - 20 $\mu g\ dm^{-3}$ As	19.71	20.02	20.04
51.83	20 $\mu g\ dm^{-3}$ As in 0.10% v/v HNO_3	19.08	19.39	19.40
59.10	20 $\mu g\ dm^{-3}$ As in 0.50% v/v HNO_3	20.57	20.90	20.90
66.42	20 $\mu g\ dm^{-3}$ As in 1.00% v/v HNO_3	20.09	20.41	20.41
73.68	20 $\mu g\ dm^{-3}$ As in 1.50% v/v HNO_3	20.03	20.34	20.34
80.95	20 $\mu g\ dm^{-3}$ As in 2.00% v/v HNO_3	19.65	19.95	19.94
88.22	20 $\mu g\ dm^{-3}$ As in 2.50% v/v HNO_3	20.33	20.64	20.63
142.48	20 $\mu g\ dm^{-3}$ As in 0.10% v/v HCl	18.43	18.70	18.68
149.82	20 $\mu g\ dm^{-3}$ As in 0.50% v/v HCl	18.11	18.37	18.35
157.18	20 $\mu g\ dm^{-3}$ As in 1.00% v/v HCl	19.61	19.89	19.87
164.55	20 $\mu g\ dm^{-3}$ As in 1.50% v/v HCl	12.57	12.76	12.74
171.92	20 $\mu g\ dm^{-3}$ As in 2.00% v/v HCl	18.14	18.40	18.38
179.30	20 $\mu g\ dm^{-3}$ As in 2.50% v/v HCl	12.67	12.85	12.83
188.58	Drift control - 20 $\mu g\ dm^{-3}$ As	19.43	19.71	19.69
220.02	20 $\mu g\ dm^{-3}$ As in (0.10% v/v HNO_3 + 0.10% v/v HCl)	18.46	18.72	18.71
227.40	20 $\mu g\ dm^{-3}$ As in (0.50% v/v HNO_3 + 0.50% v/v HCl)	16.52	16.75	16.75
234.78	20 $\mu g\ dm^{-3}$ As in (1.00% v/v HNO_3 + 1.00% v/v HCl)	20.53	20.81	20.81
244.08	Drift control - 20 $\mu g\ dm^{-3}$ As	20.21	20.49	20.50
296.78	Drift control - 20 $\mu g\ dm^{-3}$ As	19.52	19.77	19.83

Table 4.71: Results of quantitative determination of As using ^{139}La as internal standard and the molecular correction factor (mass 75 / mass 77) at (1.00% v/v HNO_3 + 1.00% v/v HCl). Results are also shown for time drift corrected values. First order equation used: ($y = 0.0049x + 19.630$) and second order equation used: ($y = -2x10^{-5}x^2 + 0.0115x + 19.285$)

Time difference (minutes)	Sample name	[As] ($\mu g\ dm^{-3}$)	Corrected with first order drift curve ($\mu g\ dm^{-3}$)	Corrected with second order drift curve ($\mu g\ dm^{-3}$)
44.57	Drift control - 20 $\mu g\ dm^{-3}$ As	19.78	19.93	20.03
51.83	20 $\mu g\ dm^{-3}$ As in 0.10% v/v HNO_3	19.65	19.76	19.82
59.10	20 $\mu g\ dm^{-3}$ As in 0.50% v/v HNO_3	20.73	20.81	20.84
66.42	20 $\mu g\ dm^{-3}$ As in 1.00% v/v HNO_3	20.20	20.25	20.24
73.68	20 $\mu g\ dm^{-3}$ As in 1.50% v/v HNO_3	20.08	20.09	20.06
80.95	20 $\mu g\ dm^{-3}$ As in 2.00% v/v HNO_3	19.80	19.77	19.71
88.22	20 $\mu g\ dm^{-3}$ As in 2.50% v/v HNO_3	20.53	20.46	20.38
142.48	20 $\mu g\ dm^{-3}$ As in 0.10% v/v HCl	19.31	19.00	18.82
149.82	20 $\mu g\ dm^{-3}$ As in 0.50% v/v HCl	19.61	19.26	19.08
157.18	20 $\mu g\ dm^{-3}$ As in 1.00% v/v HCl	21.91	21.48	21.27
164.55	20 $\mu g\ dm^{-3}$ As in 1.50% v/v HCl	14.06	13.76	13.63
171.92	20 $\mu g\ dm^{-3}$ As in 2.00% v/v HCl	20.56	20.08	19.89
179.30	20 $\mu g\ dm^{-3}$ As in 2.50% v/v HCl	14.82	14.45	14.31
188.58	Drift control - 20 $\mu g\ dm^{-3}$ As	20.53	19.98	19.80
220.02	20 $\mu g\ dm^{-3}$ As in (0.10% v/v HNO_3 + 0.10% v/v HCl)	19.63	18.96	18.83
227.40	20 $\mu g\ dm^{-3}$ As in (0.50% v/v HNO_3 + 0.50% v/v HCl)	18.35	17.69	17.59
234.78	20 $\mu g\ dm^{-3}$ As in (1.00% v/v HNO_3 + 1.00% v/v HCl)	23.38	22.50	22.39
244.08	Drift control - 20 $\mu g\ dm^{-3}$ As	21.22	20.38	20.30
296.78	Drift control - 20 $\mu g\ dm^{-3}$ As	20.81	19.74	19.88

^{36}Ar, ^{35}Cl and ^{37}Cl as internal standards

The correlation coefficients obtained were 0.9998, 1.0000 and 0.9999 when using ^{36}Ar, ^{35}Cl and ^{37}Cl as internal standards. The detection limits calculated for these three cases were 1.931 μg dm^{-3} As, 1.199 μg dm^{-3} As and 1.818 μg dm^{-3} As respectively. The results obtained from the quantitative analysis can be seen in tables 4.72 to 4.74.

With only nitric acid present in the sample matrix good results were obtained for ^{36}Ar and ^{37}Cl as internal standards. In the case of ^{35}Cl the time drift correction procedure resulted in too high values. With ^{35}Cl and ^{37}Cl as internal standards very poor values were obtained and with ^{36}Ar as internal standard the values obtained showed generally to be slightly less than 20 μg dm^{-3}.

Table 4.72: Results of quantitative determination of As using ^{36}Ar as internal standard and the molecular correction factor (mass 75 / mass 77) at (1.00% v/v HNO_3 + 1.00% v/v HCl). Results are also shown for time drift corrected values. First order equation used: ($y = -0.0182x + 19.892$) and second order equation used: ($y = 6x10^{-5}x^2 - 0.0365x + 20.854$)

Time difference (minutes)	Sample name	[As] (μg dm^{-3})	Corrected with first order drift curve (μg dm^{-3})	Corrected with second order drift curve (μg dm^{-3})
44.57	Drift control - 20 μg dm^{-3} As	19.36	20.29	20.01
51.83	20 μg dm^{-3} As in 0.10% v/v HNO_3	18.01	19.01	18.83
59.10	20 μg dm^{-3} As in 0.50% v/v HNO_3	19.02	20.21	20.12
66.42	20 μg dm^{-3} As in 1.00% v/v HNO_3	19.13	20.48	20.47
73.68	20 μg dm^{-3} As in 1.50% v/v HNO_3	18.58	20.03	20.10
80.95	20 μg dm^{-3} As in 2.00% v/v HNO_3	18.12	19.67	19.81
88.22	20 μg dm^{-3} As in 2.50% v/v HNO_3	19.09	20.88	21.10
142.48	20 μg dm^{-3} As in 0.10% v/v HCl	15.35	17.74	18.19
149.82	20 μg dm^{-3} As in 0.50% v/v HCl	13.50	15.73	16.14
157.18	20 μg dm^{-3} As in 1.00% v/v HCl	12.99	15.25	15.65
164.55	20 μg dm^{-3} As in 1.50% v/v HCl	7.80	9.24	9.48

Time difference (minutes)	Sample name	[As] (μg dm^{-3})	Corrected with first order drift curve (μg dm^{-3})	Corrected with second order drift curve (μg dm^{-3})
171.92	20 μg dm^{-3} As in 2.00% v/v HCl	11.02	13.15	13.48
179.30	20 μg dm^{-3} As in 2.50% v/v HCl	7.01	8.43	8.64
188.58	Drift control - 20 μg dm^{-3} As	15.78	19.18	19.60
220.02	20 μg dm^{-3} As in (0.10% v/v HNO_3 + 0.10% v/v HCl)	13.98	17.60	17.78
227.40	20 μg dm^{-3} As in (0.50% v/v HNO_3 + 0.50% v/v HCl)	11.43	14.51	14.60
234.78	20 μg dm^{-3} As in (1.00% v/v HNO_3 + 1.00% v/v HCl)	13.25	16.96	16.99
244.08	Drift control - 20 μg dm^{-3} As	15.51	20.08	19.99
296.78	Drift control - 20 μg dm^{-3} As	14.83	20.47	19.37

Table 4.73: Results of quantitative determination of As using ^{35}Cl as internal standard and the molecular correction factor (mass 75 / mass 77) at (1.00% v/v HNO_3 + 1.00% v/v HCl). Results are also shown for time drift corrected values. First order equation used: ($y = -0.0432x + 20.301$) and second order equation used: ($y = 0.0003x^2 - 0.1461x + 25.713$)

Time difference (minutes)	Sample name	[As] (μg dm^{-3})	Corrected with first order drift curve (μg dm^{-3})	Corrected with second order drift curve (μg dm^{-3})
44.57	Drift control - 20 μg dm^{-3} As	20.04	21.81	20.24
51.83	20 μg dm^{-3} As in 0.10% v/v HNO_3	19.45	21.54	20.53
59.10	20 μg dm^{-3} As in 0.50% v/v HNO_3	20.31	22.89	22.41
66.42	20 μg dm^{-3} As in 1.00% v/v HNO_3	20.20	23.18	23.31
73.68	20 μg dm^{-3} As in 1.50% v/v HNO_3	20.20	23.60	24.37
80.95	20 μg dm^{-3} As in 2.00% v/v HNO_3	19.73	23.48	24.89
88.22	20 μg dm^{-3} As in 2.50% v/v HNO_3	20.41	24.76	26.93
142.48	20 μg dm^{-3} As in 0.10% v/v HCl	2.99	4.23	5.44
149.82	20 μg dm^{-3} As in 0.50% v/v HCl	1.26	1.82	2.38

Time difference (minutes)	Sample name	[As] (μg dm^{-3})	Corrected with first order drift curve (μg dm^{-3})	Corrected with second order drift curve (μg dm^{-3})
157.18	20 μg dm^{-3} As in 1.00% v/v HCl	1.07	1.59	2.11
164.55	20 μg dm^{-3} As in 1.50% v/v HCl	0.97	1.47	1.97
171.92	20 μg dm^{-3} As in 2.00% v/v HCl	0.97	1.51	2.06
179.30	20 μg dm^{-3} As in 2.50% v/v HCl	0.94	1.49	2.04
188.58	Drift control - 20 μg dm^{-3} As	7.50	12.34	16.99
220.02	20 μg dm^{-3} As in (0.10% v/v HNO_3 + 0.10% v/v HCl)	2.94	5.45	7.28
227.40	20 μg dm^{-3} As in (0.50% v/v HNO_3 + 0.50% v/v HCl)	1.21	2.31	3.02
234.78	20 μg dm^{-3} As in (1.00% v/v HNO_3 + 1.00% v/v HCl)	1.08	2.12	2.71
244.08	Drift control - 20 μg dm^{-3} As	11.39	23.35	28.75
296.78	Drift control - 20 μg dm^{-3} As	8.87	23.71	20.21

Table 4.74: Results of quantitative determination of As using ^{37}Cl as internal standard and the molecular correction factor (mass 75 / mass 77) at (1.00% v/v HNO_3 + 1.00% v/v HCl). Results are also shown for time drift corrected values. First order equation used: ($y = -0.0107x + 19.870$) and second order equation used: ($y = 7x10^{-5}x^2 - 0.0340x + 21.095$)

Time difference (minutes)	Sample name	[As] (μg dm^{-3})	Corrected with first order drift curve (μg dm^{-3})	Corrected with second order drift curve (μg dm^{-3})
44.57	Drift control - 20 μg dm^{-3} As	19.78	20.39	20.06
51.83	20 μg dm^{-3} As in 0.10% v/v HNO_3	19.20	19.88	19.67
59.10	20 μg dm^{-3} As in 0.50% v/v HNO_3	19.86	20.65	20.55
66.42	20 μg dm^{-3} As in 1.00% v/v HNO_3	19.82	20.69	20.71
73.68	20 μg dm^{-3} As in 1.50% v/v HNO_3	19.24	20.16	20.28
80.95	20 μg dm^{-3} As in 2.00% v/v HNO_3	18.60	19.58	19.79
88.22	20 μg dm^{-3} As in 2.50% v/v HNO_3	19.25	20.35	20.66

Time difference (minutes)	Sample name	[As] (μg dm^{-3})	Corrected with first order drift curve (μg dm^{-3})	Corrected with second order drift curve (μg dm^{-3})
142.48	20 μg dm^{-3} As in 0.10% v/v HCl	14.41	15.71	16.31
149.82	20 μg dm^{-3} As in 0.50% v/v HCl	7.19	7.88	8.19
157.18	20 μg dm^{-3} As in 1.00% v/v HCl	4.70	5.17	5.38
164.55	20 μg dm^{-3} As in 1.50% v/v HCl	2.33	2.57	2.68
171.92	20 μg dm^{-3} As in 2.00% v/v HCl	2.64	2.93	3.05
179.30	20 μg dm^{-3} As in 2.50% v/v HCl	1.62	1.81	1.88
188.58	Drift control - 20 μg dm^{-3} As	16.72	18.73	19.47
220.02	20 μg dm^{-3} As in (0.10% v/v HNO_3 + 0.10% v/v HCl)	13.66	15.59	16.06
227.40	20 μg dm^{-3} As in (0.50% v/v HNO_3 + 0.50% v/v HCl)	6.33	7.26	7.45
234.78	20 μg dm^{-3} As in (1.00% v/v HNO_3 + 1.00% v/v HCl)	4.87	5.61	5.74
244.08	Drift control - 20 μg dm^{-3} As	17.72	20.54	20.89
296.78	Drift control - 20 μg dm^{-3} As	16.96	20.31	19.75

4.6 Conclusion

It was shown that very good calibration curves together with detection limits that varied from 0.493 μg dm^{-3} to 1.939 μg dm^{-3} arsenic are attainable for the quantitative determination of mono-isotopic arsenic in acidic matrices.

As it is known that instrumental drift occurs with time in ICP-MS the extent thereof was measured and the results were adjusted accordingly. It was seen that correction for this drift phenomena resulted in accurate analytical results. Internal standards that resulted in acceptable analytical results were ^{45}Sc, ^{89}Y, ^{139}La and ^{36}Ar, while the use of ^{35}Cl and ^{37}Cl as internal standards did not always have the desired effect.

Nitric acid concentrations were varied from 0.10% v/v to 2.50% v/v and this caused no problems or interferences in quantitative analyses.

The hydrochloric acid concentration in solution was varied from 0.10% v/v to 2.50% v/v. It was shown that correction procedures are necessary when chlorine is present in the matrix and arsenic has to be determined quantitatively. It was shown that the use of internal standards could not compensate for the chlorine interference on mono-isotopic arsenic at mass 75, as the values are not effected by only instrumental drift, but are the result of dimer formation.

Molecular correction factors were determined at different acid concentrations and the results were adjusted accordingly. The effects of the internal standards together with these correction factors on the arsenic determinations were also studied. Most of the correction factors compensated for the effect of the dimer formation at mass 75 for hydrochloric acid concentrations of less than 1.50% v/v. Under normal conditions the acid concentration of samples prepared for ICP-MS analysis do not exceed 1.00% v/v. For such samples the proposed dimer correction procedures together with instrumental drift monitoring proved to result in acceptable results. For samples with a hydrochloric acid content of more than 1.00% v/v the correction procedures do not compensate for the dimer formation adequately, effectively resulting in unacceptable values.

CHAPTER 5

THE QUANTITATIVE DETERMINATION OF THE PLATINUM GROUP ELEMENTS AND GOLD IN A CERTIFIED REFERENCE MATERIAL

5.1 Introduction

In order to assess the validity of the ICP-MS methods developed in chapter 3 it was decided to analyse a certified reference material for its content of the platinum group elements and gold. It was decided to analyse the certified reference material SARM 7 because it has certified values for all the platinum group elements and gold. The platinum group elements and gold will be extracted by means of the lead fire assay technique and the resulting prills will be dissolved and analysed by means of the ICP-MS methods as developed in chapter 3. The results obtained will also be discussed and compared to those of other researchers who employed similar techniques in the analysis of the material, SARM 7.

Certified reference materials are normally used to assess the accuracy, precision and detection limits of analytical methods. In this study the author unfortunately had very limited access to a fire assay laboratory, i.e. only four samples and a blank could be sent for analysis. Three more samples were sent to a commercial fire assay laboratory for analysis. Furthermore, the fire assay analysis was performed by laboratory assistants and not by the author herself. Due to the small number of results it was not possible to perform statistical analysis in order to assess the precision and determine detection limits. The five prills from the first laboratory and the three from the commercial fire assay laboratory were dissolved and analysed for their platinum group elements and gold content. The results reported here could therefore only be considered as preliminary.

In this text "% Recovery" refers to results obtained in terms of the certified value of the analyte in the reference material, e.g. if the reference material has a certified value of 0.31 mg kg^{-1} for Au and after analysis a value of 0.25 mg kg^{-1} was obtained for Au, this will be reported as a "% Recovery" of (0.25 / 0.31 x 100), i.e. 80.6%.

5.2 Certified reference material *[95]*

The source of the certified reference material, Platinum Ore SARM 7, is described as a composite of samples from the Merensky Reef taken from five localities in the Bushveld Complex in the Transvaal, South Africa. The material consists mainly of a felsphathic pyroxenite. Major constituents are pyroxene, olivine, serpentine and plagioclase. Minor constituents are chromite, pentlandite, chalcopyrite and pyrrhotite. The platinum minerals are mainly ferroplatinum, cooperite, sperrylite, braggite and moncheite. Silica and magnesia account for about 70% of the sample and oxides of iron, aluminium and calcium for a further 24%.

Table 5.1: Certified property values and confidence / uncertainty limits of selected elements in SARM 7.

Element	Certified value in mg kg^{-1}	Limits at 95% confidence level
Platinum	3.74	± 0.045
Palladium	1.53	± 0.032
Gold	0.31	± 0.015
Rhodium	0.24	± 0.013
Ruthenium	0.43	± 0.057
Iridium	0.074	± 0.012

5.3 Lead fire assay *[96]*

The technique consists of two consecutive pyrochemical separations. The finely ground sample is fused with a suitable flux, under reducing conditions which promote the separation of the platinum group elements and gold from the gangue, with simultaneous collection, as a lead alloy. Subsequently, the lead is removed by oxidising fusion (cupellation) and the platinum group elements and gold, thus isolated, are available for measurement.

Silver is normally employed to collect gold and the platinum group elements and added to the flux as a powder or in solution to give a ratio of Ag to total platinum group elements and gold of 20:1 *[97]*. The flux combines with the gangue to a form fluid slag and the litharge in the flux is reduced to minute globules of lead. The rain of lead globules, falling through the molten mass, collects the particles of some of the platinum group elements and gold and coalesces into a button at the bottom of the crucible. For effective collection, the composition of the flux, the

temperature and its rate of increase must be optimised. On cooling the slag solidifies and is separated from the lead button containing the platinum group elements and gold. Lead is removed by oxidation, vaporised and absorbed into the cupel thus leaving the silver prill containing the extracted platinum group elements and gold *[97]*.

5.3.1 *Flux reagents*

The selection and proportions of flux components are the most important factors in effecting a successful fusion. Hereby a summary of some of the chemical properties of the flux reagents used in this study:

Sodium carbonate: Na_2CO_3

Sodium carbonate is a powerful basic flux and readily forms alkali silicates. In the presence of air some sulphates are also formed and thus sodium carbonate may be considered an oxidising and desulphurising reagent. Sulphates are produced more readily in the presence of an oxidising reagent such as litharge:

$$FeS_2 + 7PbO + 2Na_2CO_3 \rightarrow FeO + 7Pb + 2Na_2SO_4 + 2CO_2$$

Sodium carbonate melts at 850 °C and dissociates partially at 950 °C evolving carbon dioxide and liberating some free alkali:

$$Na_2CO_3 + Na_2SiO_3 \rightleftharpoons Na_4SiO_4 + CO_2$$

Silica: SiO_2

Silica is a strongly acidic flux reagent. It combines with metallic oxides to form silicates that are fundamental to most slags. Silica slags are classified according to the ratio of oxygen in the base (metallic oxide) to the oxygen in the acid (silica). A metasilicate slag with a ratio of 1:2 is desirable because of its stability:

$$PbO + SiO_2 \rightarrow PbSiO_3$$

Borax (anhydrous sodium tetraborate): $Na_2B_4O_7$

Anhydrous borate melts at 741 °C to form a viscous slag but becomes fluid at elevated temperatures. It is a strongly acidic reagent and readily dissolves almost all metallic oxides. During fusion the dissolution by borax of metal oxides progresses through two stages: 1) the borax melts to form a colourless transparent glass consisting of sodium metaborate and boric anhydride:

$$Na_2B_4O_7 \rightarrow Na_2B_2O_4 + B_2O_3$$

and 2) the boric anhydride then reacts with the metal oxide to form metal borate:

$$MO + B_2O_3 \rightarrow MB_2O_4$$

Borax also lowers the fusion temperatures of all slags appreciably. Excess borax is detrimental to the fusion; preventing the formation of a homogenous slag and subsequent separation of the lead button.

Litharge: PbO

Litharge is a readily fusible basic flux reagent. In addition, it acts as an oxidising and desulphurising agent. It melts at 883 °C and together with the required addition of reductant (maize meal), provides the metallic lead that collects the platinum group elements and gold.

Maize meal

Maize meal acts as a reducing agent. Maize meal, which is a source of carbon, reduces litharge to metallic lead with the evolution of carbon monoxide or carbon dioxide:

At higher temperatures: $PbO + C \rightarrow Pb + CO$

At lower temperatures: $2PbO + C \rightarrow 2Pb + CO_2$

5.4 Literature survey of the analysis of SARM 7

Juvonen, Kallio and Lakomaa *[52]* determined precious metals in rocks by ICP-MS using nickel sulphide concentration with Te co-precipitation. They compared the results obtained with those obtained with other pre-treatment methods, i.e. lead fire assay (with added $AgNO_3$ as carrier for the platinum group elements and gold) and aqua regia leaching procedures. The instrument was optimised with a solution that was 10 μg dm^{-3} with respect to Mg, Rh, Pb in order to give a compromise between high sensitivity and low oxide levels. Double charged ions and oxide interferences were monitored with $^{140}Ce^{2+}$ and $^{140}CeO^{+}$. The final solutions (standards and samples) to be analysed by means of ICP-MS all contained approximately 3.6% (v/v) HNO_3 and 5.0% (v/v) HCl, as well as 50 μg dm^{-3} Tl as internal standard. They reported systematically low results for gold, which is in accordance with other workers *[98]* who also extracted gold by means of the nickel sulphide fire assay procedure. They also reported that the recoveries of Au, Pd and Pt did not differ significantly for the lead and nickel sulphide fire assay procedures. They concluded that 1) the best recoveries of Ir, Os, Rh and Ru may be obtained by means of nickel sulphide fire assay, 2) the best recoveries of Au, Pt and Pd may be achieved with lead fire assay and 3) Rh is best recovered by means of nickel sulphide fire assay with gold as collector. Aqua regia leach procedures were only recommended for preliminary studies. Their results are given in Table 5.2.

Table 5.2: Results for the analysis of SARM 7 by means of aqua regia leach, lead fire assay and nickel sulphide fire assay followed by ICP-MS.

Element	% Recovery by aqua regia leach	% Recovery by lead fire assay	% Recovery by nickel sulphide fire assay
Au	72	85	84
Ir	33	4	106
Pd	89	97	100
Pt	42	97	102
Rh	89	18	100
Ru	29	3	108

Sun, Jain, Zhou and Kerrich *[99]* analysed SARM 7 by means of nickel sulphide fire assay and Te co-precipitation. Instead of crushing the nickel sulphide button followed by open beaker dissolutions of the nickel sulphide button and the Te precipitate, they employed Teflon bombs for the mentioned dissolutions. The ion lenses of the ICP-MS were optimised so that maximum signals for Rh, Cs, Tm and Bi were obtained by using a solution that was 100 μg dm^{-3} with respect to these elements. The nebuliser gas flow rate was adjusted for maximum sensitivity while keeping the ThO^+/Th^+ ratio to 5%. The final sample solutions to be analysed by ICP-MS contained approximately 5.0% (v/v) HNO_3 and 5.0% (v/v) HCl. The acid wash that was used to rinse the system between samples contained approximately 7.1% (v/v) HNO_3 and 10% (v/v) HCl. Their results are shown in Table 5.3.

Table 5.3: Results for the analysis of SARM 7 by means of open beaker and Teflon bomb digestions of the nickel sulphide button followed by ICP-MS.

Element	% Recovery by open beaker digestion	% Recovery by Teflon bomb digestion
Au	-	88
Ir	85	108
Pd	97	100
Pt	94	104
Rh	94	106
Ru	79	104

Perry, Van Loon and Speller *[100]* used a dry-chlorination ICP-MS method to determine the platinum group elements and gold in SARM 7. They performed two point linear calibrations and the method of standard additions was used for the ICP-MS work. The prepared standards were carried in 1% (v/v) HNO_3. They reported higher recoveries, better accuracy, better precision and sensitivity for dry-chlorination than for nickel sulphide fire assay ICP-MS or lead fire assay ETAAS. Their results may be seen in Table 5.4.

Table 5.4: Results for the analysis of SARM 7 by means of chlorination and nickel sulphide fire assay followed by ICP-MS and lead fire assay followed by ETAAS. The last two methods were performed by commercial laboratories.

Element	**% Recovery by chlorination ICP-MS**	**% Recovery by nickel sulphide fire assay ICP-MS**	**% Recovery by lead fire assay ETAAS**
Au	66	not available	<65
Ir	105	43	not available
Pd	57	50	33
Pt	80	18	25
Rh	122	<79	not available
Ru	155	<44	not available

Chen, Fryer, Longerich and Jackson *[101]* analysed SARM 7 for the platinum group elements and gold using ICP-MS after ion-exchange preconcentration. They employed ion-exchange in order to separate the platinum group elements and gold from the transition elements since serious interferences from transition element argide polyatomic ions together with matrix effects from high total dissolved solids hamper the accurate determination of low concentrations of the platinum group elements and gold by ICP-MS. The nebuliser gas flow was adjusted for maximum sensitivity using a solution containing Rh, Bi and U so that $UO^+:U^+ < 0.25$, sensitivity for Rh was > 10^6 counts per second μg^{-1} and sensitivity for Bi was > 0.5×10^6 counts per second μg^{-1}. At maximum sensitivity polyatomic ion formation was higher than is normally used for trace element analysis. The internal standard solution comprised of 4031 ng g^{-1} Cd (for Ru, Rh and Pd) and 2045 ng g^{-1} Tl (for Ir, Pt and Au). The acid calibration blank solution consisted of approximately 2% (v/v) HCl and the flush solution consisted of approximately 3% (v/v) HCl and 2.8% (v/v) HNO_3. Matrix effects and drift were corrected with the internal

standards. They reported poor accuracy and precision for gold analysis. Table 5.5 shows the results they obtained with analysis of 2 mg and 20 mg fragments of nickel sulphide beads using cation exchange ICP-MS.

Table 5.5: Results for the analysis of SARM 7 by means of nickel sulphide fire assay followed by ion exchange preconcentration of fragments of the nickel sulphide beads followed by analysis by ICP-MS.

Element	**% Recovery for 2 mg fragments of a nickel sulphide bead**	**% Recovery for 20 mg fragments of a nickel sulphide bead**
Au	77	58
Ir	124	114
Pd	82	96
Pt	116	88
Rh	120	102
Ru	99	100

Enzweiler, Potts and Jarvis *[102]* determined Pt, Pd, Ru and Ir in SARM 7 by isotope dilution ICP-MS using a sodium peroxide fusion and Te co-precipitation. The final sample solutions for ICP-MS analysis contained between 10% (v/v) and 12% (v/v) aqua regia. Their results are summarised in table 5.6.

Table 5.6: Results for the analysis of SARM 7 by means of isotope dilution ICP-MS using a sodium peroxide fusion and Te co-precipitation.

Element	**% Recovery by sodium peroxide fusion and Te co-precipitation followed by isotope dilution ICP-MS**
Ir	95
Pd	98
Pt	101
Ru	96

Gowing and Potts *[51]* evaluated a rapid technique for the determination of the platinum group elements and gold based on a selective aqua regia leach. The sample solutions for analysis by

ICP-MS contained 20% (v/v) aqua regia. The ion lens settings were optimised by maximising the $^{115}In^{+}$ signal and minimising the Ce^{2+} and CeO^{+} signals. The standard solutions were also prepared in 20% (v/v) aqua regia. The data used to apply a correction for drift in instrument sensitivity was by interpolation of count data from adjacent standard solutions. They used 100 μg dm^{-3} of Re as an internal standard for Os, Ir and Pt and 100 μg dm^{-3} of In as an internal standard for Rh, Ru and Pd. A 20% (v/v) aqua regia solution was used to flush the ICP-MS system between samples. Their results are shown in Table 5.7.

Table 5.7: Results for the analysis of SARM 7 by means of an aqua regia leach followed by ICP-MS.

Element	**% Recovery by an aqua regia leach followed by ICP-MS**
Au	97
Ir	26
Pd	77
Pt	37
Rh	73
Ru	27

Jackson, Fryer, Gosse, Healy, Longerich and Strong *[98]* determined the platinum group elements and gold in SARM 7 by nickel sulphide fire assay collection followed by Te co-precipitation and ICP-MS. A solution containing approximately 8% (v/v) HCl and 7% (v/v) HNO_3 was used in the wash station of the autosampler. The ion lenses of the ICP-MS were optimised as follows: 1) lens S2 was set to 0, 2) lens P was set for minimum background readings (usually < 5 counts s^{-1}) and 3) lenses B and E were optimised for maximum signal on Rh, Cs, Tm and Bi in a solution containing 100 μg dm^{-3} of Li, Co, Rh, Cs, Tm, Bi and Th. The nebuliser gas flow was adjusted for the optimum operating conditions by monitoring Rh, Hf (background), Th and ThO. The acid calibration blank solution consisted of approximately 5% (v/v) HCl and 6% (v/v) HNO_3. Cd was employed as internal standard for Ru, Rh and Pd and Tl as internal standard for Os, Ir, Pt and Au. Drift and matrix effects were compensated for with the internal standards. Table 5.8 shows their results.

Table 5.8: Results for the analysis of SARM 7 by means of nickel sulphide fire assay and Te co-precipitation followed by ICP-MS.

Element	**% Recovery by nickel sulphide fire assay and Te co-precipitation followed by ICP-MS**
Au	82
Ir	96
Pd	88
Pt	91
Rh	88
Ru	92

Godfrey and McCurdy *[103]* analysed SARM 7 by means of flow injection ICP-MS after a sodium peroxide fusion procedure. All standard and sample solutions were prepared in 2% (v/v) HCl. 20 μg dm^{-3} of each of Cs and Bi was used as internal standards. They also made use of synthetic standards prepared by spiking the fusion blank solution at various concentrations of the platinum group elements and gold. The ion lens settings were optimised with maximum signal on In at mass 115. Table 5.9 shows their results.

Table 5.9: Results for the analysis of SARM 7 by means of a sodium peroxide fusion followed by flow injection ICP-MS.

Isotope	**% Recovery for (1g SARM 7 + 5g Na_2O_2)**	**% Recovery for (0.5g SARM 7 + 4g Na_2O_2) (with matrix matched standards)**
^{197}Au	166	103
^{193}Ir	236	215
^{105}Pd	96	118
^{194}Pt	94	97
^{195}Pt	90	-
^{103}Rh	389	85
^{101}Ru	101	87

5.5 Experimental

5.5.1 Lead fire assay procedure

Samples with a high As and/or S content require roasting at 600-800°C to volatilise these elements to prevent formation of a matte during fusion which would otherwise retain the platinum group elements and gold *[97]*. Roasting of SARM 7 samples are not necessary before the lead fire assay *[52]*. A flux similar to the one used by Hall and Pelchat *[97]* was used to extract the platinum group elements and gold from SARM 7. The flux used in the lead fire assay procedure (first assay laboratory) was composed of 105 g litharge, 45 g sodium carbonate, 5 g borax, 10 g silica and 2.5 g maize meal. Silver was used as carrier for the platinum group elements and gold in the form of approximately 1.0 ml of a 5 g dm^{-3} $AgNO_3$ solution that was added to each crucible before fusion. The fusion time for the well-mixed (25 g sample and flux) mixture was set at 60 minutes at approximately 1100°C. The lead buttons were cupelled for 30 minutes at approximately 1000°C. The prills were weighed and prepared for analysis by ICP-MS.

SARM 7 was also supplied to a commercial laboratory for lead fire assay analysis and three prills were received from the commercial laboratory. The commercial laboratory also employed a procedure whereby 25 g of sample is used as well as silver nitrate as carrier solution.

Some fire assay laboratories consider a blank to be represented by carrying reagents only through the procedures, i.e. flux only, while others would substitute "clean" silica for a sample and estimate its variation in results in order to determine the method detection limit *[97]*. In this investigation the blank comprised of reagents only, i.e. flux only. A blank was produced by the first assay laboratory but no blank was received from the commercial laboratory.

Table 5.10 shows some of the masses recorded during the procedure.

Table 5.10: The masses of SARM 7 weighed for analysis as well as the masses of the prills that were obtained. The prills from the commercial laboratory are given as p1, p2 and p3.

Sample name	Mass of SARM 7 weighed in g	Mass of prill obtained after cupellation in g
1	25.02015	0.00385
2	25.06146	0.00346
3	25.05006	0.00336
4	25.03992	0.00310
5 (Blank)	-	0.00317
p1	25	0.00669
p2	25	0.00614
p3	25	0.00561

5.5.2 *ICP-MS procedure*

Preparation of sample and standard solutions for analysis by ICP-MS

The method used to dissolve the prills is similar to that of Hall and Pelchat *[97]*. The prills produced after cupellation were prepared for ICP-MS analysis as follows: 1) The prill was heated with 2.5 ml concentrated HNO_3 in a 100 ml beaker, after which 7.5 ml concentrated HCl was added and the solution was further heated. 2) The solution was cooled and transferred quantitatively to a 50 ml volumetric flask and made to the mark with distilled water. 3) The solution was diluted 20x by transferring 5 ml of the solution to a 100 ml volumetric flask and making it up to the mark with distilled water. Internal standards, Y (Pd, Rh and Ru) and La (Au, Ir, Pt), were also added before making it up to the mark. The acid content of the solution to be analysed by ICP-MS was approximately 1% (v/v) aqua regia. The standards were prepared as set out in chapter 3. Y and La were added as internal standards.

Calculations for the platinum group elements and gold content of SARM 7

The mathematical formula used to calculate the platinum group elements and gold content of SARM 7 are derived as follows for e.g. Au:

$$P_{prill} = [(ICP\text{-}MS_{prill} \times df) / (m_{prill} / V_{prill})] \quad ...(1)$$

where P_{prill} is the purity of the prill with respect to the Au content,

$ICP\text{-}MS_{prill}$ is the result of the ICP-MS analysis of the prill with respect to the Au content in $\mu g\ dm^{-3}$,

df is the dilution factor of the solution of the dissolved prill,

m_{prill} is the mass of the prill in μg and

V_{prill} is the volume of the volumetric flask in which the solution was made up to in dm^3.

$$\text{Au content in } \mu g\ kg^{-1} = [(P_{prill} \times M_{prill}) / M_{CRM}] \times 10^9 \quad ...(2)$$

where M_{prill} is the mass of the prill in g and

M_{CRM} is the mass of SARM 7 weighed for analysis in g.

Substituting (1) into (2):

$$\text{Au content in } \mu g\ kg^{-1} = [([(ICP\text{-}MS_{prill} \times df) / (m_{prill} / V_{prill})] \times M_{prill}) / M_{CRM}] \times 10^9$$
$$= [([(ICP\text{-}MS_{prill} \times df) / (m_{prill} / V_{prill})] \times m_{prill} / 10^6) / M_{CRM}] \times 10^9$$
$$= [([(ICP\text{-}MS_{prill} \times df) / (m_{prill} / V_{prill})] \times m_{prill} / 10^6) / M_{CRM}] \times 10^9$$
$$= [(ICP\text{-}MS_{prill} \times df \times V_{prill}) / M_{CRM}] \times 10^3$$

ICP-MS: Instrument optimisation and method used

The instrument was optimised as set out in chapter 2. After the instrument was calibrated with the prepared standards, the prepared samples were analysed and the 5.0 $\mu g\ dm^{-3}$ standard was to monitor the drift of the instrument. The method used for analysis was as developed in chapter 3. The most abundant isotopes of each element were measured: ^{197}Au, ^{193}Ir, ^{106}Pd, ^{108}Pd, ^{194}Pt, ^{195}Pt, ^{103}Rh, ^{99}Ru, ^{100}Ru and ^{101}Ru.

5.6 Results and discussion

5.6.1 Results of the analysis of SARM 7

The number of samples analysed by ICP-MS was small, i.e. the drift control standard was only analysed three times because of the short time period that was necessary to analyse the samples. In order to assess whether it is necessary to apply drift correction to the results obtained, i.e. whether instrument drift affected any of the isotopes analysed, the values obtained for the drift control standards are analysed as shown in table 5.11. From table 5.11 it can be seen that drift

correction must be applied to the following isotopes: ^{197}Au, ^{106}Pd and ^{108}Pd. The results of the quantitative determination of the platinum group elements and gold in SARM 7 for the samples. 1, 2, 3, 4, p1, p2 and p3 by means of lead fire assay followed by ICP-MS are shown in tables 5.12 and 5.13.

Table 5.11: Data on the 5 μg dm^{-3} drift control standard. Standard deviation is in brackets. In the cases where the values of the drift control standard deviated significantly from a value of approximately 5.0 it was decided to apply drift correction in the form of the use of internal standards.

Isotope	**Average of the measurements of the drift control standard in μg dm^{-3}**
^{197}Au	6.15 (0.17)
^{193}Ir	5.10 (0.09)
^{106}Pd	6.98 (0.42)
^{108}Pd	6.97 (0.51)
^{194}Pt	5.38 (0.33)
^{195}Pt	5.40 (0.28)
^{103}Rh	5.45 (0.21)
^{99}Ru	5.25 (0.09)
^{100}Ru	5.35 (0.16)
^{101}Ru	5.27 (0.28)

5.6.2 *Recovery of Au*

Higher recoveries are reported for samples 1, 2, 3 and 4 than for p1, p2 and p3. The use of internal standards to correct for drift proved to be detrimental in both cases, i.e. weaker recoveries were then calculated.

The % recoveries for gold do not compare well to those obtained by some researchers who also applied lead fire assay to the analysis of SARM 7 *[52]*, but are similar to the recoveries of a commercial laboratory also using a lead fire assay procedure as reported by *[100]*.

Better extraction of gold was reported by researchers employing techniques other than lead fire assay *[51, 52, 98 - 101, 103]* in the analysis of SARM 7.

Table 5.12: Results for the analysis of SARM 7 by lead fire assay followed by ICP-MS. The results are the averages for samples 1, 2, 3 and 4. Blank values have been subtracted.

Isotope	% Recovery without the use of an internal standard	% Recovery with La as internal standard for Au and Y as internal standard for Pd
^{197}Au	58.9	42.0
^{193}Ir	0.8	no correction applied
^{106}Pd	95.7	89.1
^{108}Pd	94.4	87.9
^{194}Pt	90.6	no correction applied
^{195}Pt	90.3	no correction applied
^{103}Rh	2.6	no correction applied
^{99}Ru	0.3	no correction applied
^{100}Ru	0.1	no correction applied
^{101}Ru	0.2	no correction applied

Table 5.13: Results for the analysis of SARM 7 by lead fire assay followed by ICP-MS. The results are the averages for samples p1, p2 and p3.

Isotope	% Recovery without the use of an internal standard	% Recovery with La as internal standard for Au and Y as internal standard for Pd
^{197}Au	33.8	23.6
^{193}Ir	0.1	no correction applied
^{106}Pd	88.2	77.7
^{108}Pd	87.2	76.9
^{194}Pt	89.3	no correction applied
^{195}Pt	89.5	no correction applied
^{103}Rh	3.3	no correction applied
^{99}Ru	0.1	no correction applied
^{100}Ru	0.2	no correction applied
^{101}Ru	0.2	no correction applied

5.6.3 *Recovery of Ir*

The recovery of Ir from SARM 7 was negligible. Juvonen, Kallio and Lakomaa *[52]* also reported poor extraction of Ir by means of the lead fire assay as pre-concentration technique.

Other pre-concentration techniques are more effective than lead fire assay for the extraction of Ir from SARM 7 *[51, 52, 98 - 102]*.

5.6.4 *Recovery of Pd*

The recoveries obtained for samples 1, 2, 3 and 4 were better than those obtained for p1, p2 and p3. In both cases the use of internal standards caused lower recoveries to be reported.

The values obtained (before the application of internal standards) compare well to those obtained by other researchers *[52]* and better than those obtained by a commercial laboratory used by Perry, Van Loon and Speller *[100]* also using lead fire assay.

In some cases workers employing other pre-concentration techniques reported slightly better recoveries *[52, 99, 102]* and in some cases poorer results were obtained *[51, 52, 98, 100]*.

5.6.5 *Recovery of Pt*

Similar yields for Pt were obtained for all the samples analysed.

In some cases the values obtained compare well to those obtained by other researchers *[52]* and even better than those obtained by a commercial laboratory *[100]*.

Lead fire assay proved to be better for the pre-concentration of Pt from the matrix than other techniques *[51, 52, 100]* and in other cases other techniques proved to be superior *[52, 98, 99, 102, 103]*.

5.6.6 *Recovery of Rh*

Rh was extracted poorly, i.e. 2.6 % and 3.3 % for the samples analysed. These values do not compare well to those of other workers, i.e. Juvonen, Kallio and Lakomaa *[52]* reported a recovery of 18% for Rh by means of the lead fire assay procedure.

In general, other techniques proved to be superior to lead fire assay for the separation of Rh from the SARM 7 matrix *[51, 52, 98, 99, 103]*.

5.6.7 *Recovery of Ru*

The recovery of Ru from SARM 7 was negligible. Poor extraction was also reported by Juvonen, Kallio and Lakomaa *[52]*.

Ru is better extracted from SARM 7 by techniques other than lead fire assay *[52, 98, 99, 101 - 103]*.

5.6.8 *Lead fire assay as pre-concentration technique for the platinum group elements and gold*

According to Perry, Van Loon and Speller *[100]* the exploration industry is in general disappointed with fire assay procedures because of inaccurate results generated. However, the platinum group elements and gold must be separated from the sample matrix and concentrated before analysis *[104 - 106]* and fire assay procedures remain the most important way of doing this. Lead fire assay remains the most reliable and cost effective means of preparation for analysis of rocks, soils and sediments for Au, Pd and Pt provided certain modifications are carried out to suit the sample type *[97]*. The elements Au, Pd and Pt are effectively and quantitatively collected in a silver bead by means of the fire assay procedure *[51, 97, 104, 107]*. For the collection of Ir and Rh a gold bead is recommended *[106]*. Flux composition and assay conditions are very important if Ir and Rh are to be collected by means of the lead fire assay procedure *[51, 106]*.

Precision at low levels of the analytes is dominated by homogeneity of the elements in a particular sample rather than by the invariability inherent in the method itself *[97]*, i.e. the determination of the natural concentrations of precious metals must take into consideration their occurrence in small, rare, discrete and inhomogeneously distributed minerals *[101, 102, 107]*.

For accurate results the assay conditions and skills are very important, especially at the cupellation stage *[107]*. This may in part explain the different recoveries of the platinum group elements and gold obtained by the two fire assay laboratories employed in this study.

5.6.9 *ICP-MS procedure*

There are several potential polyatomic interferences that may influence the isotopes measured in this study: ^{197}Au ($^{181}Ta^{16}O$), ^{193}Ir ($^{177}Hf^{16}O$), ^{106}Pd ($^{90}Zr^{16}O$, $^{89}Y^{16}O^{1}H$), ^{108}Pd ($^{92}Zr^{16}O$), ^{194}Pt ($^{178}Hf^{16}O$), ^{195}Pt ($^{179}Hf^{16}O$), ^{103}Rh ($^{86}Sr^{16}O^{1}H$, $^{87}Sr^{16}O$, $^{63}Cu^{40}Ar$), ^{99}Ru (-), ^{100}Ru ($^{84}Sr^{16}O$) and ^{101}Ru ($^{84}Sr^{16}O^{1}H$, $^{61}Ni^{40}Ar$, $^{64}Ni^{37}Cl$) *[106]*. According to Hall and Pelchat *[97]* the oxides of Y and Sr were not in evidence in SARM 7 samples processed through the lead fire assay procedure. Godfrey and McCurdy *[103]* reported the oxides of Zr, Hf and Ta to be present in the system if zirconium crucibles were used during sodium peroxide fusion procedures in the analysis of SARM 7 samples. They also reported ArCu to be present due to the copper content of the SARM 7 samples. However, due to the lead fire assay procedure (separation of the platinum group elements and gold from the matrix containing base metals such as copper and nickel) none of the interferences $^{63}Cu^{40}Ar$, $^{61}Ni^{40}Ar$ or $^{64}Ni^{37}Cl$ was present in the samples that were analysed by ICP-MS.

During this study care was taken not prepare the samples in such a way that it contained a high contents of dissolved salts or high acid contents. Perry, Van Loon and Speller *[100]* reported that the signal intensity in the mass spectrometer was continuously diminished because of the gradual build-up of salts on the skimmer and sampler cones. As the salts form, the effective diameter of the sampler orifice is reduced, the amount of plasma sampled decreases and the signal diminishes. Gowing and Potts *[51]* also reported interference effects occurring due to the suppression of signals in sample solutions containing particular high contents of dissolved salt. Their samples were prepared in a 20% aqua regia matrix with > 0.1% TDS.

Some workers *[98, 101]* reported memory effects for Pd and Au when determined by ICP-MS. Due to adequate rinsing times between samples and adequate preflush times during analysis none of these memory effects were encountered in this study.

5.6.10 *Comparison of ICP-MS procedure with those of other workers*

The main differences between the ICP-MS procedures followed by other workers and that of the author may be summarised as follows:

Other workers (5.4) have a very simplistic approach to the optimisation of the ICP-MS, usually monitoring only a few isotopes. The author optimised the various parts of the instrument

(chapter 2) and not only the ion lenses. Care was also taken to keep the levels of the doubly charged ions and oxide interferences to a minimum.

Other workers (5.4) also made use of internal standards. The author however made a detailed study of various internal standards in relation to their behaviour to the platinum group elements and gold in acidic media.

One of the objectives of this study was to show that the analysis of the platinum group elements and gold may be performed in an acidic matrix of 1% (v/v) aqua regia. This is in contrast to the high acidic matrices used by other workers (5.4) (with the exception of a few *[100, 103]*). The higher acidic matrices employed by them is detrimental for the instrument, i.e. corrosion of the sampler and skimmer cones of the ICP-MS.

5.7 Recommendations

The analysis of SARM 7 by means of lead fire assay and ICP-MS proved to be relatively successful for the quantification of Au, Pd and Pt. The analysis procedure followed consisted of three steps *[102]*: 1) separation of the platinum group elements and gold from the matrix and the pre-concentration of the analytes by means of fire assay, 2) the dissolution of the silver beads and 3) detection of the isotopes of the elements by ICP-MS. However, only step 3 was studied in depth in this work. In order to obtain higher recoveries of the platinum group elements and gold from SARM 7, steps 1 and 2 need to be optimised and refined. The following suggestions and recommendations for future work are made:

As suggested by some researchers *[97, 98]* the detection capability of lead fire assay would be enhanced by the purification of flux reagents and dedication of assay equipment (furnaces, crucibles) to the processing of low-level samples only. Thus, improvement in the purity of the flux constituents and equipment would allow advantage to be taken of the excellent sensitivity of ICP-MS in the sense that less impurities would then be available to give rise to possible interferences that might interfere with the detection of the analytes. Also, reagent contamination can be reduced by the use of higher purity reagents and more rigorous clean laboratory procedures. The reagents used in the analysis of the platinum group elements and gold should be analysed for the presence of the analytes before use. Sun, Jain, Zhou and Kerrich *[99]* found their silica flux to be contaminated with Pd.

The assay conditions and parameters of the lead fire assay need to be refined when analysing for the platinum group elements and gold, e.g. some workers choose to fuse at 1000°C for 45-60

minutes and perform cupellation at 900°C for 45-60 minutes, while others fuse at 1050°C for 50-60 minutes and cupel at 950°C for 50-55 minutes *[97]*.

It is further suggested that the dissolution process of the silver beads be refined. The use of sealed tubes *[102]* or Teflon bombs *[99]* for the dissolutions proved to be successful for some researchers.

The lead fire assay procedure as a whole, i.e. flux composition, assay conditions etc. must be optimised for the analysis of samples containing low levels of the platinum group elements and gold.

5.8 Conclusion

From the analysis of the certified reference material, SARM 7, by means of lead fire assay and ICP-MS high recoveries of only Au, Pd and Pt are expected. It was shown that these three elements were indeed extracted and quantified successfully by means of the ICP-MS procedures developed in chapter 3. It was also shown that it was possible to obtain relatively good results with the lower acidic contents of standards and samples (1% (v/v) aqua regia) as employed in this study.

It was also shown that the matrix and drift correction procedures (in the form of the use of internal standards) that were developed in chapter 3 must be applied with caution. The measurements of the drift control sample must first be analysed in order to ascertain whether corrections should be applied. In this analysis of SARM 7 the time used to analyse the samples by means of ICP-MS proved to be too short for instrumental drift to have a significant effect. It was shown that the use of an internal standard was detrimental to the recoveries reported for Au and Pd.

CHAPTER 6

THE QUANTITATIVE DETERMINATION OF ARSENIC IN A CERTIFIED REFERENCE MATERIAL

6.1 Introduction

The validity of the ICP-MS method developed for the analysis of arsenic as developed in chapter 4 may be tested by the analysis of a certified reference material. The reference material Seronorm Trace Elements Urine has a certified value for the amount of arsenic it contains. As urine samples usually have relatively high concentrations of chloride present in the matrix [*79, 80*], the ICP-MS method was tested for the correction of the ArCl interference at *m/z* 75. An attempt was made to accurately determine the arsenic content of the urine samples by means of the developed ICP-MS method, i.e. using arsenic calibration standards prepared in 1% HNO_3, employing La as an internal standard, determining the correction factor at a specific chloride concentration and the application thereof to the intensities obtained at *m/z* 75, as well as the application of drift correction procedures. The urine samples will only be diluted with water. The results of other researchers who also attempted the analysis of arsenic (and specifically in a chloride medium) by means of ICP-MS will also be briefly discussed and compared to the results obtained in this study.

The certified reference material used in this study was used to assess the accuracy of the analytical method developed. As only four samples were analysed it was not possible to perform statistical analysis in order to assess the precision and determine detection limits. The results reported here could therefore only be considered as preliminary.

6.2 Certified reference material *[108]*

Seronorm Trace Elements Urine is produced from human urine collected from thoroughly controlled voluntary Norwegian donors. The reference material is stable and is a lyophilised reference urine of human origin for *in vitro* diagnostic use. The material does not contain any preservatives. After reconstitution of the reference material it is considered stable for one month at a temperature of ≤ -20°C, seven days at temperatures of between 2°C and 8°C and for eight hours at temperatures of between 15°C and 25°C. The analytical data of Seronorm Trace Elements Urine have been determined after reconstitution with 5.00 ml pure water.

Seronorm Trace Elements Urine (Lot 403125, 403125x, 403125y) has an analytical arsenic value of 101 μg dm^{-3} with a standard deviation of 3 μg dm^{-3}. It also has a certified analytical value of 4326 mg dm^{-3} with a standard deviation of 15 mg dm^{-3} for chloride. It does not have a certified value for Se.

6.3 Literature survey

McLaren *et al.* [*48*] determined arsenic in the marine sediment certified reference material PACS-1 by means of ICP-MS. They investigated the use of the background ion $^{40}Ar_2^+$ as an internal standard. With no internal standardisation applied they reported a recovery of 92.4% and with the argon dimer, $^{40}Ar_2^+$, as internal standard they achieved a recovery of 96.7%. They reported that the use of the argon dimer to compensate both for suppression (or enhancement) of ion sensitivity by concomitant elements and for induced calibration drift proved to be successful for the determination of arsenic since the mass difference between arsenic and the argon dimer is relatively small. Hydrochloric acid was however not used during sample preparation so it was not necessary to compensate for the $^{40}Ar^{35}Cl$ interference at *m/z* 75. Nitric acid, hydrofluoric acid and perchloric acid were used during sample preparation procedures.

Branch, Ebdon, Ford, Foulkes and O'Neill [*80*] determined the arsenic content of samples with a high chloride content using ICP-MS with the addition of nitrogen to the carrier gas. With the addition of nitrogen to the argon carrier gas, the level of the $^{40}Ar^{35}Cl^+$ polyatomic ion that interferes with the determination of monoisotopic arsenic is reduced to negligible levels. They showed this modification to be effective even for solutions which contain up to 1.13% chloride. All standards and samples were spiked with In to give a final concentration of 100 μg dm^{-3} and made up to volume with 2% nitric acid. The Seronorm urine samples were diluted 10x with 2% nitric acid. Their results are summarised in table 6.1.

Table 6.1: Results of the determination of arsenic in several reference materials by means of ICP-MS.

Sample	**% Recovery of arsenic without nitrogen addition**	**% Recovery of arsenic with nitrogen addition**
NIES CRM No.9 (Sargasso seaweed)	128.7	95.7
Seronorm urine	not determined	103.5
NIST 8431 (Mixed diet)	not determined	102.5
NIST 1573 (Tomato leaves)	not determined	88.9
NRCC DORM 1 (Dogfish muscle)	not determined	100.6

Kershisnik and co-workers [*78*] presented a method for the correcting the ICP-MS $^{40}Ar^{35}Cl$ interference with ^{75}As by using the $^{16}O^{35}Cl$ species. They observed that the signal intensities for the species $^{16}O^{35}Cl$ and $^{40}Ar^{35}Cl$ are proportional over a range of chloride concentrations (0 - 2.84%). They used Y as internal standard. The method is sensitive to the presence of vanadium (mass 51) in solution. They analysed a NIST standard in duplicate and reported recoveries of 102.8% and 105.2%

Branch, Ebdon and O'Neill [*88*] determined arsenic species in fish by directly coupled high performance liquid chromatography-ICP-MS. For total arsenic determinations, nitrogen addition ICP-MS was used to overcome the potential interference from $^{40}Ar^{35}Cl$. In was used as internal standard. The sample preparation procedures did however not involve the addition of hydrochloric acid. The dogfish reference material, DORM-1, was analysed and a recovery of 100.6% was reported.

Sheppard and co-workers [*93*] developed a single microwave digestion procedure for the determination of arsenic, cadmium and lead in seafood products by ICP-AES and ICP-MS. As seafood products normally have significant chloride levels, they applied the following correction at *m/z* 75 in order to obtain the intensity due to arsenic: $I_{As} = I_{75} - (3.1278 \times I_{77}) + (1.0177 \times I_{78})$ where I_n is the intensity at $m/z = n$. They analysed the dogfish muscle and liver reference material, DORM-1, and the lobster hepatopancreas marine reference material, TORT-1. They reported arsenic recoveries of 94.9% and 121.5% respectively for the two reference materials.

Larsen and Stürup [*109*] added carbon as methanol or ammonium carbonate to aqueous analyte solutions in combination with increased power input and enhanced the ICP-MS signal intensities of arsenic and selenium. They proposed that an increased population of carbon ions or carbon-containing ions in the plasma facilitates a more complete ionisation of analytes lower in ionisation energy than carbon itself. They used antimony as internal standard. The enhanced detection power for arsenic was applied to arsenic speciation by high-performance liquid chromatography ICP-MS and made possible the detection of arsenocholine (AsC) in extracts of shrimp. No reference material was analysed.

Whilst participating in some preliminary As speciation studies organised by the European Unions' Measurement and Testing group Campbell *et al.* [*79*] observed that total As levels were in excess of their certified or indicative values. They reported that the ratio of the mass to charge ratios at 75 and 77 indicated that the observed excess was not due to the formation of an isobaric polyatomic interference ($^{40}Ar^{35}Cl$) with ^{75}As. They presented evidence to support an element-specific enhancement of the As signal in the presence of a carbon matrix. They identified the source of this error as arising principally from differences in acidity between the samples and external calibrants. They obtained results using a matrix matching technique that minimised differences in acidity and carbon loading. They used microwave solubilisation (nitric acid) and mineralisation (nitric, sulphuric and perchloric acids) procedures. They analysed certified reference material CRM 422 (cod mussel) and candidate reference materials T28 (mitilus) and T25 (tuna fish). Y was used as internal standard. The presence of the polyatomic interference $^{40}Ar^{35}Cl$ was detected when a low dilution factor was employed, i.e. high matrix loading occurred. The data was then corrected on the basis of the signals at *m/z* 83 (^{83}Kr), 82 (^{82}Se + ^{82}Kr) and 77 (^{77}Se + $^{40}Ar^{37}Cl$), respectively, to derive the contribution of $^{40}Ar^{35}Cl$ to the apparent ^{75}As signal. Tables 6.2 and 6.3 show the results they obtained using external calibration, standard additions, matrix matched standards and acid matched standards.

Table 6.2: Comparison of ICP-MS results for As in certified reference and candidate reference materials by external calibration following mineralisation or solubilisation with HPLC-ICP-MS.

Sample	**Solubilisation**	**Mineralisation**	**% Recovery of arsenic by ICP-MS**	**% Recovery of arsenic by HPLC- ICP-MS**
CRM 422		x	147.4	100.0
CRM 422	x		114.2	97.2
CRM 422	x		104.3	-
T25	x		102.3	100.0
T25		x	318.2	102.3
T28		x	150.0	100.0
T28	x		136.0	97.8
T28		x	268.4	-

Table 6.3: Comparison of different calibration strategies for As in certified reference and candidate reference materials by ICP-MS. (* Denotes As values after correction for the polyatomic interference $^{40}Ar^{35}Cl$ due to high matrix-loading.)

Sample	**Solubilisation**	**Mineralisation**	**% Recovery of As (standard additions)**	**% Recovery of As (matrix matched standards)**	**% Recovery of As (acid matched standards)**
CRM 422	x		114.7*	107.1	-
CRM 422	x		115.6*	103.8*	-
CRM 422	x		-	108.5	104.3
CRM 422	x		-	100.5	-
CRM 422	x		105.2	96.7	-
CRM 422	x		-	105.2	-
CRM 422		x	100.5	100.0	97.2
CRM 422		x	-	-	96.7
CRM 422		x	-	-	99.5
T28	x		-	102.2	-
T28	x		-	105.1	-
T28	x		-	104.4	109.6
T28	x		-	106.6	-
T28	x		-	105.9	-
T28		x	100.0	-	91.9

Lasztity *et al.* determined the total arsenic in environmental, biological and food samples by ICP-MS [*94*]. Various sample preparation procedures were followed, e.g. 1) dry ashing with conventional and microwave heating and $Mg(NO_3)_2$ as ashing aid, 2) closed vessel microwave heated dissolution and 3) high temperature, pressure vapour phase acid digestion. In and Ge were used as internal standards. The following reference materials with certified As concentrations were analysed: oyster tissue (NIST SRM 1566), orchard leaves (NIST SRM 1571), pine needles (NIST SRM 1575), urban particulate matter (NIST SRM 1648), mussel

tissues (NIES no. 6) and soil (IAEA soil 7). Table 6.4 shows the recoveries of arsenic they obtained from the reference materials.

Table 6.4: Recoveries of As from reference materials by means of ICP-MS.

Sample	**Sample preparation procedure**	**% Recovery of arsenic**
Oyster tissue	Closed vessel microwave heated digestion	97.0
	High temperature, pressure vapour phase acid digestion	103.7
	Thermal furnace dry ashing	94.8
	Microwave heated ashing furnace	97.8
Orchard leaves	Closed vessel microwave heated digestion	109.0
	High temperature, pressure vapour phase acid digestion	108.0
	Thermal furnace dry ashing	102.0
	Microwave heated ashing furnace	97.9
Pine needles	Microwave heated ashing furnace	95.2
Mussel tissues	Microwave heated ashing furnace	98.2
Soil	Closed vessel microwave heated digestion	100.7
Urban particulate matter	Closed vessel microwave heated digestion	100.6
	Thermal furnace dry ashing	103.9

Nixon and Moyer [*81*] determined arsenic in urine and whole blood by ICP-MS. In order to minimise or eliminate the interference of $^{40}Ar^{35}Cl$ on arsenic they examined the classic $^{40}Ar^{37}Cl/^{82}Se/^{83}Kr$ correction and other empirical corrections, including $^{16}O^{35}Cl$. They analysed the following materials which have certified arsenic concentrations: NIST SRM 2670 (Toxic metals in freeze-dried urine, low and elevated concentrations), Lyphochek urine metals control (level 2), Lyphochek whole blood control (level 2), Urichem urine chemistry control (human level II), Sernorm whole blood III. (During preliminary investigations urine-based standards with Y as internal standard and the $^{40}Ar^{37}Cl/^{82}Se/^{83}Kr$ correction resulted in arsenic values that were 20% higher than the certified concentrations.) Isobaric correction for $^{40}Ar^{35}Cl$ was made

by measurement of the counts per second at mass 51 ($^{16}O^{35}Cl$). The intensity of $^{16}O^{35}Cl$ is approximately ten times the intensity of $^{40}Ar^{35}Cl$ and is linear with increasing chloride concentrations. The corrected As signal was obtained by subtraction of the $^{40}Ar^{35}Cl$ signal (as calculated from the $^{16}O^{35}Cl$ signal) from the total signal measured at mass 75. Results for urine analysis for As were about 13% high with the $^{16}O^{35}Cl$ correction and with Y as internal standard. Ga was then used as internal standard for the determination of As. Table 6.5 shows the arsenic results they obtained with Ga and Y as internal standards and table 6.6 shows the arsenic results after a period of seven days.

Table 6.5: % Recoveries for As in certified urines by means of ICP-MS using the $^{16}O^{35}Cl$ isobaric correction procedure.

Certified reference material	**% Recovery of As Internal standard: none**	**% Recovery of As Internal standard: Ga**	**% Recovery of As Internal standard: Y**
Urine metals control (level 2)	130.6	95.2	95.2
NIST SRM 2670	130.4	102.3	102.3

Table 6.6: Results for arsenic analyses over a seven day period. The material were analysed once a day by means of ICP-MS using the $^{16}O^{35}Cl$ isobaric correction procedure and Ga as internal standard.

Certified reference material	**% Recovery of arsenic**
Urine chemistry control (human level II)	121.3
Urine metals control (level 2)	95.2
NIST SRM 2670	102.3
Sernorm whole blood III	125.2

Madeddu and Rivoldini analysed plant tissue for arsenic by means of ICP-MS. They used a microwave digestion procedure with nitric acid and hydrofluoric acid. They used Rh and Re as internal standards. They analysed the following certified reference materials: GSV-1 and

GSV-2 (bush twigs and leaves), GSV-3 (poplar leaves) and GSV-4 (tea). Their results are shown in table 6.7.

Table 6.7: % Recoveries of arsenic from plant tissues by means of ICP-MS.

Certified reference material	**% Recovery of arsenic**
GSV-1	113.7
GSV-2	118.4
GSV-3	110.8
GSV-4	117.9

Wang, Jeng and Shieh [*110*] determined arsenic in airborne particulate matter by means of ICP-MS. They tested two closed-vessel digestion methods, i.e. high-pressure bomb digestion and microwave digestion with NIST SRM 1648 (urban particulate matter). Their results are shown in table 6.8.

Table 6.8: Comparison of As determinations in airborne particulate matter, NIST SRM 1648, by closed-vessel digestion methods under different conditions.

Digestion method	**Amount of acid mixture in ml**	**Digestion time**	**% Recovery of arsenic**
High-pressure bomb digestion:			
HNO_3	10	5 h	74.5
HNO_3-$HClO_4$	10 (1+1)	5 h	82.0
HNO_3-$HClO_4$/HF	10 (3+5/2)	7 h	96.4
HNO_3-$HClO_4$/$HClO_4$-HF	10 (3+3/2+2)	7 h	101.3
Microwave digestion:			
HNO_3-$HClO_4$-HF	5 (3+5+2)	18 min	140.2
HNO_3-$HClO_4$/$HClO_4$-HF	5 (3+3/2+2)	18 min	107.4

Sakao and Uchida [*111*] determined arsenic levels in shellfish tissue samples by ICP-MS. They analysed the following certified reference materials: NIST (USA) SRM 1566 (oyster tissue) and NIES no. 6 (mussel) with Co, Y and Bi as internal standards. They also used a sealed bomb

decomposition method (nitric acid) as a sample preparation procedure. They also employed a high resolution ICP-MS in order to overcome interferences from polyatomic ions. Table 6.9 shows their results.

Table 6.9: % Recoveries for As from oyster tissue and mussel by ICP-MS.

Technique	**% Recovery of arsenic from oyster tissue**	**% Recovery of arsenic from mussel**
Quadrupole ICP-MS	124.6	140.2
High resolution ICP-MS	103.1	103.3
Sealed decomposition method (with quadrupole ICP-MS)	-	97.2

6.4 Experimental

6.4.1 *Reconstitution of Seronorm Trace Elements Urine [108]*

The lyophilised material is sealed to ensure stability. In order to reconstitute the material, the screw cap was opened and the rubber stopper was carefully lifted without removing it completely and the air was let to enter the vial through the groove of the lower part of the stopper avoiding the loss of dry material. The rubber stopper was then removed. 5.00 ml high purity water was then added to the vial, the vial was carefully closed and let to stand for 30 minutes. The content of the vial was completely dissolved by gentle swirling, avoiding the formation of foam.

6.4.2 *ICP-MS procedure*

Preparation of sample and standard solutions for analysis by ICP-MS

The content of the vial was diluted 50x by transferring 1 ml of the solution to a 50 ml volumetric flask and making it up to the mark with distilled water. La was also added to the solution as internal standard before making it up to the mark. The chloride content of the solution to be analysed by ICP-MS was approximately 87 mg dm^{-3}.

The standards were prepared as set out in chapter 4 with La as internal standard. A solution that was blank with respect to arsenic and contained 200 mg dm^{-3} chloride (10 μl HCl transferred to

a 50 ml volumetric flask) was prepared in order to assess the correction factor to be applied to the intensities at *m/z* 75.

ICP-MS: Instrument optimisation and method used

The instrument was optimised as set out in chapter 2. After the instrument was calibrated with the prepared standards, the prepared samples were analysed. The 5.00 μg dm^{-3} arsenic calibration standard was used to monitor the drift of the instrument at *m/z* 75.The method used for analysis was as developed in chapter 4.

6.5 Results and discussion

Although the number of samples analysed by ICP-MS was small, the drift of the instrument at *m/z* 75 was monitored over a time period of 150 minutes on the day of the analyses. The 5.00 μg dm^{-3} standard were analysed at intervals of approximately 50 minutes. In the case of no internal standard being applied the measurements were 4.73 μg dm^{-3}, 4.47 μg dm^{-3}, 5.31 μg dm^{-3}, 5.48 μg dm^{-3} and the drift correction equation was calculated to be ($y = -2.278e\text{-}6x^3 + 5.596e\text{-}4x^2 - 2.756e\text{-}2x + 4.734$). In the case of La as internal standard the measurements were 4.63 μg dm^{-3}, 4.60 μg dm^{-3}, 5.88 μg dm^{-3}, 6.19 μg dm^{-3} and the drift correction equation was calculated to be ($y = -2.961e\text{-}6x^3 + 7.054e\text{-}4x^2 - 2.861e\text{-}2x + 4.630$).

The interference correction factor at *m/z* 75 was calculated as set out in chapter 4: The intensities at *m/z* 75 and *m/z* 77 were monitored for a solution consisting of water only as well as for a solution containing a small amount of chloride. The ratio of the intensities of the last solution is determined after the intensities of the water solution have been subtracted from those of the last solution. The correction factor was calculated to be 4.352. Although the interferent is usually depicted to be $^{40}Ar^{35}Cl$ it should be borne in mind that $^{38}Ar^{37}Cl$ may also be contributing to the intensity at *m/z* 75. It is therefore imperative that the interference correction factor be determined before the analyses of the samples to take into account instrument conditions and the formation of polyatomic interferences at *m/z* 75. The results of the analyses of the arsenic content of Seronorm Trace Elements Urine are shown in table 6.10.

Table 6.10: Results of the determination of the arsenic content of Seronorm Trace Elements Urine by means of ICP-MS.

Drift correction	**Internal standard**	**Interference correction**	**% Recovery of As**
Not applied	None	Not applied	110.1
Not applied	La	Not applied	120.1
Not applied	None	Applied	87.7
Not applied	La	Applied	88.2
Applied	None	Not applied	126.4
Applied	La	Not applied	137.6
Applied	None	Applied	100.3
Applied	La	Applied	101.0

From table 6.10 it may be seen that when only drift correction or interference correction was applied, unacceptable results were obtained. The recoveries that were obtained after both drift correction and interference correction were applied proved to be acceptable with and without the use of an internal standard.

6.6 Recommendations

A dilution factor of 50 was employed for the urine samples in this study. Although this reduced carbon loading as element-specific enhancement of the As signal might occur in the presence of a carbon matrix [*79*], it is recommended that smaller dilution factors are also used with the proposed method in order to test the validity of the method in matrices with a higher carbon content.

In this study the interference correction factor was determined with a solution that contained approximately the same amount of chloride (200 mg dm^{-3}) than the sample solutions (87 mg dm^{-3}). It is however recommended that the chloride content of unknown samples is determined beforehand (e.g. potentiometrically) and that the chloride content of the solution be matched exactly to those of the sample solutions.

Selenium is usually present together with arsenic in biological matrices [*79*]. The certified reference material analysed in this study did not have a certified Se content. A detailed study should be made of the effect of ^{77}Se on the interference correction procedure and the method should be modified to take into account the contribution of selenium to *m/z* 77.

6.7 Conclusion

It was shown to be possible to successfully determine the arsenic content of a biological sample that has a significant chloride concentration by means of ICP-MS. The method may be summarised as follows: 1) arsenic calibration solutions was prepared in 1% (v/v) HNO_3 and external calibration was used, 2) the interference correction factor was determined with a solution that contained a small amount of chloride and water, 3) La was used as internal standard, 4) drift correction procedures were employed and 5) the sample solutions were diluted 50x in order to reduce the carbon loading of the plasma.

REFERENCES

1. Jarvis K.E., Gray A.L., Houk R.S.; *Handbook of inductively coupled plasma mass spectrometry*; Blackie, pp.18-22, 1992.
2. Willard H.H., Merritt L.L., Dean J.A., Settle F.A.; *Instrumental methods of analysis*; 7th edition, Wadsworth, p.266, 1988.
3. Houk R.S.; *Mass spectrometry of inductively coupled plasmas*; Anal.Chem., **58**, pp.97A-105A, 1986.
4. Date A.R., Gray A.L., *Applications of inductively coupled plasma mass spectrometry*; Blackie Glasgow, pp.1-42, 1989.
5. Olivares J.A., Houk R.S.; *Suppression of analyte signal by various concomitant salts in inductively coupled plasma mass spectrometry*; Anal.Chem., **58**, pp.20-25, 1986.
6. Douglas D.J., French J.B.; *Gas dynamics of the inductively coupled plasma mass spectrometry interface*; J.Anal.Atom.Spectrom., **3**, pp.743-747, 1988.
7. Gray A.L.; *Mass spectrometry with an inductively coupled plasma as an ion source: the influence on ultratrace analysis of background and matrix response*; Spectrochim.Acta, **41B**, pp.151-167, 1986.
8. Douglas D.J., French J.B.; *An improved interface for inductively coupled plasma-mass spectrometry (ICP-MS)*; Spectrochim.Acta, **41B**, pp.197-204, 1986.
9. Gray A.L.; *Influence of load coil geometry on oxide and doubly charged ion response in inductively coupled plasma source mass spectrometry*; J.Anal.Atom.Spectrom., **1**, pp.247-249, 1986.
10. Houk R.S., Svec H.J., Fassel V.A.; *Mass spectrometric evidence for suprathermal ionization in an inductively coupled argon plasma*; Appl.Spectrosc., **35**, pp.380-384, 1981.
11. Douglas D.J.; *Fundamental aspects of ICP-MS*; In *ICPs in Analytical Atomic Spectrometry*; 2nd edition, editors Montaser A., Golightly D.W., VCH Publishers, New York, 1991.
12. Hutton R.C., Eaton A.N.; *Role of aerosol water vapour loading in inductively coupled plasma mass spectrometry*; J.Anal.Atom.Spectrom., **2**, pp.595-598, 1987.
13. Zhu G., Browner R.F.; *Study of the influence of water vapour loading and interface pressure in ICP-MS*; J.Anal.Atom.Spectrom., **3**, pp.781-789, 1988.
14. Olivares J.A., Houk R.S.; *Ion sampling for inductively coupled plasma mass spectrometry*; Anal.Chem., **57**, pp.2674-2679, 1985.

15. Lam J.W.H., Horlick G.; *Effects of sampler-skimmer separation in inductively coupled plasma-mass spectrometry*; Spectrochim.Acta, **45B**, pp.1327-1338, 1990.

16. Crain J.S., Smith F.G., Houk R.S.; *Mass spectrometric measurement of ionization temperature in an inductively coupled plasma*; Spectrochim.Acta, **45B**, pp.249-259, 1990.

17. Wilson D.A., Vickers G.H., Hieftje G.M.; *Ionization temperatures in the inductively coupled plasma determined by mass spectrometry*; Appl.Spectrosc., **41**, pp.875- 880, 1987.

18. Olivares J.A., Houk R.S.; *Ion sampling for inductively coupled plasma mass spectrometry*; Anal.Chem., **57**, pp.2674-2679, 1985.

19. Gillson G.R., Douglas D.J., Fulford J.E., Halligan K.W., Tanner S.D.; *Nonspectroscopic interelement interferences in inductively coupled plasma mass spectrometry*; Anal.Chem., **60**, pp.1472-1474, 1988.

20. Houk R.S., Fassel V.A., Flesch G.D., Svec H.J., Gray A.L., Taylor C.E.; *Inductively coupled argon plasma as an ion source for mass spectrometric determination of trace elements*; Anal.Chem., **52**, pp.2283-2289, 1980.

21. Gregoire D.C.; *Influence of instrument parameters on nonspectroscopic interferences in inductively coupled plasma-mass spectrometry*; Appl.Spectrosc., **41(5)**, pp.897-903, 1987.

22. Thompson J.J., Houk R.S.; *A study of internal standardisation in inductively coupled plasma-mass spectrometry*; Appl.Spectrosc., **41(5)**, pp.801-806, 1987.

23. Vickers G.H., Ross B.S., Hieftje G.M.; *Reduction of mass-dependent interferences in inductively coupled plasma-mass spectrometry by using flow-injection analysis*; Appl.Spectrosc., **43**, pp.1330-1333, 1989.

24. Tan S.H., Horlick G.; *Matrix-effect observations in inductively coupled plasma mass spectrometry*; J.Anal.Atom.Spectrom., **2**, pp.745-763, 1987.

25. Beauchemin D., McLaren J.W., Berman S.S.; *Study of the effects on concomitant elements in inductively coupled plasma mass spectrometry*; Spectrochim. Acta, **42B**, pp.467-490, 1987.

26. Crain J.S., Houk R.S., Smith F.G.; *Matrix interferences in inductively coupled plasma-mass spectrometry: some effects of skimmer orifice diameter and ion lens voltages*; Spectrochim. Acta, **43B**, pp.1355-1364, 1988.

27. Wang J., Shen W.-L., Sheppard B.S., Evans E.H., Caruso J.A., Fricke F.L.; *Effect of ion lens tuning and flow injection on non-spectroscopic matrix interferences in inductively coupled plasma mass spectrometry*; J.Anal.Atom.Spectrom., **5**, pp.445- 449, 1990.

28. Kawaguchi H., Tanaka T., Mizuike A.; *Continuum background in ICP-MS*; Spectrochim.Acta, **43B**, pp.955-962, 1988.

29. Horlick G., Tan S.H., Vaughan M.A., Rose C.A.; *The effect of plasma operating parameters on analyte signals in inductively coupled plasma-mass spectrometry*; Spectrochim.Acta, **40B**, pp.1555-1572, 1985.

30. Vaughan M.A., Horlick G., Tan S.H., *Effect of operating parameters on analyte signals in inductively coupled plasma mass spectrometry*; J.Anal.Atom.Spectrom., **2**, pp.765-772, 1987.

31. Zhu G., Browner R.F.; *Investigation of experimental parameters with a quadrupole ICP/MS*; Appl.Spectrosc., **41(3)**, pp.349-359, 1987.

32. Geerling R., Hattendorf B., Schmidt K.P., Krengel-Rothensee K., *Determination of trace element concentrations in water samples using the spectromass 2000*; Spectro Report, **98**, pp.1-8, 1998.

33. Long S.E., Brown R.M.; *Optimisation in inductively coupled plasma mass spectrometry*; Analyst, **111**, pp.901-906, 1986.

34. Gray A.L., Williams J.G.; *System optimisation and the effect on polyatomic, oxide and doubly charged ion response of a commercial inductively coupled plasma mass spectrometry instrument*; J.Anal.Atom.Spectrom., **2**, pp.599-606, 1987.

35. Date A.R., Gray A.L.; *Plasma source mass spectrometry using an inductively coupled plasma and a high resolution quadrupole mass filter*; Analyst (London), **106**, pp.1255-1267, 1981.

36. Date A.R., Gray A.L.; *Development progress in plasma source mass spectrometry*; Analyst (London), **108**, pp.159-165, 1983.

37. Gray A.L., Date A.R..; *Inductively coupled plasma source mass spectrometry using continuum flow ion extraction*; Analyst (London), **108**, pp.1033-1050, 1983.

38. Date A.R., Gray A.L.; *Progress in plasma source mass spectrometry*; Spectrochim.Acta, **38B**, pp.29-37, 1983.

39. Douglas D.J., Quan E.S.K., Smith R.G.; *Elemental analysis with an atmospheric pressure plasma (MIP, ICP) / quadrupole mass spectrometer system*; Spectrochim.Acta, **38B**, pp.39-48, 1983.

40. Doherty W.; *An internal standardization procedure for the determination of yttrium and the rare earth elements in geological materials by inductively coupled plasma- mass spectrometry*; Spectrochim.Acta, **44B**, pp.263-280, 1989.

41. Palmieri M.D., Fritz J.S., Thompson J.J., Houk R.S.; *Separation of trace rare earths and other metals from uranium by liquid-liquid extraction with quantitation by inductively-coupled plasma / mass spectrometry*; Anal.Chim.Acta, **184**, pp.187-196, 1986.

42. Doherty W., Van der Voet A.; *The application of inductively coupled plasma mass spectrometry to the determination of rare earth elements in geological materials*; Can.J.Spectrosc., **30(6)**, pp.135-141, 1985.

43. McLaren J., Beauchemin D., Van der Voet T.; *ICP-MS activities in Canada*; Can.J.Spectrosc., **30**, pp.29A-32A, 1985.

44. McLaren J.W., Mykytiuk A.P., Willie S.N., Berman S.S.; *Determination of trace metals in seawater by inductively coupled plasma mass spectrometry with preconcentration on silica-immobilized 8-hydroxyquinoline*; Anal.Chem., **57**, pp.2907-2911, 1985.

45. Vandecasteele C., Nagels M., Vanhoe H., Dams R.; *Suppression of analyte signal in inductively-coupled plasma / mass spectrometry and the use of an internal standard*; Anal.Chim.Acta, **211**, pp.91-98, 1988.

46. Gregoire D.C.; *The effect of easily ionizable concomitant elements on non- spectroscopic interferences in inductively coupled plasma-mass spectrometry*; Spectrochim.Acta, **42B**, pp.895-907, 1987.

47. Hall G.E.M., Park C.J., Pelchat J.C.; *Determination of tungsten and molybdenum at low levels in geological materials by inductively coupled plasma mass spectrometry*; J.Anal.Atom.Spectrom., **2**, pp.189-196, 1987.

48. McLaren J.W., Beauchemin D., Berman S.S.; *Analysis of the marine sediment reference material PACS-1 by inductively coupled plasma mass spectrometry*; Spectrochim.Acta, **43B**, pp.413-420, 1988.

49. Chen X., Houk R.S.; *Polyatomic ions as internal standards for matrix corrections in inductively coupled plasma mass spectrometry*; J.Anal.Atom.Spectrom., **10**, pp.837-841, 1995.

50. Jarvis K.E., Gray A.L., Houk R.S.; *Handbook of inductively coupled plasma mass spectrometry*; Blackie, pp.341-347, 1992.

51. Gowing C.J.B., Potts P.J.; *Evaluation of a rapid technique for the determination of precious metals in geological samples based on a selective aqua regia leach*; Analyst, **116**, pp.773-779, 1991.

52. Juvonen R., Kallio E., Lakomaa T.; *Determination of precious metals in rocks by inductively coupled plasma mass spectrometry using nickel sulfide concentration. Comparison with other pre-treatment methods*; Analyst, **119**, pp.617-621, 1994.

53. Rentoul E., Smith H.; *Toxic materials in medical jurisprudence and toxicology*; 13th edition, Churchill Livingstone, pp.537-546, 1973.

54. Calmus Y., Poupon R.; *Foie et arsenic*; Gastroenterologie Clinique et Biologique, **6**, pp.933-941, 1982.

55. Fuortes L.; *Arsenic poisoning. Ongoing diagnostic and social problem*; Postgraduate Medicine, **83(1)**, pp.234-244, 1988.

56. Levin-Scherz J.K., Patrick J.D., Weber F.H., Garabedian C.; *Acute arsenic ingestion*; Annals of Emergency Medicine, **16(6)**, pp.702-704, 1987.

57. Gerhardt R.E., Hudson J.B., Rao R.N., Sobel R.E.; *Chronic renal insufficiency from cortical necrosis induced by arsenic poisoning*; Archives of Internal Medicine, **138**, pp.1267-1269, 1978.

58. Welter A., Michaux H., Blondel A.; *Lignes de mees dans un cas d'intoxication aiguë par l'arsenic*; Dermatologica, **165(5)**, pp.482-483, 1982.

59. Quatrehomme G., Ricq O., Lapalus P., Jacomet Y., Ollier A.; *Acute arsenic intoxication: forensic and toxilogical aspects (an observation)*; J.For.Sciences, **37(4)**, pp.1163-1171, 1992.

60. Wojeck G.A., Nigg H.N., Braman R., Stamper J.M., Roussef R.; *Worker exposure to arsenic in Florida grapefruit spray operations*; Archives of Environmental Contamination and Toxicology, **11**, pp.661-667, 1982.

61. Fazekas I.G., Rengei B.; *Sur la teneur normale d'arsenic dans le cheveux, les poils axillaires, et les poils du pubis, selon sexes et ages*; Annales de Médicine Légale, **40**, pp.35-40, 1960.

62. Planques J., Brustier V., Bourbon P., Pitrt G., Broussy G.; *Contribution à l'étude de la répartition de l'arsenic dans l'organisme humain au cours d'une intoxication chronique collective*; Annales de Médicine Légale, **40**, pp.509-515, 1960.

63. Eckert W.G.; *Introduction to forensic sciences forensic toxicology*; The C.V. Mosby Company, p.99, 1980.

64. Smith H.; J.For.Medicine, **9(4)**, 1962.

65. Bagchi K.N.; Indian Med.Gazette, **72**, p.477, 1937.

66. Smales A.A., Pate E.D.; *The detection of sub-microgram quantities of arsenic by radioactivation. Part 3 The detection of arsenic in biological* material; Analyst, **77**, p.196, 1952.

67. Heydorn K.; *Environmental variation of arsenic levels in human blood determined by neutron activation analysis*; Clin.Chim.Acta, **28**, pp.349-357, 1970.

68. Espinoza E.O., Mann M-J., Bleasdell B., DeKorte S., Cox M.; *Toxic metals in selected traditional chinese medicinals*; J.For.Sciences, **41(3)**, pp.453-456, 1996.

69. Tay C.H., Seah C.S.; *Arsenic poisoning from anti-asthmatic herbal preparations*; Med.J.Australia, **2**, pp.424-428, 1975.

70. Wijesekera A.R.L., Henry K.D., Ranasinghe P.; *The detection and estimation of (a) arsenic in opium, and (b) strychnine in opium and heroin, as a means of identification of their respective sources*, For.Science Int., **36**, pp.193-209, 1988.

71. Sunshine I., *Methodology for analytical toxicology*; 2nd edition, C.C. Thomas, pp.30-33, 1978.

72. Curry A.S.; *Poison detection in human organs*; 2nd edition, C.C. Thomas, pp.159-163, 1969.

73. Kaye S.; *Handbook of emergency toxicology*; 3rd edition, C.C. Thomas, pp.48-57, 1973.

74. Sunshine I.; *CRC manual of analytical toxicology*; Chemical Rubber Company, pp.32-35, 1971.

75. Maes D., Pate B.D.; *The absorption of arsenic into single human head hairs*; J.For.Sciences, **22(1)**, pp.89-94, 1977.

76. Heitkemper D.T., Kaine L.A., Jackson D.S., Wolnik K.A.; *Practical applications of element-specific detection by inductively coupled plasma atomic emission spectroscopy and inductively coupled plasma mass spectrometry to ion chromatography of foods*; J.Chromatogr., **671A**, pp.101-108, 1994.

77. Tanaka T., Hara K., Tanimoto A., Kasai K., Kita T., Tanaka N., Takayasu T.; *Determinationof arsenic in blood and stomach contents by inductively coupled plasma / mass spectrometry(ICP/MS)*, For.Science Int., **81**, pp.43-50, 1996.

78. Kershisnik M.M., Kalamegham R., Ash K.O., Nixon D.E., Ashwood E.R., *Using $^{16}O^{35}Cl$ to correct for chloride interference improves accuracy of urine arsenic determinations by inductively coupled plasma mass spectrometry*; Clin.Chem., **38(11)**, pp.2197-2202, 1992.

79. Campbell M.J., Demesmay C., Ollé M., *Determination of total arsenic concentrations in biological matrices by inductively coupled plasma mass spectrometry*; J.Anal.Atom.Spectrom., **9**, pp.1379-1384, 1994.

80. Branch S., Ebdon L., Ford M., Foulkes M., O'Neill P., *Determination of arsenic in samples with high chloride content by inductively coupled plasma mass spectrometry*; J.Anal.Atom.Spectrom., **6**, pp.151-154, 1991.

81. Nixon D.E., Moyer T.P.; *Routine clinical determination of lead, arsenic, cadmium, and thallium in urine and whole blood by inductively coupled plasma mass spectrometry*; Spectrochim.Acta, **51B**, pp.13-25, 1996.

82. Goergen M.G., Murshak V.F., Roettger P., Murshak I., Edelman D.; *ICP-MS analysis of toxic characteristics leaching procedure (TCLP) extract: advantages and disadvantages*; At.Spectrosc., **13(1)**, pp.11-18, 1992.

83. Jarvis K.E., Gray A.L., Houk R.S.; *Handbook of inductively coupled plasma mass spectrometry*; Blackie, pp.129-134, 1992.

84. Sakata K., Kawabata K.; *Reduction of fundamental polyatomic ions in inductively coupled plasma mass spectrometry*; Spectrochim.Acta, **49B**, pp.1027-1038, 1994.

85. Vaughan M.A., Horlick G.; *Oxide, hydroxide, and doubly charged analyte species in inductively coupled plasma / mass spectrometry*; Appl.Spectrosc., **40(4)**, pp.434- 445, 1986.

86. Tan S.H., Horlick G.; *Background spectral features in inductively coupled plasma / mass spectrometry*; Appl.Spectrosc., **40(4)**, pp.445-460, 1986.

87. Prohaska T., Latkoczy C., Stingeder G., Wenzel W.W., Blum W.E.; *HR-ICPMS determination of arsenic in environmental samples - spectral interferences and matrix effects*; Presented at ISEAC26, April 1996.

88. Branch S., Ebdon L., O'Neill P., *Determination of arsenic species in fish by directly coupled high-performance liquid chromatography-inductively coupled plasma mass spectrometry*; J.Anal.Atom.Spectrom., **9**, pp.33-37, 1994.

89. Anderson S.T.G., Robért R.V.D., Farrer H.N.; *Determination of total and leachable arsenic and selenium in soils by continuous hydride generation inductively coupled plasma mass spectrometry*; J.Anal.Atom.Spectrom., **9**, pp.1107-1110, 1994.

90. Ebdon L., Fisher A.S., Worsfold P.J., *Determination of arsenic, chromium, selenium and vanadium in biological samples by inductively coupled plasma mass spectrometry using on-line elimination of interference and preconcentration by flow injection*; J.Anal.Atom.Spectrom., **9**, pp.611-614, 1994.

91. Date A.R., Cheung Y.Y., Stuart M.E.; *The influence of polyatomic ion interferences in analysis by inductively coupled plasma mass spectrometry (ICP-MS)*; Spectrochim.Acta, **42B**, pp.3-20, 1987.

92. Amarasiriwardena D., Krushevska A., Barnes R.M.; *Microwave-assisted vapor- phase nitric acid digestion of small biological samples for inductively coupled plasma spectrometry*; Appl.Spectrosc., **52(6)**, pp.900-907, 1998.

93. Sheppard B.S., Heitkemper D.T., Gaston C.M.; *Microwave digestion for the determination of arsenic, cadmium and lead in seafood products by inductively coupled plasma atomic emission and mass spectrometry*; Analyst, **119**, pp.1683- 1686, 1994.

94. Lásztity A., Krushevska A., Kotrebai M., Barnes R.M., Amarasiriwardena D.; *Arsenic determination in environmental, biological and food samples by inductively coupled plasma mass spectrometry*; J.Anal.Atom.Spectrom., **10**, pp.505-510, 1995.

95. Steele T.W.; *Certificate of analysis - Platinum Ore - SARM 7 - Certified reference material*; pp.1-4, 1975.

96. Lenahan W.C., Murray-Smith R de L.; *Assay and analytical practice in the South African mining industry*; The Chamber of Mines of South Africa, The South African Institute of Mining and Metallurgy, Monograph series M6, 1986.

97. Hall G.E.M., Pelchat J.C.; *Analysis of geological materials for gold, platinum and palladium at low ppb levels by fire assay-ICP mass spectrometry*; Chem.Geol., **115**, pp.61-72, 1994.

98. Jackson S.E., Fryer B.J., Gosse W., Healey D.C., Longerich H.P., Strong D.F.; *Determination of the precious metals in geological materials by inductively coupled plasma-mass spectrometry (ICP-MS) with nickel sulphide fire-assay collection and tellurium coprecipitation*; Chem.Geol., **83**, pp.119-132, 1990.

99. Sun M., Jain J., Zhou M., Kerrich R.; *A procedural modification for enhanced recovery of precious metals (Au, PGE) following nickel sulphide fire assay and tellurium co-precipitation: applications for analysis of geological samples by inductively coupled plasma mass spectrometry*; Can.J.Appl.Spectrosc., **38(4)**, pp.103-108, 1993.

100. Perry B.J., Van Loon J.C., Speller D.V.; *Dry-chlorination inductively coupled plasma mass spectrometric method for the determination of platinum group elements in rocks*; J.Anal.Atom.Spectrom., **7**, pp.883-888, 1992.

101. Chen Z., Fryer B.J., Longerich H.P., Jackson S.E.; *Determination of the precious metals in milligram samples of sulfides and oxides using inductively coupled plasma mass spectrometry after ion exchange preconcentration*; J.Anal.Atom.Spectrom., **11**, pp.805-809, 1996.

102. Enzweiler J., Potts P.J., Jarvis K.E.; *Determination of platinum, palladium, ruthenium and iridium in geological samples by isotope dilution inductively coupled plasma mass spectrometry using a sodium peroxide fusion and tellurium coprecipitation*; Analyst, **120**, pp.1391-1396, 1995.

103. Godfrey J., McCurdy E.; *Investigation into the feasibility of ICP-MS as an alternative to fire assay measurements for gold and the platinum group elements*; Applications of plasma source mass spectrometry II; Holland G., Eaton A.N. (editors); pp.65-71, 1993.

104. Enzweiler J., Potts P.J.; *The separation of platinum, palladium and gold from silicate rocks by the anion exchange separation of chloro complexes after a sodium peroxide fusion: an investigation of low recoveries*; Talanta, **42**, pp.1411-1418, 1995.

105. Yi Y.V., Masuda A.; *Isotopic homogenization of iridium for high sensitivity determination by isotope dilution inductively coupled plasma spectrometry*; Anal.Sciences, **12**, pp.7-12, 1996.

106. Perry B.J., Barefoot R.R., Van Loon J.C.; *Inductively coupled plasma mass spectrometry for the determination of platinum group elements and gold*; Trends in Anal.Chem., **14(8)**, pp.388-397, 1995.

107. Qu Y.B.; *Recent developments in the determination of precious metals*; Analyst, **121**, pp.139-161, 1996.

108. Seronorm Trace Elements Urine; Lot 403125, 403125x, 403125y; Analytical values; Mat.no: 800106; Certificate of analysis.

109. Larsen E.H., Stürup S.; *Carbon-enhanced inductively coupled plasma mass spectrometric detection of arsenic and selenium and its application to arsenic speciation*; J.Anal.Atom.Spectrom., **9**, pp.1099-1105, 1994.

110. Wang C., Jeng S., Shieh F.; *Determination of arsenic in airborne particulate matter by inductively coupled plasma mass spectrometry*; J.Anal.Atom.Spectrom., **12**, pp.61-67, 1997.

111. Sakao S., Uchida H.; *Determination of trace elements in shellfish tissue samples by inductively coupled plasma mass spectrometry*; Anal.Chim.Acta, **382**, pp.215-223, 1999.

ADDENDUM A

AVERAGES OF THE INTENSITIES MEASURED OF THE ISOTOPES OF THE INTERNAL STANDARDS, THE PLATINUM GROUP ELEMENTS AND GOLD

Table 3.5: Averages of the measured intensities (counts s^{-1}) of the different isotopes of Ar, Sc, Y, La, Au and Ir.

Sample	^{36}Ar	^{45}Sc	^{89}Y	^{138}La	^{139}La	^{197}Au	^{191}Ir	^{193}Ir
Blank in 1% v/v HCl	$2.06x10^{7}$	$9.83x10^{5}$	$6.98x10^{5}$	$4.58x10^{2}$	$3.53x10^{5}$	$1.16x10^{2}$	$7.12x10^{1}$	$7.44x10^{1}$
10 $\mu g\ dm^{-3}$ of element in 1% v/v HCl	$2.01x10^{7}$	$9.03x10^{5}$	$6.45x10^{5}$	$4.50x10^{2}$	$3.36x10^{5}$	$7.93x10^{2}$	$6.76x10^{2}$	$1.15x10^{3}$
50 $\mu g\ dm^{-3}$ of element in 1% v/v HCl	$2.00x10^{7}$	$8.81x10^{5}$	$6.21x10^{5}$	$4.60x10^{2}$	$3.22x10^{5}$	$3.52x10^{3}$	$3.11x10^{3}$	$5.03x10^{3}$
100 $\mu g\ dm^{-3}$ of element in 1% v/v HCl	$2.05x10^{7}$	$9.18x10^{5}$	$6.33x10^{5}$	$4.70x10^{2}$	$3.28x10^{5}$	$7.12x10^{3}$	$6.28x10^{3}$	$1.03x10^{4}$
150 $\mu g\ dm^{-3}$ of element in 1% v/v HCl	$1.97x10^{7}$	$9.22x10^{5}$	$6.63x10^{5}$	$4.24x10^{2}$	$3.39x10^{5}$	$1.10x10^{4}$	$9.76x10^{3}$	$1.60x10^{4}$
50 $\mu g\ dm^{-3}$ of element in 1% v/v HCl	$2.05x10^{7}$	$9.33x10^{5}$	$6.65x10^{5}$	$5.10x10^{2}$	$3.36x10^{5}$	$3.73x10^{3}$	$3.28x10^{3}$	$5.45x10^{3}$
50 $\mu g\ dm^{-3}$ of element in 0.35% v/v aqua regia	$1.63x10^{7}$	$8.31x10^{5}$	$6.08x10^{5}$	$4.29x10^{2}$	$3.26x10^{5}$	$3.49x10^{3}$	$3.16x10^{3}$	$5.11x10^{3}$
50 $\mu g\ dm^{-3}$ of element in 0.50% v/v aqua regia	$1.70x10^{7}$	$8.48x10^{5}$	$6.09x10^{5}$	$4.14x10^{2}$	$3.29x10^{5}$	$3.64x10^{3}$	$3.25x10^{3}$	$5.27x10^{3}$
50 $\mu g\ dm^{-3}$ of element in 1.00% v/v aqua regia	$1.86x10^{7}$	$8.73x10^{5}$	$6.42x10^{5}$	$4.49x10^{2}$	$3.33x10^{5}$	$3.58x10^{3}$	$3.17x10^{3}$	$5.25x10^{3}$
50 $\mu g\ dm^{-3}$ of element in 1% v/v HCl	$2.02x10^{7}$	$9.19x10^{5}$	$6.61x10^{5}$	$4.44x10^{2}$	$3.36x10^{5}$	$3.75x10^{3}$	$3.32x10^{3}$	$5.42x10^{3}$
50 $\mu g\ dm^{-3}$ of element in 1.50% v/v aqua regia	$2.07x10^{7}$	$9.33x10^{5}$	$6.57x10^{5}$	$4.51x10^{2}$	$3.33x10^{5}$	$3.67x10^{3}$	$3.19x10^{3}$	$5.32x10^{3}$
50 $\mu g\ dm^{-3}$ of element in 2.00% v/v aqua regia	$2.23x10^{7}$	$9.81x10^{5}$	$6.90x10^{5}$	$4.64x10^{2}$	$3.48x10^{5}$	$3.83x10^{3}$	$3.33x10^{3}$	$5.30x10^{3}$
50 $\mu g\ dm^{-3}$ of element in 2.50% v/v aqua regia	$2.27x10^{7}$	$9.75x10^{5}$	$6.76x10^{5}$	$4.80x10^{2}$	$3.44x10^{5}$	$3.71x10^{3}$	$3.20x10^{3}$	$5.45x10^{3}$
50 $\mu g\ dm^{-3}$ of element in 1% v/v HCl	$2.01x10^{7}$	$9.27x10^{5}$	$6.61x10^{5}$	$4.77x10^{2}$	$3.35x10^{5}$	$3.68x10^{3}$	$3.17x10^{3}$	$5.32x10^{3}$
Standard deviation of blank in 1% v/v HCl	$1.05x10^{6}$	$6.85x10^{4}$	$5.90x10^{4}$	$2.17x10^{1}$	$2.87x10^{4}$	$1.22x10^{1}$	$6.33x10^{0}$	$6.43x10^{0}$

Table 3.6: Averages of the measured intensities (counts s^{-1}) of the different isotopes of Pd and Pt.

Sample	^{102}Pd	^{104}Pd	^{105}Pd	^{106}Pd	^{108}Pd	^{110}Pd	^{192}Pt	^{194}Pt	^{195}Pt	^{196}Pt	^{198}Pt
Blank in 1% v/v HCl	$8.43x10^{1}$	$1.07x10^{2}$	$3.81x10^{3}$	$6.76x10^{2}$	$1.14x10^{2}$	$1.01x10^{2}$	$7.50x10^{1}$	$5.55x10^{1}$	$6.61x10^{1}$	$6.44x10^{1}$	$6.87x10^{1}$
10 μg dm^{-3} of element in 1% v/v HCl	$1.82x10^{3}$	$1.49x10^{3}$	$4.37x10^{3}$	$1.67x10^{3}$	$1.10x10^{3}$	$5.65x10^{2}$	$9.67x10^{1}$	$4.34x10^{2}$	$4.29x10^{2}$	$3.62x10^{2}$	$1.47x10^{2}$
50 μg dm^{-3} of element in 1% v/v HCl	$8.63x10^{3}$	$7.28x10^{3}$	$7.83x10^{3}$	$6.13x10^{3}$	$5.46x10^{3}$	$2.46x10^{3}$	$1.02x10^{2}$	$1.74x10^{3}$	$1.82x10^{3}$	$1.40x10^{3}$	$4.82x10^{2}$
100 μg dm^{-3} of element in 1% v/v HCl	$1.78x10^{4}$	$1.49x10^{4}$	$1.24x10^{4}$	$1.20x10^{4}$	$1.09x10^{4}$	$5.08x10^{3}$	$1.88x10^{2}$	$3.58x10^{3}$	$3.62x10^{3}$	$2.68x10^{3}$	$8.19x10^{2}$
150 μg dm^{-3} of element in 1% v/v HCl	$2.74x10^{4}$	$2.31x10^{4}$	$1.79x10^{4}$	$1.81x10^{4}$	$1.72x10^{4}$	$7.76x10^{3}$	$2.53x10^{2}$	$5.59x10^{3}$	$5.73x10^{3}$	$4.23x10^{3}$	$1.29x10^{3}$
50 μg dm^{-3} of element in 1% v/v HCl	$9.20x10^{3}$	$7.83x10^{3}$	$8.39x10^{3}$	$6.45x10^{3}$	$5.80x10^{3}$	$2.56x10^{3}$	$9.10x10^{1}$	$1.88x10^{3}$	$1.88x10^{3}$	$1.45x10^{3}$	$4.73x10^{2}$
50 μg dm^{-3} of element in 0.35% v/v aqua regia	$8.44x10^{3}$	$7.14x10^{3}$	$7.60x10^{3}$	$5.73x10^{3}$	$5.21x10^{3}$	$2.36x10^{3}$	$1.09x10^{2}$	$1.84x10^{3}$	$1.83x10^{3}$	$1.35x10^{3}$	$4.45x10^{2}$
50 μg dm^{-3} of element in 0.50% v/v aqua regia	$8.71x10^{3}$	$7.17x10^{3}$	$7.64x10^{3}$	$6.00x10^{3}$	$5.19x10^{3}$	$2.39x10^{3}$	$1.33x10^{2}$	$1.79x10^{3}$	$1.92x10^{3}$	$1.41x10^{3}$	$4.80x10^{2}$
50 μg dm^{-3} of element in 1.00% v/v aqua regia	$8.77x10^{3}$	$7.54x10^{3}$	$8.15x10^{3}$	$6.16x10^{3}$	$5.53x10^{3}$	$2.54x10^{3}$	$1.09x10^{2}$	$1.88x10^{3}$	$1.88x10^{3}$	$1.47x10^{3}$	$4.91x10^{2}$
50 μg dm^{-3} of element in 1% v/v HCl	$9.23x10^{3}$	$7.71x10^{3}$	$8.09x10^{3}$	$6.21x10^{3}$	$5.69x10^{3}$	$2.61x10^{3}$	$1.07x10^{2}$	$1.82x10^{3}$	$1.89x10^{3}$	$1.48x10^{3}$	$4.94x10^{2}$
50 μg dm^{-3} of element in 1.50% v/v aqua regia	$9.09x10^{3}$	$7.60x10^{3}$	$8.34x10^{3}$	$6.37x10^{3}$	$5.76x10^{3}$	$2.55x10^{3}$	$1.24x10^{2}$	$1.88x10^{3}$	$1.94x10^{3}$	$1.38x10^{3}$	$4.69x10^{2}$
50 μg dm^{-3} of element in 2.00% v/v aqua regia	$9.64x10^{3}$	$7.99x10^{3}$	$8.75x10^{3}$	$6.62x10^{3}$	$5.74x10^{3}$	$2.69x10^{3}$	$1.16x10^{2}$	$1.88x10^{3}$	$1.93x10^{3}$	$1.47x10^{3}$	$4.92x10^{2}$
50 μg dm^{-3} of element in 2.50% v/v aqua regia	$9.14x10^{3}$	$7.80x10^{3}$	$8.55x10^{3}$	$6.48x10^{3}$	$5.74x10^{3}$	$2.63x10^{3}$	$1.26x10^{2}$	$1.85x10^{3}$	$1.83x10^{3}$	$1.44x10^{3}$	$4.86x10^{2}$
50 μg dm^{-3} of element in 1% v/v HCl	$9.17x10^{3}$	$7.71x10^{3}$	$8.25x10^{3}$	$6.17x10^{3}$	$5.67x10^{3}$	$2.64x10^{3}$	$1.34x10^{2}$	$1.85x10^{3}$	$1.96x10^{3}$	$1.40x10^{3}$	$4.88x10^{2}$
Standard deviation of blank in 1% v/v HCl	$1.11x10^{1}$	$1.29x10^{1}$	$4.21x10^{2}$	$6.58x10^{1}$	$1.29x10^{1}$	$2.00x10^{1}$	$1.01x10^{1}$	$2.06x10^{1}$	$1.54x10^{1}$	$1.54x10^{1}$	$1.33x10^{1}$

Table 3.7: Averages of the measured intensities (counts s^{-1}) of the different isotopes of Rh and Ru.

Sample	**^{103}Rh**	**^{96}Ru**	**^{98}Ru**	**^{99}Ru**	**^{100}Ru**	**^{101}Ru**	**^{102}Ru**	**^{104}Ru**
Blank in 1% v/v HCl	1.24×10^{2}	1.06×10^{2}	1.60×10^{2}	8.42×10^{1}	1.49×10^{2}	8.99×10^{1}	9.21×10^{1}	1.05×10^{2}
10 μg dm^{-3} of element in 1% v/v HCl	4.68×10^{3}	4.29×10^{2}	2.88×10^{2}	7.95×10^{2}	8.15×10^{2}	1.04×10^{3}	1.81×10^{3}	1.53×10^{3}
50 μg dm^{-3} of element in 1% v/v HCl	2.25×10^{4}	1.49×10^{3}	6.26×10^{2}	3.36×10^{3}	3.41×10^{3}	4.69×10^{3}	8.51×10^{3}	7.24×10^{3}
100 μg dm^{-3} of element in 1% v/v HCl	4.65×10^{4}	3.09×10^{3}	1.21×10^{3}	6.83×10^{3}	6.96×10^{3}	9.26×10^{3}	1.75×10^{4}	1.50×10^{4}
150 μg dm^{-3} of element in 1% v/v HCl	7.28×10^{4}	4.53×10^{3}	1.67×10^{3}	1.05×10^{4}	1.04×10^{4}	1.42×10^{4}	2.69×10^{4}	2.26×10^{4}
50 μg dm^{-3} of element in 1% v/v HCl	2.41×10^{4}	1.55×10^{3}	6.80×10^{2}	3.72×10^{3}	3.74×10^{3}	4.90×10^{3}	9.34×10^{3}	7.72×10^{3}
50 μg dm^{-3} of element in 0.35% v/v aqua regia	2.23×10^{4}	1.55×10^{3}	6.24×10^{2}	3.38×10^{3}	3.35×10^{3}	4.48×10^{3}	8.25×10^{3}	7.18×10^{3}
50 μg dm^{-3} of element in 0.50% v/v aqua regia	2.26×10^{4}	1.52×10^{3}	6.31×10^{2}	3.38×10^{3}	3.43×10^{3}	4.54×10^{3}	8.42×10^{3}	7.09×10^{3}
50 μg dm^{-3} of element in 1.00% v/v aqua regia	2.33×10^{4}	1.53×10^{3}	7.12×10^{2}	3.49×10^{3}	3.43×10^{3}	4.72×10^{3}	9.02×10^{3}	7.51×10^{3}
50 μg dm^{-3} of element in 1% v/v HCl	2.41×10^{4}	1.69×10^{3}	7.18×10^{2}	3.58×10^{3}	3.55×10^{3}	4.79×10^{3}	9.12×10^{3}	7.60×10^{3}
50 μg dm^{-3} of element in 1.50% v/v aqua regia	2.37×10^{4}	1.62×10^{3}	7.04×10^{2}	3.57×10^{3}	3.59×10^{3}	4.75×10^{3}	9.03×10^{3}	7.55×10^{3}
50 μg dm^{-3} of element in 2.00% v/v aqua regia	2.47×10^{4}	1.64×10^{3}	7.54×10^{2}	3.75×10^{3}	3.64×10^{3}	5.20×10^{3}	9.50×10^{3}	8.03×10^{3}
50 μg dm^{-3} of element in 2.50% v/v aqua regia	2.43×10^{4}	1.65×10^{3}	7.38×10^{2}	3.58×10^{3}	3.82×10^{3}	4.97×10^{3}	9.46×10^{3}	7.75×10^{3}
50 μg dm^{-3} of element in 1% v/v HCl	2.39×10^{4}	1.53×10^{3}	6.77×10^{2}	3.65×10^{3}	3.64×10^{3}	4.70×10^{3}	9.18×10^{3}	7.66×10^{3}
Standard deviation of blank in 1% v/v HCl	3.67×10^{1}	6.44×10^{0}	2.41×10^{1}	2.00×10^{1}	3.08×10^{1}	3.42×10^{1}	1.40×10^{1}	2.89×10^{1}

ADDENDUM B

CALIBRATION DATA FOR THE ISOTOPES OF THE PLATINUM GROUP ELEMENTS AND GOLD

Table 3.8: Calibration data for Au and Ir isotopes when no internal standard was used.

	^{197}Au			^{191}Ir			^{193}Ir		
[Element] ($\mu g\ dm^{-3}$)	Intensity ratio	Calculated concentration ($\mu g\ dm^{-3}$)	% difference (certified value - calculated value)	Intensity ratio	Calculated concentration ($\mu g\ dm^{-3}$)	% difference (certified value - calculated value)	Intensity ratio	Calculated concentration ($\mu g\ dm^{-3}$)	% difference (certified value - calculated value)
0	$1.16x10^{2}$	1.32	-	$7.12x10^{1}$	1.18	-	$7.44x10^{1}$	1.03	-
10	$7.93x10^{2}$	10.65	6.52	$6.76x10^{2}$	10.59	5.92	$1.15x10^{3}$	11.21	12.09
50	$3.52x10^{3}$	48.21	-3.59	$3.11x10^{3}$	48.50	-3.01	$5.03x10^{3}$	47.96	-4.08
100	$7.12x10^{3}$	97.80	-2.20	$6.28x10^{3}$	97.81	-2.19	$1.03x10^{4}$	97.60	-2.40
150	$1.10x10^{4}$	152.02	1.35	$9.76x10^{3}$	151.92	1.28	$1.60x10^{4}$	152.20	1.47
Correlation coefficient	0.9996			0.9996			0.9995		
Slope (counts s^{-1} ($\mu g\ dm^{-3}$)$^{-1}$)	$7.25x10^{1}$			$6.43x10^{1}$			$1.06x10^{2}$		
Intercept (counts s^{-1})	$2.06x10^{1}$			$-4.67x10^{0}$			$-3.45x10^{1}$		
Detection limit ($\mu g\ dm^{-3}$)	0.5028			0.2955			0.1827		
Standard error	2.1813			2.0399			2.3983		

Table 3.9: Calibration data for ^{102}Pd, ^{104}Pd and ^{105}Pd when no internal standard was used.

	^{102}Pd			^{104}Pd			^{105}Pd		
[Element] ($\mu g\ dm^{-3}$)	**Intensity ratio**	**Calculated concentration ($\mu g\ dm^{-3}$)**	**% difference (certified value - calculated value)**	**Intensity ratio**	**Calculated concentration ($\mu g\ dm^{-3}$)**	**% difference (certified value - calculated value)**	**Intensity ratio**	**Calculated concentration ($\mu g\ dm^{-3}$)**	**% difference (certified value - calculated value)**
0	$8.43x10^{1}$	1.06	-	$1.07x10^{2}$	1.38	-	$3.81x10^{3}$	3.84	-
10	$1.82x10^{3}$	10.62	6.16	$1.49x10^{3}$	10.43	4.32	$4.37x10^{3}$	9.78	-2.21
50	$8.63x10^{3}$	48.18	-3.64	$7.28x10^{3}$	48.33	-3.35	$7.83x10^{3}$	46.76	-6.48
100	$1.78x10^{4}$	98.74	-1.26	$1.49x10^{4}$	98.00	-2.00	$1.24x10^{4}$	95.56	-4.44
150	$2.74x10^{4}$	151.41	0.94	$2.31x10^{4}$	151.86	1.24	$1.79x10^{4}$	154.05	2.70
Correlation coefficient	0.9997			0.9996			0.9981		
Slope (counts s^{-1} ($\mu g\ dm^{-3}$)$^{-1}$)	$1.81x10^{2}$			$1.53x10^{2}$			$9.37x10^{1}$		
Intercept (counts s^{-1})	$-1.08x10^{2}$			$-1.03x10^{2}$			$3.45x10^{3}$		
Detection limit ($\mu g\ dm^{-3}$)	0.1836			0.2524			13.4835		
Standard error	1.6710			2.0298			4.5156		

Table 3.10: Calibration data for ^{106}Pd, ^{108}Pd and ^{110}Pd when no internal standard was used.

	^{106}Pd			^{108}Pd			^{110}Pd		
[Element] ($\mu g\ dm^{-3}$)	Intensity ratio	Calculated concentration ($\mu g\ dm^{-3}$)	% difference (certified value - calculated value)	Intensity ratio	Calculated concentration ($\mu g\ dm^{-3}$)	% difference (certified value - calculated value)	Intensity ratio	Calculated concentration ($\mu g\ dm^{-3}$)	% difference (certified value - calculated value)
0	$6.76x10^2$	1.50	-	$1.14x10^2$	1.60	-	$1.01x10^2$	1.44	-
10	$1.67x10^3$	10.02	0.15	$1.10x10^3$	10.32	3.18	$5.65x10^2$	10.53	5.33
50	$6.13x10^3$	48.33	-3.35	$5.46x10^3$	48.67	-2.65	$2.46x10^3$	47.58	-4.84
100	$1.20x10^4$	98.79	-1.21	$1.09x10^4$	96.96	-3.04	$5.08x10^3$	99.02	-0.98
150	$1.81x10^4$	151.36	0.91	$1.72x10^4$	152.45	1.63	$7.76x10^3$	151.42	0.95
Correlation coefficient	0.9997			0.9994			0.9996		
Slope (counts s^{-1} ($\mu g\ dm^{-3}$)$^{-1}$)	$1.17x10^2$			$1.14x10^2$			$5.11x10^1$		
Intercept (counts s^{-1})	$5.01x10^2$			$-6.78x10^1$			$2.73x10^1$		
Detection limit ($\mu g\ dm^{-3}$)	1.6930			0.3418			1.1743		
Standard error	1.6697			2.5588			1.9301		

Table 3.11: Calibration data for ^{192}Pt, ^{194}Pt and ^{195}Pt when no internal standard was used.

	^{192}Pt			^{194}Pt			^{195}Pt		
[Element] ($\mu g\ dm^{-3}$)	Intensity ratio	Calculated concentration ($\mu g\ dm^{-3}$)	% difference (certified value - calculated value)	Intensity ratio	Calculated concentration ($\mu g\ dm^{-3}$)	% difference (certified value - calculated value)	Intensity ratio	Calculated concentration ($\mu g\ dm^{-3}$)	% difference (certified value - calculated value)
0	$7.50x10^{1}$	3.67	-	$5.55x10^{1}$	1.21	-	$6.61x10^{1}$	1.38	-
10	$9.67x10^{1}$	22.27	122.68	$4.34x10^{2}$	11.57	15.65	$4.29x10^{2}$	11.08	10.80
50	$1.02x10^{2}$	26.93	-46.14	$1.74x10^{3}$	47.20	-5.60	$1.82x10^{3}$	48.26	-3.47
100	$1.88x10^{2}$	100.77	0.77	$3.58x10^{3}$	97.58	-2.42	$3.62x10^{3}$	96.31	-3.69
150	$2.53x10^{2}$	156.36	4.24	$5.59x10^{3}$	152.44	1.63	$5.73x10^{3}$	152.96	1.98
Correlation coefficient	0.9776			0.9993			0.9991		
Slope ($counts\ s^{-1}\ (\mu g\ dm^{-3})^{-1}$)	$1.17x10^{0}$			$3.66x10^{1}$			$3.74x10^{1}$		
Intercept ($counts\ s^{-1}$)	$7.07x10^{1}$			$1.12x10^{1}$			$1.46x10^{1}$		
Detection limit ($\mu g\ dm^{-3}$)	26.0360			1.6907			1.2346		
Standard error	15.3245			2.7999			3.0762		

Table 3.12: Calibration data for ^{196}Pt, ^{198}Pt and ^{103}Rh when no internal standard was used.

	^{196}Pt			^{198}Pt			^{103}Rh		
[Element] ($\mu g\ dm^{-3}$)	Intensity ratio	Calculated concentration ($\mu g\ dm^{-3}$)	% difference (certified value - calculated value)	Intensity ratio	Calculated concentration ($\mu g\ dm^{-3}$)	% difference (certified value - calculated value)	Intensity ratio	Calculated concentration ($\mu g\ dm^{-3}$)	% difference (certified value - calculated value)
0	$6.44x10^{1}$	0.47	-	$6.87x10^{1}$	0.32	-	$1.24x10^{2}$	1.40	-
10	$3.62x10^{2}$	11.36	13.61	$1.47x10^{2}$	10.15	1.51	$4.68x10^{3}$	10.85	8.53
50	$1.40x10^{3}$	49.34	-1.32	$4.82x10^{2}$	52.14	4.28	$2.25x10^{4}$	47.87	-4.26
100	$2.68x10^{3}$	96.08	-3.92	$8.19x10^{2}$	94.33	-5.67	$4.65x10^{4}$	97.67	-2.33
150	$4.23x10^{3}$	152.74	1.83	$1.29x10^{3}$	153.06	2.04	$7.28x10^{4}$	152.20	1.47
Correlation coefficient	0.9992			0.9985			0.9994		
Slope ($counts\ s^{-1}\ (\mu g\ dm^{-3})^{-1}$)	$2.73x10^{1}$			$7.98x10^{0}$			$4.82x10^{2}$		
Intercept ($counts\ s^{-1}$)	$5.14x10^{1}$			$6.61x10^{1}$			$-5.51x10^{2}$		
Detection limit ($\mu g\ dm^{-3}$)	1.6948			4.9849			0.2284		
Standard error	2.9059			3.9211			2.4137		

Table 3.13: Calibration data for ^{96}Ru, ^{98}Ru and ^{99}Ru when no internal standard was used.

	^{96}Ru			^{98}Ru			^{99}Ru		
[Element] ($\mu g\ dm^{-3}$)	Intensity ratio	Calculated concentration ($\mu g\ dm^{-3}$)	% difference (certified value - calculated value)	Intensity ratio	Calculated concentration ($\mu g\ dm^{-3}$)	% difference (certified value - calculated value)	Intensity ratio	Calculated concentration ($\mu g\ dm^{-3}$)	% difference (certified value - calculated value)
0	$1.06x10^{2}$	0.32	-	$1.60x10^{2}$	-0.39	-	$8.42x10^{1}$	0.73	-
10	$4.29x10^{2}$	11.23	12.29	$2.88x10^{2}$	12.26	22.63	$7.95x10^{2}$	11.03	10.28
50	$1.49x10^{3}$	47.14	-5.72	$6.26x10^{2}$	45.74	-8.52	$3.36x10^{3}$	48.20	-3.60
100	$3.09x10^{3}$	101.33	1.33	$1.21x10^{3}$	103.37	3.37	$6.83x10^{3}$	98.54	-1.46
150	$4.53x10^{3}$	149.98	-0.01	$1.67x10^{3}$	149.03	-0.65	$1.05x10^{4}$	151.51	1.00
Correlation coefficient	0.9996			0.9989			0.9997		
Slope ($counts\ s^{-1}\ (\mu g\ dm^{-3})^{-1}$)	$2.96x10^{1}$			$1.01x10^{1}$			$6.90x10^{1}$		
Intercept ($counts\ s^{-1}$)	$9.65x10^{1}$			$1.64x10^{2}$			$3.41x10^{1}$		
Detection limit ($\mu g\ dm^{-3}$)	0.6533			7.1587			0.8686		
Standard error	1.9616			3.4455			1.7533		

Table 3.14: Calibration data for ^{100}Ru, ^{101}Ru and ^{102}Ru when no internal standard was used.

	^{100}Ru			^{101}Ru			^{102}Ru		
[Element] ($\mu g\ dm^{-3}$)	Intensity ratio	Calculated concentration ($\mu g\ dm^{-3}$)	% difference (certified value - calculated value)	Intensity ratio	Calculated concentration ($\mu g\ dm^{-3}$)	% difference (certified value - calculated value)	Intensity ratio	Calculated concentration ($\mu g\ dm^{-3}$)	% difference (certified value - calculated value)
0	$1.49x10^{2}$	0.73	-	$8.99x10^{1}$	0.39	-	$9.21x10^{1}$	1.01	-
10	$8.15x10^{2}$	10.44	4.35	$1.04x10^{3}$	10.57	5.68	$1.81x10^{3}$	10.64	6.42
50	$3.41x10^{3}$	48.28	-3.44	$4.69x10^{3}$	49.48	-1.05	$8.51x10^{3}$	48.29	-3.42
100	$6.96x10^{3}$	100.04	0.04	$9.26x10^{3}$	98.27	-1.73	$1.75x10^{4}$	98.59	-1.41
150	$1.04x10^{4}$	150.52	0.35	$1.42x10^{4}$	151.29	0.86	$2.69x10^{4}$	151.47	0.98
Correlation coefficient	0.9999			0.9998			0.9997		
Slope ($counts\ s^{-1}\ (\mu g\ dm^{-3})^{-1}$)	$6.86x10^{1}$			$9.37x10^{1}$			$1.78x10^{2}$		
Intercept ($counts\ s^{-1}$)	$9.86x10^{1}$			$5.29x10^{1}$			$-8.83x10^{1}$		
Detection limit ($\mu g\ dm^{-3}$)	1.3473			1.0966			0.2361		
Standard error	1.1463			1.3409			1.6850		

Table 3.15: Calibration data for ^{104}Ru when no internal standard was used.

	^{104}Ru		
[Element] ($\mu g\ dm^{-3}$)	Intensity ratio	Calculated concentration ($\mu g\ dm^{-3}$)	% difference (certified value - calculated value)
0	$1.05x10^{2}$	0.87	-
10	$1.53x10^{3}$	10.33	3.35
50	$7.24x10^{3}$	48.26	-3.48
100	$1.50x10^{4}$	99.92	-0.08
150	$2.26x10^{4}$	150.61	0.41
Correlation coefficient	0.9999		
Slope (counts s^{-1} ($\mu g\ dm^{-3}$)$^{-1}$)	$1.51x10^{2}$		
Intercept (counts s^{-1})	$-2.69x10^{1}$		
Detection limit ($\mu g\ dm^{-3}$)	0.5755		
Standard error	1.1944		

Table 3.16: Calibration data for Au and Ir when ^{36}Ar is used as internal standard.

	^{197}Au			^{191}Ir			^{193}Ir		
[Element] ($\mu g\ dm^{-3}$)	**Intensity ratio**	**Calculated concentration ($\mu g\ dm^{-3}$)**	**% difference (certified value - calculated value)**	**Intensity ratio**	**Calculated concentration ($\mu g\ dm^{-3}$)**	**% difference (certified value - calculated value)**	**Intensity ratio**	**Calculated concentration ($\mu g\ dm^{-3}$)**	**% difference (certified value - calculated value)**
0	$5.64x10^{-6}$	1.79	-	$3.45x10^{-6}$	1.66	-	$3.61x10^{-6}$	1.51	-
10	$3.94x10^{-5}$	11.02	10.23	$3.36x10^{-5}$	10.96	9.58	$5.71x10^{-5}$	11.56	15.64
50	$1.76x10^{-4}$	48.37	-3.25	$1.56x10^{-4}$	48.66	-2.69	$2.52x10^{-4}$	48.12	-3.76
100	$3.46x10^{-4}$	95.02	-4.98	$3.06x10^{-4}$	95.04	-4.96	$5.00x10^{-4}$	94.84	-5.16
150	$5.61x10^{-4}$	153.79	2.53	$4.96x10^{-4}$	153.69	2.46	$8.15x10^{-4}$	153.96	2.64
Correlation coefficient	0.9986			0.9986			0.9984		
Slope $((\mu g\ dm^{-3})^{-1})$	$3.65x10^{-6}$			$3.24x10^{-6}$			$5.32x10^{-6}$		
Intercept	$-8.93x10^{-7}$			$-1.91x10^{-6}$			$-4.45x10^{-6}$		
Detection limit ($\mu g\ dm^{-3}$)	0.4840			0.2845			0.1758		
Standard error	3.9116			3.8119			4.1012		

Table 3.17: Calibration data for ^{102}Pd, ^{104}Pd and ^{105}Pd when ^{36}Ar is used as internal standard.

	^{102}Pd			^{104}Pd			^{105}Pd		
[Element] ($\mu g\ dm^{-3}$)	Intensity ratio	Calculated concentration ($\mu g\ dm^{-3}$)	% difference (certified value - calculated value)	Intensity ratio	Calculated concentration ($\mu g\ dm^{-3}$)	% difference (certified value - calculated value)	Intensity ratio	Calculated concentration ($\mu g\ dm^{-3}$)	% difference (certified value - calculated value)
0	$4.09x10^{-6}$	1.54	-	$5.20x10^{-6}$	1.86	-	$1.85x10^{-4}$	3.85	-
10	$9.02x10^{-5}$	10.98	9.77	$7.40x10^{-5}$	10.80	7.97	$2.17x10^{-4}$	10.59	5.91
50	$4.31x10^{-4}$	48.34	-3.32	$3.64x10^{-4}$	48.48	-3.03	$3.92x10^{-4}$	47.38	-5.24
100	$8.66x10^{-4}$	95.96	-4.04	$7.23x10^{-4}$	95.23	-4.77	$6.04x10^{-4}$	92.04	-7.96
150	$1.39x10^{-3}$	153.18	2.12	$1.17x10^{-3}$	153.63	2.42	$9.08x10^{-4}$	156.14	4.09
Correlation coefficient	0.9990			0.9987			0.9961		
Slope $((\mu g\ dm^{-3})^{-1})$	$9.13x10^{-6}$			$7.69x10^{-6}$			$4.75x10^{-6}$		
Intercept	$-1.00x10^{-5}$			$-9.07x10^{-6}$			$1.67x10^{-4}$		
Detection limit ($\mu g\ dm^{-3}$)	0.1768			0.2430			12.8949		
Standard error	3.2914			3.7481			6.3785		

Table 3.18: Calibration data for ^{106}Pd, ^{108}Pd and ^{110}Pd when ^{36}Ar is used as internal standard.

	^{106}Pd			^{108}Pd			^{110}Pd		
[Element] ($\mu g\ dm^{-3}$)	**Intensity ratio**	**Calculated concentration ($\mu g\ dm^{-3}$)**	**% difference (certified value - calculated value)**	**Intensity ratio**	**Calculated concentration ($\mu g\ dm^{-3}$)**	**% difference (certified value - calculated value)**	**Intensity ratio**	**Calculated concentration ($\mu g\ dm^{-3}$)**	**% difference (certified value - calculated value)**
0	$3.28x10^{-5}$	1.92	-	$5.53x10^{-6}$	2.07	-	$4.89x10^{-6}$	1.90	-
10	$8.28x10^{-5}$	10.44	4.42	$5.48x10^{-5}$	10.69	6.86	$2.81x10^{-5}$	10.91	9.12
50	$3.07x10^{-4}$	48.55	-2.91	$2.73x10^{-4}$	48.83	-2.35	$1.23x10^{-4}$	47.76	-4.47
100	$5.85x10^{-4}$	95.90	-4.10	$5.33x10^{-4}$	94.22	-5.78	$2.47x10^{-4}$	96.21	-3.79
150	$9.21x10^{-4}$	153.19	2.12	$8.76x10^{-4}$	154.20	2.80	$3.94x10^{-4}$	153.21	2.14
Correlation coefficient	0.9990			0.9982			0.9989		
Slope $((\mu g\ dm^{-3})^{-1})$	$5.87x10^{-6}$			$5.72x10^{-6}$			$2.57x10^{-6}$		
Intercept	$2.15x10^{-5}$			$-6.32x10^{-6}$			$-6.97x10^{-9}$		
Detection limit ($\mu g\ dm^{-3}$)	1.6288			0.3290			1.1305		
Standard error	3.3111			4.3593			3.3694		

Table 3.19: Calibration data for ^{192}Pt, ^{194}Pt and ^{195}Pt when ^{36}Ar is used as internal standard.

	^{192}Pt			^{194}Pt			^{195}Pt		
[Element] ($\mu g\ dm^{-3}$)	Intensity ratio	Calculated concentration ($\mu g\ dm^{-3}$)	% difference (certified value - calculated value)	Intensity ratio	Calculated concentration ($\mu g\ dm^{-3}$)	% difference (certified value - calculated value)	Intensity ratio	Calculated concentration ($\mu g\ dm^{-3}$)	% difference (certified value - calculated value)
0	$3.64x10^{-6}$	3.47	-	$2.69x10^{-6}$	1.68	-	$3.20x10^{-6}$	1.84	-
10	$4.80x10^{-6}$	23.07	130.73	$2.16x10^{-5}$	11.92	19.25	$2.13x10^{-5}$	11.45	14.46
50	$5.11x10^{-6}$	28.22	-43.57	$8.69x10^{-5}$	47.37	-5.25	$9.09x10^{-5}$	48.42	-3.15
100	$9.17x10^{-6}$	96.55	-3.45	$1.74x10^{-4}$	94.81	-5.19	$1.76x10^{-4}$	93.57	-6.43
150	$1.29x10^{-5}$	158.69	5.79	$2.84x10^{-4}$	154.21	2.81	$2.91x10^{-4}$	154.72	3.14
Correlation coefficient	0.9773			0.9982			0.9978		
Slope $((\mu g\ dm^{-3})^{-1})$	$5.95x10^{-8}$			$1.84x10^{-6}$			$1.88x10^{-6}$		
Intercept	$3.43x10^{-6}$			$-4.12x10^{-7}$			$-2.71x10^{-7}$		
Detection limit ($\mu g\ dm^{-3}$)	24.8009			1.6274			1.1882		
Standard error	15.4003			4.3943			4.8748		

Table 3.20: Calibration data for ^{196}Pt, ^{198}Pt and ^{103}Rh when ^{36}Ar is used as internal standard.

	^{196}Pt			^{198}Pt			^{103}Rh		
[Element] ($\mu g\ dm^{-3}$)	Intensity ratio	Calculated concentration ($\mu g\ dm^{-3}$)	% difference (certified value - calculated value)	Intensity ratio	Calculated concentration ($\mu g\ dm^{-3}$)	% difference (certified value - calculated value)	Intensity ratio	Calculated concentration ($\mu g\ dm^{-3}$)	% difference (certified value - calculated value)
0	$3.12x10^{-6}$	0.95	-	$3.33x10^{-6}$	0.73	-	$6.03x10^{-6}$	1.88	-
10	$1.80x10^{-5}$	11.73	17.28	$7.31x10^{-6}$	10.60	5.99	$2.32x10^{-4}$	11.21	12.07
50	$7.00x10^{-5}$	49.50	-0.99	$2.41x10^{-5}$	52.34	4.68	$1.13x10^{-3}$	48.02	-3.96
100	$1.30x10^{-4}$	93.31	-6.69	$3.99x10^{-5}$	91.46	-8.54	$2.26x10^{-3}$	94.93	-5.07
150	$2.15x10^{-4}$	154.51	3.01	$6.54x10^{-5}$	154.88	3.25	$3.70x10^{-3}$	153.96	2.64
Correlation coefficient	0.9978			0.9968			0.9984		
Slope ($(\mu g\ dm^{-3})^{-1}$)	$1.38x10^{-6}$			$4.03x10^{-7}$			$2.43x10^{-5}$		
Intercept	$1.82x10^{-6}$			$3.04x10^{-6}$			$-3.97x10^{-5}$		
Detection limit ($\mu g\ dm^{-3}$)	1.6309			4.7914			0.2199		
Standard error	4.7953			5.8438			4.0889		

Table 3.21: Calibration data for ^{96}Ru, ^{98}Ru and ^{99}Ru when ^{36}Ar is used as internal standard.

	^{96}Ru			^{98}Ru			^{99}Ru		
[Element] ($\mu g\ dm^{-3}$)	Intensity ratio	Calculated concentration ($\mu g\ dm^{-3}$)	% difference (certified value - calculated value)	Intensity ratio	Calculated concentration ($\mu g\ dm^{-3}$)	% difference (certified value - calculated value)	Intensity ratio	Calculated concentration ($\mu g\ dm^{-3}$)	% difference (certified value - calculated value)
0	$5.13x10^{-6}$	0.78	-	$7.75x10^{-6}$	-0.04	-	$4.08x10^{-6}$	1.21	-
10	$2.13x10^{-5}$	11.62	16.19	$1.43x10^{-5}$	12.77	27.73	$3.95x10^{-5}$	11.39	13.91
50	$7.45x10^{-5}$	47.36	-5.27	$3.13x10^{-5}$	46.14	-7.73	$1.68x10^{-4}$	48.37	-3.26
100	$1.51x10^{-4}$	98.40	-1.60	$5.88x10^{-5}$	100.09	0.09	$3.32x10^{-4}$	95.73	-4.27
150	$2.30x10^{-4}$	151.84	1.22	$8.47x10^{-5}$	151.04	0.69	$5.32x10^{-4}$	153.29	2.20
Correlation coefficient	0.9995			0.9993			0.9989		
Slope ($(\mu g\ dm^{-3})^{-1}$)	$1.49x10^{-6}$			$5.10x10^{-7}$			$3.47x10^{-6}$		
Intercept	$3.97x10^{-6}$			$7.77x10^{-6}$			$-1.16x10^{-7}$		
Detection limit ($\mu g\ dm^{-3}$)	0.6289			6.8785			0.8362		
Standard error	2.3158			2.8093			3.4160		

Table 3.22: Calibration data for ^{100}Ru, ^{101}Ru and ^{102}Ru when ^{36}Ar is used as internal standard.

	^{100}Ru			^{101}Ru			^{102}Ru		
[Element] ($\mu g\ dm^{-3}$)	**Intensity ratio**	**Calculated concentration ($\mu g\ dm^{-3}$)**	**% difference (certified value - calculated value)**	**Intensity ratio**	**Calculated concentration ($\mu g\ dm^{-3}$)**	**% difference (certified value - calculated value)**	**Intensity ratio**	**Calculated concentration ($\mu g\ dm^{-3}$)**	**% difference (certified value - calculated value)**
0	$7.20x10^{-6}$	1.20	-	$4.36x10^{-6}$	0.88	-	$4.46x10^{-6}$	1.50	-
10	$4.04x10^{-5}$	10.82	8.17	$5.18x10^{-5}$	10.93	9.33	$8.97x10^{-5}$	11.00	10.02
50	$1.71x10^{-4}$	48.47	-3.06	$2.34x10^{-4}$	49.63	-0.73	$4.26x10^{-4}$	48.45	-3.10
100	$3.39x10^{-4}$	97.18	-2.82	$4.51x10^{-4}$	95.48	-4.52	$8.50x10^{-4}$	95.81	-4.19
150	$5.29x10^{-4}$	152.33	1.56	$7.22x10^{-4}$	153.08	2.05	$1.37x10^{-3}$	153.25	2.16
Correlation coefficient	0.9994			0.9990			0.9989		
Slope $((\mu g\ dm^{-3})^{-1})$	$3.46x10^{-6}$			$4.72x10^{-6}$			$8.97x10^{-6}$		
Intercept	$3.06x10^{-6}$			$1.99x10^{-7}$			$-8.96x10^{-6}$		
Detection limit ($\mu g\ dm^{-3}$)	1.2972			1.0557			0.2274		
Standard error	2.4372			3.2474			3.3519		

Table 3.23: Calibration data for ^{104}Ru when ^{36}Ar is used as internal standard.

	^{104}Ru		
[Element] ($\mu g\ dm^{-3}$)	**Intensity ratio**	**Calculated concentration ($\mu g\ dm^{-3}$)**	**% difference (certified value - calculated value)**
0	5.08×10^{-6}	1.36	-
10	7.59×10^{-5}	10.70	7.02
50	3.62×10^{-4}	48.43	-3.14
100	7.31×10^{-4}	97.10	-2.90
150	1.15×10^{-3}	152.41	1.61
Correlation coefficient	0.9994		
Slope $((\mu g\ dm^{-3})^{-1})$	7.58×10^{-6}		
Intercept	-5.21×10^{-6}		
Detection limit ($\mu g\ dm^{-3}$)	0.5542		
Standard error	2.5168		

Table 3.24: Calibration data for Au and Ir when ^{45}Sc is used as internal standard.

	^{197}Au			^{191}Ir			^{193}Ir		
[Element] ($\mu g\ dm^{-3}$)	**Intensity ratio**	**Calculated concentration ($\mu g\ dm^{-3}$)**	**% difference (certified value - calculated value)**	**Intensity ratio**	**Calculated concentration ($\mu g\ dm^{-3}$)**	**% difference (certified value - calculated value)**	**Intensity ratio**	**Calculated concentration ($\mu g\ dm^{-3}$)**	**% difference (certified value - calculated value)**
0	$1.18x10^{-4}$	0.58	-	$7.25x10^{-5}$	0.46	-	$7.58x10^{-5}$	0.33	-
10	$8.79x10^{-4}$	10.25	2.50	$7.49x10^{-4}$	10.17	1.73	$1.27x10^{-3}$	10.80	7.95
50	$3.99x10^{-3}$	49.91	-0.18	$3.53x10^{-3}$	50.19	0.39	$5.71x10^{-3}$	49.62	-0.76
100	$7.75x10^{-3}$	97.75	-2.25	$6.85x10^{-3}$	97.75	-2.25	$1.12x10^{-2}$	97.55	-2.45
150	$1.20x10^{-2}$	151.51	1.01	$1.06x10^{-2}$	151.42	0.95	$1.74x10^{-2}$	151.71	1.14
Correlation coefficient	0.9998			0.9998			0.9997		
Slope $((\mu g\ dm^{-3})^{-1})$	$7.86x10^{-5}$			$6.96x10^{-5}$			$1.14x10^{-4}$		
Intercept	$7.32x10^{-5}$			$4.06x10^{-5}$			$3.82x10^{-5}$		
Detection limit $(\mu g\ dm^{-3})$	0.4725			0.2777			0.1717		
Standard error	1.6081			1.5639			1.8085		

Table 3.25: Calibration data for ^{102}Pd, ^{104}Pd and ^{105}Pd when ^{45}Sc is used as internal standard.

	^{102}Pd			^{104}Pd			^{105}Pd		
[Element] ($\mu g\ dm^{-3}$)	Intensity ratio	Calculated concentration ($\mu g\ dm^{-3}$)	% difference (certified value - calculated value)	Intensity ratio	Calculated concentration ($\mu g\ dm^{-3}$)	% difference (certified value - calculated value)	Intensity ratio	Calculated concentration ($\mu g\ dm^{-3}$)	% difference (certified value - calculated value)
0	$8.58x10^{-5}$	0.37	-	$1.09x10^{-4}$	0.69	-	$3.88x10^{-3}$	1.03	-
10	$2.01x10^{-3}$	10.18	1.84	$1.65x10^{-3}$	10.00	0.02	$4.84x10^{-3}$	10.41	4.10
50	$9.80x10^{-3}$	49.84	-0.32	$8.26x10^{-3}$	49.99	-0.01	$8.90x10^{-3}$	50.17	0.33
100	$1.94x10^{-2}$	98.69	-1.31	$1.62x10^{-2}$	97.95	-2.05	$1.35x10^{-2}$	95.44	-4.56
150	$2.97x10^{-2}$	150.91	0.61	$2.50x10^{-2}$	151.37	0.91	$1.94x10^{-2}$	152.96	1.97
Correlation coefficient	0.9999			0.9998			0.9990		
Slope ($(\mu g\ dm^{-3})^{-1}$)	$1.96x10^{-4}$			$1.65x10^{-4}$			$1.02x10^{-4}$		
Intercept	$1.28x10^{-5}$			$-4.43x10^{-6}$			$3.77x10^{-3}$		
Detection limit ($\mu g\ dm^{-3}$)	0.1726			0.2372			12.5941		
Standard error	0.9573			1.4796			3.2028		

Table 3.26: Calibration data for ^{106}Pd, ^{108}Pd and ^{110}Pd when ^{45}Sc is used as internal standard.

	^{106}Pd			^{108}Pd			^{110}Pd		
[Element] ($\mu g\ dm^{-3}$)	Intensity ratio	Calculated concentration ($\mu g\ dm^{-3}$)	% difference (certified value - calculated value)	Intensity ratio	Calculated concentration ($\mu g\ dm^{-3}$)	% difference (certified value - calculated value)	Intensity ratio	Calculated concentration ($\mu g\ dm^{-3}$)	% difference (certified value - calculated value)
0	$6.88x10^{-4}$	0.54	-	$1.16x10^{-4}$	0.89	-	$1.03x10^{-4}$	0.69	-
10	$1.85x10^{-3}$	9.71	-2.86	$1.22x10^{-3}$	9.89	-1.10	$6.26x10^{-4}$	10.15	1.46
50	$6.96x10^{-3}$	50.23	0.46	$6.20x10^{-3}$	50.36	0.73	$2.79x10^{-3}$	49.28	-1.45
100	$1.31x10^{-2}$	98.73	-1.27	$1.19x10^{-2}$	96.90	-3.10	$5.54x10^{-3}$	98.98	-1.02
150	$1.97x10^{-2}$	150.79	0.52	$1.87x10^{-2}$	151.95	1.30	$8.41x10^{-3}$	150.91	0.61
Correlation coefficient	0.9999			0.9995			0.9999		
Slope ($(\mu g\ dm^{-3})^{-1}$)	$1.26x10^{-4}$			$1.23x10^{-4}$			$5.53x10^{-5}$		
Intercept	$6.21x10^{-4}$			$6.16x10^{-6}$			$6.46x10^{-5}$		
Detection limit ($\mu g\ dm^{-3}$)	1.5897			0.3212			1.1033		
Standard error	0.9393			2.1875			0.9810		

Table 3.27: Calibration data for ^{192}Pt, ^{194}Pt and ^{195}Pt when ^{45}Sc is used as internal standard.

	^{192}Pt			^{194}Pt			^{195}Pt		
[Element] ($\mu g\ dm^{-3}$)	**Intensity ratio**	**Calculated concentration ($\mu g\ dm^{-3}$)**	**% difference (certified value - calculated value)**	**Intensity ratio**	**Calculated concentration ($\mu g\ dm^{-3}$)**	**% difference (certified value - calculated value)**	**Intensity ratio**	**Calculated concentration ($\mu g\ dm^{-3}$)**	**% difference (certified value - calculated value)**
0	$7.63x10^{-5}$	-0.31	-	$5.65x10^{-5}$	0.47	-	$6.73x10^{-5}$	0.62	-
10	$1.07x10^{-4}$	23.80	138.01	$4.81x10^{-4}$	11.19	11.86	$4.75x10^{-4}$	10.69	6.88
50	$1.16x10^{-4}$	30.78	-38.43	$1.97x10^{-3}$	48.86	-2.27	$2.07x10^{-3}$	49.98	-0.05
100	$2.05x10^{-4}$	100.71	0.71	$3.90x10^{-3}$	97.53	-2.47	$3.94x10^{-3}$	96.25	-3.75
150	$2.75x10^{-4}$	155.01	3.34	$6.06x10^{-3}$	151.94	1.30	$6.22x10^{-3}$	152.46	1.64
Correlation coefficient	0.9821			0.9996			0.9993		
Slope ($(\mu g\ dm^{-3})^{-1}$)	$1.28x10^{-6}$			$3.96x10^{-5}$			$4.05x10^{-5}$		
Intercept	$7.67x10^{-5}$			$3.78x10^{-5}$			$4.21x10^{-5}$		
Detection limit ($\mu g\ dm^{-3}$)	24.2390			1.5887			1.1601		
Standard error	13.7187			2.0643			2.6417		

Table 3.28: Calibration data for ^{196}Pt, ^{198}Pt and ^{103}Rh when ^{45}Sc is used as internal standard.

	^{196}Pt			^{198}Pt			^{103}Rh		
[Element] ($\mu g\ dm^{-3}$)	**Intensity ratio**	**Calculated concentration ($\mu g\ dm^{-3}$)**	**% difference (certified value - calculated value)**	**Intensity ratio**	**Calculated concentration ($\mu g\ dm^{-3}$)**	**% difference (certified value - calculated value)**	**Intensity ratio**	**Calculated concentration ($\mu g\ dm^{-3}$)**	**% difference (certified value - calculated value)**
0	$6.55x10^{-5}$	-0.35	-	$7.00x10^{-5}$	-0.87	-	$1.27x10^{-4}$	0.73	-
10	$4.01x10^{-4}$	10.98	9.78	$1.63x10^{-4}$	9.89	-1.14	$5.18x10^{-3}$	10.42	4.22
50	$1.59x10^{-3}$	51.15	2.30	$5.48x10^{-4}$	54.36	8.71	$2.56x10^{-2}$	49.50	-1.01
100	$2.92x10^{-3}$	96.00	-4.00	$8.92x10^{-4}$	94.20	-5.80	$5.07x10^{-2}$	97.63	-2.37
150	$4.58x10^{-3}$	152.22	1.48	$1.40x10^{-3}$	152.42	1.61	$7.89x10^{-2}$	151.72	1.15
Correlation coefficient	0.9993			0.9981			0.9997		
Slope $((\mu g\ dm^{-3})^{-1})$	$2.96x10^{-5}$			$8.65x10^{-6}$			$5.22x10^{-4}$		
Intercept	$7.58x10^{-5}$			$7.74x10^{-5}$			$-2.57x10^{-4}$		
Detection limit $(\mu g\ dm^{-3})$	1.5926			4.6804			0.2146		
Standard error	2.7855			4.4352			1.7865		

Table 3.29: Calibration data for ^{96}Ru, ^{98}Ru and ^{99}Ru when ^{45}Sc is used as internal standard.

	^{96}Ru			^{98}Ru			^{99}Ru		
[Element] ($\mu g\ dm^{-3}$)	Intensity ratio	Calculated concentration ($\mu g\ dm^{-3}$)	% difference (certified value - calculated value)	Intensity ratio	Calculated concentration ($\mu g\ dm^{-3}$)	% difference (certified value - calculated value)	Intensity ratio	Calculated concentration ($\mu g\ dm^{-3}$)	% difference (certified value - calculated value)
0	$1.08x10^{-4}$	-0.55	-	$1.63x10^{-4}$	-1.94	-	$8.57x10^{-5}$	-0.01	-
10	$4.75x10^{-4}$	10.90	9.00	$3.19x10^{-4}$	12.29	22.86	$8.80x10^{-4}$	10.62	6.22
50	$1.69x10^{-3}$	48.92	-2.15	$7.11x10^{-4}$	48.06	-3.88	$3.82x10^{-3}$	49.91	-0.19
100	$3.37x10^{-3}$	101.29	1.29	$1.32x10^{-3}$	103.29	3.29	$7.44x10^{-3}$	98.48	-1.52
150	$4.92x10^{-3}$	149.44	-0.37	$1.81x10^{-3}$	148.30	-1.13	$1.14x10^{-2}$	151.00	0.67
Correlation coefficient	0.9999			0.9992			0.9999		
Slope ($(\mu g\ dm^{-3})^{-1}$)	$3.21x10^{-5}$			$1.10x10^{-5}$			$7.47x10^{-5}$		
Intercept	$1.25x10^{-4}$			$1.84x10^{-4}$			$8.66x10^{-5}$		
Detection limit ($\mu g\ dm^{-3}$)	0.6137			6.7135			0.8162		
Standard error	1.1885			2.9688			1.1112		

Table 3.30: Calibration data for ^{100}Ru, ^{101}Ru and ^{102}Ru when ^{45}Sc is used as internal standard.

	^{100}Ru			^{101}Ru			^{102}Ru		
[Element] ($\mu g\ dm^{-3}$)	Intensity ratio	Calculated concentration ($\mu g\ dm^{-3}$)	% difference (certified value - calculated value)	Intensity ratio	Calculated concentration ($\mu g\ dm^{-3}$)	% difference (certified value - calculated value)	Intensity ratio	Calculated concentration ($\mu g\ dm^{-3}$)	% difference (certified value - calculated value)
0	$1.51x10^{-4}$	-0.06	-	$9.15x10^{-5}$	-0.35	-	$9.37x10^{-5}$	0.32	-
10	$9.02x10^{-4}$	10.04	0.44	$1.16x10^{-3}$	10.14	1.35	$2.00x10^{-3}$	10.21	2.10
50	$3.87x10^{-3}$	50.03	0.07	$5.32x10^{-3}$	51.23	2.46	$9.67x10^{-3}$	49.96	-0.09
100	$7.59x10^{-3}$	99.99	-0.01	$1.01x10^{-2}$	98.21	-1.79	$1.90x10^{-2}$	98.54	-1.46
150	$1.13x10^{-2}$	149.99	0.00	$1.54x10^{-2}$	150.78	0.52	$2.92x10^{-2}$	150.98	0.65
Correlation coefficient	1.0000			0.9998			0.9999		
Slope $((\mu g\ dm^{-3})^{-1})$	$7.43x10^{-5}$			$1.01x10^{-4}$			$1.93x10^{-4}$		
Intercept	$1.56x10^{-4}$			$1.27x10^{-4}$			$3.19x10^{-5}$		
Detection limit ($\mu g\ dm^{-3}$)	1.2659			1.0306			0.2219		
Standard error	0.0482			1.3509			1.0402		

Table 3.31: Calibration data for ^{104}Ru when ^{45}Sc is used as internal standard.

	^{104}Ru		
[Element] ($\mu g\ dm^{-3}$)	**Intensity ratio**	**Calculated concentration ($\mu g\ dm^{-3}$)**	**% difference (certified value - calculated value)**
0	$1.07x10^{-4}$	0.17	-
10	$1.69x10^{-3}$	9.90	-0.96
50	$8.22x10^{-3}$	49.94	-0.12
100	$1.64x10^{-2}$	99.87	-0.13
150	$2.46x10^{-2}$	150.11	0.07
Correlation coefficient	1.0000		
Slope $((\mu g\ dm^{-3})^{-1})$	$1.63x10^{-4}$		
Intercept	$7.85x10^{-5}$		
Detection limit ($\mu g\ dm^{-3}$)	0.5408		
Standard error	0.1544		

Table 3.32: Calibration data for Au and Ir when ^{89}Y is used as internal standard.

	^{197}Au			^{191}Ir			^{193}Ir		
[Element] ($\mu g\ dm^{-3}$)	Intensity ratio	Calculated concentration ($\mu g\ dm^{-3}$)	% difference (certified value - calculated value)	Intensity ratio	Calculated concentration ($\mu g\ dm^{-3}$)	% difference (certified value - calculated value)	Intensity ratio	Calculated concentration ($\mu g\ dm^{-3}$)	% difference (certified value - calculated value)
0	$1.67x10^{-4}$	0.11	-	$1.02x10^{-4}$	0.00	-	$1.07x10^{-4}$	-0.13	-
10	$1.23x10^{-3}$	9.74	-2.57	$1.05x10^{-3}$	9.67	-3.31	$1.78x10^{-3}$	10.29	2.94
50	$5.66x10^{-3}$	49.92	-0.15	$5.01x10^{-3}$	50.21	0.41	$8.10x10^{-3}$	49.63	-0.74
100	$1.12x10^{-2}$	100.53	0.53	$9.93x10^{-3}$	100.52	0.52	$1.62x10^{-2}$	100.31	0.31
150	$1.67x10^{-2}$	149.69	-0.21	$1.47x10^{-2}$	149.60	-0.26	$2.42x10^{-2}$	149.90	-0.07
Correlation coefficient	1.0000			1.0000			1.0000		
Slope ($(\mu g\ dm^{-3})^{-1}$)	$1.10x10^{-4}$			$9.78x10^{-5}$			$1.61x10^{-4}$		
Intercept	$1.54x10^{-4}$			$1.02x10^{-4}$			$1.28x10^{-4}$		
Detection limit ($\mu g\ dm^{-3}$)	0.4738			0.2785			0.1722		
Standard error	0.3907			0.4406			0.3392		

Table 3.33: Calibration data for ^{102}Pd, ^{104}Pd and ^{105}Pd when ^{89}Y is used as internal standard.

	^{102}Pd			^{104}Pd			^{105}Pd		
[Element] ($\mu g\ dm^{-3}$)	Intensity ratio	Calculated concentration ($\mu g\ dm^{-3}$)	% difference (certified value - calculated value)	Intensity ratio	Calculated concentration ($\mu g\ dm^{-3}$)	% difference (certified value - calculated value)	Intensity ratio	Calculated concentration ($\mu g\ dm^{-3}$)	% difference (certified value - calculated value)
0	$1.21x10^{-4}$	-0.09	-	$1.54x10^{-4}$	0.23	-	$5.46x10^{-3}$	0.49	-
10	$2.82x10^{-3}$	9.68	-3.16	$2.31x10^{-3}$	9.50	-4.96	$6.77x10^{-3}$	9.58	-4.16
50	$1.39x10^{-2}$	49.84	-0.32	$1.17x10^{-2}$	50.00	0.01	$1.26x10^{-2}$	50.31	0.61
100	$2.81x10^{-2}$	101.47	1.47	$2.35x10^{-2}$	100.70	0.70	$1.96x10^{-2}$	99.08	-0.92
150	$4.13x10^{-2}$	149.10	-0.60	$3.48x10^{-2}$	149.56	-0.29	$2.70x10^{-2}$	150.54	0.36
Correlation coefficient	0.9999			1.0000			0.9999		
Slope ($(\mu g\ dm^{-3})^{-1}$)	$2.76x10^{-4}$			$2.32x10^{-4}$			$1.43x10^{-4}$		
Intercept	$1.45x10^{-4}$			$1.01x10^{-4}$			$5.39x10^{-3}$		
Detection limit ($\mu g\ dm^{-3}$)	0.1730			0.2379			12.6231		
Standard error	1.0164			0.5725			0.7369		

Table 3.34: Calibration data for ^{106}Pd, ^{108}Pd and ^{110}Pd when ^{89}Y is used as internal standard.

	^{106}Pd			^{108}Pd			^{110}Pd		
[Element] ($\mu g\ dm^{-3}$)	Intensity ratio	Calculated concentration ($\mu g\ dm^{-3}$)	% difference (certified value - calculated value)	Intensity ratio	Calculated concentration ($\mu g\ dm^{-3}$)	% difference (certified value - calculated value)	Intensity ratio	Calculated concentration ($\mu g\ dm^{-3}$)	% difference (certified value - calculated value)
0	$9.70x10^{-4}$	0.06	-	$1.63x10^{-4}$	0.43	-	$1.45x10^{-4}$	0.22	-
10	$2.59x10^{-3}$	9.17	-8.30	$1.71x10^{-3}$	9.39	-6.07	$8.76x10^{-4}$	9.64	-3.64
50	$9.87x10^{-3}$	50.25	0.50	$8.79x10^{-3}$	50.38	0.76	$3.96x10^{-3}$	49.28	-1.45
100	$1.90x10^{-2}$	101.63	1.63	$1.73x10^{-2}$	99.64	-0.36	$8.04x10^{-3}$	101.79	1.79
150	$2.74x10^{-2}$	148.88	-0.74	$2.60x10^{-2}$	150.16	0.10	$1.17x10^{-2}$	149.07	-0.62
Correlation coefficient	0.9999			1.0000			0.9998		
Slope ($(\mu g\ dm^{-3})^{-1}$)	$1.77x10^{-4}$			$1.73x10^{-4}$			$7.77x10^{-5}$		
Intercept	$9.58x10^{-4}$			$8.86x10^{-5}$			$1.27x10^{-4}$		
Detection limit ($\mu g\ dm^{-3}$)	1.5940			0.3221			1.1063		
Standard error	1.2468			0.5350			1.2623		

Table 3.35: Calibration data for ^{192}Pt, ^{194}Pt and ^{195}Pt when ^{89}Y is used as internal standard.

	^{192}Pt			^{194}Pt			^{195}Pt		
[Element] ($\mu g\ dm^{-3}$)	Intensity ratio	Calculated concentration ($\mu g\ dm^{-3}$)	% difference (certified value - calculated value)	Intensity ratio	Calculated concentration ($\mu g\ dm^{-3}$)	% difference (certified value - calculated value)	Intensity ratio	Calculated concentration ($\mu g\ dm^{-3}$)	% difference (certified value - calculated value)
0	$1.08x10^{-4}$	-0.85	-	$7.96x10^{-5}$	0.02	-	$9.48x10^{-5}$	0.16	-
10	$1.50x10^{-4}$	22.75	127.46	$6.73x10^{-4}$	10.68	6.80	$6.65x10^{-4}$	10.18	1.83
50	$1.65x10^{-4}$	30.87	-38.25	$2.80x10^{-3}$	48.87	-2.26	$2.93x10^{-3}$	50.00	0.00
100	$2.98x10^{-4}$	105.10	5.10	$5.66x10^{-3}$	100.31	0.31	$5.72x10^{-3}$	99.00	-1.00
150	$3.82x10^{-4}$	152.13	1.42	$8.43x10^{-3}$	150.12	0.08	$8.65x10^{-3}$	150.65	0.44
Correlation coefficient	0.9828			0.9999			1.0000		
Slope ($(\mu g\ dm^{-3})^{-1}$)	$1.80x10^{-6}$			$5.56x10^{-5}$			$5.69x10^{-5}$		
Intercept	$1.09x10^{-4}$			$7.88x10^{-5}$			$8.55x10^{-5}$		
Detection limit ($\mu g\ dm^{-3}$)	24.2669			1.5933			1.1637		
Standard error	13.4226			0.7854			0.7032		

Table 3.36: Calibration data for ^{196}Pt, ^{198}Pt and ^{103}Rh when ^{89}Y is used as internal standard.

	^{196}Pt			^{198}Pt			^{103}Rh		
[Element] ($\mu g\ dm^{-3}$)	**Intensity ratio**	**Calculated concentration ($\mu g\ dm^{-3}$)**	**% difference (certified value - calculated value)**	**Intensity ratio**	**Calculated concentration ($\mu g\ dm^{-3}$)**	**% difference (certified value - calculated value)**	**Intensity ratio**	**Calculated concentration ($\mu g\ dm^{-3}$)**	**% difference (certified value - calculated value)**
0	$9.23x10^{-5}$	-0.81	-	$9.85x10^{-5}$	-1.35	-	$1.78x10^{-4}$	0.28	-
10	$5.61x10^{-4}$	10.46	4.58	$2.28x10^{-4}$	9.31	-6.91	$7.25x10^{-3}$	9.93	-0.71
50	$2.25x10^{-3}$	51.19	2.38	$7.76x10^{-4}$	54.45	8.90	$3.63x10^{-2}$	49.50	-1.00
100	$4.23x10^{-3}$	98.78	-1.22	$1.29x10^{-3}$	97.10	-2.90	$7.36x10^{-2}$	100.37	0.37
150	$6.38x10^{-3}$	150.39	0.26	$1.94x10^{-3}$	150.50	0.33	$1.10x10^{-1}$	149.93	-0.05
Correlation coefficient	0.9999			0.9990			1.0000		
Slope $((\mu g\ dm^{-3})^{-1})$	$4.16x10^{-5}$			$1.21x10^{-5}$			$7.33x10^{-4}$		
Intercept	$1.26x10^{-4}$			$1.15x10^{-4}$			$-2.49x10^{-5}$		
Detection limit $(\mu g\ dm^{-3})$	1.5974			4.6946			0.2152		
Standard error	1.1437			3.2005			0.3961		

Table 3.37: Calibration data for ^{96}Ru, ^{98}Ru and ^{99}Ru when ^{89}Y is used as internal standard.

	^{96}Ru			^{98}Ru			^{99}Ru		
[Element] ($\mu g\ dm^{-3}$)	Intensity ratio	Calculated concentration ($\mu g\ dm^{-3}$)	% difference (certified value - calculated value)	Intensity ratio	Calculated concentration ($\mu g\ dm^{-3}$)	% difference (certified value - calculated value)	Intensity ratio	Calculated concentration ($\mu g\ dm^{-3}$)	% difference (certified value - calculated value)
0	$1.52x10^{-4}$	-1.02	-	$2.29x10^{-4}$	-2.44	-	$1.21x10^{-4}$	-0.48	-
10	$6.64x10^{-4}$	10.36	3.62	$4.46x10^{-4}$	11.63	16.27	$1.23x10^{-3}$	10.11	1.12
50	$2.40x10^{-3}$	48.92	-2.16	$1.01x10^{-3}$	48.08	-3.84	$5.41x10^{-3}$	49.92	-0.17
100	$4.89x10^{-3}$	104.22	4.22	$1.91x10^{-3}$	106.59	6.59	$1.08x10^{-2}$	101.28	1.28
150	$6.84x10^{-3}$	147.53	-1.65	$2.52x10^{-3}$	146.14	-2.57	$1.58x10^{-2}$	149.17	-0.56
Correlation coefficient	0.9992			0.9978			0.9999		
Slope $((\mu g\ dm^{-3})^{-1})$	$4.50x10^{-5}$			$1.54x10^{-5}$			$1.05x10^{-4}$		
Intercept	$1.98x10^{-4}$			$2.67x10^{-4}$			$1.71x10^{-4}$		
Detection limit ($\mu g\ dm^{-3}$)	0.6152			6.7259			0.8185		
Standard error	2.9548			4.8410			0.9275		

Table 3.38: Calibration data for ^{100}Ru, ^{101}Ru and ^{102}Ru when ^{89}Y is used as internal standard.

	^{100}Ru			^{101}Ru			^{102}Ru		
[Element] ($\mu g\ dm^{-3}$)	Intensity ratio	Calculated concentration ($\mu g\ dm^{-3}$)	% difference (certified value - calculated value)	Intensity ratio	Calculated concentration ($\mu g\ dm^{-3}$)	% difference (certified value - calculated value)	Intensity ratio	Calculated concentration ($\mu g\ dm^{-3}$)	% difference (certified value - calculated value)
0	$2.13x10^{-4}$	-0.53	-	$1.29x10^{-4}$	-0.82	-	$1.32x10^{-4}$	-0.14	-
10	$1.26x10^{-3}$	9.52	-4.76	$1.62x10^{-3}$	9.62	-3.76	$2.80x10^{-3}$	9.71	-2.90
50	$5.49x10^{-3}$	50.04	0.07	$7.55x10^{-3}$	51.25	2.50	$1.37x10^{-2}$	49.96	-0.08
100	$1.10x10^{-2}$	102.84	2.84	$1.46x10^{-2}$	101.00	1.00	$2.76x10^{-2}$	101.31	1.31
150	$1.57x10^{-2}$	148.13	-1.25	$2.15x10^{-2}$	148.94	-0.70	$4.06x10^{-2}$	149.16	-0.56
Correlation coefficient	0.9996			0.9999			0.9999		
Slope ($(\mu g\ dm^{-3})^{-1}$)	$1.04x10^{-4}$			$1.43x10^{-4}$			$2.71x10^{-4}$		
Intercept	$2.68x10^{-4}$			$2.45x10^{-4}$			$1.70x10^{-4}$		
Detection limit ($\mu g\ dm^{-3}$)	1.2692			1.0335			0.2225		
Standard error	2.0072			1.2224			0.9187		

Table 3.39: Calibration data for ^{104}Ru when ^{89}Y is used as internal standard.

	^{104}Ru		
[Element] ($\mu g\ dm^{-3}$)	**Intensity ratio**	**Calculated concentration ($\mu g\ dm^{-3}$)**	**% difference (certified value - calculated value)**
0	$1.50x10^{-4}$	-0.29	-
10	$2.37x10^{-3}$	9.40	-6.01
50	$1.17x10^{-2}$	49.94	-0.12
100	$2.37x10^{-2}$	102.68	2.68
150	$3.42x10^{-2}$	148.27	-1.15
Correlation coefficient	0.9997		
Slope $((\mu g\ dm^{-3})^{-1})$	$2.29x10^{-4}$		
Intercept	$2.17x10^{-4}$		
Detection limit ($\mu g\ dm^{-3}$)	0.5423		
Standard error	1.8812		

Table 3.40: Calibration data for Au and Ir when ^{138}La is used as internal standard.

	^{197}Au			^{191}Ir			^{193}Ir		
[Element] ($\mu g\ dm^{-3}$)	**Intensity ratio**	**Calculated concentration ($\mu g\ dm^{-3}$)**	**% difference (certified value - calculated value)**	**Intensity ratio**	**Calculated concentration ($\mu g\ dm^{-3}$)**	**% difference (certified value - calculated value)**	**Intensity ratio**	**Calculated concentration ($\mu g\ dm^{-3}$)**	**% difference (certified value - calculated value)**
0	$2.54x10^{-1}$	3.01	-	$1.56x10^{-1}$	2.87	-	$1.63x10^{-1}$	2.73	-
10	$1.76x10^{0}$	11.98	19.80	$1.50x10^{0}$	11.92	19.16	$2.56x10^{0}$	12.50	25.01
50	$7.65x10^{0}$	46.98	-6.03	$6.77x10^{0}$	47.26	-5.48	$1.09x10^{1}$	46.75	-6.49
100	$1.51x10^{1}$	91.47	-8.53	$1.34x10^{1}$	91.50	-8.50	$2.19x10^{1}$	91.31	-8.69
150	$2.61x10^{1}$	156.56	4.37	$2.30x10^{1}$	156.45	4.30	$3.79x10^{1}$	156.71	4.47
Correlation coefficient	0.9957			0.9958			0.9955		
Slope $((\mu g\ dm^{-3})^{-1})$	$1.68x10^{-1}$			$1.49x10^{-1}$			$2.45x10^{-1}$		
Intercept	$-2.51x10^{-1}$			$-2.72x10^{-1}$			$-5.05x10^{-1}$		
Detection limit ($\mu g\ dm^{-3}$)	0.4738			0.2785			0.1721		
Standard error	6.7496			6.6405			6.9172		

Table 3.41: Calibration data for ^{102}Pd, ^{104}Pd and ^{105}Pd when ^{138}La is used as internal standard.

	^{102}Pd			^{104}Pd			^{105}Pd		
[Element] ($\mu g\ dm^{-3}$)	Intensity ratio	Calculated concentration ($\mu g\ dm^{-3}$)	% difference (certified value - calculated value)	Intensity ratio	Calculated concentration ($\mu g\ dm^{-3}$)	% difference (certified value - calculated value)	Intensity ratio	Calculated concentration ($\mu g\ dm^{-3}$)	% difference (certified value - calculated value)
0	$1.84x10^{-1}$	2.75	-	$2.34x10^{-1}$	3.06	-	$8.33x10^{0}$	5.58	-
10	$4.04x10^{0}$	11.93	19.28	$3.31x10^{0}$	11.75	17.53	$9.71x10^{0}$	11.87	18.66
50	$1.88x10^{1}$	46.98	-6.04	$1.58x10^{1}$	47.11	-5.78	$1.70x10^{1}$	45.18	-9.64
100	$3.79x10^{1}$	92.39	-7.61	$3.16x10^{1}$	91.70	-8.30	$2.64x10^{1}$	87.68	-12.32
150	$6.46x10^{1}$	155.95	3.97	$5.45x10^{1}$	156.38	4.25	$4.22x10^{1}$	159.69	6.46
Correlation coefficient	0.9964			0.9959			0.9906		
Slope ($(\mu g\ dm^{-3})^{-1}$)	$4.20x10^{-1}$			$3.54x10^{-1}$			$2.20x10^{-1}$		
Intercept	$-9.72x10^{-1}$			$-8.48x10^{-1}$			$7.10x10^{0}$		
Detection limit ($\mu g\ dm^{-3}$)	0.1731			0.2379			12.5505		
Standard error	6.1337			6.5650			9.9640		

Table 3.42: Calibration data for ^{106}Pd, ^{108}Pd and ^{110}Pd when ^{138}La is used as internal standard.

	^{106}Pd			^{108}Pd			^{110}Pd		
[Element] ($\mu g\ dm^{-3}$)	**Intensity ratio**	**Calculated concentration ($\mu g\ dm^{-3}$)**	**% difference (certified value - calculated value)**	**Intensity ratio**	**Calculated concentration ($\mu g\ dm^{-3}$)**	**% difference (certified value - calculated value)**	**Intensity ratio**	**Calculated concentration ($\mu g\ dm^{-3}$)**	**% difference (certified value - calculated value)**
0	$1.48x10^{0}$	3.20	-	$2.49x10^{-1}$	3.27	-	$2.20x10^{-1}$	3.12	-
10	$3.71x10^{0}$	11.45	14.51	$2.46x10^{0}$	11.65	16.47	$1.26x10^{0}$	11.87	18.71
50	$1.33x10^{1}$	47.06	-5.88	$1.19x10^{1}$	47.43	-5.14	$5.34x10^{0}$	46.40	-7.19
100	$2.56x10^{1}$	92.22	-7.78	$2.33x10^{1}$	90.72	-9.28	$1.08x10^{1}$	92.60	-7.40
150	$4.28x10^{1}$	156.07	4.05	$4.07x10^{1}$	156.93	4.62	$1.83x10^{1}$	156.01	4.00
Correlation coefficient	0.9963			0.9952			0.9963		
Slope $((\mu g\ dm^{-3})^{-1})$	$2.70x10^{-1}$			$2.63x10^{-1}$			$1.18x10^{-1}$		
Intercept	$6.12x10^{-1}$			$-6.12x10^{-1}$			$-1.49x10^{-1}$		
Detection limit ($\mu g\ dm^{-3}$)	1.5938			0.3221			1.1068		
Standard error	6.2606			7.1359			6.2202		

Table 3.43: Calibration data for ^{192}Pt, ^{194}Pt and ^{195}Pt when ^{138}La is used as internal standard.

	^{192}Pt			^{194}Pt			^{195}Pt		
[Element] ($\mu g\ dm^{-3}$)	Intensity ratio	Calculated concentration ($\mu g\ dm^{-3}$)	% difference (certified value - calculated value)	Intensity ratio	Calculated concentration ($\mu g\ dm^{-3}$)	% difference (certified value - calculated value)	Intensity ratio	Calculated concentration ($\mu g\ dm^{-3}$)	% difference (certified value - calculated value)
0	$1.64x10^{-1}$	5.46	-	$1.21x10^{-1}$	2.90	-	$1.44x10^{-1}$	3.07	-
10	$2.15x10^{-1}$	23.99	139.93	$9.65x10^{-1}$	12.85	28.52	$9.54x10^{-1}$	12.39	23.93
50	$2.22x10^{-1}$	26.60	-46.81	$3.78x10^{0}$	46.03	-7.94	$3.96x10^{0}$	47.02	-5.96
100	$4.01x10^{-1}$	91.25	-8.75	$7.61x10^{0}$	91.25	-8.75	$7.69x10^{0}$	90.06	-9.94
150	$5.98x10^{-1}$	162.70	8.47	$1.32x10^{1}$	156.97	4.64	$1.35x10^{1}$	157.46	4.97
Correlation coefficient	0.9696			0.9951			0.9944		
Slope $((\mu g\ dm^{-3})^{-1})$	$2.76x10^{-3}$			$8.48x10^{-2}$			$8.68x10^{-2}$		
Intercept	$1.49x10^{-1}$			$-1.25x10^{-1}$			$-1.22x10^{-1}$		
Detection limit ($\mu g\ dm^{-3}$)	24.0620			1.5929			1.1628		
Standard error	17.8035			7.2072			7.6676		

Table 3.44: Calibration data for ^{196}Pt, ^{198}Pt and ^{103}Rh when ^{138}La is used as internal standard.

	^{196}Pt			^{198}Pt			^{103}Rh		
[Element] ($\mu g\ dm^{-3}$)	Intensity ratio	Calculated concentration ($\mu g\ dm^{-3}$)	% difference (certified value - calculated value)	Intensity ratio	Calculated concentration ($\mu g\ dm^{-3}$)	% difference (certified value - calculated value)	Intensity ratio	Calculated concentration ($\mu g\ dm^{-3}$)	% difference (certified value - calculated value)
0	$1.41x10^{-1}$	2.22	-	$1.50x10^{-1}$	2.13	-	$2.72x10^{-1}$	3.07	-
10	$8.05x10^{-1}$	12.69	26.89	$3.27x10^{-1}$	11.66	16.63	$1.04x10^{1}$	12.15	21.45
50	$3.05x10^{0}$	48.01	-3.97	$1.05x10^{0}$	50.54	1.09	$4.90x10^{1}$	46.68	-6.64
100	$5.69x10^{0}$	89.79	-10.21	$1.74x10^{0}$	87.87	-12.13	$9.90x10^{1}$	91.41	-8.59
150	$9.98x10^{0}$	157.29	4.86	$3.04x10^{0}$	157.79	5.20	$1.72x10^{2}$	156.69	4.46
Correlation coefficient	0.9946			0.9933			0.9955		
Slope ($(\mu g\ dm^{-3})^{-1}$)	$6.34x10^{-2}$			$1.86x10^{-2}$			$1.12x10^{0}$		
Intercept	$-1.70x10^{-4}$			$1.11x10^{-1}$			$-3.16x10^{0}$		
Detection limit ($\mu g\ dm^{-3}$)	1.5956			4.6824			0.2153		
Standard error	7.5661			8.4189			6.8868		

Table 3.45: Calibration data for ^{96}Ru, ^{98}Ru and ^{99}Ru when ^{138}La is used as internal standard.

	^{96}Ru			^{98}Ru			^{99}Ru		
[Element] ($\mu g\ dm^{-3}$)	**Intensity ratio**	**Calculated concentration ($\mu g\ dm^{-3}$)**	**% difference (certified value - calculated value)**	**Intensity ratio**	**Calculated concentration ($\mu g\ dm^{-3}$)**	**% difference (certified value - calculated value)**	**Intensity ratio**	**Calculated concentration ($\mu g\ dm^{-3}$)**	**% difference (certified value - calculated value)**
0	$2.31x10^{-1}$	2.06	-	$3.49x10^{-1}$	1.45	-	$1.84x10^{-1}$	2.44	-
10	$9.53x10^{-1}$	12.58	25.82	$6.40x10^{-1}$	13.81	38.10	$1.77x10^{0}$	12.34	23.41
50	$3.24x10^{0}$	45.98	-8.05	$1.36x10^{0}$	44.52	-10.95	$7.31x10^{0}$	46.98	-6.03
100	$6.58x10^{0}$	94.64	-5.36	$2.57x10^{0}$	95.93	-4.07	$1.45x10^{1}$	92.15	-7.85
150	$1.07x10^{1}$	154.74	3.16	$3.94x10^{0}$	154.29	2.86	$2.48x10^{1}$	156.08	4.05
Correlation coefficient	0.9975			0.9974			0.9963		
Slope $((\mu g\ dm^{-3})^{-1})$	$6.86x10^{-2}$			$2.35x10^{-2}$			$1.60x10^{-1}$		
Intercept	$9.01x10^{-2}$			$3.15x10^{-1}$			$-2.07x10^{-1}$		
Detection limit ($\mu g\ dm^{-3}$)	0.6157			6.7238			0.8186		
Standard error	5.0941			5.2013			6.2785		

Table 3.46: Calibration data for ^{100}Ru, ^{101}Ru and ^{102}Ru when ^{138}La is used as internal standard.

	^{100}Ru			^{101}Ru			^{102}Ru		
[Element] ($\mu g\ dm^{-3}$)	Intensity ratio	Calculated concentration ($\mu g\ dm^{-3}$)	% difference (certified value - calculated value)	Intensity ratio	Calculated concentration ($\mu g\ dm^{-3}$)	% difference (certified value - calculated value)	Intensity ratio	Calculated concentration ($\mu g\ dm^{-3}$)	% difference (certified value - calculated value)
0	$3.24x10^{-1}$	2.44	-	$1.96x10^{-1}$	2.13	-	$2.01x10^{-1}$	2.71	-
10	$1.81x10^{0}$	11.79	17.92	$2.32x10^{0}$	11.90	19.04	$4.02x10^{0}$	11.95	19.54
50	$7.42x10^{0}$	47.06	-5.87	$1.02x10^{1}$	48.18	-3.64	$1.85x10^{1}$	47.08	-5.84
100	$1.48x10^{1}$	93.52	-6.48	$1.97x10^{1}$	91.91	-8.09	$3.72x10^{1}$	92.25	-7.75
150	$2.46x10^{1}$	155.18	3.45	$3.36x10^{1}$	155.87	3.91	$6.35x10^{1}$	156.01	4.01
Correlation coefficient	0.9973			0.9965			0.9964		
Slope ($(\mu g\ dm^{-3})^{-1}$)	$1.59x10^{-1}$			$2.17x10^{-1}$			$4.13x10^{-1}$		
Intercept	$-6.42x10^{-2}$			$-2.67x10^{-1}$			$-9.17x10^{-1}$		
Detection limit ($\mu g\ dm^{-3}$)	1.2701			1.0335			0.2226		
Standard error	5.3568			6.0714			6.1948		

Table 3.47: Calibration data for ^{104}Ru when ^{138}La is used as internal standard.

	^{104}Ru		
[Element] ($\mu g\ dm^{-3}$)	**Intensity ratio**	**Calculated concentration ($\mu g\ dm^{-3}$)**	**% difference (certified value - calculated value)**
0	$2.29x10^{-1}$	2.58	-
10	$3.40x10^{0}$	11.67	16.66
50	$1.57x10^{1}$	47.06	-5.87
100	$3.19x10^{1}$	93.49	-6.51
150	$5.35x10^{1}$	155.21	3.47
Correlation coefficient	0.9973		
Slope $((\mu g\ dm^{-3})^{-1})$	$3.49x10^{-1}$		
Intercept	$-6.69x10^{-1}$		
Detection limit ($\mu g\ dm^{-3}$)	0.5428		
Standard error	5.3898		

Table 3.48: Calibration data for Au and Ir when ^{139}La is used as internal standard.

	^{197}Au			^{191}Ir			^{193}Ir		
[Element] ($\mu g\ dm^{-3}$)	Intensity ratio	Calculated concentration ($\mu g\ dm^{-3}$)	% difference (certified value - calculated value)	Intensity ratio	Calculated concentration ($\mu g\ dm^{-3}$)	% difference (certified value - calculated value)	Intensity ratio	Calculated concentration ($\mu g\ dm^{-3}$)	% difference (certified value - calculated value)
0	$3.30x10^{-4}$	0.47	-	$2.02x10^{-4}$	0.34	-	$2.11x10^{-4}$	0.21	-
10	$2.36x10^{-3}$	9.90	-1.03	$2.01x10^{-3}$	9.83	-1.71	$3.42x10^{-3}$	10.45	4.49
50	$1.09x10^{-2}$	49.65	-0.70	$9.66x10^{-3}$	49.93	-0.13	$1.56x10^{-2}$	49.37	-1.27
100	$2.17x10^{-2}$	99.59	-0.41	$1.91x10^{-2}$	99.58	-0.42	$3.13x10^{-2}$	99.37	-0.63
150	$3.26x10^{-2}$	150.40	0.27	$2.88x10^{-2}$	150.31	0.21	$4.73x10^{-2}$	150.60	0.40
Correlation coefficient	1.0000			1.0000			1.0000		
Slope ($(\mu g\ dm^{-3})^{-1}$)	$2.15x10^{-4}$			$1.91x10^{-4}$			$3.13x10^{-4}$		
Intercept	$2.29x10^{-4}$			$1.36x10^{-4}$			$1.44x10^{-4}$		
Detection limit ($\mu g\ dm^{-3}$)	0.4799			0.2821			0.1744		
Standard error	0.4776			0.3745			0.6842		

Table 3.49: Calibration data for ^{102}Pd, ^{104}Pd and ^{105}Pd when ^{139}La is used as internal standard.

	^{102}Pd			^{104}Pd			^{105}Pd		
[Element] ($\mu g\ dm^{-3}$)	**Intensity ratio**	**Calculated concentration ($\mu g\ dm^{-3}$)**	**% difference (certified value - calculated value)**	**Intensity ratio**	**Calculated concentration ($\mu g\ dm^{-3}$)**	**% difference (certified value - calculated value)**	**Intensity ratio**	**Calculated concentration ($\mu g\ dm^{-3}$)**	**% difference (certified value - calculated value)**
0	$2.39x10^{-4}$	0.25	-	$3.04x10^{-4}$	0.56	-	$1.08x10^{-2}$	1.48	-
10	$5.41x10^{-3}$	9.85	-1.50	$4.43x10^{-3}$	9.67	-3.29	$1.30x10^{-2}$	9.32	-6.75
50	$2.68x10^{-2}$	49.58	-0.85	$2.26x10^{-2}$	49.73	-0.53	$2.43x10^{-2}$	49.78	-0.45
100	$5.42x10^{-2}$	100.52	0.52	$4.53x10^{-2}$	99.77	-0.23	$3.78x10^{-2}$	97.89	-2.11
150	$8.07x10^{-2}$	149.80	-0.13	$6.81x10^{-2}$	150.27	0.18	$5.28x10^{-2}$	151.53	1.02
Correlation coefficient	1.0000			1.0000			0.9997		
Slope $((\mu g\ dm^{-3})^{-1})$	$5.38x10^{-4}$			$4.53x10^{-4}$			$2.80x10^{-4}$		
Intercept	$1.06x10^{-4}$			$4.87x10^{-5}$			$1.04x10^{-2}$		
Detection limit $(\mu g\ dm^{-3})$	0.1753			0.2410			12.7873		
Standard error	0.4380			0.4547			1.7771		

Table 3.50: Calibration data for ^{106}Pd, ^{108}Pd and ^{110}Pd when ^{139}La is used as internal standard.

	^{106}Pd			^{108}Pd			^{110}Pd		
[Element] ($\mu g\ dm^{-3}$)	Intensity ratio	Calculated concentration ($\mu g\ dm^{-3}$)	% difference (certified value - calculated value)	Intensity ratio	Calculated concentration ($\mu g\ dm^{-3}$)	% difference (certified value - calculated value)	Intensity ratio	Calculated concentration ($\mu g\ dm^{-3}$)	% difference (certified value - calculated value)
0	$1.92x10^{-3}$	0.48	-	$3.23x10^{-4}$	0.77	-	$2.86x10^{-4}$	0.58	-
10	$4.96x10^{-3}$	9.29	-7.14	$3.28x10^{-3}$	9.56	-4.41	$1.68x10^{-3}$	9.79	-2.13
50	$1.90x10^{-2}$	49.95	-0.11	$1.70x10^{-2}$	50.11	0.21	$7.63x10^{-3}$	49.01	-1.98
100	$3.66x10^{-2}$	100.65	0.65	$3.33x10^{-2}$	98.71	-1.29	$1.55x10^{-2}$	100.84	0.84
150	$5.35x10^{-2}$	149.63	-0.25	$5.09x10^{-2}$	150.86	0.57	$2.29x10^{-2}$	149.79	-0.14
Correlation coefficient	1.0000			0.9999			0.9999		
Slope ($(\mu g\ dm^{-3})^{-1}$)	$3.46x10^{-4}$			$3.37x10^{-4}$			$1.52x10^{-4}$		
Intercept	$1.75x10^{-3}$			$6.27x10^{-5}$			$1.98x10^{-4}$		
Detection limit ($\mu g\ dm^{-3}$)	1.6146			0.3263			1.1206		
Standard error	0.6607			1.0327			0.8390		

Table 3.51: Calibration data for ^{192}Pt, ^{194}Pt and ^{195}Pt when ^{139}La is used as internal standard.

	^{192}Pt			^{194}Pt			^{195}Pt		
[Element] ($\mu g\ dm^{-3}$)	**Intensity ratio**	**Calculated concentration ($\mu g\ dm^{-3}$)**	**% difference (certified value - calculated value)**	**Intensity ratio**	**Calculated concentration ($\mu g\ dm^{-3}$)**	**% difference (certified value - calculated value)**	**Intensity ratio**	**Calculated concentration ($\mu g\ dm^{-3}$)**	**% difference (certified value - calculated value)**
0	$2.13x10^{-4}$	0.58	-	$1.57x10^{-4}$	0.37	-	$1.87x10^{-4}$	0.52	-
10	$2.88x10^{-4}$	22.04	120.45	$1.29x10^{-3}$	10.82	8.21	$1.28x10^{-3}$	10.33	3.29
50	$3.17x10^{-4}$	30.44	-39.13	$5.39x10^{-3}$	48.61	-2.78	$5.65x10^{-3}$	49.72	-0.56
100	$5.74x10^{-4}$	103.66	3.66	$1.09x10^{-2}$	99.37	-0.63	$1.10x10^{-2}$	98.07	-1.93
150	$7.48x10^{-4}$	153.28	2.19	$1.65x10^{-2}$	150.83	0.55	$1.69x10^{-2}$	151.36	0.90
Correlation coefficient	0.9831			0.9999			0.9998		
Slope $((\mu g\ dm^{-3})^{-1})$	$3.51x10^{-6}$			$1.09x10^{-4}$			$1.11x10^{-4}$		
Intercept	$2.10x10^{-4}$			$1.17x10^{-4}$			$1.29x10^{-4}$		
Detection limit ($\mu g\ dm^{-3}$)	24.5744			1.6137			1.1785		
Standard error	13.3378			1.1304			1.4151		

Table 3.52: Calibration data for ^{196}Pt, ^{198}Pt and ^{103}Rh when ^{139}La is used as internal standard.

	^{196}Pt			^{198}Pt			^{103}Rh		
[Element] ($\mu g\ dm^{-3}$)	Intensity ratio	Calculated concentration ($\mu g\ dm^{-3}$)	% difference (certified value - calculated value)	Intensity ratio	Calculated concentration ($\mu g\ dm^{-3}$)	% difference (certified value - calculated value)	Intensity ratio	Calculated concentration ($\mu g\ dm^{-3}$)	% difference (certified value - calculated value)
0	$1.82x10^{-4}$	-0.43	-	$1.95x10^{-4}$	-0.86	-	$3.52x10^{-4}$	0.61	-
10	$1.08x10^{-3}$	10.59	5.92	$4.38x10^{-4}$	9.39	-6.08	$1.39x10^{-2}$	10.09	0.95
50	$4.34x10^{-3}$	50.89	1.79	$1.50x10^{-3}$	54.07	8.15	$6.99x10^{-2}$	49.24	-1.52
100	$8.15x10^{-3}$	97.85	-2.15	$2.49x10^{-3}$	96.14	-3.86	$1.42x10^{-1}$	99.44	-0.56
150	$1.25x10^{-2}$	151.10	0.73	$3.80x10^{-3}$	151.26	0.84	$2.15x10^{-1}$	150.62	0.42
Correlation coefficient	0.9998			0.9989			0.9999		
Slope ($(\mu g\ dm^{-3})^{-1}$)	$8.11x10^{-5}$			$2.37x10^{-5}$			$1.43x10^{-3}$		
Intercept	$2.17x10^{-4}$			$2.15x10^{-4}$			$-5.15x10^{-4}$		
Detection limit ($\mu g\ dm^{-3}$)	1.6177			4.7542			0.2180		
Standard error	1.5467			3.3730			0.7443		

Table 3.53: Calibration data for ^{96}Ru, ^{98}Ru and ^{99}Ru when ^{139}La is used as internal standard.

	^{96}Ru			^{98}Ru			^{99}Ru		
[Element] ($\mu g\ dm^{-3}$)	Intensity ratio	Calculated concentration ($\mu g\ dm^{-3}$)	% difference (certified value - calculated value)	Intensity ratio	Calculated concentration ($\mu g\ dm^{-3}$)	% difference (certified value - calculated value)	Intensity ratio	Calculated concentration ($\mu g\ dm^{-3}$)	% difference (certified value - calculated value)
0	$3.00x10^{-4}$	-0.62	-	$4.53x10^{-4}$	-1.81	-	$2.39x10^{-4}$	-0.12	-
10	$1.28x10^{-3}$	10.48	4.81	$8.56x10^{-4}$	11.59	15.93	$2.36x10^{-3}$	10.26	2.63
50	$4.63x10^{-3}$	48.65	-2.71	$1.94x10^{-3}$	47.74	-4.51	$1.04x10^{-2}$	49.64	-0.71
100	$9.42x10^{-3}$	103.22	3.22	$3.68x10^{-3}$	105.48	5.48	$2.08x10^{-2}$	100.33	0.33
150	$1.34x10^{-2}$	148.27	-1.15	$4.93x10^{-3}$	146.99	-2.01	$3.09x10^{-2}$	149.88	-0.08
Correlation coefficient	0.9995			0.9984			1.0000		
Slope ($(\mu g\ dm^{-3})^{-1}$)	$8.79x10^{-5}$			$3.01x10^{-5}$			$2.05x10^{-4}$		
Intercept	$3.54x10^{-4}$			$5.07x10^{-4}$			$2.63x10^{-4}$		
Detection limit ($\mu g\ dm^{-3}$)	0.6231			6.8131			0.8290		
Standard error	2.2946			4.0773			0.3339		

Table 3.54: Calibration data for ^{100}Ru, ^{101}Ru and ^{102}Ru when ^{139}La is used as internal standard.

	^{100}Ru			^{101}Ru			^{102}Ru		
[Element] ($\mu g\ dm^{-3}$)	Intensity ratio	Calculated concentration ($\mu g\ dm^{-3}$)	% difference (certified value - calculated value)	Intensity ratio	Calculated concentration ($\mu g\ dm^{-3}$)	% difference (certified value - calculated value)	Intensity ratio	Calculated concentration ($\mu g\ dm^{-3}$)	% difference (certified value - calculated value)
0	$4.21x10^{-4}$	-0.16	-	$2.55x10^{-4}$	-0.46	-	$2.61x10^{-4}$	0.20	-
10	$2.42x10^{-3}$	9.67	-3.28	$3.10x10^{-3}$	9.78	-2.16	$5.38x10^{-3}$	9.87	-1.26
50	$1.06x10^{-2}$	49.76	-0.48	$1.46x10^{-2}$	50.97	1.93	$2.64x10^{-2}$	49.69	-0.61
100	$2.12x10^{-2}$	101.87	1.87	$2.82x10^{-2}$	100.05	0.05	$5.32x10^{-2}$	100.37	0.37
150	$3.08x10^{-2}$	148.85	-0.76	$4.20x10^{-2}$	149.66	-0.23	$7.94x10^{-2}$	149.86	-0.09
Correlation coefficient	0.9998			1.0000			1.0000		
Slope $((\mu g\ dm^{-3})^{-1})$	$2.04x10^{-4}$			$2.78x10^{-4}$			$5.29x10^{-4}$		
Intercept	$4.53x10^{-4}$			$3.82x10^{-4}$			$1.56x10^{-4}$		
Detection limit ($\mu g\ dm^{-3}$)	1.2856			1.0467			0.2254		
Standard error	1.2925			0.6609			0.3174		

Table 3.55: Calibration data for ^{104}Ru when ^{139}La is used as internal standard.

	^{104}Ru		
[Element] ($\mu g\ dm^{-3}$)	**Intensity ratio**	**Calculated concentration ($\mu g\ dm^{-3}$)**	**% difference (certified value - calculated value)**
0	2.97×10^{-4}	0.05	-
10	4.55×10^{-3}	9.56	-4.35
50	2.25×10^{-2}	49.67	-0.66
100	4.57×10^{-2}	101.73	1.73
150	6.68×10^{-2}	148.99	-0.67
Correlation coefficient	0.9999		
Slope $((\mu g\ dm^{-3})^{-1})$	4.47×10^{-4}		
Intercept	2.74×10^{-4}		
Detection limit $(\mu g\ dm^{-3})$	0.5493		
Standard error	1.1972		